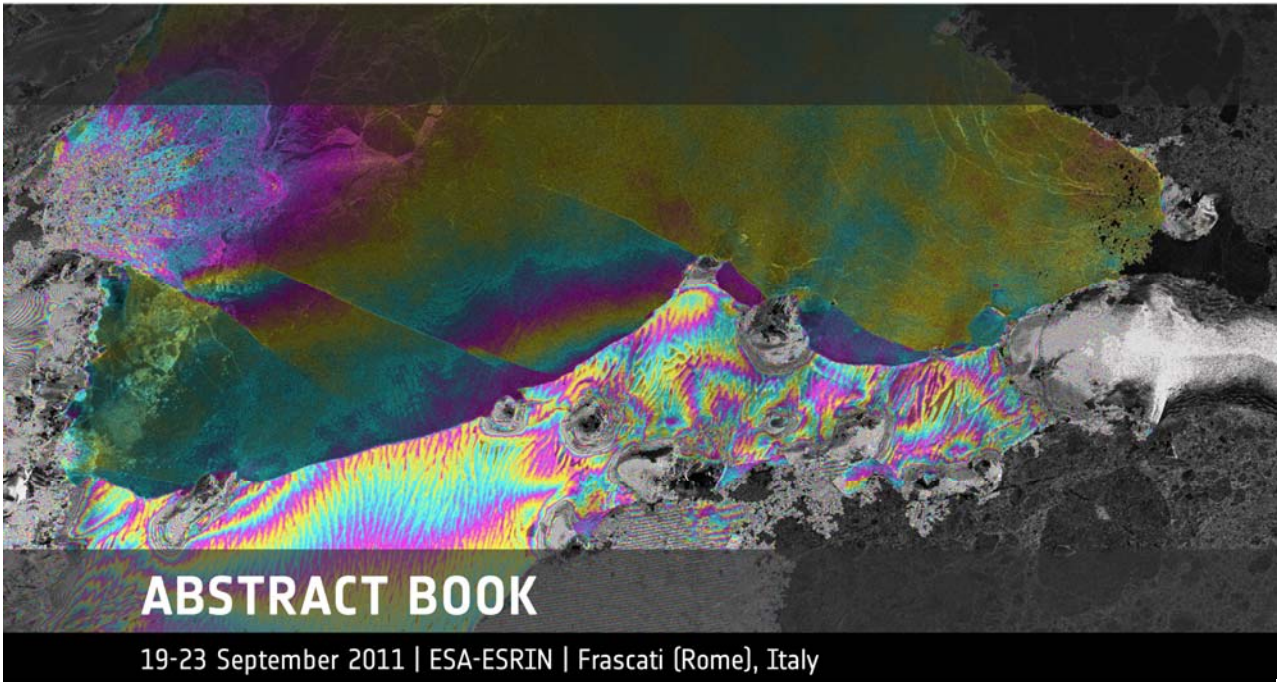


## → **FRINGE 2011 WORKSHOP**

**Advances in the Science and Applications of SAR Interferometry  
and Sentinel-1 Preparatory Workshop**





# FRINGE2011

## 8th International Workshop on “Advances in the Science and Applications of SAR Interferometry”

19<sup>th</sup> September -23<sup>rd</sup> September 2011  
ESA-ESRIN  
Frascati  
Italy

Organised by:  
The European Space Agency (ESA)

*Last Update: 12 September 2011*



# Table of Contents

<b>Day 1, Monday 19 September 2011</b> .....	1
<b>Session: Opening</b> .....	3
InSAR-capabilities of the ESA SAR Toolbox NESTa.....	3
<b>Session: Sentinel-1</b> .....	3
Sentinel-1 Mission Implementation .....	3
Sentinel-1 Mission Operations Concept.....	4
Sentinel-1 In-orbit Calibration and Performance Verification .....	5
Sentinel-1 Payload Data Ground Segment operations concept.....	6
<b>Session: InSAR Methods</b> .....	6
Bi-directional Interferometric SAR Acquisition with .....	6
TanDEM-X .....	6
The impact of second generation SAR sensors on the deformation time series analysis via DInSAR techniques: The COSMO-SkyMed study case .....	7
Generation and calibration of high resolution DEMs from single baseline spaceborne interferometry: the 'split-swath' approach .....	9
Interferometric multi chromatic analysis of high resolution X-BANDA data.....	10
How accurately can current and future InSAR missions map tectonic strain?.....	11
ERS-Envisat Tandem Cross-Interferometry Campaigns: systematic CInSAR processing and studies over extended areas .....	12
Multi-pass ERS-ENVISAT Cross-Interferometry methods and results .....	13
Design of a geosynchronous SAR system for water-vapour maps and deformation estimation.....	14
<b>Day 2, Tuesday 20 September 2011</b> .....	15
<b>Session: Earthquakes and Tectonics I</b> .....	17
Interseismic strain accumulation across strike-slip faults in the Middle East .....	17
Monitoring of interseismic creep of the Longitudinal Valley Fault (Eastern Taiwan) using Persistent Scatterer InSAR with ALOS PALSAR data.....	18
Shallow creep along the Haiyuan fault (Gansu, China) revealed by InSAR time series analysis.....	19
Mapping fault creep on the faults of northern California using persistent scatterer InSAR .....	20
Interseismic strain accumulation across an active thrust system: an InSAR case study in the Himalayas .....	21
Constraints on fault and lithosphere rheology from the coseismic slip and postseismic afterslip of the 2006 Mw7.0 Mozambique earthquake.....	22
Inter-Seismic Deformation, Volcanic Uplift and Post-Rifting Relaxation in North Iceland, derived from GPS and InSAR Time-Series .....	23
Three-dimensional time-varying crustal velocity and strains in the Afar triangle .....	24
Fault activity in the Manda Hararo rift in Afar (Ethiopia) using Interferometric Synthetic Aperture Radar.....	25
Multi-track InSAR Time Series of Plate Boundaries: The Zagros Mountains and Makran Subduction Zone, Southern Iran.....	26
Determining large scale crustal velocity field from GPS and InSAR: With application to Tibet .....	27
Two Contrasting InSAR Studies of Recent Earthquakes in Tibet .....	28
Magmatically driven normal faulting: A comparison of cumulative vs. incremental fault growth derived from high-resolution LiDAR and InSAR data .....	29
DLR's Activities to Support the GEO Supersite Initiative with TerraSAR-X Data .....	30
Tensile Strength of Rock from InSAR Observations.....	31
Earthquake slip distribution estimation from InSAR data, using a random field approach.....	32
Imaging recent complex earthquake ruptures with combined InSAR and seismic analysis.....	33
Geodetic Imaging, Seismic Hazard and Mountain Building Across the Sierra Nevada/Great Basin Transition Using InSAR and GPS .....	34
<b>Session: Pol-InSAR &amp; Tomography</b> .....	35
Diff-Tomo Opening of the Urban SAR Pixel: Single-look 4D and Non-uniform Motion "5D" Extensions.....	35
Polarimetric SAR Tomography with TerraSAR-X by means of Distributed Compressed Sensing .....	37
3D SAR Tomography of the Paracou Forest: Methods and Results .....	38

Underlying Topography Estimation and Separation of Scattering Contributions over Forests Based on PolInSAR Data .....	40
Sub-Canopy Topography Estimation With Multibaseline Pol-InSAR Data: A RELAX-Based Solution .....	41
<b>Session: Ice and snow</b> .....	43
Increased ocean melting and retreat of the Pine Island Glacier.....	43
Antarctic Ice Motion Unveiled with InSAR.....	43
Mapping Ice Shelf Flow with Interferometric Synthetic Aperture Radar Stacking.....	44
Grounding line mapping in Antarctica using 15 years of DInSAR data .....	44
Detecting Ice Motion in Grove Mountain, East Antarctica with ALOS/PALSAR Interferometry .....	45
Short-term glacier velocity changes at West Kunlun Mountains, NW Tibet.....	46
Airborne and satellite-based InSAR observations of Icelandic Ice Caps .....	47
Monitoring ice flow surface velocities of the Inylchek Glacier (Kyrgyzstan) using TerraSAR-X Data .....	48
ERS-EnvisatTandem Cross-Interferometry results from the EET northern hemisphere and Antarctic campaigns .....	48
A review of the 2011 ERS-2 3-day mission.....	49
Ice velocity fluctuations of Greenland's Jacobshavn Isbrae from ERS-2 3-day SAR imagery.....	49
Displacement of periglacial landforms on Svalbard observed with high-resolution RADARSAT-2 and TerraSAR-X InSAR time series.....	49
<b>Day 3, Wednesday 21 September 2011</b> .....	51
<b>Session: Atmosphere I and II</b> .....	53
OSCAR: Online Services for Correcting Atmosphere in Radar.....	53
InSAR integrated water vapour variational assimilation in mesoscale model MM5: a step for improving model initial conditions at high resolution .....	54
Validation of Centimeter-Level SAR Geolocation Accuracy after Correction for Atmospheric Delay using ECMWF Weather Data.....	55
InSAR Time Series with Atmospheric Estimation Model for Regional Deformation Mapping.....	56
Numerical Weather Model Assisted Time Series InSAR Processing for Geophysical Application .....	57
IP-STATS – A System for Deriving Statistical Models of Ionospheric Signals in Low-Frequency SAR.....	58
Spatio-temporal variability of Water Vapor as seen by InSAR, GPS, Meris and MM5.....	60
Systematic InSAR tropospheric phase delay corrections from global meteorological reanalysis data.....	61
Correcting DInSAR ALOS data using atmospheric delay estimated by GPS signals to constrain the surface deformation in the Longitudinal Valley (Taiwan Island).....	62
Pushing the accuracy limit for CO2 sequestration monitoring: Statistically optimal spatio-temporal removal of the atmospheric component from InSAR Networks.....	63
<b>Session: Earthquakes &amp; Tectonics II</b> .....	65
Satellite Constraints & Field Observations of slip in the Canterbury Earthquakes, New Zealand: Implications for future seismic hazard in Christchurch.....	65
The whole 2010-2011 New Zealand seismic sequence revealed by DInSAR and time-series data .....	66
Coseismic and postseismic deformation analysis of the 2010 Mw 7.1 Darfield and 2011 Mw 6.3 Christchurch earthquakes in New Zealand from combined GPS and InSAR observations.....	66
Damage Proxy Map of the 2011 M6.3 Christchurch Earthquake using InSAR Coherence .....	67
How sharp is our source image of the 2010 Haiti earthquake?.....	68
Postseismic deformation following the 2010 Haiti earthquake: Time-dependent surface subsidence induced by groundwater flow in response to a sudden uplift.....	69
Slip distribution and postseismic deformation of the April 14, 2010 Mw 6.9 Yushu (Qinghai, China) earthquake constrained using InSAR observations .....	70
Transient slip on the Hayward fault from SBAS-InSAR and GPS .....	71
Coseismic Deformations of the 2011 Tohoku, Japan, Earthquake and triggered events derived from ALOS/PALSAR71	
Wide area deformation map generation with TERRASAR-X data. the Tohoku-Oki earthquake 2011 case.....	72
The March 11, 2011, Tohoku-oki earthquake (Japan): surface displacement and source modeling.....	73
The Tohoku-oki (Japan) Earthquake imaged through 3-days repeat cycle ERS-2 SAR data .....	74
<b>Session: Terrain Subs. &amp; Landslides</b> .....	77
Surface deformation of the whole Netherlands after PSI analysis .....	77
Subsidence mapping in Jakarta - PSI processing of L-band ALOS PALSAR data.....	78

Satellite SAR interferometry for the measurement of surface subsidence above deep tunnels in metamorphic basement rocks of the Alps .....	79
DORIS FP7-EU project: exploitation of 20 years DInSAR data archive for landslide monitoring.....	80
TSX InSAR assessment for slope instabilities monitoring in Alpine periglacial environment (Western Swiss Alps, Switzerland).....	81
Long term analysis of strong non linear deformations induced by coal mining using the SBAS technique .....	82
Quantification of subsidence rates associated with groundwater flow using SAR interferometry .....	83
<b>Session: Methods – Unwrapping</b> .....	<b>85</b>
New improvements of the EMCF phase unwrapping algorithm for surface deformation analysis at full spatial resolution scale .....	85
Multibaseline gradient ambiguity resolution using graph-cuts for TANDEM-X phase unwrapping .....	86
Redundant Phase Unwrapping and Integration of Finite Differences on a Sparse Multidimensional Domain: Theory and Validation .....	87
Quality-guided segmentation for phase unwrapping of sparse differential interferograms.....	90
<b>Day 4, Thursday 22 September 2011</b> .....	<b>93</b>
<b>Session: Methods - DInSAR/PSI</b> .....	<b>95</b>
Wide Area Persistent Scatterer Interferometry: Algorithms and Examples .....	95
Virtual reconstruction and validation of Sentinel-1 Interferometric WideSwath mode: InSAR/PSI algorithms perspective.....	96
TOPS Differential SAR Interferometry with TerraSAR-X.....	96
Mapping 3D Surface Deformation by Combining Multiple Aperture InSAR and Conventional InSAR .....	97
Combination of X-band high resolution SAR data from different sensors to produce ground deformation maps .....	98
Bridge Health Monitoring using Persistent Scatterer Interferometry (PSI).....	99
Deformation estimation in non urban areas exploiting high resolution SAR data .....	100
InSAR partially coherent targets: multiplicity of approaches .....	101
Deformation rate estimation on changing landscapes using Temporarily Coherent Point InSAR.....	102
Exploitation of temporary coherent scatterers in SQUEESAR analyses.....	103
Noise covariance model for time series InSAR analysis .....	104
Detecting regular patterns in urban PS sets.....	105
A comparative study of corner reflectors, compact active transponders and I2GPS for monitoring deformation in areas with low spatial density of persistent scatterers: the Delft field experiment.....	106
<b>Session: Volcanoes</b> .....	<b>109</b>
InSAR and thermal monitoring of lava fountain episodes at Mt. Etna: the case study of the ASI-SRV Pilot project during the January 2001 episode.....	109
3D temporal evolution of displacements recorded on Mt. Etna from the 2007 to 2010 through the SISTEM method .....	110
Long-term experience gathered on Etna for volcano monitoring using radar and optical remote sensing, in preparation for Sentinel Missions .....	111
Source models for the March 5-9, 2011 Kamoamoia fissure eruption, Kilauea Volcano, Hawaii, constrained by InSAR and in-situ observations.....	112
Subsidence of the collapsed caldera of Miyakajima, Japan, 2006-2009.....	113
Pulses of Deformation Reveal Frequently Recurring 1 Shallow Magmatic Activity Beneath the Main Ethiopian Rift .....	114
Long-term uplift due to deep magma bodies: Insights from ERS and ENVISAT observations .....	115
Eighteen years of InSAR observations at Fernandina volcano, Galápagos: dynamics of magma storage and eruption .....	115
Tectonic control of magma ascent in volcanic arcs: Space-geodetic evidence from the West-Sunda arc, Indonesia .....	117
InSAR measurements of volcanoes in the tropics: examples from a survey of the Central American Volcanic Arc.....	118
High resolution monitoring of Campi Flegrei (Naples, Italy) by exploiting TerraSAR-X data: an application to Solfatara crater.....	119
Analysis of the Eyjafjallajökull 2010 eruption through InSAR time series .....	120
<b>Session: Methods- General</b> .....	<b>123</b>
Effect of Unmodelled Reference Frame Motion on InSAR Deformation Estimates .....	123

Revising vegetation scattering theories: Adding a rotated dihedral double bounce scattering to explain cross-polarimetric SAR observations over wetlands .....	124
Recent advances on InSAR temporal decorrelation: theory and observations using UAVSAR.....	124
Mining Very High Resolution InSAR Data based on Complex-GMRF Cues and Relevance Feedback .....	126
<b>Poster Session 1</b> .....	<b>129</b>
<b>Posters on ESA Sentinel-1 constellation</b> .....	<b>129</b>
End to End Sentinel-1 Toposar interferometric experiment based on simulated data.....	129
Space adaptive quantizer for interferometric applications.....	130
<b>Posters on Ground-based InSAR</b> .....	<b>131</b>
Use of Ground based InSAR for mapping unstable rock walls above a road in Norway .....	131
MODE TInSAR: an ESA incubation project dedicated to the Terrestrial SAR Interferometry.....	132
Advanced data analysis procedures for Ground-Based SAR (GBSAR) data .....	133
IBIS, an innovative ground-based interferometric radar for monitoring engineered and natural slopes .....	133
Design of the ground based array for the TropiScat experiment.....	134
Examples of precise detection and visualization of landslide related surface deformations with the Gamma Portable Radar Interferometer (GPRI).....	135
Monitoring of a building in the city of Rome by Terrestrial SAR Interferometry .....	136
2D Atmospheric Artifact Compensation with Multiple Regression Model in Ground-Based SAR over mountainous areas .....	137
<b>Posters on Earthquakes and tectonics</b> .....	<b>139</b>
Transient deformation in the Eastern California Shear Zone in Northern Mojave, California.....	139
Persistent Scatterer InSAR applied to the South West of Taiwan: neotectonic implications .....	140
L'Aquila earthquake: would an early warning have been possible? .....	140
Comparing Long and Short Term Deformation in the Krafla Fissure System, NE Iceland .....	141
Surface deformation in the Western Basin and Range Province .....	142
Co-seismic deformation due to the Tohoku-Oki earthquake measured by ENVISAT-ASAR data and GPS.....	142
Using SBAS-InSAR to Investigate tectonic activities along Chamn Fault .....	143
Inferring Complete (3D) Surface Deformation Field from Fusion of MAI and DInSAR Measurements: Application to 2010 Darfield Earthquake .....	144
The relationship between coseismic and postseismic deformation associated with the 2010 Mw 8.8 Maule, Chile Earthquake .....	144
InSAR observation and inversion of the 2011 three large earthquakes.....	145
InSAR analysis of active deformation related to the 2008 Nura earthquake, Pamir-Alai mountains .....	146
How well can InSAR derived earthquake source parameters explain observed seismic data? .....	146
Comparison of multi-temporal INSAR and coherent targets INSAR methods for post-seismic crustal deformation detection: a case study in east Kunlun fault after 2001 KOKOXILI earthquake .....	147
Time-series analysis of interseismic deformation across the Ganos segment of the North Anatolian Fault (NAF) zone, Turkey, from ERS and Envisat InSAR.....	148
The Study of Marine Terraces, SE of Iran using InSAR .....	148
3D ground motion detection combining different methods, sensors and geometries using SAR data.....	149
Measurement of interseismic strain accumulation in the Southern Andes (25°-35°S).....	149
Estimation of the surface deformation due to the 2009-2010 slow slip event at Guerrero seismic gap (Mexico) by satellite SAR Interferometry.....	150
Assessing variability in the slip rate of the Altyn Tagh Fault using InSAR data .....	152
Stability assessment of Rio-Antirio cable-stayed bridge (Western Greece) using C- and X-band SAR Interferometry .....	152
Towards mapping crustal deformation across North Africa: Examples from Algeria and Libya.....	153
Surface displacement time series analysis of the Afar rift zone retrieved through phase and amplitude SAR data .....	154
InSAR-GPS optimization for mapping high resolution 3-D crustal deformation of the 2011 Mw=9.0 Tohoku earthquake.....	155
Visco-elastic deformation of the lithosphere around the lake Siling Co in Tibet.....	156
Imaging crustal deformation and faulting processes in central and southern California.....	157
Co-seismic Displacement of 24-March-2011 Mw 6.8 Mong Hpayak Earthquake, Myanmar .....	158
Surface deformation in the western rift of Corinth, Greece, from InSAR data .....	159



Slip Distribution of the Giant 2011 Tohoku-oki Earthquake from Joint Inversion of Tsunami Waveforms and GPS Data .....	160
Error Analysis in Calculating 3D Displacement of Gaize Earthquake (Tibet) with ASAR Images of Different Viewing Angles.....	160
Coseismic deformation of Ahl (Kodian) earthquake derived from InSAR, Zagros-Iran.....	161
Investigation of different strategies for fault parameters and slip distribution retrieval of the 2005 Kashmir earthquake using SAR imagery.....	162
The effects of vegetation coverage, topography and coastal orientation on the 2011 Tohoku-Oki (Japan) tsunami inundation investigated by satellite data .....	163
The September 2010, Darfield earthquake, and the February 2011, Christchurch "aftershock": is there a cause and effect?.....	164
The lowest place on Earth is rising due to Dead Sea water level drop: Evidence from SAR Interferometry.....	164
An new approach for modeling fault dislocation from wrapped interferometric SAR data .....	165
Co-seismic deformation and Source characteristics of the Yushu Ms7.1 earthquake using InSAR and observation data.....	167
Fault-slip evolution during the 2009 earthquake sequence in the northern Malawi Rift, East Africa.....	168
Recent tectonic activity over the Marmara sea region from time series InSAR .....	168
Time series in Cascadia .....	170
DINSAR co-seismic and post-seismic analysis of the March,11th 2011 Tohoku (Japan) earthquake by using COSMO-SkyMed data .....	170
InSAR results from North America by the WInSAR Consortium.....	171
<b>Posters on Polarimetric Interferometry, Tomography and other Advanced Topics.....</b>	<b>172</b>
Just beyond PSI: Multi-dimensional SAR focusing for imaging and monitoring vertical structures.....	172
Three Dimensional SAR Tomography in Shanghai Using High Resolution Space-borne SAR Data.....	173
An improved crosstalk estimation algorithm of polarimetric and interferometric SAR calibration .....	174
Accurate Interferometric processing of PALSAR Wide-Beam SCANSAR Data.....	175
Evolutions of Diff-Tomo for Sensing Subcanopy Deformations and Height-varying Temporal Coherence.....	177
Urban 3D Reconstruction using COSMO-SkyMed high-resolution data.....	178
Different approaches for PSI target characterization for monitoring urban infrastructure.....	180
Theoretical Performance Bounds on the Estimation of Forest Structure Parameters From Multibaseline SAR Data .....	181
A Modified Model Based SAR Target Decomposition Method for Polarimetric Data .....	182
Statistical Edge Detection in Urban Areas Exploiting X-Band SAR data .....	183
<b>Posters on Ice and Snow .....</b>	<b>184</b>
Tide Model Accuracy in the Amundsen Sea, Antarctica, from InSAR Observations of Ice Shelf Motion.....	184
The application of time Series InSAR on the Antarctic Peninsula: first results .....	184
Monitoring Glacial Rebound using InSAR in Iceland .....	186
Dynamics of fast glaciers in the Patagonia Icefields derived from TerraSAR-X and TanDEM-X data .....	186
Periglacial Mass Wasting in the Antarctic Peninsula: Displacement detection at the South Shetlands Islands with DInSAR.....	187
Studies of ice motion and drainage of glaciers in Iceland using high resolution X-Band SAR .....	188
Ice flow mapping in Grove Mountains, East Antarctica using multi-temporal Inteferometric SAR dat.....	189
Glacier-surface deformation in alpine terrain based on PS-InSAR method in Siachen Glacier .....	190
Melt-induced speedup of Greenland Ice Sheet offset by efficient subglacial drainage.....	191
Estimation of Ice Flow Velocity of Calving Glaciers Using Feature Tracking and SAR Interferometry.....	192
<b>Posters on Terrain Subsidence and Landslides.....</b>	<b>193</b>
Local Phase Anomalies associated with the 2011 Tohoku-Oki Earthquake detected by PALSAR Interferometry ...	193
Monitoring slow-movement landslides in Central Taleghan region, Iran, by using SAR Interferometry.....	193
Land subsidence in Mahyar plain, Central Iran, studied using SBAS-InSAR method.....	194
Landslide creep monitoring using the integration of GPS and InSAR .....	195
InSAR Products in Support of Urban Monitoring – Case Study: Lüneburg.....	195
Landslides monitoring by means of DInSAR, SBAS and PSI, in the Prefecture of Peloponnesus, Greece .....	196
A geotechnical approach to the analysis of building settlements via DInSAR data.....	196
Deformation monitoring in Aghajari oil field using DINSAR-SBAS approach .....	197
Sinking cities in Indonesia: Space-geodetic evidence of rates and spatial distribution of land subsidence.....	197
Long Term, Operational Monitoring of Enhanced Oil Recovery in Harsh Environments with InSAR.....	198
INSAR Study of Landslides in the region of lake Sevan – Armenia.....	198
Detection and monitoring of landslide creep in Semirom, Central Iran, using SAR Interferometry.....	199

Monitoring of the landslide in the vicinity of the railway - highway road to Sochi Olympic 2014 site "Krasnaya Polyana".....	200
InSAR assessment of pipeline stability using compact active transponders.....	201
Recent results of subsidence in Khoy (Iran) - Ability of ALOS data in agricultural regions .....	201
Monitoring anthropogenic and natural ground deformation in Grand Duchy of Luxembourg and the "Greater Region" by the advanced Interferometric Synthetic Aperture Radar.....	202
Land subsidence monitoring in the southern Spanish coast using satellite radar interferometry .....	202
Persistent Scatterers Interferometry study of Roznow Lake area with ERS-1/2 archival data .....	203
InSAR and PSI results improvements with detailed LIDAR data.....	203
Landslide dynamics monitoring with TerraSAR-X interferometry and LIDAR data. Case studies of Klodne and Zbyszyce landslide (Southern Poland) .....	204
Bulging of the gypsum dome at Lesina Marina (Southern Italy) revealed by PSI techniques.....	205
The SBAS-DInSAR approach for the spatial and temporal analysis of sinkhole phenomena.....	206
InSAR time series analysis of coal mining field in Zonguldak city, NW Turkey .....	207
Factors that have an influence on time series.....	208
Integrated GNSS and InSAR processing over a landslide target near Koroška-Bela, NW Slovenia.....	209
Monitoring Stability of Levee with Time-series ENVISAT/ASAR Images.....	210
Geodynamic monitoring of oil-and-gas fields using radar Interferometric data .....	211
PSI helps to map relative susceptibility to ground and slope instabilities in the Lanzhou loess area of Gansu Province, China .....	212
Soil water storage change inferred from clay expansion as detected by satellite radar interferometry.....	213
Potential contribution of radar remote sensing for landslide monitoring in mountainous environment.....	214
Satellite vs Ground Based SAR Interferometry for landslide monitoring .....	214
Comparison of ground movements in coal mining areas (Belgium) observed by the PSI technique.....	215
Application of advanced InSAR time series for monitoring seasonal and long-term peatland surface change .....	216
Application of SAR interferometric methods to identify the mobility of the area above salt diapir in Inowroclaw City , Kujawy Region (Poland).....	217
Landslide mapping with SqueeSAR: from local to national scale .....	218
Modeling of Small Scale Surface Deformation based on DInSAR result.....	219
Subsidence due to fluid extraction, measured by small baseline InSAR in the Yellow River Delta, China.....	220
Application of Differential SAR Interferometry technique in a Dynamic Neural Network-based simulation-optimization model for subsidence prediction .....	221
Landslide detection in the Three Gorges region (China) using Small Baseline InSAR time-series techniques .....	222
DInSAR analysis of aquifer compaction due to ground water extraction in the Segura River Basin.....	224
Non-linear land subsidence in Morelia, Mexico, imaged through Synthetic Aperture Radar Interferometry .....	224
Operational Validation of the Accuracy of InSAR Measurements over an Enhanced Oil Recovery Field .....	225
<b>Posters on Cross Interferometry.....</b>	<b>226</b>
ERS – ENVISAT cross-interferometry over the Athens metropolitan area.....	226
<b>Poster Session II .....</b>	<b>227</b>
<b>Posters on Atmosphere I and II .....</b>	<b>227</b>
Atmospheric effects detection by short baseline processing in RADARSAT time series over Manaus city, Amazon region.....	227
Mitigation of atmospheric phase delay artefacts in interferometric SAR time series .....	228
Estimating ASAR atmospheric propagation phase delay from MERIS data: a case study.....	229
Atmospheric corrections of Interferometric Synthetic Aperture Radar observations: comparison of GPS Radio Occultation, Global Atmospheric Models (GAM), MODIS and MERIS .....	230
Comparison of Interferometric SAR and Multispectral time series for determination of Atmospheric Phase Screen .....	231
Atmospheric phase delay estimation from multiple SAR interferometry measurements .....	232
Water vapor distribution during heavy rain detected by InSAR and GPS.....	233
Atmospheric Water Vapor determination by the integration of InSAR and GNSS observations .....	233
Separating non-linear deformation and atmospheric phase screen (APS) for InSAR time series analysis using least-squares collocation.....	234
<b>Posters on Methods- General .....</b>	<b>236</b>
InSAR time series analysis of land deformation, North West of Iran.....	236

Landslides forecasting analysis by time series displacement derived from satellite InSAR data: preliminary results .....	236
MATSAR: a Matlab-based INSAR processor .....	237
Application of novel SAR interferometry techniques for the retrieval of ice velocity and ice topography.....	238
Empirical study of the sensitivity of measuring horizontal displacements of point-like targets using C- and X-band SAR.....	238
Joint inversion of INSAR and GPS times series : Application to monitoring ground motions related to volcanic or tectonic activities.....	239
Impulse response correlation, a new method for Signal to Clutter Ratio estimation of point scatterers .....	239
Automatic coregistration and simulated FRINGE removal by a direct estimation from high resolution DEM and ORBITAL data .....	240
An Adaptive and Iterative Filter Based on Local SNR for Strong Noise Reduction in SAR Interferogram.....	241
Monitoring Ground Deformation on Carbon Sequestration Reservoirs in North America .....	242
Frequency and Space Domain Orbit Error Corrections: A case study in Coseismic Deformations of 2011 Tohoku Earthquake .....	242
Interferometric coherence analysis with high resolution space-borne synthetic aperture radar .....	243
ALOS SAR interferometry for landslide monitoring in the Republic of Georgia .....	243
Landslide Monitoring for German Infrastructure Construction Site using Concrete Corner Reflector InSAR .....	244
InSAR Time series Analysis of Interseismic deformation of Eastern part of Iran .....	245
SAR inteferometry with seasonally changing snow cover .....	246
Interferometric Crossing Orbit Experiment using TerraSAR-X and TanDEM-X .....	247
InSAR interferogram real-time generation using optronic processor: initial concept.....	248
The InSAR Scientific Computing Environment: a processing tool for interferometric and polarimetric radar data..	249
DEM-based SAR pixel area estimation for enhanced geocoding refinement and radiometric normalization.....	250
The Introduction Of ICDINSAR Software For DINSAR And PSINSAR Application .....	251
On the Use of Radargrammetry in SAR Interferometry .....	252
Multiple Aperture InSAR (MAI) With C-Band and L-Band Data: Noise and Precision.....	252
Structure and Object Recognition using Very High Resolution InSAR Observations.....	253
Coregistration between Small Baseline InSAR Image Subsets using Pointwise Targets.....	254
<b>Posters on Methods - DInSAR/PSI .....</b>	<b>256</b>
Performance Evaluation of SBAS and PS to study land surface deformation in agricultural regions, case study: Western Tehran plain .....	256
Combining Continuous GPS and InSAR Data for the Analysis of Dynamic Aleutian Volcanoes.....	257
Towards repeatability, reliability and robustness in time-series InSAR .....	258
A Kalman Filter Based MTInSAR Methodology for Deriving 3D Surface Displacement Evolutions .....	259
SBAS bounds evaluation: a case study .....	260
Salt mining induced subsidence mapping of Lueneburg (DE) using PSI and SBAS techniques exploiting ERS and TERRASAR-X data .....	261
<b>Posters on Volcanoes .....</b>	<b>262</b>
The 2007-8 Volcanic Eruption on Jebel at Tair Island (Red Sea) studied by InSAR .....	262
SAR Interferometric analysis of ground deformation at Santorini Volcano (Greece).....	263
Correlated volcano deformation detected by InSAR .....	263
Evaluation of deformation processes in Tenerife volcanic island: the role of the troposphere.....	264
Beyond elasticity: the continuous to discontinuous deformation transition and its importance for InSAR data modeling in volcanology .....	265
Analysis of long-wavelength deformation in central Kamchatka, Russia, with combined InSAR and GPS time series .....	265
Permanent Scatterers and Small Baselines ( SBAS ) applications over ETNA .....	266
Time series of volcanic deformation in the Galápagos: A perspective from InSAR, GPS, and seismic data .....	267
Volcanic Deformation in Kenya, East African Rift.....	267
Surface displacement time series at Kilauea volcano, Hawaii using space-based synthetic aperture radar .....	268
1993-2010 InSAR measurements at Aso caldera (Japan). .....	269
The integration of multi-sensor interferometric observations for monitoring ground deformation in Damavand volcano, Iran .....	270
Envisat Extended mission" continues the InSAR monitoring of Mt. Etna .....	270
InSAR observations of post-rifting deformation around the Dabbahu rift segment, Afar, Ethiopia.....	271
Detachment depth revealed by rollover deformation: an integrated approach at Mount Etna.....	272
The April 3, 2010 earthquake along the Pernicana Fault (mt. Etna - IT): analysis of satellite and in situ ground deformation data integrated by the system approach .....	272

Improving the determination of volumetric sources from InSAR data.....	274
High-resolution interferometric monitoring of Piton de la Fournaise with TERRASAR-X and COSMO-SKYMED data .....	275
Anatomy of an unstable volcano from InSAR: multiple processes affecting flank instability at Mt. Etna, 1994-2008 .....	276
Volcanic activity in Eastern Turkey investigated by using InSAR.....	276
Deformation at Katla volcano, Iceland, 2003-2009: Disentangling surface displacements due to ice load reduction and magma movement using InSAR time series analysis .....	278
<b>Posters on Cross-Interferometry.....</b>	<b>279</b>
ERS-ENVISAT Cross-Interferometry Results over the Jangtsekiang delta in China.....	279
ERS-ENVISAT Cross-Interferometry signatures over deserts.....	280
<b>Posters on 3<sup>rd</sup> Party Missions.....</b>	<b>281</b>
An overview of MetaSensing SAR interferometric capabilities at L, C, X and Ku band.....	281
<b>Posters on Thematic mapping and DEM.....</b>	<b>282</b>
Inter-Tidal flats segmentation of SAR images using waterfall hierarchical algorithm .....	282
Contribution of Flash Floods to the Interannual Variability of Dust Emission in the Sahara.....	283
High resolution digital surface model for production of airport obstruction charts using spaceborne SAR sensors	283
Void filling and APS removal for DEM reconstruction from high-resolution INSAR data .....	285
InSAR DEM Reconstruction with ICESat GLAS Data.....	286
Enhancing Building Reconstruction by Adaptive Filtering of Interferometric Phases.....	287
<b>Posters on DInSAR &amp; PSI.....</b>	<b>288</b>
Report on ENVISAT Wide Swath interferometry beyond 2010.....	288
Ocean Tide Loading corrections applied to Persistent Scatterer Interferometry processing at tide gauges in the United Kingdom.....	288
Mapping of water level changes in Anzali wetland, North Iran, using multi-sensor InSAR observations .....	289
Models to predict Persistent Scatterers data distribution and their capacity to register movement along the slope .....	290
PS and SBAS Interferometry over the broader area of Thessaloniki, Greece, using the 20-year archive of ERS and Envisat data.....	291
Satellite and ground based InSAR studies of the Åknes rockslide in Norway.....	292
Urban deformation monitoring using X-band Persistent Scatterer Interferometry.....	293
Mexico city subsidence monitoring aided by interferometry: summary and discussion of the different achieved results.....	293
Thermal Response of Buildings with TerraSAR-X Stripmap Data.....	294
Detection of ground deformation in the Porto metropolitan area with persistent scatterer interferometry (PSI) .....	294
InSAR for early warning of possible highway instability over undermined area of Ostrava.....	295
Long term monitoring of mining induced subsidence in Thuringia, Germany by DInSAR .....	295
DInSAR Application: Subsidence of the Cerro Blanco Caldera .....	296
Assessment of surface deformation associated with CO <sub>2</sub> Storage at the Ketzin test site, Germany: Results from TerraSAR-X time-series analysis.....	296
Radar Interferometry Time Series Analysis to Evaluate the Source Modeling of the City Uplift in Staufen i. Br. (Germany) .....	297
Near Real-time Deformation Monitoring based on Persistent Scatterer Interferometry.....	297
Testing with real data a weighted LEAST-SQUARES Method for PSI .....	298
Evaluation of spatial interpolation of PSI datasets for continuous displacement field characterization .....	299
Experiences about the COSMO-SkyMed Stripmap Himage data processing – First Results of COSMO-SkyMed A0 research Project .....	300
Space based monitoring and analysis of the geological and geomorphological processes influencing the surficial dynamics of the Danube Delta .....	301
Complex investigation of the moderate seismicity in the Mediterranean .....	301
PS-analysis of COSMO SAR data stacks through a fast and simple technique .....	302
Presentation of the small baseline NSBAS processing chain on a case example: the Etna deformation monitoring from 2003 to 2010 using Envisat data.....	303
Multi-scale InSAR Time Series (MInTS) analysis of the creeping section of the San Andreas Fault .....	304
Applications using CEA SAR interferometry software package CIAO .....	305
3-D phase unwrapping for satellite radar interferometry .....	306

High Resolution Ground Deformations Monitoring by Cosmo-SkyMed PSP SAR Interferometry: Accuracy Analysis and Validation .....	307
Correction of Ionospheric Effects on InSAR Images Using Multiple Aperture InSAR.....	309
Estimation of the Persistent Scatterer density using optical remote sensing data and land cover data .....	309
Comparative analyses of PSI ground deformation measurements derived from multi-frequency satellite acquisitions .....	310
Performance of a combined pixels selection method in DinSAR.....	311
The thermal dilation component of X-band PSI observations .....	312
Retrieve ground parameters from QUASI-COHERENT targets for SAR interferometry .....	313
Ground Deformation Analysis by Persistent Scatterer Interferometry over the Whole Italian Territory: the Pst-A/2 Project .....	314
Time Series InSAR: an Integer Least Squares approach for slowly decorrelating pixels.....	316
An improved persistent scatterer method for high deformation estimation .....	317
Ground Deformation Time Series Analysis from Temporarily Coherent Point InSAR.....	318
DInSAR Pixel Selection based on Spectral Correlation in Time between Sublooks .....	319
A simulated annealing (SA) algorithm to efficiently select the interferometric SAR data pairs used by the EMCF phase unwrapping technique.....	320
<b>NOTES.....</b>	<b>323</b>



**Day 1, Monday 19 September 2011**





# Session: Opening

## InSAR-capabilities of the ESA SAR Toolbox NESTa

### Author(s)

Petar Marinkovic <sup>(1)</sup>, Andrea Minchella <sup>(2)</sup>,

### Department

<sup>(1)</sup> PPO.labs, NL

<sup>(2)</sup> RSAC c/o ESA-Esrin Via Galileo Galilei 64, IT

### Abstract

The Next ESA SAR Toolbox (NEST) is an user friendly open source toolbox for reading, processing, analysing and visualising ESA (ERS-1&2, ENVISAT) and other spaceborne (TerraSAR-X, RADARSAT 1&2, COSMO-SkyMed, JERS-1, ALOS PALSAR) SAR data processed to Level-1 or higher. The toolbox provides both basic and advanced tools for SAR user community such as absolute calibration, automatic coregistration of detected and complex products, multilooking, speckle filtering, ASAR WSS product debursting, external precise orbit ingestion, geocoding, mosaicking and a Product Library Metadata Database. In addition to these capabilities, NEST offers basic routines for oil spill detection, ship detection and wind field estimation from SAR data. Currently also InSAR and DInSAR tools are being developed through the porting of the functionality of the DORIS software developed in TU-Delft University. NEST shares the architecture of the BEAM Earth Observation Toolbox and Development Platform and it is fully portable to multiple hardware platforms and operating systems thanks to a 100% pure Java implementation. The modular design allows easy modifications and upgrades. Through APIs users can add their own modules and extend the capabilities of NEST. NEST is being developed by Array Systems Computing Inc. of Toronto Canada under ESA Contract number 20698/07/I-LG. InSAR functionalities are being developed by a joint effort of PPO.labs, Delft University of Technology and Array. For documentation and more information regarding NEST project, please visit the website at <http://earth.esa.int/nest>.

# Session: Sentinel-1

## Sentinel-1 Mission Implementation

### Author(s)

Paul Snoeij <sup>(1)</sup>, Ramon Torres <sup>(1)</sup>, Dirk Geudtner <sup>(1)</sup>, Malcolm Davidson <sup>(1)</sup>,

Mike Brown <sup>(1)</sup>

### Department

<sup>(1)</sup> ESA, NL

### Abstract

The Sentinel-1 synthetic aperture radar (SAR) constellation represents a completely new approach to SAR mission design by ESA in direct response to the operational needs for SAR data expressed under the EU-ESA Global Monitoring for Environment and Security (GMES) programme. The Sentinel-1 constellation is expected to provide near daily coverage over Europe and Canada, global coverage all independent of weather with delivery of radar data within 1 hour of acquisition – all vast improvements with respect to the existing SAR systems. Data products from the Agency's successful ERS-1, ERS-2 and Envisat missions form the basis for many of the GMES services. Consequently Sentinel-1 data products need to maintain data quality levels of the Agency's

previous SAR missions in terms of spatial resolution, sensitivity, accuracy, polarisation and wavelength. In addition to responding directly to current needs of the GMES program, the design of the Sentinel-1 satellite mission with its focus on stability, reliability, global coverage, consistent operations and quick data delivery is expected to enable the development of new applications and meet the evolving needs of GMES, for instance in the area of climate change and associated monitoring needs. The Sentinel-1 satellite carries a Synthetic Aperture Radar (SAR) instrument with four standard operational modes: Interferometric Wide Swath Mode, Wave Mode, Strip Map Mode, and Extra-wide Swath Mode. It is expected that Sentinel-1A be launched in 2013 and Sentinel-1B 18 months later. Once in orbit the Sentinel-1 satellites will be operated from two centres on the ground. The Agency's facilities in Darmstadt, Germany will command the satellite ensuring its proper functioning along the orbit. The mission exploitation will be managed at the Agency's facilities in Frascati, Italy, including the planning of the acquisitions by the SAR instrument according to the mission requirements, the processing of the acquired data and the provision of the resulting products to the users. This paper will describe the mission and systems aspects of the Sentinel-1 constellation. The status of the current development phase will be presented.

## Sentinel-1 Mission Operations Concept

### Author

Pierre Potin<sup>(1)</sup>,

Department

<sup>(1)</sup>ESA. IT

### Abstract

The main objective of the Sentinel operations concept is to ensure systematic and routine operational activities, with a high level of automation and with pre-defined operations to the maximum extent possible. The Sentinel-1 mission will provide C-band SAR observation continuity of the ERS and ENVISAT missions and will support a wide range of applications, including: monitoring sea ice zones and the arctic environment; surveillance of marine environment (e.g. oil spill monitoring); maritime security (e.g. ship detection); wind, wave, current monitoring; monitoring of land surface motion (subsidence, landslide, tectonics, volcanoes, etc.); support to emergency / risk management (e.g. flooding, etc.) and humanitarian aid in crisis situations; mapping of land surfaces: forest, water and soil, agriculture, etc.

The objective of the Sentinel-1 observation strategy is to implement a pre-defined and conflict-free observation plan aiming at fulfilling the observation requirements from the GMES services and from Member States. In addition, and in order to ensure continuity of ERS/ENVISAT, requirements from the science community are also considered, as well as the contribution to international activities. This approach for the Sentinel-1 observation scenario requires the need to find a priori the solutions on the potential conflict among users (e.g. different SAR operation modes / polarisation required over same geographical area, etc.).

The Sentinel-1 operations strategy is based on the optimum use of the SAR duty cycle (25 min/orbit), taking into account the various technical constraints (e.g. limitation in the number of X-band RF switches, mode transition times, etc.). The Wave Mode is planned to be continuously operated over open oceans, with lower priority versus the other modes, while the other modes will be the Interferometric Wide Swath (IWS) mode and the Extra Wide Swath (EWS) mode, which will be operated over predefined geographical areas: IWS over land, and EWS or IWS over seas, polar areas, and ocean relevant areas. In exceptional cases only, emergency observation requests may alter the pre-defined observation scenario, with e.g. the use of the Strip Map (SM) mode.

The presentation also provides the status of collection of the Sentinel-1 observation requirements and addresses the objectives of the planned cooperation between ESA and CSA regarding the respective Sentinel-1 and Radarsat Constellation Mission.

## Sentinel-1 In-orbit Calibration and Performance Verification

### Author(s)

Paul Snoeij <sup>(1)</sup>, Ramon Torres <sup>(1)</sup>, Dirk Geudtner <sup>(1)</sup>, Dave Bibby <sup>(1)</sup>,  
Allan Ostergaard <sup>(1)</sup>, Ignacio Navas Traver <sup>(1)</sup>, Mike Brown <sup>(1)</sup>,  
Berthyl Duesmann <sup>(1)</sup>

Department

<sup>(1)</sup>ESA, NL

### Abstract

The ESA Sentinels constitute the first series of operational satellites responding to the Earth Observation needs of the EU-ESA Global Monitoring for Environment and Security (GMES) programme. The GMES space component relies on existing and planned space assets as well as on new complementary developments by ESA. ESA is developing the Sentinel-1 European Radar Observatory, a constellation of two polar orbiting satellites for operational SAR applications. The two C-band radar satellites will provide continuous all-weather day/night imagery for user services, especially those identified in ESA's GMES service elements programme and on projects funded by the European Union (EU) Framework Programmes. Three priorities ('fast-track services') have been identified by EU user working groups: marine core services, land monitoring services and emergency services. Radiometric calibration must be performed as part of the normal operation of the SAR. The calibration process is divided into two components: internal and external calibration. Internal calibration provides an assessment of radar performance using internally generated calibrated signal sources, especially in the context of pre-flight testing. The Sentinel-1 SAR instrument has demanding requirements for measurement stability. Considering in orbit conditions and ageing effects, the hardware alone can not provide sufficient stability to fulfil these requirements. Therefore an internal calibration system is implemented to measure the actual instrument gain and phase changes in order to apply them later, in the ground processing, for correction of the image data. The parameter to be derived by internal calibration is the so called PG product, a quantity proportional to the product of transmit power and receiver gain. It is to be noted that the PG product is complex and allows correcting both amplitudes and phases of the image data. External calibration makes use of ground targets of known RCS to render an end-to-end calibration of the SAR system, thereby assessing the impact of those elements that are difficult, if not impossible, to assess using internal methods. External calibration methods can involve the use of: passive and precisely constructed targets, such as corner reflectors and spheres; natural terrain with known backscattering properties, such as the Amazon rainforest; or active transponders. The most important point with respect to the in-orbit calibration and performance verification of this flexible SAR system is the tight performance with an absolute radiometric accuracy of only 1 dB [3 dB] for all operational modes. Never before such a strong requirement (a few tenths of dB) has been defined for a satellite SAR system. Following the experience gained with ERS and ENVISAT it is necessary to have a set of precision radar transponders to act as point targets which can be automatically programmed and accessed during the Sentinel-1 commissioning phase and the remainder of the mission lifetime in order to achieve the absolute radiometric accuracy requirement. This paper will describe aspects of the in-orbit calibration and performance verification of the Sentinel-1 constellation.

# Sentinel-1 Payload Data Ground Segment operations concept

Author(s)

Betlem Rosich<sup>(1)</sup>,

Department

<sup>(1)</sup>ESA. IT

## Abstract

The Sentinel-1 Payload data Ground Segment (PDGS) will be responsible during the Sentinel-1 mission operations for the Sentinel-1 mission planning, X-Band data downlink, data processing, quality performance, data dissemination and archiving activities and user interface, with the main objective to make the core ground segment products available to the Sentinel-1 users within the expected timeliness and quality.

To achieve this objective, the Sentinel-1 mission planning will follow a stable but yet configurable, mission observation scenario fulfilling to the best possible extend (within the available spacecraft and ground segment resources), the GMES services requirements, national requirements and continuity requirements with ERS/ENVISAT.

The data downlinked over a set of Core Ground Stations (CGS) will be systematically processed at the CGSs or at the Processing and Archiving Centres (PAC) depending on their timeliness, into a configured set of L1/L2 core ground segment products, depending on the regional area and/or instrument mode. Registered Sentinel-1 users will have on line access to the systematic data flow according to their specific interests.

Although planning and processing approach is mainly based on a systematic approach, the pre-defined planning may be interrupted in case of emergency to satisfy specific observation needs whenever feasible, and on-request processing remains possible.

The presentation will provide an overview of the overall Sentinel-1 PDGS operations concept, in line with above considerations and with the operational nature of the Sentinel-1 mission.

## Session: InSAR Methods

### Bi-directional Interferometric SAR Acquisition with TanDEM-X

Author(s)

Josef Mittermayer <sup>(1)</sup>

Department

<sup>(1)</sup>DLR-IHR Muenchener Str. 20, D-82230 Wessling, DE

## Abstract

The paper presents the new interferometric Bi-directional SAR acquisition mode (InBiDi) and the first TanDEM-X interferograms obtained in this mode. The paper aims to raise a discussion about possible InBiDi applications by presenting the InBiDi principle and first results in along and across track interferometry. In the Bi-directional SAR acquisition (BiDi) the antenna pattern illuminates simultaneously into forward and backward azimuth direction. The same image area is acquired twice and with an along track offset of several seconds. A simple linear phase can be applied onto the antenna excitation which results in an antenna main beam and a grating lobe with the same gain as the main lobe. More sophisticated antenna pattern shaping and/or acquisition commanding with several azimuth patterns provides even more than two repeated

acquisitions. If one BiDi antenna configuration is kept during the whole acquisition, in principle repeated images can be acquired with an arbitrary azimuth extension. One acquisition example for TerraSAR-X / TanDEM-X geometry with a near range elevation beam results in an azimuth offset of 50 km or 7 s, achieved with simultaneous forward and backward illumination into  $\pm 2^\circ$  azimuth directions. This corresponds to about  $\pm 20$  kHz of Doppler centroid. The principal InBiDi acquisition geometry is discussed and the separation of the signals arriving simultaneous from different azimuth directions is explained. The separation is performed in Doppler domain and requires a PRF considerably higher than the azimuth bandwidth, e.g. by a factor of two. A dedicated timing parameter commanding is required which considers the acquisition geometry. In an interferometric constellation with two satellites providing an along and/or cross track baseline, the InBiDi mode allows for the repeated acquisition of two or more interferograms. The paper reports interferometric results obtained with TerraSAR-X and TanDEM-X during the so-called pursuit commissioning phase which is characterized by an along track separation of the two satellites of about three seconds. Several interferometric time series are presented showing several cross-track interferograms of the same scene with an acquisition offset in the range of seconds. Detailed analysis of the interferograms shows the differences between the interferograms and first hypotheses are made with respect to the possible origin of the differences as well as to possible new InBiDi applications. The first example is a series of interferograms acquired from the Upsala Glacier in Argentina/Chile. During the acquisition, both satellites were commanded to first illuminate in the BiDi mode, then switched to boresight illumination and finally returned to the BiDi mode. With this acquisition scheme it was possible to obtain three interferograms with an azimuth time offset of 3.6s and 7.2s. The azimuth extension of the common area in the interferograms is 20 km. The second example is a series of two interferograms acquired over Singapore including land, sea, urban area and several ships. Ships are either moving or anchoring near the harbour. These two interferograms show an azimuth offset of 6s and the azimuth extension of the common area is 100 km. Several fringes can be identified e.g. on the ships and detailed analysis is performed on the differences in the interferograms of the ships for forward and backward looking acquisition.

## The impact of second generation SAR sensors on the deformation time series analysis via DInSAR techniques: The COSMO-SkyMed study case

### Author(s)

Eugenio Sansosti <sup>(1)</sup>, Manuela Bonano <sup>(1)</sup>, Francesco Casu <sup>(1)</sup>, Riccardo Lanari <sup>(1)</sup>, Michele Manunta <sup>(1)</sup>, Luca Paglia <sup>(1)</sup>, Giuseppe Solaro <sup>(1)</sup>

### Department

<sup>(1)</sup>IREA-CNR Via Diocleziano 328, Napoli, Italy, IT

### Abstract

Differential SAR Interferometry (DInSAR) is a remote sensing technique that allows detecting and monitoring ground displacements with centimeter to millimeter accuracy by exploiting the phase difference (interferogram) between two SAR images relevant to the same area. During the last decade, advanced DInSAR techniques appeared in the literature. They are able to generate deformation time series and velocity maps, thus allowing to follow the detected deformation over time, with evident advantages from the geophysical point of view. Applications of those techniques to several real case studies have been possible by exploiting the large SAR data archives acquired, during the last 20 years, by the so-called "first generation" SAR sensors (e.g., ERS, ENVISAT, ALOS, RADARSAT-1), characterized by a nearly monthly revisit time and by ground resolutions ranging from few meters to tens of meters. The use of advanced DInSAR techniques

and first generation SAR data allow an almost continuous and complete coverage of the Earth's surface with measurement accuracies ranging within the 5-10 millimetre interval. Based on this experience, a "second generation" of SAR sensors have been recently launched (TerraSAR-X, Cosmo-SkyMed, RADARSAT-2) and/or will be launched in the near future (Sentinel, ALOS-2). Although some of them differ for the operating band and the achievable ground resolution, all these new systems exhibit a common characteristics: a reduced repeat time with respect to previous generation sensors. In this work, we discuss the present DInSAR scenario and how the availability of second generation SAR sensors is impacting on it. For our analysis, we focus on the Small Baseline Subset (SBAS) algorithm (Berardino et al., 2002) that relies on the combination of DInSAR data pairs, characterized by a small separation between the acquisition orbits (baseline), and is capable to work at two spatial resolution scales (Lanari et al., 2004): regional scale (with a spatial resolution up to 100m by 100m), and local scale (at the full sensor spatial resolution). Our test sites are the volcanic areas of Mt. Etna and Naples Bay (both in Italy), the latter including two volcanoes (Campi Flegrei and Vesuvius) and the urban area of Naples. In particular, as far as the Mt. Etna test site is concerned, we compare recent time series results from first generation sensors (ERS/ENVISAT) to those obtained by using 78 COSMO-SkyMed data acquired on descending orbit from July 2009 to December 2010. The analysis of the relative ground displacement between points across the Pernicana Fault computed by using COSMO-SkyMed data reveal a clear discontinuity in the deformation time series in correspondence to the  $M = 3.6$  earthquake (occurred on April 3, 2010), which, instead, is barely detectable by ENVISAT measurements. This is a clear and expected effect of the very short revisit time of the COSMO satellites, which was 8-days for this dataset. Moreover, despite the use of X-band, the computed velocity map exhibits a significantly increase of the number of measureable points with respect to typical C-band results; again, this is due to the short revisit time that allows circumventing the temporal decorrelation phenomenon, particularly significant for X-band data. For the Naples Bay test site, we carried out a full resolution analysis in order to investigate also the impact of the second generation sensors on the measurement of deformation phenomena affecting single structures or buildings. We compared ERS-ENVISAT and RADARSAT-1 time series with that obtained by processing 81 ascending images acquired by COSMO-SkyMed between July 2009 and November 2010. The obtained results show that the improved spatial resolution and the reduced revisit time of the COSMO-SkyMed dataset dramatically increase the performances of the advanced DInSAR techniques also for the full resolution processing, thus allowing detection and assessment of intra-building displacements and, therefore, investigation of portions of single structures, too. References Berardino, P., G. Fornaro, R. Lanari, and E. Sansosti, "A new Algorithm for Surface Deformation Monitoring based on Small Baseline Differential SAR Interferograms", IEEE Transactions on Geoscience and Remote Sensing, Vol. 40, No 11, pp. 2375-2383, 2002. Lanari, R., Mora, O., Manunta, M., Mallorqui, J.J., Berardino, P. and Sansosti, E., "A small baseline approach for investigating deformations on full resolution differential SAR interferograms", IEEE Transactions on Geoscience and Remote Sensing, Vol. 42, pp. 1377-1386, 2004.

# Generation and calibration of high resolution DEMs from single baseline spaceborne interferometry: the 'split-swath' approach

## Author(s)

Davide Giudici <sup>(1)</sup>, Andrea Monti Guarnieri <sup>(2)</sup>, Daniele Mapelli <sup>(1)</sup>, Fabio Rocca <sup>(2)</sup>

## Department

<sup>(1)</sup>Aresys , IT

<sup>(2)</sup>Politecnico di Milano , Italy

## Abstract

The generation of Digital Elevation Models (DEMs) through single pass SAR interferometry is a well known application that has been demonstrated by the success of SRTM mission and the recent results from TANDEM-X. While these DEMs meet the requirements of a wide community of users, they pave the road for better DEM with finer planimetric and altimetric resolutions. The generation of such DEM is nowadays made possible by the higher bandwidth available for civil applications. However, the finer resolution results in smaller swaths and at the same time in more stringent requirements of DEM calibration. Thus, even if coarse resolution DEMs are exploited for calibration, the precise estimation of normal baselines becomes a challenge. In the paper, we consider the case of single-pass spaceborne SAR interferometer, like a constellation or a single satellite with boom, like SRTM. The paper is focused on the main limits to the performances of the DEM, measured in terms of horizontal resolution and vertical accuracy. A mathematical model is developed to assess the accuracy of the location in 3D, given the two SAR images and a set of calibrated references, or Ground Control Point, with known accuracy, whereas we assume that the geometry of the interferometer, say the baselines, are known only at a very rough approximation. The mathematical model expresses the final accuracy as the combination of: - the noise on the interferometric phases - the accuracy of the GCP - the contribution of images coregistration. In the case of single pass interferometry, the phase error coming from thermal noise is the unavoidable term leading to the lower bound in the altimetric quality. This in turns leads to requirements to the system performance such as bandwidth, ambiguity rejection and the noise equivalent sigma zero. Volume decorrelation can be reduced by getting fine resolution cell, and minimizing penetration (say X band or higher). However, the error introduced by the limited knowledge of the interferometric baselines, can be hardly handled at system level (i.e. by imposing tight requirements to the boom stability). In fact, the normal baseline should be known with accuracy from millimeter to tens of micron, the most critical case being the boom configuration. Moreover this estimate should be enough frequent than the the dynamic of the boom itself. In the paper we describe a technique called 'split-swath', where the two interferometric images are acquired by scanning in TOPSAR mode two swaths separated by several tens of kilometers across track. The method exploits the same idea of Wavemill, to calibrate the across-track baseline by angular difference, yet with a very different configuration. Here the two swaths come from the same antenna pair, and the GCP there located by the coarse DEM in the two swaths combined together with coregistration information in a Mimimum Mean Square Estimator to derive the two components of the baseline. In that way, The main point of interest is the number of GCP needed to obtain the desired accuracy. With the limited swath size that can be obtained at low wavelengths, this is related also to the azimuth length of the calibration. It is found that, through the exploitation of the distance between the two split swaths, this calibration technique can reach micrometric accuracy in few seconds of acquisition. The advantage is to avoid complex evolution models for the baseline allowing a simple two-parameters calibration. In the paper, the derivation of the model for the evaluation of the vertical accuracy is described, the description of the calibration technique is reported and a numerical case

is reported. Namely, the characteristics of a Ka-band single pass interferometer aimed at the generation of high resolution DEMs are considered and discussed.

## Interferometric multi chromatic analysis of high resolution X-BANDA data

### Author(s)

Fabio Bovenga <sup>(1)</sup>, Vito Martino Giacobazzi <sup>(1)</sup>, Alberto Refice <sup>(1)</sup>,  
Oscar Davide Nitti <sup>(2)</sup>, Nicola Veneziani <sup>(1)</sup>

### Department

<sup>(1)</sup>National Research Council of Italy , IT

<sup>(2)</sup>Politecnico di Bari , Italy

### Abstract

The Multi-Chromatic Analysis, as introduced in [1], uses interferometric pairs of SAR images processed at range sub-bands and explores the phase trend of each pixel as a function of the different central carrier frequencies. The phase of stable scatterers evolves linearly with the sub-band central wavelength, the slope being proportional to the absolute optical path difference. Unlike the standard “monochromatic” InSAR approach, this new multi-chromatic technique allows performing spatially independent and absolute topographic measurements, if the attention is focused on single targets exhibiting stable phase behaviour across the frequency domain. Potential applications for the study of frequency-stable targets include topographic measurement, atmospheric research, and urban monitoring. Through a simplified model [2], we obtained a first evaluation of the impact of the MCA processing parameters on the height estimation performances. Results show that the estimation is improved by using wider bandwidths for the sub-look images, and by increasing the number of sub-looks. Moreover, a total bandwidth of at least 300 MHz seems to be required to provide reliable results. Thus, the technique appears optimally suited for the new generation of satellite sensors, which operate with larger bandwidths than those of previously available instruments, generally limited to about 20 MHz. SAR sensors such as those mounted on TerraSAR-X or COSMO/SkyMed spacecrafts, all pose great expectations on the potential use of multi-chromatic methods. Previous work [2] has started demonstrating the practical feasibility of the technique by using a set of SAR data collected by the airborne AES-1 radar interferometer, operating at X-band by multi-channel electronics, which provides a total radar bandwidth of 400 MHz. First successful applications of the technique to satellite data were performed by processing interferometric datasets acquired by TerraSAR-X as well as COSMO/SkyMed, both satisfying the processing requirements derived from the theoretical modelling and the prototype processing of the AES-1 dataset. In particular, it was possible to validate the use of MCA for performing PU as well as for absolute height measurement on a pixel by pixel basis. In principle the MCA method works independently on each single pixel. Nevertheless, due to temporal and geometrical decorrelation, a smoothing filtering in the spatial domain is required to derive a continuous unwrapped phase surface. Concerning absolute height retrieval, this may be theoretically possible on single pixels that show an adequate mean square error on the intercepts in the phase vs. frequency linear fit, provided that orbital parameters are known with sufficient accuracy, and atmospheric contributions are negligible or compensated for. Reaching metric absolute vertical precisions appears however problematic, given the required precision on the sensor position. Calibration procedures through independent measurements (e.g. reference points) are still required to fully retrieve the absolute heights. This work presents results obtained by processing both COSMO/SkyMed and TerraSAR-X SAR data with bandwidth ranging from 160 MHz up to 380 MHz, and acquired over a few test sites showing different characteristics in terms of topography as well as ground coverage. The MCA technique has been explored in order to check the limits of applicability. Moreover, a comparison between pixels



behaving temporally as Persistent Scatterers (PS) and pixels showing stable phase linear trends along the frequency is attempted by analyzing a TerraSAR-X spotlight image stack. -  
Acknowledgments - Work supported by both ESA ESTEC Contr. N. 21319/07/NL/HE and ASI Contr. I/047/09/0. TerraSAR-X data provided by DLR under a Scientific Use License for the proposal MTH0397. COSMO/SkyMed data provided by ASI under the AO-COSMO Project ID-1820. -  
References - [1] N. Veneziani, F. Bovenga, and A. Refice, "A wide-band approach to absolute phase retrieval in SAR interferometry". *Multidimensional Systems and Signal Processing*, vol. 14, no. 1-2, 2003. [2] Bovenga, F., Giacobazzo, V. M., Refice, A., Veneziani, N., Vitulli, R., "Multi-Chromatic Analysis of InSAR data: validation and potential". *Proceedings of FRINGE 2009, ESRIN, Frascati, Italy, Nov.30 – Dec. 4, 2009.*

## How accurately can current and future InSAR missions map tectonic strain?

### Author(s)

Tim Wright <sup>(1)</sup>, Matthew Garthwaite <sup>(1)</sup>, Andrew Shepherd <sup>(1)</sup>, Hyung-Sup Jung <sup>(2)</sup>, Andy Hooper <sup>(3)</sup>

### Department

<sup>(1)</sup>University of Leeds Leeds, UK, GB

<sup>(2)</sup>The University of Seoul 90 Jeonnong-dong, Dongdaemun-gu, The Republic of Korea

<sup>(3)</sup>Delft University of Technology Kluuyverweg 1, 2629 HS Delft, The Netherlands

### Abstract

By exploiting phase measurements from multiple acquisitions of Synthetic Aperture Radar (SAR) data, interferometric SAR (InSAR) can be used to measure the build up of tectonic strain around locked faults. Here we assess the accuracy of InSAR missions that are currently flying and planned for the future. We first identify a target level of strain using the global strain rate model of Kreemer et al (2003). We find that 90% of earthquake deaths occur in regions straining at rates higher than  $1.2 \times 10^{-8} \text{ yr}^{-1}$ . Because the accuracy of InSAR measurements is critically dependent on the length scale over which the observations are made, we also define a critical length scale of 100 km, based on the observed distribution of surface deformation around locked faults. We then review the error budget of individual interferograms; atmospheric noise dominates at length scales of 100 km. We discuss methods for optimum combination of multiple SAR acquisitions to estimate linear deformation rates, and show that methods using connected networks of short-interval interferograms are more accurate than simple stacking. We find that the error on the linear rate is proportional to the  $(\text{mission length})^{-3/2}$  and  $(\text{revisit time})^{1/2}$ . i.e. to half the error on linear deformation rates, the revisit time must be cut by a factor of four, or the mission duration increased by ~60%. Accuracies of 1.2 mm/yr over 100 km in the satellite line of sight can be achieved with a revisit time of 12 days with a 5 year mission, but to achieve this accuracy with a 3 year mission would require a 3 day repeat. The ability to measure tectonic strain on particular faults depends critically on the viewing geometry of satellite missions. Conventional SAR missions are poor at resolving surface deformation oriented north-south, since they fly in near polar orbits and have look directions that are near east-west at most latitudes. If we assume coherence can be maintained in all straining areas, Sentinel-1A should be able to resolve tectonic strain for 68% of the surface area straining above our target threshold of  $1.2 \times 10^{-8} \text{ yr}^{-1}$  on length scales of 100 km, although this increases to ~80% if ascending and descending data area both acquired. The archive of 7 years of Envisat data should be sufficient to resolve 39% of the area straining above the threshold. The proposed configuration of the shelved DESDYNI mission would be capable of measuring 89% of tectonic strain after 5 years. By contrast, an optimised, dual-beam SAR system, with forward and rear squinted beams, would be capable of resolving all three components of surface deformation with comparable accuracies. We show that 5 years of observations from such a system would be sufficient to resolve strain for

97% of the tectonic zones. We recommend that (i) Sentinel-1 acquire both ascending and descending data in areas of earthquake hazard, (ii) future SAR mission lengths should be extended for as long as possible, and (iii) dual beam radars are considered as possible a future design.

## ERS-Envisat Tandem Cross-Interferometry Campaigns: systematic CInSAR processing and studies over extended areas

Author(s)

Paolo Pasquali <sup>(1)</sup>, Paolo Riccardi <sup>(1)</sup>, Alessio Cantone <sup>(1)</sup>, Massimo Barbieri <sup>(1)</sup>, Marcus Engdahl <sup>(2)</sup>, Stefano Monaco <sup>(1)</sup>

Department

<sup>(1)</sup>Sarmap s.a. Cascine di Barico, 6989 Purasca, Switzerland, CH

<sup>(2)</sup>ESA, IT

### Abstract

The availability of ERS-Envisat 28minute tandem acquisitions from the dedicated ERS –ENVISAT - Tandem campaigns, thanks to the large geometrical baseline and very short temporal separation, provides highly valuable information for different applications, including among others: - very precise DEMs generation in areas with moderate topography; - monitoring of very fast displacements, including fast glaciers and sea ice; - better understanding of volume decorrelation phenomena, for example over densely vegetated areas or in areas of significant penetration due to the terrain dryness; - discrimination of different land cover types; - better understanding of atmospheric artifacts in the interferometric phase. The goal of this article is to summarize the results obtained within the “ERS-Envisat Tandem Cross-Interferometry Campaigns: CInSAR processing and studies over extended areas” project, aiming at evaluating the interferometric quality of the whole ERS-Envisat tandem data archive acquired during the four EET campaigns, run by ESA in the 2007-2010 period, and at demonstrating their suitability for different applications. In particular, a summary of the outcomes of the following different activities will be provided: 1) Systematic screening of the whole EET archive. A two-steps screening has been performed on the whole archive of data acquired during these campaigns (approximately 6'000 + 6'000 + 800 + 8'000 ERS – ENVISAT frame pairs), by first exploiting (when available and reliable enough) the nominal information available from the ESA EOLI-SA archive concerning normal baseline and Doppler Centroid difference, and then by performing interferometric processing and estimating the coherence statistics of all the pairs selected in the first screening step. This activity allowed to create a complete catalogue of the pairs suitable for interferometric exploitation, including both synthetic and detailed information for each pair: average baseline – Doppler Centroid and coherence as well as coherence maps for the whole frames. The results of this screening activity have been made available on-line, for direct consultation by the scientific community to help the selection of pairs suitable for exploitation in different applications. 2) Generation of large area products for the whole EET archive, including Digital Elevation Maps, Land Cover Maps, geocoded amplitude images and coherence maps. All the data that during the systematic screening resulted as suitable for CInSAR processing had been exploited for generation of different base products over large areas. 3) Validation of the results obtained during the generation of the large area products. Due to the location of the acquisitions obtained during the EET campaigns, in most of the cases in very Northern or Southern Areas, the validation of the large area products generated during the systematic processing is not so evident due to the lack of reference information. For this reason, alternative validation strategies have been exploited, in particular for assessing the accuracy of the obtained DEMs. On one hand products from repeated acquisitions (both on the same and on overlapping but different tracks) on the same area have been generated and compared, and on the other hand DEMs obtained from CInSAR processing

have been compared with height measurements derived from the interferometric stacking (PS + SBAS) processing of long time series on the same areas. 4) Results of studies related to different applications. A gallery of results obtained during the validation of the EET data suitability for different applications will be shown.

## Multi-pass ERS-ENVISAT Cross-Interferometry methods and results

### Author(s)

Urs Wegmüller <sup>(1)</sup>, Charles Werner <sup>(1)</sup>, Othmar Frey <sup>(1)</sup>, Tazio Strozzi <sup>(1)</sup>,  
Maurizio Santoro <sup>(1)</sup>

### Department

<sup>(1)</sup>Gamma Remote Sensing, CH

### Abstract

ERS-ENVISAT Tandem (EET) cross-interferometry (CInSAR) pairs are characterized by long 2km baselines and short 28 minute time intervals [1,2]. Over some sites multiple pairs are available. In our work we investigated for a variety of applications the use of multiple EET pairs.

One important CInSAR application is the generation of DEMs over relatively flat areas. Having multiple pairs permits improving the accuracy of the DEMs generated. The main error, the atmospheric path delay, does typically not correlate between multiple pairs, so that better accuracies can be achieved by combining multiple pairs. While features observed in all available pairs rather relate to the surface elevation features only observed in one pair are very likely caused by atmospheric effects. In EET CInSAR phase unwrapping is not trivial even in rather flat areas because of the high phase to elevation sensitivity with height ambiguities around 5 meter. Having multiple pairs with different baselines available helps with the phase unwrapping. Apart from the EET pairs combinations can be considered. Combinations with a shorter baseline can more easily be unwrapped, which helps avoiding unwrapping errors.

In the case of fast moving areas, e.g. for glaciers, multiple pairs are also useful. Assuming that the glacier flow rate is the same for the multiple EET pairs considered, it is possible to separate topographic and deformation phase terms, if the baselines differ significantly. If the baselines differ only slightly the combined interferogram without displacement phase has a much shorter effective baseline. This facilitates phase unwrapping, but up-scaling of the resulting topographic phase to long baselines may not be accurate enough to fully compensate the topographic phase of a 2km baseline pair. Using specific data we could derive the topography over large glaciers, but we could not accurately estimate the glacier velocity because the baselines of the available pairs differed only by less than 200m.

In the case of tidal motion of ice sheets the situation is different. For different EET pairs the tidal motion usually differs because of the tidal cycle. The estimation of grounding lines should therefore be more straightforward than the estimation of glacier motion and in this case very similar baselines are ideal. In the difference between two EET cross interferograms the topographic phase is largely reduced if the baselines are similar, so that the tidal phase will dominate. The topographic and the displacement phase can be separated and the grounding line determined.

### References

[1] Wegmüller U., M. Santoro, C. Werner, T. Strozzi, A. Wiesmann and W. Lengert, "ERS-2 Zero-Gyro-Mode Data Application Showcases", Proc. FRINGE 2007 Workshop, Frascati, Italy, 26. – 30. Nov., 2007 (<http://earth.esa.int/workshops/fringe2007>).

[2] Wegmüller U., M. Santoro, C. Werner, T. Strozzi, A. Wiesmann, and W. Lengert, "DEM generation using ERS-ENVISAT interferometry", Journal of Applied Geophysics Vol. 69, pp 51–58, 2009, doi:10.1016/j.jappgeo.2009.04.002.

# Design of a geosynchronous SAR system for water-vapour maps and deformation estimation

## Author(s)

Andrea Monti Guarnieri <sup>(1)</sup>, Fabio Rocca <sup>(1)</sup>, Luca Perletta <sup>(1)</sup>, Diego Scapin <sup>(1)</sup>, Antoni Broquetas <sup>(2)</sup>

## Department

<sup>(1)</sup> Politecnico di Milano Piazza Leonardo da Vinci, 32, IT

<sup>(2)</sup> Universitat Politècnica de Catalunya Jordi Girona 1-3, Spain

## Abstract

Envisaged geosynchronous SARs are peculiar for their twice daily revisit and for their near north-south Line Of Sight. Their low orbiting velocity allows for exploiting very small PRF and getting images free of ambiguities even if small antennas of one or two meters are exploited. The orbit stability of current geosynchronous satellites for telecommunications limits the azimuth resolution to say 10 m in X band, whereas the range resolution is limited by the available power and the targets RCS. Thus, the use of user antennas for targets of opportunity makes the system attractive even at the shorter wavelengths. One of the features of major interest is their capabilities of making coarse resolution images in very short time, say hundreds of meters in ten-twenty minutes. These images lead to the generation of water vapour maps finely sampled in space and time that can augment the value of weather forecast products like ECMWF. However, the atmospheric turbulence introduces an apparent motion of the target that impacts the image quality into different ways. A first effect of the random delay whose power is linearly increasing with time is a resolution loss, that depends on the wavelength, the turbulence and the satellite velocity, and has been addressed in literature. The second effect is however the spreading of the targets energy over the whole aperture, that causes a clutter like from moving targets (here motion is due to the fluctuation of the delay). This effect is significant when the scene is much larger than the APS lobe, say a few km, hence in the geosynchronous case. In this paper we evaluate the impact of the APS on both the resolution and the Signal to Clutter Ratio. In particular we discuss an algorithm to provide the estimation of the Atmospheric Phase Screen in the time-space domain, a necessary step to get fine resolution focused images. Such algorithm operates by processing raw data in a sequence of steps arranged in a hierarchical iterative approach from the coarser resolutions, and shorter time intervals, to the finer resolution, and longer intervals. At each step, the residual APS power is reduced up to the time-frequency resolution allowed by data themselves. At a final step, the residual high-pass components of the APS power would leave an high pass clutter at a resolution comparable with the focused data. Particular attention should be given to the conditions necessary for a bootstrap of the algorithms, in dependence of the wavelengths, by deriving the APS statistics from meteo stations and SAR data, and the satellite velocity from the existing geosynchronous systems.

**Day 2, Tuesday 20 September 2011**



# Session: Earthquakes and Tectonics I

## Interseismic strain accumulation across strike-slip faults in the Middle East

### Author(s)

Richard Walters <sup>(1)</sup>, John Elliott <sup>(1)</sup>, Rachel Holley <sup>(2)</sup>, Barry Parsons <sup>(1)</sup>,  
Tim Wright <sup>(3)</sup>

### Department

<sup>(1)</sup>University of Oxford Department of Earth Sciences, South Parks Road, OX1 3AN, GB

<sup>(2)</sup>Fugro NPA Ltd. Crockham Park, Edenbridge, TN8 6SR, UK

<sup>(3)</sup>University of Leeds School of Earth and Environment, LS2 9JT, UK

### Abstract

Large strike-slip faults play an important role in accommodating continental deformation and pose a significant seismic hazard in the Middle East, but to date there are few geodetic slip-rate estimates for many of these faults. We use Envisat InSAR measurements to study interseismic strain accumulation on strike-slip faults in Turkey and Iran, including the North Anatolian Fault (NAF). The NAF is a major feature of Middle Eastern tectonics, and it is important to accurately determine the slip rate across the fault in order to understand the role that the NAF plays in regional tectonics. In eastern Turkey, existing GPS data are sparse, and all previous InSAR studies of the NAF have used SAR data acquired from only one look direction. We make use of Envisat ASAR data from two satellite tracks, one ascending and one descending, that overlap across the NAF. We construct satellite radar interferograms from these data in order to measure ground displacements around the NAF and hence estimate the slip rate across it (Walters et al., 2011). We mitigate the effects of atmospheric errors by constructing multiple interferograms over the fault and summing them, effectively creating longer timespan interferograms and improving the signal-to-noise ratio. We empirically correct for orbital errors by flattening the radar swaths on the Anatolian Plateau, an area with little expected deformation. Our measurements of rates of displacement are consistent with an interseismic model for the NAF where deformation occurs at depth on a narrow shear zone below a layer in which the fault is locked. We jointly invert data from both satellite tracks to solve for best fitting model parameters, estimating both the slip rate and the depth to which the fault is locked. We have been able to reduce uncertainties on model parameters from those in previous studies by around 60 %. Our measurements show that the NAF is moving at a rate of  $23 \pm 3$  mm/yr below a locking depth of  $19 \pm 6$  km, which is in agreement both with a previous estimate made from a single track of ERS SAR data (Wright et al., 2001), and with existing GPS data. In addition, by using data acquired from two look directions, along with geological estimates of negligible vertical motion across the NAF, we have been able to calculate profiles of fault-parallel and fault-normal motion across the fault. Our results show negligible fault-normal convergence, validating the assumption of purely horizontal strike-slip movement that has previously been used in interseismic modelling of the NAF. We also show early results from InSAR analysis of strain accumulation across other strike-slip faults in Iran, where the slip rates are much smaller, and where the fault geometry is often unfavourable. R. J. Walters, R. J. Holley, B. Parsons and T. J. Wright (2011), Interseismic strain accumulation across the North Anatolian Fault from Envisat InSAR measurements, *Geophys. Res. Lett.*, V.38, L05303. Wright, T., B. Parsons, and E. Fielding (2001), Measurement of interseismic strain accumulation across the North Anatolian Fault by satellite radar interferometry, *Geophys. Res. Lett.*, 28(10), 2117–2120

# Monitoring of interseismic creep of the Longitudinal Valley Fault (Eastern Taiwan) using Persistent Scatterer InSAR with ALOS PALSAR data

## Author(s)

Champenois Johann <sup>(1)</sup>, Bénédicte Fruneau <sup>(2)</sup>, Erwan Pathier <sup>(3)</sup>,  
Benoit Deffontaines <sup>(2)</sup>, Kuan-Chuan Lin <sup>(4)</sup>, Jyr-Ching Hu <sup>(4)</sup>

## Department

<sup>(1)</sup>University Paris-Est 5 Bd Descartes, Bat IFI, FR

<sup>(2)</sup>Université Paris-Est 5 Bd Descartes, FRANCE

<sup>(3)</sup>Université Joseph Fourier , FRANCE

<sup>(4)</sup>National Taiwan University ,

## Abstract

The Longitudinal Valley, located in the eastern part of Taiwan, corresponds to the suture zone between the Eurasian and Philippine Sea plates, where an active collision occurs associated to an important seismicity. A series of historical large earthquakes occurred on the Longitudinal Valley, especially in autumn 1951 with four earthquakes  $M_s > 7$  and more recently, with the  $M_s \sim 6.5$  Chengkung earthquake (December the 10th, 2003). Since the 80's, several studies have showed a strain accumulation associated with interseismic deformation across the Longitudinal Valley. Firstly monitored by local trilateration networks [1], the deformation has been then measured by regional GPS network [2], leveling data, and in a few places by ground geodetic measurements, like at Chihshang where two creepmeters installed since 1998 show 30mm/year of localized creep, mainly thrust with left-lateral component [3]. This tectonic activity is usually attributed to the Longitudinal Valley Fault (LVF), which is one of the most active tectonic structures in Taiwan. However, different traces of the LVF segments have been proposed and other tectonic structures localized in the valley can also accommodate part of the deformation. Regarding the creeping activity, if it is locally well documented in a few places, its temporal and spatial variability along the Valley remains still unclear. To address these issues, an increase of the density of measurements over the whole valley is needed. Synthetic Aperture Radar Interferometry (InSAR) methods have proved their capacities to detect and to measure with great accuracy (cm to mm) ground surface deformations. A first InSAR study, using ERS C-band data [4], has confirmed on few local profiles, the existence of surface creep along the LVF. A more recent study, also conducted with ERS data but using a more recent method called Persistent Scatterer InSAR (PS-InSAR) [5], revealed more continuously the interseismic deformation along the LVF. However, the density of measurements is still too low in some places of the valley (especially over mountains or over area with high density of vegetation) to estimate precisely the interseismic deformation. This study presents new results on creep measurement and analysis on the southern part of the Longitudinal Valley from InSAR techniques with more recent data provided by ALOS satellite in L-Band (from JAXA). We use 10 SAR images acquired from January 2007 to February 2010 by the PALSAR sensor, an L-band radar (wavelength = 23cm) which provides a much better coherence than in C-band (5.6 cm) over the Longitudinal Valley (a rural area surrounded by mountainous tropical areas with a dense vegetal cover). Data are processed with the "Stanford Method for Persistent Scatterers" (StaMPS) that can perform time series analysis on a set of selected points called Persistent Scatterers (PS) [6]. We obtain more than 73 000 points of measurement in this area, which corresponds to an unprecedented spatial density (42 points per  $\text{km}^2$  in average). These results show clearly the interseismic activity of the Longitudinal Valley in good agreement with GPS measurement (RMS = 2.58), marked by a continuous discontinuity in the mean Line Of Sight (LOS) velocities, which has a location in global agreement with the published traces of the LVF. However there are locally significant discrepancies (up to several hundreds of meters) between the location of present-day interseismic creep and the published traces mainly based on



geological and geomorphological evidences. A first outcome allowed by the high spatial density of the ALOS PS-INSAR, is an improvement of the creeping faults traces map (with a location accuracy of about 100m). This helped us finding new field evidences of the fault activity based on markers of deformation affecting man-made structures close to the improved fault trace. PS-InSAR results also allow us to better quantify the deformations occurring in the valley between 2007 and 2010 and to analyze its temporal variability. We use a series of 58 close profiles along the major segment of the fault to estimate the LOS offset between both sides of the LVF. The relative change of LOS velocity is up to 2.4 cm/year but shows significant variations along the fault. On some part of the fault, the LOS offset occurs in less than a few ten's of meters across the fault, but in other part it can be distributed on 2-2.5 km. In the southern termination of the LVF, in the Peinanshan area, the deformation is more widely distributed amongst several active structures. These LOS offsets can be compared with GPS data and interpreted in terms of creep rates. Over the 2007 to 2010 period, no significant temporal variability of the creep rate can be shown in the PS-INSAR data. Due to the low temporal sampling of the ALOS data, this remains consistent with the seasonal variability shown in GPS or creepmeters time series. These results over the Longitudinal Valley gives new constraints to better understand the seismic cycle over the Taiwan orogen. They also provide original observations for studying creeping phenomena through a rare case of an onland creeping thrust fault. It also confirm the interest of using L-band ALOS data with PS-InSAR method to measure ground deformation in rural and mountainous area with a dense vegetal cover. [1] Yu, S.-B., C. Lee, 1986. Geodetic measurement of horizontal crustal deformation in Eastern Taiwan. *Tectonophysics*, 125, 73-85. [2] Yu, S.-B., Chen, H.-Y. & Kuo, L.-C., 1997. Velocity field of GPS stations in the Taiwan area, *Tectonophysics*, 274, 41-59. [3] Lee, J.-C., J. Angelier, H.-T. Chu, J.-C. Hu, F.-S. Jeng, and R.-J. Rau (2003), Active fault creep variations at Chihshang, Taiwan, revealed by creep meter monitoring, 1998-2001, *J. Geophys. Res.*, 108(B11), 2528, doi:10.1029/2003JB002394. [4] Hsu, L., and R. Bürgmann (2006), Surface creep along the Longitudinal Valley fault, Taiwan from InSAR measurements, *Geophys Res. Lett.*, 33, L06312, doi:10.1029/2005GL024624. [5] Peyret, M., Dominguez, S., Cattin, R., Champenois, J., Leroy, M. & Zajac, A., 2011. Present-day interseismic surface deformation along the Longitudinal Valley, eastern Taiwan, from a PS-InSAR analysis of the ERS satellite archives, *J. Geophys. Res.*, 116, B03402. [6] Hooper, A. J., Persistent scatterer radar interferometry for crustal deformation studies and modeling of volcanic deformation, Ph.D. thesis, Stanford University, 2006.

## Shallow creep along the Haiyuan fault (Gansu, China) revealed by InSAR time series analysis

### Author(s)

Romain Jolivet <sup>(1)</sup>, Cécile Lasserre <sup>(1)</sup>, Marie-Pierre Doin <sup>(2)</sup>, Gilles Peltzer <sup>(3)</sup>, Stephane Guillaso <sup>(4)</sup>, Jianbao Sun <sup>(5)</sup>, Rong Dailu <sup>(5)</sup>, Zheng-Kang Shen <sup>(6)</sup>

### Department

<sup>(1)</sup>ISTerre - CNRS , FR

<sup>(2)</sup>Ecole Normale Supérieure Paris , France

<sup>(3)</sup>University of California, Los Angeles , United States of America

<sup>(4)</sup>University of Technology, Berlin ,

<sup>(5)</sup>Chinese Earthquake Administration Beijing, China

<sup>(6)</sup>Peking University Beijing, China

### Abstract

Recent improvements on satellite based geodetic methods allow to measure spatial and temporal variations of the strain during different phases of the seismic cycle. Finer observations of fault behavior will lead to a better understanding of the mechanisms governing the strain evolution and to a better assessment of the seismic hazard. We use SAR interferometry to measure the strain evolution along the left-lateral Haiyuan fault system, that marks the north-eastern

boundary of the tibetan plateau. The last major earthquakes that occurred along the Haiyuan fault system are the M-8 1920 Haiyuan earthquake (strike-slip mechanism) and the M-8 1927 Gulang earthquake that ruptured a thrust fault system. There has been no known large earthquake on the central section of the Haiyuan fault, the "Tianzhu seismic gap", in the last ~1000 years. We focus here on the particular junction between the millennial seismic gap and the 1920 rupture. We first analyze the complete ENVISAT SAR data archive along 3 descending and 2 ascending tracks for the 2003-2009 period and construct InSAR-based mean line-of-sight velocity maps around the Haiyuan fault system from the eastern end of the Qilian Shan (102° E), to the west, to the Liupan Shan (106° E), to the east. From raw data, we compute the single look complex images and coregister them to a single master image, chosen on the basis of the total correlation. We then apply a local adaptive range filtering to generate the interferograms, which are then filtered, and unwrapped. We empirically correct our interferograms for propagation delays associated with changes on the stratified atmospheric structure, using a joint inversion to estimate biases between deformation, residual orbits and atmospheric phase delays. We then estimate, pixel by pixel, the mean line-of-sight velocity for each track, using a constrained time series analysis. The obtained LOS mean velocity maps show a dominant left-lateral motion across the fault with along-strike variations: some fault sections are locked at shallow depth while others are creeping and local vertical movements are observed. We model the shallow velocity by inverting the mean LOS velocities for both strike-slip and dip-slip motion on vertical, 2.5km x 2.5km discretized patches as well as the interseismic loading rate, using a least-square method with an appropriate degree of smoothing. The fault geometry follows the surface trace determined from SPOT images, with two main segments: one along the M-8 1920 rupture to the east and one along the "Tianzhu gap". We assess the influence of atmospheric noise on our velocity solution. Along a 35 km long segment, the creep rate is estimated to reach  $8 \pm 2$  mm/yr locally and is higher than the long term loading rate of the Haiyuan fault, estimated geodetically at  $5 \pm 1$  mm/yr, suggesting that creep is transient. The surface extension of the creeping segment is collocated with strong micro- and moderate seismic activity. At the junction between the 1920 rupture and the seismic gap, the Jingtai pull-apart basin shows a 2 to 3 mm/yr subsidence rate, limited by the Haiyuan fault to the south. We then explore the potential creep rate variations between 1993 and 2009. We first compare the inferred fault parallel velocity map on the 2003-2009 time period with that determined by Cavalieri et al. 2008, over the 1993-1998 period from ERS data. This reveals creep migration to shallower depth, and a possible creep rate increase through time. We also investigate for short term creep rate variations during the 2003-2009 period, applying a gaussian time filtering on ENVISAT time series. It reveals a creep rate increase during the 2007-2008 period which seems to correlate with a high cumulative seismic moment release. We finally model the creep rate evolution using the Principal Components Analysis Inversion Method (Kositsky & Avouac, 2010).

## Mapping fault creep on the faults of northern California using persistent scatterer InSAR

### Author(s)

Gareth Funning <sup>(1)</sup>, Lizhen Jin <sup>(2)</sup>, Brad Lipovsky <sup>(1)</sup>

### Department

<sup>(1)</sup>University of California, Riverside, US

<sup>(2)</sup>University of California, USA

### Abstract

Shallow aseismic fault creep is a behaviour exhibited by very few faults in the world. Instead of the stick-slip frictional regime that most faults follow, creeping faults move, steadily or episodically, throughout the interseismic period of the earthquake cycle. Creep effectively reduces

the fault surface area capable of rupture in earthquakes, and thus knowledge of its extent is critical for the correct assessment of seismic hazard. In addition, by comparing the geographical locations of creeping fault areas with mapped lithologies, we may be able to better understand the underlying causes or mechanisms. We present here the results of our ongoing research into the distribution of creeping fault areas in northern California, where the majority of reported cases are located. We map the surface deformation field of the plate boundary system south and north of the San Francisco Bay Area applying persistent scatterer InSAR (PSI) to the full archive of Envisat ASAR data, generating a dense spatial coverage of surface deformation measurements across the region, with both ascending and descending lines of sight where possible. Using a principal component analysis, we are able to characterise and exclude a variety of non-tectonic signals, such as surface subsidence due to mud settling and compaction, and periodic uplift and subsidence due to aquifer recharge and discharge. In the data that remain, we identify deformation consistent with right-lateral shallow creep on sections of five major faults (the Hayward, Calaveras, San Andreas, Rodgers Creek and Concord faults). On the Hayward fault, we are able to map both the extent and distribution of creep rates at depth, constraining the location of a locked zone that is presumably the source of major earthquakes on the fault. We are not able to identify a consistent lithological control for the creep behaviour.

## Interseismic strain accumulation across an active thrust system: an InSAR case study in the Himalayas

### Author(s)

Raphael Grandin <sup>(1)</sup>, Laurent Bollinger <sup>(2)</sup>, Marie-Pierre Doin <sup>(1)</sup>, Gabriel Ducret <sup>(1)</sup>, Romain Jolivet <sup>(3)</sup>, Cécile Lasserre <sup>(3)</sup>, Béatrice Pinel-Puysségur <sup>(2)</sup>

### Department

<sup>(1)</sup>Ecole Normale Supérieure, Paris , FR

<sup>(2)</sup>Commissariat à l'Energie Atomique , France

<sup>(3)</sup>ISTerre-CNRS-Université Joseph Fourier , France

### Abstract

The major active thrust system underlying the Himalayan range produces recurrent large earthquakes, representing a significant threat to the densely populated Indo-Gangetic basin. Measuring the interseismic deformation associated with this fault system should provide important constraints on the geometry of the locked faults that are bound to rupture in future earthquakes. This has so far been considered out of reach of InSAR techniques, due to strong temporal decorrelation, prominent topographic features, and unfavourable climatic conditions. However, preliminary tests carried out with the archived ASAR data provided by ESA's ENVISAT satellite since 2002 have shown that recent advances in InSAR processing may now allow geodesists to tackle most of these perturbations. In this context, applying these advanced techniques to the case of the Himalayas is both a challenging and necessary task. In this communication, we will present the methodology and the first results of an InSAR study of interseismic strain accumulation across the Himalayas. Small-baseline processing of ENVISAT data using a combination of ROI\_PAC software, NSBAS processing chain and MuSAR post-processing technique yields a sufficient number of coherent interferograms to compute a preliminary average velocity map of interseismic uplift. Time-space variations of stratified tropospheric delay observed in these interferograms are mitigated using both an a priori correlation between phase and topography, and a prediction using outputs of the ECMWF global meteorological reanalysis ERA-Interim. Finally, a correction of DEM errors from the wrapped InSAR data set further improves the coherence of interferograms with a large perpendicular baseline. Comparison of the InSAR LOS velocity maps with microseismic activity detected near the transition zone at the base of the seismogenic portion of the Main Himalayan Thrust is expected to provide constraints on the

process of elastic strain accumulation during the interseismic period. This will help in understanding the interaction between the construction of topography, damage near the active fault zone, and the role of fluids in controlling seismic activity, and will allow us to determine the relationship between these features and the ramp-flat geometry of the plate interface.

## Constraints on fault and lithosphere rheology from the coseismic slip and postseismic afterslip of the 2006 Mw7.0 Mozambique earthquake

### Author(s)

Alex Copley <sup>(1)</sup>, James Hollingsworth <sup>(2)</sup>, Eric Bergman <sup>(3)</sup>

### Department

<sup>(1)</sup>University of Cambridge Madingley Rise, Cambridge, CB3 0EZ, UK, GB

<sup>(2)</sup>Caltech ,

<sup>(3)</sup>Global Seismological services ,

### Abstract

We have studied the 2006 Mw 7.0 Mozambique (Machaze) normal-faulting earthquake using SAR data, SPOT optical images, and seismic waveforms. By performing a joint inversion of Envisat coseismic interferograms and P and SH teleseismic waveforms we can constrain the dip of the fault plane to be unusually steep (~75 degrees). Such a steep dip suggests the reactivation of a pre-existing structure, of less than half the strength of the surrounding material. The amount of slip in the earthquake decreased from depths of ~10 km to the surface, which corresponds to the depth extent of the thick sedimentary sequence in the region. The analysis of postseismic ALOS SAR data shows that this shallow slip deficit was at least partly recovered by postseismic afterslip on the shallow part of the coseismic fault plane. The postseismic deformation shows an unusual evolution through time. Rapid deformation immediately after the mainshock for ~250 days was followed by a long phase of constant-rate displacement. This steady motion abruptly stopped ~1000 days after the event. These observations of the temporal evolution of fault slip suggest possible refinements to mechanical models of fault rheology. The cross-correlation of SPOT 5 optical satellite images shows that an adjacent normal fault segment slipped post-seismically at shallow depths in a strike-slip sense. Models of the evolution of stress in the region show that this motion occurred in response to the stresses generated by the coseismic slip and postseismic afterslip on the main earthquake fault plane. Our observations of postseismic deformation on the coseismic fault plane, and on the adjacent fault, suggest that where the faults cut through the thick sedimentary sequence in the region they accumulate less displacement during earthquakes than occurs at depth. The shallow parts of the faults then slip postseismically in response to the stresses imposed by coseismic slip. Comparison with published dynamic models of earthquake rupture imply that the shallow part of the fault, within the sedimentary layer, is usually creeping (i.e. showing 'velocity-strengthening' behaviour), and that the coseismic rupture dynamically propagated into this region from the stick-slip ('velocity-weakening') region in the underlying crystalline basement. We discuss the implications of such behavior, if widespread in other fault zones, for the rheology of the continental lithosphere. Although the signal of shallow postseismic slip on the fault is clearly visible in the postseismic InSAR results, there is no long-wavelength signal of the type often observed after large earthquakes. This lack of signal, used in conjunction with models of viscoelastic relaxation, can be used to place constraints on the viscosity of the ductile portion of the lithosphere, which must be greater than  $\sim 2 \times 10^{19}$  Pa s. We have also examined satellite-derived optical images and topographic data for the region. By doing this we have been able to identify geomorphological features along the fault plane indicative of previous faulting. These observations suggest ways in which similar faults could be recognized before they rupture in future earthquakes. However, we also discuss the potentially misleading

features that the unusual coseismic and postseismic deformation in the Mozambique earthquake would leave recorded in the landscape.

## Inter-Seismic Deformation, Volcanic Uplift and Post-Rifting Relaxation in North Iceland, derived from GPS and InSAR Time-Series

Author(s)

Sabrina Metzger <sup>(1)</sup>, Sigurjón Jónsson <sup>(2)</sup>

Department

<sup>(1)</sup>ETH Zürich Sonneggstrasse 5, CH

<sup>(2)</sup>King Abdullah University of Science and Technology , Saudi Arabia

### Abstract

The Tjörnes Fracture Zone is a 100-km-long transform zone that connects two rift segments of the Mid-Atlantic Ridge: the onshore volcanic zone in North Iceland and the offshore Kolbeinsey Ridge to the North. The transform motion between these two rift segments is accommodated mainly by two parallel transform lineaments. One of them, the Húsavík-Flatey fault, is partly onshore and has not ruptured in a major earthquake for nearly 140 years. Thus Húsavík, a town located right on the fault, is exposed to a significant seismic risk. Using InSAR and GPS time-series, we want to identify the different signals that contribute to the overall deformation pattern in North Iceland and consequently constrain the kinematics of the Tjörnes Fracture Zone. The dominating deformation signal seen in the ERS1/2 (1992-2010) and ENVISAT (2002-2010) data are associated with two volcanic systems, Theistareykir and Krafla located south of the Tjörnes Fracture Zone. Uplift due to magmatic pressure increase is seen at Theistareykir (mainly between 2007 and 2008) and the effects of the 1975-1984 Krafla rifting episode are still present. These include local subsidence at Krafla central volcano and a decaying extensional post-rifting pulse emerging from the rift-axis. The expected subtle LOS inter-seismic deformation rate ( $\sim 2$  mm/yr) across the Húsavík Flatey fault is hardly detectable in the InSAR data among these strong transient signals. In contrast, accurate horizontal velocities from both continuous (2006-2011) and campaign GPS observations (1997-2010) clearly show inter-seismic strain accumulation across the fault. We use a combination of a back-slip model and Mogi sources (for the volcanic uplift/subsidence) to describe the observed deformation. The key model parameters define the kinematics of the transform motion on the Húsavík-Flatey fault. We find that  $34 \pm 3\%$  of the full transform motion is accommodated by this fault, indicating accumulating horizontal slip-deficit of  $6.9 \pm 0.7$  mm each year. Together with a locking depth of  $6.8 \text{ km} +2.3/-1.6 \text{ km}$ , the accumulated seismic potential of the fault corresponds to a magnitude  $6.8 \pm 0.1$  earthquake.

# Three-dimensional time-varying crustal velocity and strains in the Afar triangle

## Author(s)

Carolina Pagli <sup>(1)</sup>, Tim Wright <sup>(1)</sup>, Hua Wang <sup>(2)</sup>, Eric Calais <sup>(3)</sup>, Laura Bennati <sup>(3)</sup>, Cindy Ebinger <sup>(4)</sup>, Manahloh Belachew <sup>(4)</sup>, Elias Lewi <sup>(5)</sup>

## Department

<sup>(1)</sup>University of Leeds , GB

<sup>(2)</sup>Guangdong University of Technology , China

<sup>(3)</sup>Purdue University , USA

<sup>(4)</sup>University of Rochester , USA

<sup>(5)</sup>Addis Ababa University , Ethiopia

## Abstract

The start of a rifting episode in Dabbahu in 2005 prompted a renewed wave of interest in the tectonics of Afar. Here we use satellite geodesy to investigate the distribution of strain in time and space, the width of the plate boundary deformation zone, its variability in the different volcanic systems of Afar, and the style of deformation of individual volcanoes. The remoteness of the Afar region and its barren morphology makes it an ideal target for geodetic studies. As a result, the InSAR catalogue has seen a ten-fold increase in only five years, jumping from a few tens of acquisitions in 2005 to hundreds of images collected to date. Afar has also been the target of other crustal deformation techniques and continuous GPS sites and seismic stations have been collected all over the Afar triangle. Today, geodesists are faced with the problem of having to extract information from an extensive dataset, acquired in different reference frames (different acquisition geometry for each track and yet a different one for the GPS) and covering an area 700x500 km large. The approach has been to analyze individual interferograms spanning the time of episodic dyke intrusions and/or eruptions. However, this method has become impractical for studies of regional-scale tectonics, in particular when using such large datasets. Here, we use a method that combines all the different InSAR and GPS measurements in one common 3-dimensional framework. We use InSAR data from 12 different Envisat tracks and all the available GPS data to obtain large-scale 3D velocity and strain-rate maps in Afar. We obtain line-of-sight (LOS) deformation rates and the associated uncertainties for each InSAR track using a network approach to mitigate planar orbital and linear topographically correlated atmospheric delay errors in the interferograms. Unreliable pixels are not included in the rate maps by removing pixels with uncertainties of deformation larger than an a priori value, about 3-4 mm/yr. The network approach allows inversion for time-varying linear patterns and discrete offsets. Thus our rate maps preserve both linear deformation patterns as well as sudden deformations, ie. due to dyke intrusions, eruptions or faulting. We combine the LOS rate maps with the GPS data and invert for the three-dimensional velocity field based on Tikhonov regularization, following the method of England and Molnar (1), as adapted by Wang and Wright (2) to incorporate InSAR data. A triangular mesh is constructed over the Afar area and then we solve for the best-fit horizontal and vertical velocities on each node. Our analysis shows that strain in Afar is accumulated not only around the Dabbahu segment. A high strain rate is also observed towards the north in the Erta 'Ale range. This may be caused by high magma flow towards the segment as two eruptions occurred in Erta Ale since 2008. All 3D components of the velocity field are high around the Dabbahu segment, as a result of repeated dyke intrusions and accelerated post-rifting extension. Interestingly, the north component of the velocity field sharply ends between the Tat Ale Erta Ale segments, matching the main cluster of earthquakes in the area. One interpretation is that the east-west trending faults, as expected in a shear zone act as a bound to the northward velocity.

The strain map also highlights the extent of the area affected by post-rifting deformation around Dabbahu, with high strain rates observed over a 400 km wide area centred at the Dabbahu segment. On the other hand, the width of the plate boundary deformation zone over the non-currently rifting Erta Ale volcanic range is ~100 km, comparable to values observed in SE Iceland. We further adapt the velocity field method to solve for time-varying strain. The input data are from time series of deformation on each InSAR track and continuous GPS sites. We assume the deformation is smooth in time except at the known times of each dyke intrusion, and solve for the smooth 3D velocities at each node and the steps that occur during each dyke event. Preliminary results suggest that the post-rifting relaxation signal from the Dabbahu rifting episode consists of two components – a visco-elastic relaxation signal that decays only very slowly with time, and a magmatic signal that has high temporal variability. References 1- England P. and P. Molnar (2005), Late Quaternary to decadal velocity fields in Asia, *J. Geophys. Res.*, 110, B12401. 2- Wang H. and T.J. Wright, Crustal velocity field from InSAR and GPS reveals internal deformation of Western Tibet, *Nature Geoscience* (in review).

## Fault activity in the Manda Hararo rift in Afar (Ethiopia) using Interferometric Synthetic Aperture Radar.

### Author(s)

Stéphanie Dumont <sup>(1)</sup>, Anne SOCQUET <sup>(2)</sup>, Yann KLINGER, Eric JACQUES, Raphaël GRANDIN <sup>(3)</sup>, Cécile DOUBRE <sup>(4)</sup>

### Department

<sup>(1)</sup>Institut de Physique du Globe 1 rue Jussieu, FR

<sup>(2)</sup>Institu de Physique du Globe 1 rue jussieu, France

<sup>(3)</sup>ENS , France

<sup>(4)</sup>IPGS 5 rue René Descartes, France

### Abstract

A major rifting episode began in September 2005 in the northern part of the Manda Hararo rift with the intrusion of a 65-km-long mega-dike. This dike intruded at depth, over 10 km height and induced an average opening of 5 m at the surface (Grandin et al., 2009 ; Wright et al., 2006). From 2006 to present, 13 successive intrusions took place in the Manda Hararo Northern part of the rift. They were less voluminous (total volume for the last 12 dikes : 1.013 km<sup>3</sup> that is 55 % of the volume of the mega-dike). Grandin et. al (2010) highlighted transient deformations during the inter-diking periods at the center of the Manda Hararo rift segment. This signal may be associated with the recharge of the central magma reservoir involved in feeding the 2005-2009 dikes. During this inter-diking period creeping on faults is observed from InSAR data. These observations raise the questions relative to magmato-tectonic and fault interactions: Is the fault activity triggered by the magmatic intrusions at depth ? How do the faults interact ? What is the role of fault segmentation on the slip variations along fault strike ? The Manda Hararo rift area presents an important amount of normal faults and cracks, that were mapped using optical images (SPOT images, QUICKBIRD images) together with SAR interferograms and coherence images. This rift has been surveyed by repeated acquisitions of C-band data since the first dike in September 2005. With such a database [ >150 RADAR acquisitions in 4 tracks], we first focus our fault analysis on the period which follows the mega-dike intrusion and stops just before the next dike (June 2006). We consider the individual fault scale to investigate fault growth and then the interactions within a fault population. Then, we set the fault activity back in the rifting context: we consider its potential relation with the previous dikes injections and with the active magmatic system located at the center of the segment. We extract the displacement along the fault from the interferograms by performing a series of profiles normal to the fault. The preliminary results indicate two areas presenting a continuous activity : the first one is located in the northern part

of the segment, the second one above the magmatic chamber. We separately analyze the fault behavior of these regions in order to understand the dynamics of faulting in the rifting context.

## Multi-track InSAR Time Series of Plate Boundaries: The Zagros Mountains and Makran Subduction Zone, Southern Iran

Author(s)

William Barnhart <sup>(1)</sup>, Rowena Lohman <sup>(1)</sup>

Department

<sup>(1)</sup>Cornell University , US

### Abstract

We present interferometric synthetic aperture radar (InSAR) time series maps that span the eastern Zagros Mountains and western Makran of Southern Iran. We constrain the spatial and temporal characteristics of surface displacements across single structures over 7+ year time spans using 10 multi-frame (2-4 frames) Envisat descending tracks (335, 63, 20, 292, 249, 478, 206, 435, 163, 120). We invert for line-of-sight displacement at each acquisition date using an algorithm, similar to the Small Baseline Subset (SBaS) technique, to construct orogen-wide LOS rate maps. We can then extract full time series of pixels in deforming features of interest. We are able to image displacements related to hydrocarbon and hydrologic extraction, exposed diapir flow, transpressional motion across the Minab-Zendan fault zone, small (M~4-4.5) shallow earthquakes, post-seismic deformation from the 2003 Bam and 2005/2008 Qeshm Island Earthquakes, and, possibly, strain across the Main Zagros Thrust. Deformation in the Zagros/Alborz Mountains and the Makran Subduction Zone currently accommodates convergence between the Eurasian and Arabian plates. Modern convergence rates across the plate boundary vary from 25 mm/yr in the northern Zagros to 41 mm/yr in the eastern Makran. GPS observations suggest that the Zagros Fold and thrust belt (ZFTB) accommodates half of the Zagros/Alborz total shortening while convergence across the Makran subduction zone is accommodated by deformation of the Makran accretionary prism (MAP), which experiences great (>M8) earthquakes. Although GPS and seismic observations constrain the first order characteristics of convergence between Arabia and Eurasia, there is currently little geodetic data that is able to constrain deformation on small scales across single structures. Active structures identified through sparse campaign GPS surveys include the Minab-Zendan and Jiroft fault zones and the inferred Kazerun strike slip zone. Shallow, moderate sized (M~5.5-6) earthquakes occur in the ZFTB, but the nature of deformation across these thrust faults in the interseismic period as well as their relation to seismic folding are poorly constrained. InSAR observations over southern Iran provide comparatively higher spatial and temporal measurements than campaign GPS at a lower measurement precision. InSAR time series techniques exploit repeated acquisitions to minimize the effects of correlated atmospheric noise while imaging small magnitude and temporally variable deformation that is not apparent in single InSAR pairs. Furthermore, excellent phase coherence over southern Iran permits nearly spatially continuous measurements and few ambiguities due to unwrapping errors. We demonstrate the potential errors associated with incorrect orbital corrections induced by varying correlated noise scales in tests involving synthetic data. We also use independent observations of atmospheric water vapor from the MODIS and MERIS instruments to constrain error bounds of observed displacements given correlated atmospheric noise.



# Determining large scale crustal velocity field from GPS and InSAR: With application to Tibet

## Author(s)

Hua Wang <sup>(1)</sup>, Tim Wright <sup>(2)</sup>

## Department

<sup>(1)</sup>Guangdong University of Technology Guangzhou, China, CN

<sup>(2)</sup>University of Leeds Leeds, LS2 9JT, UK,

## Abstract

How continental lithosphere is deforming has been the subject of much debate since the birth of plate tectonics. Two end-member views dominate the debate in Tibet: (i) The deformation is primarily localized on major faults separating crustal blocks [e.g. Tapponnier et al., 1982, 2001; Meade, 2007; Thatcher, 2007], or (ii) deformation is distributed throughout the continental lithosphere [e.g. England and Houseman, 1986; England and Molnar, 1997, 2005]. These two views suggest rather different crustal deformation patterns in the vicinity of the plateau: block models predict all crustal strain will be concentrated around major fault zones, which will have relatively high slip rates, whereas continuum models predict lower slip rates, distributed over multiple fault zones. Although some studies combined the above two models [e.g. Chen et al., 2004; Loveless and Meade, 2011], the conclusion remains enigmatic due to sparse GPS data in central and western Tibet. InSAR offers an independent means of measuring present-day crustal deformation with a spatial resolution of a few tens of meters and accuracy comparable to GPS [e.g., Wright et al., 2001, 2004; Wang et al 2009]. The combination of GPS and InSAR provides constraints on the velocity field and allows us to test continental deformation models. Here we adapt the method by England and Molnar [2005] and incorporate most published InSAR data to determine the velocity field of Tibet. The InSAR data include a track covering the northwestern Xianshuihe fault (Wang et al., 2009), six tracks in western Tibet (Wang and Wright, 2011), a ~1000-km-long track across central Tibet (Garthwaite et al., 2011), and four tracks that cover the Altyn Tagh Fault (Elliott et al., 2008; Cavalie et al., 2008; Jolivet et al., 2008). Initially, we set up a triangular mesh spanning the whole plateau; we then solve for the horizontal velocities on each node, as well as additional orbital and atmospheric terms for the InSAR data. The solution is regularised using Laplacian smoothing, whose weight is determined as a compromise between solution roughness and data misfit. The resultant velocity field satisfies the InSAR and GPS data with a RMS misfit of ~1 mm/yr. The incorporation of InSAR data reveals a series of focused strain zones by the influence of the earthquake cycles, e.g. the transient deformation associated with the 1996 Mw 6.8 Hetian earthquake and the 2001 Mw 8.0 Kokoxili earthquake, and the interseismic strain accumulation on the Xianshuihe fault. The velocity field shows high strain rates along the Himalayan thrust zone and fast clock-wise rotation along the Eastern Himalayan Syntaxis, but it also shows smoothly distributed strain and low slip rates along the major strike-slip faults in the interior of the plateau. Though blocks exist and the models may fit the observations equally well, more and more earthquakes and high strain zones have been identified on unknown faults. Therefore it is neither realistic nor useful to model Tibet by blocks bounded by known faults. We conclude that it is more approximate to describe Tibet with continuum models of continental deformation modified by the short-term influence of the earthquake cycle.

# Two Contrasting InSAR Studies of Recent Earthquakes in Tibet

## Author(s)

Barry Parsons <sup>(1)</sup>, John Elliott <sup>(1)</sup>, Zhenhong Li <sup>(2)</sup>, Wanpeng Feng <sup>(3)</sup>,  
James Jackson <sup>(4)</sup>, Xinjiang Shan <sup>(3)</sup>, Alastair Sloan <sup>(4)</sup>, Richard Walker <sup>(1)</sup>,  
Richard Walters <sup>(1)</sup>

## Department

<sup>(1)</sup>University of Oxford , GB

<sup>(2)</sup>University of Glasgow , UK

<sup>(3)</sup>China Earthquake Administration , China

<sup>(4)</sup>University of Cambridge , UK

## Abstract

A large earthquake ( $M_w = 6.9$ ) struck the county of Yushu, Qinghai, China on 13 April 2010, causing 2,220 fatalities and over 12,000 injured. The reason this was such a damaging earthquake can be understood from the fault geometry and slip distribution determined using ALOS and Envisat SAR data. In contrast, two smaller earthquakes (both  $M_w = 6.3$ ) that occurred on 10th November 2008 and 28th August 2009 in almost the same location in the North Qaidam thrust system did little damage. However, Envisat InSAR studies of these events provide direct evidence for the first time of fault segmentation with depth in the seismogenic crust. Such fault segmentation with depth can allow a significant seismic hazard to remain even the occurrence of a strong to major earthquake.

The fault on which the Yushu earthquake occurred is one of a number of strike slip faults in eastern Tibet accommodating the deformation of the Tibetan plateau. It can be traced precisely using SPOT 5 (2.5 m resolution) imagery and SAR image offsets, interferometric coherence and phase discontinuities. On this basis, the fault was most simply divided into three segments, and the dips of the fault segments were obtained from elastic dislocation models with uniform slip. The fault geometry was then fixed and the slip distribution that best-fits the InSAR phase measurements determined. Slip that is almost pure left-lateral occurs mainly in the upper 10 km, with a maximum slip of  $\sim 2$  m at a depth of 3 km on the southeast segment. Near-surface slip (upper 1 km of the model) agrees well with field observations of offsets on the southeast segment.

The geodetically-determined and seismic moments are in reasonable agreement ( $2.1 \pm 0.2 \times 10^{19}$  N m). However, rupture lengths of 35-40 km were estimated immediately after the earthquake from the seismic moment together with magnitude of slip at the surface observations and assumed seismogenic layer thicknesses, whereas the interferograms showed slip must have occurred over a length of 70-75 km. The apparent discrepancy can be explained in terms of the non-uniform distribution of moment release on the fault. There are three main patches of moment release along the length of the fault. We believe the northwest patch may be due to the aftershock ( $M_0 = \sim 0.2 \times 10^{19}$  N m) that occurred about two hours after the main event.

The other two patches of moment release would then correspond to the two peaks in the source-time function determined by body-wave modelling. The best fits to the body waves are found if a speed of propagation of the rupture of  $2.5 \text{ km s}^{-1}$  to the southeast is assumed. The lengths of the moment-release patches along strike and the widths of the two peaks in the source-time function are roughly consistent at this rupture speed. The location of the town of Yushu at the end of the fault rupture, towards which it propagated, can explain the extensive damage to the town. The placement of the town relative to the rupture is very similar to that in the 2003 Bam (Iran) earthquake.

The 2008 and 2009 Qaidam earthquakes occurred within the North Qaidam thrust system, south of the Qilian Shan/Nan Shan thrust belt and on the northern margin of the Qaidam basin, NE Tibet.

This fold-and-thrust belt is the result of the ongoing northward convergence of India with Eurasia, with the rate of NE-SW convergence across it of approximately 10 mm/yr. The coseismic displacements due to each earthquake were measured by constructing radar interferograms using a combination of SAR ENVISAT acquisitions spanning each event separately. For each earthquake, we utilised two look directions on ascending and descending satellite passes, and derived fault and slip models using both look directions simultaneously. The models suggest that the two earthquakes occurred on a near coplanar fault that was segmented in depth, resulting in the arrested rupture of the initial deeper segment of the fault, and only allowing the failure of the upper portion of the crust ten months later.

The depth at which the segmentation occurs is approximately coincident with the intersection of the down-dip projection of a range-bounding thrust fault. Similar fault interactions at depth can also explain the occurrence of the 1981 Sirch and 1998 Fandoqa earthquakes on the same section of the Gowk fault in SE Iran. In addition, a similar fault geometry may have prevented the failure of the lower part of the seismogenic layer during the 2003 Bam (Iran) earthquake. These observations suggests that where either an interacting fault geometry or lithological properties allow only part of the seismogenic layer to rupture, the occurrence of a large earthquake does not necessarily result in a reduction of the immediate seismic hazard.

## Magmatically driven normal faulting: A comparison of cumulative vs. incremental fault growth derived from high-resolution LiDAR and InSAR data

### Author(s)

Barbara Hofmann, Tim Wright, Douglas Paton, Julie Rowland <sup>[1]</sup>

### Department

<sup>[1]</sup>The University of Auckland School of Environment, Private Bag 92019, Auckland, NZ, NZ

### Abstract

The influence of magma in extensional tectonic settings is widely recognised. Magmatic intrusions can cause surface fault displacement in the range of meters accompanied by only moderate seismicity. In such circumstances there is a large difference between seismic and geodetic moment release [e.g. Ebinger et. al., 2010]. Hazard estimates are based on paleoseismological analyses which relate fault slip to seismic moment release without considering the influence of magmatic processes on fault development. Due to the nature of fault growth, which is caused by multiple slip events, we can usually only study a snapshot during its evolution. The ongoing Dabbahu (Afar) rifting episode, which commenced in 2005 within the Afar Depression, is providing a unique opportunity to study progressive magmatically-driven fault growth. Here we compare cumulative fault slip from airborne LiDAR data with slip measured using InSAR during individual dyke intrusions. Analyses of the initial dyke intrusion on the base of satellite radar data (SAR) obtained by the ENVISAT satellite of the European Space Agency (ESA) were carried out by Wright et al. [2006] and Ayele et al. [2007]. They inferred a 25km-wide zone along most of the Dabbahu segment was uplifted by up to 1.5 m at the flanks of the rift while a central 2-3 km-wide zone subsided by up to 2 m. A maximum of 6 m horizontal opening was estimated. Surface displacement as well as observed seismicity were characteristic of laterally propagating magmatic dyke intrusions [Keir et. al., 2009]. Simple elastic modelling [Wright et al., 2006] infers the dyke intrusion to be situated between depths of 2 and 9 km with a volume of  $\sim 2 \text{ km}^3$ . Estimates of moment release show a significant difference of an order of magnitude between the geodetic moment release ( $\sim 8.0 \times 10^{19} \text{ Nm}$ ) and the seismic moment release ( $\sim 6.7 \times 10^{18} \text{ Nm}$ ). Since its onset, a total of 14 individual dyking events have been identified through InSAR and seismicity intruding the same section of the segment [Hamling et. al. 2010]). Surface fault displacement is

considered to be closely related to fault length and the shape of its distribution along the length of the fault has been thought to bear information on the processes of fault growth. For a single unconnected fault, elliptical or bell-shaped slip distributions are expected with their maxima at the centre gradually tapering off towards the fault tips. Alterations of this shape are thought to be due to interactions with neighbouring faults [e.g. Kim et. al., 2005] or in the case of magmatically-driven faults might indicate the direction of magma transport [Manighetti et al, 2001]. In addition to InSAR observations, a high-resolution airborne LiDAR survey was carried out in October 2009 covering the central section of the Dabbahu segment. The resulting DEM covers 600 km<sup>2</sup> with a resolution of 0.5 m. It enabled us to re-evaluate InSAR observations and process the InSAR data at the full resolution. Specifically, we have used available data from Envisat and ALOS that span individual dyke intrusions to estimate the surface deformation caused by dyke intrusion on each fault. This allows us to directly quantify incremental slip distribution on these faults and investigate how they grow. In combination with the cumulative fault displacement-length patterns extracted from the same data set it gives us new insight into the evolution of magmatically-driven normal faults. Ayele, A., Jacques, E., Kassim, M., Kidane, T., Omar, A., Tait, S., Nercessian, A., de Chabaliere, J.B. and King, G., The volcanoseismic crisis in Afar, Ethiopia, starting September 2005. *Earth and Planetary Science Letters* 255, 177-187, (2007) Ebinger, C., Ayele, A., Keir, D., Rowland, J., Yirgu, G., Wright, T., Belachew, M. and Hamling, I., Length and timescales of rift faulting and magma intrusion: The Afar rifting cycle from 2005 to present. *Annual Review of Earth and Planetary Sciences* 38, 439-466, (2010) Hamling, I., Wright, T., Calais, E., Bennati, L. and Lewi, E., Stress transfer between thirteen successive dyke intrusions in Ethiopia. *Nature Geoscience* 3, 713–717, (2010) Keir, D., Hamling, I.J., Ayele, A., Calais, E., Ebinger, C.J., Wright, T.J., Jacques, E., Mohamed, K., Hammond, J.O.S, Belachew, M., Baker, E., Rowland, J.V., Lewi, E. and Bennati, L., Evidence for focused magmatic accretion at segment centers from lateral dike injections captured beneath the Red Sea rift in Afar. *Geology* 37, 59-62, (2009) Kim, Y and Sanderson, D.J., The relationship between displacement and length of faults: a review. *Earth-Science Reviews* 68, 317-334, (2005). Manighetti, I., King, G.C.P., Gaudemer, Y., Scholz, C.H. and Doubre, C., Slip accumulation and lateral propagation of active normal faults in Afar. *Journal of Geophysical Research* 106, 13667-13696, (2001). Wright, T.J., Ebinger, C., Biggs, J., Ayele, A., Yirgu, G., Keir, D. and A. Stork, A., Magma-maintained rift segmentation at continental rupture in the 2005 Afar dyking episode. *Nature* 442, 291-294, (2006)

## DLR's Activities to Support the GEO Supersite Initiative with TerraSAR-X Data

### Author(s)

Michel Eineder <sup>(1)</sup>, Achim Roth <sup>(2)</sup>, Christian Minet <sup>(2)</sup>, Falk Amelung <sup>(3)</sup>

### Department

<sup>(1)</sup>DLR IMF-SV, DE

<sup>(2)</sup>Deutsches Zentrum für Luft- und Raumfahrt e.V. (DLR) , Germany

<sup>(3)</sup>University of Miami ,

### Abstract

Abstract: In this contribution we explain the mechanisms implemented by DLR to support the GEO Supersite initiative by providing TerraSAR-X data to the community at reduced cost and simplified access procedures. The Supersites are an initiative of the Group of Earth Observations (GEO) to study natural hazards in geologically active regions using information from Synthetic Aperture Radar (SAR), GNSS, geophysical models and other data sources. The data are provided in the spirit of GEO, ESA, NASA and DLR that easy access to Earth science data will promote their use and advance scientific research, ultimately leading to improved geo-risk modelling and the prediction of hazards. Seven Supersites have been defined initially with different threat

mechanisms: Hawaii (volcanic), Vancouver (tectonic), Los Angeles (tectonic), Etna (volcanic), Vesuvius (volcanic), Istanbul (tectonic) and Tokyo (tectonic). Triggered by tragic earthquakes, additional sites such as Port'o Prince (Haiti, 2010) and Tohoku-oki (Japan, 2011) have been recently added to the list. The TerraSAR-X mission is carried out under a public-private partnership (PPP) between the German Federal Ministry of Education and Research (Bundesministerium für Bildung und Forschung; BMBF), the German Aerospace Center (Deutsches Zentrum für Luft- und Raumfahrt; DLR) and Astrium GmbH. DLR is responsible for the scientific usage of the data (<http://sss.terrasar-x.dlr.de/>), and it takes care of design, implementation and operation of the mission. Data for commercial use are made available through Astrium GEO-Information Services GmbH (<http://www.infoterra.de/>). The satellite's total data-collecting capacity is divided equally between science and industry. In order to support research in the georisk domain, DLR allocated a quota of TerraSAR-X products to the Geo-supersite initiative that will be provided free of charge. It mainly utilizes the data provision mechanism in place applicable for scientific applications (AO) in order to satisfy as well the German Satellite Data Security Act (SATDSiG) as to protect the commercial interests of the PPP. For each Supersite, a dedicated principal investigator takes care of - justifying the scientific use of the requested data in the AO proposal, - SAR data acquisition planning, - negotiation of acquisition requests in case of conflicts with other scientists, - acquisition planning and - regular reporting. For the task of data ordering the PI gets a special account in DLR's Science Service System with low priority but rather large number of scenes free of charge that will be used for filling the archive. In order to work with the data, the scientists write a simplified AO proposal with reference to the supersite AO proposal. He may then order a certain number of scenes from the catalogue for free. This mechanism has already proven successful at some supersites and first results are available, e.g. from Hawaii, Haiti and Tohoku-oki. For the latter, a time sequence of TerraSAR-X data is currently being acquired and jointly released to the public by DLR and Astrium GEO-Information Services GmbH in an even more simplified procedure. An overview of DLR's supersite process and first scientific results are given in the presentation.

## Tensile Strength of Rock from InSAR Observations

Author(s)

Sigurjon Jonsson <sup>(1)</sup>

Department

<sup>(1)</sup>KAUST, SA

### Abstract

Rock is much weaker under tension than compression. The failure strength is usually determined in the laboratory using cm-scale cylindrical samples of rock material that are subjected to differential stress under various pressure and temperature conditions. The strength of small-scale samples is, however, significantly higher than large-scale (meters to km) rock (bulk) strength, as small-scale samples are typically free of cracks and other imperfections. The problem is that rock bulk strength is impossible to determine in the laboratory and it is therefore unclear how small-scale laboratory strength values scale to large-scale rock strength. In this study we use InSAR measurements of a recent dyke intrusion in western Saudi Arabia to provide unusual insights into tensional bulk strength of rocks. The dyke intrusion occurred in a lava province called Harrat Lunayyir in western Saudi Arabia in April-July 2009 and caused a number of small to moderate-sized earthquakes along with extensive surface faulting. The most intensive earthquake activity took place on 17-20 May when six magnitude 4.6-5.7 earthquakes occurred, resulting in some structural damage and prompting the Saudi civil protection authorities to evacuate more than 40000 people from the area. InSAR data of the area show that large-scale (40 km x 40 km) east-west extension of over 1 m took place as well as broad uplift amounting to over 40 cm. The

center of the uplifted area was transected by northwest-trending graben subsidence of over 50 cm, bounded by a single fault to the southwest showing up to ~1 m of normal faulting and by multiple smaller faults and cracks to the northeast. The observed deformation is well explained with a near-vertical dyke intrusion with a volume of ~0.1 cubic-km and a NW-SE orientation, approximately parallel to the Red Sea. The modeling suggests that the shallowest part of the dyke reached within only 2 km of the surface, resulting in the extensive surface faulting. We use ascending and descending Envisat interferograms and ascending ALOS data, along with Envisat and ALOS multiple aperture radar interferometry (MAI) to determine the 3D displacements of the surface caused by the intruding dyke. From the 3D displacements we generate strain maps that show a large amount of extension above the intrusion. The interferometric data of this arid region are almost perfectly correlated, such that lineations due to faulting and fractures can be accurately mapped by tracing abrupt phase discontinuities. The discontinuity map and the 3D displacement map confirm that up to 1 m of normal faulting occurred to the southwest of the dyke on a single fault, while in contrast, multiple fractures are seen to the northeast of the dyke, exhibiting limited amount of vertical throw. Field observations affirm that the discontinuities to the northeast are indeed tensional cracks with no significant vertical displacement. Comparison of observed tensional strain with the occurrence of tensional fractures shows where tension exceeded the tensional strength limit of the surface rocks. Surface strain is found to be larger than 0.2 millistrain in places, although this high amount of surface strain is clearly coincident with tensional fractures, implying that the surface bulk rock strength was exceeded. Other locations, which are free of surface fractures, exhibit extensional strain up to 0.05-0.08 millistrain. Assuming a shear modulus of 10 GPa of the surface rocks in the area, the results show that the tensional bulk strength of the rock is close to 1-2 MPa, a value that is ~10% of the strength that typically is estimated from small cm-scale intact rock samples of similar rock types in the laboratory.

## Earthquake slip distribution estimation from InSAR data, using a random field approach

Author(s)

Andrew Hooper <sup>(1)</sup>

Department

<sup>(1)</sup>Delft University of Technology , NL

### Abstract

InSAR data are routinely used to invert for the slip distribution on faults that rupture during earthquakes. Here we propose a new approach for constraining the slip distribution in a way that gives more physically reasonable results, which are also in better agreement with previously studied fault distributions. We demonstrate our approach on the 2011 Mw=9.0 Tohoku earthquake in Japan and the Mw=6.8 Mong Hpayak earthquake in Burma. In modelling slip distributions, deformation at the surface is usually assumed to be the elastic response to slip on discretised patches distributed over the fault. In order to ensure physically reasonable slip distributions, extra constraints are required. The first is that slip should be of the same mechanism throughout e.g., there should not be left-lateral movement on a right-lateral fault. The second constraint is that the slip should vary smoothly over the fault. Without these conditions the slip can vary drastically from patch to patch in trying to fit errors in the data. The usual way to impose the smoothness constraint is to simultaneously minimize both the fit to the data and the Laplacian of the slip. As the two cost functions trade off against each other, the relative weighting of the two has to be selected in some way. This is typically chosen either arbitrarily with a trade-off curve, or by minimising the cross validation sum of squares (CVSS). Fukuda and Johnson (2002) have incorporated the estimation of the relative weighting of smoothness into a Bayesian approach implemented with a Markov chain Monte Carlo algorithm. Not only does this

approach include the relative weighting as a parameter to be estimated, but the full posterior probability density function that is estimated also includes the uncertainty in the weighting. Some assumption has to be made about the expected distribution of the Laplacians however, and Fukuda and Johnson (2008) assume it is Gaussian. When we apply this method to real faults we get slip distributions that superficially look reasonable. However, if we calculate the stress drop over the fault (i.e., the change in stress across the fault before and after the earthquake), we sometimes find unrealistic scenarios, with patches of negative stress drop (i.e. stress increase) in areas that have slipped significantly and that are interspersed with areas showing positive stress drops. Analysis of many different slip distributions derived from seismic finite-source slip inversions led Mai and Beroza (2002) to conclude that slip distributions can be stochastically characterised as a spatial random field following a von Karman autocorrelation function. We therefore incorporate this model in our geodetic inversions using the Bayesian approach of Fukuda and Johnson (2008), modified to estimate the Hurst number and correlation lengths that characterise the von Karman model. We apply our approach to our test cases in Japan and Burma and find slip distributions that result in more reasonable stress drop distributions. Fukuda, J., and K. Johnson (2008), A Fully Bayesian Inversion for Spatial Distribution of Fault Slip with Objective Smoothing, *Bull. Seis. Soc. Am.* 98(3), 1128-1146. Mai, P. M., and G. C. Beroza (2002), A spatial random field model to characterize complexity in earthquake slip, *J. Geophys. Res.*, 107(B11), 2308.

## Imaging recent complex earthquake ruptures with combined InSAR and seismic analysis

### Author(s)

Eric Fielding <sup>(1)</sup>, Anthony Sladen <sup>(2)</sup>, Shengji Wei <sup>(2)</sup>, Mark Simons <sup>(2)</sup>, Piyush Shanker Agram <sup>(2)</sup>, Sang-Ho Yun <sup>(1)</sup>, Walter Szeliga <sup>(1)</sup>

### Department

<sup>(1)</sup>Jet Propulsion Laboratory, Caltech MS 300-233, US

<sup>(2)</sup>California Institute of Technology, USA

### Abstract

Geodetic measurements of surface displacements with InSAR, pixel tracking, and ground-based methods such as GPS provide strong constraints on the locations of fault ruptures and distribution of total slip on the faults during earthquakes. Seismic waveforms record the timing of fault slip but have poor spatial resolution. Joint inversions of the geodetic and seismic data together can resolve the earthquake fault slip in both spatial location and in time to provide a picture of the fault slip evolution during large earthquakes. High-resolution InSAR and pixel tracking also provides valuable information on the locations of surface ruptures that can aid field investigations. The newly available TerraSAR-X and COSMO-SkyMed satellite systems and UAVSAR airborne InSAR are now joining Envisat and the recently deceased ALOS-1 in providing data on earthquake ruptures. We find that nearly all of the recent earthquakes on the continents with magnitudes greater than 6 have significant complexity in the fault ruptures, with the amount of complexity generally increasing with magnitude as the larger events over M 7 often rupture many fault segments. The rupturing of several faults in one event significantly increases the area of damage and in many cases means that seismic hazard models may need to be revised. We present highlights of analysis of several recent major earthquakes, including the 2010 Mw 7.0 Haiti earthquake, the 2010 Mw 7.2 El Mayor-Cucapah earthquake in Baja California, Mexico and the 2011 Mw 9.0 Tohoku, Japan earthquake and some of its shallow aftershocks that struck on land. We also studied a sequence of two earthquakes Mw 6.5 and Mw 6.0 in southeast Iran in December 2010 and January 2011. For the devastating Mw 7.0 Haiti earthquake, interferograms from ALOS-1 PALSAR showed that the main fault rupture involved a previously unmapped north-dipping fault, the Léogâne Fault, with significant thrust slip during the earthquake, and lesser

amounts of strike slip on a part of the microplate boundary fault in southern Haiti, the Enriquillo Fault. Seismic data analysis indicates that the earthquake most likely started on the Enriquillo Fault, and the Léogâne Fault rupture followed. Because most of the 2010 slip did not occur on the Enriquillo Fault, the interseismic stress buildup on that fault was only partially released and it could have a future large earthquake in the same area or an adjacent segment. The 2010 earthquake in Baja California also ruptured a previously unmapped fault, the Indiviso Fault beneath the Colorado River Delta, in addition to three other faults in the Sierra Cucapah. Seismic analysis shows that the earthquake began with a M 6 normal fault that then triggered oblique slip on the other faults. This complex set of ruptures is subparallel to the main plate boundary fault in Mexico. The two earthquakes in SE Iran are interesting because they ruptured nearly perpendicular conjugate strike-slip faults, a pattern that is similar to previous moderately large events in southernmost California and the triggered slip on faults near the Baja earthquake. The complexity of the Iran ruptures is apparently limited to minor secondary faulting. The great 2011 Tohoku earthquake was imaged by Envisat ASAR and ALOS-1 PALSAR interferograms. The interferograms reveal details of a sequence of M5 to M6.6 aftershocks near the city of Iwaki, all on normal faults activated by the large coseismic stress change of the M9 earthquake.

## Geodetic Imaging, Seismic Hazard and Mountain Building Across the Sierra Nevada/Great Basin Transition Using InSAR and GPS

### Author(s)

William Hammond <sup>(1)</sup>, Geoffrey Blewitt <sup>(1)</sup>, Zhenhong Li <sup>(2)</sup>, Corné Kreemer <sup>(3)</sup>, Hans-Peter Plag <sup>(3)</sup>

### Department

<sup>(1)</sup>Nevada Geodetic Laboratory University of Nevada, Reno, US

<sup>(2)</sup>University of Glasgow Glasgow G12 8QQ, United Kingdom

<sup>(3)</sup>University of Nevada, Reno , USA

### Abstract

The rate and timing of uplift of the Sierra Nevada have been the subject of vigorous debate. Estimates of the age of the modern topography based on geologic and geochronologic data vary by over one order of magnitude, from less than 3 to as old as 60 million years. Present peak elevations exceed 4 km, and thus the most rapid of the possible uplift rates are >1 mm/yr, which is large enough to be detected by precise space geodetic measurements. Interferometric Synthetic Aperture radar (InSAR) can improve constraints on interseismic crustal deformation and fault slip rates, in both the horizontal and vertical dimensions. In particular, when InSAR time series line-of-sight (LOS) velocity maps are aligned with 3-component GPS velocities, the complementary strengths of the two techniques provide a comprehensive model for secular solid Earth surface motion. This can be used to infer slip rates on faults (for input into seismic hazard analysis), or used to resolve the rate of uplift of large tectonic blocks such as the Sierra Nevada. In this study we used ERS and ENVISAT data collected over 19 years, accessed from the WinSAR and GeoEarthScope archives, to estimate vertical motions across the Sierra Nevada/Great Basin transition. We used data from three overlapping tracks 442, 170, 399 in frame 2871 that form a transect from east of Yucca Mountain, Nevada to the Sierra Nevada in California. All the interferograms were formed from raw images using the JPL/Caltech ROI\_PAC software (version 3.1 beta) and unwrapped with the SNAPHU algorithm. To these interferograms we applied the InSAR Time Series with Atmospheric Estimation Model, based on the SBAS algorithm, which partitions the unwrapped phase into five terms: topographic error, time invariant constant motion, non-linear surface motion, atmospheric effects and noise. GPS data were obtained from high precision western U.S. networks including the continuously recording BARGEN, BARD, SCIGN, and EarthScope Plate Boundary Observatory, and semi-continuous MAGNET networks. These data were processed with the latest version of the GIPSY/OASIS software as a part of a global



solution that includes over 9000 stations worldwide, and aligned with a North America fixed reference frame. A significant fraction of the stations in the Great Basin have collected data since 1999, and offer extremely stable reference three-component velocity field, while the remaining stations provide almost complete coverage of the western Great Basin at ~20 km spacing. Thus the GPS station distribution is sufficient to provide a strong alignment of the InSAR line-of-sight velocity maps to the GPS velocity field. We apply linear transformations (linear ramps) that place the InSAR velocity maps into the GPS reference frame. The degree of internal consistency between GPS and InSAR, after alignment, is a measure of the accuracy of the integrated LOS rate map. We compare the InSAR LOS rate maps to both point GPS measurements and to a tensor strain rate map that provides an interpolation of the horizontal GPS velocities. The results show that InSAR LOS rate maps agree with GPS measurements to within 0.5 mm/yr RMS misfit at the stations and 0.5 mm/yr RMS misfit to the strain map obtained from the GPS velocities. This close agreement between InSAR and GPS suggests that 1) the corrections for atmosphere and orbits errors in the InSAR time series analysis are working well, 2) that the GPS network is dense enough to accurately constrain the alignment of the InSAR to the GPS rate field, 3) that short-wavelength features in the InSAR velocity map are real and thus that 4) strain maps estimated directly from InSAR and GPS point velocities will provide higher resolution three-component surface motion maps that will improve constraints on deformation and uplift. Our InSAR results show that the southern Sierra Nevada is moving upward by  $1.4 \pm 0.7$  mm/yr with respect to the Owens Valley directly to the east, and with respect to eastern Nevada. The strongest gradient in the velocity map coincides with the eastern edge of the Sierra Nevada/Great Valley microplate. About one dozen continuous GPS stations on the west slope of the Sierra Nevada have upward rates between 1.1 and 1.9 mm/yr and independently corroborate the rate of uplift, and are similar along most of the length of the Sierra Nevada. These rates are therefore sufficient to generate the entire elevation of the modern Sierra Nevada in 3 Myr or less, and are most consistent with a model of active east-up tilting of a tectonic microplate that drives growth of the modern Sierra Nevada.

## Session: Pol-InSAR & Tomography

### Diff-Tomo Opening of the Urban SAR Pixel: Single-look 4D and Non-uniform Motion "5D" Extensions

#### Author(s)

Fabrizio Lombardini <sup>(1)</sup>, Federico Viviani <sup>(1)</sup>

#### Department

<sup>(1)</sup>University of Pisa Dept. of Information Eng., via Caruso 16, 56122 Pisa, IT

#### Abstract

Differential interferometry and 3D SAR tomography are a mature operational and an emerging interferometric SAR mode, respectively. The former is based on multiple pass satellite SAR acquisition to accurately measure terrain deformation motions (scatterer velocity), see e.g. [1,2]. SAR tomography is a more recent interferometric technique, it is based on multibaseline acquisition to produce full 3D imaging for elevation/reflectivity analysis of semitransparent scattering layers, or complex urban and infrastructure scenarios with layover ("garbled") scatterers, see e.g. [3,4]. It is an elevation beamforming i.e. spatial (baseline) spectral estimation technique, and it represents a very promising extension of classical interferometry for topographic mapping in the more general framework of coherent complex (i.e. amplitude and phase) data combination [5]. Recently, a new coherent data combination mode crossing the differential SAR interferometry and multibaseline SAR tomography concepts, termed differential SAR tomography

(Diff-Tomo) or 4D (3D + time) imaging, has been introduced by University of Pisa [6]. Its potentials for deformation monitoring in garbled scenarios, coming from the joint elevation-velocity resolution capability of multiple layover scatterers, i.e. the “opening of the SAR pixel”, have been demonstrated both theoretically and with real data [6-8]. Processing is based on a two-dimensional baseline-time spectral analysis, to separate and identify the spatial-temporal harmonics originated by each scattering component. Interestingly, adaptive two-dimensional spectral estimation has been shown to allow - at a moderate computational load - Diff-Tomo processing with controlled sidelobes despite the typical very sparse sampling in the baseline-time plane, and also elevation-velocity superresolution [6,8]. However, this method requires coherent multilooking to work properly, i.e. it can not operate at the full range-azimuth data resolution. While this framework is well suited for possible applications of Diff-Tomo to natural scenarios [9], it may be less satisfactory for applications where full horizontal resolution products are often desirable, typically in urban scenarios [2,5,7]. More recently, other solutions have been proposed and tested for Diff-Tomo imaging, the limited elevation-velocity resolution regularized linear inversion [7], and the complex compressive sensing [10]. In this work, two extensions are presented and investigated of superresolution adaptive Diff-Tomo, in the single-look operation and non-uniform motion context. The pursued goal is to fully match possible future requirements for applications to garbled urban/infrastructure scenarios, still keeping a moderate computational load, and to extend the application range and performance of deformation monitoring in these or other garbled scenarios in case of deviations from the common constant velocity assumption (e.g. for nonlinear subsidences [2] or seasonal effects [7]). In particular, a novel single-look adaptive Diff-Tomo processor is presented, allowing full horizontal resolution jointly with the good elevation-velocity sidelobe and superresolution capabilities of the previous multilook adaptive processing. To get this coupling, the sparse baseline knowledge-based interpolation approach in [11], exploiting a light a-priori information about the multiple scatterers scenario and able to reduce sidelobes even at full horizontal resolution processing, is integrated with adaptive two-dimensional spectral estimation. Concerning possible non-uniform motion components after proper atmospheric compensation [7], a novel semiparametric adaptive Diff-Tomo processor is presented, to extract different (average) accelerations of garbled scatterers. In this case, the adaptive Diff-Tomo output is in the joint range-azimuth-elevation-initial velocity-acceleration domain, i.e. a “5D” image is produced. First results of these superresolution Diff-Tomo extensions (patent pending) are reported, both simulated with realistic baseline-time satellite sampling patterns and with real C-band ERS-1/2 data over an area of Rome, Italy. Experiments will be carried out also with spaceborne X-band data ([12-13]) when delivered. The simulations, carried out for different acquisition patterns both monostatic and multistatic [13], and various motion and signal parameters, yield good results of the new full resolution adaptive Diff-Tomo 4D processor. Both low elevation-velocity sidelobes and superresolution starting from single-look data are obtained, at moderate computation burden. First cut experiments with the ERS-1/2 data are also promising. First preliminary results regarding the new adaptive Diff-Tomo 5D processor with accelerated motions show interesting potentials. ACKNOWLEDGEMENT The authors thank Dr. G. Fornaro from CNR-IREA for providing the ERS-1/2 calibrated data set. REFERENCES [1] P. Berardino, G. Fornaro, R. Lanari, E. Sansosti, “A New Algorithm for Surface Deformation Monitoring based on Small Baseline Differential SAR Interferograms,” *IEEE Trans. Geosci. and Remote Sens.*, vol. 40 (11), pp. 2375-2383, Nov. 2002. [2] A. Ferretti, C. Prati, F. Rocca, “Nonlinear Subsidence Rate Estimation using the Permanent Scatterers in Differential SAR Interferometry”, *IEEE Trans. Geosci. and Remote Sens.*, vol. 38 (5), pp. 2202-2212, Sept. 2000. [3] A. Reigber, A. Moreira, “First Demonstration of Airborne SAR Tomography using Multibaseline L-band Data,” *IEEE Trans. Geosci. and Remote Sensing*, vol. 38 (5), pp. 2142-2152, Sept. 2000. [4] F. Gini, F. Lombardini, M. Montanari, “Layover Solution in Multibaseline SAR Interferometry,” *IEEE Trans. Aerospace and Electronic Systems*, vol. 38 (4), pp. 1344–1356, Oct. 2002. [5] F. Lombardini, M. Pardini, G. Fornaro, F. Serafino, L. Verrazzani, M. Costantini, “Linear and Adaptive Spaceborne Three-dimensional SAR

Tomography: A Comparison on Real Data”, IET Radar, Sonar and Navigation, special issue of IEEE RadarCon’08, vol. 3 (4), pp. 424-436, Aug. 2009. [6] F. Lombardini, “Differential Tomography: a New Framework for SAR Interferometry,” IEEE Trans. Geosci. and Remote Sensing, vol. 43 (1), pp. 37-44, Jan. 2005. [7] G. Fornaro, F. Serafino, D. Reale, “4D SAR Imaging for Height Estimation and Monitoring of Single and Double Scatterers,” IEEE Trans. on Geosci. and Remote Sensing, vol. 47 (1), pp. 224-237, Jan. 2009. [8] F. Lombardini, M. Pardini, “Superresolution Differential Tomography: Experiments on Identification of Multiple Scatterers in Spaceborne SAR Data,” submitted to IEEE Trans. Geosci. and Remote Sensing. [9] F. Lombardini, “New Potentials of Differential SAR Tomography: Volumetric Differential Interferometry and Robust DEM Generation,” Proc. 2007 IEEE Int. Geosci. and Remote Sensing Symp., Barcelona, Spain, July 2007. [10] X. Zhu, R. Bamler, “Tomographic SAR Inversion by L1-norm Regularization: the Compressive Sensing Approach,” IEEE Trans. Geosci. and Remote Sensing, vol. 48 (10), pp. 3839-3846, Oct. 2010. [11] F. Lombardini, M. Pardini, “3-D SAR Tomography: The Multibaseline Sector Interpolation Approach,” IEEE Geosci. and Remote Sensing Letters, vol. 5 (4), pp. 630-634, Oct. 2008. [12] S. Mezzasoma, A. Gallon, F. Impagnatiello, G. Angino, S. Fagioli, A. Capuzi, F. Caltagirone, R. Leonardi, I. Ziliotto, “COSMO-SkyMed System Commissioning: End-to-end System Performance Verification,” Proc. IEEE RadarCon’08, Rome, Italy, May 2008. [13] G. Krieger, A. Moreira, H. Fiedler, I. Hajnsek, M. Werner, M. Younis, M. Zink, “TanDEM-X: A Satellite Formation for High-Resolution SAR Interferometry”, IEEE Trans. Geosci. and Remote Sens., vol. 45 (11), pp. 3317-3341, Nov. 2007.

## Polarimetric SAR Tomography with TerraSAR-X by means of Distributed Compressed Sensing

Author(s)

Matteo Nannini <sup>(1)</sup>, Arthur Antonello <sup>(1)</sup>, Esteban Aguilera <sup>(1)</sup>, Luca Marotti <sup>(1)</sup>,  
Pau Prats <sup>(1)</sup>, Andreas Reigber <sup>(1)</sup>

Department

<sup>(1)</sup>German Aerospace Center , DE

### Abstract

In recent years, synthetic aperture radar tomography has become a leading technique to solve for layover and obtain three-dimensional (3D) reconstructions of a viewed scene. This technique overcomes the limitations of SAR interferometry that suffer such phenomenon and cannot deal with the related distortions on the interferometric phase. SAR tomography represents a step forward when compared to classical polarimetric SAR interferometry since this technique fails to perform phase center separation if the scatterers within the observed resolution cell exhibit the same polarimetric signature. In SAR tomography, the vertical reflectivity function for every azimuth-range pixel is recovered by processing data acquired from a special tomographic imaging geometry, that basically builds an aperture in the direction perpendicular to the flight paths allowing a resolution in the perpendicular line-of-sight or cross-range direction. This imaging technique is appealing, since it is very simple and applicable also in the space-borne case, but has the drawback that, for some applications (e.g. if imaging of large volumetric structures is desired), it cannot always be implemented since it generally requires the acquisition of a large number of SAR images over the area of interest. Some work has been addressed to reduce the number of required acquisitions based on super-resolution subspace based methods, like the MUSIC algorithm, where resolution and ambiguity rejection constraints permit to define the correspondent tomographic geometry such that, also in the worst case of large volume, allows one to define the noise subspace (mandatory for subspace methods). Another important field of study which has the goal to reduce the number of tracks and achieves super-resolution, applies to SAR tomography the compressed sensing (CS) theory. In principle, a set of azimuth-range pixels out of a tomographic stack of SAR images, corresponds to the Fourier transform of the vertical

complex reflectivity as a function of the baselines. In particular, if this vertical signal is sparse, i.e. if only a few point targets are identifiable within the considered resolution cell (assumption generally true for urban areas), the complex reflectivity can be completely recovered with a considerably reduced number of samples in comparison to the number required to fulfill the Nyquist criterion. Moreover, a new tomographic focusing methodology, that trades the number of SAR images for correlations between neighboring azimuth-range pixels and polarimetric channels has been recently addressed. One can exploit these additional information under the framework of Distributed Compressed Sensing (DCS), which stems from the CS theory. In addition to the standard CS, in this case, the polarimetric signature of the scatterers is also retrieved, leading to an easier interpretation of the 3D profile. For this purpose, two novel methods that consider different assumptions about the targets to be focused have been developed. Specifically, the first method, which applies to point scatterers, scans neighboring pixels in the elevation direction seeking for scatterers with common complex amplitudes located at approximately the same height. The second method scans neighboring pixels in the elevation direction as well, but this time seeking for scatterers at approximately the same elevation across all polarimetric channels that may not have common complex amplitudes. Clearly, tomographic focusing of speckled targets is most likely to benefit from this last technique. The high quality data provided by the TerraSAR-X and its flexibility to image areas also in dual polarized mode makes it possible, for the first time, to test DCS techniques with space-borne polarimetric data and to compare the related 3D reconstructions to the ones obtained by means of the MUSIC algorithm. In addition also fully polarimetric L-band data acquired by the E-SAR sensor of DLR will be exploited for validating the results.

## 3D SAR Tomography of the Paracou Forest: Methods and Results

### Author(s)

Mauro Mariotti Dalessandro <sup>[1]</sup>, Stefano Tebaldini <sup>[1]</sup>

### Department

<sup>[1]</sup>Politecnico di Milano Via Ponzio 34/5, IT

### Abstract

Synthetic Aperture Radar (SAR) systems are widely used for geophysical exploration because of their capability to investigate a large areas nevertheless providing good spatial resolution; furthermore, longer wavelength SARs are able to sense scattering contributions coming from different depths within volumetric scatterers, according to wave penetration. Such features make longer wavelength SARs a major tool for the characterization of the vegetation layer above the ground level. In order to obtain a tomographic (three dimensional) reconstruction of the scene, many observation of the same area are needed. The performances depend on the geometric displacement between the radar position during the different acquisitions, that is the total aperture of the SAR array and the sampling interval. Typical surveys are characterized by a resolution comparable or even larger than the vegetation layer itself: such data volumes have to be processed by means of algorithms able to overcome such poor resolution. As a consequence many model based algorithms have been developed ([1], [2], [3], [4], [5]): they are able to incorporate the a-priori information as well as to enable super-resolution within the vegetation layer. There are cases, however, where the vertical resolution is actually smaller than the vegetation extent, which makes it possible to process the data without assuming physical or statistical models. Such an approach frees the results from modeling error, so enabling a direct observation of the spatial distribution of the scatterers. In particular it is well known that the signal received by a multibaseline SAR array is related to the vertical distribution of the scatterers via Fourier transform. Such a relation enables to easily move the original data volume from its original domain (slant range, azimuth, baseline) to the three dimensional space, and so to

associate a synthetic slc (single look complex) value with any point over the ground level. The aim of this work is to show some interesting properties of the vegetation layer that emerge after the processing described above, basing on the P-Band dataset collected by ONERA over French Guyana during the ESA campaign TropiSAR. Such a dataset is characterized by an almost constant vertical resolution of about 20 m, whereas forest height ranges from 20 m to 40 m. By considering these values it is clear that it is possible to obtain up to three independent slices (each one characterized by a constant height above the ground) of the forest layer and to process them separately in order to associate different physical properties to different heights above the ground. Before extracting the physical parameters, two preliminary processing steps have been performed. In order to remove the impact of possible propagation disturbances and to refer any height specification to the ground level, the approach proposed in [6] has been applied. To further improve the accuracy of the results, the displacement of the aircraft from its nominal trajectory has been corrected by linearly interpolating the baselines on a uniform grid. The first interesting result is about the different behavior of the backscattered power coming from the ground, from the middle of the vegetation layer and from the tree top with respect to topographic slope. It is observed that the backscattered power is strongly correlated with the slope of the ground surface only for the top and for the bottom slices whereas the slice associated with the middle of the forest is much more homogeneous. We also propose the comparison between the copolar phase ([7]) associated with the ground level slice and the one associated with the original (i.e.: non tomographic) slc image: the latter is clearly the result of the combination of the copolar phases characterizing the canopy layer and the one characterizing the ground backscattering whereas the former appears less noisy and leads to a better characterization of the underlying scattering mechanism. In particular, by looking at the histograms relating copolar phase and ground slope it is possible to clearly appreciate the range of ground slopes that makes the ground trunk double bounce the dominant scattering mechanism. References [1] R.N. Treuhaft, P.R. Siqueira, "Vertical structure of vegetated land surfaces from interferometric and polarimetric radar," *Radio Science*, vol. 35, pp. 141–177, 2000. [2] K. Papathanassiou and S. Cloude, "Single-baseline polarimetric SAR interferometry," *Geoscience and Remote Sensing, IEEE Transactions on*, vol. 39, no. 11, pp. 2352–2363, Nov 2001. [3] M. Neumann, L. Ferro-Famil, and A. Reigber, "Estimation of forest structure, ground, and canopy layer characteristics from multibaseline polarimetric interferometric sar data," *Geoscience and Remote Sensing, IEEE Transactions on*, vol. 48, no. 3, pp. 1086 –1104, 2010. [4] S. Tebaldini, "Single and multipolarimetric SAR tomography of forested areas: A parametric approach," *Geoscience and Remote Sensing, IEEE Transactions on*, vol. 48, no. 5, pp. 2375 –2387, may 2010. [5] —, "Algebraic synthesis of forest scenarios from multibaseline polinsar data," *Geoscience and Remote Sensing, IEEE Transactions on*, vol. 47, no. 12, pp. 4132 –4142, dec. 2009. [6] S. Tebaldini and F. Rocca, "On the impact of propagation disturbances on SAR tomography: Analysis and compensation," in *Radar Conference, 2009 IEEE*, 4-8 2009, pp. 1 –6. [7] A. Freeman, "Fitting a two-component scattering model to polarimetric SAR data from forests," *Geoscience and Remote Sensing, IEEE Transactions on*, vol. 45, no. 8, pp. 2583–2592, Aug. 2007.

# Underlying Topography Estimation and Separation of Scattering Contributions over Forests Based on PolInSAR Data

## Author(s)

Carlos López-Martínez <sup>(1)</sup>, Kostantinos Papathanassiou <sup>(2)</sup>, Alberto Alonso <sup>(1)</sup>, Xavier Fabregas <sup>(1)</sup>

## Department

<sup>(1)</sup>Universitat Politècnica de Catalunya Campus Nord, D3-203, Jordi Girona, 1-3, ES

<sup>(2)</sup>German Aerospace Center P.O. Box 1116, Germany

## Abstract

Forest areas cover approximately 30% of the Earth's solid surface, with a mean tree height of about 20 m. Any attempt to provide global surface mapping based on SAR Interferometry (InSAR) is affected by the presence of the vegetation cover, in such a way, that the interferometric phase due to the surface scattering presents a bias, respect to the actual value, due to vegetation. The magnitude of this bias error depends on the systems parameters, mainly the used frequency, and on the forest characteristics, mainly the extinction coefficient. From a quantitative point of view, this error may range up to the mean tree height. The evaluation of volume decorrelation effects in multi-baseline InSAR data has demonstrated that there is no conventional frequency (from P- up to X-band) able to be sensitive only the ground under a vegetation layer without being affected by any volume, i.e., vegetation scattering contribution. In consequence, all Digital Elevation Models (DEM's) generated by means of conventional InSAR are affected by a more or less significant vegetation bias. The correction of this inherent vegetation bias, always present in conventional interferometric data, and the estimation of the underlying ground topography is an essential improvement of the topographic information provided by SAR interferometry, with great ecological as well as commercial impact. In this work, we will propose an alternative implementation of the Random Volume over Ground (RVoG) coherent scattering model inversion to estimate underlying ground topography from Polarimetric Interferometric SAR data (PolInSAR) [1-2] without being biased by the presence of vegetation. A theoretical analysis of the RVoG model shows that it is possible to obtain algebraic expressions to derive an unbiased estimation of the ground topography, making possible to eliminate the volume bias when the ground topography is estimated. This new processing technique presents several advantages respect the conventional use of the RVoG model, namely, the proposed approach presents a more robust (by means of parameter estimation) implementation and an unambiguous estimation of the ground topography. The first section of this work will present the theoretical foundations of the proposed technique, as well as its limitations. Of special importance will be the determination of the effects of the speckle noise component on the estimation of the ground topography. Accordingly, a special emphasis will be paid to the statistical characterization of the information retrieved by the proposed technique. This study will make possible to determine the minimum number of independent samples necessary for a correct estimation of the ground topography. The second part of the present work will focus on the quantitative evaluation of the proposed technique. In a first stage, an evaluation considering simulated PolInSAR data, based on the RVoG model, shall be conducted. On a second stage, this evaluation shall be extended to a variety of forest conditions using repeat-pass Pol-InSAR data acquired by DLR's airborne E-SAR system. The obtained results shall be validated against available ground-truth. Critical issues shall be presented and analyzed. Finally, optimized system and acquisition scenarios shall be presented based on the conclusions of this work. References: [1] S. R. Cloude and K. P. Papathanassiou, "Polarimetric SAR interferometry," *Geoscience and Remote Sensing, IEEE Transactions on*, vol. 36, no. 5, pp. 1551–1565, Sep. 1998 [2] S. Cloude and K. Papathanassiou, "Three-stage inversion

## Sub-Canopy Topography Estimation With Multibaseline Pol-InSAR Data: A RELAX-Based Solution

Author(s)

Matteo Pardini <sup>(1)</sup>, Konstantinos Papathanassiou <sup>(1)</sup>

Department

<sup>(1)</sup>German Aerospace Center (DLR) , DE

### Abstract

New opportunities for the radar remote sensing of forests are arising from L-band and P-band SAR systems given their capability of penetrating deep into volumes. A key objective is estimating the sub-canopy topography, which finds a primary application in the derivation and/or interpretation of vertical radar profiles of the vegetation. Noteworthy, the systematic and reliable vertical forest distribution estimation is one of the essential goals of the German mission proposal TanDEM-L consisting of two cooperating L-band space borne radars flying in close formation.

Concerning the ground height estimation problem, a significant processing advance has been achieved in the last decade by coherently combining SAR data acquired in polarization and baseline diversity. For instance, already operating with a single baseline, coherent scattering models can be related to the polarimetric interferometric (Pol-InSAR) complex coherences in order to retrieve the forest height, the extinction coefficient and the sub-canopy topography [1]. In parallel to the single baseline Pol-InSAR, different strategies were investigated. In particular, SAR Tomography (Tomo-SAR) [2-3] and its polarimetric version PolTomo-SAR [4] are experimental techniques which in the last years demonstrated their potential in the 3-D analysis of volumetric scenarios. Tomo-SAR is a multibaseline (MB) extension of conventional cross-track SAR interferometry, employing many passes over the same area. Differently from conventional interferometry, which can only furnish a measure of the terrain topography, (Pol)Tomo-SAR can resolve multiple scatterers at different heights in each given range-azimuth cell, and outputs a continuous profile along the height dimension. Up to now, the performance of Tomo-SAR techniques (parametric and not) for ground topography estimation has been quantitatively assessed mostly with P-band data, proving the possibility to reach a precision in the order of magnitude of 1 m (see e.g. [3, 5]).

This work proposes the use and investigates the performance of an iterative ground topography estimation technique employing Pol-InSAR MB data, with particular reference to L-band acquisitions. More in detail, the proposed algorithm aims at separating the ground component (reasonably modeled as a point-like scatterer) from the dominant spatial spectral component of the canopy by means of a superresolution RELAX-based iteration [6-7]. For each iteration, an objective function is optimized with respect to one single height, thus the global algorithm implementation results simple and fast. It is worth remarking that in the signal processing literature it has been demonstrated that while RELAX is asymptotically statistically efficient when dealing with point-like scatterers, it is also robust to a model mismatch [6], which in the specific case happens with the canopy height-extended scatterer. Moreover, in contrast with MB covariance matching techniques like the ones in [5], the ground topography is estimated without making any particular hypothesis on the canopy coherence model, thus without the need of estimating its parameters. In other words, ground and canopy estimations are decoupled. The accuracy in ground topography retrieval is evaluated quantitatively with real data experiments by processing a DLR E-SAR L-band dataset over the Traunstein temperate forest. The dataset consists of 5 fully polarimetric SAR images acquired in June 2008 with a time span of

1 hour, hence with limited temporal decorrelation effects. The maximum baseline measures 20 m. A digital terrain model acquired through LiDAR measurements is also available, and it is used as a benchmark in the performance analysis. A comparison will be carried out of the accuracy obtained by combining single and full polarization MB data. Different baseline distributions, obtained by thinning the original one, will also be considered.

References:

- [1] S. R. Cloude, K. Papathanassiou, "Polarimetric SAR Interferometry," IEEE Trans. on Geoscience and Remote Sensing, vol. 36, 1998.
- [2] A. Reigber, A. Moreira, "First Demonstration of Airborne SAR Tomography Using Multibaseline L-Band Data," IEEE Trans. on Geoscience and Remote Sensing, vol. 38, 2000.
- [3] F. Lombardini, M. Pardini, "Experiments of Tomography-Based SAR Techniques with P-Band Polarimetric Data", Proc. of 2009 ESA PolInSAR Workshop.
- [4] S. Sauer, F. Kugler, et al., "Polarimetric Decompositions Applied to 3D SAR Images of Forested Terrains," Proc. of EUSAR 2010.
- [5] S. Tebaldini, "Single and Multipolarimetric SAR Tomography of Forested Areas: A Parametric Approach," IEEE Trans. on Geoscience and Remote Sensing, vol. 48, 2010.
- [6] M. Pardini, "Advances and Experiments of Tomographic SAR Imaging for the Analysis of Complex Scenarios". PhD thesis, University of Pisa, 2010.
- [7] J. Li, P. Stoica, "Efficient Mixed-Spectrum Estimation With Application to Target Feature Extraction," Proc. of 1996 ASILOMAR Conference.



# Session: Ice and snow

## Increased ocean melting and retreat of the Pine Island Glacier

### Author(s)

J. W. Park <sup>(1)</sup>, N. Gourmelen <sup>(2)</sup>, A. Shepherd <sup>(3)</sup>, S.W. Kim <sup>(4)</sup>, D.G. Vaughan <sup>(5)</sup>,  
D. J. Wingham <sup>(6)</sup>

### Department

<sup>(1)</sup>Department of Earth System Sciences, Yonsei University, Seoul 120-749, Korea.

<sup>(2)</sup>Ecole et Observatoire des Sciences de la Terre, University of Strasbourg, Strasbourg, France

<sup>(3)</sup>School of Earth and Environment, University of Leeds, Leeds, LS2 9JT, UK.

<sup>(4)</sup>Department of Geoinformation Engineering, Sejong University, Seoul 143-747, Korea.

<sup>(5)</sup>British Antarctic Survey, Natural Environment Research Council, Cambridge, CB3 0ET, UK.

<sup>(6)</sup>Department of Earth Sciences, University College London, London, WC1E 6BT, UK.

### Abstract:

The presence of warm water on the Amundsen Sea continental shelf has caused rapid melting at the terminus of the Pine Island Glacier, triggering retreat, thinning, speed-up, and accelerated loss of ice. Projections of the glaciers' future sea level contribution range widely between 2 and 15 cm by the year 2100 because of uncertainties as to how the ocean forcing will evolve and how the glacier will respond. Here, we use satellite observations to investigate the long-term trajectory of glacier retreat, making use of the latest ice phase of the ERS-2 satellite. Between 1992 and 2011, the hinge-line retreated at a constant rate despite a progressive steepening and shoaling of the glacier surface and bedrock slopes, respectively, which impede retreat. The retreat has remained constant because the glacier terminus has thinned at an accelerating rate, with comparable changes upstream. We explore the relation between the observed acceleration and oceandrive melting within the cavity beneath the floating section of the glacier.

## Antarctic Ice Motion Unveiled with InSAR

### Author(s)

Eric Rignot <sup>(1)</sup>, Jeremie Mouginot <sup>(1)</sup>, Bernd Scheuchl <sup>(1)</sup>

### Department

<sup>(1)</sup>UC Irvine Croul Hall, US

### Abstract

We present a reference, first, complete, high-resolution, digital mosaic of ice motion in Antarctica assembled from multiple satellite interferometric synthetic-aperture radar data acquired during the International Polar Year 2007-2009 by ESA's Envisat ASAR, CSA's RADARSAT-2 and JAXA's ALOS PALSAR systems. Each satellite made a unique and critical contribution to this digital mosaic. The data reveal complex, widespread streaming flow with tributary glaciers reaching hundreds to thousands of kilometers inland, over the entire continent. This new view of ice sheet motion emphasizes the importance of bed-slip dominated tributary flow over shear-stress dominated ice sheet flow, redefines our understanding of ice sheet dynamics, and has far-reaching implications for the reconstruction and prediction of ice sheet evolution.

# Mapping Ice Shelf Flow with Interferometric Synthetic Aperture Radar Stacking

## Author(s)

Malcolm McMillan <sup>(1)</sup>, Andrew Shepherd <sup>(1)</sup>, Noel Gourmelen <sup>(1)</sup>, Peter Nienow <sup>(2)</sup>, Jeong-Won Park <sup>(1)</sup>, Eero Rinne <sup>(2)</sup>, Amber Leeson <sup>(1)</sup>

## Department

<sup>(1)</sup>University of Leeds , GB

<sup>(2)</sup>University of Edinburgh ,

## Abstract

Interferometric Synthetic Aperture Radar (InSAR) observations of ice shelf flow are contaminated by ocean tide and atmospheric pressure signals. A model-based correction can be applied, but this method is limited by its dependency upon model accuracy, which in remote regions can be uncertain. Here we describe a method to determine 2-d ice shelf flow vectors independently of model predictions of tide and atmospheric pressure, by stacking conventional and multiple aperture (MAI) InSAR observations from the ERS-1 satellite. We apply this technique to the Dotson Ice Shelf in West Antarctica. By stacking we synthesise a longer observation period, which enhances long-period (flow) displacement signals, relative to rapidly-varying (tide and atmospheric pressure) ones. To estimate the error introduced by any remaining tidal- and atmospheric pressure- displacement of the ice shelf, we model the distribution of errors arising from these residual signals. Along- and across-track errors are shown to be of comparable magnitude (~ 22 m/yr), demonstrating that by utilising MAI processing, 2-d ice shelf velocity can be estimated from SAR data acquired from a single viewing direction, without compromising the accuracy of one of the vector components. These methods can improve estimates of ice shelf velocity, and better constrain the associated error, particularly in regions where model accuracy is low or uncertain.

# Grounding line mapping in Antarctica using 15 years of DInSAR data

## Author(s)

Jeremie Mouginot <sup>(1)</sup>, Eric Rignot <sup>(1)</sup>, Bernd Scheuchl <sup>(1)</sup>

## Department

<sup>(1)</sup>University of California Earth System Science, US

## Abstract

The grounding line is where the glacier switches from being grounded to being afloat in the ocean waters. This line migrates back and forth with changes in oceanic tides that varies in width depending on the slopes of the glacier bed and surface, and the amplitude of tides. The delineation of an ice sheet grounding line is critical to ice sheet mass budget calculations, numerical modeling of ice sheet dynamics, ice-ocean interactions, oceanic tides, and subglacial environments. Here, we present 15 years of mapping of grounding lines in Antarctica using differential satellite synthetic-aperture radar interferometry (DInSAR) data from the Earth Remote Sensing Satellites 1 and 2 (ERS-1/2), RADARSAT-1 and 2, and the Advanced Land Observing System (ALOS) PALSAR for years 1994 to 2009. To do so, we difference two interferograms spanning the same time interval with the exact same imaging geometry. A key component of this

analysis is to migrate image pixels before forming the interferograms by first calculating the motion field using a speckle tracking technique (Michel and Rignot, 1999) and then displace the image pixels accordingly to reconstitute phase coherence. Each interferogram measures range displacements caused by surface topography, interferometric baseline, glacier flow, tidal motion, plus noise. The differencing removes the glacier flow signal. Surface topography if known is removed, otherwise we select interferograms with a short differential baseline so no topographic correction is required. After that, tidal motion is easily recognizable by its distinct signature of elastic bending from other effects (atmospheric/ionospheric errors, glacier acceleration, etc ..). Using this technique, we mapped 1.4 million grounding line points. Ice reaches the ocean at over 28,600 km of the coastline, or 76% of Antarctica, of which 22,600 km experiences tidal flexure. Grounding line mapping is complete in the Peninsula and West Antarctica, gaps still exist for glaciers crossing the transAntarctic mountains and on a few East Antarctic ice shelves. We compare our DInSAR mapping with the mappings from MOA (Bohlander and Scambos, 2007) and from ICESat (Brunt et al, 2010). While a good agreement exists between DInSAR and MOA in areas of slow flow or steep surface gradients. In nearly all areas of fast flow, the MOA delineation is in large disagreement with tidal motion recorded by DInSAR. Grounding lines are mislocated inland or seaward, by several km up to 100-150 km. A better agreement is found with ICESat's data, also based on measurements of vertical motion, but with a detection noise one order of magnitude larger than with DInSAR. Overall, the DInSAR mapping of Antarctic grounding lines completely redefines the coastline of Antarctica. The DInSAR grounding line will be available at the National Snow and Ice Data Center (NSIDC) and will be regularly updated. Bohlander, J. and T. Scambos. Antarctic coastlines and grounding line derived from MODIS Mosaic of Antarctica (MOA). Boulder, Colorado USA: National Snow and Ice Data Center, Digital media (2007). Brunt, K., H. A. Fricker, L. Padman, T. Scambos and S. O'Neel, Mapping the grounding zone of the Ross Ice Shelf, Antarctica, using ICESat laser altimetry. *Ann. Glaciol.* 51(55) (2010). Michel, R. and E. Rignot. Flow of Glacier Moreno, Argentina, from repeat-pass Shuttle Imaging Radar images: comparison of the phase correlation method with radar interferometry. *J. Glaciol.* 45(149), 93-100 (1999). Bohlander and Scambos, 2007

## Detecting Ice Motion in Grove Mountain, East Antarctica with ALOS/PALSAR Interferometry

### Author(s)

Xin Tian <sup>(1)</sup>, Chunxia Zhou <sup>(2)</sup>, Yu Zhou <sup>(3)</sup>, Mingsheng Liao <sup>(1)</sup>

### Department

<sup>(1)</sup>State Key Laboratory of Information Engineering in Surveying, Mapping and Remote Sensing (LIESMARS), Wuhan University 129 Luoyu Road, Wuhan 430079, Hubei, China, CN

<sup>(2)</sup>Chinese Antarctic Center of Surveying and Mapping (CACSM), Wuhan University 129 Luoyu Road, Wuhan 430079, Hubei, China,

<sup>(3)</sup>School of Geodesy and Geomatics, Wuhan University 129 Luoyu Road, Wuhan 430079, Hubei, China,

### Abstract

It is well known that the Antarctic environment can significantly reflect global climate changing, since glacier ablation is a sensitive symbol of the global warming impacts. Within the Antarctic region, monitoring ice flow is very important for the study of glacier dynamics and allows us to inverse the mechanism of Antarctic ice sheet. Scientists have been keeping a watch on the Antarctic ice sheet for a long time. It is necessary to accurately measure the change and movement of glaciers, ice streams and so forth. The conventional measures, such as GPS and leveling network, are limited in the scale of area, time, cost, accuracy and so on especially in the Antarctic region. Due to the fact that Synthetic Aperture Radar (SAR) has all time, all weather data acquisition capability and thus is able to cover large areas with high-resolution imagery, SAR

has proven to be an effective tool for topographic mapping and deformation measurement in large, difficult and inaccessible areas. Synthetic Aperture Radar Interferometry (InSAR) is a relatively new technique with a high potential in earth observation. The use of InSAR techniques can give a more detailed view of the glaciers motion. And this technique has the capability of mapping the subtle change of Antarctic surface in centimeter even millimeter level. In this work, we present the complicated ice flow measurement result using Advanced Land Observing Satellite (ALOS) PALSAR data. The test area is selected around Grove Mountain in East Antarctica. Grove Mountain is located about 400-500 kilometers to the south of the Chinese Zhongshan Station in Antarctic inland areas. We choose a pair of ALOS images acquired on May 18th, 2007 and Oct 3rd, 2007 respectively according to their spatial/temporal baseline and Doppler spectrum. And the improved InSAR generated DEM corrected with ICESAT GLAS data by Zhou etc. will be used in our work as well. The ice flow pattern is complicated in Grove Mountain area. In this presentation, we investigate the relationship between the displacement of the radar look-of-sight and actual ice flow displacement and describe the model of glacier velocity as well as its calculation method. As the coherence of L-band data can be well kept and the effect of topographic phase can be suppressed effectively, taking L-band data as reference, the advantages of long wavelength data in detecting Antarctic ice sheet are then discussed. Meanwhile, some field measurement data of glacier velocity in Grove Mountain area is available for cross validation. The GPS benchmark data of ice flow velocity has been acquired during the past decade by Chinese National Antarctic Research Expedition (CHINARE). The result of the glacier velocity field in our experiment will be compared with the GPS data. The comparison shows the result derived from InSAR approach is consistent with the in-situ data. In addition, the characteristics of the glacier surface motion will be analyzed according to the derived glacier velocity. The demonstration of InSAR approach in Antarctic is prospective in environment assessment in Antarctic area and it should be applied more widely to Antarctic research.

## Short-term glacier velocity changes at West Kunlun Mountains, NW Tibet

Author(s)

Masato Furuya <sup>(1)</sup>, Takatoshi Yasuda <sup>(1)</sup>

Department

<sup>(1)</sup>Hokkaido University 8-316, JP

### Abstract

Glacier surface velocity is a combination of plastic internal deformation of the ice and basal slip, the latter of which consists of basal sliding over the bed and deformation of the bed itself. Because plastic ice cannot deform rapidly, short-term surface velocity changes are often attributed to basal slip caused by penetration of surface melt water to the bed, which will enhance basal water pressure and reduce basal friction. Such rapid signals that were detected over the past decade across the High Arctic, including Greenland Ice sheet, have been attracting a great deal of attention. It remains uncertain, however, if and how much short-term variability exists in the glaciers in High Asia that are equally important contributor to the eustatic sea-level rise. Short-term glacier velocity changes in the tectonically active High Asia, if any, will have another important implication for the interaction between internal dynamics of mountain building and surface erosion processes. This is because subglacial basal slip controls the efficiency of glacial erosion, which significantly influences the evolution of tectonically active mountain belts but remains to be quantified at High Asia. Satellite-based radar imagery analysis reveals short-term velocity changes at the largest glacier in West Kunlun Mountains at the northern edge of Tibetan Plateau, exhibiting seasonal periodicities with deviations from the minimum by up to ~20 m/yr. The inferred basal slip magnitude suggests that the erosion rate is at least ~1 mm/yr in

summer. We further detected surge-like rapid advance in the nearby valley glaciers. These observations provide us with evidences for significant basal slip and efficient glacial erosion even at these high-elevation cold glaciers.

## Airborne and satellite-based InSAR observations of Icelandic Ice Caps

### Author(s)

Mark Simons <sup>(1)</sup>, Brent Minchew <sup>(1)</sup>, Scott Hensley <sup>(2)</sup>, Eric Larour <sup>(2)</sup>

### Department

<sup>(1)</sup>Seismological Laboratory, Caltech 1200 E. California Blvd, Pasadena CA 91125, USA, US

<sup>(2)</sup>Jet Propulsion Laboratory/Caltech 4800 Oak Grove Dr, Pasadena CA 91109, USA, USA

### Abstract

Repeat-pass InSAR provides one of the better ways to construct surface velocity fields of glaciers and ice caps. These velocity fields can be used in conjunction with existing ancillary data, such as basal and surface topography, to constrain models of basal tractions and glacier rheology. Here, we focus on Hofsjokull and Langjokull icecaps in Iceland where we conducted a multi-day campaign to acquire repeat pass InSAR data using the NASA UAVSAR platform—a fully polarimetric L-band SAR system currently mounted on a GIII airplane. The data acquisition campaign lasted 5 days in June of 2009. Thus far, more than 125 interferograms have been processed at all polarization channels. These interferograms have temporal baselines that span from approximately 1 to 3 days and cover the entire surface area of Hofsjokull and Langjokull from multiple look angles. Another 270 interferograms remain to be processed for three long east-west trending flight tracks covering both Hofsjokull and Langjokull. When completed, the east-west interferograms, with temporal baselines ranging from less than 4 hours to more than 4 days, will provide unprecedented data on the temporal stability of L-band InSAR over temperate glaciers as well as the sufficient coverage to allow a construction of a complete 3D velocity field for Hofsjokull without along-topographic gradient assumptions for the velocity vector. Where possible, observations from the UAVSAR experiment is compared with ERS 1 and 2 C-band observations from the three-day repeat ice phase. From the existing interferograms, we have constructed several time series of the interferometric correlation over Hofsjokull. We find that over much of the glacier, a large amount of decorrelation occurs between one- and two-day repeat-pass intervals and continues at a reduced rate between two- and three-day baselines. The area around the equilibrium line shows the most significant change in correlation from one-day to three-day repeat pass intervals while areas at the highest and lowest elevations have consistently poor correlation. Based on these correlation data, weather data provided by the Icelandic Meteorological Office for stations located near Hofsjokull, and PolSAR inversion techniques, we are investigating the relationship between the relative surface moisture, roughness, and interferometric correlation. We present initial models of 3D surface velocity for selected regions as well as models incorporating the available velocity field observations into finite element models (FEM) of glacier flow of Hofsjokull to estimate rheological and basal properties. For the FEM modeling we rely on the ISSM code suite. Results from this initial experiment will form the basis for a more extensive set of campaigns conducted at different seasons.

# Monitoring ice flow surface velocities of the Inylchek Glacier (Kyrgyzstan) using TerraSAR-X Data

## Author(s)

Julia Neelmeijer <sup>(1)</sup>, Mahdi Motagh <sup>(1)</sup>

## Department

<sup>(1)</sup>GFZ Helmholtz-Zentrum Potsdam Telegrafenberg, 14473 Potsdam, DE

## Abstract

The glaciated mountains of Central Asia are home to one of the highest concentration of permanent snow and ice in the mid-latitudes of the Northern Hemisphere. Mountain glaciers are the only renewable fresh water resource in this region, dominated by semi-arid lowlands with low precipitation and dry climate. The Tien Shan mountain range in Central Asia hosts numerous glaciers including the Inylchek as the largest glacier with a length of approx. 60 km. The objective of this work is to evaluate the kinematics of the Inylchek glacier using radar data from TerraSAR-X satellite imagery. Due to their high spatial and temporal resolution TerraSAR-X data yield a great potential for deriving detailed information about the spatio-temporal pattern of ice flow surface velocity rates. Measurements are done using Amplitude Tracking, a sub-pixel correlation analysis of backscatter intensity values. Our data set covers the time period from April to October 2009 and February to September 2010 and includes both ascending and descending tracks. We investigate seasonal variations of the ice flow surface velocity and its correlation with meteorological parameters and also examine the significant contrast in ice-flow kinematics between different parts of the glacier.

# ERS-Envisat Tandem Cross-Interferometry results from the EET northern hemisphere and Antarctic campaigns

## Author(s)

Paolo Pasquali <sup>(1)</sup>, Paolo Riccardi <sup>(1)</sup>, Alessio Cantone <sup>(1)</sup>, Marcus Engdahl <sup>(2)</sup>

## Department

<sup>(1)</sup>Sarmap s.a. Cascine di Barico, 6989 Purasca, Switzerland, CH

<sup>(2)</sup>ESA, IT

## Abstract

The availability of ERS-Envisat 28minute tandem acquisitions from dedicated campaigns, covering large areas in the northern and southern latitudes with large geometrical baseline and very short temporal separation, allows among others the precise estimation of snow and ice displacement fields with an accuracy that cannot be obtained on large scale from any other instrument. The fusion of conventional differential interferometric techniques and multi-aperture approaches furthermore allows to estimate the full two dimensional displacement fields. The large overlap of adjacent tracks at northern and southern latitudes provides also a finer temporal resolution respect to the standard repeat cycle of ERS and ENVISAT. These factors open up the possibility of fine monitoring of glaciers and sea ice displacements, and to identify the boundary of the grounded ice areas. This article presents different results of snow and ice dynamic monitoring over Antarctica, Alaska and northern Canada obtained within the "ERS-Envisat Tandem Cross-Interferometry Campaigns: CInSAR processing and studies over extended areas" project from data acquired during the different ERS – ENVISAT Tandem campaigns performed in the 2007 – 2010 period.

# A review of the 2011 ERS-2 3-day mission

Author(s)

Andrew Shepherd <sup>[1]</sup>

Department

<sup>[1]</sup>University of Leeds , GB

## Abstract

The 3-day orbit repeat cycle missions of ERS-1 and ERS-2 have proven to be of wide benefit for a range of scientific applications due to the high degree of phase coherence that is maintained over short time periods. The data are useful for mapping rates of ice motion over wide areas and over short intervals, glacier grounding lines, and for studies of interferometric coherence as a precursor to the Sentinel-1 mission. This presentation reviews the main scientific achievements of the 2011 ERS-2 3-day campaign including studies of rapid and decadal flow variations of the principal outlet glaciers in Greenland and Antarctica.

# Ice velocity fluctuations of Greenland's Jakobshavn Isbrae from ERS-2 3-day SAR imagery

Author(s)

Aud Sundal <sup>[1]</sup>, Andrew Shepherd <sup>[1]</sup>, Noel Gourmelen <sup>[1]</sup>

Department

<sup>[1]</sup>University of Leeds Leeds, LS2 9JT, GB

## Abstract

Jakobshavn Isbrae is Greenland's largest outlet glacier, draining about 6.5 per cent of the total ice-sheet area. In March 2011, ERS-2 was moved to a 3 days repeat cycle, and here we apply InSAR and offset tracking techniques to the available 3-day SAR dataset to measure ice velocity fluctuations of Jakobshavn Isbrae. We detect maximum surface ice velocities near the glacier front of ~13000 meters per year, and short-term changes in ice speed of ~1000 meters per year. The velocity time-series will be extended to include all SAR data acquired by the ERS-2 3-day campaign.

# Displacement of periglacial landforms on Svalbard observed with high-resolution RADARSAT-2 and TerraSAR-X InSAR time series

Author(s)

Tom R. Lauknes <sup>[1]</sup>, Yngvar Larsen <sup>[1]</sup>, Hanne H. Christiansen <sup>[2]</sup>

Department

<sup>[1]</sup>Norut P.O. Box. 6434 Forskningsparken, NO-9294 Tromsø, NO

<sup>[2]</sup>UNIS P.O. Box. 156, NO-9171 Longyearbyen, NO

## Abstract

In Norway, permafrost represents a significant element of the landscape mainly in mountainous areas, but in high arctic Svalbard is continuous of nature and thus also occur in lowland sediment-filled valleys. As permafrost contains varying amounts of ground ice, thawing of particularly ice-rich permafrost will lead to subsidence of the ground surface, having a substantial impact on infrastructures, on the stability of northern ecosystems and on periglacial landforming processes. Permafrost degradation may affect slope stability, and to evaluate certain geohazards (rock slides and mudflows), improved knowledge on permafrost is essential to increase the understanding of

geohazards in Norway and Svalbard. Collection of in-situ field data quantifying periglacial landform activity on Svalbard is ongoing, but rather expensive and time consuming, despite the reasonably extensive research infrastructure available particularly in the vicinity of Longyearbyen. In the presented work the objective is to use time series interferometric synthetic aperture radar (InSAR) to detect, characterize, and quantify landscape displacement related to permafrost on both regional and local scales. Our results show that InSAR using ERS and Envisat ASAR data, with its 35 day repeat cycle, and relatively low resolution, are unable to capture the significant seasonal ground displacement happening relatively quickly mainly during spring thawing and autumn refreezing of the active layer above the permafrost. As part of the project, we have since summer 2009 acquired both Radarsat-2 Ultra-Fine and TerraSAR-X Stripmap and Spotlight modes over two study sites on Svalbard, the Longyearbyen and Kapp Linné areas, and the Nordnes site in northern Norway. Our results show that the high spatial resolution and short revisit time of TerraSAR-X is particularly well suited for monitoring the fine scale and highly nonlinear displacement that happens during the autumn refreezing and summer thawing of the active layer. We are acquiring data from both ascending and descending orbits, which enable separation of vertical and east-west displacement components. This makes it possible to distinguish different movement patterns between individual periglacial landforms, from solifluction sheets and rock glaciers with a significant horizontal component to landforms characterized by vertical displacement due to frost heave, such as beach ridges. The TerraSAR-X satellite provides data with 11 days repeat cycle, enabling us to prepare for the Sentinel-1 a/b satellites, which will provide operational InSAR products with a repeat cycle of 12 days (or 6 days with both satellites). We will present results from using the small baseline subset (SBAS) multitemporal interferometric method to detect surface displacements in different periglacial landforms of the study areas. We will compare different spatial resolution data from very high resolution Radarsat-2 and TerraSAR-X to medium resolution ERS, Envisat ASAR, and ALOS data with different radar frequency (X/C/L band), and different temporal resolutions (from days to weeks). Data from 2009, 2010, and 2011 will be presented. Proper ground verification and validation is mandatory for understanding of the interaction between the measured InSAR displacement signal and the variety of field movements recorded in the different periglacial landforms. We present field verification from the Nordenskiöld Land Permafrost Observatory installations of solifluction sheet ground movements and ground temperatures in Endalen/Adventdalen and at Kapp Linné in Svalbard.



**Day 3, Wednesday 21 September 2011**



# Session: Atmosphere I and II

## OSCAR: Online Services for Correcting Atmosphere in Radar

### Author(s)

Paul Von Allmen <sup>(1)</sup>, Evan Fishbein <sup>(1)</sup>, Eric Fielding <sup>(1)</sup>, Zhenhong Li <sup>(2)</sup>,  
Zhangfan Xing <sup>(1)</sup>, Lei Pan <sup>(1)</sup>, Martin Lo <sup>(1)</sup>, Virgil Adumitroaie <sup>(1)</sup>

### Department

<sup>(1)</sup>Jet Propulsion Laboratory , US

<sup>(2)</sup>University of Glasgow , UK

### Abstract

The atmosphere produces significant delays in the propagation of radar signals. The dominant delay source for short wavelength radar is due to tropospheric water vapor, the distribution of which is affected by large temporal and spatial variations and the amount of which is modulated by topography. These effects introduce noise in deducing ground motion from InSAR imaging which limits the thresholds of detectability. Ground-based GPS receivers provide the most accurate delay corrections but are useful only in densely monitored regions. Otherwise, meteorological data, such as satellite-derived near-IR total column water vapor, radiosonde profiles and numerical weather forecasts provide alternatives on a more global scale. The question is to determine what meteorological data are available, how to obtain them, and how to derive an optimal InSAR delay corrections. We have developed an Information Technology system that addresses these problems in a seamless and transparent way to the user. This set of Online Services for Correcting Atmosphere in Radar (OSCAR) consists of a client-server architecture that takes as input only the times of overpass and the corners of InSAR images. The system is extensible and currently works with MODIS near-IR water vapor data and ECMWF numerical weather forecasts (NWF). The MODIS data has 1 km spatial resolution, overpasses on the Terra and Aqua satellites typically twice per day (during daylight) and is biased in cloudy pixels. ECMWF data currently has 1/8° spatial resolution and has global coverage eight times daily. In the first step of calculating a map of delays, OSCAR uses its web services to retrieve the URL of available data. It then gets the data, subsets and merges it, lays it out on a common latitude-longitude grid, corrects for biases, computes maps of uncertainties, merges the data and finally creates a map of atmospheric delay differences which it delivers to the user to be used in the processing of InSAR images. The merging algorithm is Bayesian, but few data sets have point error estimates. Using provided quality control parameters, if available, or intercomparison studies, we create empirical error estimates for use in the merge. Currently we have a constant diagonal error matrix for the ECMWF analyses and a point estimate for the MODIS NIR water vapor that depends on cloudiness, and the fraction of high quality water vapor data points in the surrounding region. OSCAR is highly modular and uses IT tools such as webification, RESTful web services, and the workflow tool SCIFLO. We have validated our algorithms using comparison with GPS data and have found that near-IR vapor data leads to accurate values for the delays. On the other hand, we have seen that computing delays from uncorrected NWF data leads to sizeable inaccuracies due to the coarse spatial resolution of topography in the NWF models. We have developed and tested a set of topographic correction algorithms that improve the accuracy of NWF delays. In addition to presenting a detailed description of OSCAR's IT architecture, we will discuss the algorithms for quality controlling, bias and topography correcting and error estimation and

merging. A real-time demonstration of OSCAR will conclude the presentation. Future developments will include MERIS and NAM datasets.

## InSAR integrated water vapour variational assimilation in mesoscale model MM5: a step for improving model initial conditions at high resolution

### Author(s)

Nazzareno Pierdicca <sup>(1)</sup>, Emanuela Pichelli <sup>(2)</sup>, Rossella Ferretti <sup>(2)</sup>,  
Domenico Cimini <sup>(3)</sup>, Daniele Perissin <sup>(4)</sup>, Fabio Rocca <sup>(5)</sup>, Bjorn Rommen <sup>(6)</sup>

### Department

<sup>(1)</sup>Sapienza University of Rome Via Eudossiana 18, Rome, IT

<sup>(2)</sup>Univ. of L'Aquila L'Aquila, IT

<sup>(3)</sup>CNR, IT

<sup>(4)</sup>Chinese Univ. of Hong Kong, CN

<sup>(5)</sup>Polytechnic of Milan, IT

<sup>(6)</sup>ESA, NL

### Abstract

The high spatial resolution Numerical Weather Prediction (NWP) models are able to reproduce realistic atmospheric scenarios, but one of their most limiting factor is the poor resolution of the initial conditions (IC). In particular, the lack of both precise and continuous water vapour data is one of the major sources of error in short-term forecast of precipitation. An improvement in monitoring the atmospheric water vapour and its assimilation in NWP models would lead to more accurate forecasts of precipitation and severe weather. In this context, benefits from InSAR high resolution phase wet delay can be employed by obtaining integrated water vapour (IWV) maps from InSAR data and assimilating them in NWP. In this study a preliminary experiment of variational assimilation of InSAR data has been performed to correct initial condition of the mesoscale model MM5. The basic procedure for GPS assimilation has been adapted to InSAR data, suitably converted into IWV information. A case study of the 2008 campaign of ESA METAWAVE (Mitigation of Electromagnetic Transmission errors induced by Atmospheric Water Vapour Effects) project has been simulated. A sensitivity study is performed using different error matrix of the measured data; the impact on both IC and simulated results has been investigated. Variations on the initial horizontal and vertical distribution of water vapor have been discussed. Moreover a comparison of MM5 simulations with experimental data by radiosondes, surface stations and RADAR has been performed to the aim of establishing the impact of InSAR assimilation on model results. Among the others, an impact on the rain distribution and amount has been also detected: InSAR assimilation allows to correct MM5 overestimation of accumulated rain, but it doesn't show any improvement in reducing temporal bias on rain cells evolution. These results are anyway promising and further experiments will be performed. The work has been performed in the frame of ESA-ESTEC Contract N. 21207/07/NL/HE. In more details, the first problem to be faced when trying to assimilate InSAR Atmosphere Phase Screen data (APS) is translating the differential information provided by InSAR into an absolute value of the Integrated Water Vapour (IWV). Since an interferogram from SAR represents the path delay difference in both time and space and the InSAR APS at any given time is obtained by removing noise and phase ramp, it is not trivial to derive absolute IWV from InSAR APS images. Beside a conversion from phase difference to path delay, which can be assumed roughly a proportional factor, the basic idea is to estimate the mean (average in time) distribution of IWV in a given area and within a time frame by relying on an external source, such as IWV maps from Earth Observation missions (we have used MERIS maps in this work). It is easily to demonstrate that a reliable estimation of the actual IWV at time  $i$  can be derived from the differential IWV provided by APS at that time

(dIWWiAPS), a comparable average of the differential IWV  $\bar{I}$  provided by a multipass interferometric stack, and the external average  $\bar{I}$  by using the following equation:  $IWWiAPS = \bar{I} - \bar{I}_{dIWWiAPS}$ . To assess the impact of the InSAR data assimilation on the forecast, the most difficult field to predict was analyzed, that is the hourly precipitation. Comparisons between the model hourly precipitation, 8 hours after the model start time with (MM5\_SAR) and without (MM5\_NOSAR) InSAR data assimilation are shown. Furthermore, the outputs are compared with observed rainfall to better verify the impact. In one specific case, the MM5\_NOSAR clearly shows a precipitating cell in the south east corner of the domain producing more than 18mm/h; a similar structure is produced by MM5\_SAR, but a reduction of the rainfall is clearly produced by the InSAR assimilation. The comparison with the observation clearly suggests that the cell position is well reproduced by both MM5 simulations, but a 3 hour anticipation is found. Moreover, an overestimation by MM5\_NOSAR is produced: the maximum observed precipitation is approximately 16mm/h. Moreover, both MM5 simulations miss the precipitation in the eastern part of the central domain. The time shift is a well known MM5 structural problem that barely would be corrected by the InSAR assimilation; on the contrary, the IWV assimilation clearly reduces the rainfall overestimation by lowering it to 16mm/h.

## Validation of Centimeter-Level SAR Geolocation Accuracy after Correction for Atmospheric Delay using ECMWF Weather Data

### Author(s)

Xiaoying Cong <sup>(1)</sup>, Michael Eineder <sup>(2)</sup>, Ramon Brcic <sup>(2)</sup>, Nico Adam <sup>(2)</sup>,  
Christian Minet <sup>(2)</sup>

### Department

<sup>(1)</sup>Technische Universitaet Muenchen Arcisstr. 21, DE

<sup>(2)</sup>German Aerospace Center Muenchner Strasse 20, DE

### Abstract

As reported in [Eineder et al., 2011], absolute ranging with centimetre level accuracy can be achieved in TerraSAR-X images after correcting for 1) solid earth and ionospheric delay, both in the centimeter range and the 2) atmospheric delay of about 3 m in slant range due to air refractivity. The latter could be compensated for directly by using the total zenith path delay (ZPD) provided by the Regional Reference Frame Sub - Commission for Europe (EUREF) permanent GPS network. Unfortunately, this GPS network is quite sparse and in some regions, such as Africa and South America, not present. In order to accurately correct for atmospheric delay on a global scale another solution is needed.

To solve this problem, we have used the 3D global weather data available from the European Centre for Medium - Range Weather Forecasts (ECMWF) which is sampled every 6 hours and has 60 vertical layers. Since the atmospheric refractivity [Hanssen, 2001]; can be modelled as a function of temperature, air pressure and water vapour pressure provided by the atmospheric model, the total ZPD can be found by integrating the atmospheric refractivity in each vertical layer from the bottom to the top of the atmosphere.

In order to validate the accuracy of the total ZPD obtained by using ECMWF data, a comparison was made with respect to that obtained from two GPS stations selected from the EUREF network, namely Ponta Delgada (PDEL), Portugal and Bad Koetzing (WTZR), Germany. 120 ECMWF entries from PDEL and 500 from WTZR were collected. The weather data was interpolated to the GPS location and the surface pressure was adjusted to GPS height. After integration along the zenith path, we compared the ECMWF ZPD with the EUREF GPS ZPD measurements taken at the nearest sample time. The standard deviation of the differences between the two ZPDs was 1.31 cm at PDEL and 0.96 cm at WTZR. The ZPD obtained using the ECMWF atmospheric model hence shows good agreement with GPS ZPD measurements.

Afterwards, we repeated the experiments carried out at Fogo, Azores Portugal and in Venice, Italy as described in [Eineder et al., 2011], where the slant range delay in the SAR image was obtained as described above using the 3D ECWMF atmospheric model in conjunction with the ray tracing method. The ionospheric delay was also updated using freely available global ionospheric models [CODE]. For the two test sites, instead of using the angle corrected ZPD from the GPS network, the range delay at the corner reflector was obtained by integrating along the line of sight to the sensor the refractivity obtained from the 3D atmospheric model. After this updated slant range delay correction the absolute ranging accuracy at Fogo and in Venice was in both cases found to be approximately 3 cm.

In this paper, an alternative method to effectively compensate for the atmospheric delay in SAR images using 3D weather data was presented. With this method, we could also achieve centimeter-level accuracy without having to rely on ZPD information from a GPS station.

References:

[Eineder et al., 2011]: Michael Eineder, Christian Minet, Peter Steigenberger and Xiaoying Cong, Imaging Geodesy—Toward Centimeter-Level Ranging Accuracy With TerraSAR-X. IEEE Transactions on Geoscience and Remote Sensing, Vol. 49 (Iss. 2), pp. 661-671. IEEE. DOI: 10.1109/TGRS.2010.2060264. ISSN 0196-2892

[Hanssen, 2001]: Ramon F. Hanssen, Radar Interferometry – Data Interpretation and Error Analysis. Kluwer Academic Publishers, 2001

[CODE]: CODE Research on the homepage of the Astronomisches Institut at Universität Bern, [http://cmslive2.unibe.ch/unibe/philnat/aiub/content/research/gnss/code\\_\\_\\_research/](http://cmslive2.unibe.ch/unibe/philnat/aiub/content/research/gnss/code___research/).

## InSAR Time Series with Atmospheric Estimation Model for Regional Deformation Mapping

Author(s)

Zhenhong Li <sup>(1)</sup>, William Hammond <sup>(2)</sup>, Geoffrey Blewitt <sup>(2)</sup>, Corné Kreemer <sup>(2)</sup>, Hans-Peter Plag <sup>(2)</sup>, Yangmao Wen <sup>(3)</sup>, Caijun Xu <sup>(3)</sup>

Department

<sup>(1)</sup>COMET+, School of Geographical and Earth Sciences, University of Glasgow , UK

<sup>(2)</sup>Nevada Geodetic Laboratory, Nevada Bureau of Mines and Geology, University of Nevada , US

<sup>(3)</sup>School of Geodesy and Geomatics, Wuhan University , CN

**Abstract**

InSAR has difficulties in measuring small deformation signals over a wide region such as postseismic motion and interseismic strain accumulation because of its two major sources of error: (a) Atmospheric water vapour and (b) orbital uncertainties. Difference in radar signal propagation delays between SAR acquisitions attributable to tropospheric water vapour can cause errors as large as 10-20 cm in deformation retrievals. The knowledge of satellite orbits is limited; after known geometrical contributions have been removed using precise orbits, residual phase ramps remain in interferograms. The impact of orbit separation (i.e. baseline) error on surface deformation increases with areal extents of SAR images. InSAR Time Series analysis with Atmospheric Estimation Models (InSAR TS + AEM), developed at the University of Glasgow, is an advanced InSAR time series analysis approach that uses multiple interferograms with small geometric baselines to minimize the effects of decorrelation and inaccuracies in topographic data. InSAR TS + AEM can be used to separate deformation signals from atmospheric effects and orbital ramps in order to recover surface deformation evolution. The principal purpose of this study is to assess the accuracy of the InSAR TS + AEM derived deformation time series and atmospheric path delays through two case studies: (1) crustal deformation of the Southern Walker Lane, western Great Basin, United States; and (2) postseismic motion after the 2001 Mw 7.8 Kokoxili (Tibet) earthquake. (1) Case study 1: The southern Walker Lane (SWL) and Yucca

Mountain region of the western Great Basin in the United States is chosen as a study site because (a) it is a zone of active crustal extension and shear deformation with a magnitude of 2-4 mm/yr and (b) it has a dense, high-precision continuous GPS network and extensive radar archives. Presently the archives include >11 years of continuous GPS data and >19 years of ERS and ENVISAT radar acquisitions. Interferometric coherence is generally high owing to the relatively arid environment, even for long temporal baselines that span the existing C-band radar archives. In this study, GPS data was used to remove orbital ramps on InSAR derived line of sight (LOS) mean velocity maps. Our results show that: (1) the InSAR LOS deformation map agrees with GPS measurements to within 0.46 mm/yr RMS misfit at the stations over a wide region (250 km x 100 km), and (2) the RMS differences between InSAR and GPS derived path delays are about 5 mm. (2) Case study 2: The Mw 7.8 Kokoxili earthquake ruptured more than 400 km along the western part of the Kunlun fault with a maximum of 8 m left-lateral slip on 14 November 2001. In this study, five adjacent descending tracks of ENVISAT images with an coverage of 350 km x 350 km collected between 2003 and 2008 were employed to study its postseismic motion, and a peak deformation signal of 5 cm was observed in the satellite line of sight with the 2-6 years after the large event. As there was no GPS data available for validation, comparisons between measurements of the overlaps between two adjacent tracks were performed, suggesting an accuracy of c. 0.4 cm for InSAR derived displacements (equivalent to an accuracy of c. 1mm/yr for deformation rates). It is clear from the above two case studies that InSAR is not only a powerful geodetic tool for detecting small surface movements over a wide region, but also an unparalleled remote sensing technique for mapping high spatial resolution atmospheric water vapour.

## Numerical Weather Model Assisted Time Series InSAR Processing for Geophysical Application

Author(s)

Wenyu Gong <sup>(1)</sup>, Franz Meyer, Shizhuo Liu <sup>(2)</sup>

Department

<sup>(1)</sup>University of Alaska Fairbanks 903 Koyukuk Drive, PO Box 757320, USA

<sup>(2)</sup>Delft University of Technology Kluyverweg 1, 2629 HS Delft, NL

### Abstract

The interferometric Synthetic Aperture Radar (InSAR) technique shows significant potential and capability to provide fine resolution and high accuracy measurements of centimeter-scale surface deformation. It is helpful to recognize, monitor, interpret and understating tectonic movement especially subtle signals from ground, e.g. volcano inflation precursor and earthquake movement. In recent years, the so-called time-series InSAR shows improvement in reducing the sensitive of InSAR technique to temporal decorrelation and electromagnetic path delay variations (atmospheric artifacts). For atmospheric signal mitigation, this group of methods rely on a set of assumptions that atmospheric signals are un-correlated in time but correlated within certain spatial scales (less than 2~3km), to successfully separate atmospheric signals from other interferometric phase components in large stacks of multi-temporal SAR datasets (approx. 20-100 SAR images). The presence of highly non-linear surface motion additionally requires the SAR data stack to have high temporal sampling frequency to enable the separation of atmospheric signals from non-linear motion components. For highly dynamic systems, like volcanoes, these requirements render conventional InSAR time-series analysis methods impractical. Not only does the presence of non-linear motion cause strict requirements on data volume and sampling, the atmosphere phase signal in these areas additionally does not match the statistical assumptions that are used for their detection and mitigation. Atmospheric artifacts are often spatially correlated with the surface deformation signatures. Also, in certain areas, atmospheric phase

signals show temporal persistence (e.g., persistent cloud patterns near volcanic cones) complicating their detection and mitigation based on spatio-temporal statistics. Therefore, atmospheric interference still is a main limitation in advance time-series InSAR methods especially when applied to complex systems such as volcanic vents. More research on atmospheric corrections of interferograms is required to improve the performance of InSAR for dynamics in geophysical application. With this paper, we focus on the development of mitigation methods for atmospheric artifacts in interferograms using Numerical Weather Prediction (NWP) models. We will present both an optimized parameterization and the achievable performance of the Weather Research and Forecasting Model (WRF) for this application. The performance of WRF is studied using two study areas, Unimak Island in Aleutian Arc, Alaska and Los Angeles City, California, both in USA. The motion signatures and geophysics properties of the two study sites are highly different, one showing strong seasonal fluctuations and the other one showing strong linear trends. For both test sites, InSAR data is strongly affected by partially persistent atmospheric artifacts that are difficult to mitigate using conventional InSAR time-series analysis methods. The WRF model was applied to forecast absolute atmospheric delay maps for each SAR image acquisition time. These simulated signals were then used in time-series InSAR processing to support master image selection and perform model-based atmospheric signal correction. We will present the development and performance assessment of efficient concepts for incorporating WRF simulations into time-series analyzes of InSAR data. Our previous research results indicate significant potential of NWPs for this task, including a significant improvement of the reliability, accuracy, and sensitivity of InSAR-based deformation measurements. NWPs seem particularly useful for predicting statistical properties of atmospheric signals and may therefore provide a convenient means for completing statistical models of InSAR data. A quality analysis of NWP assisted time-series processing will be presented. This includes a relative cross-validation of WRF- and InSAR-derived atmospheric delay maps to determine similarities of signals at different spatial scales. Whenever available, both GPS data and MODIS products are used as a reference to determine accuracy and precision of the derived atmospheric signals. Also, as the second step of performance assessment, the results are analyzed in statistical fashion, including extraction and comparison of structure functions of atmosphere phase screens. Finally, deformation signals are calculated both using a conventional setup and NWP-assisted time-series analysis. The resulting deformation signals are compared to observations of GPS permanent stations to assess the performance improvement achieved by the inclusion of NWPs into the InSAR processing flow. The expected contribution of the proposed paper includes: 1) Analysis of the benefit of WRF-assisted master image selection; 2) NWP predicted delay map and atmospheric signal correction for master image in time-series InSAR processing; 3) Comparison of correction performance with and without NWP model inclusion in time-series InSAR analysis; and 4) Conclusion of troposphere effects mitigation by using NWPs.

## IP-STATS – A System for Deriving Statistical Models of Ionospheric Signals in Low-Frequency SAR

Author(s)

Franz Meyer <sup>(1)</sup>, Brenton Watkins <sup>(1)</sup>

Department

<sup>(1)</sup>University of Alaska Fairbanks , USA

### Abstract

1. ABSTRACT: This paper focuses on deriving a realistic statistical model for ionospheric effects in low-frequency Synthetic Aperture Radar (SAR) data. The approach used to develop this statistical model is based on the assumption that, for a certain range of scales, ionospheric plasma turbulence can be considered a scale-invariant process that can be described by power-law



functions or fractal statistics. Based on the parameters of a power law model, covariance functions and ionospheric variance-covariance matrices are derived. An ionospheric phase statistics simulator (IP-STATS) is presented that is capable of calculating a variety of statistical descriptors and is able to predict representative ionospheric phase screens. To demonstrate its functionality and performance, the IP-STATS system is used to derive statistical models for a 10 year time series of L-band SAR data over the area of Alaska.

2. APPROACH: The irregularities in the ionosphere, as measured by a microwave signal, are modeled by a power-law function  $P(k)$  that is parameterized by its spectral index  $\nu$  and a height-integrated turbulence strength parameter  $P_0$ . Values for  $P_0$  and  $\nu$  vary with signal frequency, geographic location, solar activity, and time of day. Typically reported values for  $\nu$  range between  $\nu = 2.2$  and  $\nu = 3.5$ . In this paper, representative parameters  $P_0$  and  $\nu$  are derived using the global ionospheric scintillation model WBMOD (WideBand MODel). Given a set of parameters describing solar activity (namely the Smoothed Zurich Sunspot Number (SSN) and the Planetary Geomagnetic Activity Index (KP)) and using a number of system parameters, WBMOD is capable of simulating electron density fluctuations and propagating them to scintillation effects on a user-defined system. Under the assumption that the ionospheric signal within a SAR image is a second-order stationary signal, the power-law models  $P(k)$  defined in this study are converted to covariance functions  $C(r)$ . The calculated  $C(r)$  are then used to construct variance-covariance matrices  $Q$  to be entered into the stochastic model of parameter estimations. In this paper, adequate methods for the required transformations ( $P(k) \rightarrow C(r) \rightarrow Q$ ) are presented. Power-law functions are additionally converted to fractal statistics, which is an elegant tool for visualization and simulation. In fractal statistics, the spatial behavior of a process is parameterized by the fractal dimension  $D$ , a parameter that is equivalent to the spectral exponent  $\nu$  mentioned previously. Using fractal theory, ionospheric phase delay signals are simulated by approximating their power spectra with fractal regimes. Each consistent spectral regime is represented by its corresponding fractal dimension, which allows assigning different fractal behavior for different spatial scales.

3. THE IONOSPHERIC PHASE STATISTICS SIMULATOR (IP-STATS): Based on the mentioned mathematical concepts, an Ionospheric Phase STATistics Simulator (IP-STATS) was developed that enables the calculation of statistical models describing ionospheric phase delay patterns in SAR acquisitions. It also allows simulating representative two-dimensional ionospheric phase screens that can be used to analyze potential effects of ionospheric signals on a SAR application, e.g., monitoring of surface deformation. The work flow of the IP-STATS system will be presented in the paper. In IP-STATS the calculation of ionospheric phase statistics is based on a set of ionospheric parameters as well as geometry and system-related input. Output parameters of IP-STATS are i) ionospheric power law model  $P(k)$ , ii) ionospheric covariance function  $C(r)$ , iii) ionospheric variance-covariance matrix  $Q$ , and iv) simulated ionospheric phase screens. The IP-STATS simulator can be used to determine statistical properties of ionospheric propagation effects throughout the lifetime of a SAR system and for any location on the globe. To demonstrate its performance, the IP-STATS system was used to analyze ionospheric signals affecting L-band SAR data acquired in the auroral-zone. Ionospheric phase statistics were calculated for a 10 year time span between 1/19/2001 and 4/01/2010 covering the full range of solar activity from the last solar maximum in 2001 to the recent solar minimum in 2008. ALOS PALSAR-like system and geometry parameters were used for simulation. Acquisition dates were simulated in 46 day periods resulting in a total of 74 acquisition scenarios. The ionospheric parameters SSN and KP were derived from published observations. For this time series of data, IP-STATS output parameters will be presented in the paper for various ionospheric conditions.

4. SIGNIFICANCE AND CONCLUSIONS: A framework for deriving statistical descriptors of ionospheric signals in SAR data was introduced. Based on this framework, an ionospheric phase statistics simulator (IP-STATS) was developed that is capable of predicting statistical ionospheric parameters and simulating ionospheric phase screens. The statistical and mathematical descriptors presented in this paper have a wide range of potential applications ranging from data simulation, statistical modeling of SAR data, identification of

potentially affected imagery, and sensitivity assessment of existing spaceborne SAR systems. Due to the dependence on quantifiable ionospheric conditions and system parameters, IP-STATS can also support mission planning efforts as its outputs can be used to define mission parameters like system wavelength and the timing of ascending and descending orbit nodes.

## Spatio-temporal variability of Water Vapor as seen by InSAR, GPS, Meris and MM5

### Author(s)

Daniele Perissin <sup>(1)</sup>, Fabio Rocca <sup>(2)</sup>, Emanuela Pichelli <sup>(3)</sup>, Rossella Ferretti <sup>(3)</sup>, Nico Cimini <sup>(3)</sup>, Giovanna Venuti <sup>(4)</sup>, Nazzareno Pierdicca <sup>(5)</sup>

### Department

<sup>(1)</sup>CUHK Hong Kong, HK

<sup>(2)</sup>POLIMI Milano, IT

<sup>(3)</sup>CETEMPS L'Aquila, IT

<sup>(4)</sup>POLIMI, DIAR Milano, IT

<sup>(5)</sup>La Sapienza Roma, IT

### Abstract

Electromagnetic signals are delayed by the Water Vapor (WV) content in the atmosphere and this causes a space-varying bias on interferograms generated with spaceborne SAR images. The feasibility of estimating the atmospheric water vapor with alternative instruments for compensating the corresponding interferometric delay is strictly linked to its variability in space and time. In this work we exploit the results of the ESA Metawave project (Mitigation of Electromagnetic Transmission errors induced by Atmospheric Water Vapour Effects) to study the space-time variability of water vapor. The results got in the Metawave project are relative to two test-sites in Italy: Roma and Como. In the Roma experiment, we processed 27 ERS images taken at 3 days time distance, 41 Envisat images acquired along ascending Track 172 and 29 images acquired along the Track 352, descending. Twenty five WV maps have been taken by Meris during the descending passes (morning time) in correspondence of SAR images. Finally, 24 hours simulations of WV evolution have been generated with the Numerical Weather Prediction model MM5 at the same date of more than 30 Envisat images. In the Como test site, 28 and 38 images have been processed in descending (480) and ascending (487) tracks respectively. Eight GPS stations have been deployed for the experiment, at distance levels of 100m, 1km and 10km. The temporary stations have been connected to the regional GPS permanent network, comprising 17 spots. Permanent and temporary stations are mainly at low altitudes, but high ones are present as well. From the two datasets, WV vertical stratification and turbulence have been estimated and compared among the different instruments. Spatio-temporal characteristics have been extracted and analyzed. The WV temporal evolution retrieved by GPS and MM5 shows that a synchronization better than half an hour is required to mitigate the delay in the interferometric phase. The estimated WV spectral content in space makes it clear that no other instrument has the capacity to resolve the turbulence frequencies as the Permanent Scatterers technique. However, Meris has good performances in clear sky conditions and in absence of topography. NWP models can be of great help in mitigating long WV wavelengths and in reducing the vertical stratification component. Finally, GPS Zenith Wet Delays have the highest correlation with the InSAR Atmospheric Phase Screen, assessing their usefulness in integrating InSAR analyses where multi-temporal techniques fail.

# Systematic InSAR tropospheric phase delay corrections from global meteorological reanalysis data

## Author(s)

Romain Jolivet <sup>(1)</sup>, Raphael Grandin <sup>(2)</sup>, Cécile Lasserre <sup>(3)</sup>, Marie-Pierre Doin <sup>(2)</sup>, Gilles Peltzer <sup>(4)</sup>

## Department

<sup>(1)</sup>ISTerre - CNRS , FR

<sup>(2)</sup>Ecole Normale Supérieure, Paris 24, rue Lhomond, FR

<sup>(3)</sup>ISTerre-CNRS-Université Joseph Fourier 1381, rue de la piscine - Campus Universitaire, FR

<sup>(4)</sup>UCLA-JPL 595 Charles Young Drive East, Box 951567 , USA

## Abstract

Differential InSAR has achieved prominent successes in recent years, particularly for the retrieval of surface deformation maps induced by most of the major continental earthquakes since the mid-1990s. Extension of the technique to cases where a smaller signal is expected is more challenging because of errors due to atmospheric phase delays. In order to enhance the signal-to-noise ratio in InSAR data, the commonly used method is to combine a large number of images in a stack or a time-series analysis, and to rely on the redundancy of interferograms to estimate the atmospheric phase screen associated with each acquisition. However, these methods often fail in tackling any atmospheric stationary component that cannot be efficiently cancelled by averaging over a large number of measurements, such as spatial and temporal variations of the stratified atmospheric delay, which result in fringe patterns that correlate with the topography of the imaged area. In areas of high relief, their influence can dominate most of the signal induced by tectonic or volcanic processes of moderate magnitude. The empirical removal of topography-correlated phase delays yields satisfactory results in most cases, but provides biased results when the deformation signal correlates with the topography, for example over a volcano or along a mountain range. In this communication, we describe the capability of recent advances in the field of meteorology and weather forecasting in allowing for prediction of the spatial and temporal distribution of the three main parameters controlling the observed topography-correlated tropospheric effects in interferograms (i.e. temperature, geopotential and partial pressure in water vapor). The ERA-Interim reanalysis of the ECMWF provides the spatial distribution of these meteorological parameters at 37 pressure levels, 4 times daily, with a horizontal grid spacing of ~ 75 km over the globe. Using these data, we compute the predicted daily tropospheric delay as a function of altitude, taking into account lateral variations. A horizontal bilinear- and vertical spline-interpolation scheme is applied to simulate smooth atmospheric delay maps that can be readily compared to observed interferograms. To validate this approach, we examine two regions where strong tropospheric delays are observed in InSAR data. These regions are chosen to lie on the periphery of the Tibetan plateau, where deformation and topography are chiefly correlated. The first area of interest is the Kunlun area (North-East Tibet), where a major strike-slip fault separates two blocks with a 2 km elevation difference (the Qaidam basin to the North, and the Tibetan Plateau to the South). Unwrapped interferograms are successfully corrected using predicted tropospheric delays, with no significant degradation compared to an empirical correction estimated from a joint inversion of orbital errors and phase-elevation ratio. The second test case is the Himalayan range (between the Tibetan plateau to the North and the Indo-Gangetic basin to the South), where phase unwrapping across the 5 km high mountain range is impossible without a priori correction of tropospheric effects. Removal of the predicted phase delay significantly enhances the interferometric phase coherence, and allows for phase unwrapping in a few cases. The resulting accuracy on the residual LOS deformation signal is of the order of magnitude of the expected underlying interseismic strain across the range.

# Correcting DInSAR ALOS data using atmospheric delay estimated by GPS signals to constrain the surface deformation in the Longitudinal Valley (Taiwan Island).

## Author(s)

Rana Charara <sup>(1)</sup>, Marie-Pierre Doin <sup>(1)</sup>, Bénédicte Fruneau <sup>(2)</sup>, Erwan Pathier <sup>(3)</sup>, Johann Champenois <sup>(2)</sup>, Jyr-Ching Hu <sup>(4)</sup>, Kuan-Chuan Lin <sup>(5)</sup>

## Department

<sup>(1)</sup>Ecole Normale Supérieure 24, rue Lhomond 75005 Paris, France, FR

<sup>(2)</sup>Université Paris-Est Bd Descartes, 77454 Marne-la-Vallée cedex 2, FR

<sup>(3)</sup>Université Joseph Fourier BP 53 - 38041 Grenoble Cedex 9, France, FR

<sup>(4)</sup>National Taiwan University P.O. Box 13-318, Taipei 106, Taiwan, TW

<sup>(5)</sup>University of Nice - Sophia Antipolis , FR

## Abstract

DInSAR has proven its potential in detecting not only large coseismic or postseismic deformation, but also small deformation signals, such as interseismic deformation. However, atmospheric phase screens are the main limitation in detecting such small deformations, and can even mask them, especially in areas of large relief. Various methods have been tested to correct the atmospheric perturbation: i/ stacking of several interferograms to reduce artefacts related to the turbulent variation of the water vapor contained in the atmosphere (Peltzer et al., 2001, Schmidt et al., 2005); ii/ using empirical law between interferometric phase and elevation to correct the topographic dependent atmospheric delays (Cavalié et al., 2007), and iii/ estimating directly the atmospheric delays using global atmospheric models (e.g., ERA40), meso-scale dynamic meteorological models (e.g., MM5) or MERIS satellite images to reduce both topography-dependent and turbulent atmospheric effects (Doin et al., 2009, Li et al., 2006). In the Longitudinal Valley, in the East of Taiwan, surface deformation has been detected using DInSAR all along the Longitudinal Valley Fault, the main seismically active fault zone in this region. This has been done with ERS C-band images (Hsu et Bürgmann, 2006; Peyret et al., 2011), and with PALSAR L-band images provided by ALOS (Champenois et al., 2011). However, because of the large topographic variations over the valley and the proximity of the sea, strong atmospheric phase delays can affect the InSAR measurements of surface displacement and have to be accurately corrected. Moreover, while the use of L-band data allows improving considerably the coherence in such area characterized by luxuriant vegetation, they may also be severely affected by ionospheric heterogeneities, compared to C-band images. The aim of this study is to estimate tropospheric and ionospheric signals that corrupt differential interferograms computed with ALOS PALSAR images on the Longitudinal Valley, and correct them. The final objective is to better constrain the surface deformation in this area. We processed all available images (14) acquired by ALOS on the 2007-2010 period using the NSBAS (New Small temporal and spatial BASelines) chain (Lopez-Quiroz et al., 2008). 44 interferograms were generated. Direct measurements of atmospheric delays using local meteorological data are not enough accurate because of the low density of weather stations equipped with water vapor radiometer (WVR). However, Taiwan has one of the most important permanent GPS network in the world with inter-station distance lesser than 5-10km. Thus, we propose to estimate the atmospheric delays affecting the GPS signal and to use these direct estimations to reduce the atmospheric effects in the interferograms. Taiwan, with its high density of GPS stations, is an ideal case to test this method. GPS data are processed with GAMIT-GLOBK 10.35 software (King et Bock, 1999) to extract the ionosphere and troposphere delays at 100 permanent GPS chosen stations and for each date that a radar image is acquired. This work needs to follow several steps: 1/ to accurately estimate the position of each GPS sites following the strategy used for tectonics applications, the difficulty residing in the number of available GPS stations that require to divide the network in several sub-networks and

to realize a combination of these sub-networks to obtain consistent positions over the whole network, 2/ based on the calculated positions, to estimate the tropospheric zenithal delays for each date an ALOS image was acquired following the method developed in Champollion et al. (2004) and Walpersdorf et al. (2007), 3/ estimate the total electron content (TEC) along the path satellite-receiver (Calais,1998) to calculate the ionospheric zenithal delays. Then, for each SAR acquisition date, two maps of ionosphere and troposphere delay are computed in the line of sight of the radar, using the GPS atmospheric zenithal delays and a SRTM DEM. Interpolation of troposphere delay maps is based on elevation. Those maps are then used to reduce the atmospheric phase in all interferograms. We analyse and quantify statistically the improvement of the 44 formed interferograms after atmospheric corrections. We calculate the reduction of the interferograms phase variability, and the reduction of the difference between the GPS and InSAR derived displacements. At the same time, different attempts are also carried out to estimate, from the SAR data directly, ionospheric contributions to the interferometric phase, the difference of ionospheric states at two SAR acquisitions giving rise to azimuth and range shifts, as well as phase differences (Meyer et al., 2006). This is done through the estimates of range and azimuth offsets values between the two images forming an interferogram, as well as the phase difference between the forward- and backward-looking interferograms (AZISAR, Barbot et al.,2008). Finally, a comparison between all different delays obtained by GPS, global meteorological models and interferometric phase allows to quantify the added-value of using GPS data. All these steps lead us to quantify more precisely the surface deformation in the longitudinal valley of Taiwan Island, which is a crucial issue to improve seismic hazard assessment.

## Pushing the accuracy limit for CO<sub>2</sub> sequestration monitoring: Statistically optimal spatio-temporal removal of the atmospheric component from InSAR Networks

Author(s)

Bernhard Rabus <sup>(1)</sup>, Jayson Eppler <sup>(2)</sup>

Department

<sup>(1)</sup>Simon Fraser University Canada, CA

<sup>(2)</sup>MDA Canada, CA

### Abstract

Continued monitoring of CO<sub>2</sub> sequestered underground poses substantial challenges with regard to InSAR measurement accuracy. This is due to the inevitable weakening of the uplift signal over time (at constant injection rate) as increasing reservoir maturation due to CO<sub>2</sub> emplacement shortens diffusion times and spatially spreads the uplift footprint. We found that there is no advantage to using X-band over C-band due to the higher sensitivity to subsidence of the former being offset by a proportional increase in atmospheric noise. On the other hand we found that choosing a steep incidence angle is an important a-priori measure to boost accuracy as this maximizes the uplift signal while minimizing atmospheric path length. However, the crucial increase of InSAR measurement accuracy must come from better removal of the atmospheric component from the network. Choosing sensors with small revisit intervals is an obvious solution to remove temporally uncorrelated atmospheric noise, however temporally dense data stacks are expensive and unnecessary to capture the generally slowly varying uplift signals from CO<sub>2</sub> sequestration. We found that the most robust and efficient way to boost InSAR accuracy is through using an optimum spatio-temporal filter to remove atmospheric noise. Spatial frequencies belonging exclusively to the atmospheric noise signal are identified and removed for each data layer in an optimum way while temporal filtering has been optimized to handle temporally irregular data stacks as well as temporal edge effects at the end of an evolving data stack.

Spatial and temporal filters are iteratively coupled in our processing chain to improve robustness and allow for joint processing of interleaved data stacks from different geometries and sensors. By comparing results between different data stacks we demonstrate that final accuracy levels achieved with the new atmospheric filtering scheme for non-linear time series are on the order of 0.6 mm per year.

# Session: Earthquakes & Tectonics II

## Satellite Constraints & Field Observations of slip in the Canterbury Earthquakes, New Zealand: Implications for future seismic hazard in Christchurch

### Author(s)

John Elliott <sup>(1)</sup>, James Jackson <sup>(2)</sup>, Philip England <sup>(1)</sup>, Simon Lamb <sup>(3)</sup>,  
Zhenhong Li <sup>(4)</sup>, Nissen Edwin <sup>(2)</sup>, Mike Oehlers <sup>(5)</sup>, Kirill Palamartchouk <sup>(1)</sup>,  
Barry Parsons <sup>(1)</sup>

### Department

<sup>(1)</sup>University of Oxford The Earth Sciences Building, South Parks Road, UK

<sup>(2)</sup>University of Cambridge Bullard Laboratories, Madingley Rise, UK

<sup>(3)</sup>Victoria University of Wellington Antarctic Research Centre, NZ

<sup>(4)</sup>University of Glasgow, UK

<sup>(5)</sup>FugroNPA, UK

### Abstract

The pair of recent earthquakes to strike southern New Zealand occurred on previously unknown faults. On the 3rd September 2010, a Mw 7.1 shallow strike-slip earthquake occurred on the South Island of New Zealand, 40 km west of Canterbury. This was followed less than 6 months later by a large aftershock (Mw 6.3) which ruptured beneath the city of Christchurch. We use field mapping, satellite optical imagery, SAR amplitude offsets and teleseismic bodywave modelling to constrain fault segmentation used in slip models based upon InSAR phase measurements. Field measurements of the distribution of surface ruptures and surface slip (augmented by those offsets mapped from high-resolution satellite imagery) of up to 4 m dextral motion generally agree with that predicted from the InSAR constrained fault models. The InSAR measurements reveal complex faulting in the first event, with slip on multiple strike-slip segments and secondary thrust faults. Fault orientations are consistent with that expected from the GPS derived strain field. The main fault rupture is constrained largely to the upper 10 km of the crust and is relatively short at 45 km. However high slip on the individual faults segments and a peak slip of over 8 m at 4 km depth indicate large stress drops. The combined models and satellite observations of both the Darfield and Christchurch events reveal a significant spatial gap in fault slip south-west of Christchurch which presents a continuing seismic hazard if a further unknown fault structure should exist there. The identification of such possible structures of which slip could occur in the vicinity of Christchurch is now a priority as the current gap in the fault rupture is similar in length to that which ruptured in the latter Christchurch event. The shallow magnitude 7 earthquake that ruptured across the northern Canterbury Plains in September 2010 occurred only 40 km west of the city of Christchurch (population 330,000), but fortunately resulted in no loss of life. However, less than 6 months later a smaller earthquake (Mw 6.3) occurred right beneath the city and despite the high standards of building codes, the extreme ground shaking due to the shear proximity of the event resulted in the loss of 186 lives. The ruptures in both these events occurred on previously unknown faults, and the main seismic hazard for the region was presumed to be due to the major mapped faults to the north-west in the Alpines, structures which are capable of even larger earthquakes. The current priority is to now assess the nature and extent of faulting in the immediate area, which can help direct research to focus on determining potential fault structures that could fail in future ruptures and which present a risk in particular to the relative populous city of Christchurch. To this end, we combine InSAR geodetic observations, with field mapping and seismological solutions to examine the distribution of rupture and model the

previously unknown fault orientations. This is essential to identify not only the structures which failed in this event, but also to identify the regions around Christchurch that have now been brought closer to failure by these two events. Furthermore, we examine the GPS derived velocity field for this part of New Zealand, and show that the complex rupture that occurred in these events is however, still consistent with the overall strain field.

## The whole 2010-2011 New Zealand seismic sequence revealed by DInSAR and time-series data

### Author(s)

Cristiano Tolomei <sup>(1)</sup>, Elisa Trasatti <sup>(1)</sup>, Stefano Salvi <sup>(1)</sup>, Paolo Pasquali <sup>(2)</sup>, John Peter Merryman <sup>(1)</sup>, Alessio Cantone <sup>(2)</sup>, Andrea Antonioli <sup>(1)</sup>, Simone Atzori <sup>(1)</sup>

### Department

<sup>(1)</sup>Istituto Nazionale di Geofisica e Vulcanologia Via di Vigna Murata,605, IT

<sup>(2)</sup>SARMAP ,

### Abstract

This presentation is based on the results obtained with standard DInSAR and time-series SBAS approach for the seismic sequence that interested New Zealand from September 2010 to February 2011. We start from the analytical modeling of the displacement obtained with C-, L- and X-band DInSAR for the Darfield and Christchurch events, giving new insights into their slip distribution and their interaction by means of Coulomb Failure Function. We then focus on the deformation occurred between the two events; the latter has been investigated with 14 descending and 9 ascending COSMO-SkyMed images. The analysis of the time evolution of the displacement between the two main events shows strong horizontal components, reaching cumulated values up to 5 centimeters. The observed deformation can be attributed to the post-seismic behavior following the first event and possibly triggering the incoming Christchurch earthquake. We investigate the time-series SBAS data by means of numerical approaches, accounting for the crust rheology, thus including poro-elastic effects and visco-elastic relaxation. The overall analysis is intended to fill the gap in interpreting geodetic and tectonic implications between the two events.

## Coseismic and postseismic deformation analysis of the 2010 Mw 7.1 Darfield and 2011 Mw 6.3 Christchurch earthquakes in New Zealand from combined GPS and InSAR observations

### Author(s)

John Beavan <sup>(1)</sup>, Mahdi Motagh <sup>(2)</sup>, Sergey Samsonov <sup>(3)</sup>, Eric Fielding <sup>(4)</sup>, Andrea Celentano <sup>(5)</sup>

### Department

<sup>(1)</sup>GNS Science, Lower Hutt, New Zealand , NZ

<sup>(2)</sup>Department of Geodesy and Remote Sensing, Helmholtz Center Potsdam, GFZ German Research Center for Geosciences, Potsdam, DE

<sup>(3)</sup>ECCGS, L-7256 Walferdange, Luxembourg , LU

<sup>(4)</sup>Jet Propulsion Laboratory, California Institute of Technology, Pasadena, California, USA <sup>(5)</sup>E-GEOS, Italy , IT

### Abstract

We study coseismic and postseismic deformation associated with the September 2010 Darfield and February 2011 Christchurch earthquakes in New Zealand from combined interferometric synthetic aperture radar (InSAR) and global positioning system (GPS) data. High-quality campaign



and continuous GPS measurements and differential InSAR from C-band and L-band radar data are inverted jointly to derive a variable-slip source model for the 4 September, 2010 Darfield earthquake. We find that the coseismic geodetic data indicate a very complex source model. The main rupture, slipping by as much as 5 m between depths of 3 and 8 km, occurred on the previously unrecognized strike-slip Greendale Fault extending east-west for ~ 30 km across alluvial plains west of Christchurch. A number of other faults were also active during this event including a northeast-striking blind reverse fault near Charing Cross that initiated the rupture process, and another blind reverse fault west of the Greendale fault near Hororata. TerraSAR-X observations of postseismic deformation indicate various processes in the first two months after the Darfield earthquake including shallow deformation on the Charing Cross reverse fault and a small amount of afterslip on the Greendale Fault. For the 22 February 2011 Christchurch earthquake, which is a large and late aftershock of the Darfield event, we inverted GPS together with X-band InSAR from Cosmo-Skymed and L-band InSAR from ALOS to investigate its source parameters. We find that the deformation pattern observed can be well explained by a slip on a single planar fault running into Christchurch city with a peak slip of ~ 2.5 m occurring at a depth of ~ 5 km. We report on postseismic deformation following this event analyzed by the integration of TerraSAR-X and GPS measurements.

## Damage Proxy Map of the 2011 M6.3 Christchurch Earthquake using InSAR Coherence

### Author(s)

Sang-Ho Yun <sup>(1)</sup>, Eric Fielding <sup>(1)</sup>, Mark Simons <sup>(2)</sup>, Paul Rosen <sup>(1)</sup>, Susan Owen <sup>(1)</sup>, Frank Webb <sup>(1)</sup>

### Department

<sup>(1)</sup>Jet Propulsion Laboratory , USA

<sup>(2)</sup>California Institute of Technology , USA

### Abstract

The 2011 ML 6.3 Christchurch earthquake killed 181 people as of May 3, 2011 and its strong ground acceleration (with the highest recording of 2.2g) caused widespread damage in Christchurch, New Zealand's second-most populated city, and its eastern suburbs. Extensive liquefaction damage was reported with about 200,000 tons of silt coming out of the ground. Various degrees of building damage, from partial failure to complete collapse, were photographed and reported by the public media as well as by local residents through social networking websites and blogs. Several large rock falls and local landslides were also reported to have damaged houses under hills. When a major earthquake hits an area with significant human population, a critical component of the situational awareness for rescue operations and disaster size estimation is rapid, accurate, and comprehensive assessment of building damage. Spaceborne or airborne remote sensing techniques can be crucial for this purpose. At present, private companies and government agencies have been mostly interpreting manually high-resolution optical images acquired before and after the event to create damage assessment maps. Radar remote sensing has all-day and all-weather capability as opposed to optical remote sensing. However, its applicability to operational production of damage proxy maps has not been verified yet, partly because of its quality being sensitive to imaging conditions such as perpendicular and temporal baselines. InSAR coherence, a measure of similarity of two radar echoes, provides a quantitative measure of surface and subsurface scattering properties. Major damage to building structures significantly changes scattering properties, which are often detectable with InSAR coherence change. However, perpendicular baselines vary from one interferometric pair to another, and temporal decorrelation occurs everywhere at various rates. The doppler centroid changes at every data acquisition, and volume scattering causes different amount of decorrelation depending on perpendicular and temporal baselines. These factors challenge the ability to isolate coherence

change due to building collapse. Under the ARIA (Advanced Rapid Imaging and Analysis) project at JPL & Caltech, we developed an algorithm to produce comprehensive and reliable damage proxy maps of earthquakes using InSAR coherence despite the possible presence of other effects that cause coherence changes. We applied the algorithm to the 2011 Christchurch earthquake with ALOS PALSAR data and detected three different types of damage: liquefaction, building collapse, and landslide. The detected liquefaction damage is extensive in the eastern suburbs of Christchurch, showing Bexley as one of the most significantly affected areas as was reported in the media. Some places show sharp boundaries of liquefaction damage, indicating different type of ground materials that might have been formed by the meandering Avon River in the past. Well reported damaged buildings such as Christchurch Cathedral, Canterbury TV building, Pyne Gould building, and Cathedral of the Blessed Sacrament were detected by the algorithm. A landslide in Redcliffs was also clearly detected. The detected damage signals were verified by comparing it with optical images provided by Google Earth and anecdotal damage reports available on the Internet. We plan to compare it with more comprehensive ground truth data as they become available. Rapidly produced accurate damage assessment maps will help saving people, assisting effective prioritization of rescue operations at early stage of response, and significantly improve timely situational awareness for emergency management and national / international assessment and response for recovery planning. Results of this study will also inform the design of future InSAR missions including DESDynI.

## How sharp is our source image of the 2010 Haiti earthquake?

### Author(s)

Henriette Sudhaus <sup>(1)</sup>, Frank Krueger <sup>(2)</sup>, Thomas R. Walter <sup>(1)</sup>

### Department

<sup>(1)</sup>German Research Centre for Geosciences GFZ ,DE

<sup>(2)</sup>University of Potsdam , DE

### Abstract

The main source characteristics of the devastating M7.2 Haiti earthquake in 2010 have been reported in a number of recent studies. The data used by the earlier studies is dominated by similar combinations of surface displacement measurements, e.g. InSAR and GPS data. According to these analyses, a considerable part of the seismic energy radiated by the oblique left-lateral strike-slip earthquake was apparently not released on a segment of the Enriquillo-Plantain Garden Fault (EPGF), a major strike-slip fault crossing Hispaniola. Instead, a large portion of slip is thought to have occurred on a northward-dipping thrust fault located slightly north of the EPGF. Apart from these common characteristics, however, the Haiti earthquake source models differ widely. For instance, it remains unclear whether the earthquake ruptured multiple distinguishable fault segments, and whether these might have included a part of the EPGF. Furthermore, the modeled dip of the northward located thrust fault differs substantially, by tens of degrees, in the previous studies. The variety of source models points to significant uncertainties in the model parameters, but a rigorous estimation of these uncertainties is missing so far. Since regional hazard assessment depends heavily on establishing the statistically most likely source model, our new study of the 2010 Haiti earthquake aims to provide a more robust source model with quantified uncertainties. Similarly to the earlier Haiti source studies, we combined measurements of the surface displacement from coseismic interferograms of the ALOS satellite with coseismic GPS data, to which we added pixel offset measurements from TerraSAR-X data. This data assembly comprises surface displacement vectors of various directions and can therefore capture the three-dimensional surface displacement field to a better degree. Difficulties in the source modeling, however, arise from the absence of directly observed surface ruptures, and from the complexity of local fault systems that are only partly exposed on-land. Also, the 2010 rupture

apparently extends off-shore, such that large parts of co-seismically deformed surface are beyond reach of our geodetic measurement techniques. Due to this limited data coverage, we find that there is a strong model parameter trade-off between the fault dip and the displacement on the fault. Therefore, we aim to reduce the coupling between these model parameters in our optimization through a weighted combination of geodetic and seismic data. The seismic recordings of the Haiti earthquake are limited to far-field observations, but nevertheless provide important information on the main source characteristics. A meaningful data combination implies that we consider the seismic data errors and the errors of surface deformation measurements in the same fashion. This we achieve by weighting the data on the basis of empirically estimated data error covariances. In studies of either geodetic or seismic source modeling it has been shown that such weighting significantly improves the model parameter estimations, e.g. by reducing model parameter trade-offs. Accordingly, from a combined optimization of geodetic and seismic data, we expect to find a robust source model for the Haiti earthquake. These results may then help to better understand the processes at the Enriquillo-Plantain-Garden Fault zone and to evaluate the seismic hazard in the densely populated areas around the Haitian capital Port-au-Prince.

## Postseismic deformation following the 2010 Haiti earthquake: Time-dependent surface subsidence induced by groundwater flow in response to a sudden uplift

### Author(s)

Shimon Wdowinski <sup>(1)</sup>, Sang-Hoon Hong <sup>(2)</sup>

### Department

<sup>(1)</sup>University of Miami , USA

<sup>(2)</sup>Korea Aerospace Research Institute , KR

### Abstract

The 2010, M=7.0 Haiti earthquake was one of the worst natural disasters of the past century with more than 300,000 fatalities. The earthquake ruptured a 40 km long fault and had a seismic moment of  $5.44 \times 10^{26}$  dyne cm. A magnitude 7 earthquake typically displaces the Earth's crust by 3-5 meters and deforms the crust over a wide area along the fault. It can also induce large transient displacements, termed postseismic deformation. In this research project we used Synthetic Aperture Radar observations acquired by the German TerraSAR-X (TSX) and the Japanese ALOS satellites to detect postseismic deformation induced by the 2010 Haiti earthquake. The advantages of using TSX data are their very high spatial resolution (1-5 meters) and short repeat time (11 days). However, the satellite acquires data over a narrow swath (30 km) and its X-band signal (3 cm wavelength) degrades within short time, except over open areas. The ALOS satellite uses L-band (24 cm wavelength) radar, which maintains interferometric coherence over long time periods (months and years) even over vegetated areas. However the repeat orbit of ALOS is 46 days, which provides limited temporal resolution. We obtained 8 TSX and 5 ALOS scenes covering the eastern portion of the earthquake rupture area, from before and after the earthquake. Interferometric data processing, which compares phase observations between pairs of acquisitions, allows us to detect surface deformation induced by the earthquake. Our analysis shows an elongated patch of postseismic deformation at the northeastern extent of the Leogane delta. The deformation is time-dependent and occurred in the first 45 days after the earthquake. We suggest that the deformation occurred due to sediment compaction induced by groundwater withdrawal as the watertable adjusted to the hydraulic conditions imposed by the sudden uplift of the delta by ~80 cm with respect to unchanged sea level. Using an analytical model of aquifer discharge due to a sudden change in boundary head (Lockington, 1997), we calculated the

expected water table height changes and surface subsidence, which are time dependent. A comparison between the observed and modeled subsidence show a very good agreement when the model's hydraulic conductivity is in the range of 1000-2000 m/day and sediment compaction is 15-20%. The observed postseismic deformation following the 2010 Haiti earthquake is a new mode postseismic deformation, which we explain by sediment compaction induced groundwater withdrawal in response to the sudden uplift. Unlike the other three known postseismic deformation modes, afterslip, viscoelastic relaxation and poroelastic response, which occur within deeper crustal levels, the new mode occurs at a very shallow depth, within the first meter beneath the surface. Because postseismic deformation started right after the earthquake, coseismic interferograms spanning from before the earthquake till several days after the earthquake are contaminated by postseismic signal. Thus, the coseismic deformation of the 2010 Haiti earthquake has been under-estimated (up to ~10%) due to the unaccounted postseismic subsidence.

## Slip distribution and postseismic deformation of the April 14, 2010 Mw 6.9 Yushu (Qinghai, China) earthquake constrained using InSAR observations

### Author(s)

Jianbao Sun <sup>(1)</sup>, Zhengkang Shen <sup>(2)</sup>

### Department

<sup>(1)</sup>Institute of Geology, China Earthquake Admin. , CN

<sup>(2)</sup>Peking University , CN

### Abstract

A devastating Mw6.9 earthquake struck the Yushu area in the interior of the eastern Tibetan Plateau on April 14, 2010 and claimed more than 2500 human lives. We produce three coseismic interferograms using radar data from C-band and L-band satellites and identify three areas with concentrated deformation along the rupture. The easternmost one with the highest fringe rate lies around Yushu-Jiegu town where most casualties and damage occurred. By adopting a two-step Maximum-A Posterior (MAP) probability kinematic inversion method and using the fault surface traces obtained from field investigations to constrain the model, we obtain a preferred slip model composed of three segments. The eastern segment has slip near the surface with maximum left-lateral slip of up to ~1.72 m. The middle segment has a similar faulting style with its slip up to ~1.0 m at shallow depth but without reaching to the surface. The western segment is offset to the south on a parallel fault across a pull-apart basin, and has only small amounts of slip (< 0.6 m) reaching to the surface. Most of the slip occurred within 15 km depth, and is predominantly left-lateral. The total seismic moment release is estimated to be  $2.23 \times 10^{19}$  Nm, consistent with the seismic estimate of  $2.50 \times 10^{19}$  Nm. This earthquake attests to the active tectonic deformation process of the Xianshuihe- Ganzi-Yushu fault zone, which accommodates the eastward extrusion of the southeast domain of the Tibetan Plateau. Following the coseismic study, we collected two-path ALOS data covering the main portion of the coseismic rupture and detect the postseismic deformation activated by the strong coseismic stress changes using the SBAS time-series analysis techniques. We find very subtle postseismic signals up to max ~1-3 cm identified on the interferograms, which is comparable to the few available GPS measurements. We implement afterslip, pore-elastic and visco-elastic modeling (including Maxwell, SLS and Burgers body configurations) on the data using both BEM and FEM methods. The final results will be presented on the meeting.

# Transient slip on the Hayward fault from SBAS-InSAR and GPS

## Author(s)

Ingrid Johanson <sup>[1]</sup>, Coauthor: Roland Bürgmann <sup>[1]</sup>

## Department

<sup>[1]</sup>University of California, Berkeley, 215 McCone Hall, Berkeley, CA 94720, USA

## Abstract:

We present the results of our analysis of two decades of regional crustal deformation data in the San Francisco Bay region of California, USA, with a focus on providing a detailed investigation of slow slip events on the Hayward fault. Geodetic measurements provide information on the nature of strain accumulation and release on seismogenic faults, including locking depth and slip rates, and any variations of those parameters in space and time. This project incorporates time series processing of InSAR data spanning 18 years and three satellites, together with 17 years of GPS acquisitions processed in a consistent manner to form BAVU. BAVU is the primary source of central-California data used in ongoing compilations of California-wide velocity fields. The sparsely distributed, but continuously operating CGPS BARD and PBO networks provide a precise geodetic backbone with high temporal resolution into which we integrate campaign-mode measurements collected by our and other groups. The Small Baseline Subset (SBAS) approach is a method for extracting time series of range change at certain locations from a large set of InSAR data. The SBAS approach is well suited to revealing time varying deformation without a known functional form.

These data are used to investigate slow slip events (SSEs) on the Hayward fault. Alinement array measurements have shown that surface creep on the Hayward fault varies on both short (days to weeks) and long (decade) time scales. Here we single out a localized SSE in 1996 on the southern Hayward fault and a larger scale event in 2007 on the northern Hayward fault for targeted analysis. The spatial density of SBAS-InSAR gives us more information on the spatial extent of the SSEs, both along strike and with depth, while GPS data (particularly for 2007) provides improved temporal resolution. Our work so far shows that the 1996 event may have been very shallow, but that a post-2001 creep rate increase at the same location may have included more slip at 4-5 km depth than at the surface. However it is not yet clear how much vertical motion is affecting the InSAR measurements and that will need to be investigated. Our eventual goal is to put together a set of well-described slow-slip events, which will give us a better understanding of where and how much slow slip occurs on the Hayward fault and an idea of the types of events that may happen in the future. This will contribute to improved estimates of earthquake potential on San Francisco Bay Area faults.

# Coseismic Deformations of the 2011 Tohoku, Japan, Earthquake and triggered events derived from ALOS/PALSAR

## Author(s)

Manabu Hashimoto <sup>[1]</sup>, Yo Fukushima <sup>[1]</sup>, Youichiro Takada <sup>[1]</sup>

## Department

<sup>[1]</sup>Kyoto University, JP

## Abstract

The Tohoku earthquake of March 11, 2011, caused a remarkably large deformation over Honshu. Up to 3.5 m range increase at the tip of the Ojika peninsula, the closest point to the epicenter, were detected from the ascending orbits, which is consistent with displacements derived from continuous GPS. Combining descending interferograms, this peninsula was confirmed to have subsided and shifted eastward. Curiously, tidal records showed a long-term subsidence of the

Pacific coast of northern Honshu. These observations imply complicated recurrence of great and large interplate earthquakes. This large deformation induced activities of local earthquakes of which are of magnitude 6 or larger, and volcanic unrests. For example, a M6.7 event hit the northern Nagano Prefecture, central Japan, on March 12. On March 15, a M6.4 earthquake occurred in the vicinity of Mt. Fuji. On March 19, a M6.1 event occurred northern Ibaraki Prefecture, where no shallow seismicity had been reported before the March 11 mainshock. On April 11, a M7.0 event occurred in southern Fukushima Prefecture, near the March 19 event. It is highly important to reveal the associated deformation and their mechanism for the understanding of triggering process and forecast of activities. We carefully investigated interferograms of the pairs of ALOS/PALSAR images spanning the March 11 mainshock and found disturbances in fringes associated with the mainshock at several spots. The most prominent ones are the concentric fringes near the epicenters of the Fukushima event of April 11. More than 9 fringes showing range increase were found in the vicinity of the epicenter of the Fukushima event. This observation is consistent with normal faulting on faults, whose motion was previously not recognized.

## Wide area deformation map generation with TERRASAR-X data. the Tohoku-Oki earthquake 2011 case.

### Author(s)

Nestor Yague-Martinez <sup>(1)</sup>, Christian Minet <sup>(1)</sup>, Michael Eineder <sup>(1)</sup>,  
Birgit Schaettler <sup>(1)</sup>

Department

<sup>(1)</sup>DLR, DE

### Abstract

The German TerraSAR-X satellite, launched in 2007, acquires high resolution SAR data at X-band. Every scene acquired in Stripmap mode covers an area of ca. 30 km x 50 km, which is too small to study wide area deformation phenomena. In this paper the authors propose a way to overcome the limitation of the TerraSAR-X image dimensions by acquiring data spread over the whole area of interest. Cross-correlation technique is applied. The Tohoku-Oki earthquake has been taken as case study. Japan was struck by a M9.0 undersea megathrust earthquake on the 11th of March 2011, with its epicenter situated approximately 72 km east of the Oshika Peninsula of Tohoku and the hypocenter at a depth of ca. 32 km. It was the most powerful known earthquake to have hit Japan. The whole archipelago has been affected, according to GPS measurements. Such a large geophysical event could not even be covered in ScanSAR acquisition mode, therefore an alternative approach is necessary. A total of ten interferometric co-seismic pairs in Stripmap mode have been acquired distributed over the Japanese archipelago with different geometries. Cross-correlation technique is used to derive absolute displacements in slant-range and azimuth directions for each scene. A quality assessment of the displacement maps has to be performed carefully due to the quite large time span between pre- and post-seismic acquisitions (ranging 2 to 6 months). The displacement maps are also corrected for solid earth tides and atmospheric path delays.

# The March 11, 2011, Tohoku-oki earthquake (Japan): surface displacement and source modeling

## Author(s)

Salvatore Stramondo <sup>(1)</sup>, Christian Bignami <sup>(1)</sup>, Sven Borgstrom <sup>(1)</sup>, Marco Chini <sup>(1)</sup>, Francesco Guglielmino <sup>(1)</sup>, Daniele Melini <sup>(1)</sup>, Giuseppe Puglisi <sup>(1)</sup>, Valeria Siniscalchi <sup>(1)</sup>

## Department

<sup>(1)</sup>Istituto nazionale di Geofisica e Vulcanologia - INGV , IT

## Abstract

We have studied the disastrous earthquake (M 9.0) occurred on March 11th, 2011 (at 05:46:23 UTC) offshore the coast of Honshu island (Japan). It has been generated along the subduction plate boundary between the Pacific and the North America plates. The earthquake was followed by a tsunami of rare destructive power that caused most of damages along the coastline of most of Honshu island. The epicenter has been located at about 130 km East of Sendai city at a depth of about 32 km. The location, the geometric parameters, the focal mechanism, all these data are in agreement with the occurrence of the seism along the subduction plate boundary. The mainshock ruptured about 300 km x 150 km along the fault plane, with a maximum slip estimated up to 30-40 m. Soon after the seism some of the most important Space Agencies have made available their data all over the epicentral region. JAXA (Japanese Space Agency), ESA (European Space Agency), DLR (German Space Agency), NASA (National AeroSpace Agency) and CNES (French Space Agency) provided a large number of SAR and Optical data, each one applying its own data policies. We have processed a dataset composed of 27 Envisat IS6 frames along three adjacent tracks and a set of ALOS PALSAR FBS (Fine Beam Single pol.) and FBD (Fine Beam Dual pol.) along ascending and descending paths. We have applied the Differential SAR Interferometry (DInSAR) technique to such data, elaborating each strip as a single frame. The resulting interferograms have been unwrapped over each track. We then measured a maximum displacement of about 2.5 m along the Envisat IS6 LOS. We have parallelly applied the same approach to the ALOS PALSAR dataset. To obtain the displacement along North, East and Up directions, we have applied the SISTEM approach that simultaneously integrate DInSAR and GPS vectors. Finally we used the output from SISTEM for the inversion of seismic moment release. In this occasion, ESA made available also data from the ERS2 satellite, previously moved on a new three days revisiting time orbit, providing also precise orbit files based on Laser Range data with only two days delay. The optimal ERS2 orbital control allowed getting very short baseline values as well. This three days revisiting time means a chance to get an almost continuous monitoring system, with data and orbit files dissemination policy allowing a near-real-time data processing, besides the possibility to extract just the coseismic deformation field with the postseismic deformation filtered out, unlike other spaceborne sensors with long revisiting times. The choice of the ERS2 processed interferograms, has been done based on the occurrence of some strong aftershocks (April 7th, M7.4 and May 5th, M6.3) after the mainshock of March 11st.

# The Tohoku-oki (Japan) Earthquake imaged through 3-days repeat cycle ERS-2 SAR data

## Author(s)

Michele Manunta <sup>(1)</sup>, Francesco Casu <sup>(1)</sup>, Luca Paglia <sup>(1)</sup>, Riccardo Lanari <sup>(1)</sup>

## Department

<sup>(1)</sup>IREA-CNR Via Diocleziano, 328, 80124, Napoli, IT

## Abstract

Differential SAR Interferometry (DInSAR) has demonstrated to be an effective technique for studying and monitoring deformation phenomena affecting Earth's surface. In particular, the DInSAR technique has been successfully applied for analyzing the displacements due to natural and anthropic hazards, such as volcanic and earthquake events, subsidence, landslides, and urban consolidation. In this context, ERS-1/2 and ENVISAT SAR satellites have played a key role in DInSAR development thanks to the huge archive availability and to relatively easy access to the data. Indeed, this has significantly contributed to build up several advanced DInSAR techniques that effectively exploit this large amount of SAR data for the generation of deformation maps and time-series. Among these techniques, the advanced DInSAR approach, referred to as Small Baseline Subset (SBAS) algorithm (Berardino et al., 2002), has been successfully applied to several volcanic (Solaro et al., 2010) and seismic events (Lanari et al., 2010) and has demonstrated its capability to precisely detect and monitor these deformation phenomena. The SBAS-DInSAR algorithm relies on the combination of DInSAR data pairs, characterized by a small separation between the acquisition orbits (baseline), in order to produce mean deformation velocity maps and the corresponding time-series, maximizing the coherent pixel density of the investigated area. Moreover, the SBAS-DInSAR algorithm allows investigating very large scale deformation phenomena, such as tectonic movements and seismic events, with a spatial resolution of about 100 m by 100 m. In this work, we use the SBAS-DInSAR approach to study the post-seismic displacements occurred in Tōhoku-oki (Japan) area, interested by a 9.0 magnitude earthquake on 11 March 2011. This earthquake was one of the largest measured in the 20th century and caused a large tsunami that struck the Japanese coast. Because of its importance, Tōhoku-oki area has been also included in the GEO Geohazard Supersites. Accordingly, we exploit the new 3-days repeat cycle ERS-2 data acquired on that area since March 2011, in order to generate post-seismic deformation time-series through the SBAS-DInSAR approach. Since launch back in 1995, ERS-2 has been operated in a 35-days repeat cycle called 'multi-disciplinary' mission phase with the same ground track as ENVISAT IS2 until the orbital change in October 2010. For the few remaining months of ERS-2 activity, ESA wanted to focus on achieving the maximum scientific benefits and ERS-2 has been moved to a 3-days repeat cycle to reproduce the ERS-1 Ice Phases of 1992 and 1994. The new ERS-2 acquisition mode is aimed for studying ice-stream dynamics, glaciers, geo-hazard (post-seismic deformation, fault creep, volcanic deformation), fast-moving landslides. In this work we show that a very short revisit time C-band SAR dataset allows us to significantly improve not only the temporal sampling of the investigated deformation phenomena, but also the coherent pixel density. Indeed, the 3-days configuration permits the generation of very small temporal baseline interferograms that are strongly less affected by temporal decorrelation with respect to the 35-days standard ERS-2 mission data. Nevertheless the ERS-2 3-days mission has been conceived for ice sheet monitoring, this work demonstrates that the availability of SAR scenes acquired with a very short revisit time is strategic also in land applications for investigating fast deformation phenomena. Finally, this experiment represents a good simulation of the forthcoming Sentinel SAR mission, characterized, in the final configuration, by a constellation of 2 C-band satellites able to acquire the same area



with a 6-days revisit time. References Berardino, P., G. Fornaro, R. Lanari, and E. Sansosti, "A new Algorithm for Surface Deformation Monitoring based on Small Baseline Differential SAR Interferograms", *IEEE Trans. Geosci. Remote Sens.*, Vol. 40, No 11, pp. 2375-2383, 2002. Lanari R., Berardino P., Bonano M., Casu F., Manconi A., Manunta M., Manzo M., Pepe A., Pepe S., Sansosti E., Solaro G., Tizzani P., and . Zeni G, "Surface displacements associated with the L'Aquila 2009 Mw 6.3 earthquake (central Italy): New evidence from SBAS-DInSAR time series analysis", *Geophysical Research Letters*, Vol. 37, L20309, doi:10.1029/2010GL044780, 2010. Solaro, G., V. Acocella, S. Pepe, J. Ruch, M. Neri, and E. Sansosti, "Anatomy of an unstable volcano from InSAR: Multiple processes affecting flank instability at Mt. Etna, 1994–2008", *J. Geophys. Res.*, 115, B10405, doi:10.1029/2009JB000820, October 2010.



# Session: Terrain Subs. & Landslides

## Surface deformation of the whole Netherlands after PSI analysis

### Author(s)

Miguel Caro Cuenca <sup>(1)</sup>, Ramon Hanssen <sup>(1)</sup>, Mahmut Arikan <sup>(1)</sup>, Andy Hooper <sup>(1)</sup>

### Department

<sup>(1)</sup>Delft University of Technology , NL

### Abstract

The Netherlands is a coastal country with very low topography, 60% of the territory is below mean sea level. Flooding risks are therefore a major concern. Hence, monitoring surface deformation is highly required. Surface displacement are measured by Dutch authorities mainly through leveling, with the intrinsic limitation of being spatially sparse and having a low temporal resolution. Other techniques have also been applied in the Netherlands to study land deformation, in particular, Persistent Scatterer InSAR (PSI) because it provides an unmatched density of observations with large coverage (100 x 100 km<sup>2</sup>) and high measurement frequency (usually 1 observation~ every 35 days) . PSI has been successfully applied in the Netherlands to measure land deformation caused by, e.g., gas production, water extraction and poroelastic rebound in abandoned coal mines. Until now InSAR coverage, although extensive, has been limited to the nominal image size (100 x 100 km<sup>2</sup>). Better comprehension of the deformation phenomena can be achieved by studying a wider area. In this contribution, we employ PSI to produce rate estimates over the whole Netherlands, covering a total area of 200 x 350 km<sup>2</sup>. The radar images used in this study were acquired by the European Satellites ERS1/2 and Envisat. The radar data covers the time range from April 1992 to January 2001, and from November 2003 to September 2010, for ERS1/2 and Envisat, respectively. We produce two rate maps of the Netherlands corresponding to each satellite period. To do so, we employ an image length larger than the nominal one. With this scene type, the images, which are provided by ESA, are in RAW format and therefore require to be focused. We process in total 8 descending tracks (3 Envisat and 5 ERS1/2), which include 599 images. Each track has a width of 100 km and a length that changes from 100 to 350 km to cover accordingly the whole Dutch territory. The final number of observations that are detected by PSI to be reliable (persistent scatters) is around 2 millions. The tracks are processed independently. We initially produce 8 different rate maps (one per track), that need to be combined. In this process the fact that , PSI estimates are not absolute but relative to a PS (or area) selected as reference, must be taken into account. Furthermore, GPS data are also added in the integration to be able estimate spurious longwavelength signals (such as orbital errors) that usually affect InSAR data and separate these from large scale deformation. To integrate multi-track PSI rate maps and GPS velocities, we propose a least square approach where longwavelength deformation is constrained with GPS data. The GPS velocities are obtained by 8 permanent stations that belong to the EUREF network. This work is performed in the framework of Subcoast, where different European research institutes join efforts to provide a service for coastal management, deformation studies, and flood risk predictions.

# Subsidence mapping in Jakarta - PSI processing of L-band ALOS PALSAR data

## Author(s)

Rachel Holley <sup>(1)</sup>, Richard Burren <sup>(1)</sup>

Department

<sup>(1)</sup>Fugro NPA Ltd. , UK

## Abstract

Jakarta is a heavily populated city, which has been experiencing ongoing ground subsidence for several decades, due to heavy use of groundwater, soil characteristics and tectonic motion. It is expected that this ground motion will increasingly impact upon flood risk management and ongoing development of the city, in particular critical infrastructure. InSAR measurement has the potential to enhance the information available from conventional surveying techniques, increasing spatial and temporal coverage at low cost, with potential for both historical information and ongoing monitoring. Persistent Scatterer Interferometry (PSI) is an ideal technique for deriving accurate and detailed historical motion studies over urban areas. The available archive of C-band data is rather limited over Jakarta, with a maximum stack of 10 suitable ERS images available between 1996-1998, and 8 Envisat from 2007-2009. This restricts both temporal coverage and processing options, since neither archive contains enough SAR images for persistent scatterer processing. This work instead applied PSI processing to a stack of 18 archived L-band images from the PALSAR (Phased Array type L-band Synthetic Aperture Radar) instrument aboard JAXA's ALOS (Advanced Land Observing Satellite) platform. To enable use of a sufficient number of SAR images, a combination of single- and dual-polarisation images have been used. The HH component of the dual-polarisation images is interferometrically compatible with the HH single-polarisation images, but requires over-sampling prior to InSAR processing. PSI processing produced a high point density across the urban area of Jakarta, and retained sufficient points across the majority of surrounding rural areas for patterns of deformation to be examined. Eighteen images would normally be considered toward the smaller end of suitable stack sizes for PSI, particularly in areas with high potential for atmospheric artefacts from strong topographic contrasts. This prevented robust analysis in the mountainous terrain south of the city, but the urban area has low relief and residual atmospheric influence appears minimal. Residual orbital gradients must also be considered when utilising relatively small data stacks, particularly since the presence of relatively wide areas of deformation have the potential to bias empirical orbital corrections. The PSI results show a variety of subsidence features across the city at various spatial scales, with some areas experiencing average annual velocities of up to ~180 mm/yr. The available archives of ERS and Envisat SAR data were processed using DifSAR, to provide a cross-comparison and to place the results in a longer temporal context. Comparisons with Envisat and ERS DifSAR interferograms show a promising agreement in both the spatial distribution and magnitude of deformation within the city. Results are also compared with existing GPS measurements from the city. Accumulation of sufficient numbers of images to form a suitable stack has only recently made ALOS PSI feasible. The Jakarta results are therefore a promising demonstration of the capabilities of this approach.

# Satellite SAR interferometry for the measurement of surface subsidence above deep tunnels in metamorphic basement rocks of the Alps

## Author(s)

Tazio Strozzi <sup>(1)</sup>, Reynald Delaloye <sup>(2)</sup>, Andrew Kos <sup>(3)</sup>, Jürgen Hansmann <sup>(3)</sup>, Simon Loew <sup>(3)</sup>, Hugo Raetzo <sup>(4)</sup>, Urs Wegmüller <sup>(1)</sup>

## Department

<sup>(1)</sup>Gamma Remote Sensing -, CH

<sup>(2)</sup>University of Fribourg -, CH

<sup>(3)</sup>Engineering Geology - ETH Zürich -, CH

<sup>(4)</sup>Federal Office for the Environment -, CH

## Abstract

Surface subsidence related to fluid extraction, mining, or tunnel drainage is commonly experienced in loosely consolidated sediments or high porosity rocks. However, the development of surface settlements above low-porosity, fractured rock is less recognized, even though large reductions in pore pressure can occur when driving a deep tunnel. In Switzerland, examples were reported in the cases of the driving of an investigation adit 1.5 km away of the Zeuzier arch dam (Lombardi, 1988), of the construction of the Gotthard highway tunnel (Zangerl et al., 2008a, 2008b), and of the excavation of the Gotthard Basetunnel (Löw et al., 2007). Although settlements of a few centimetres appear to be small compared to those associated with ground water or oil and gas withdrawal from more compliant porous media, they are large enough to adversely affect the structural integrity of sensitive concrete structures on the surface like thin arch dams. With ERS SAR interferometry we were able to detect the surface subsidence associated with the construction of a headrace tunnel for a hydroelectric scheme in the Swiss Alps (Strozzi et al., 2011). In two areas located at more than 2000 m above sea level maximum displacements of about 4 cm between 1995 and 1997 have been observed above the tunnel. Large-scale consolidation associated with pore-pressure reduction in the rock mass arising from tunnel drainage at about 200–400 m depth beneath the topographical surface is believed to be the contributing mechanism. Evidence for this process is based on pore pressure recordings in nearby deep wells. In both areas, the subsidence was followed by a small uplift of about one centimeter between 1997 and 1999, after the tunnel was cased with permeable concrete segments. This partial recovery is also visible in pore pressure records and relates to the elastic components of rock mass deformation. Our observations above the headrace tunnel indicate that the spatial and temporal evolution of surface subsidence associated with tunnel drainage induced pore pressure changes in metamorphic rock masses can be successfully surveyed with satellite SAR interferometry in alpine regions above the tree line, i.e. where only small vegetation is present. Current investigations are concentrated at the detection of transient surface settlements above the Gotthard Basetunnel with ENVISAT ASAR, ALOS PALSAR and TerraSAR-X interferometry.

Lombardi, G. (1988). Les tassements exceptionnels au barrage de Zeuzier. Publication de la Société Suisse de Mécanique des Sols et des Roches, 118, 39–47. Löw, S., Ebnetter, F., Bremen, R., Herfort, M., Lützenkirchen, V., & Matousek, F. (2007). Annual opening and closure of Alpine valleys. Felsbau – Rock and Soil Engineering, 25, 6. Strozzi, T., Delaloye, R., Poffet, D., Hansmann, J., & Loew S. (2011). Surface subsidence and uplift above a headrace tunnel in metamorphic basement rocks of the Swiss Alps as detected by satellite SAR interferometry. Remote Sensing of Environment, 115(6), 1353-1360. Zangerl, C., Eberhardt, E., Evans, K., & Loew, S. (2008a). Consolidation settlements above deep tunnels in fractured crystalline rock: Part 2 – Numerical analysis of the Gotthard highway tunnel case study. International Journal of Rock Mechanics and

Mining Sciences, 45, 1211–1225. Zangerl, C., Evans, K., Eberhardt, E., & Loew, S. (2008b). Consolidation settlements above deep tunnels in fractured crystalline rock: Part 1 – Investigations above the Gotthard highway tunnel. *International Journal of Rock Mechanics and Mining Sciences*, 45, 1195–1210.

## DORIS FP7-EU project: exploitation of 20 years DInSAR data archive for landslide monitoring

### Author(s)

Michele Manunta <sup>(1)</sup>, Fabiana Calò <sup>(1)</sup>, Luca Paglia <sup>(1)</sup>, Manuela Bonano <sup>(1)</sup>, Riccardo Lanari <sup>(1)</sup>

### Department

<sup>(1)</sup>IREA-CNR Via Diocleziano, 328, 80124, Napoli, IT

### Abstract

Differential Synthetic Aperture Radar Interferometry (DInSAR) techniques have opened new perspectives in the field of Earth Sciences and in particular of environmental hazards, greatly contributing to the assessment and mitigation of the associated risks. However, while these interferometric techniques have been extensively applied to volcanology and earthquake studies, a few DInSAR studies concern with landslide applications. The advanced DInSAR technique referred to as Small BAseline Subset (SBAS) algorithm (Berardino et al., 2002) is able to carry out a multi-scale and multi-sensor analysis of surface deformation, providing more insights on the spatial and temporal pattern of the phenomena under investigation. The SBAS approach, in fact, allows analyzing mass movements at two spatial scales, i.e. at regional and local scale (Lanari et al., 2004). In particular, at regional scale, the SBAS technique exploits average (multi-look) interferograms to produce mean deformation maps of wide areas (about 100 km x 100 km) at low spatial resolution (about 100 m x 100 m), while at local scale it focuses on single-look interferograms for generating full spatial resolution products (about 5 m x 20 m). At both scales, time-series showing the temporal behaviour of the analyzed deformation phenomena are produced. Furthermore, the SBAS technique allows a multi-sensor processing of SAR data collected by different radar systems acquiring with the same illumination geometry (ERS-1/2 and ENVISAT satellites) (Pepe et al., 2005). The key point is to consider the images acquired by the ERS and ENVISAT sensors as belonging to independent subsets; accordingly, no ERS/ENVISAT cross-interferograms, characterized by heavy decorrelation effects due to slightly different carrier frequencies of the two radar systems, are generated and the integration of ERS/ERS and ENVISAT/ENVISAT interferograms is effectively performed by applying the conventional SBAS strategy without major changes. The multi-sensor SBAS approach has been extended to the full spatial resolution scale, in order to produce deformation time-series from large archives of full resolution ERS-1/2 and ENVISAT SAR data (Bonano et al., 2011). In particular, the doppler centroid variations of the post-2000 ERS-2 acquisitions and the carrier frequency difference between the ERS-1/2 and the ENVISAT systems have been exploited, thus maximizing the number of investigated SAR pixels, identifying also those exhibiting a response significantly deviating from a single scatterer backscattering, and improving their geocoding as well. In this work, developed within the framework of the DORIS FP7-EU project, we apply such a comprehensive SBAS approach for investigating slope instability phenomena in Umbria region (Central Italy) during the last 20 years; in particular, we exploit both descending and ascending ERS-1/2 and ENVISAT SAR data spanning the 1992-2010 time interval. The presented results highlight the high potentialities of such integrated interferometric analysis in landslide studies, since their capability to provide valuable long-term monitoring dataset of displacement measurements, thus significantly contributing to the interpretation of landslide mechanisms as well as to the understanding of their kinematics. References Berardino, P., Fornaro, G., Lanari, R.,

Sansosti, E., 2002, A new Algorithm for Surface Deformation Monitoring based on Small Baseline Differential SAR Interferograms, IEEE Trans. Geo. Rem. Sens., 40 (11), 2375-2383. Bonano, M., Manunta M., Marsella M., Lanari R., 2011, Long Term ERS/ENVISAT Deformation Time-Series Generation at Full Spatial Resolution via the Extended SBAS Technique, Int. J. of Remote Sensing, in press. Lanari, R., Mora, O., Manunta, M., Mallorqui, J.J., Berardino, P. and Sansosti, E., 2004, A small baseline approach for investigating deformations on full resolution differential SAR interferograms, IEEE Trans. Geo. Rem. Sens., 42, 1377-1386. Pepe, A., Sansosti, E., Berardino, P. and Lanari, R., 2005, On the Generation of ERS/ENVISAT DInSAR Time-Series Via the SBAS Technique, IEEE Geo. Rem. Sens. Letters, 2(3), 265-269.

## TSX InSAR assessment for slope instabilities monitoring in Alpine periglacial environment (Western Swiss Alps, Switzerland)

### Author(s)

Chloé Barboux <sup>(1)</sup>, Reynald Delaloye <sup>(1)</sup>, Tazio Strozzi <sup>(2)</sup>, Claude Collet <sup>(1)</sup>, Hugo Raetzo <sup>(3)</sup>

### Department

<sup>(1)</sup>University of Fribourg Ch. du musée 4 CH-1700 Fribourg, CH

<sup>(2)</sup>Gamma Remote Sensing Worbstrasse 225, CH-3073 Gümligen, CH

<sup>(3)</sup>Swiss Federal Office for the Environment Worblentalstrasse 68, CH-3063 Ittigen, CH

### Abstract

The topography of the Western Swiss Alps, mainly consisting of north-south oriented valleys has proved to be optimal for an application of the InSAR technique. Since 2005 several inventories of InSAR detected slope instabilities have been compiled at a regional scale in this test region [1,2,3] using a large set of ERS-1/2 data (archive data from 1991 to 2000). Velocities of the detected landforms range from a few centimetres to several meters per year. In particular, fast moving slopes were detected thanks to 3 days repeat cycle of ERS-1 in 1991 and to the 1 day repeat cycle of ERS-1/2 Tandem data in 1995-1999. The main objective now is to update inventories with actual data.

The use of InSAR, especially ERS-1/2 InSAR, to estimate magnitude and spatial pattern of slope motion has been evaluated and shows the efficiency of this remote sensing for inventorying creeping landforms in mountain periglacial environment, but also estimating and categorizing their displacement velocities [4,5]. However, since the extinction of ERS-1/2 tandem, the higher deformation rate of rapidly moving rockglaciers (>1 m/y) can no longer be detected or surveyed correctly on C-band and L-band monthly SAR interferograms [3,4]. Thus, the aim target of this study is to investigate the potential of TSX InSAR allowing to acquire high resolution X-band interferograms with 11 days time interval for slope motion monitoring at local scale, and to use these data for further investigations at a regional scale.

We are currently surveying about 30 landforms annually or seasonally in the Western Swiss Alps by GPS field measurements since 2001 for the longest series. In order to give a reliable assessment of InSAR visibility for slope motion monitoring, an index of visibility RdHS characterizing the velocity compression for each landform is calculated. Under the hypothesis that the landform flow is directed toward the highest slope direction at 25m scale resolution, RdHS is defined as the dot product between the unit vector in the maximum slope direction and the unit vector in the LOS direction. Then the maximal observable velocity Vmax of each landform could be easily calculated, compared and validated by combining InSAR observations and differential GPS measurements. The influence of the incidence angle of TSX (full capacity between 20° to 55°) is investigated for each landform.

For most of the west-oriented landforms, first results show that Vmax can reach 1 m/y in descending mode, and 3.5 m/y in ascending mode. In ascending mode the incidence angle has

generally few influences on Vmax which can reach even so 7 to 8 m/y for some of these landforms. However, due to high topography, large layover and distortions could occur on landforms for this mode. In the descending mode, the incidence angle has usually no influence on Vmax. The reverse phenomenon appears for east-oriented landforms and Vmax usually reaches about 1 m/y in both ascending and descending modes for north-oriented slopes.

As a conclusion, it seems to be possible to monitor some very active rockglaciers (1-2.5m/y) when layover or distortions does not hide them. Higher rate velocities appear decorrelated in most of the cases. Moreover the high resolution of TSX looks suitable to monitor small slope instabilities (average of the studied landforms 14 ha). Lower velocity rates could be still well monitored. Finally by observing fringes on interferograms for some active landforms we can notice that it is possible to identify fluctuations on 11 days repeat cycle, which is not the case with differential GPS measurement. Thus, even if field measurements are still in most of the case needed to validate and confirm observations at local scale, TSX InSAR appears to be an efficient remote sensing method for creeping landforms monitoring of the alpine periglacial belt.

TERRASAR-X data courtesy LAN0411 (c) DLR, DHM25 (c) 2003 swisstopo

#### References :

- (1) Reynald Delaloye, Christophe Lambiel, Ralph Lugon, Hugo Raetzo, Tazio Strozzi. "ERS InSAR for detecting slope movement in a periglacial mountain environment (western Valais Alps, Switzerland)". High Mountain Remote Sensing and Cartography IX, Graz, 14-15 Sept. 2006
- (2) Reynald Delaloye, Tazio Strozzi, Christophe Lambiel, Eric Perruchoud, Hugo Raetzo. "Landslide-like development of rockglaciers detected with ERS1-2 SAR interferometry". Proceedings of FRINGE 2007 Workshop, Frascati, Italy, 26 – 30 November 2007 (ESA SP-649, February 2008)
- (3) Delaloye R., Strozzi T., Lambiel C., Barboux C., Mari S., Stocker A., Techel F., Raetzo H. 2010 : The contribution of InSAR Data to the early detection of potentially hazardous active rock glaciers in mountain areas. Proceedings ESA Living Planet Symposium, Bergen, Norway, June28 – July2, 2010 (ESA SP-686, December 2010)
- (4) Christophe Lambiel, Reynald Delaloye, Tazio Strozzi, Ralph Lugon, Hugo Raetzo. "ERS InSAR for Assessing Rock Glacier Activity" Proceedings of the 9th International Conference on Permafrost, Fairbanks, Alaska, USA, June 29 - July 3, 2008
- (5) Reynald Delaloye, Christophe Lambiel, Ralph Lugon, Hugo Raetzo, Tazio Strozzi. "Typical ERS InSAR signature of slope movements in a periglacial mountain environment (Swiss Alps)". Proceedings of the Envisat Symposium, Montreux, Switzerland, 23-27 April 2007

## Long term analysis of strong non linear deformations induced by coal mining using the SBAS technique

#### Author(s)

Kanika Goel <sup>(1)</sup>, Nico Adam <sup>(1)</sup>, Christian Minet <sup>(1)</sup>

#### Department

<sup>(1)</sup>Remote Sensing Technology Institute (IMF), German Aerospace Center (DLR), DE

#### Abstract

This paper demonstrates the application of differential interferometric SAR (D-InSAR) for monitoring strong non-linear subsidence induced by coal mining. We present eleven years (1993-2004) of deformation estimation results for Gardanne coal mine in France exploiting SAR data acquired by ERS-1 and ERS-2 satellites. The mine is located in southern France between Aix-en-Provence and Marseille. The mining started in the 17th century and went on till 2003. Due to the continuous mining, this region experienced strong non-linear subsidence ranging from zero (in stable areas) to a few centimetres per year. During the considered time period, the mining was based on the long wall technique which resulted in a faster and larger deformation as compared to the chamber and pillar techniques used previously in this area. Monitoring the subsidence



induced by mining is important for geological and hazard analysis and D-InSAR has been used for mapping Earth's surface displacement time series using advanced techniques such as Persistent Scatterer Interferometry (PSI) and Small Baseline Subset Algorithm (SBAS). Gardanne coal mine represents a difficult test case for deformation monitoring using the C-band ERS sensors with 5.6 cm wavelength, a revisit time of 35 days and a maximum detectable deformation rate of 14.6 cm/year in radar's line-of-sight (LOS). Reasons include the strong non-linear motion occurring in the region, low density of point scatterers (PSs) present in this rural area and difficult to compensate atmospheric effects. C-band PSI is difficult to implement as many points experienced fast subsidence in the considered time period with sudden non-linear movements and it is difficult to fit a model to the actual deformations. This has been demonstrated in the study conducted by the European Space Agency (ESA) for PSIC4 (PSI Codes Cross-Comparison and Certification for Long-Term Differential Interferometry) project. In fact, Gardanne coal mine is an application test case for the SBAS technique which makes use of small baseline differential interferogram subsets. Using this approach, non-linear deformation can be estimated without any modelling and prior knowledge even in non-urban areas where point scatterer (PS) density is low and temporal decorrelation is faster. We used 72 ERS images from 1993-2004 and generated 165 interferograms based on spatial baseline threshold of 150 m and maximum temporal baseline of 700 days for the SBAS processing. We present the deformation results obtained using SBAS for Gardanne coal mine. Validation of the processing is performed with levelling data used in the PSIC4 project. The estimated deformation consists of two subsidence bowls, one covering a larger area and having a larger subsidence. The cumulative deformation is largest in the center of the bowls and gradually decreases as we go away from the center. Most of the subsidence occurs in the beginning of the considered time period and the area becomes stable gradually. A maximum of 273.5 millimeters of cumulative deformation over the eleven years has been measured at the center of the bigger subsidence bowl. We report on precision of our results and show visualizations of the geocoded deformation time series in Google Earth. The results illustrate that SBAS is well suited for monitoring mining induced strong non-linear deformations and similar applications as compared to PSI.

## Quantification of subsidence rates associated with groundwater flow using SAR interferometry

### Author(s)

Joao Catalao <sup>(1)</sup>, Giovanni Nico <sup>(2)</sup>, Vasco Conde <sup>(1)</sup>, Miguel Miranda <sup>(1)</sup>

### Department

<sup>(1)</sup>IDL, University of Lisbon, PT

<sup>(2)</sup>Consiglio Nazionale delle Ricerche, Istituto per le Applicazioni del Calcolo Bari, IT

### Abstract

In the scope of Terrafirma experiment significant ground subsidence was detected north of Lisbon area. This was interpreted as the result of neotectonic activity and generated a major concern. In this work we processed a long time series of SAR interferograms, minimizing atmospheric artefacts in each interferogram of the time series using the available measurements of atmospheric delay at the permanent GPS stations installed in the Lisbon area at the time of SAR acquisition and the results of a Numerical Weather Model ran to compute the temporal changes of the water vapour spatial distribution. The aim of this work is to quantify as best as possible the magnitude of the subsidence rates, and to study its source. We claim that there is a relationship between ground subsidence and regional groundwater flow regime, possibly induced by the construction of the subway infrastructures, and the urban development around it. A time series of 46 ERS SAR images, acquired between May 1995 and January 2001, and 20 ENVISAT ASAR images, acquired between September 2008 and September 2010 were interferometrically

processed using the Persistent Scatterers (PS) technique. Terrain deformation velocities were estimated at the location of the permanent scatterers. The first data set shows a quadrangular area where there is subsidence, with a maximum subsidence rate of about -4.8 mm/year. In the second period there is no evidence of ground deformation in the same area. Furthermore a topographic survey was carried out in 2010, in the urban area interested by the subsidence phenomenon, and compared with previous levelling measurements made at different times, 1976 and 1996. As a first result, levelling measurements confirmed both the location of the subsidence area and the amplitude of ground deformation velocity estimated by our InSAR analysis. As far as the temporal evolution of the phenomenon is concerned, we found that the ground deformation occurred mainly in the period 1996-2010 since the differences from the 1976 levelling are on the same order of that from the 1996 levelling. The time occurrence of this phenomenon seems to indicate that it could be related to the construction of the subway whose operations were carried between 1988 and 2002. The subway lines were built across the subsiding area and could be interfered with the piezometric level that in this area is only 6 m depth. To confirm the hypothesis that operations related to the construction of the subway caused the observed subsidence phenomenon, we correlated the piezometric measurements to the volumetric distribution of geology in the area interested by the subsidence and around it. The idea is to understand if the available piezometric measurements in the area are consistent with the scenario of a change in the groundwater flow and drainage gradients caused by a change in the stress state and porewater stress distribution. If confirmed, this scenario could explain the terrain subsidence measured by SAR interferometry. This would open new perspective and give the possibility to quantitatively compare the terrain subsidence measured by SAR interferometry to that obtained by a numerical model of underground water circulation ran using the piezometric measurements and volumetric distribution of geological properties as constraints.

# Session: Methods – Unwrapping

## New improvements of the EMCF phase unwrapping algorithm for surface deformation analysis at full spatial resolution scale

Author(s)

Antonio Pepe <sup>(1)</sup>

Department

<sup>(1)</sup>IREA-CNR, IT

### Abstract

Pepe A 1, Manunta M 1, Euillades L 2, Paglia L 1, Yang Y 1,3 and Lanari R 1 [1] Istituto per il Rilevamento Elettromagnetico dell'Ambiente, CNR, 328 Diocleziano, I-80124 Napoli, Italy; e-mail:{pepe.a, manunta.m, paglia.l, yang.y,manunta.m,lanari.r@irea.cnr.it} [2] Instituto de Capacitación Especial y Desarrollo de la Ingeniería Asistida por Computadora, Universidad Nacional de Cuyo, 5500 Mendoza, Argentina {leuillades@cediac.uncu.edu.ar} [3] National University of Defense Technology, P.R. China ABSTRACT We present a new space-time Phase Unwrapping (PhU) algorithm allowing us to analyze sequences of multitemporal full resolution differential Synthetic Aperture Radar (SAR) interferograms for the generation of surface deformation time-series. The core of the proposed technique is represented by the Extended Minimum Cost Flow (EMCF) PhU algorithm [1] which was originally developed for analyzing sequences of multi-look interferograms. In particular, our method performs a joint analysis of the spatial and temporal relationships among a set of multi-temporal differential interferograms, compatible with the Small Baseline Subset (SBAS) algorithm [2]. It exploits the SAR data representation in the Temporal/Perpendicular baseline plane, where a Delaunay triangulation is computed. Each arc of this triangulation allows us to identify a SAR data pair to be exploited in the interferogram generation. Unfortunately, this approach may also lead to generate interferograms with large temporal and/or spatial baselines, which may be drastically corrupted by decorrelation phenomena. Accordingly, to avoid these effects, we also impose constraints on the maximum allowed interferogram baseline values, and we discard from the triangulation all the triangles that involve at least one "large baseline" interferogram. Equivalently, we also remove triangles which involve SAR data pairs characterized by doppler centroid differences exceeding a selected threshold. The proposed PhU approach allows us to apply the SBAS inversion to the unwrapped full resolution differential synthetic aperture radar interferometry (DInSAR) phase sequences, with no need to pass through the analysis of the corresponding sequences of multi-look DInSAR interferograms [3]. On the other hand, the straightforward application of the MCF and EMCF techniques to unwrap sequences of full resolution interferograms is unfortunately often not feasible due to the large amount of "phase residues" [4] to be compensated, which often leads to high-computing time or even unfeasible solutions of the network flow problems [4]. To properly cast this PhU problem, we suggest to use an effective divide-and-conquer approach to the space-time phase unwrapping problem. The key idea is to split our complex minimum cost flow network problem, implementing the whole PhU step, into that of simplex sub-networks, which are solved by applying the EMCF approach. More precisely, we start by identifying, and solving, a primary network that involves a properly selected set of coherent pixels of our interferograms, which are characterized by phase signals with very limited spatial high-pass components. The results of this primary network minimization, representing the backbone structure of the overall network, are subsequently used to constrain the solution of the remaining sub-networks, including the whole set of coherent pixels. These PhU sub-networks are built relying on the generation of a

Constrained Delaunay Triangulation (CDT) [5], whose constrained edges are relevant to the set of successfully unwrapped pixels analyzed during the first PhU operation. To clarify this issue, let us provide some basic information about CDT, which is a triangulation of a given set of vertices with the following properties: 1) a pre-specified set of non-crossing edges (referred to as constraints, or constrained edges) is included in the triangulation, and (2) the triangulation is as close as possible to a Delaunay one. The experimental results were achieved by applying the proposed approach to a dataset consisting of European Remote Sensing (ERS) SAR data acquired, from June 1992 to August 2007, over the Napoli (Italy) bay area. As a final remark, we want to stress that the availability of precise and computationally efficient PhU tools, when dealing with data processed at the full spatial resolution scale, may be very relevant for the future development of innovative interferometric processing techniques. For instance, the knowledge of the phase information associated to the set of successfully unwrapped points, as retrieved via the propose PhU technique at the full spatial resolution scale, may be exploited to perform “enhanced” multi-look operations. REFERENCES [1] A. Pepe, and R. Lanari R., “On the extension of the minimum cost flow algorithm for phase unwrapping of multitemporal differential SAR interferograms,” *IEEE Trans. Geosci. Remote Sens.*, vol. 44, no. 9, pp. 2374-2383, Sept. 2006. [2] P. Berardino, G. Fornaro, R. Lanari, and E. Sansosti, “A new algorithm for surface deformation monitoring based on small baseline differential SAR interferograms,” *IEEE Trans. Geosci. Remote Sens.*, vol. 40, no. 11, pp. 2375–2383, Nov. 2002. [3] R. Lanari, O. Mora, M. Manunta, J. J. Mallorquí, P. Berardino, and E. Sansosti, “A Small Baseline Approach for Investigating Deformation on Full resolution Differential SAR Interferograms,” *IEEE Trans. Geosci Remote Sens.*, vol. 42, no. 7, Jul. 2004. [4] M. Costantini and P. A. Rosen, “A Generalized Phase Unwrapping Approach for Sparse Data”, in *Proc. Geosc. and Rem. Sensing Symposium (IGARSS)*, Hamburg (Germany), Jun. 1999, pp. 267–269. [5] L. P. Chew, “Constrained Delaunay triangulations,” in *Algorithmica*, vol. 4, Springer. Verlag. New York 1989, pp. 97–108.

## Multibaseline gradient ambiguity resolution using graph-cuts for TANDEM-X phase unwrapping

Author(s)

Marie Lachaise <sup>(1)</sup>, Richard Bamler <sup>(2)</sup>

Department

<sup>(1)</sup>DLR; german Aerospace Center Münchner strasse 22, 82234 Oberpfaffenhofen; DE

<sup>(2)</sup>DLR German Aerospace Center, Münchner strasse 22, 82234 Oberpfaffenhofen; DE

**Abstract**

The TanDEM-X Mission has as primary objective to generate a high resolution global Digital Elevation Model (DEM). To carry out this goal, two global interferometric coverages with different baselines will be acquired in two years. We propose a new method for multibaseline phase unwrapping which is the critical point of this DEM generation. Our algorithm combines Minimum Cost Flow (MCF) and Maximum a Posteriori (MAP) estimation. MAP is used to solve phase gradient ambiguities whereas MCF is used to integrate the unwrapped gradients and resolve possible remaining residues. We work in the Markov random Field (MRF) framework so that the MAP problem can become an energy minimization problem over the (integer) ambiguity bands separately for gradients in range and in azimuth. The energy is composed of two terms: the data energy represented by the likelihood term is a link between the estimated and observed gradients; the second term, also called penalty energy, introduces contextual information or prior knowledge on the data for example a certain smoothness. This minimization problem can be carried out efficiently by using graph-cuts. In our case, the negative log joint probability density function (pdf) of the gradients is used for the likelihood term. The gradient pdf is the convolution of the pdf of two neighbouring phase pixels. It allows us to combine all interferograms. They are

uncorrelated since they are independent measurements of the same terrain with different baselines. Thus the noise is different for every measurement). This negative log likelihood is first minimized in the different ambiguity gradient bands of the reference interferogram. The interferogram with the smallest height of ambiguity is chosen as reference in order to avoid the presence of several local minima inside an ambiguity band. The space in which the energy will be minimized is thus much smaller (only some few ambiguity bands instead of several hundreds of pdf samples). The penalty or prior term is the mean over the different interferograms of the absolute differences of two neighbouring pixels gradients. It is written as a function of the gradient ambiguity bands. In fact, unwrapped gradients – scaled by the baseline - of all interferograms must have the same variation at the same position. The attractive property of this prior term is its convexity w.r.t to the ambiguity band. Therefore Ishikawa's exact algorithm [1] can be used to solve the min-cut max-flow problem. Usually it cannot be applied with remote sensing data due to the prohibitive size in memory of the graph to construct. In our case of ambiguity resolution, the graphs are much smaller and can be stored in memory (on the very powerful processing computers used for the TanDEM-X mission). Two graphs are then constructed: one for range gradients and one for azimuth gradients. Moreover, it is possible to adapt the prior to allow discontinuities, i.e. only a piecewise smooth solution, for range gradients since they are subject to layover and shadow phenomena (in this case an approximate algorithm similar to alpha-expansion [2] has to be used). After having unwrapped both gradients in range and azimuth, the last step is to integrate them with MCF to obtain the unwrapped phase. Since ambiguities of both gradients are solved separately, the gradient field conservativeness condition has been lost. However, MCF allows us to reintroduce it. An interesting issue of dual baseline data separated by one year (as in TanDEM-X) are temporal and terrain changes. For example, a mine is deeper after one year or there could be some snow on a mountain even if the acquisition period in the year is more or less the same. This issue will be addressed and our algorithm demonstrated on real TanDEM-X data. [1] Ishikawa, H.; Exact optimization for Markov random fields with convex priors; IEEE Transactions on Pattern Analysis and Machine Intelligence, 2003, 25, 1333-1336 [2] Boykov, Y.; Veksler, O. & Zabih, R.; Fast approximate energy minimization via graph cuts; IEEE Transactions on Pattern Analysis and Machine Intelligence, 2001, 23, 1222-1239

## Redundant Phase Unwrapping and Integration of Finite Differences on a Sparse Multidimensional Domain: Theory and Validation

### Author(s)

Mario Costantini <sup>(1)</sup>, Fabio Malvarosa <sup>(1)</sup>, Federico Minati <sup>(1)</sup>

### Department

<sup>(1)</sup>E-GEOS - an ASI/Telespazio Company Via Cannizzaro, 71, Rome, IT

### Abstract

1. INTRODUCTION In SAR interferometry phase unwrapping and finite difference integration are still key problems for reconstruction of elevations and ground displacements [1-2]. We propose a novel approach capable to guarantee more accurate and reliable solutions to the problems above mentioned, as required by operational applications. The proposed approach exploits more redundant information than previous methods (that are included as particular cases in the general formulation), and is efficiently solved by linear or quadratic programming methods. The improvements obtained with the proposed method with respect to the previous ones are significant, and can make a big difference in operational applications, for example in reconstruction of elevations and ground displacements, where accuracy and reliability are mandatory. In SAR interferometry, the starting data for phase unwrapping and finite difference

integration are differential measurements (finite differences between neighboring points), typically obtained, in the first case, by assuming that the difference of phases in neighboring points are smaller than half a cycle, in the second case, by maximizing the so-called temporal coherence. Therefore, the two problems can be formulated identically as the problem of reconstructing a function given preliminary estimates of its finite differences, which in general are not consistent, i.e. their integration depends on the integration path. In the case of phase unwrapping there is the additional constraint that the corrections should be integer multiple of  $2\pi$ , which makes the phase unwrapping problem more difficult, with a lot of literature produced on this topic (see [1-4] and references therein). In SAR interferometry, in particular in persistent scatterer interferometry [5], often a stack of images acquired at different times, baselines or frequencies are available, which form a three-dimensional (3D) domain. However, phase unwrapping is usually performed independently for each image or, at most, working on different 2D domains at once [6], [7]. Some techniques for 3D phase unwrapping have been proposed, [8] and [9], but they need a preliminary data calibration to compensate atmosphere and orbital phase contributions. In this work we describe a general formulation for the integration of finite differences and phase unwrapping problems. The proposed approach (comprising standard phase unwrapping techniques as special cases), allows obtaining a robust and accurate solution by exploiting redundant information, obtained working with differences between not only nearest neighboring pixels. Moreover, the proposed formulation allows to exploit multi-dimensional information (2D space + time, multi-frequency, multi-baseline, etc.), and to integrate external information if available (e.g. GPS). In all cases the solution can be efficiently obtained by solving a linear or a quadratic programming (LP or QP) problem. Based on the proposed general formulation, we propose and validate different solutions for: \* redundant 2D and 3D phase unwrapping and finite difference integration \* joint phase unwrapping of a multi-temporal series of interferograms (e.g. in persistent scatterer interferometry) robustly with respect to atmospheric or orbital contributions in the phase \* joint phase unwrapping of multi-baseline and multi-frequency (band-split wide-band) SAR data. The validation tests performed on real and simulated SAR data confirm the validity of the proposed method, and show that the improvement with respect to previous techniques is significant (the error reduce by an order of magnitude), and can be essential in several cases. We presented a first version of our approach at the Fringe 2009 Workshop [10], where a similar formulation, limited to the basic extension of the minimum cost flow phase unwrapping to an LP problem, was independently proposed [11]. Here a more mature version currently under peer review [12], with a rigorous theory description and a detailed validation, is presented. In the following sections a summary of the method and of the validation results are given.

## 2. METHOD

Consider the problem of reconstructing a function on a set of sparse points in a multidimensional domain from preliminary estimates for the values of linear combinations (in the simplest case neighboring point differences) of the function at the points to be reconstructed. This reconstruction problem is formulated as the inversion of a linear system of equations, where the constraint matrix defines the linear relations between the function values at different points, and the right hand side terms represent the corresponding estimates (and in case the constant term of the linear combination). In the cases of interest the system is over-determined and the preliminary estimates are inconsistent. The solution can be determined by minimizing, according to a given metric (e.g. L1, L2), the residuals of the different determinations. The problem can be efficiently solved with quadratic and linear programming (QP and LP) solving algorithms in the case of the norm L1 and L2, respectively. The classical problems of SAR interferometry, i.e. phase unwrapping and mean velocity/elevation reconstruction are included in this formulation. The L2 metric is more appropriate when a normal distribution of the errors it is expected, whereas the L1 norm guarantees solutions more robust to outliers, avoiding error spreading, and is therefore very useful for the applications examined in this paper. In particular, the L1 norm guarantees that the phase unwrapping corrections are integer multiples of  $2\pi$ , as expected. Our approach allows using a very redundant set of preliminary estimates of differences between nearby points, and not only

the nearest neighboring points. As a result, phase unwrapping and mean velocity/elevation reconstruction are more accurate and robust to noise and outliers. Moreover, if a multi-temporal series of interferometric phases are available, in the proposed formulation a 3D (2D space + 1D time) redundant problem, with differences between phases acquired at different times, can be straightforwardly written. This solution would require calibrating the interferometric phases in order to reduce atmospheric and orbital systematic errors. But the proposed general formulation also allows a more flexible use of the available multidimensional information. We propose a solution for multi-temporal phase unwrapping of a series of interferograms (e.g. in persistent scatterer interferometry) that overcomes the phase calibration problem by considering double-differences of phases in order to cancel atmospheric and orbital contributions. Finally, we propose also solutions for phase unwrapping of multi-baseline and multi-frequency (band-splitting wide-band) SAR data, based on different scaling factors for the information layers corresponding to different baselines or frequencies.

### 3. EXAMPLES AND VALIDATION

The proposed approach was extensively validated on data from real and simulated SAR acquisitions, and integrated in our production chain, with successful use also in massive productions. The tests performed confirm the validity of the approach: the quality of the results significantly improve with respect to standard techniques, with higher robustness to noise, which guarantees more reliable and accurate results, thanks to the additional information exploited in the proposed formulation. The computational time remains affordable also in very large problems as those arising in SAR interferometry. We performed several validation tests, comparing the performance obtained by the standard minimum cost flow technique with those obtained by the methods based on the new approach proposed in this paper: 2D redundant, multi-temporal, multi-baseline and multi-frequency phase unwrapping. The tests performed on simulated data allowed to quantitatively evaluate the performance of the different methods. With real data, for which the correct solution was not known, we devised some indirect tests that gave us important indications on the performance of the proposed methods in real cases. The quantitative tests performed on simulated data confirm that the use of redundant information in the space/time domain considerably reduces, by an order of magnitude, the unwrapping errors with respect to standard methods. With real data, we performed different tests. First we applied a consistency check on a stack of images, based on the fact that the results should not depend on the integration path in the temporal domain: i.e. for each triplet of images the temporal circuitation should be null. The consistency check is verified by definition for multi-temporal phase unwrapping. In fact, the consistency is one of the conditions enforced in this case, which help finding a better solution. The percentages of inconsistencies found in the obtained unwrapped phases confirm the results obtained with the simulated data, showing that much better results are obtained when the equations are more redundant and can better condition the solution. Further tests with real data showed that small variations of the weighting costs in the minimization influence the solution much less than with standard techniques. Finally, we also verified that the solution tends to stabilize when the level of redundancy become sufficient high. The algorithm is currently implemented in an automatic processing chain installed on a parallel platform (computer cluster), successfully tested in operative projects with massive productions.

### 4. REFERENCES

- [1] P. A. Rosen, S. Hensley, I. R. Joughin, F. K. Li, S. N. Madsen, E. Rodriguez, R. M. Goldstein, "Synthetic aperture radar interferometry," *Proceedings of the IEEE*, vol. 88, pp. 333-382, March 2000.
- [2] R. Bamler and H. Philipp, "Synthetic aperture radar interferometry," *Inverse Problems*, vol. 14, pp. R1-R54, 1998.
- [3] Costantini, M, "A novel phase unwrapping method based on network programming," *Geoscience and Remote Sensing*, *IEEE Transactions on* Volume 36, Issue 3, May 1998 Page(s):813 – 821
- [4] M. Costantini and P. A. Rosen, "A generalized phase unwrapping approach for sparse data," in *Proc. Int. Geosci. Remote Sensing Symp. (IGARSS)*, Hamburg, Germany, June 28–July 2 1999, pp. 267–269.
- [5] A. Ferretti, C. Prati, and F. Rocca, "Permanent scatterers in SAR interferometry," *IEEE Trans. Geosci. Remote Sensing*, vol. 39, no.1, pp. 8-20, Jan. 2001.
- [6] A. Pepe, R. Lanari, "On the Extension of the Minimum Cost Flow Algorithm for Phase

Unwrapping of Multitemporal Differential SAR Interferograms," *Geoscience and Remote Sensing, IEEE Transactions on* Volume 44, Issue 9, Sept. 2006 Page(s):2374 – 2383 [7] G. Fornaro, A. Pauciullo, D. Reale, "A new algorithm for the phase unwrapping of interferogram stacks", in *Proc. Int. Geosci. Remote Sensing Symp. (IGARSS '09)*, vol.5, pp. 21-24, July 2009 [8] M. Costantini, F. Malvarosa, F. Minati, L. Pietranera, G. Milillo, "A three-dimensional phase unwrapping algorithm for processing of multitemporal SAR interferometric measurements," *Geoscience and Remote Sensing Symposium, 2002. IGARSS '02. 2002 IEEE International Volume 3*, 24-28 June 2002 Page(s):1741 - 1743 vol.3 [9] A. Hooper , H. A. Zebker "Phase unwrapping in three dimensions with application to InSAR time series," *J. Opt. Soc. Am. A* 24, 2737-2747 (2007) [10] M. Costantini, F. Malvarosa, F. Minati, "A general formulation for robust and efficient integration of finite differences and phase unwrapping on sparse multidimensional domains," in *Proc. ESA Fringe 2009 Workshop (ESA SP-677, also at <http://earth.eo.esa.int/workshops/fringe09>)*, Frascati, Italy, Nov.-Dec. 2009. [11] P. Agram, H. Zebker, "The edgelist phase unwrapping algorithm and its application to time-series InSAR," in *Proc. ESA Fringe 2009 Workshop, (ESA SP-677)*, Frascati, Italy, Nov.-Dec. 2009. [12] M. Costantini, F. Malvarosa, F. Minati, "A general formulation for redundant integration of finite differences and phase unwrapping on a sparse multidimensional domain", *Geoscience and Remote Sensing, IEEE Transactions*, submitted on July 2010.

## Quality-guided segmentation for phase unwrapping of sparse differential interferograms

Author(s)

Tom Grydeland <sup>[1]</sup>, Yngvar Larsen <sup>[1]</sup>, Tom Rune Lauknes <sup>[1]</sup>

Department

<sup>[1]</sup>Norut Tromsø , NO

### Abstract

When two-dimensional phase unwrapping is performed using Minimum Cost Flow (MCF) formulation [Costantini, 1998], a two-stage approach has already been suggested [Carballo and Fieguth, 2002] in order to keep the problem tractable. We have found that there are multiple advantages to segmentation besides making the computations simpler: Having segments that are highly connected in some sense means that the unwrapping of each segment is very robust, and the unwrapping of disjoint segments is completely independent and perfectly parallelizable. There is also an advantage to have segments already unwrapped when assembling the combined unwrapped interferogram, as will be described below. Blind segmentation (e.g. cutting an interferogram into rectangular sections) brings problems, however. This is especially true if the interferogram has large decorrelated regions, e.g. water or vegetation. In these cases one might end up with pieces of an interferogram which are incorrectly wrapped in their own segment, and where the correct wrapping would be clear from neighbouring pixels in the larger interferogram. We have devised a procedure for unsupervised segmentation which is quick and robust, and produces segments which are connected in a way which makes segment unwrapping (using MCF) very robust also. We begin with a sparse differential interferogram and a layover mask (computed from a DEM) which is used to exclude layover pixels. The grid formed by the selected pixels (including layover pixels) is triangulated. Next, we compute the `_quality_` of each edge connecting two phase pixels. This quality is the product of three factors, based on 1) the coherence of the endpoints, edges connecting high-coherence pixels have higher quality than when either or both endpoints have low coherence; 2) on the wrapped phase difference between the endpoints, phase differences close to zero have high quality, while phase differences close to  $\pm\pi$  have low quality; and 3) the geometric length of the edge, where quality quickly diminishes as the length approaches an estimated atmospheric correlation distance. Layover pixels are defined to have coherence zero, which means that edges which have an endpoint on an layover pixel have a



quality of zero. During quality-guided segment building, only segments with quality above a certain threshold are considered. We begin with the pixel with highest coherence in the interferogram. The next pixel added to the segment is the one which is reached from any pixel already in the segment along the highest-quality edge, and which is not already assigned to a different segment. The segment is completed when no further pixels can be reached, or when the number of pixels in the segment has reached a segment size limit. The next segment is then seeded with the highest-coherence unsegmented pixel and the process continues until at least 90% of all eligible pixels have been segmented. Finally, segments below a certain size are discarded (their pixels are considered unsegmented). The segments are now unwrapped separately, using a MCF approach. Since the segments are strongly connected and layover regions are explicitly excluded, many segment of small or intermediate size end up with no residues, and can be integrated directly. When there are residues and the flow problem must be solved, we use the same quality metric again. Each arc in the flow graph crosses one and only one edge in the phase triangulation, and we set the cost of flow along this arc equal to the quality of the edge it crosses. In this way, branch cuts are guided along paths of low coherence and ambiguous phase differences, and prefers to cut a few long edges rather than a larger number of shorter edges. After unwrapping the segments, we enter the growth and combination stage. Lowering the edge quality threshold, we consider the highest-quality unused edge from a segmented pixel in the entire interferogram. If the pixel reached is unsegmented, it is added to the segment and given phase according to the edge used to reach it. If it was already in the same segment, we can check that the integration along this edge corresponds to the phase already assigned and flag any discrepancies. If the pixel belongs to a different segment, a collision is recorded, along with the wrapping number difference (a small, signed integer) of this collision. Once two segments have collided a specific number of times, the wrapping number differences are inspected. If they all agree (with at most a tiny number of dissenting values), the relative wrapping of the two segments is considered decided and the segments combined. Otherwise, the decision regarding these two segments will be left to the final combination stage. In this stage, segments which were arbitrarily and artificially divided in the segmentation stage (by the maximum segment size) are in all cases reassembled with no ambiguity. At the end of this stage, we have a very small number of segments which are all strongly connected internally and with weak or unreliable connections between them. Attempts at a "voting" strategy in this stage has had moderate success, and final combination might be better done using heuristic methods, or perhaps even a flow approach. The technique recently introduced by Zhang et al [2011] is likely to be of interest. For this approach to be useful for the unwrapping of topographical phase, the quality measure associated with wrapped phase difference must be modified. Carballo, G. F., & Fieguth, P. W. (2002). Hierarchical network flow phase unwrapping. *IEEE Transactions on Geoscience and Remote Sensing*, 40(8), 1695-1708. doi: 10.1109/TGRS.2002.800279. Costantini, M. (1998). A novel phase unwrapping method based on network programming. *Geoscience and Remote Sensing, IEEE Transactions on*, 36(3), 813–821. Zhang, K., Ge, L., Hu, Z., Ng, A. H.-M., Li, X., & Rizos, C. (2011). Phase Unwrapping for Very Large Interferometric Data Sets. *Geoscience and Remote Sensing, IEEE Transactions on*, doi: 10.1109/TGRS.2011.2130530.



**Day 4, Thursday 22 September 2011**



# Session: Methods - DInSAR/PSI

## Wide Area Persistent Scatterer Interferometry: Algorithms and Examples

### Author(s)

Nico Adam <sup>(1)</sup>, Fernando Rodriguez Gonzalez <sup>(2)</sup>, Alessandro Parizzi <sup>(2)</sup>,  
Werner Liebhart <sup>(3)</sup>

### Department

<sup>(1)</sup>German Aerospace Center (DLR) Remote Sensing Technology Institute (IMF), DE

<sup>(2)</sup>DLR IMF-SV, DE

<sup>(3)</sup>Technische Universität München Remote Sensing Technology, DE

### Abstract

Sentinel-1 constitutes ESA's follow-up mission to the successful ERS and Envisat SAR satellites. In the course of these radar missions, SAR interferometry has been evolved into an operational monitoring technique for the generation of digital elevation models and for displacement of the Earth's surface. The state of the art processing for the observation of subtle deformation with Millimetre accuracy is the persistent scatterer interferometry (PSI). By using large stacks of data and a time series analysis, this processing technique can separate the different interferometric phase contributions topography, atmosphere and motion of the scatterer. For the upcoming Sentinel-1 mission, Terrain Observation by Progressive Scans (TOPS) is foreseen the standard acquisition mode to guarantee a continuous, repeated without gap and global mapping of the Earth's surface with conventional resolution. The idea at ESA is consequent to extend the interferometric processing also to such a large coverage. Subject is to map countries and continents based on the PSI technique. In spite, PSI is a well established and validated processing technique, this is a difficult task. Actually, this technique has been developed for urban areas with a typical persistent scatterer (PS) density of 100 PSs per square kilometre. This high scatterer density makes the atmosphere effect compensation straight forward. Now, non-urban areas need to be processed also. These are characterized by a rare occurrence of PSs and a spatially varying PS density as well as a low PS quality with respect to their phase stability. As a consequence of the increased distance between the usable scatterers, the correction for the troposphere propagation effect is not optimal any more. Besides, the number of outliers and estimation noise increases for the estimation on arcs too. As a result, spatial error propagation can become a significant problem. This is the reason, a wide area product (WAP) for the PSI monitoring is developed at DLR. It is foreseen to be the standard level 1 product for the Sentinel-1 mission and is developed in the course of ESA's TerraFirma project. Practically, it is an update of DLR's operational PSI GENESIS system. Subject is an operator interaction free processing and quality assessment and an error propagation characteristic which meets the end users requirements. The key algorithms which need to be updated for the wide area processing are the PS detection and characterization, the reference network setup and its robust inversion as well as the troposphere effect mitigation. This paper presents the developed algorithms to avoid significant spatial error propagation and presents first WAP processing examples based on available ERS data from the TerraFirma project.

# Virtual reconstruction and validation of Sentinel-1 Interferometric WideSwath mode: InSAR/PSI algorithms perspective

Author(s)

Petar Marinkovic <sup>(1)</sup>, Yngvar Larsen <sup>(2)</sup>

Department

<sup>(1)</sup>PPO.labs , NL

<sup>(2)</sup>NORUT , NO

## Abstract

For InSAR applications, a default imaging mode of Sentinel-1 is an Interferometric WideSwath (IWS) mode, the mode based on principles of TOPS (Terrain Observation by Progressive Scans). The TOPS is a wide swath mode that has the same coverage and resolution as of the ScanSAR mode, but without scalloping effect. As a consequence of the signal properties of the mode, i.e., large Doppler centroid variations within a burst, it is expected that some modifications of well established InSAR processing algorithms would have to be performed. Specifically, regarding potential issues due to high Doppler centroid with, e.g., coregistration, persistent scatters point selection, signal interpretation, etc.

In order to fine-tune and upgrade the computational algorithms for the TOPS mode, the access to simulated and real data is a must. However, except for the images of TerraSAR-X acquired in TOPS mode there is no other real data source; and unfortunately, for most of the researchers and developers, TerraSAR-X TOPS mode data is not easily accessible. Therefore, in order to have an early-access and get a feeling for the InSAR performance of Sentinel-1 IWS mode, we designed an algorithm that is effectively capable of converting any SAR acquisition mode to another one. The algorithm builds on the TOPS azimuth spectral characteristics, where time varying bandpass filtering is utilized to mask out the the azimuth time-frequency spectrum not corresponding to the TOPS mode. The algorithm is designed to perform in a SLC domain, with obvious restriction due to coverage in azimuth time and frequency of the input data (e.g., ScanSAR to Stripmap conversion mode can be problematic).

Considering the context of the workshop, apart from the algorithmic description of the conversion model and discussion on the optimization needed for InSAR processing of IWS mode; the contribution will focus more on the application and demonstration studies. An implementation and open source prototype in NEST-DORIS will be presented. Furthermore, results of algorithmic studies of InSAR/PSI processing algorithms using simulated IWS data obtained from ERS/ENVISAT StripMap and TerraSAR-X SpotLight data will be reviewed. Furthermore, the contribution will also discuss the performance of IWS mode, based on the simulated data, for the long-term monitoring applications, e.g., subsidence monitoring.

## TOPS Differential SAR Interferometry with TerraSAR-X

Author(s)

Luca Marotti <sup>(1)</sup>, Pau Prats <sup>(1)</sup>, Rolf Scheiber <sup>(1)</sup>

Department

<sup>(1)</sup>German Aerospace Center (DLR) , DE

## Abstract

Differential SAR Interferometry (DINSAR) is a remote sensing technique that allows the investigation of the deformation phenomena occurring on the Earth surface. Conventionally

DINSAR investigations have been performed on data acquired in Stripmap mode. Clearly a wider coverage of the investigated area might be an advantage for seismology, subsidence monitoring and civil protection purposes. For these reasons we investigate, for the first time, the analysis of the DINSAR technique by means of data acquired in the TOPS mode. In this mode the acquisition is performed steering the antenna in the along track direction from backward to forward. At the end of the burst the antenna look angle is changed to illuminate a second subswath, pointing again backward. When the last subswath is imaged, the antenna points back to the first subswath, so that no gaps are left between bursts of the same subswath. The fast steering leads to a reduction of the observation time and, consequently, to a worsening of the azimuth resolution. However all targets are observed by a complete antenna pattern and, therefore, it is possible to overcome the problems of scalloping and azimuth varying signal-to-noise ratio of the conventional ScanSAR mode. It is worth to remark that the TOPS DINSAR processing presents several critical points (i.e. coregistration) since, due to the TOPS signal characteristics, the interferometric chain is very sensitive to small implementation errors. The analysis will be conducted with a stack of data acquired both in TOPS and in Stripmap mode by the TerraSAR-X sensor over the Mexico City area. Part of the city area is suffering from severe subsidence due to ground water extraction. In the first part of the study the DINSAR procedure will be applied to the TOPS and Stripmap data independently, in order to compare the deformations estimated by means of the two datasets. In the second part a step forward will be achieved performing the DINSAR analysis by generating cross interferograms between TOPS and Stripmap data. This combination might be of interest for several reasons. On the one hand, when using TOPS mode, it would be possible not to break the data continuity of data acquired in Stripmap mode by previous sensors. On the other hand, the use of two different modes over the same area at different time instants might be of interest due to different applications or user needs. Due to the different acquisition modes, only a part of the azimuth frequencies of the signal spectra acquired in TOPS mode will overlap with the one acquired in Stripmap mode. For this reason it is clear that, for distributed targets, a cross-interferogram will result totally decorrelated at the burst edges. Therefore, the exploitation of such interferograms will be performed by means of ideal point-like scatterers. Such targets are commonly known as permanent scatterers (PS), persistent scatterers, or coherent scatterers (CS). Note that the latter refer to the method used to detect those targets, not to be mistaken by the interferometric coherence. Indeed, the method consists in computing the coherence between independent spectral bands of the same image. Therefore, by definition, only CS (PS) will have correlation between independent spectral looks, either in the range or the azimuth dimension. Acknowledgement: The work presented in this study was funded under ESA-ESTEC contract number 22243/09/NL/JA.

## Mapping 3D Surface Deformation by Combining Multiple Aperture InSAR and Conventional InSAR

### Author(s)

Zhong Lu <sup>(1)</sup>, Hyung-Sup Jung <sup>(2)</sup>

### Department

<sup>(1)</sup>U.S. Geological Survey , USA

<sup>(2)</sup>The University of Seoul , KR

### Abstract

Mapping 3D Surface Deformation by Combining Multiple Aperture InSAR and Conventional InSAR  
Hyung-Sup Jung (1) & Zhong Lu (2) (1) The University of Seoul, Seoul, Korea (2) U.S. Geological Survey, Vancouver, Washington, USA InSAR technique has demonstrated a great success in mapping surface deformation, but is limited to the measurement of displacement along the radar line-of-sight (LOS) direction. Because SAR satellites have near-polar orbits, it is difficult to

construct 3D surface deformation from LOS InSAR data alone. Multiple aperture InSAR (MAI) technique represents a remarkable improvement in measuring along-track deformation than the pixel offset tracking method [1]. We show here a method that combines MAI and LOS InSAR measurements of one ascending and one descending interferometric datasets to retrieve 3D surface deformation. We present examples of mapping volcanic and earthquake deformation fields using ALOS and ERS/Envisat images and comparison of the derived 3D deformation fields with those from GPS measurements [2]. We demonstrate that MAI does not depend on SAR image resolution while the azimuth pixel offset method relies on SAR azimuth pixel resolution, which has a significant implication for measuring 3D deformation fields from ESA Sentinel-1 SAR mission. [1] Jung, H.S., Won, J.S., & Kim, S.W. (2009). An improvement of the performance of multiple aperture SAR interferometry (MAI), *IEEE Trans. Geosci. Remote Sens.*, 47, 2859-2869. [2] Jung, H.S., Lu, Z., Won, J.S., Poland, M.P., & Miklius, A. (2011) Mapping Three-Dimensional Surface Deformation by Combining Multiple-Aperture Interferometry and Conventional Interferometry: Application to the June 2007 Eruption of Kilauea Volcano, Hawaii, *IEEE Geosci.& Remote Sens. Lett.*, 8, 34-38, 10.1109/LGRS.2010.2051793

## Combination of X-band high resolution SAR data from different sensors to produce ground deformation maps

### Author(s)

Javier Duro <sup>(1)</sup>, Marc Gaset <sup>(1)</sup>, Oscar Mora <sup>(1)</sup>, Alain Arnaud <sup>(1)</sup>

### Department

<sup>(1)</sup>ALTAMIRA INFORMATION C/ Còrsega, 381-387 E-08037 Barcelona, ES

### Abstract

The successful launch of TerraSAR-X and Cosmo-Skymed in 2007 put available high resolution Synthetic Aperture Radar images with a reduced revisit time. These new sensor characteristics influence the benefits of ground deformation estimation by means of advanced DInSAR or Persistent Scatterers Interferometric techniques. The improvement, in terms of spatial resolution, of these new X-band sensors compared with the precedent C-band sensors on board ERS-1/2 or ENVISAT satellites is noted in an increase of Persistent Scatterers density. As a result, more detailed deformation maps can be obtained with a better delimitation of the areas affected by ground motion. Another improvement of using X-band data is in term of precision. Thanks to the shorter wavelength there is an increase of the sensitivity to detect and monitor millimetric changes of the distance between the sensor and the ground targets. The last advantage is the reduced revisit time which increase the monitoring capabilities of non-linear ground motion and in some way (jointly with the increase of spatial resolution) it compensates the maximum gradient of deformation that could be detected with such a short wavelength. Nevertheless the use of these sensors presents some limitations. For example, acquisitions are not systematically done over major areas of interest (as in the case of the past C-band missions), therefore it is necessary to set up acquisitions in background mode in order to have the possibility to benefit of one of the great advantages of InSAR technology, the capacity of looking into the past. This makes that before having the possibility to perform a monitoring of an area of interest, a data archive should first be created. A minimum number of SAR imagery should then be available before that the first maps ground movements could be generated using PSI techniques. In normal conditions, considering the fast repeat cycles of the high resolution sensors this could take less than half a year (with approximately three images per month and considering the processing time). Another important limitation in using these satellites is that they are intended for civil, military and scientific use. This make that quite often one could be in conflict with the scientific/military mode losing one or even several consecutive acquisitions. This situation can originate serious problems in monitoring projects which requires systematic acquisitions. This paper presents one possible



solution to this particular problem. It is based on the combination of two different stacks of SAR data acquired by different sensors over the same ground area. In that way, in case of conflicts the gaps of acquisitions can be filled with data gathered with the other X-band satellite, ensuring the continuity in the measurements. This is possible because both sensors operate with the same carrier frequency and are wide-band systems. Their respective StripMap mode of acquisition has similar resolutions. In the paper it is demonstrated that with the selection of the appropriate orbital pass it is possible to have acquisitions with approximately the same incidence angle with the two sensors. Keeping the same geometry of observation is mandatory to preserve the coherent targets in the two stacks of data allowing the merging procedures. One key point of the processing is the coregistration of the two datasets. To have acquisitions with a similar incidence angle implies a baseline of several kilometers with respect to the orbital passes of the two satellites. Fine coregistration procedures are then necessary in order to estimate properly the distortions between the two geometries. The performance of this solution is tested and evaluated with a real test site.

## Bridge Health Monitoring using Persistent Scatterer Interferometry (PSI)

Author(s)

Adrian McCardle <sup>[1]</sup>

Department

<sup>[1]</sup>3v Geomatics Inc. 4350 Arbutus st, CA

### Abstract

The widespread deterioration and some recent collapses of highway bridges have highlighted the importance of developing effective bridge monitoring technologies that can help identify structural problems before they become critical and endanger public safety. Bridges are designed to exhibit ductile failure modes that manifest as a temporally continuous motion profile at distinct locations along a bridge span. However, monitoring bridges using PSI presents unique challenges. Double and triple bounce echo effects must be overcome to identify reliable bridge targets for displacement monitoring. Moreover, targets must be accurately positioned in 3D space to enable bridge engineers to pinpoint the location of suspicious displacement. 3v Geomatics acquired RADARSAT-2 images over Vancouver bridges using three distinct beam modes. Different point target identification techniques were investigated and optimized to maximize the density and quality of measurable scatterers in each dataset. Spatio-temporal characteristics of amplitude and differential phase were evaluated for bridge targets in order to correct their horizontal and vertical positions. External bridge CAD (Computer Aided Design) models have been imported and geo-located to visualize interferometry-enabled bridge information in the paradigm of bridge engineers. This paper presents results of these foregoing analyses and discusses key issues pertaining to interpretation of PSI information products for structural health monitoring of bridge superstructures.

# Deformation estimation in non urban areas exploiting high resolution SAR data

## Author(s)

Kanika Goel <sup>(1)</sup>, Nico Adam <sup>(1)</sup>

## Department

<sup>(1)</sup>Remote Sensing Technology Institute (IMF), German Aerospace Center (DLR), DE

## Abstract

In this paper, we present a technique for high resolution deformation monitoring with a focus on non-urban areas characterized by fast temporal decorrelation caused by agricultural fields, forests and soil and rock surfaces. With the launch of high resolution SAR satellites such as TerraSAR-X with smaller orbital tubes, higher bandwidth and shorter revisit times; Distributed Scatterer (DS) interferometry is now supported by a practical data basis. Typical application areas include mines, reservoirs (oil, gas, water etc.), volcanoes and seismic zones. The technique we present here for deformation mapping is a two step approach. In the first step, we use an object adaptive spatial phase filtering algorithm for generating high resolution coherent differential interferometric stacks. The aim is an accurate phase estimation even in the presence of error sources (e.g. temporal and spatial decorrelation, topographic errors and atmospheric effects). Additionally, coherence estimation of the interferograms is also performed as it is important for various applications such as guiding phase unwrapping algorithms and selection of pixels for deformation monitoring. The object adaptive estimation maintains the high geometric resolution provided by new satellites such as TerraSAR-X (meter resolution). Practically, the algorithm is based on the identification of statistically homogenous pixels in a neighbourhood using a stack of coregistered (upto sub-pixel accuracy) and calibrated SAR amplitude images. Anderson-Darling test is used to identify if two pixels statistically arise from the same distribution. It is a non-parametric test with no assumption about the probability density function (pdf) generating the data. The homogenous pixels identified are then used for adaptive phase flattening of single look small baseline differential interferograms to compensate for topographic errors (due to errors in Digital Elevation Model (DEM) etc.). The phase flattening or denoising is important because the topographic errors affect subsequent estimation of an improved phase and coherence. We use a periodogram approach in spatial domain for a robust estimation of the local slope pixel wise (similar to periodogram used in Persistent Scatterer Interferometry (PSI) in time domain) and removing it from the interferograms. This is then followed by phase filtering of the flattened interferometric phase via adaptive complex averaging. In the second step, we use these phase estimates to retrieve the line-of-sight (LOS) deformation and residual topography using the Small Baseline Subset Algorithm (SBAS). In this processing step, the L1 norm minimization for phase inversion is used instead of the standard least squares (L2 norm minimization). This results in a more robust solution with respect to the often occurring and difficult to detect phase unwrapping errors found in non-urban areas. We demonstrate our new proposed technique using high resolution TerraSAR-X data of Bierwang gas storage reservoir located near Chiemsee lake in Germany. This is a rural region with many agricultural fields and forests, and thus, is ideal for testing our technique to illustrate its advantages. We use 55 TerraSAR-X images of the test site from January, 2008 to May, 2010 and generate 123 high resolution differential interferograms using the adaptive spatial phase filtering algorithm. These are then used for deformation monitoring using the SBAS approach. The applicability of our technique is shown by presenting results for the adaptive spatial phase filtering and estimated deformation time series.

# InSAR partially coherent targets: multiplicity of approaches

Author(s)

Daniele Perissin <sup>(1)</sup>, Zhiying Wang <sup>(2)</sup>

Department

<sup>(1)</sup>CUHK Hong Kong, HK

<sup>(2)</sup>Harbin Institute of Technology Shenzhen, CN

## Abstract

In recent years several researchers have introduced methods for processing series of InSAR data to estimate terrain displacement and elevation in order to improve or extend the pioneer Permanent Scatterers technique (Ferretti et al 2001). Just to mention a few of them, SBAS (Berardino et al 2002), StamPS (Hooper et al 2004) and QPS (Perissin et al 2007). Starting from the QPS technique, we want to analyze here several options to choose for processing InSAR data stacks in order to solve a variegated set of nontrivial cases. The experience brought here comes from the analysis of several test-sites in China, whose territory is at times extremely complex. The main challenging terrain characteristics that we dealt with are: degree of urbanization, degree of vegetation, elevation, degree of temporal change. We met several kinds of terrain changes (that prevent from positively using the PS technique): construction/demolition of buildings (in China renovating is not a common practice), land use change, snow cover, agricultural management (e.g. in some Chinese regions there are areas where fields are covered in winter and left open in summer). On the other side, the processing approach to choose is also determined by the available data-set: number of images, frequency, band, baseline dispersion, time span, time sampling. In our QPS method, some of the options that can be chosen to process areas with different characteristics and with different data are: the images graph (how to combine the images of the dataset to form interferograms), the PSC graph (how to connect PS candidates in the area of interest), which weights to use in the estimation process (amplitude, spatial coherence or nothing). In particular, we distinguish the following images graph: (A) star graph (single master, used in the PS technique), (B) small normal baselines (used in SBAS), (C) small temporal baselines, (D) Minimum Spanning Tree (obtained maximizing the spatial coherence of all possible interferograms), (E) Delaunay graph (generated in the baseline-time space) or (F) simply a set of coherent interferograms with no particular topology. Among the possible ways to connect PSC's, there are (a) the common Delaunay graph, (b) a redundant graph formed by many close connections and (c) a smart configuration that connects aggregates of close points. Finally, each space-time double difference (a connection between two images and between two PSC's) can be weighted using either amplitude information or the interferometric spatial coherence. It can be shown that each combination of options has different performances in different cases, and that, when the terrain complexity is particularly high, the choice makes the difference. The discussion about the possible processing approaches here reported will go through the following analyzed sites: Shanghai, in which we processed Cosmo-SkyMed and TerraSAR-X images; Tianjin, analyzed with ALOS and TerraSAR-X data; Hong Kong and neighborhood areas, observed by TerraSAR-X and Envisat; Tibet, with Envisat and ALOS data. Options and methods here reported are implemented by the research software SARPROZ.

[http://ihome.cuhk.edu.hk/~b122066/index\\_files/download.htm](http://ihome.cuhk.edu.hk/~b122066/index_files/download.htm)

# Deformation rate estimation on changing landscapes using Temporarily Coherent Point InSAR

## Author(s)

Lei Zhang <sup>(1)</sup>, Xiaoli Ding <sup>(1)</sup>, Zhong Lu <sup>(2)</sup>, Jun Hu <sup>(3)</sup>

## Department

<sup>(1)</sup>The Hong Kong Polytechnic University Hung Hom, KLN, HK

<sup>(2)</sup>U.S. Geological Survey, USA

<sup>(3)</sup>Central South University Changsha, CN

## Abstract

Persistent scatterers are the stable natural reflectors that keep coherent during the whole observation time span which can usually be identified densely in developed urban areas. However in areas undergoing large scale redevelopments like the cities in most developing countries there are a large number of scatterers that only are visible temporarily in the observation period [1]. In fact these scatterers still carry high-quality phase information at least in a subset of interferograms allowing us to estimate the deformation rates from them. Here the persistent scatterers as well as the partially coherent scatterers are termed as Temporarily Coherent Points (TCPs). The usage of TCPs can apparently increase the density of deformation signals, which is expected to provide us more information on the deformation pattern and help us to make better risk assessment over the research area. In this paper, besides the approach presented in [2] we provide two alternatives to select the so called TCPs. One is based on interferometric coherence which works well for images pairs with short baselines and can be performed efficiently. The other one is based on the amplitude intensity of SLC images which is similar with the method used in [3]. However we design the amplitude dispersion index with the median and median absolute deviation of the amplitude values instead of the mean and the standard deviation, which can successfully pick up the pixels that appear visible in a partial observation time. Since the TCPs might keep coherent in a subset of interferograms, deformation parameter estimation must either be performed only with coherent phases of TCPs or have the ability to suppress the effect of random phases that are considered as outliers when taking all interferograms as observations. Based on the algorithm presented in [4], we present in this paper two reliable approaches to estimate the deformation rate from these TCPs. All the proposed approaches have been applied with real datasets and results have been verified by the ground measurements. References [1] D. Perissin, A. Ferretti, R. Piantanida, D. Piccagli, C. Prati, F. Rocca, A. Rucci, F. de Zan, Repeat-pass SAR interferometry with partially coherent targets, Proceedings of Fringe 2007, Frascati (Italy), 26-30 November, 2007. [2] Zhang, L., Ding, X.L., & Lu, Z. (2011a). Ground settlement monitoring based on temporarily coherent points between two SAR acquisitions. *ISPRS Journal of Photogrammetry and Remote Sensing*, 66, 146-152 [3] Ferretti, A., Prati, C., & Rocca, F. (2001). Permanent scatterers in SAR interferometry. *IEEE Transactions on Geoscience and Remote Sensing*, 39(1), 8-20. doi: 10.1109/36.898661. [4] Zhang, L., Ding, X.L., & Lu, Z. (2011b). Modeling PSInSAR time series without phase unwrapping. *IEEE Transactions on Geoscience and Remote Sensing*, 49, 547-556

# Exploitation of temporary coherent scatterers in SQUEESAR analyses

## Author(s)

Fabrizio Novali <sup>(1)</sup>, Alfio Fumagalli <sup>(1)</sup>, Fabio Rocca <sup>(2)</sup>, Claudio Prati <sup>(2)</sup>,  
Alessandro Ferretti <sup>(1)</sup>, Alessio Rucci <sup>(1)</sup>

## Department

<sup>(1)</sup>Tele-Rilevamento Europa - T.R.E. s.r.l. , IT

<sup>(2)</sup>Politecnico di Milano , IT

## Abstract

During the last decade, Permanent Scatterer SAR interferometry (PSInSAR) – and, in general, other Persistent Scatterer algorithms, based on a similar approach - has been widely used for monitoring surface deformation phenomena, such as subsidence and uplift, seismic fault creeping, volcano inflation and landslides. As well known, the algorithm aims at identifying and then exploiting PS, i.e. radar targets only slightly affected by temporal and geometrical decorrelation, where very precise displacement measurements can be carried out. The operational use of PSInSAR has originated the request for a more effective monitoring tool over non-urban areas, where the density of measurement points (i.e. PS) is usually low. These areas, are characterized by the presence of distributed scatterers (DS), affected by both temporal and geometrical decorrelation phenomena, but still exhibiting good coherence levels in some interferograms. In order to identify the best InSAR algorithm for each family of scatterers, it is important to obtain a complete statistical characterization of all image pixels belonging to the area of interest, by estimating, for each of them, the so-called coherence matrix (CM). The CM, where each element is related to a certain interferogram, becomes a roadmap to identify and select useful interferometric pairs and to design proper InSAR algorithms. In SqueeSAR, recently developed by POLIMI and TRE, the CM is used to optimally estimate the time series of the optical ray-path of each DS, preserving at the same time the information associated to point-wise PS. This new technique is based on the selection of statistically homogeneous pixels (for DS identification), followed by a Maximum Likelihood (ML) estimation of a vector of phase values (one vector for each DS), fitting all interferograms (i.e. the CM elements). The SqueeSAR approach allows to jointly process PS and DS, using the best approach for each of them. The results provided by this processing chain have shown a significant increase in coverage extent and number of measurement points over non-urban areas. In order to retrieve a time series of displacement values for each DS, it is important to have a “connected path” from the first to the last acquisition of the dataset, via high-coherence interferograms. However, this is not possible for “temporary coherent scatterers” (TCS), i.e. targets whose SNR varies dramatically over time due, for example, to snow coverage in certain period of the year. TCS can still prove useful in InSAR analyses, by taking advantage of the estimated CM to extract not the time series of displacement, but to perform a Maximum Likelihood (ML) estimation of their elevation and average displacement rate. This approach allows to extract information also for DS exhibiting high coherence values only in a few interferograms, and results in a significant increase in the density of measurement points. As already mentioned, the drawback is that it is not possible to reconstruct the displacement time series of a TCS, at least without prior information. This paper will show how the combination of PS, DS and TCS allow the user to get an extremely powerful tool to characterize surface deformation phenomena affecting an area of interest. While the velocity map estimated using all types of scatterers makes it possible a detailed characterization of the footprints of unstable areas, thanks to the very high spatial coverage of measurement points, displacement time-series provided by SqueeSAR allow to monitor the temporal evolution of motion. Results obtained by

applying this new approach to different scenarios, with special attention to landslide monitoring, will be presented.

## Noise covariance model for time series InSAR analysis

### Author(s)

Piyush Agram <sup>(1)</sup>, Mark Simons <sup>(1)</sup>

### Department

<sup>(1)</sup>California Inst of Tech MC 252-21, Caltech, Pasadena, CA, USA

### Abstract

Interferometric Synthetic Aperture Radar (InSAR) Time-series methods estimate the spatio-temporal evolution of surface deformation using multiple SAR interferograms. While various noise models have been developed to describe statistics of interferometric phase and correlation for individual interferograms, there has been no concerted effort to develop covariance models for application to networks of multiple interferograms.

Building on existing InSAR noise models, we develop a simple covariance model (over space and time) for interferometric phase that can be exploited to analyze the performance of time-series InSAR techniques. We combine established atmospheric phase screen models [1,2] and decorrelation noise models [3,4] into a simple framework allowing us to estimate error bounds in InSAR time-series products. A natural outcome from our new covariance model is that phase observation noise in a connected network of interferograms is correlated. Inclusion of the correct noise covariance matrix in the inversion process can significantly improve estimates of deformation time-series. In particular, we can exploit spatial correlation to significantly improve the signal-to-noise ratio in estimated deformation time-series relative to traditional individual pixel-based time-series InSAR techniques. We illustrate this improvement with results obtained by applying a multi-scale interferometric time-series (MInTS) algorithm [7] over the Parkfield region in California, USA. The MInTS technique reduces the set of InSAR observations to a set of almost uncorrelated observations at various spatial scales using wavelets. Traditional pixel-based inversion techniques can then be applied to the wavelet coefficients more effectively, thus significantly improving the signal-to-noise ratio.

Our covariance model, in combination with a reliable decorrelation model, can also be used to determine trade-offs between redundancy in interferogram networks and error in deformation estimates from traditional pixel-based time-series techniques. The proposed framework can also be used to determine the optimal extension of pre-existing interferogram networks with newer SAR acquisitions, allowing for faster generation of time-series InSAR products. We apply our framework to compare the performances of single-master based interferogram networks (traditionally used in persistent scatterer techniques [5]) and multi-master based networks (used in short baseline techniques [6]).

### References

1. Hanssen, R. F. 2001. Radar Interferometry: Data Interpretation and Error Analysis. First edn. Springer.
2. Emardson, T. R., Simons, M., Webb, F. H., 2003. Neutral atmospheric delay in interferometric synthetic aperture radar applications: Statistical description and mitigation. JGR 15 (B5), 2231.
3. Zebker, H. A., Villasenor, J., 1992. Decorrelation in interferometric radar echoes. IEEE TGRS 30 (5), 950-959.
4. Bamler, R., Just, D., August 1993. Phase statistics and decorrelation in sar interferograms. IGARSS' 93. Vol. 3. pp. 980-984.
5. Ferretti, A., Prati, C., Rocca, F., 2001. Permanent scatterers in sar interferometry. IEEE TGRS 39 (1), 8-20.
6. Berardino, P., Fornaro, G., Lanari, R., Sansosti, E., 2002. A new algorithm for surface

deformation monitoring based on small baseline differential sar interferograms. IEEE TGRS 40 (11), 2375-2383.

7. Hetland, E., Muse, P., Simons, M., Shanker, P., Lin, N., & DiCaprio, C. J. 2011. A multi-scale approach to InSAR time-series analysis. In preparation.

## Detecting regular patterns in urban PS sets

### Author(s)

Alexander Schunert <sup>(1)</sup>, Eckart Michaelsen <sup>(2)</sup>, Uwe Sörgel <sup>(1)</sup>

### Department

<sup>(1)</sup>Leibniz Universitaet Hannover Nienburger Strasse 1, DE

<sup>(2)</sup>Fraunhofer IOSB Gutleuthausstr. 1, DE

### Abstract

Recent years have seen the advent of a new generation of space-borne high resolution SAR sensors like COSMO-SkyMed or TerraSAR-X. The latter provides a resolution in the order of one meter in the finest mode. Considering this tremendous improvement in resolution, a plethora of new mapping applications, which are particularly interesting for urban areas, becomes possible. One example for that is the exploitation of TerraSAR-X data stacks featuring very high resolution to map topography and deformation on a very dense grid. A typical method to achieve that is the Persistent Scatterer Interferometry (PSI), which provides the height and the deformation for a set of stable radar targets, referred to as Persistent Scatterers (PS). Due to the resolution, the PS density is very high in urban areas. It was shown, that a trihedral corner reflector having a side length of 6cm is enough to induce a PS. In view of this fact a large number of PS can be expected for a common building facade exhibiting structures like balconies or windows. These structures are usually arranged in a rectilinear setup, leading to a regular PS distribution in SAR data. These patterns formed by the PS contain lots of information, which is not used in current PSI processing schemes. Our research aims at extracting those patterns and use the obtained information in PSI processing. We propose here a scheme to extract horizontal groups of PS to facilitate height estimation. For that purpose a simple building model, consisting of the part of the building footprint visible to the SAR sensor and the maximum building height, is used as prior knowledge. In a first step PS, which possibly belong to the building under investigation, are selected. For that the distance in range-direction for the PS at hand to the next building outline is calculated and compared to the assumed maximum building height. In a second step the PS set is searched for regular patterns in the direction of the building outline (if the building facade consists of many parts having different orientation to the sensor, every part is investigated separately). The search is essentially conducted in one dimension for all possible rows of the facade. In every search step a starting PS - referred to as triggering PS - is chosen and a search area for a possible successor is defined based on a pre-defined spatial frequency. If a PS is found in this area, it is added to the group and a new search area is defined. Otherwise the search is terminated. This procedure is repeated until every PS has been used as triggering PS once. In case a PS is contained in several groups, it is removed from all but the biggest group. Finally the height of PS, that have been assigned to a group, is recalculated as a function of the height of all points in this group (in the simplest case just the arithmetic mean of all points is taken as height estimate for all points). After visual inspection the results look quite promising. Currently, an evaluation of the results against ground truth is carried out, to investigate the benefit of the proposed method numerically.

# A comparative study of corner reflectors, compact active transponders and I2GPS for monitoring deformation in areas with low spatial density of persistent scatterers: the Delft field experiment

## Author(s)

Pooja Mahapatra <sup>(1)</sup>, Ramon Hanssen <sup>(1)</sup>, Hans Van der Marel <sup>(1)</sup>, Ling Chang <sup>(1)</sup>, Prabu Dheenathayalan <sup>(1)</sup>, Jose-Manuel Delgado Blasco <sup>(1)</sup>, Joana Esteves Martins <sup>(1)</sup>, Rachel Holley <sup>(2)</sup>, Marko Komac <sup>(3)</sup>, Chris Prior <sup>(4)</sup>, Alan Fromberg <sup>(4)</sup>

## Department

<sup>(1)</sup>Delft University of Technology , NL

<sup>(2)</sup>Fugro NPA Ltd. , UK

<sup>(3)</sup>Geological Survey of Slovenia , SI

<sup>(4)</sup>System Engineering & Assessment Ltd. , UK

## Abstract

Persistent Scatterer Interferometry (PSI) has emerged over the last decade as a technique capable of very accurate (millimetric) measurements of ground deformation occurring at radar scatterers (persistent scatterers or PS) that are phase coherent over a period of time. PSI studies using C-band SAR data have shown that the PS spatial density in urban areas is usually very high (100-300 PS/km<sup>2</sup>). However, many ground deformation phenomena (e.g. tectonic motion, volcanoes, landslides, mining, gas extraction, CO<sub>2</sub> sequestration) occur in uninhabited or rural areas with few man-made structures, leading to much lower PS density because of significant phase decorrelation between subsequent SAR acquisitions. In order for PSI to be effective in monitoring these areas, it has been found that a PS density greater than about 10 PS/km<sup>2</sup> is required. Artificial amplitude- and phase-stable radar scatterers may thus have to be introduced in non-urbanised geodynamic areas that have too low a density of PS points.

Conceptually the simplest of these artificial PS points are corner reflectors. Several experiments have been performed in the past using these reflectors, with conclusive results about their amplitude and phase stability. They suffer, however, from the disadvantage of large size (in the order of a metre in case of C-band SAR). To make these artificial PS points easy to deploy and maintain, especially in poorly accessible areas, Compact Active Transponders (CATs) have been designed to be used in lieu of corner reflectors. These CATs are small (in the order of a few tens of centimetres), lightweight (<3 kg), less obtrusive, and have the added advantage of a better link budget due to signal amplification by the transponder. They are sealed, function autonomously with internal power and over a wide temperature range, and can operate unattended for more than a year. Additionally, since a CAT is transmitter-specific and is only turned on at the time of the satellite overpass, it offers little interference to other radar or radio targets. However, it is of paramount importance in geodetic applications to ensure that the phase of the CAT remains stable in all operating and environmental conditions.

Towards this goal, an experiment to validate the phase stability of CATs has been set up in a farmland in Delft (The Netherlands). The setup comprises three CATs and three corner reflectors, which are installed at distances of a couple of hundred metres from each other. SAR data from the ERS-2 Ice-Phase Mission are being acquired every three days between March and June 2011. Since the area does not exhibit steady ground deformation, some of the units are displaced vertically by a controlled amount. Levelling is performed between the CATs and the corner reflectors as close as possible to each SAR acquisition, in order to validate the height differences



obtained from the radar phase information. As a second means of validation, campaign-style GPS is performed on each of the devices to accurately position them in WGS-84 coordinates. One of the CATs in the Delft field experiment has an integrated GPS antenna, to ensure millimetric coregistration and a coherent cross-reference. This novel unit called I2GPS (Integrated Interferometry and GNSS for Precision Survey) has been developed with the objective of producing a fully-integrated deformation map. In addition to providing absolute calibration for PSI data, the high temporal sampling rate of GPS data imparts the capability of accurately detecting abrupt ground motion in three dimensions. With adequate GPS/I2GPS units, the vertical components of the local velocity field can be derived from single-track InSAR line-of-sight displacements. The results and conclusions of this experiment consisting of corner reflectors, CATs and I2GPS will be presented and analysed here.



# Session: Volcanoes

## InSAR and thermal monitoring of lava fountain episodes at Mt. Etna: the case study of the ASI-SRV Pilot project during the January 2001 episode

### Author(s)

Giuseppe Puglisi <sup>(1)</sup>, Massimo Aranzulla <sup>(1)</sup>, Boris Behncke <sup>(1)</sup>, Stefano Branca <sup>(1)</sup>,  
M. Fabrizia Buongiorno <sup>(1)</sup>, Mauro Coltelli <sup>(1)</sup>, Francesco Casu <sup>(2)</sup>,  
Emanuela De Beni <sup>(1)</sup>, Francesco Guglielmino <sup>(1)</sup>, Massimo Musacchio <sup>(1)</sup>,  
Cristina Proietti <sup>(1)</sup>, Eugenio Sansosti <sup>(2)</sup>, Malvina Silvesti <sup>(1)</sup>, Giuseppe Solaro <sup>(2)</sup>, Letizia Spampinato <sup>(1)</sup>,  
Simona Zoffoli <sup>(3)</sup>

### Department

<sup>(1)</sup>Istituto Nazionale di Geofisica e Vulcanologia , IT

<sup>(2)</sup>Consiglio Nazionale delle Ricerche , IT

<sup>(3)</sup>Agenzia Spaziale Italiana , IT

### Abstract

Mt. Etna is characterized by almost continuous volcanic activity at the summit craters, which ranges from quiet degassing to periodic explosions. Intensity of the explosions varies from strombolian activity to fire fountains. Lava fountain episodes are controlled by processes that originate in the shallow part of the plumbing system and their geophysical effects may give information on the eruptive dynamics, as well as on the geometry of conduits and stocking volumes in the plumbing system. Recent fountain episode occurred during the night between 12 and 13 January 2011 allowed applying EO techniques, implemented in the frame of the ASI-SRV Project, for monitoring its effects both on ground deformations, thermal anomalies and emplaced volcanic products. In particular, in this contribution we consider a) the results of the analysis SAR data either from Cosmo Sky-Med and ASAR ENVISAT sensors, to define the ground deformation pattern associated with the lava fountain episode and the distribution of the volcanic deposits associated with it, b) the results of the NOAA-AHVRR and MODIS data to estimate the effusion rate of the eruption and the distribution of the thickness of the volcanic aerosols (AOT) and c) the volcanological and geophysical ground data suitable to validate the EO results (e.g., volcanic deposits, path delay). In particular, the Cosmo-SkyMed sensors SAR2 and SAR3, which are in a 1-day tandem configuration, acquired just across the mentioned fountain episode. In the framework of the CAT-1. 5843, we also produced an interferogram relevant to the 12 December 2010 – 20 January 2011 passes, profiting of the ENVISAT mission extension beyond the end of 2010, which allows to (a) operate the mission for an additional 3 years (until end of 2013 or early 2014) and (b) ensure the continuity of the InSAR applications at latitude of around 38° North for descending passes. Both interferometric products (Cosmo-SkyMed and ENVISAT) show a relatively small and limited deformation around the summit area, at elevations above the 1500-2000 m. The interferometric fringes, suggest a deflation that might be related to the emptying of the shallow magmatic reservoir, although an atmospheric component cannot be definitively excluded. In the framework of the ASI-SRV project, the analysis of the NOAA-AVHRR data provide the effusion rate of the lava fountain, which show a maximum in the late evening of 12 January, while the analysis of MODIS data allow estimating the optical thickness of the AOT. Furthermore, the interferometric products show two highly decorrelated areas: the first, in the “Valle del Bove” area, trending ESE, corresponds to the lava flow emplaced during the fire fountain episode; the second, in the summit area, trending SSW, corresponds to the fall-out deposit of the largest (> 3 cm) pyroclasts around the SEC. These preliminary analyses well fit with the data acquired by the monitoring systems

managed by the INGV Sezione di Catania – Osservatorio Etneo (GPS, tilt, seismic) and field and helicopter surveys. Working in progress are aimed at evaluating the atmospheric effects on the interferograms using the GPS signals acquired by the permanent network of INGV and at modelling the ground deformations by integrating InSAR and other geodetic data.

## 3D temporal evolution of displacements recorded on Mt. Etna from the 2007 to 2010 through the SISTEM method

### Author(s)

Francesco Guglielmino <sup>(1)</sup>, Alessandro Bonforte <sup>(1)</sup>, Giuseppe Puglisi <sup>(1)</sup>

### Department

<sup>(1)</sup>INGV Istituto Nazionale di Geofisica e Vulcanologia, Piazza Roma, 2, Catania, IT

### Abstract

A study of the ground deformation pattern of Mount Etna volcano, based on the results of the SISTEM (Simultaneous and Integrated Strain Tensor Estimation from geodetic and satellite deformation Measurements) integration method is reported. This new approach is aimed to combine geodetic and satellite data in order to derive the 3D ground displacement components and the complete strain tensor. Combining GPS and DInSAR data allows us to take advantage of their complementary nature. Indeed, GPS measures are point-wise three dimensional data characterized by high time resolution. On the other hand, DInSAR measures provide mono-dimensional spatially distributed data characterized by a low time resolution (namely 35 days for Envisat data). Adequately integrating these data it is possible to produce high resolution three dimensional ground deformation maps over the whole investigated area. In this work ground motion data provided by GPS surveys are integrated with the interferometric synthetic aperture radar (InSAR) Envisat data, collected from 2007 to 2010, to provide 3D displacements maps. We imaged the time evolution of ground displacement measured along the Line Of Sight (LOS) of the Envisat satellite also using the Permanent Scatterers (PS) technique developed into the StaMPS (Stanford Method for PS) package for both ascending and descending Envisat geometries. The main deformation episode occurred on Mt. Etna during the 2007-2010 time period was the 2008-2009 eruption. It started on May 13th, 2008, with the opening of an eruptive fissure propagating inside the topographical depression of the Valle del Bove, where the lava flows expanded. The eruption produced a lava flow of about 6 Km length, and it was preceded and accompanied by strong seismic release, and lava fountaining activity. The 3D temporal evolution of ground deformation was analyzed in order to define the dynamics preceding, accompanying and following the 2008-2009 Mt. Etna eruption. In particular, this analysis reveals a slight inflation visible on the upper western side of the volcano in the pre-eruptive period (from June 2007 to May 2008) characterized by a small amplitude of the ground deformation, except on the eastern flank. In the period across the eruption onset, the main ground deformation occurred around the summit craters, in the nearby of the eruptive fissures. The displacement pattern reveals also a rapid decay of the deformation gradient with the altitude confirming the shallow depth of the intrusion. The northward dyke propagation, occurred after the beginning of the eruption, was well detected by reconstructed displacement maps; it was confirmed by on field structural surveys that revealed a dry fracture field, propagating from the summit area towards the NNW direction for about 2.5 km. In the post-intrusion period (from May to November 2008), a slight deflation of the volcano is visible, suggesting the presence of a depressurizing source, localized beneath the upper south-western area, feeding the eruption. The last period analyzed (from 2009 to 2010) was characterized by a new inflation phase of the volcano, coupled with an acceleration of the eastern flank seawards motion. In this work, the SISTEM method was efficiently applied to integrate the GPS and InSAR data sets, and the results show that the reconstructed deformation pattern is in

good agreement with the geophysical and volcanological knowledge of the dynamics of Mt. Etna during the 2007-2010 period.

## Long-term experience gathered on Etna for volcano monitoring using radar and optical remote sensing, in preparation for Sentinel Missions

### Author(s)

Giuseppe Puglisi <sup>(1)</sup>, Pierre Briole <sup>(2)</sup>, M. Fabrizia Buongiorno <sup>(1)</sup>,  
Fabiano Costantini <sup>(3)</sup>, Francesco Guglielmino <sup>(1)</sup>, Valerio Lombardo <sup>(1)</sup>,  
Mattia Marconcini <sup>(3)</sup>, Antonio Mouratidis <sup>(3)</sup>, Francesco Sarti <sup>(3)</sup>,  
Claudia Spinetti <sup>(1)</sup>, Salvatore Stramondo <sup>(1)</sup>

### Department

<sup>(1)</sup>Istituto Nazionale di Geofisica e Vulcanologia , IT

<sup>(2)</sup>Ecole Normale Supérieure , FR

<sup>(3)</sup>ESA, IT

### Abstract

The implementation of the future ESA Sentinel missions represents a unique opportunity for improving the capabilities of the Earth Observation (EO) systems for geophysical monitoring, and in particular for active volcanoes. The different satellites and sensors planned within the mission will greatly increase the amount and quality of available information on volcanic areas. The first satellites of the Sentinel missions (Sentinel-1A and 1B) will continue the SAR operational application by using C-band sensors to monitor the ground deformations, which began with ERS1/2 and continued with Envisat. This constellation, when fully implemented, will allow a revisit time of six days at the latitudes of Mt. Etna, which represent a significant step forward of the monitoring capabilities with respect to the current operative conditions, by using either single interferograms or time series analysis. Sentinel-2 constellation is aimed at continuing and enhancing the SPOT- and Landsat-type multi-spectral data set particularly suitable for map volcanic plume features and for land-cover mapping of volcanic areas. In this presentation, the experience gathered during the last decade by using the data of past and current EO systems on the Mt. Etna volcano is discussed in view of providing essential guidelines for the Sentinel missions. The large datasets available for Mt. Etna, both from optical and radar sensors, together with its almost continuous volcanic activity gave the opportunity to scientists to implement, test and apply many algorithms and methods for processing EO data, confirming the role of Mt. Etna as a natural laboratory. Indeed, on Mt. Etna was applied for the first time the SAR Interferometry for studying ground deformation on volcanic area. This early study spurred the investigation on tropospheric effects on SAR signals, which produced a long series of worldwide researches that continue until now. Finally, among the numerous algorithms or approaches planned, implemented and/or tested on this volcano, for ground deformation monitoring, we include also the algorithm for the SAR time series analysis (PS and SBAS). Analogous fundamental studies were carried out on thermal monitoring of this volcano on the detection of both the lava flow and the vents. Furthermore, the large number of ground data collected by INGV was also crucial to assess the EO data. Thanks to the continuous volcanic activity of Mt. Etna, a few study cases, relevant to significant eruptive periods, are considered for showing the capability of EO system to provide valuable data for studying active volcanoes. The EO data discussed in this presentation indicate that the 2001 eruption was the event that characterizes the activity of this volcano during the last decade. Particular care is also devoted to discuss the extension of the Envisat mission through to 2013, considered as a bridge between the current and the future missions for Mt. Etna and many other significant geodynamic areas located at +/- 38° +/- 4° of latitude. Finally, the new

possibilities offered by the sensors on board the Sentinel mission are discussed, focusing particular attention on radar (Sentinel 1) and optical (multispectral; Sentinel 2) sensors, performing also some simulations considering similar data already acquired on Mt. Etna during past airborne missions.

## Source models for the March 5-9, 2011 Kamoamoia fissure eruption, Kilauea Volcano, Hawaii, constrained by InSAR and in-situ observations

### Author(s)

Paul Lundgren <sup>(1)</sup>, Michael Poland <sup>(2)</sup>, Asta Miklius <sup>(2)</sup>, Sang-Ho Yun <sup>(1)</sup>, Eric Fielding <sup>(1)</sup>, Zhen Liu <sup>(1)</sup>, Akiko Tanaka <sup>(3)</sup>, Walter Szeliga <sup>(1)</sup>

### Department

<sup>(1)</sup>California Institute of Technology , USA

<sup>(2)</sup>USGS - Hawaiian Volcano Observatory , USA

<sup>(3)</sup>AIST , JP

### Abstract

On March 5, 2011, the Kamoamoia fissure eruption began along the east rift zone (ERZ) of Kilauea Volcano. It followed several months of pronounced inflation beneath Kilauea's summit and was the first dike intrusion into the ERZ since June 2007. The eruption began in the late afternoon of March 5, 2011 (Hawaii Standard Time; UTC-10:00 hrs) with rapid deflation beginning at Pu'u 'O'o on the ERZ and about 30 minutes later at the summit. Magma from both locations fed the intrusion and an eruption that included lava fountaining along a set of eruptive fissures ~2 km in length between Napau and Pu'u 'O'o. The eruption continued, jumping between fissure segments, until all activity terminated on the night of March 9. A rich InSAR data set exists for this eruption from the COSMO-SkyMed (CSK), TerraSAR-X (TSX), ALOS PALSAR, and UAVSAR sensors. CSK data acquired on March 7 and processed that same day provided the earliest, quasi-real-time SAR data for this event. By March 10, when the eruption had ended, we had three CSK acquisitions and one ALOS scene acquired and processed. At present we have the following satellite data (UTC dates): ALOS March 6, 9, 11; CSK March 7, 10, 11; TSX March 11; from a mixture of ascending and descending tracks. UAVSAR airborne SAR data that were acquired in early May 2011 should provide enhanced resolution and viewing geometries perpendicular to the satellite look directions. SAR data were acquired on all days of the eruption except March 8, allowing us to examine the progression of the dike opening beneath the surface with excellent spatial and temporal resolution. We use a combination of unwrapped differential interferograms, azimuthal pixel offsets, and in-situ data from GPS and borehole tiltmeters. GPS and tilt data are from the Hawaiian Volcano Observatory's continuous network, augmented by survey GPS occupations closer to the eruption area. Continuous tilt measurements are concentrated near Kilauea's summit and Pu'u 'O'o, with one site in between to help constrain dike propagation. SAR data were processed using the JPL/Caltech ROI\_PAC software. To model the sources we use a Markov Chain Monte Carlo optimization. At Kamoamoia, we fixed the surface location of the dike based on field observations and solved for the opening distribution using Laplacian smoothing for a multi-patch dike. Preliminary models of the dike show 1-2 meters of dike opening at the beginning of the eruption, reaching 2-3 meters of opening by the end of the eruption. The shape of the dike is somewhat irregular, extending from the surface to a depth of roughly 3 km with a tail of opening that extends back toward Kilauea's summit in the 2-3 km depth range and a less clearly resolved extension toward Pu'u 'O'o crater to the east, where the floor collapsed by about 115 m at the start of the eruption. Separately, we solve for Kilauea caldera source(s) that produced clear and distinct fringe patterns, especially at X-band. Preliminary results for the summit favor a shallow source centered at roughly 1.5 km depth beneath the eastern rim of Halemaumau crater and

extending in a SW-NE direction. Initial estimates of the volume changes indicate less than 2 MCM (million cubic meters) at the summit compared to nearly 20 MCM for the dike. This difference suggests that much of the magma came from sources other than the shallow Kilauea summit reservoir.

## Subsidence of the collapsed caldera of Miyakajima, Japan, 2006-2009

### Author(s)

Yosuke Aoki <sup>(1)</sup>, Emily Montgomery-Brown <sup>(2)</sup>

### Department

<sup>(1)</sup>University of Tokyo, JP

<sup>(2)</sup>University of Wisconsin-Madison, USA

### Abstract

Miyakejima is one of an active volcano along the Izu-Bonin arc with major eruptions in 1940, 1962, 1983, and 2000-2009. In 2000, lateral magma migration out of the volcano created a caldera with a diameter of 1.7 km and depth of 500 m (e.g., Nakada et al., 2005). The caldera is formed more or less to the present shape in about a month. The shape of the collapsed caldera is bowl-shaped but asymmetric with a floor to the northwest (Geshi, 2009). Abundant gas emission accompanied the activity. The amount of SO<sub>2</sub> emission rose up to 25,000 t/day right after the eruption; it decreased afterwards but still at a level of 1000-3000 t/day during 2006-2009. Such abundant and sustained gas emission would result in subsidence of the surface. Here we derived the deformation field of Miyakejima between 2006 and 2009 from Synthetic Aperture Radar (SAR) data taken from PALSAR on the ALOS satellite. Note that SAR data is the only way to delineate the deformation field around the summit because no continuous Global Positioning System sites exist there. We first processed all possible pairs of SAR data between September 2006 and December 2009 taken from the ascending and descending orbits. Note that the observed line-of-sight (LOS) change is a linear combination of horizontal and vertical components of deformation as  $dLOS = 0.616U_e + 0.111U_n - 0.780U_v$  for ascending interferograms and  $dLOS = -0.616U_e + 0.111U_n - 0.780U_v$  for descending images, respectively, where  $dLOS$  is the observed LOS change, and  $U_e$ ,  $U_n$ , and  $U_v$  represent the east, north, and vertical component of the deformation, respectively. We picked up interferograms with good coherences. Next we performed a time series analysis (Schmidt and Burgmann, 2003) with the interferograms picked up above. Our result shows that the deformation rate is small with less than 20 mm/yr of LOS change everywhere on the island except for an area around the summit. The rate of LOS change is the largest at the lowest part of the collapsed caldera and gradually became smaller toward the caldera rim and beyond. It is larger in 2007-2008 than 2008-2009. At the caldera bottom, the observed rate of the LOS change between 2007 and 2008 is 143.2±1.3 mm/yr from ascending images and 120.7±1.8 mm/yr from descending images, respectively. As a next step, we constructed a model to explain the observed deformation field. We first examined an appropriate source to explain the observed deformation by examining the ratio of the horizontal to vertical displacement. Note that we can roughly extract the east and vertical components by taking advantages of the observations from both ascending and descending orbits. The observed deformation field shows that the horizontal displacement is too small to be explained by a spherical source and that the observed deformation field should be explained by a closing sill. The sill that best fits to the observation is located at 500 meters below sea level with its closing rate at 0.3 million cubic meters per year. To have the observed sulfur dioxide emission of 1000 tons/day solely from the sill compaction requires a closing rate of 40 million cubic meters per year when assuming a sulfur dioxide concentration of 0.17 % (Saito et al., 2005), much larger than the modeled sill compaction rate. This indicates that the observed degassing cannot be explained

by the sill compaction modeled in this study but another mechanisms need to be invoked. The observed subsidence can be physically interpreted as gravity compaction of a piston column which has been fractured when the collapsed caldera was formed during the 2000 eruption due to the magma outflow. The column was presumably fractured both at shallow and deeper levels right after the collapse, and deeper part was consolidated earlier than the shallower part due to the higher compressional stress, leading to the observation that the compaction is ongoing at shallower level only during 2006-2009.

## Pulses of Deformation Reveal Frequently Recurring 1 Shallow Magmatic Activity Beneath the Main Ethiopian Rift

### Author(s)

Juliet Biggs <sup>(1)</sup>, Derek Keir <sup>(2)</sup>, Ian Bastow <sup>(1)</sup>, Elias Lewi <sup>(3)</sup>

### Department

<sup>(1)</sup>University of Bristol Wills Memorial Building, UK

<sup>(2)</sup>National Oceanography Centre Southampton, UK

<sup>(3)</sup>University of Addis Ababa , ET

### Abstract

Pulses of Deformation Reveal Frequently Recurring Shallow Magmatic Activity Beneath the Main Ethiopian Rift Magmatism strongly influences continental rift development yet the mechanism, distribution and timescales on which melt is emplaced and erupted through the shallow crust are not well characterised. The Main Ethiopian rift has experienced significant volcanism during the past 30 Ma and the mantle beneath is characterised by high temperatures and partial melt. Despite its magma-rich geological record, only one eruption has been historically recorded, and no dedicated monitoring networks exist. Consequently, the present-day magmatic processes in the region remain poorly documented, and the associated hazard neglected. As part of the ESA Changing Earth Science Network, we use data from the ERS and Envisat background mission to systematically study the East African Rift. We demonstrate that significant deformation has occurring at 4 volcanic edifices in the MER (Alutu, Corbetti, Bora and Haledebi) from 1993- 2010. This raises the number of volcanoes known to be deforming in East Africa beyond 12, comparable to many subduction arcs despite the smaller number of recorded eruptions. The largest displacements are at Alutu volcano, the site of a geothermal plant, which showed two pulses of rapid inflation (10-15 cm) in 2004 and 2008 separated by gradual subsidence. Our observations indicate a shallow (<10 km), frequently replenished zone of magma storage associated with volcanic edifices and add to the growing body of observations that indicate shallow magmatic processes operating on a decadal timescale are ubiquitous throughout the East African Rift. Furthermore, this study demonstrates the power of systematically exploring data archived during the ERS and Envisat background missions, and suggests that many more exciting signals remain to be discovered.



# Long-term uplift due to deep magma bodies: Insights from ERS and ENVISAT observations

## Author(s)

Yuri Fialko <sup>(1)</sup>, Jill Pearce <sup>(2)</sup>

## Department

<sup>(1)</sup>UCSD, USA

<sup>(2)</sup>Canadian Geological Survey, CA

## Abstract

We present InSAR observations of long-term deformation due to the two largest known magma bodies in the Earth's continental crust, the Socorro Magma Body (SMB) in New Mexico, USA, and the Altiplano-Puna Magma Body in South America. ERS and ENVISAT spanning 18 years (1992-2010) reveal that both magma bodies are associated with a steady uplift surrounded by a broader zone of subsidence. The rate of uplift is 2-3 mm/yr in case of the Socorro Magma Body, and 8-10 mm/yr in case of the Altiplano-Puna Magma Body. In both cases the inferred sources of inflation appear to reside in the middle crust at depth of 18-19 km. Peripheral subsidence is most likely associated with melt withdrawal from an extended source region in the middle or lower crust. We interpret the apparent constancy of the present-day uplift rate in terms of slow heat transfer and viscous deformation in a metamorphic aureole of a large mid-crustal intrusion, rather than due to a steady increase in the magma overpressure. We propose that the observed uplift and peripheral subsidence are associated with formation and buoyant ascent of large granitic diapirs. We present results of finite element simulations of "ballooning" of diapirs in the viscoelastic middle/lower crust underlying the elastic upper crust. Our numerical models indicate that ductile deformation associated with deep magma bodies may bias inversions of surface uplift for the source geometry that are based on the assumption of a pressurized source in an elastic half-space. In particular, viscous relaxation below the brittle-ductile transition decreases the ratio of maximum horizontal to maximum vertical displacements at the Earth's surface, thereby biasing elastic half-space inversions toward more oblate (sill-like) source geometries. InSAR observations of deformation due to deep magmatic unrest may shed light on the mechanisms and dynamics of generation and transport of granitoid magmas from the source regions to their final emplacement levels in the upper crust.

# Eighteen years of InSAR observations at Fernandina volcano, Galápagos: dynamics of magma storage and eruption

## Author(s)

Marco Bagnardi <sup>(1)</sup>, Falk Amelung <sup>(1)</sup>, Scott Baker <sup>(1)</sup>

## Department

<sup>(1)</sup>University of Miami 4600 Rickenbacker Cswy, 33149 Miami, FL, USA

## Abstract

Six volcanoes in the western Galápagos Islands of Isabela and Fernandina have been actively deforming since at least 1992 and three of them have erupted in the last decade. Among these, Fernandina can be considered the most active volcano in the archipelago, having experienced 25 eruptions since 1813 and three eruptions in the last sixteen years: 1995, 2005 and 2009. Because of their geographic isolation and difficult working conditions, permanent geodetic monitoring for Fernandina and the other western Galapagos volcanoes began only ten years ago. The use of

detailed Interferometric Synthetic Aperture Radar (InSAR) measurements of surface deformation represents a unique opportunity to study magmatic processes in such a location. We used SAR data acquired by the European Space Agency satellites ERS-1, ERS-2 and ENVISAT between 1992 and 2010, when the two satellites changed their orbits. Data from five different tracks that fully cover Fernandina Island provided independent measurements of ground deformation. The advantage of using different viewing geometries is that by combining ascending and descending interferograms we can infer the vertical and one horizontal component of the surface displacement, and better constrain the geometry of subsurface sources of deformation. We generated more than 600 interferograms and we applied the Small Baseline Subset (SBAS) method to investigate the temporal evolution of ground deformation. Fernandina Island is characterized by an almost continuous displacement of an elliptical area limited by the caldera rim; this pattern is occasionally interrupted by short-lived episodes that displace a larger surface that extends to almost the entire island. These episodes are mostly related to eruptive and major seismic events: co-eruptive/co-seismic deformation is characterized by the subsidence of almost the entire portion above sea level of the island; post-eruptive/post-seismic interferograms show the re-inflation of the same area. LOS displacements inside and outside the caldera show different characteristics: while fringes inside the caldera have small amplitude and suggest a relatively shallow source, those that extend outside of it, when present, cover an elliptical area whose major axis is perpendicular to the one of the caldera, and have larger amplitude. These characteristics suggest the presence of a second, distinct, deeper source of deformation also centered under the summit. We performed a non-linear inversion of the InSAR data and modeled the observed deformation as the surface expression of intra-crustal magmatic activity of multiple sources. We inferred the presence of a sill-like reservoir at ~1 km depth and of a deeper source at ~6 km depth. Both magmatic sources are located below the summit caldera and do not show important variations in their geometry and position through time. We also studied the details of the last three eruptions, in particular the most recent one: during the night between 10-11 April, 2009 a radial fissure about 200 meters long, opened on the southwestern flank of the volcano. An image acquired on April 10, at 8am local time, does not show any signs of deformation except for the years-long caldera uplift. A second SAR image acquired on the same day, at 9pm and just a few hours before the opening of the first eruptive vent, shows distinct uplift (maximum displacement: ~0.40 m) of a circular area centered below the southwestern caldera rim. This pattern of deformation represents the surface displacement generated by the intrusion of a sheet-like body from a shallow magma reservoir towards the surface. The eruption ended on April 28, and the SAR interferograms produced using images acquired before, during (April 17) and after (May 5-15-16-22) the eruption, allow us to study its effects. The pattern of deformation generated by this event resulted to be very similar to the one generated by the January 1995 eruption. Further insight into the structure of Fernandina volcano is provided by SAR acquisitions spanning the May 2005 eruption: they represent the first circumferential dike intrusion ever observed by InSAR and a unique opportunity to study these particular structures very common on Galápagos volcanoes.

# Tectonic control of magma ascent in volcanic arcs: Space-geodetic evidence from the West-Sunda arc, Indonesia

Author(s)

Estelle Chaussard <sup>(1)</sup>, Falk Amelung <sup>(1)</sup>

Department

<sup>(1)</sup>Rsmas, USA

## Abstract

A large proportion of the world's population lives on or near active volcanoes. Ground deformation measurements are key observations for volcano monitoring because they can identify precursory uplift caused by ascent of new magma towards the surface. Moreover interpretations of geodetic data in terms of depth of magma accumulation play a major role in volcanic hazard assessment. If a volcanic chamber is located close to the surface it is usually associated with a higher risk for significant eruption. We conducted the first global survey of the West-Sunda volcanic arc using differential InSAR combined with SBAS-time series analysis. The D-InSAR survey covers an area of about 500 000 km<sup>2</sup> and 3000 km long on the islands of Sumatra, Java and Bali. We used ALOS data from 35 tracks and more than 1500 granules to complete more than 1000 interferograms spanning a period from late 2006 to early 2009. L-band SAR images (such as PALSAR onboard ALOS) enable deformation mapping at global scales even in highly vegetated areas where C-band signal experiences loss of coherence. The compiled ground velocity map reveals the background level of activity of the 84 volcanic centers of the arc and provides data for previously unmonitored volcanoes. We identified uplift at 6 volcanic centers and subsidence at 2 edifices. Interestingly, 3 of the 6 uplifting centers erupted after the time period of our survey, suggesting that edifice inflation is a precursor of eruptions. The 3 uplifting centers that have not yet erupted have all been historically active, emphasizing the importance of this type of surveys to improve hazard assessment and warning. Models of the measured deformation give quantitative estimates of the depths of the magmatic sources. By assuming that deformation is caused by changes of pressure at depth due to injection or withdrawal of magma or hydrothermal fluids, we inverted the time-series for magma chambers geometries in an elastic half-space. McTigue models reveal that the sources of deformation at the 6 inflating centers are located at shallow depths, less than 3km under the sea level. Magma is less dense than the rocks in the upper mantle and lower crust and rises from depth towards the Earth's surface because of buoyancy. If the contrast of density, and the associated forces of buoyancy, controls the depth at which magma chambers typically develop, magma is expected to pond around the depth where it first encounters a crustal density similar to its density, in the lower part of the range of neutral buoyancy. When an Andesitic magma rises from depths, it encounters a crustal density similar to its density (2.5-2.6 g/cm<sup>3</sup>) at depths starting 7 to 4km, depending on the crustal thickness and its associated density distribution. Magma chambers around these depths are found in most volcanic arcs, such as the Central Andes [Pritchard, 2004; Pritchard and Simons, 2004] but other arcs, such as the Aleutian and Costa-Rica, present, in addition to magma chambers around 4km depth, shallow chambers, above 4km, in the upper level of the range of neutral buoyancy [Lu et al., 2002; Lu, 2007; Alvarado et al., 2006]. Our survey of the West-Sunda arc additionally revealed that six volcanoes in Sumatra, Java and Bali, present magma reservoirs above 4km depth. A global analysis shows an inverse correlation between the observed reservoir depth in volcanic arcs and the vertical stress and an inverse correlation between chamber depth and heat flow. This suggests that volcanoes in extensional and strike slip settings are more likely to accumulate magma in shallow reservoirs, because of a reduced shear stress needed to break through the crust, an elevated heat flow and the presence of tectonic structures creating pathways for the rising magma. The virtue of shallow magma

chambers is that volume changes related to the arrival of new magma can be readily detected using space geodetic measurements without any ground-based monitoring networks, facilitating volcanic hazard assessment.

## InSAR measurements of volcanoes in the tropics: examples from a survey of the Central American Volcanic Arc

### Author(s)

Susanna K Ebmeier <sup>(1)</sup>, Juliet Biggs <sup>(2)</sup>, Tamsin A Mather <sup>(1)</sup>, Falk Amelung <sup>(3)</sup>

### Department

<sup>(1)</sup>University of Oxford South Parks Road, Oxford, OX1 3AN, UK

<sup>(2)</sup>University of Bristol Queen's Road, Bristol, BS8 1RJ, UK

<sup>(3)</sup>University of Miami 4600 Rickenbacker Causeway, FL 33149, USA

### Abstract

InSAR measurements of deformation from the Central American Volcanic Arc appear to show less deformation than other arcs with similar levels of volcanic activity. We use three years of L-band ALOS (2007-2010) interferograms to test whether this is a result of the inherent ambiguities in interpreting interferometric data from tropical volcanoes, or is indicative of differences in volcanic processes between Central America and other parts of the world. L-band ALOS data provide the first opportunity for arc-scale surveys of Central America, as C-band radar is unable to penetrate dense vegetation. We now have a dataset of three years of interferograms over Central America, allowing an early comparison with other volcanic arcs. Volcanoes in the tropics present particular challenges for InSAR measurement. On top of the potential for decorrelation presented by steep, unstable slopes, volcano morphology commonly causes highly variable ramps in tropospheric water vapour, creating phase delays over the volcano summit. These are of particularly high magnitude in the tropics, where seasonal variations in water vapour are the largest in the world. In Central America, phase variation over the majority of volcanoes is dominated by topographically correlated, stratified tropospheric water vapour. The root mean squared variation in phase delay in time-series for active volcanoes shows a correlation with edifice height and has a maximum value of about 8 and a mean of  $\sim 2$  cm. We also observe phase artefacts caused by DEM errors at a few volcanoes. The most significant of these is at Santiaguito lava dome in Guatemala, where we were able to estimate the thickness of lavas emplaced since 2000 from the DEM error. We develop a systematic method to distinguish between atmospheric or geometric artefacts and actual ground deformation, based on identifying diagnostic characteristics for artefacts in the spatial and temporal structure of phase. We do this using evidence from a range of tools, including time series analysis, stacking and tests of phase properties. We find no measurable magmatic deformation in Central America. The Central American Volcanic Arc is made up of over 70 Holocene volcanoes, of which 26 are historically active. InSAR measurements were possible at 19 of these active volcanoes, which include a diverse range of systems: both basic and sillicic, open and closed and passively and explosively degassing. Of these, persuasive evidence for deformation was found only at Arenal, Costa Rica, where it is confined to a section of the volcano edifice loaded by young lavas and is structural, rather than magmatic in origin (Ebmeier et al., 2010). We estimate upper bounds for any deformation taking place at other active volcanoes which could lie below the limits of our measurement. These limits depend both on the atmospheric variability at different volcanoes and on the duration and spatial extent of any deformation, and are therefore different for transient and steady deformation. We expect to observe any permanent deformation above a magnitude of 1-2 cm (corresponding, for example, to a steady rate deformation  $> 0.7$  cm/yr over three years), while any transient deformation may have to significantly exceed a magnitude of  $\sim 8$ cm to be detectable above atmospheric variation at some volcanoes. Of the 35 InSAR observations of deformation in the Aleutians and Andes made

to date [e.g. Fournier et al., 2010], only about 9 would have been unobservable with the average limitations of deformation and rate found in Central America. This seems to suggest that there is a lack of significant shallow magma storage in Central America relative to other parts of the world. However, the short survey time (3 years) relative to periods of observation in other areas (e.g. ~18 years in parts of the Andes) means that this conclusion remains tentative. References: Ebmeier, S.K., J. Biggs, T. A. Mather, F. Amelung. (2010) Steady downslope movement on the western flank of Arenal volcano, Costa Rica. *Geochemistry, Geophysics, Geosystems*, 11, 12, Q12004. Fournier, T. J., M.E. Pritchard and S.N. Riddick. (2010) Duration, magnitude, and frequency of subaerial volcano deformation events: New results from Latin America using InSAR and a global synthesis, *Geochemistry, Geophysics, Geosystems*, 11, 1, Q01003.

## High resolution monitoring of Campi Flegrei (Naples, Italy) by exploiting TerraSAR-X data: an application to Solfatara crater

### Author(s)

Christian Minet <sup>(1)</sup>, Kanika Goel <sup>(1)</sup>, Ida Aquino <sup>(2)</sup>, Rosario Avino <sup>(2)</sup>,  
Giovanna Berrino <sup>(2)</sup>, Stefano Caliro <sup>(2)</sup>, Giovanni Chiodini <sup>(2)</sup>,  
Prospero De Martino <sup>(2)</sup>, Carlo Del Gaudio <sup>(2)</sup>, Ciro Ricco <sup>(2)</sup>, Valeria Siniscalchi <sup>(2)</sup>, Sven Borgstrom <sup>(2)</sup>

### Department

<sup>(1)</sup> German Aerospace Center (DLR) IMF, Münchner Strasse 20, 82234 Wessling, DE

<sup>(2)</sup> INGV OV, via Diocleziano, 328, 80124 Naples, IT

### Abstract

Geodetic monitoring of Campi Flegrei caldera, to the west of Naples (Italy), has been historically carried out via an integration between ground based networks and space-borne Differential InSAR (D-InSAR) techniques, exploiting the SAR sensors onboard ERS1-2 and ENVISAT satellites. Unfortunately, the use of C-band sensors could result sometimes in no information when dealing with very low deformation rates. To overcome this problem, from December 2009 we decided to use TerraSAR-X from DLR, a high resolution SAR sensor operating in the X-band. TerraSAR-X Spotlight scenes covering the main part of the Campi Flegrei caldera and centred on the Solfatara crater were used for a D-InSAR analysis, using DLR's operational InSAR software GENESIS. The first two scenes (Dec. 15 and 26, 2009) of the dataset were acquired with a temporal baseline of only one repetition cycle (11 days) and formed an interferogram with a very small perpendicular baseline (16.5 m). Apart from some minor atmospheric effects, the interferogram shows a small but clear deformation signal in the Pisciarelli area, close to the east side of the Solfatara crater. The deformation event highlighted by D-InSAR analysis is consistent with geochemical observations carried out in the area, which is seat of a fumarolic field systematically monitored in the frame of the volcanic surveillance of the Campi Flegrei caldera. Starting from this period, many field surveys highlighted a strong fumarolic activity, recorded also by seismic stations and borehole tiltmeters with clear temperature variations. Considering the particular trend of the Solfatara - Pisciarelli area in the last period, we decided to increase monitoring activities. Many geodetical and geochemical observations, including new levelling and gravimetric measurements are integrated with data from GPS and tiltmetric permanent stations. Furthermore, the growing stack of high-resolution spotlight TerraSAR-X data is processed using the Small Baseline Subset Algorithm (SBAS). DLR's GENESIS InSAR system has been upgraded for this technique which is especially suited to detect and monitor non-linear deformations, as they can be expected in a highly active fumarolic field. SBAS makes use of small baseline differential interferograms to limit spatial and temporal decorrelation and then applying single value decomposition (SVD) to link independent interferogram subsets in time. Non-linear deformation can be estimated without any modelling and prior knowledge even in areas where coherence is low. Finally, the 2009 event proves the high potential of TerraSAR-X High Resolution Spotlight data in monitoring volcanic

activity with a resolution suitable for detecting also minor, but possibly dangerous, changes of the systems, as it could be in the early recognition of the signals generated by impending phreatic eruptions. First results of the SBAS processing and the combination of different observation techniques will be presented.

## Analysis of the Eyjafjallajökull 2010 eruption through InSAR time series

### Author(s)

Joana Martins <sup>(1)</sup>, Andrew Hooper <sup>(1)</sup>, Karsten Spaans <sup>(1)</sup>,  
Freysteinn Sigmundsson <sup>(2)</sup>, Kurt Feigl <sup>(3)</sup>

### Department

<sup>(1)</sup>Delft University of Technology , NL

<sup>(2)</sup>Nordic Volcanological Center , IS

<sup>(3)</sup>University of Wisconsin , USA

### Abstract

After a period of quiescence since a sill intrusion in 1999-2000, a subtle deformation signal was again detected at a continuous GPS station on the southern flank of Eyjafjallajökull in Iceland, beginning in the summer of 2009. At our request the German Space Centre (DLR) immediately began tasking the TerraSAR-X satellite to acquire three SAR images every 11 days, giving a time series of SAR images prior to the eruption with unprecedented temporal sampling (although interrupted by snow during the winter). Previously we modelled individual interferograms between August 2009 and March/April 2010, which showed a large uplift signal. We modelled this signal as a series of sills and a dike with a total volume of  $\sim 0.05 \text{ km}^3$ . During the flank eruption beginning on 20 March 2010, we detected no significant deformation. However, coinciding with the start of the explosive eruption on 14 April 2010, we detected subsidence centred on the caldera. What we modelled showed us that Eyjafjallajökull was an unusual case, because this subsidence does not relate to pressure changes within a single magma chamber. Here we extend our analysis of deformation by applying InSAR time series to the full eruptive period. After correcting for DEM errors and reducing the atmospheric signal, we have found a number of signals that we interpreted in terms of magma movement. The time series displacement from 18 June 2009 to 4 February 2010 shows an inflation-deflation action, reaching a line-of-sight shortening of up to 2 cm on the southwestern flank (4 February 2010). The displacement signal is present in a set of interferograms and has a consistent behaviour in time, implying that it is not due to atmospheric contamination. To check how much of the signal is correlated with topography, we estimated the correlation coefficients between phase values and height over two test areas; one around the southwestern flank and another on the southeastern flank where we did not find any abnormal deformation. The correlation coefficient over the southwestern flank was found to be very small compared to that of the southeastern flank. We can, therefore, say that in the southwestern flank, not much of the atmospheric effects related with topography are present, suggesting that the signal could be deformation. For the co/post-eruptive phases, we also calculated the phase differences between nearby sets of points to study their temporal behaviour. On the southeastern flank we observe deflation all through the period 20 March - 1 September 2010. While on the western flank we observe inflation during effusive eruption, followed by deflation during explosive eruption, and a new inflation pattern between 5 June and 19 July that requires further research. Additionally, in contrast with the previous model, the magma chamber could no longer be fitted by a 2D source, and required a 3D source. In our model, we fit the post-eruptive phase with a pressure decrease of an ellipsoidal source, equivalent to a volume reduction of  $\sim 0.03 \text{ km}^3$ .

The analysis of the TerraSAR-X dataset faced some limitations, mainly concerning the phase unwrapping performance through ice- and ash-covered areas. This is caused by decorrelation due to the ash cover where there is an almost complete loss of coherence. We applied new methods to overcome these limitations. We combined Persistent Scatterer (PS) and Small Baseline (SB) methods to improve point density over the area. By using combinations of highly coherent interferograms, there is a clear increase in the number of distributed scatterers and the phase unwrapping performance is improved.

In this paper, we will present a comprehensive analysis of the Eyjafjallajökull eruption of 2010 as studied using InSAR time series and the resulting geophysical models.





# Session: Methods- General

## Effect of Unmodelled Reference Frame Motion on InSAR Deformation Estimates

### Author(s)

Hermann Bähr <sup>(1)</sup>, Sami Samiei-Esfahany <sup>(2)</sup>, Ramon F. Hanssen <sup>(2)</sup>

### Department

<sup>(1)</sup>Karlsruhe Institute of Technology Englerstrasse 7, 76131 Karlsruhe, DE

<sup>(2)</sup>Delft University of Technology Kluyverweg 1, 2629 HS Delft, NL

### Abstract

Deformation analysis by synthetic aperture radar interferometry (InSAR) is based on comparing the measured interferometric phase from two images to the reference phase computed from acquisition geometry. The latter is deduced from precise orbit ephemerides, which are commonly expressed in the International Terrestrial Reference Frame (ITRF). This frame is a realisation of a global coordinate system and defined by a number of geodetic stations close to the earth surface. To account for secular tectonic motion, not only positions but also linear velocities are attributed to the ITRF stations. A common assumption for InSAR processing is that the reference system of the orbit data does not move with respect to the earth surface in the region of interest. Due to tectonics, this assumption is not valid at the centimetre level though. Observing from a viewpoint on a tectonic plate, the coordinate frame of the orbits performs a relative motion in the order of centimetres per year. Neglecting this in InSAR processing is comparable to an error in the interferometric baseline, the size of which is increasing with the temporal baseline. The effect on the interferometric phase is an almost linear trend in range suggesting a large scale tilt of the surface. In contrast to temporally uncorrelated ramps caused by orbital errors, this kind of trend is correlated in time and cannot be separated from spatio-temporally correlated deformation signals. Hence, it can be mistakenly interpreted as an actual deformation signal in applications where the signal of interest is a large scale deformation over long time period, e. g., in monitoring interseismic tectonic motions. In order to evaluate the effect induced by this relative motion, baseline error rates for ENVISAT have been inferred from the velocity vectors of all ITRF stations, which are in most cases representative for the tectonic ground movement of a whole scene. The predicted bias of deformation estimates mainly depends on the respective tectonic plate and the heading of the sensor. It is most significant for the Pacific, the Indian and the Australian plate. Depending on the temporal baseline, the perpendicular component of the interferometric baseline can be biased by up to 6 cm/a. This accumulates to an error signal of one fringe spanning a whole scene for a temporal baseline of four years and corresponds to a relative error in the estimated displacement rates of 6 mm/a between near range and far range. An effective way to correct for this systematic error is to apply the relative motion of the tectonic plate to the orbital state vectors, provided that the motion is homogeneous over the whole scene. In inter-plate deforming zones, this simple approach would fail though. The contribution covers a global evaluation of the effect based on ITRF data. In light of the limitation that ITRF velocities are only available for discrete stations, it is further demonstrated that for most locations on earth, a good approximation can be obtained by using velocities from the geophysical plate kinematic model NNR-NUVEL-1A. The correction approach is tested and evaluated on ENVISAT persistent scatterer interferometry results over Groningen area in the Netherlands.

# Revising vegetation scattering theories: Adding a rotated dihedral double bounce scattering to explain cross-polarimetric SAR observations over wetlands

Author(s)

Sang-Hoon Hong <sup>(1)</sup>, Shimon Wdowinski <sup>(2)</sup>

Department

<sup>(1)</sup>Korea Aerospace Research Institute , KO

<sup>(2)</sup>University of Miami , USA

## Abstract

Common vegetation scattering theories indicate that short wavelength Synthetic Aperture Radar (SAR) observations (X- and C-band) measure mainly vegetation canopies as the short-wavelength radar signal interacts mostly with upper sections of the vegetation. Furthermore, these theories also suggest that SAR cross-polarization (cross-pol) observations reflect only volume scattering. Consequently most SAR decomposition techniques assume that the cross-pol signal represents solely volume scattering. However, short-wavelength and cross-pol observations from the Everglades wetlands, south Florida, suggest that a significant portion of the SAR signal scatters from the surface and not only from the upper sections of the vegetation. The indication for surface scattering in wetland environment is derived from phase observable processed using interferometric techniques. The interferometric SAR (InSAR) observations reveal coherent phase signal in all polarizations and all wavelengths, reflecting water level changes beneath the vegetation. This coherent phase signal cannot be explained by neither volume scattering nor radar signal interaction with the upper sections of the vegetations, because canopies and branches are frequently move by wind. The only way that such coherent signal can be maintained and represents surface water level changes is when a multiple bounce from the vegetation and surface occurs. The simplest multi-bounce scattering mechanism that generate cross-pol signal occurs by rotated dihedrals. Thus, we use the rotated dihedral mechanism to explain the InSAR wetland observations and to revise the current vegetation scattering theories to accounts also for double bounce component in cross-pol observations.

# Recent advances on InSAR temporal decorrelation: theory and observations using UAVSAR

Author(s)

Marco Lvalle <sup>(1)</sup>, Scott Hensley <sup>(1)</sup>, Marc Simard <sup>(1)</sup>

Department

<sup>(1)</sup>JPL/Caltech , USA

## Abstract

Synthetic aperture radar (SAR) interferometry [1] is an imaging technique with important applications in the measurement of geophysical parameters, such as topography, deformations and vegetation properties. A repeat-pass SAR interferometer is realized with two observations of an area of the Earth surface from slightly different positions and at different times. The correlation between two received signals, also called interferometric coherence, carries information about the imaged medium and is one of the measurement observables of a SAR interferometer. Several factors contribute to the value of the interferometric coherence and are often referred to as decorrelation sources. The most common decorrelation sources are the geometric surface decorrelation, the geometric volume decorrelation, the temporal decorrelation, and the thermal noise decorrelation [3]. One major limitation of SAR interferometry and

polarimetric SAR interferometry over land surfaces is temporal decorrelation [1, 2]. Temporal decorrelation originates from physical changes of vegetation and ground properties between two acquisitions, potentially reducing the interferometric coherence. Physical changes can be anthropogenic or natural. Examples of anthropogenic changes are deforestation, ploughing and irrigation, which usually destroy the coherence. Natural changes may arise from biological growth and variations of weather conditions. As an example, the wind perturbs the location and the orientation of the scattering elements in the radar resolution cell, and the rain and the transition of temperature alter the moisture content and the dielectric constant. Some temporal phenomena have short temporal scales, of the order of seconds or minutes, such as the wind, while others have longer scales such as the natural growth. In previous works, an exponential model of temporal decorrelation assuming Gaussian-statistic motion of the scatterers was derived and validated using L-band SEASAT data [3]. This model was then extended to the Brownian motion, which implies that the motion variance of the scatterers increases linearly with the time interval [4]. The exponential model was shown to be valid also for birth-and-death processes of the scatterers, and validated using C-band ERS data [5]. As the motion variance was assumed equal for all scatterers, other authors proposed to associate different temporal decorrelation levels to different components of vegetation, but without providing an explicit expression for the temporal decorrelation [6]. Here we present a new forward physical model of temporal decorrelation based on a Gaussian-statistic motion that varies along the vertical profile of the vegetation [7, 8]. Relaxing the constraint of uniform temporal decorrelation along the vertical direction is particularly useful for modeling the effects of the wind on vegetated land surfaces. As a result, it is shown that the temporal decorrelation depends on the structural parameters of the vegetation, such as vegetation height, and on the wave polarization. The dependence of temporal decorrelation on the system frequency results also modified with respect to the uniform temporal decorrelation model published in [3]. In addition to the new model, we discuss how temporal decorrelation depends on the spatial baseline as a consequence of the range spectral shift applied to the interferometric dataset. We validate the model and illustrate our findings using L-band data acquired by the JPL/UAVERSAR airborne radar. [1] R. Bamler and P. Hartl, "Synthetic aperture radar interferometry," *Inverse Problems*, vol. 14, pp. R1–R54, 1998. [2] S. Cloude and K. Papathanassiou, "Polarimetric SAR interferometry," *Geoscience and Remote Sensing, IEEE Transactions on*, vol. 36, no. 5, pp. 1551–1565, 1998. [3] H. Zebker and J. Villasenor, "Decorrelation in interferometric radar echoes," *Geoscience and Remote Sensing, IEEE Transactions on*, vol. 30, no. 5, pp. 950–959, Sep. 1992. [4] F. Lombardini and H. Griffiths, "Effect of temporal decorrelation on 3D SAR imaging using multiple pass beamforming," in *Proc. IEE-EUREL Meeting on Radar and Sonar Signal Processing*, Peebles, UK, July 1998, pp. 34/1–34/4. [5] F. Rocca, "Modeling interferogram stacks," *Geoscience and Remote Sensing, IEEE Transactions on*, vol. 45, no. 10, pp. 3289–3299, Oct. 2007. [6] J. O. Hagberg, L. M. H. Ulander, and J. Askne, "Repeat-pass SAR interferometry over forested terrain," *IEEE Transactions on Geoscience and Remote Sensing*, vol. 33, no. 2, pp. 331–340, Mar. 1995. [7] M. Lavalle, "Full and compact polarimetric radar interferometry for vegetation remote sensing," Ph.D. dissertation, University of Rennes 1 and University Tor Vergata of Rome, Dec. 2009. [8] M. Lavalle, M. Simard, S. Hensley, "A temporal decorrelation model for polarimetric radar interferometers," submitted to *Geoscience and Remote Sensing, IEEE Transaction on*, 2010.

# Mining Very High Resolution InSAR Data based on Complex-GMRF Cues and Relevance Feedback

Author(s)

Jagmal Singh <sup>(1)</sup>, Mihai Datcu <sup>(1)</sup>

Department

<sup>(1)</sup>DLR Oberpfaffenhofen, DE

## Abstract

Automatic retrieval of SAR images using query by image content from a large repository is of great interest due to availability of huge volume of high-resolution SAR images from satellites such as TerraSAR-X and TanDEM-X. Moreover, sub-meter resolution of these images has increased the diversity of the structures and the objects in the scenes to a great extent thus opening new challenges for image understanding and Information Mining systems. In this paper, we propose a concept of Image Information Mining (IIM) system which uses InSAR data to recognize the structures and the objects in the scenes with a Relevance-Feedback (RF) Support Vector Machine (SVM) active learning. This concept is based on the knowledge-driven Information Mining (KIM) system, which is a prototype of a knowledge-driven content-based information mining system produced to manage and explore the large volumes of remote sensing image data, mainly optical and detected SAR images [1]. Experimental results obtained from analysis of complex-valued SAR data presented in [2] proves that phase information in complex-valued SAR can provide added information for IIM, thus motivated us to extend KIM concept to InSAR data. The Markov-Random Field model characterizes spatial statistical dependencies of 2-D data by a symmetric set called the neighbor set [3]. Gauss-Markov random field (GMRF) can also be modeled by selecting a suitably sized neighborhood system and clique structure. The neighborhood size defines the maximum limits of the structural complexity of GMRF model, also termed as order of model. In [4] and [5] are presented application of feature extraction using GRMF model for the detected SAR data. SAR images are bi-dimensional complex signals and reveal structures both in magnitude. However, a neighborhood system around a center pixel for the detected data cannot make use of phase information as it is not present in detected data. We propose using InSAR data instead of detected data to exploit the complete information of SAR because Interferogram is complex-valued signal generated by exploiting the phase difference between two coherent complex-valued SAR images preserving the special structural information otherwise lost in detected data. We estimate the complex-GMRF for InSAR data. Model evidence and model parameter are used as primitive features for RF-SVM active learning and indexing categories. Proposed Information Mining concept consists of cutting the Interferogram in patches along with a quick-look file corresponding to every patch. Primitive features are estimated based on complex-GMRF for all Interferogram patches. Patch parameter-files and corresponding quick look files are imported into RF-SVM classifier. From RF we mean that the results will be generated based on the user judgment. This way we try to link visual similarity of images and their information content [6] to incorporate active learning concept in the system. Graphical User Interface (GUI) of RF-SVM Classifier gives us the possibility of searching by category generation (relevant and irrelevant), equivalent to two classes classification. Thus broadly the IIM systems will have main blocks as: (a) Interferogram and SAR image data-base, (b) primitive feature extraction block, and (c) classifier-user communication block. Based on the user feedback, categories will be generated. For the performance evaluation, we use the standard metric used to evaluate the performance of a retrieval systems such as Precision-Recall, F-measure and/or ROC Curve. Preliminary results are encouraging and proposed concept is an important step towards using Interferometric SAR for IIM. References: [1] M. Datcu, H. Daschiel, A. Pelizzari, M. Quartulli,

A. Galoppo, A. Colapicchioni, M. Pastori, K. Seidel, P.G. Marchetti, and S. D'Elia, "Information Mining in Remote Sensing Image Archives- Part A: System Concepts," IEEE Transactions on Geoscience and Remote Sensing, vol. 41(12), pages 1-14, 2003. [2] J. Singh and M. Datcu, "SAR Target Analysis based on Multiple Sub-Look Decomposition: A Visual Exploration Approach," Submitted to IEEE Geoscience and Remote Sensing Letters. [3] R. Chellappa, S. Chatterjee and R. Bagdazian, "Texture Synthesis and Compression using Gaussian-Markov Random Field Models," IEEE Transactions on Systems, Man, and Cybernetics., vol.-15, no. 2, pages 298-303, Mar./Apr. 1985. [4] M. Datcu, K. Seidel and M. Walessa, "Spatial Information Retrieval from Remote-Sensing Images - Part I: Information Theoretical Perspective," IEEE Transactions on Geoscience and Remote Sensing, vol. 36, no. 5, pages 1431-1445, 1998. [5] M. Walessa and M. Datcu, "Model-based despeckling and information extraction from SAR images," IEEE Transactions on Geoscience and Remote Sensing, vol. 38, no. 5, pages 2258- 2269, 2000. [6] M. Costache, H. Maitre and M. Datcu, "Categorization based Relevance Feedback Search Engine for Earth Observation Images Repositories," Proc. IGARSS, 2006.



# Poster Session 1

## Posters on ESA Sentinel-1 constellation

### End to End Sentinel-1 Topsar interferometric experiment based on simulated data

#### Author(s)

Daive Giudici <sup>(1)</sup>, Francesco Andriani <sup>(2)</sup>, Davide Riva <sup>(1)</sup>, Davide D'Aria <sup>(1)</sup>

#### Department

<sup>(1)</sup>Aresys , IT

<sup>(2)</sup>Politecnico di Milano , IT

#### Abstract

TOPSAR (Terrain Observation by Progressive Scans) is a scanning SAR mode first proposed in 2006 by Monti Guarnieri et al., with the purpose of solving scalloping and azimuth-varying ambiguities shown by ScanSAR. While the latter obtains wide-swath coverage by switching the antenna elevation beam to points in several subswaths, this new acquisition mode is characterized by a backward-to-forward antenna movement in the squint direction. This rotation is opposite with respect to spotlight (SPOT) SAR, resulting in the opposite effect: gathering returns from a much longer strip within the same time span, at the cost of a worse azimuth resolution. It can be furtherly combined with ScanSAR, allowing for additional flexibility in terms of acquisition planning: long burst can achieve wide coverage in the azimuth direction and subswath switching can extend the same coverage by integer factors; on the other hand, repeated passes over the same swath provides for better noise attenuation and/or different polarizations. Sentinel -1, the next ESA SAR mission, shall implement 2 Topsar acquisition modes: the Interferometric Wide Swath mode, an high resolution Topsar mode acquiring over 3 sub-swaths, and the Extra Wide Swath, the medium resolution topsar mode acquiring over 5 swaths. From a spectral point of view, TOPSAR acquired data are characterized by a linearly azimuth-varying spectrum, as a consequence of continuous shifting in the antenna pointing direction. This peculiar time-frequency relationship, requires customisation to both the focusing chain and the interferometric chain. In this paper we present an end-2-end Sentinel-1 specific interferometric experiment that has been carried out exploiting Sentinel-1 simulated data. The simulation has been carried out by the Sentinel-1 Instrument Software Simulator that is capable of providing realistic Sentinel-1 Instrument Source Packets with point and distributed scenarios. It is able to reproduce the correct Sentinel-1 instrument acquisition timeline and reconstruct the antenna pattern. Moreover, it also takes into account the electronic transmission and receiver chain in order to reproduce all the foreseen signal characteristics. To simulate a real scene, the ISS ingests a simulated orbit and a proper ASAR scene in order to provide a realistic  $\sigma_0$ . Using this information, the simulator is able to create, on a DEM, complex cell responses with the foreseen (expected?) characteristics. The contribution of all the cells on ground, using the bistatic start and stop approximation, are then coherently summed to create raw data. The simulated data, have then been processed by the TOPSAR prototype processor in order to generate a sentinel-1 IW SLC product. The last step of the process is the interferogram generation that, for Topsar (and ScanSAR) modes, must take into account an additional synchronisation constraint. Further, another not-nominal step within the topsar interferometric chain, is the data coregistration step, which compels an ad-hoc interpolation stage. For the aforementioned reasons, a complete TOPSAR burst spans a very large frequency interval. Thus, in order to make it compatible with any kind of interpolation (i.e. sinc-based, linear, etc), data must be brought back to zero-Doppler baseband

across the whole burst, and brought back to original frequency band after coregistration. Moreover, to reduce noise in the resulting interferogram, common band is to be selected between the master and each slave acquisition.

## Space adaptive quantizer for interferometric applications

### Author(s)

Pietro Guccione <sup>(1)</sup>, Andrea Monti Guarnieri <sup>(2)</sup>

### Department

<sup>(1)</sup>Politecnico di Bari Via Orabona, 4, IT

<sup>(2)</sup>Politecnico di Milano , IT

### Abstract

Modern and future spaceborne Synthetic Aperture Radar systems exploit large bandwidths, high pulse repetition frequencies and multiple polarizations, resulting in a stringent demanding of efficient on-board compression schemes. Persistent Scatterers (PS) and interferometric applications, especially in urban context, require, on the other side, the availability of high SNR to have temporal series of stable targets affected by low phase noise. The limit of the Block Adaptive Quantizer (BAQ) in maintaining phase preservation has been already remarked in [1], [2]. To this aim a Space Adaptive Flexible Block Quantizer (SA-FBQ) is presented. This quantizer is actually an extension of the Flexible Dynamic Block Adaptive Quantizer (FDBAQ), [3], that in turn is an extension of the BAQ, which can be considered the optimal quantizer for a homogeneous target. The FDBAQ gets better performances on heterogeneous target by adaptively selecting the best BAQ according to the local Signal to-Thermal-Noise Ratio (STNR): the worst the STNR, the lower the quantizer rate. The quantizers selection are pre-computed in a Look-Up-Table (LUT), by assuming a fixed and known Probability Distribution Function (PDF) of the reflectivity  $\sigma_0$ . The SA-FBQ extends further this concept allowing the reflectivity PDF to vary, coping with this by exploiting many quantizers sets, each adapted to the local statistics. We introduce here two degree of improvement w.r.t. original FDBAQ proposed for Sentinel-1. The design of the FDBAQ is improved by looking for a solution that maximizes the average SNR and selects the optimal quantizers between a continuous set, instead than a finite, small one. Moreover we extend the FDBAQ to cope for the variation of the shape of SAR reflectivity PDF, from zone to zone, i.e. a non-stationary shape. The resulting scheme makes use of a set of LUTs in place of a single one, where each LUT is adapted to a particular PDF. We introduce an algorithm to adaptively find the best set of quantizers constrained on the mean bit rate; discuss the implementation of the SA-FBQ and estimate its performances w.r.t. the FDBAQ and the BAQ. Results are shown by exploiting the word-wide mosaic of C-band reflectivity derived from ENVISAT data and Sentinel-1 system parameters. [1] G. Krieger S. Huber, "The TanDEM-X mission: Overview and interferometric performance," in Radar Conference, 2009. EuRAD 2009, 2009. [2] R. Metzger S. Wollstadt J. M. Martinez J. Mittermayer, M. Younis and A. Meta, "TerraSAR-X system performance characterization and verification," Geoscience and Remote Sensing, IEEE Transactions on, vol. 48, 2010. [3] M. Gottwald P. Guccione A. Monti Guarnieri F. Rocca P. Snoeij E. Attema, C. Cafforio, "Flexible Dynamic Block Adaptive Quantization for Sentinel-1 SAR missions," IEEE Geoscience and Remote Sensing Letters, vol. PP, 2010.



# Posters on Ground-based InSAR

## Use of Ground based InSAR for mapping unstable rock walls above a road in Norway

Author(s)

Lene Kristensen <sup>(1)</sup>

Department

<sup>(1)</sup>Aknes Early Warning Centre , NO

### Abstract

The Norwegian Road Authorities register between 1500-2000 slide events/ yr on the road network, of which the majorities are snow avalanches and rockslides. Presented here is a test study to see if ground based InSAR can be used to detect larger areas of movement in rock walls along road sections that are prone to large rock falls. Areas of active movement are likely the source areas for rock falls or slides, so if they are identified, it may be easier to install physical barriers, such as rock nets, or by releasing the loose blocks in a controlled manner. The work is carried out by Åknes Early Warning Centre - a Norwegian national centre for monitoring of large rock slides. The centre have used ground based radar systems successfully to measure distributed displacement in large rock instabilities, both for mapping purposes and as a permanent early warning system. The centre is building the capacity to perform radar surveying jobs also from external sources and this study was carried out on commission from the Norwegian road authorities. The radar used is a LiSALab system from Ellegi Srl. The company has assisted on various steps of the data gathering and processing, in order to build competence of the use of GB radar at Åknes. The system operated with a central frequency on 17.25 and a bandwidth between 0.25 and 0.3 GHz. The range to the measured rock wall varied from 160 to 1300 m, and the range resolution between 0.5 – 0.75 m. The scan time was around 7 minutes. The system was placed on each site for approximate 1 week, and daily and weekly averages of the measurements used forward. This carries the assumption that no significant displacement occur during each measurement on a particular location. 3 surveys of each site were made: Spring 2010, autumn 2010 and spring 2011. Thus the measurements were periodic and the same radar moved from site to site. The radar was placed on well founded steel beams and covered by a plastic tent for protection. Interferograms were created on the basis of the measurements between each campaign, and the data was then projected on a DEM for 3D display of the movement. Noise in the data was filtered using limits to the power level and coherence. The studied road stretch (rv. 70 between Sunndalsøra and Oppdølstranda, Møre and Romsdal) has suffered 3 large rockslides between 2007 and 2009. A tunnel will be opened in 2013-2014, but until then the road remains open. Four different rock-faces above the road (A, B, C & D) were scanned, in locations where previous rock slides/rock falls have occurred. At stretches A, B and C, the system was located close below the slope at the roadside, as the slope continues steeply into the fjord. On stretch C the most interesting displacement was observed. In one place, movement of about 6 – 7 mm was measured from May to October 2010. An additional 8 mm of movement occurred between October 2010 and April 2011. The interferograms suggest that the movement is a toppling of a large block of around 15 x 30 m, but observations of geological structures and signs of deformation need to be more closely evaluated. Unfortunately this area is quite inaccessible by foot, and we therefore plan to make use of a laser-scan. On stretch A, an area showed displacement of c. 4 mm. The instability was confirmed by a field inspection that revealed two hanging blocks loosened by faults and fractures. On Stretch B no displacement was observed and

on stretch D a couple of small areas may indicate displacement of 1 – 2 mm. Snow and vegetation proved to be the biggest challenges to the measurements. The entire snow season must be avoided, which for this site means approximately from October to March. Vegetation causes some noise in the data and may obscure the view to important parts of a dangerous rock wall. However, when the conditions allows, this study suggest that the method can be very useful to document movements in larger areas on rockwalls above road sections. The identification of active areas is important in order to improve mitigation measures, which will lead to an improved safety along roads.

## MODE TInSAR: an ESA incubation project dedicated to the Terrestrial SAR Interferometry

### Author(s)

Paolo Mazzanti <sup>(1)</sup>, Alessandro Brunetti <sup>(1)</sup>, Gabriele Scarascia Mugnozza <sup>(2)</sup>

### Department

<sup>(1)</sup>NHAZCA S.r.l. Via Cori snc, 00177 Rome, IT

<sup>(2)</sup>Dipartimento di Scienze della Terra, "Sapienza" University of Rome Piazzale Aldo Moro 5, 00185 Rome; IT

### Abstract

MODE TInSAR (MOnitoring DEformation by Terrestrial SAR Interferometry) is an incubation project which NHAZCA S.r.l. (Spin-off Company of "Sapienza" University of Rome) is carrying out in the frame of the ESA (European Space Agency) Business Incubation Platform. The project, that has been technically and financially supported by ESA (European Space Agency) and BIC Lazio (Business Innovation Centre Lazio), started in January 2010 and it is going to end on September 30th 2011. The main project purposes were the following: a) identification of new technological solutions for the application of the TInSAR technique to static and dynamic monitoring of buildings, structures and natural elements; b) commercial development of services by TInSAR technique. The first pilot site was the monitoring of the Basilica di Massenzio (Rome) by Terrestrial Radar Interferometry, committed by IMG S.r.l. (promoting partner of NHAZCA) on behalf of Metro C S.c.p.A. The starting point of the project was the analysis and the identification of the main limitations of TInSAR technique. Then, new methodologies and software were designed and developed aiming to reduce the atmospheric noise in the radar signal propagation and to improve the accuracy in the displacement detection, also by the comparison and integration with conventional Laser and GPS monitoring techniques. Within this step, a fundamental support was offered by ESA-ESRIN experts in the radar signals processing. So far, an automatic software suitable for the data acquisition, transfer, storage, processing and visualisation of Terrestrial Interferometric Radar data was realized. Furthermore, algorithms for data sampling, filtering and correction of atmospheric artefacts were developed by NHAZCA technicians and then imported in the software. The validation of the achieved results and the estimation of improvements were performed by the comparison with data processed by commercial software. Further technological solutions, specifically dedicated to the improvement in data dissemination and service providing, were also developed and realized by NHAZCA in the frame of the MODE TInSAR Project such as: a) the LARAM tools for the 3D TInSAR data visualization by the integration of TInSAR and Terrestrial Laser Scanner DTM; b) the QUIB (Quick Installation Basement) Equipment for the spreading of the TInSAR technique by the realization of a quick installation basement (QUIB) for the quick installation of a TInSAR monitoring platform. Performance analyses were then led in several test sites (both buildings and natural slopes) in order to evaluate the efficacy of Terrestrial Radar Interferometry for the static and dynamic monitoring of displacements. A comparison with data collected by conventional monitoring instrumentations installed on the same test sites allowed to confirm the reliability of TInSAR results. As regards the market and business plan, the following actions were done, with the

support of BIC Lazio: a) the NHAZCA official website was designed and published; b) a commercial partnership between NHAZCA S.r.l. and Microgeo S.r.l. has been activated in order to increase the customers portfolio of NHAZCA; c) seminars and workshops on TInSAR monitoring techniques were organized in Rome and Foggia (Italy). In the frame of the incubation project, a formal monitoring contract was stipulated with the Province and the Municipality of Bolzano (Italy) for the static monitoring of a rock scarp, and with the University of Padua for the monitoring of a landslide. Moreover, technical and financial offers were submitted for the monitoring of historical buildings and heritages in Italy.

## Advanced data analysis procedures for Ground-Based SAR (GBSAR) data

### Author(s)

Oriol Monserrat <sup>(1)</sup>, Guido Luzi <sup>(1)</sup>, Michele Crosetto <sup>(1)</sup>, Núria Devanthy <sup>(1)</sup>

### Department

<sup>(1)</sup>Institut de Geomàtica Av. del Canal Olímpic, s/n, ES

### Abstract

In the last years Ground-Based SAR (GBSAR) interferometry has demonstrated to be a reliable microwave remote sensing technique in several application fields, especially in deformation monitoring. The technique can provide displacement measurements over few squared kilometers areas and with a very high spatial resolution. In the first part of the paper we will cover all the relevant aspects of GBSAR data analysis to understand advantages and limitations of this technique. All main components of the whole GBSAR chain, including the design of the campaign, data acquisition, screening, processing, analysis, geocoding and visualization, will be discussed. The paper will discuss two different and complementary data processing approaches: an interferometric approach and a non-interferometric approach. In the second part of the paper an overview on the GB-SAR some acquired data and the results obtained in the last six years, at different sites, by the Institute of Geomatics, IG, will be given. These results have been obtained within different national and international projects. The data collected have been obtained by two different sensors: a C-band GB-SAR developed by the University of Florence and the Ku band IBIS-L system bought by the IG to the company IDS.

## IBIS, an innovative ground-based interferometric radar for monitoring engineered and natural slopes

### Author(s)

Paolo Farina <sup>(1)</sup>, Lorenzo Leoni <sup>(1)</sup>, Francesco Babboni <sup>(1)</sup>, Francesco Coppi <sup>(1)</sup>, Lorenzo Mayer <sup>(1)</sup>, Pier Paolo Ricci <sup>(1)</sup>

### Department

<sup>(1)</sup>Ingegneria dei Sistemi SpA IDS, IT

### Abstract

The need for effective monitoring systems for both engineered and natural slopes is a critical component in risk management practices for urbanized areas threatened by active landslides, critical infrastructure management and mineral resources production. Ground-based interferometric radar technology has emerged in the last ten years as a leading edge tool for this purpose. The success of interferometric radar technology is attributed to its ability to rapidly measure slope movements with sub-millimeter accuracy over wide areas in any weather conditions, obviating the need to install artificial reflectors. As a result, slope monitoring radar is

effectively used to get a better understanding of the spatial distribution of slope movements and for the provision of alerts in the event of progressive movements that can potentially lead to slope failure as well. Slope stability monitoring radar is today commonly used by prominent mining groups internationally, by civil protection authorities in developed countries and also by academics for the provision of high level consultancy to end users involved in landslide risk management. Historically especially in the mining industry, radar systems have been designed with parabolic dish antennas that are mechanically moved to achieve a full scan of the observed area. These designs presented the following constraints: • limited working distance from the target resulting in the need to move the radar frequently to cover the entire active wall • consequent difficulties in historic data retention on the slope behavior, • limited spatial resolution owing to dish footprint size, • stability problems induced by strong wind • potential reliability problems caused by numerous moving parts. IDS have overcome the above mentioned limitations with the introduction of an innovative radar system, known as IBIS. Owing to the unique radar technologies used in its design and its high reliability connected to highest military standards used for its production, IBIS is able to significantly improve the performance of slope monitoring radar by providing higher spatial resolution, longer working distances and faster acquisition time. In addition to its alarm generation capability for rapid slope movement, long-term monitoring can be provided as well, facilitated by the erection of permanent installations remote or through precise re-positioning of the system after re-deployment and data stitching of different surveys. The low power consumption of IBIS is advantageous in that the system is able to be powered by solar panels with the generator used only as a back up. Thanks to the high acquisition frequency of the radar, IBIS can be used also for the measurements of vibrations of civil engineering structures or slopes. The system is available in different configurations, from a very portable solution to a trailer-based version, making possible to satisfy the specific needs of different type of users. Today more than 70 systems have been deployed around the world for different applications. The main technical features of the IBIS system will be presented in this paper along with recent case studies for different applications, from landslide monitoring to slope monitoring in very large open pit mines.

## Design of the ground based array for the TropiScat experiment

### Author(s)

Dinh Ho Tong Minh <sup>(1)</sup>, Stefano Tebaldini <sup>(1)</sup>, Fabio Rocca <sup>(1)</sup>

### Department

<sup>(1)</sup>Politecnico di Milano Dipartimento di Elettronica e Informazione, IT

### Abstract

In the framework of the BIOMASS mission [1], many airborne surveys had been performed. More recently, the TropiSAR 2009 campaign in the area of Paracou in French Guiana [2] has been carried out for studying the vertical structure of forest areas which would be one of the key elements for the assessment of the forest biomass [3]. In order to complement the airborne TropiSAR dataset, the TropiScat ground based experiment has been proposed to acquire the polarimetric intensity and the complex coherence in HH, VV, and HV, together with a vertical imaging capability. The Guyaflux tower (55m) has been selected to support this experiment and antennas will be placed on the top of the tower to radiate P to L band signals to the forest below. A preliminary test was carried out in October 2010 using a Vector Network Analyser (VNA) with 2 P band antenna instruments [4]. The vertical aperture for tomographical imaging is formed by progressively moving downwards the couple of antennas. The first successful test results are the inputs for a stable configuration designed to ensure the quality of the results of the experiments to dure more than one year. This paper will discuss this design. This configuration will be designed to accomplish three requirements: the full polarimetric imaging capability, vertical

imaging capability, and temporal stability so as to allow the investigation of the temporal coherence as a function of polarimetry and height. These requirements will allow in depth understanding the vertical structure and the scattering mechanisms in airborne and in the possibly coming spaceborne BIOMASS observations. The constraints for such configuration are: placing 20 antennas, reducing antenna coupling effects, keeping the operational system as simple as possible and stable. The most important point for implementation of the system configuration is to ensure the absence of the antenna coupling effects. In order to avoid such effects, it has been decided the minimum distance between two antennas would not be less than 0.8m as the first test [4]. At this vertical sampling, however, the height ambiguity appears as a serious problem. Since the vertical sampling requirement to have a safe height of ambiguity, say a half of wavelength, is broken if we place antennas in 1D vertical direction. In this paper, we intend to provide a multi-static configuration design which solves the minimum distance between antennas problem based on the idea of a virtual array. Roughly speaking, the virtual array is the array relating to the center positions between any transmitter and receiver positions. We propose an array which is approximately equivalent to a 1D vertical array having a 20 cm spacing. This spacing, at P band, yields an ambiguous return appearing at an angle close to 135 degree from the target, well distinguished from the forest. No cross range ambiguity affects the imaging of the rest of the scene. Assuming that the forest height is below 40m, then the system can work from 500 MHz to 900MHz. The vertical resolution in far range (100m) is about 10m in P band and proportionally higher at higher frequencies. Furthermore, such configuration preserves the best coherence for co-polar HH-VV as their virtual arrays coincide. The VH and HV virtual arrays are separate and allow to double the available number of cross polar looks. Each antenna belongs to either the receiver or the transmitter groups, simplifying the switch boxes. The performance assessment will be based on a simulated scenario. References [1]. M. Davidson, A. Thompson, and C. Lin, "Report for Assessment: BIOMASS," ESA SP-1313/3 Candidate Earth Explorer Core Missions 2008, 2008. [Online]. Available: <http://www.congrex.nl/09c01> [2]. P. Dubois-Fernandez, H. Oriot, C. Coulombeix, H. Cantalloube, O. Ruault du Plessis, T. Le Toan, S. Daniel, J. Chave, L. Blanc, M. Davidson, and M. Petit, "Tropisar: Exploring the temporal behavior of p-band sar data," in Geoscience and Remote Sensing Symposium (IGARSS), 2010 IEEE International, July 2010, pp. 1319 –1322. [3]. S. Tebaldini, M. Mariotti D'Alessandro, H.T.M. Dinh and F. Rocca, "P band penetration in tropical and boreal forest: Tomographical results". Submitted in Geoscience and Remote Sensing Symposium (IGARSS), 2011 IEEE International. [4]. T. Koleček, P. Borderies, L. Villard, C. Albinet, Y. Lasne, S. Tebaldini, F. Rocca, and L. T. Thuy, "TROPISCAT: a polarimetric scatterometer experiment in tropical forests," PolInSAR, 2011. Frascati, January 2011.

## Examples of precise detection and visualization of landslide related surface deformations with the Gamma Portable Radar Interferometer (GPRI)

### Author(s)

Rafael Caduff <sup>[1]</sup>, Andreas Wiesmann <sup>[1]</sup>, Tazio Strozzi <sup>[1]</sup>

### Department

<sup>[1]</sup>Gamma Remote Sensing AG Gümligen, Switzerland, CH

### Abstract

Erosion and accumulation processes on the topographic surface form the landscape of alpine environments. In temperate zones, the major mass wasting processes with regard to the net mass balance are permanently active land- and rockslides. Under favorable geologic and hydrological conditions, unstable slopes can have areas of more than several tens of square kilometers. Within these areas urban settlements are often located. If the rates of deformation

suddenly change, e.g. because of significant variations in temperature and/or the hydrological system (precipitation, groundwater level), unexpectedly high mass movement hazards might occur, possibly causing damages to the settlements or infrastructural buildings within or near this environment. Satellite SAR interferometry has a high potential in detecting and outlining slope instabilities. But the relatively long repeat cycles of the satellites currently in orbit do not allow high resolution time series collection. In addition, the geometry of an object of interest (e.g. steep slopes) often prevents a survey with satellite radar interferometry. The Gamma Portable Radar Interferometer (GPRI), offers the possibility to detect slope deformation rates in steep areas and to measure the spatial and temporal variations of the surface deformations. The GPRI operates at Ku-band with real aperture fan beam antennas rotating around its vertical axis. Range resolution is 0.8 m and azimuth resolution is 0.4 degrees. The image acquisition time for a 360° scan is only a few seconds and thus very dense time series can be collected. While most of the observed landslides show deformation rates of 1 mm/day or less, the oversampling in scenes can be used for atmospheric corrections and to enhance the interferometric signatures. In our contribution we will present different case studies from the Swiss Alps. Time series of GPRI measurements were obtained from a deep seated rock slide (Zervreila, Canton of Grison), a deep seated landslide with dense vegetation cover (Lumnezia, Canton of Grison), and an very localized instability in the escarpment area of a major debris-flow catchment area (Illgraben, Canton of Valais). The average surface deformation rates of the Zervreila rock slide and the instability at the Illgraben are approximately 1 mm/day. Several GPRI images from different sampling positions have been acquired with different temporal baselines ranging from 2 to 20 minutes with a total duration of up to 60 hours. The distinct topographic situation and therefore the changing illumination situations with shadowing lead to distinct atmospheric signatures in the interferometric pattern. Atmospheric filtering and removal of scenes containing high amount of atmospheric disturbances had to be applied. After phase unwrapping, displacement maps have been generated. In a final step, the displacement maps showing the spatial distribution of areas with different LOS-displacement rates have been projected with a new geocoding approach to a three dimensional surface obtained from other sources (Terrestrial or airborne Laser Scanner and photogrammetric surface reconstruction). Penalties in spatial resolution in steep (almost vertical) areas can be so avoided, and the interpretation of the data is more straightforward.

## Monitoring of a building in the city of Rome by Terrestrial SAR Interferometry

### Author(s)

Paolo Mazzanti <sup>(1)</sup>, Ivan Cipriani <sup>(2)</sup>

### Department

<sup>(1)</sup>NHAZCA S.r.l., spin-off "Sapienza" Università di Roma Via Cori snc, 00177 Rome, IT

<sup>(2)</sup>Department of Earth Sciences, "Sapienza" Università di Roma P.le Aldo Moro 5, 00185, Rome, IT

### Abstract

Communications in large developed cities are mainly controlled by subways and the realization of new metro lines is continuously increasing. Hence, several thousands of passengers can be moved around large cities in a short time and noise and air pollution can be significantly reduced. However, the excavation of tunnels in urban areas can lead to the destabilization of surface buildings. Therefore, the deformation monitoring of the ground and the buildings and structures is strongly recommended before, during and after the construction works. One of the main underground line under construction in Italy is the METRO C of Rome (Italy) which is characterized 18 kms of tunnels that run below the historical centre of Rome. Along the route of the tunnel there are several historical buildings and heritages such the Colosseum and the Venezia Palace, as well as strategic buildings (schools, churches etc). A very complex monitoring

project has been developed which includes different types of instrumentations and monitoring systems (i.e. extensometers, inclinometers, automatic levelling and total stations). Furthermore, innovative techniques such as Ground Based and Satellite radar have been tested on strategic buildings. During the activities for the realization of the underground sectors T7 to T4 of the METRO C, particular attention has been devoted to buildings already characterized by structural problems. Among them the Carducci School located at the intersection between Via La Spezia and Via Altamura streets has been selected as the ideal test site for the application of the Terrestrial SAR Interferometry. An IBIS-L equipment manufactured by IDS S.p.A. was installed in front of the building over a concrete basement and then covered by a wood structure. The monitoring platform was located inside the Metro C yard, 40 m far from the building. One month 24/continuous monitoring (from March 6th to April 4h 2009) was performed with a data sample rate of about 5 minutes thus collecting an amount of 7229 SAR images. Processed data allowed us to achieve 2D images of LOS (line of sight) displacement of the overall building and time series of displacement of each pixel of the SAR images. The back-scattering stability of the signal were negatively affected by the transit and parking of the work's vehicles especially during the working hours. Hence, two different processing methodologies were used in order to reduce the noise of data: 1) multi-stacks analysis of images collected during stable hours (by using data not affected by working activities); 2) differential SAR Interferometry analysis over couple of SAR images. Data collected by Terrestrial SAR Interferometry (TInSAR) allowed to infer a displacement of about 1,5 mm along one side of the building and zero displacement on the other side. Results obtained by TInSAR technique were compared with data collected by two robotic total stations that were continuously monitoring 20 prisms installed on the building external faces. However, TInSAR measured displacements only along the line of sight direction, while total station were able to measure the real displacement of the mini-prisms along three directions (North, East and Height). Total displacement measured by TInSAR and total station data were compared by taking into the different geometry of acquisition, thus achieving similar results. Furthermore, also the temporal series of displacement of the SAR interferometric pixels located close to the prisms showed a similar behaviour over time.

## 2D Atmospheric Artifact Compensation with Multiple Regression Model in Ground-Based SAR over mountainous areas

### Author(s)

Xavier Fabregas <sup>(1)</sup>, Rubén Iglesias <sup>(1)</sup>, Albert Aguasca <sup>(1)</sup>, Josep Gili <sup>(1)</sup>

### Department

<sup>(1)</sup>Universitat Politècnica de Catalunya (UPC) Campus Nord Edifici D3 C/ Jordi Girona 31 08034, ES

### Abstract

This paper deals with atmospheric artifact compensation in Ground-Based SAR (GB-SAR) zero-baseline acquisitions in presence of steep topography. Ground-Based Differential Interferometric SAR (DInSAR) is a remote sensing technique in which the high stability of the sensor platform, the lack of revisiting-time constrains and its high resolution possibilities are translated as a promising alternative to a satellite based solution when small scenarios are considered. The most relevant decorrelation source for targets that exhibit a stable phase behavior (stable amplitude dispersion or high coherence) in these types of data is the atmospheric phase screen [1]. In order to apply any differential interferometric technique for the deformation map retrieval, the atmospheric effects must be compensated. Traditionally this issue has been solved studying the refractivity index variations. Under the assumption of atmosphere spatial homogeneity (constant refractivity index for the whole scene), the atmosphere artifact estimation consists of a linear range phase-ramp that can be theoretically described by just two parameters: an offset and a slope coefficient. The projection onto a range-line of the phase of all the pixels whose coherence

value are higher than a reference threshold shows a linear behavior due to the atmosphere spatial homogeneity. In these conditions we could compensate the atmospheric phase contribution with a regression-line estimator [2]. Another possibility to the compensation is a linear model approximation method based on available meteorological information [3]. In scenes with steep topographic variations, fluctuations of atmospheric parameters as temperature, pressure and humidity can be observed on the spatial domain for each acquisition mainly due to changes in height. This aspect introduces a second-order term in the differential interferometric phase which depends on the range distance and height. The consequence is that now atmosphere spatial homogeneity cannot be considered and any linear model approximation solution fails. A new model to estimate the atmospheric phase screen is considered under this type of scenarios. To solve the problem, the well-known empirical relationship between atmospheric parameters (temperature, pressure, humidity) and refractive index have been taken into account, but now considering that the refractive index can be supposed to be a function of space too (height-dependent). The absolute delay of the backscattered wave at each range distance from the radar sensor can be expressed as the integral of the refractivity index along the space which now will have a term related with the range distance (as in the atmosphere spatial homogeneity case) and a second-order term related with the product of range distance with height. Using an external DEM and solving a 2D Multiple Regression Model (least squares) the atmospheric phase screen can be estimated. In the particular case of smooth topography this new model trends to the 1D phase-ramp solution so it is a generalization of the linear model approximation. The Remote Sensing Laboratory (RSLab) in collaboration with The Department of Geotechnical Engineering and Geosciences of the Universitat Politècnica de Catalunya (UPC) is carrying out a one-year measuring campaign (October 2010 – October 2011) in the landslide of 'El Forn de Canillo', Andorra, using the polarimetric UPC GB-SAR sensor (RISKSAR) [7]. The results of the new atmospheric compensation technique will be analyzed in this environment. This work is being carried out in the frame of the fourth area of Safeland project funded by The Seventh Framework Program for research and technological development (FP7) of the European Commission. 'El Forn de Canillo' is an ancient landslide with a complex movement that took place in more than one episode. Nowadays it is quite stable, with some residual movement (of the order of millimeters per year). In the North-East extreme of the landslide exists a sector that nowadays is active and it is reactivated coinciding with strong rains and big increases of the piezometric conditions episodes of the zone [4]. In order to validate the model, several meteorological measurement profiles of pressure, temperature and relative humidity have been collected every second by a weather station along different spatial points with different heights along the mountain. These measurements helped us to demonstrate that the atmosphere spatial homogeneity assumption in this type of scenarios is wrong. Through single simulations the second-order term in the phase delay observed in the GB-SAR real acquired data has been confirmed. Unlike the most of the other GB-SAR systems available in the remote sensing scientific community, which are based on a Vector Network Analyzer (VNA) for the stepped-frequency sweeping of the transmitted signal bandwidth [7], the UPC CW-FM radar is based on a Digital Direct Synthesizer (DDS) chipset that generates it at once. This kind of solution allows performing PolSAR or PolInSAR measurements without increasing the temporal decorrelation effects during a single scan and this extra information will provide higher densities to phase atmosphere estimation and removal. The improvement of atmosphere phase estimation using polarimetric acquisitions will be presented.

[1] Luca Pipia, Albert Aguasca, Xavier Fabregas et al., "Temporal Decorrelation in Polarimetric Differential Interferometry using a Ground-Based SAR Sensor", IGARSS'05, Seoul, Korea, 25-29 July 2005 [2] Luca Pipia, Xavier Fabregas, Albert Aguasca et al., "Atmospheric Artifact Compensation in Ground-Based DInSAR Applications", *Geoscience and Remote Sensing Letters*, IEEE, vol.5, no.1, pp.88-92, Jan. 2008 [3] Iannini, L.; Monti Guarnieri, A., "Atmospheric Phase Screen in Ground-Based Radar: Statistics and Compensation", *Geoscience and Remote Sensing Letters*, IEEE, vol.8, no.3, pp.537-541, May 2011 [4] J. Torrebadella, J. Corominas, X. Planas et. al., "El Deslizamiento



del Forn de Canillo en Andorra. Un Ejemplo de Gestión del Riesgo Geológico en Zonas Habitadas en Grandes Deslizamientos", VII Simposio Nacional sobre Taludes y Laderas Inestables. October 2009 [5] Zheng-Shu Zhou, Wolfgang-Martin Boerner, "Development of a Ground-Based Polarimetric Broadband SAR System for Noninvasive Ground-Truth Validation in Vegetation Monitoring", IEEE TGRS, Vol. 42, No. 9, September 2004 [6] Nico, D. Leva et al., "Generation of Digital Terrain Models With a Ground-Based SAR System", IEEE TGRS, Vol. 43, No. 1, January 2005 [7] Albert Aguasca, Antoni Broquetes, Jordi Mallorqui, Xavier Fabregas, Jordi Mallorqui et al. "A Solid State L to X-band Flexible Ground-based SAR System for Continuous Monitoring Applications", IGARSS 2004, Anchorage, Alaska

## Posters on Earthquakes and tectonics

### Transient deformation in the Eastern California Shear Zone in Northern Mojave, California

#### Author(s)

Gilles Peltzer <sup>(1)</sup>, Zhen Liu <sup>(2)</sup>, Paul Lundgren <sup>(2)</sup>

#### Department

<sup>(1)</sup>University of California, Los Angeles Geology, USA

<sup>(2)</sup>JPL-Caltech MS-300-210, USA

#### Abstract

Previous results obtained with InSAR data suggest that during the 1992-2000 decade, a prominent fault system in the Eastern California Shear Zone (ECSZ), the Blackwater - Little Lake fault system, accommodated strain at a rate exceeding its long-term (geologic) rate by a factor of at least 3. During the same period, the study also suggests that the Garlock fault, cutting across the ECSZ as a conjugate fault, accumulated strain at a slower rate than its geological rate, or even not at all in its eastern section. This intriguing observation raised a number of questions about the temporal behavior of faults in the northern Mojave and stress transfer between near-by structures. With an InSAR archive of almost 18 years, we revisit the northern Mojave Desert area to determine the temporal history of the strain observed along the Blackwater fault. To correct atmospheric errors, we use the North America Regional Reanalysis (NARR) global atmospheric model distributed by NOAA to estimate the radar phase delay produced by the stratified atmosphere. For each epoch of radar acquisition, a vertical profile of the air index of refraction is computed at each of the NARR grid nodes. The phase delay at each image pixel is then estimated by interpolation within the NARR grid and integration along the atmospheric column above the elevation of the pixel. The complete ERS/ENVISAT archive is processed and corrected using the approach above. The set of interferograms is used to compute a time series of the LOS displacement field using the SBAS approach. The linear trend adjusted in the entire series indicates that strain is concentrated along the Blackwater fault over a width of 60-80km, consistent with right-lateral shear on the fault. The template approach using an atan function shape adjusted to all interferograms reveals the temporal history of the strain along the fault: two periods of accelerated deformation seem to coincide with the co- and post-seismic periods after the Landers 1992 and the Hector Mine 1999 earthquakes, which occurred on faults located SE of the Blackwater fault. A fraction of the signal may be due to post-seismic mantle flow subsequent to the two near-by earthquakes but the width of the strained zone suggests a local response of the Blackwater fault to the stress change produced by these events.

# Persistent Scatterer InSAR applied to the South West of Taiwan: neotectonic implications

## Author(s)

Champenois Johann <sup>(1)</sup>, Benoit Deffontaines <sup>(2)</sup>, Bénédicte Fruneau <sup>(2)</sup>, Erwan Pathier <sup>(3)</sup>, Jyr-Ching Hu <sup>(4)</sup>, Kuan-Chuan Lin <sup>(4)</sup>

## Department

<sup>(1)</sup>University Paris-Est 5 Bd Descartes, Bat IFI, FR

<sup>(2)</sup>Université Paris-Est 5 Bd Descartes, FR

<sup>(3)</sup>Université Joseph Fourier , FR

<sup>(4)</sup>National Taiwan University , TW

## Abstract

The island of Taiwan is the result of the ongoing collision between the Philippines Sea Plate and the Eurasian Plate. The South West of Taiwan, composed by the Coastal Plain and the Foothills, is the area where occur the deformation front of the Taiwan mountain belt. This orogeny is associated with destructive earthquakes (example of the 1999 Mw 7.6 Chi-Chi earthquake) and several blind fault systems. The precise location and the knowledge of newly active structures are crucial in this densely populated area. Several studies based on geodetic data and Synthetic Aperture Radar Interferometry has shown the uplift of the Tainan pop-up structure [1, 2], the subsidence of the Pingtung plain (essentially due to water pumping [3]) the activity of the Hengchun Peninsula situated at the top of the accretion prism, and the creep activity of the Fengshan transfer fault zone, where the Kaohsiung block situated in the south bounded to the north-east by an active fault zone NW-SE verging [2]. This study uses the recent Persistent Scatterer (PS-InSAR) [4] method which allows us to obtain a high density of points of measure with a huge dataset, composed of ERS, ENVISAT and ALOS data, allowing us to cover the large period between 1996 and 2011 (pre and post Chi-Chi earthquake). The analysis of maps of mean Line Of Sight displacement (toward the satellite) combined with the monitoring of temporal variations (through the time series of displacement), give major keys for the structural information for better understanding the mechanism of the South West Taiwan active faults system. [1] Fruneau, E. Pathier, D. Raymond, B. Deffontaines, C.T. Lee, H.T. Wang, J. Angelier, J.P. Rudant, and C.P. Chang, Uplift of Tainan Tableland (SW Taiwan) revealed by SAR interferometry, *Geophys. Res. Lett.*, Vol. 28, No. 16, p.3071-3074, 2001. [2] Lacombe O., Mouthereau F., Deffontaines B., Angelier J., Chu H.T., Lee C.T., 1999. Geometry and quaternary kinematics of fold-and-thrust units of southwestern Taiwan, *Tectonics*, 18, 6 : 1198-1223. [3] Chang, C.P., Chang, T.Y., Wang, C.T., Kuo, C.H. & Chen, K.S., 2004. Land-surface deformation corresponding to seasonal ground-water fluctuation, determining by SAR interferometry in the SW Taiwan, *Mathematics and Computers in Simulation*, 67, 351-359. [4] Hooper, A. J., Persistent scatterer radar interferometry for crustal deformation studies and modeling of volcanic deformation, Ph.D. thesis, Stanford University, 2006.

# L'Aquila earthquake: would an early warning have been possible?

## Author(s)

Licia Mangione <sup>(1)</sup>

## Department

<sup>(1)</sup>University of Rome "La Sapienza", IT

## Abstract

The Italian town of L'Aquila, capital of the Abruzzi Region in the central part of Italy, underwent a major seismic devastation on 6 April 2009, when an earthquake of 6.3 magnitude of Richter scale destroyed a large part of the city and surroundings. The objective of this work is twofold: on

the one side to analyse a recent earthquake that occurred in an area of particular seismic interest and that has been well documented, on the other side to check whether it would be possible to identify a posteriori a possible seismic signal that could have occurred before the earthquake and that could have been used as a sort of “early warning” of the event. Differential interferometry technique has been used on several Envisat ASAR image pairs: the latter have been selected with short baseline, all, but with different time separation. From the several pairs used, two have been selected here to illustrate the results of this investigation. The first ASAR pair considered included one image acquired on 1 February 2009 (master) and one on 12 April 2009 (slave), from the first Envisat pass after the event: it shows a noisy coherence image in general, except in a couple of sites, where the InSAR images show few semicircular fringes in the centre and in the bottom right corner. It is interesting to note that on the same dates but from ERS-2 SAR data good interferograms were instead obtained, for instance by R. Lanari of IREA. Master of another interferogram was the ASAR image acquired on 27 April 2008, used as a reference image of a normal situation, and the slave image was the same of the previous exercise (12 April 2009): it was certainly the best result obtained from the ASAR interferograms generated, with a good coherence image, as it shows neat fringes in most locations where a vertical terrain movement was detected after the earthquake (some 25 cm in L’Aquila and in Fossa). Results of this work confirm the excellent contribution that InSAR methodology can provide to an “a posteriori” characterisation of an earthquake and to the analysis of its impact on the environment. However, they also make clear that, to date, InSAR cannot help in detecting possible terrain signals “before” the event, for example fringes that could be interpreted as a sort of soil vibration. A similar investigation will be carried out for the area of Ardea (Latium) where low intensity seismic phenomena have been detected in the last years.

## Comparing Long and Short Term Deformation in the Krafla Fissure System, NE Iceland

### Author(s)

Emma Bramham <sup>(1)</sup>, Tim Wright <sup>(1)</sup>, Douglas Paton <sup>(1)</sup>, Freysteinn Sigmundsson <sup>(2)</sup>, Carolina Pagli <sup>(1)</sup>

### Department

<sup>(1)</sup>University of Leeds School of Earth and Environment, Leeds LS2 9JT, GB

<sup>(2)</sup>University of Iceland Volcanological Centre, Institute of Earth Sciences, IS

### Abstract

The Krafla volcanic system is situated on the divergent plate boundary separating Eurasia from North America in the Northern Volcanic Zone of Iceland. It is a 5-10 km wide and 100 km long region consisting of a central volcano and fissure swarm. Dyke intrusions and fissure eruptions characterise the activity in Krafla. A rifting episode in 1975-1984 activated an 80 km long segment of the Krafla fissure swarm. The eruptive history suggests that the Krafla fissure swarm may not have been active for the whole of the last 10 ka, and that other rift segments may accommodate extension during periods of quiescence. To better understand the deformation in this region we have attempted to determine whether faulting has been proceeding at a steady rate during this time period by examining both the long term (10 ka) and short term (10s of years) vertical deformations. To study the short-term vertical deformation in the Krafla system we have combined a series of interferometric synthetic aperture radar (InSAR) images, acquired by ERS and Envisat, with GPS data. The GPS data constrain the horizontal deformation – we remove the contribution of horizontal motion from the InSAR data to isolate the current vertical surface deformation rates. For the long term deformation, we have acquired high resolution LiDAR surveys over the Krafla fissure swarm in August 2007 and September 2008. These data have been interpolated to create a 1,300 km<sup>2</sup> high resolution (~0.5 m) Digital Elevation Model (DEM) of

the area. Using the DEM and ages of known lavas, we have estimated the average rate of vertical deformation during the post-glacial period (10 ka). We will present a comparison of the long-term rates with the present-day deformation to determine whether the present-day deformation can be used as a reliable indicator of long-term rates of activity.

## Surface deformation in the Western Basin and Range Province

### Author(s)

Fernando Greene <sup>(1)</sup>, Falk Amelung <sup>(1)</sup>, Shimon Wdowinski <sup>(1)</sup>

### Department

<sup>(1)</sup>University of Miami 4600 Rickenbacker Cswy, USA

### Abstract

We present the contemporary velocity field in the western Basin and Range province observed by satellite radar interferometry. A recent study in the Central Nevada Seismic Belt (CNSB) reported a broad area of uplift (~ 2-3 mm/yr) explained by postseismic mantle relaxation after a sequence of four earthquakes (M ~ 7) that occurred in the first half of the 20th century. To investigate the contemporary crustal deformation at the CNSB we use SAR imagery that covers a swath nearly 700 km long (seven conventional SAR frames) acquired by the European Remote Sensing Satellites ERS-1 and ERS-2 between 1992 and 2009, and Envisat between 2004 and 2010. Time-Series results suggest that the uplift velocity decreased for the last 7 years, which is consistent with models of postseismic relaxation. We also produce line of sight (LOS) velocity fields for different time periods (1992 – 2000, 1995 – 2009 and 1992 - 2009) by averaging independent interferograms with small perpendicular baselines (< 150 m). Additionally we identify high rates of deformation related to land subsidence due to water pumping on mines and agricultural exploitation areas, and ground deformation associated with moderate earthquakes

## Co-seismic deformation due to the Tohoku-Oki earthquake measured by ENVISAT-ASAR data and GPS

### Author(s)

Fabio Bovenga <sup>(1)</sup>, Oscar Davide Nitti <sup>(2)</sup>, Athanassios Ganas <sup>(3)</sup>,  
Kostas Chousianitis <sup>(3)</sup>

### Department

<sup>(1)</sup>National Research Council of Italy , IT

<sup>(2)</sup>Politecnico di Bari , IT

<sup>(3)</sup>National Observatory of Athens , GR

### Abstract

On March 11th, 2011, 05:46 UTC, a giant earthquake of magnitude Mw=9.0 occurred off the Pacific coast of Tohoku, Honshu Island, Japan. It has been followed by a series of powerful aftershocks, with 31 earthquakes of magnitude higher than 6 in 3 days (EMSC special web site). The earthquake epicenter is located approximately 150 km off Sendai at a depth of 22 km. A tsunami wave was generated in the Pacific, with wave heights reported at more than 4 m high. Massive damage has been reported, mainly related to the subsequent tsunami. This is the largest earthquake ever recorded in Japan, and is among the 5 largest earthquakes recorded worldwide. Two days earlier, on March 9th, another large earthquake (Mw=7.2) occurred in the same area, approximately 40 km to the southwest from the main earthquake of March 11th. The Differential Interferometric SAR (DInSAR) technique has been routinely applied to analyze co-seismic data relative to many earthquakes. Main advantage of SAR Interferometry are the synoptic view of wide area on the ground as well as the periodic surveying of the area which guarantees long time

monitoring. The SAR sensors launched by ESA (ERS-1/2, ASAR ENVISAT) provided great impulse in experimentation and development of InSAR based techniques devoted to disaster monitoring. In the present work we present results concerning the displacement induced by the Tohoku-oki earthquake by using C-band ASAR ENVISAT data acquired few days before and after the event.. In particular we used a set of 8 InSAR couples acquired in Stripmap mode along descending track 347, frames from 2763 to 2907, on February 19, 2011 and March 21, 2011. The resultant ground coverage is a strip 750 km long and 70 km wide. GPS measurements were also available thanks to the GPS Earth Observation Network (GEONET) of Japan, which consists of 1200 GPS permanent stations and is the largest GPS network of the world with average spacing between stations of about 20 km. Regional continuous GPS networks designed mainly to monitor strain for earthquake research and forecasting have operated in Japan for several years. In the present case, the displacements derived by GPS are used both to support InSAR processing as well as to validate the DInSAR results. Our results show that, after removing artifacts due to strong orbital errors, the resultant displacement field is mainly related to the coseismic ground deformation. The work points out the reliability of ASAR ENVISAT data to provide interferometric-based displacement field even though the satellite is recently came into a new operative phase with degraded orbital control and, SAR data were processed in an emergency framework soon after the acquisition without precise orbital records. - Acknowledgments - ENVISAT data are provided by ESA through the GEO Geohazards Supersite (<http://supersites.earthobservations.org>). Preliminary GPS time series provided by the ARIA team at JPL and Caltech. All original GEONET RINEX data provided to Caltech by the Geospatial Information Authority (GSI) of Japan.

## Using SBAS-InSAR to Investigate tectonic activities along Chamn Fault

### Author(s)

Heresh Fattahi <sup>(1)</sup>, Falk Amelung <sup>(1)</sup>

### Department

<sup>(1)</sup>University of Miami , USA

### Abstract

The Chaman fault is the transform boundary between the Indian and Eurasian plates located at the border between Afghanistan and Pakistan. The relative slip velocity of the Chaman fault is 2-4 cm/yr based on geological observations. Furuya et al., [2008] used InSAR to study the 2005 M6.X earthquake and observed long-lasting afterslip of several tens of centimeter over two years time period following the earthquake. Due to a lack of geodetic data, it is not yet known whether the Chaman fault is accumulating strain along its entire length or whether it is seismically creeping along parts of the fault. In this poster we will present preliminary results based on 2004 to 2010 Envisat-ASAR acquisitions processed using the SBAS technique. Our initial results shows creeping along some segments of the fault and strain accumulation at rates below our detection threshold at other segments.

# Inferring Complete (3D) Surface Deformation Field from Fusion of MAI and DInSAR Measurements: Application to 2010 Darfield Earthquake

## Author(s)

Jun Hu <sup>(1)</sup>, Zhiwei Li <sup>(1)</sup>, Xiaoli Ding <sup>(2)</sup>, Jianjun Zhu <sup>(1)</sup>, Lei Zhang <sup>(2)</sup>, Qian Sun <sup>(1)</sup>

## Department

<sup>(1)</sup>Central South University, CN

<sup>(2)</sup>The Hong Kong Polytechnic University, CN

## Abstract

Recently, DInSAR technology is frequently used to measure crustal deformation induced by geophysical or engineering processes. However, azimuth surface deformation vector, which is perpendicular to the line-of-sight (LOS) direction, is completely blind to DInSAR measurements. Although multiple observations with different imaging geometry can be combined to resolve vertical and east-south surface displacements, but is almost helpless to north-south surface displacement, which is nearly parallel to the azimuth direction. Multi-Aperture InSAR (MAI) technology can be an effective complement to DInSAR by providing azimuth displacements from the same interferometric pair. As the accuracies of MAI measurements depend on wavelength of SAR image as DInSAR measurements, improvement in precision have been yielded when comparing with conventional offset tracking method, which accuracies rely on the spatial resolution. In this paper, MAI and DInSAR techniques had been applied to investigate the complete coseismic surface deformation caused by Darfield earthquake in 3 September 2010. In order to derive three-dimensional surface displacement, total 12 PALSAR scenes acquired from ascending and descending orbits had been exploited and integrated by weighted least squares adjustment. We found that the MAI measurements were affected by ionospheric anomalies in the ascending data processing. An ionospheric effect detection and reduction approach was then introduced to improve the precision of MAI measurements. It is demonstrate that the three-dimensional displacement fields are of benefit to exhibit the comprehensive ground movements due to the earthquake and therefore have great potential in source parameters inversion.

Keywords: InSAR, MAI, ionospheric anomaly, three-dimension, Darfield earthquake

# The relationship between coseismic and postseismic deformation associated with the 2010 Mw 8.8 Maule, Chile Earthquake

## Author(s)

Nina Lin <sup>(1)</sup>, Mark Simons <sup>(1)</sup>, Anthony Sladen <sup>(1)</sup>, Sarah Minson <sup>(1)</sup>, Junle Jiang <sup>(1)</sup>, Francisco Ortega <sup>(1)</sup>, Jean-Philippe Avouac <sup>(1)</sup>, Eric Fielding <sup>(2)</sup>, Benjamin Brooks <sup>(3)</sup>, Mike Bevis <sup>(4)</sup>

## Department

<sup>(1)</sup>Caltech MC100-23 1200 E California Blvd, Pasadena, CA91125, USA

<sup>(2)</sup>Jet Propulsion Laboratory 4800 Oak Grove Drive Pasadena, CA 91109, USA

<sup>(3)</sup>University of Hawaii 1680 East-West Road, POST 602 Honolulu, HI 96822,

<sup>(4)</sup>Oregon State University 275 Mendenhall Laboratory, 125 South Oval Mall, Columbus, Ohio 43210, USA

## Abstract

Coseismic and postseismic deformation associated with large megathrust earthquakes can be used to unveil a mosaic frictional properties and stress states along a subduction interface. The 2010 Mw 8.8 Maule earthquake in south-central Chile and its aftermath, together with the 1835

Concepcion earthquake and the 1960 Valdivia earthquake, provide key constraints on the distribution of seismogenic asperities and apparent barriers. The Arauco Peninsula appears to be a barrier for seismogenic slip between the 1835 and 2010 event in the north and the 1960 event in the south. To explore the relationship between coseismic and postseismic deformation of the Maule earthquake, we exploit survey and continuous GPS, InSAR images, teleseismic data and tsunami waveforms to constrain the coseismic slip. We also carry out a joint inversion using GPS and InSAR data to estimate the spatial and temporal evolution of afterslip. We find two major regions of post-seismic slip down-dip of the regions that slipped during the earthquake. The northern patch near Constitucion, is at depths greater than 35 km, with another deep slip patch further down dip . A southern region of afterslip encircles the region that slipped coseismically beneath the Arauco Peninsula and extends all the way to the trench . The near-trench slip patch, however, may be related to the slip on secondary structures in the upper crust. These two regions of afterslip are spatially separated from regions that slipped coseismically. Aftershocks are distributed along the borders between the patches that slip coseismically and postseismically . We find a high misfit in the vertical component of the postseismic GPS data east of the Andes, which may indicate aseismic deformation in the upper crust or viscoelastic relaxation. Our models for the Arauco Peninsula predict ~3 m coseismic uplift, followed by 0.1 m gradual postseismic subsidence within the first six months. By correlating the deformation and uplift of the peninsula with coseismic and postseismic slip distribution, we make the linkage between seismic cycles and peninsular building and determine the long-term spatial stability of the seismic barrier under Arauco.

## InSAR observation and inversion of the 2011 three large earthquakes

### Author(s)

Jianbao Sun <sup>(1)</sup>, Shaozhuo Liu <sup>(1)</sup>, Xuwei Luo <sup>(2)</sup>, Zhengkang Shen <sup>(2)</sup>

### Department

<sup>(1)</sup>Institute of Geology, China Earthquake Admin. , CN

<sup>(2)</sup>Peking University , CN

### Abstract

We studied three large earthquakes happened in 2011 in Asia and Pacific region, which produce large crust deformation and led to heavy damages to the local residences in these regions. Using InSAR data, combing with GPS data if available, we generated the coseismic interferograms of the March 1 Mw6.3 New Zealand earthquake, March 11 Mw9.0 Sendai earthquake and the March 24 Mw6.8 Myanmar earthquake. We use both InSAR and GPS data collected near the earthquake area before and after those earthquakes and implement detailed deformation inversion and get the fault slip solutions for these events. The March 11 Mw9.0 Sendai earthquake in the Japanese trench has max fault slip as much as ~42.0 m from our inversion. The fault slip is thrust dominated, but there are also some strike-slip components to the north (sinistral) and south (dextral). Given the very density GPS and InSAR observations, it's still non-objective to determine the smoothing parameter because the fault plane is far away from land observations (~60-80 km away). Both the March 1 Mw6.3 New Zealand earthquake and the March 24 Mw6.8 Myanmar earthquakes have simple strike-slip motion and InSAR results give high quality results. We use these data sets for the coseismic slip distribution inversion. The work is supported by the Dragon2 project of ESA and NRSCC and the Sentinel Asia framework in Asia. The results may be helpful for understanding the earthquake mechanisms and shed light on the earthquake hazard assessment in these areas. The details will be reported on the meeting.

# InSAR analysis of active deformation related to the 2008 Nura earthquake, Pamir-Alai mountains

## Author(s)

Kanayim Teshebaeva <sup>(1)</sup>, Mahdi Motagh <sup>(2)</sup>, Sigrid Roessner <sup>(2)</sup>, Helmut Echtler <sup>(2)</sup>, Aleksander Zubovich <sup>(1)</sup>, Bernd Schurr <sup>(2)</sup>

## Department

<sup>(1)</sup>Central Asian Institute for Applied Geosciences Timur Frunze 73/2, KZ

<sup>(2)</sup>GFZ Telegrafenberg D 14473, IR

## Abstract

On October 5, 2008, a 6.6 magnitude Nura earthquake struck the eastern Alai region, causing human fatalities and considerable destructions in the southern province of Osh, Kyrgyzstan. No ground-based geodetic monitoring system were available in the area at the time of the earthquake to assess the coseismic deformation field and source parameters of the earthquake. In this study, we use space-based interferometric observations from Envisat and ALOS to analyze ground surface deformation associated with the Nura earthquake. We processed 22 ascending ALOS/PALSAR and 10 descending ENVISAT/ASAR images covering the east part of the Pamir Alai region. For this high altitude region L-band PALSAR interferograms proved to preserve coherence for time periods longer than one year and perpendicular baseline less than 1000 meter, while C-band ENVISAT interferograms lost coherence quickly month due to extensive snow cover. The measured line-of-sight uplift and subsidence amounts to about 36 cm and 30 cm in the hanging and footwall, respectively, with a clear activation of the NE-SW oriented Irkeshtam thrust fault. Interferometric measurements show a clear localization of surface deformation due to the rupture of a south-dipping thrust fault, accommodating part of the convergence between Pamir and Eurasia with the reverse movement of Trans Alay range onto Alai basin and ridge. Long-term GPS observations over the Pamir-Alay zone indicate NNW-SSE oriented shortening with a velocity of 10 up to 15 mm/yr along this thrust, collecting the main part of about 25 mm/yr of convergence between the Pamir and Eurasia. The present results provide updated insights into the processes of mountain building at the eastern end of Trans Alay range with strain partitioning in the footwall of the Pamir.

## How well can InSAR derived earthquake source parameters explain observed seismic data?

## Author(s)

Jennifer Weston <sup>(1)</sup>, Ana Ferreira <sup>(1)</sup>

## Department

<sup>(1)</sup>University of East Anglia School of Environmental Sciences, UEA, Norwich NR4 7TJ, UK

## Abstract

Earthquake source parameters that are calculated from the inversion of InSAR data are often compared with results from the inversion of seismic data, such as those in the Global Centroid Moment Tensor (GCMT) catalogue. A recent comparison of this nature for 58 events (Weston et al. 2011) showed an overall agreement between the two datasets. However, for several earthquakes there were significant discrepancies in fault geometry, location or seismic moment. Here it is investigated whether despite these differences the geodetically determined source parameters are able to explain the observed seismic data. CMT parameters from InSAR and seismic data are forward modelled in a 1D earth model (PREM, Dziewonski and Anderson, 1981) using normal mode summation (e.g. Dahlen and Tromp, 1998) and in a 3D earth model (S2ORTS, Ritsema et al.,



1999) using the spectral element method (Komatitsch and Tromp, 1999). The synthetic and observed waveforms are filtered at 150s, 80s and 40s to enhance long period surface waves, moderate-long period surface waves and long period body waves respectively. Phase, amplitude and waveform misfits between data and synthetics are subsequently calculated. Initial results for the Landers earthquake (28th June 1992, Mw 7.3) indicate that both sets of source parameters explain the observed data equally well, with waveform misfit values ranging from 0.3-0.4. The implications of these results and preliminary results for five other earthquakes (Mw 6.1 - 8.1) in different tectonic settings will be discussed.

## Comparison of multi-temporal INSAR and coherent targets INSAR methods for post-seismic crustal deformation detection: a case study in east Kunlun fault after 2001 KOKOXILI earthquake

Author(s)

Xiao Cheng <sup>(1)</sup>

Department

<sup>(1)</sup>Beijing Normal University , CN

### Abstract

On 14/11/2001 a strike-slip earthquake, with Ms 8.1, occurred along the western Kunlun fault (Tibet, China). The earthquake produced a surface rupture about 400km long, in a very remote area. The Kunlun fault is active and also after the heavy earthquake, it will definitely undergo a relaxation and balancing process. So the post-seismic deformation detection is rather important for the evolvement study of Kunlun fault. The high altitude and remote nature of the terrain meant that the traditional observation technologies are inefficient for continuous observation. Commonly processed InSAR data also encounters heavy decorrelation when the time gap is long or the seasonal difference induces large change of ground surface. In this paper, we adopted two methods for deformation detection, one is multi-temporal InSAR, the other is Coherent Target D-InSAR. 14 scenes of ENVISAT ASAR data acquired from 2003 to 2007 are adopted in this research to study the post-seismic surface deformation in Kusai Lake region after the 2001 Ms 8.1 Kunlun earthquake. Coherent Target D-InSAR aims at resolving the problems caused by loss of coherence and atmospheric inhomogeneity which restrained the InSAR to be more effective on terrain deformation monitoring. The advantage of using point targets is that these do not exhibit geometric decorrelation such as distributed targets, permitting a more complete use of the data as even pairs with very long baselines can be interpreted, resulting in improved accuracies and temporal coverage. PS InSAR has been successfully applied on some urban areas to measure the terrain deformation. But it is not easy to use it in the mountainous and humid areas due to the uncorrelated and atmospheric errors. In this paper, we take on a PS InSAR application in Kusai Lake area for crustal deformation with the ENVISAT ASAR data from ESA. Also SRTM DEM data is included and a cooperative SAR image registration method is used for pre-processing of multi-temporal ASAR data in later two-pass differential InSAR pairs. After a long calculation and regression progress, we got deformation and some relevant information of hundreds of coherent target points. However, since the density of PS is too low, it is impossible to interpolate to make a continuous deformation image. However, multi-temporal fine-baseline 2-pass INSAR got better results and good interpretation for deformations. The results showed that: (1) cooperative registering multi-temporal InSAR is an efficient tool for continuous surface deformation detection in this area. (2) the post-seismic deformation adjustment of the rupture belt is a dynamic process. During the period of 2003, 2004 and from Sep. 2005 to Feb. 2006, the amplitude of adjustment was large. The rupture belt was relatively stable during the period from Nov. 2004 to Sep. 2005. (3) In 2006 and 2007, the adjustment was weakening gradually.

# Time-series analysis of interseismic deformation across the Ganos segment of the North Anatolian Fault (NAF) zone, Turkey, from ERS and Envisat InSAR

Author(s)

Mahmud Haghshenas <sup>(1)</sup>, Mahdi Motagh <sup>(2)</sup>, Mohammad-Ali Sharifi <sup>(1)</sup>

Department

<sup>(1)</sup>University of Tehran Department of Surveying and Geomatics Engineering, University of Tehran, Tehran, Iran, IR

<sup>(2)</sup>Helmholtz-Zentrum Potsdam Department of Geodesy and Remote Sensing, Helmholtz-Zentrum Potsdam, Potsdam, Germany, DE

**Abstract**

In this study, we use time-series analysis of ERS and Envisat SAR data to measure more than 15 years of interseismic strain accumulation across the Ganos segment of the North Anatolian Fault (NAF) zone in Turkey. North Anatolian fault is one of the most active continental strike-slip faults in the world and the Ganos segment is the westernmost part of this fault between the Marmara Sea and the Gulf of Saros. This segment was last ruptured in 1912 with a large Ms 7.4 earthquake. Previous space and ground-based geodetic studies show a zone of high strain rate across the fault, a few kilometers wide, consistent with right-lateral slip on Ganos fault. East-west orientation of this fault and the sense of expected motion in the region make it a suitable target for InSAR measurement. However, vegetation coverage, steep topography in the eastern part of the fault zone, and the influence of decorrelation noise and atmospheric artifacts make it impossible for the classic repeat-pass InSAR to provide reliable measurements of the rate of interseismic deformation in the Ganos area. Advanced InSAR time-series methods of Persistent Scatterer (PS) and SBAS can overcome these problems. Here we apply both PS and SBAS methodologies to measure interseismic deformation rate in the Ganos fault and compare the results. We utilize more than 15 years of SAR data acquired by the ERS and Envisat satellites in the region to produce multi-sensor long time-series of deformation. The resultant deformation field is then inverted using elastic and visco-elastic interseismic models to constrain coupling depth and slip rate of the fault.

## The Study of Marine Terraces, SE of Iran using InSAR

Author(s)

Alireza Kiani <sup>(1)</sup>, Mahasa Roustaei <sup>(1)</sup>

Department

<sup>(1)</sup>Geological Survey of Iran(GSI) , IR

**Abstract**

The Makran accretionary prism is the site of low-angle subduction of Oman Sea beneath the Lut and Afghan continental blocks at the rate of about 25 mmyr<sup>-1</sup> (e.g. Stoneley 1974; White 1982; Kidd & McCall 1985). East 58E, most of shortening is 19.5±2 mmyr<sup>-1</sup> (Varnent et al., 2004). Sub Makran region composed of 25 terrace and platform areas. Marine terraces are striking features along the Makran coast and rise at least 245m above the flat coastal plain. The uplifted terraces are just part of active tectonics; repeated pulses of vertical movement which is associated with sea level fluctuation. Landscapes are not entirely due to the present day deformation (e.g. Page et al. 1979; Hosseini-Barzi & Talbot 2003). The study area located around Chabahar Bay; Konarak and Chabahar Terraces. An attempt to explore the recent deformation was hampered by a lack of seismic and geodetic data. In our first preliminary investigation, ascending images (track 199 with incident angle ~41 degree) were ordered from a decade of SAR data. The main problem for

processing SAR data is atmospheric water vapor as well as orbital, unwrapping errors, topography distortion. The primary aim is to estimate regional deformation which can fruitfully link with field observations. Key words: Makran, Marine terraces, uplift, Chabahar Bay, SAR data

## 3D ground motion detection combining different methods, sensors and geometries using SAR data

### Author(s)

Gopika Suresh <sup>(1)</sup>, Christian Minet <sup>(2)</sup>, Michael Eineder <sup>(2)</sup>, Alessandro Parizzi <sup>(2)</sup>, Nestor Yague-Martinez <sup>(2)</sup>

### Department

<sup>(1)</sup>Technical University, Munich Arcisstr. 21, 80333, München, DE

<sup>(2)</sup>German Aerospace Center (DLR) Münchner Strasse 20, Oberpfaffenhofen, DE

### Abstract

Over the past years, InSAR has become a powerful technique for mapping surface deformations by earthquakes. However, it has the disadvantage that the interferograms are only sensitive to surface movements towards or away from the satellite's line of sight. This problem can be eliminated by using multiple observations which have different imaging geometries such as ascending and descending or different incidence angles. 3D motion detection methods attempt to resolve the displacement by providing information in the North, East and Up directions. The Haiti M7.0 Earthquake occurred at the Enriquillo-Plantain Garden Fault zone (EPGF) on the 12th of January 2010 and resulted in wide spread structural damage and loss to human life in and around Port-au-Prince. The aim of our study is to analyse the co- and post-seismic deformation caused by the Haiti Earthquake using different methods of processing, on data acquired from different SAR sensors with different geometries. InSAR methods that use phase information are shown to be affected by temporal decorrelation and topography while Cross Correlation methods only make use of the amplitude of the signal and are shown to provide better results in forest regions than InSAR methods. TerraSAR-X data provided by the DLR, Oberpfaffenhofen and ALOS PALSAR data provided by JAXA (Japanese Space Agency) will be used. For the 3D ground motion detection, the data will be processed mainly using Incoherent Cross Correlation and InSAR. The results will then be inverted to derive the 3D motion vectors that show the displacements of the surface. To conclude this project, an error analysis will be done for the 3 motion directions.

## Measurement of interseismic strain accumulation in the Southern Andes (25°-35°S).

### Author(s)

Gabriel Ducret <sup>(1)</sup>, Marie Pierre DOIN <sup>(1)</sup>, Raphaël GRANDIN <sup>(1)</sup>, Anne Socquet <sup>(2)</sup>, Christophe Vigny <sup>(1)</sup>, Marianne Metois <sup>(1)</sup>, Marta Bejar Pizarro <sup>(3)</sup>

### Department

<sup>(1)</sup>Ecole Normale Supérieure, FR

<sup>(2)</sup>Institut de Physique du Globe de Paris, FR

<sup>(3)</sup>Instituto Geologico y Minero de Espana, ES

### Abstract

The Chilean subduction zone is one of the most active in the world. The Nazca plate subducts under South America plate with a velocity around 7cm/year. The subduction is divided into segments with laterally varying coupling width. Rupture of these segments or of consecutive segments may produce earthquakes of magnitude greater than 8.0. However, the definition of the segmentation geometry in the particular case of Chilean subduction and its relation to earthquake

genesis in general is a debated topic. We focus on an area extending over 1000 km in latitude, located between Copiapo (25°S) and Santiago (35°S), which has been accumulating tectonic strain since the mid-20th century. Two main earthquakes occurred in the last decade around the boundaries of this segment : the 2007 Tocopilla earthquake to the North (M=7.7) and the 2010 Maule earthquake to the South (M=8.8). The 25-35°S part of the subduction zone presents since 38 years a background seismicity (given by USGS catalogs) rather homogeneously distributed in the North and higher in the South, mainly located along the plate interface and less frequently within the overriding plate. The seismicity does not clearly delineate intraplate features, which are also not yet related to clear geodetic strain measurements. Two seismic swarms occurred in recent years, the Puntaqui crisis in 1997, and the episode of Valparaiso in 1985. It has been recently suggested that seismicity can be related to variations of interplate coupling along the subduction. Around La Serena (32°S-29°S), the coupling distribution is constrained by an important GPS dataset. In contrast, further North or South, the GPS network is sparse and data indicate that coupling is heterogeneous there. InSAR (Interferometric Synthetic Aperture Radar) data is expected to provide additional constraints on interseismic strain accumulation and the coupling coefficient in this desert area. We ordered all archived ERS and ENVISAT satellite images (1992-2010) on 3 tracks (53, 282 and 325) between 25° and 35° S of latitude and with longitude varying with the track from 73° to 67° E : the track 325 covers the coast, the track 53 is inland in the North and covers the coast in the South and the track 282 is completely inland, mostly in Argentina. The ESA archive contains 150 images (39 ENVISAT and 104 ERS) unequally distributed for each track, with a very large number of ERS data on track 282. Moreover, the doppler centroid of all recent ERS data is screened to select useful 2002-2010 ERS scenes. We compute interferograms with a small baseline strategy. Due to the small number of data per track, the perpendicular baseline must reach up to 600m and the temporal baseline sometimes exceeds 7 years, thus limiting the interferometric coherence. The interferograms are corrected before unwrapping, whenever possible, from DEM errors effects and from stratified atmospheric delays (the phase-elevation correlation). The unwrapping step is done by ROI\_PAC on adaptatively filtered interferograms. The data scarcity hinders a temporal analysis, but the time series is used to derive an average velocity map in the satellite line of sight that can be compared with GPS velocity vectors projected on the same direction. The results, combined with GPS permanent stations and GPS campaigns points since 2004, give us a new and continuous geodetic data set to invert the coupling distribution on the subduction interface.

## Estimation of the surface deformation due to the 2009-2010 slow slip event at Guerrero seismic gap (Mexico) by satellite SAR Interferometry.

### Author(s)

Bacques Guillaume <sup>(1)</sup>, Erwan Pathier <sup>(2)</sup>, Cécile Lasserre <sup>(2)</sup>, Marie-Pierre Doin <sup>(3)</sup>, Nathalie Cotte <sup>(2)</sup>, Romain Jolivet <sup>(2)</sup>, Mathilde Radiguet <sup>(2)</sup>

### Department

<sup>(1)</sup>CNES/BRGM/ISTERRE BP53 Grenoble CEDEX9, FR

<sup>(2)</sup>ISTerre BP53 38041 Grenoble CEDEX 9, FR

<sup>(3)</sup>Laboratoire de Géologie, Ecole Normal Supérieur 24 Rue Lhomond 75231 Paris, FR

### Abstract

The Guerrero seismic gap is located along the Pacific coast of Mexico in a subduction zone where the Cocos plate subducts under the North American plate with a 5.5cm per year convergence rate. Along this 100 km long band located between Acapulco to the East and Zihuatanejo West side, no major earthquake has occurred since at least 1911 in the seismogenic zone of the subduction interface. In contrast, the surrounding areas of the Guerrero gap have been the location of large

seismic events like the one of 1985 (Mw 8), which destroyed Mexico City. Based on the plate convergence rate, a slip deficit of about 5 meters has been estimated in the seismogenic zone of the gap since the last major earthquake (Lowry et al. 1998), making a large earthquake possible in this location. However, the Guerrero gap was also the location of four slow slip events (SSE) with an approximately four years periodicity (1998, 2002, 2006, 2009-2010) since it has been instrumented by GPS permanent network in January 1997. Slow slip events are commonly interpreted as aseismic slip on the subduction plane. An important issue for seismic hazard assessment is to know whether the slip occurs in the seismogenic zone and then release part of the accumulated interseismic strain or if it occurs only deeper. To address this issue, geodetic measurements from GPS or space-borne Sar interferometry (InSAR) can be used to retrieve the SSE slip distribution on the subduction plane. Up to now mainly GPS data has been used. The continuous GPS network provides high temporal sampling data (better than daily) of the ground displacement. However the low spatial density of the stations (a few tens of stations irregularly distributed in an area of about 300km\*300km) cannot give a continuous spatial distribution that is critical for the slip estimation onto the subduction plane. A previous study concerning the 2006 SSE using InSAR with ENVISAT C-band data has shown the ability of the technique to provide complementary information with respect to GPS data (Cavalié, 2009), despite the presence of vegetation and of strong atmospheric artifacts. The aim of this study is to measure by InSAR the ground displacement of the 2009-2010 slow slip event from ENVISAT data. To do this we designed an Envisat acquisition plan to complete the available archive on this area for the 2009-2010 event with an acquisition programming effort during the event. The data set represents, between 5 and 10 images per track over 5 tracks covering spatially and temporally the 2010 slow slip event (C band, polarisation VV, I2 acquisition mode, 3 to 5 frames per track). We processed the SAR data by using a small baseline approach (NSBAS) based upon the ROI\_pac chain. One of the main encountered difficulties comes from unwrapping problems in the coastal range parallel to the coast where topography and dense vegetal cover are responsible for signal decorrelation and where strong atmospheric effects occur. To mitigate the unwrapping problems we tried to reduce the phase gradient due to atmosphere correlated to topography directly from the wrapped interferogram. We estimate the local density of fringe related to topography gradient and we fit these coefficients values with a linear model along the azimuth line (North to South) to remove it from the interferogram. This method applied for each interferogram reduces fringes gradient of the image making the unwrapping process easier and increasing significantly the proportion of unwrapped area. As we get our unwrapped interferograms, we apply a time series analysis based upon the Quiroz et al. approach [2009]. This method aims to retrieve the phase time evolution associated to each date of acquisition for each pixel by using the redundant information contained into each interferogram and by constraining the missing information with a phase evolution model. Thanks to this method, we can retrieve the time phase evolution for each pixel. This provides maps of the ground displacement at each date with respect to a reference date and a reference area. These measurements can be compared to the GPS measurement. Acknowledgments: This work is supported by a CNES/BRGM funding program and also by the G-GAP ANR. References: Lowry, A., K. M. Larson, V. Kostoglodov, and R. Bilham, Transient fault slip in Guerrero, southern Mexico, *Geophysical Research Letters*, 2001. doi:10.1029/2001GL013238. M. Radiguet, F. Cotton, M. Vergnolle, M. Campillo, B. Valette, V. Kostoglodov, N. Cotte, Spatial and temporal evolution of a long term slow slip event: the 2006 Guerrero slow slip event, *Geophysical Journal International*, 2010, Doi: 10.1111/j.1365-246X.2010.04866.x López-Quiroz, P., Marie-Pierre Doin, Florence, Pierre Briole and Jean-Marie Nicolas, Time series analysis of Mexico City subsidence constrained by radar interferometry, *Journal of Applied Geophysics* (2009), doi:10.1016/j.jappgeo.2009.02.006 Cavalié, O., E. Pathier, F. Cotton, M.-P Doin, N. Cotte, M. Vergnolle, and A. Walpersdorf. Mapping of the 2006 silent slow event in the Guerrero (Mexico) seismic gap by InSAR *Geophysical Research Abstracts*, Vol. 11, EGU2009-5133, 2009, EGU General Assembly 2009

# Assessing variability in the slip rate of the Altyn Tagh Fault using InSAR data

## Author(s)

Joanna Hamlyn <sup>(1)</sup>, Tim Wright <sup>(1)</sup>

## Department

<sup>(1)</sup>University of Leeds Leeds, UK, UK

## Abstract

The Altyn Tagh Fault in Tibet is a major left-lateral strike-slip fault that marks the northern boundary of the Tibetan plateau. The slip rate of the fault is controversial - the few measurements that exist (from geology and geodesy) show markedly different slip rates (Wright et al., 2004). An open question is whether the slip rate of the Altyn Tagh fault varies in time and space, or whether the discrepancy between the differing estimates simply reflects the uncertainties of the methods. The slip rate is important as it is a primary indicator of the mode of deformation of the plateau - a high slip rate, constant along the fault, would suggest that plate tectonic block models are appropriate, with most of the deformation accommodated by slip on major faults. A low slip rate, varying in space, would be more consistent with continuum models of continental deformation. We have analysed radar data collected from the European Space Agency's Envisat satellite to determine the slip rate of the fault at several locations. For each track, average deformation rate maps have been produced using a network algorithm (pi-rate) following the method of Elliott et al. (2008). We have modelled the data using simple elastic dislocation theory, and compared the results with existing geodetic constraints and geologic estimates of slip rate. References Elliott, JR; Biggs, J; Parsons, B; Wright, TJ (2008) InSAR slip rate determination on the Altyn Tagh Fault, northern Tibet, in the presence of topographically correlated atmospheric delays, *Geophysical Research Letters*, 35, . doi:10.1029/2008GL033659 Wright, TJ; Parsons, B; England, PC; Fielding, E (2004) InSAR Observations of Low Slip Rates on the Major Faults of Western Tibet, *Science*, 305(5681), pp236-239. doi:10.1126/science.1096388

# Stability assessment of Rio-Antirio cable-stayed bridge (Western Greece) using C- and X-band SAR Interferometry

## Author(s)

Issaak Parcharidis <sup>(1)</sup>, Michael Foumelis <sup>(1)</sup>, Penelope Kourkouli <sup>(1)</sup>,  
Salvatore Stramondo <sup>(2)</sup>, Urs Wegmuller <sup>(3)</sup>

## Department

<sup>(1)</sup>Harokopio University of Athens 70, El. Venizelou Str., 17671 Athens, Greece, GR

<sup>(2)</sup>INGV Via di Vigna Murata 605 00143, Rome, IT

<sup>(3)</sup>GAMMA REMOTE SENSING Worbstrasse 225, CH-3073 Gümligen, CH

## Abstract

In late '90s the Permanent or Persistent Scatterers Interferometry (PSI) technique was introduced to overcome limitations of conventional repeated-pass interferometry, related primarily to temporal and geometric decorrelation as well as to atmospheric path delays. By temporal analysis interferometric phase at coherent point-like targets, it was possible to monitor ground deformation over areas characterized by the low levels of coherence. Displacements at millimeter level accuracy along the line-of-sight direction of the satellite became feasible, allowing measurements of slow terrain motion even for specific infrastructures. The Rio-Antirio Bridge is the longest multi-span cable-stayed bridge of the world with 2,252 m of suspended deck and two viaducts of 392 m on Rio and another of 239 m on Antirio side. The area of the strait presents a

combination of hazards such as deep soil strata of weak alluviums, strong seismic activity, tectonic movements etc, which make the area of great ground deformation susceptibility and the bridge an element at risk. The present work concerns PSI analysis over Rio-Antirio cable-stayed bridge in order to estimate potential deformation occurring along the structure using C- and X-bands SAR observations. This activity is carried out in the framework of ESA's GMES project Terrafirma-X. Two different datasets of 37 ENVISAT ASAR scenes and 20 TerraSAR-X Stripmap scenes covering the periods 2002-2010 and 2008-2011 respectively were utilized. The interferometric processing was performed using GAMMA's Interferometric Point Target Analysis (IPTA) software packages. The IPTA is rather a toolbox than a simple processing sequence that supports various analysis schemes, including different approaches for point target selection, spatial and temporal phase unwrapping. For the Rio-Antirio bridge due to its characteristics (suspended deck), coherent targets could only be detected on the four pylons and the two viaducts. The generated preliminary results consist of height corrections, linear deformation rates, atmospheric phase, refined baselines, temporal coherence estimates and non-linear deformation histories for each geocoded point target. Results obtained from ENVISAT provide information on the deformation pattern of the surrounding area and the two viaducts as well. On the contrary high resolution TerraSAR-X interferometric observations provide valuable information about the main bridge stability through a number of targets detected.

## Towards mapping crustal deformation across North Africa: Examples from Algeria and Libya

### Author(s)

Ian Hamling <sup>(1)</sup>, Abdelkrim Aoudia <sup>(1)</sup>

### Department

<sup>(1)</sup>ICTP Strada Costiera 11, IT

### Abstract

Deformation along the north African plate boundary, related to the closure of the Tethys Ocean and subsequent collision between the Nubian and Eurasian plates, is complex and poorly understood. During the last century there have been a number of large (>6 Mw) earthquakes including the 2003 Zemmouri earthquake in Algeria and the 1935, Mw 7.1, earthquake in Northern Libya. Despite this history of large earthquakes, there have been very few studies of active faulting and consequently very little is known about which structures are actively accumulating strain. Previous studies in Algeria, examining historical seismicity, have suggested that seismicity is concentrated in four main areas: Oran, Cheliff, Mitijda, and Guelma. Although many existing fault structures, responsible for past earthquakes, have been identified across the region there are no estimates of inter-seismic strain accumulation making it difficult to assess the potential seismic hazard. Using SAR images acquired over the last ~18 years we have constructed a series of interseismic interferograms in an attempt to better understand the tectonics of this region. The study focusses on the Hun Graben, situated in north-west Libya, and the regions of Oran, Guelma, Mitijda and Cheliff in Algeria. To determine the interseismic deformation we first generate interseismic interferograms and correct each interferogram using the SRTM DEM and precise orbits. To maximise the number of coherent pixels in the time series we try to select SAR images with the shortest possible spatial and temporal baselines. Each of the interferograms is then checked for unwrapping errors and is corrected where necessary. To remove any residual orbital errors and reduce tropospheric phase delays, we perform a network atmospheric and orbital correction. To determine the interseismic strain accumulation we invert for the best fitting displacement, at every coherent pixel, and at each epoch. Next we generate line of sight rate maps to identify actively deforming regions. Analysis over the Hun graben in northern Libya suggests that neither of the two border faults are actively deforming. However, displacement

rates of ~10 mm/yr are observed in both ascending and descending datasets along a ~30 km section of the western fault. The pattern of deformation does not appear to be a result of tectonic activity but is instead a result of water extraction in the region. We find that the observed subsidence pattern correlates well with the location of well sites, which, over the past few decades, have been extracting water from the North-Western Sahara Aquifer System (SASS). In Algeria, preliminary analysis shows a number of interesting features. Line of sight displacement rates of ~ 5 mm/yr are observed close to Algeria's second city of Oran. The observed displacements appear to be related to a ~60 km-long, east west trending, reverse fault. Similarly, displacement rates of up to 5-6 mm/yr are observed around the Cheliff and Mitijda basins. As with Oran, the observed deformation seems to concentrate along ~EW trending reverse faults. With few ground based measurements across the region we hope that this study will provide new constraints on the tectonics along the north African plate boundary.

## Surface displacement time series analysis of the Afar rift zone retrieved through phase and amplitude SAR data

### Author(s)

Francesco Casu <sup>(1)</sup>, Luca Paglia <sup>(1)</sup>, Carolina Pagli <sup>(2)</sup>, Tim Wright <sup>(2)</sup>,  
Riccardo Lanari <sup>(1)</sup>

### Department

<sup>(1)</sup>IREA - CNR Via Diocleziano 328, 80124 Napoli, Italy, IT

<sup>(2)</sup>University of Leeds Earth Sciences Building, LS2 9JT Leeds, UK,

### Abstract

Continental rifting between the African and Arabian plates started 30 Myr ago, creating the Afar depression. A series of volcanic rift segments run across the Afar depression marking the axis of the plate boundary. The Dabbahu rift segment has been in active since 2005 when a 2.5 km<sup>3</sup> dyke intrusion and hundreds of earthquakes marked the onset a rifting episode [1] which continues to date [2-3]. At Dabbahu, 14 dyke intrusions and 4 eruptions have occurred so far. The dykes have caused massive ground breaks along faults and fissures. At least three shallow magma chambers have experienced cyclic emptying and replenishment, while a deep (~10 km) chamber has been continuously deflating. To analyze such complex deformations, we use Differential SAR Interferometry (DInSAR). This technique allows us to produce Earth surface deformation maps through the use of the phase difference (interferogram) of SAR image pairs. In particular, we use the advanced DInSAR algorithm referred to as Small BAseLine Subset (SBAS) [4] that combines a set of small baseline interferograms, to generate ground deformation maps and time series along the satellite Line-Of-Sight (LOS), with accuracies on the order of 5mm. Application of SBAS to the extensive ENVISAT data archive collected over Afar from 2003 to 2010, is ideal to show and test the capability of the technique. A common problem with large and rapid deformations, such as caused by dyke intrusions in Afar, is that the phase information degrades. In particular, some of the areas in the interferograms may be affected by high fringe rates, leading to difficulties in the phase unwrapping, and/or to complete loss of coherence due to significant misregistration errors [5]. This limitation can be overcome by exploiting the SAR image amplitude information instead of the phase, and by calculating the Pixel-Offset (PO) field. This is retrieved from the amplitude information of a given SAR image pair. When the deformation causes geometric distortions without significantly affecting the SAR image reflectivity, then the displacements can be retrieved by measuring the distortion of the scene, as observed in the amplitude images of a SAR pair. Moreover, after computing the POs for each image pair, it is possible to combine them, following the same rationale of the SBAS technique, to finally retrieve the offset-based deformation time series. Furthermore, as the POs are calculated in both the range and azimuth directions, this approach, referred to as PO-SBAS [6], permits us to generate



deformation time series not only in the satellite LOS (range) but also along the sensor flight direction (azimuth) which is mostly sensitive to the North-South component of the deformation. The PO-SBAS permits to retrieve the deformation field in areas affected by very large displacements at an accuracy on the order of 1/30th of a pixel. In this work we use both the phase and amplitude information of a set of ENVISAT images acquired over the Afar rift region, to retrieve a spatially and temporally detailed map of deformation. First, we apply the SBAS-DInSAR technique that, by exploiting differential SAR interferograms, permits us to generate ground deformation maps and time series with high accuracies in areas not affected by large displacement. In addition, we also use the PO-SBAS technique that, taking advantage of the amplitude information, allows us to retrieve the displacement field in areas affected by loss of coherence due to the large deformations. Moreover, we improve the N-S accuracy of our deformation maps using the azimuth PO which is commonly not used with standard DInSAR techniques. Our results show that by jointly exploiting the phase (SBAS) and amplitude (PO-SBAS) information of SAR pairs, we can fully characterize the deformation occurred in an area affected by large ground displacements, as the Afar rift region. Finally, it is worth noting the impact that such analysis may have for the interpretation and modeling of the ongoing phenomena.

References [1] Wright T.J. et al. (2006), Magma-maintained rift segmentation at continental rupture in the 2005, *Nature* 442, 291-294. [2] Hamling I.J. et al. (2009), Geodetic observations of the ongoing Dabbahu rifting, *Geophys. J. Int.*, 178, 989–1003. [3] Grandin R. et al. (2009), September 2005 Manda Hararo-Dabbahu rifting event, *J. Geophys. Res.*, 114, B08404. [4] Berardino P. et al. (2002), A new algorithm for Surface Deformation Monitoring based on Small Baseline Differential SAR Interferograms, *IEEE Trans. Geosci. Remote Sens.*, vol. 40, 11, pp. 2375-2383. [5] Yun S-H. et al. (2007), Interferogram formation in the presence of complex and large deformation, *Geophys. Res. Lett.*, vol. 34, L12305. [6] Casu F. et al. (2011), Deformation time-series generation in areas characterized by large displacement dynamics: the SAR amplitude Pixel-Offset SBAS technique, *IEEE Trans. Geosci. Remote Sens.*, doi: 10.1109/TGRS.2010.2104325.

## InSAR-GPS optimization for mapping high resolution 3-D crustal deformation of the 2011 Mw=9.0 Tohoku earthquake

Author(s)

Liming Jiang <sup>(1)</sup>, Hansheng Wang <sup>(1)</sup>, Bo Hu <sup>(1)</sup>

Department

<sup>(1)</sup>Institute of Geodesy and Geophysics, Chinese Academy of Sciences (CAS) 340 XuDong Rd., CN

### Abstract

Three-dimensional (3-D) crustal deformation maps allow us to improve the knowledge of the parameters of co-seismic models. We present here a revised method to derive continuous 3-D high resolution velocity maps with corresponding errors by combining sparse GPS measurements and InSAR observations. It is based on Bayesian statistical approach and Markov random field (MRF) theory. Three key steps are required in the proposed method: 1) interferometric baselines are refined with GCPs from GPS data to mitigate long wavelength errors related to inaccuracy SAR satellite orbits; 2) sparse GPS measurements are interpolated in order to fill in GPS displacements in the InSAR data grid; 3) 3-D continuous deformation velocity maps are estimated with a MRF-MPM optimization technique. This fusion method of GPS and InSAR data is applied to investigate the co-seismic deformation of the 2011 Mw=9.0 Tohoku earthquake in Japan. In the case study, we use a long-strip co-seismic interferogram (~750 km) produced with two ENVISAT ASAR acquisitions from 19th February and 21th March, and sparse GPS 3-D deformation measurements of the Japanese GEONET. The preliminary results show that not only a continuous 3-D deformation velocity field with high resolution is derived, but significant improvements in the

accuracy of the vertical component of velocity are achieved in comparison with the GPS data alone. Key words: Co-seismic 3-D deformation, the 2011 Mw=9.0 Tohoku earthquake, InSAR, GPS

## Visco-elastic deformation of the lithosphere around the lake Siling Co in Tibet

### Author(s)

Marie-Pierre Doin <sup>(1)</sup>, Cedric Twardzik <sup>(2)</sup>, Gabriel Ducret <sup>(1)</sup>, Cecile Lasserre <sup>(3)</sup>, Stephane Guillaso <sup>(4)</sup>, Jianbao Sun <sup>(5)</sup>

### Department

<sup>(1)</sup>Ecole Normale Supérieure 24 rue Lhomond, FR

<sup>(2)</sup>University of Oxford, United Kingdom

<sup>(3)</sup>Univ. Joseph Fourier, France

<sup>(4)</sup>Technische Universität Berlin, Germany

<sup>(5)</sup>Chinese Earthquake Administration, China

### Abstract

The lithospheric strength in Central Tibet is constrained from the rebound of the lithosphere and uppermost mantle subjected to loading or unloading due to lake Siling Co water level fluctuations. This lake is a large endoreic lake at 4500 m elevation located North of the strike-slip right lateral Gyaring Co fault, and South of the Bangong Nujiang suture zone, on which numerous left-lateral strike slip faults are branching. The Siling Co water level has strongly changed in the past, as testified by numerous traces of palaeo-shorelines, clearly marked until 60 m above present-day level. Altimetric measures show that during the period 1995-1999 the Siling Co water level remained stable while it increased by about 0.8-m/yr in the period 2000-2008, a remarkably fast rate given the large lake surface (1600-km<sup>2</sup>). To extend the lake level observation duration, we extract the lake contour from all cloud-free LANDSAT images available on the USGS GLOVIS server. The lake surface, used as a proxy for lake elevation, shows that the water level in the Siling Co lake in Tibet was more or less stagnant from 1973 to 1999 and increased between 2000 and 2010 at an average rate of 0.8 m/yr. A clear seasonal signal is superimposed on the interannual trend. The ground motion associated to the water level increase is studied by InSAR using all available 56 ERS and 51 Envisat data on descending tracks 491 and 219 in the period 1992-2010, obtained through the Dragon ESA-MOST cooperation program. A redundant network of small baseline differential interferograms is computed with perpendicular baseline smaller than 500-m. The ERS and Envisat networks overlap in time, thus insuring measurement continuity. The coherence is quickly lost with time (over one year), particularly to the North of the lake because of freeze-thaw cycles. Interferograms are corrected for stratified atmospheric effect and residual orbital trends. The interferograms covering the period 1992-1999 show no detectable deformation, whereas the ones covering the period 2000-2010 present a clear bowl shape pattern centered on the lake that extend from the shore to about ~100 km from the lake center. The amplitude is about 5 mm/yr close to the lake shores. To increase the signal to noise ratio, the interferograms are first analysed in time assuming a constant deformation shape. We then obtain the temporal evolution of the deformation amplitude : it remains constant for the period 1992-1999, and increases from 2000 until 2010. This curve follows closely the lake level temporal evolution. An average velocity map for the period 2000-2010 is also produced to better assess the shape of the ground displacement. Both the amplitude temporal evolution and the average velocity map are used to explore possible rheological models. The elastic model is based on dynamic moduli extracted from Vp/Vs profile from INDEPTH III experiment. It could explain the observed subsidence rates if static moduli were about 1.6 times lower than the dynamic moduli derived from the lithosphere seismic velocity profiles. On the other hand, a visco-elastic model with a low viscosity lower crust (about  $5 \times 10^{18}$  Pa.s) provides a good fit to the data. Although the ground

motion appears well correlated to water level fluctuations, delays resulting from viscous relaxation do not strongly change the temporal evolution and in fact yields a slightly better fit to the observed temporal evolution than the elastic model. We will discuss to what extent the models can be constrained by the available data, given the data noise amplitude and properties. In particular, we explore the model sensitivity to the layered rheological properties and past load history, and present model trade-off between elastic thickness, lower crust viscosity, and mantle viscosity. Furthermore, we provide and discuss uncertainties on ground motion time series, focusing on the quantification of turbulent atmospheric noise and of the azimuthal phase ramp.

## Imaging crustal deformation and faulting processes in central and southern California

### Author(s)

Zhen Liu <sup>(1)</sup>, Paul Lundgren <sup>(1)</sup>, Scott Hensley <sup>(1)</sup>

### Department

<sup>(1)</sup>Jet Propulsion Laboratory California Institute of Technology, 4800 Oak Grove Dr., Pasadena, CA 91109, USA, USA

### Abstract

We use satellite and airborne synthetic aperture radar (SAR) repeat pass interferometry (RPI) observations and GPS to image crustal deformation and fault slip behaviors in central and southern California. The major plate boundary fault (San Andreas) in central California displays a spectrum of complex fault slip behaviors. The central San Andreas fault (CSAF) is creeping in its central segment and transitions from creeping to locked towards the north and south, respectively. It branches into two sub-parallel faults in the north (northern SAF and Calaveras-Paicines fault) that are all actively accommodating plate motion. In the southern transition zone near Parkfield, regular earthquakes have occurred, with at least six Mw ~6.0 events since 1857, the most recent in 2004. Further south the Cholame segment is locked and ruptures only in large earthquakes. The complexity and variety of the observed fault slip behaviors have made the CSAF a natural laboratory to understand fault mechanics and fault zone rheology and to advance our knowledge and capability in earthquake hazard assessment. Existing Envisat and ERS-1/2 SAR data provide the longest archive of SAR data over the region but are subject to severe decorrelation. The L-band ALOS has less frequent acquisitions (5-6/yr per track) since 2006 but higher coherence than shorter wavelength radar data. In particular, the UAVSAR airborne SAR has repeated lawn-mowing (fault perpendicular adjacent swaths imaged from opposing look directions) flights over the CSAF for the past two years. Initial analysis of UAVSAR RPI reveals fault slip related deformation at much finer spatial resolution (~6m at 12 azimuth x 3 range looks) and clear variability along strike. We integrate available ALOS and UAVSAR observations with in-situ GPS measurements from the Plate Boundary Observatory (PBO) and regional campaign networks to estimate fault slip rate and shallow slip deficits along the CSAF. In addition, we will present InSAR-based time series analysis of crustal deformation in southern California using an ~18-year catalog of ERS-1/2 and Envisat data. We observe a clear transient variation across the Eastern California Shear Zone. We test the hypotheses whether this is due to broad scale postseismic deformation following Hector Mine earthquake or time dependent local fault response.

# Co-seismic Displacement of 24-March-2011 Mw 6.8 Mong Hpayak Earthquake, Myanmar

## Author(s)

Itthi Trisirisatayawong <sup>(1)</sup>, Itthi Trisirisatayawong <sup>(1)</sup>, Andy Hooper <sup>(2)</sup>,  
Anuphao Aobpaet <sup>(3)</sup>

## Department

<sup>(1)</sup>Chulalongkorn University Phayathai rd., Pathumwan, Bangkok 10330, TH

<sup>(2)</sup>Delft University of Technology, Kluyverweg 1, 2629 HS, Delft, NL

<sup>(3)</sup>Geo-Informatics and Space Technology Development Agency (Public Organization) 120 The Government Complex, Chaeng Wattana Road, Lak Si, Bangkok 10210, TH

## Abstract

The 2011 Mw=6.8 Mong Hpayak earthquake occurred on the western segment of the Nam Ma fault, one of many left-lateral faults in the region where Myanmar, China, Laos and Thailand meet. All faults in this system lie nearly parallel, trending in a south-east north-west direction, between two major faults in the region: the Sagaing fault in Myanmar and the Red River fault in Vietnam. Being a remote and mountainous area in less developed countries, the majority of these left-lateral faults are poorly studied. As there are no IGS or international CGPS in the earthquake-affected region, SAR images are probably the only available geodetic data for the scientific community to study the co-seismic motion. We present here a preliminary analysis of InSAR data acquired by ALOS PALSAR. Two SLCs in ascending path (fine beam mode, single polarization, path 486, frame 400) acquired on 26 February and 2 April 2011 are used in 2-pass DInSAR analysis with 3-second resolution SRTM DEM for topographic phase removal. We find coherence is generally good even though the Nam Ma fault area is highly vegetated and situated in a tropical zone. Distinct fringes shown in the interferogram demonstrate the applicability of L-band SAR for this kind of land cover that has been problematic for 2-pass DInSAR with shorter wavelength radar data. From the interferogram, a 1.2 m left-lateral offset in the radar look direction can be estimated across the fault. Further from the fault, smaller offsets around 10 cm are still observable at distance more than 20 km from the epicenter (20.705N, 99.949E; depth 10km as estimated by USGS). The interferogram reveals a rupture 26 km long. Since the Mong Hpayak earthquake, numerous small quakes, many of which have magnitude greater than 4.0, have been occurring in the area of this fault system.. The situation is particularly worrisome as segments of some of the nearby faults, including the Mae Chan fault in Chiang Rai, northern Thailand, pass through populated areas. We model the slip distribution on the inferred fault plane using the InSAR data as a constraint. We treat the surface displacements as the elastic response to slip on a planar fault, assuming a model of vertically varying stiffness. We divide the fault into a series of rectangular patches and calculate the Greens functions for unit slip of each patch at each downsampled interferogram pixel. We then apply a Markov chain Monte Carlo algorithm to find the posterior probability distribution of the slip. In order to restrict the range of solutions to distributions of slip that are physically reasonable, we apply an additional smoothing constraint; we assume that the probability distribution of the Laplacian of the slip is Gaussian, and simultaneously solve for the variance of this distribution. The resulting probability distribution of slip allows us to calculate the probability distribution of stress change due to the earthquake. We use this to calculate the distribution of Coulomb stress change for other faults in the region and evaluate the risk of future seismic hazard in this area.

# Surface deformation in the western rift of Corinth, Greece, from InSAR data

## Author(s)

Panagiotis Elias <sup>(1)</sup>, Pierre Briole <sup>(2)</sup>

## Department

<sup>(1)</sup>National Observatory of Athens , GR

<sup>(2)</sup>Ecole Normale Supérieure , FR

## Abstract

The rift of Corinth has been long identified as a site of major importance in Europe due to its intense tectonic activity. It is one of the world's most rapidly extending continental regions and it has one of the highest seismicity rates in the Euro-Mediterranean region, having produced a number of earthquakes with magnitude greater than 5.8: Alkyonides (1981, M=6.7), Aigio (1995, Mw=6.1), and Galaxidi (1992, Mw=5.8). It produces in average, an earthquake of magnitude 6 per decade. The GPS studies conducted since 1990 indicate a North–South extension rate across the rift of ~1.5 cm year<sup>-1</sup> around its western termination. Geological evidences show that the South coast of the rift is uplifting whereas the North part is subsiding. The rifting mechanism observed is crucial for the stability of the region as it can lead to submarine slope failures and possible damaging tsunamis. The western termination of the rift in the Patras broader area presents a major scientific and socio-economic importance, with the Psathopyrgos fault zone which is considered to be a presently active structure, the Rion-Patras fault zone, the city of Patras and the Rion-Antirion bridge. Psathopyrgos fault zone acts as a transfer zone between the Patras fault and Corinth rift. On 18th of January 2010, an Mw=5.1 (NOA) earthquake occurred near Efpalio and 25 km NE of Patras. Another strong event occurred on 22nd of January 2010, with Mw= 5.1 (NOA) approximately 3 km NE of the first event. Intense post-seismic activity followed. Despite their low magnitudes those events show a small signature in C-band DInSAR. Modelling of the deformation source has been used provides constraints on the location, size and azimuth of the faults. On June 8th, 2008 an Mw=6.4 earthquake occurred in NW Peloponnesus, western Greece, at a distance of 17km SW of the city of Patras. This seismic event is the largest strike-slip earthquake that taken place in western Greece during the past 25 years. The days following the main shock, the seismicity were propagating northward towards the city of Patras. Patra is the third most populated city in Greece with more that 200,000 citizens. The bridge of Rion-Antirion is 2,880m long (its width is 28m) and connects the eastern and western Greece. The bridge has been designed and constructed taking into consideration the raised seismicity of the area. Recent seismic and aseismic ground deformations of the area have been measured using series of ASAR/ENVISAT, PALSAR/ALOS and RASARSAT-2 acquisitions. All datasets were processed by means of PSI, SBAS and DInSAR techniques. In addition to common software processing software (ROI-PAC, DORIS, STAMPS e.t.c.) in-house tools and SARscape have been also used. Ascending and descending tracks have been used in order to extract the East-West and Up-Down deformation components. The discontinuities (in terms of abrupt changes of relative ground deformation rates) and co-seismic deformations detected in the Western Corinth rift area constitute the major observations discussed in the present study. In the city of Patras such observed discontinuities are located in the South area (Ag. Triada discontinuity) striking E-W, having a linear rate in the LOS direction of ~3 - ~6mm year<sup>-1</sup>. In the North area of the city of Patras the Rion-Patras (striking NE-SE, an oblique-slip transfer zone between the Patra fault and Corinth rift) fault zone, the Psathopyrgos (striking E-W) and Lambiri-Rododafni segments in the east, present relative linear deformation rate of ~2 - ~5 mm year<sup>-1</sup> in the LOS direction. Moreover the segment of the fault system falling inside the University of Patras has been investigated in more detail. Finally, in the South Area of Etoloakarnania an observed discontinuity striking NEE-SWW, with a linear slip rate in the LOS direction of ~4 - ~5mm year<sup>-1</sup> have been investigated.

The deformation occurred by the two forth-mentioned seismic events of January 2010, near Nafpaktos has been also observed and investigated. The SAR observations have been validated, calibrated and completed with measurements acquired from both permanent and non permanent GPS network. The presence of a triple junction with a portion of the relative micro-plate motion being accommodated across a) the western end of the Corinth rift, b) the strike-slip zone beneath Patra connected to the fault of the forthmentioned 2008 earthquake and c) to the Trichonida graben, striking NW, towards the Agrinion area, the Aetoliko valley and the Amvrakikos Gulf, has been investigated and discussed.

## Slip Distribution of the Giant 2011 Tohoku-oki Earthquake from Joint Inversion of Tsunami Waveforms and GPS Data

### Author(s)

Fabrizio Romano <sup>(1)</sup>, Alessio Piatanesi <sup>(1)</sup>, Stefano Lorito <sup>(1)</sup>, Nicola D'Agostino <sup>(1)</sup>, Kenji Hirata <sup>(2)</sup>, Simone Atzori <sup>(1)</sup>, Massimo Cocco <sup>(1)</sup>

### Department

<sup>(1)</sup>INGV, IT

<sup>(2)</sup>Meteorological Research Institute/JMA, JP

### Abstract

On 11 March 2011 a giant earthquake (Mw 9.0) occurred near the northeast coast of Tohoku (Japan). The hypocenter is located at 142.861 °E 38.1035 °N and at a depth of about 24 km (Japan Meteorological Agency). This earthquake ruptured the interface between the Pacific and North America plates, and generated a huge tsunami that devastated parts of the northeastern Honshu Island for up to 5 km inland. This is probably the best instrumentally recorded great earthquake ever. In fact, the extraordinarily dense and high-quality Japanese network provided a huge amount of seismological, geodetic, and tsunami recordings. In particular, a network of bottom pressure recorders and GPS-buoys, specifically designed for measuring tsunami waves close to the Japanese coasts and in the open Pacific Ocean, together with the Japanese GPS network, allow an unprecedented resolution on the slip distribution for this earthquake. The results show an unexpected amount of slip concentrated in a very narrow region with the rupture probably reaching to the trench, consistently with analogous results obtained with seismic data.

## Error Analysis in Calculating 3D Displacement of Gaize Earthquake (Tibet) with ASAR Images of Different Viewing Angles

### Author(s)

Jingfa Zhang <sup>(1)</sup>, Bin Liu <sup>(1)</sup>

### Department

<sup>(1)</sup>Institute of Crustal Dynamics,CEA #1 Anningzhuang RD, Haidian, Beijing, China, CN

### Abstract

The Ms6.9 earthquake followed with an Ms6.0 aftershock on 16 January 2008 struck Gaize in Tibet, China on 9 January 2008, which was the largest magnitude earthquake in this area since 1973 reported by China Earthquake Networks Center (CENC). The earthquake occurred near the western end of the ENE-WSW-trending left-lateral Riganpei Co fault, which is the northern branch of one of these conjugate strike-slip systems. One of the limitations of displacement measurements made with interferometric synthetic aperture radar (InSAR) is that an interferogram is only sensitive to LOS displacement of the surface displacement, which means

lack of information. However, 3D displacement can provide more information of crustal displacement processes, so we investigate strategies for analyzing error characteristics and improving accuracy of surface displacement in three dimensions based on multiple interferograms with different imaging geometries. ENVISAT ASAR is known to have the capability to image the same area on the ground from several different viewing angles. If we can obtain three observations of ground displacement from different viewing angles, it is possible to construct a three-dimensional model of the displacement of Gaize earthquake. However, the radar antenna is fixed with respect to the satellite, which may lead to the different LOS observations with nearly identical viewing angles in each of the ascending and descending orbits. As a result, ill-conditioned system of equations in calculating 3D displacement may result in the inaccurate results. InSAR accuracy and ill-conditioned system of equations are the major perturbing factors limiting the accuracy of 3D displacement. InSAR processing has usually been affected by orbit indetermination (baseline errors), atmospheric propagation and phase unwrapping errors, et al. A common objective of all InSAR processing schemes is to distinguish the contributions due to the geophysical signals of interest from the above-mentioned error sources. In this study, we firstly use ENVISAT ASAR data set to investigate the characteristics of orbital and atmospheric errors and phase unwrapping errors in monitoring Gaize earthquake, and then different techniques may be applied to remove these major errors. Moreover, some integrated models of different viewing angles are analyzed due to potential ill-conditioned system of equations. Ultimately, accurate 3D displacement signals are extracted from complex error sources, which may allow us to understand focal mechanism and failure mode as well as post seismic reconstruction in Gaize areas. In this study, the synthetic aperture radar (SAR) data consists of image mode and wide swath mode collected by the European Space Agency (ESA) ENVISAT spacecraft on the descending pass (Image mode: track 348) and ascending pass (Image mode: track 69, 155, 341 and 427, Wide Swath mode: track 112, 155, 341, 384, 427). The strip and wide-swath images are processed with the two-pass method using the JPL/Caltech ROI\_PAC 3.0.1 software and ENVISAT ASAR ScanSAR Processor contributed by Liang, respectively. The interferograms are corrected using preliminary DORIS satellite orbits from the European Space Agency. Effects of topography are removed from the interferograms using a 3-arc-sec (~90 m) resolution Shuttle Radar Topography Mission Digital Elevation Model (SRTM DEM). SNAPHU software contributed by Chen is used in phase unwrapping. The unwrapped interferograms are geocoded to a geographic coordinate system and then converted to LOS displacement.

## Coseismic deformation of Ahl (Kodian) earthquake derived from InSAR, Zagros-Iran

### Author(s)

Mahasa Roustaei <sup>(1)</sup>, Behnam Oveisi <sup>(1)</sup>, Majid Nemati <sup>(1)</sup>, Alireza Kiani <sup>(1)</sup>

### Department

<sup>(1)</sup>Geological Survey of Iran(GSI) , IR

### Abstract

The 2010 July 20 Ahl (Kodian) earthquake (Mw ~6) provides an excellent opportunity to study coseismic deformation in the Zagros Simply Folded Belt (ZSFB) using InSAR. This event occurred over the active ramp of a Mountain Front Fault (MFF) and was followed by 11 aftershocks. The MFF as a “blind master thrust” is composed of discontinuous, complex thrust segments and make a clear major topographic step with a clear structural, topographic, geomorphic and seismotectonic expression. The southwestern edge of the ZSFB is being uplifted mainly along the underlying MFF and the frontal asymmetric surface folds associated with it. In order to analyze the Ahl seismic event, the Envisat ASAR data descending track 249 (incident angle ~23o) was ordered and processed with GAMMA software. The shape of signal, however, is ellipsoid and very

similar to Fin earthquake which occurred on 25 March 2006, but here syncline core-extrusion is not a significant mechanism for the superficial deformation (depth to the Max ~ 4 km). Maximum uplift is approximately 2.5 Fringe (~ 7 cm). The conjugate shear zone covered upper part of signal where the elevation is zero and shows maximum intensity. The active Kodian anticline and its NW lateral continuation in the Lamerd anticline are asymmetric high-relief structures have been created by thrusting and folding in association with MFF and their long-term growth may be controlled primarily by repeated earthquakes on the ramp of this part of MFF. In the other word, the coseismic displacement during Ahl (Kodian) earthquake displays ongoing hanging-wall anticline growing over the MFF. Key words: Coseismic deformation, Zagros, Thrust, Mountain Front Fault, InSAR, Conjugate shear zone

## Investigation of different strategies for fault parameters and slip distribution retrieval of the 2005 Kashmir earthquake using SAR imagery

### Author(s)

Yajing Yan <sup>(1)</sup>, Virginie Pinel <sup>(2)</sup>, Emmanuel Trouvé <sup>(1)</sup>, Erwan Pathier <sup>(3)</sup>

### Department

<sup>(1)</sup>Université de Savoie–Polytech Annecy-Chambéry , FR

<sup>(2)</sup>ISTerre-IRD , FR

<sup>(3)</sup>ISTerre-UJF , FR

### Abstract

The geometry as well as the slip distribution of the fault responsible for the 2005 Kashmir earthquake, have been previously estimated by using 6 measurements from sub-pixel correlation of SAR images through an inversion of an elastic deformation model (Pathier et al., 2006). One measurement corresponds to a map of the ground displacement between two given dates (one before and one after the earthquake) projected along a given direction. In this paper, we increase the amount of data by using 22 measurements from sub-pixel image correlation (accuracy of the order of dm) and 5 measurements from differential interferometry (D-InSAR, accuracy of the order of cm) to retrieve the fault geometry parameters and the slip distribution. Firstly, two strategies: joint inversion and pre-fusion are applied. Joint inversion is the strategy commonly used by most of geophysicists and consists of combining all of the available measurements within the inversion. On the contrary, pre-fusion consists of a step of fusion before inversion. In this strategy, the fusion step is a selection: the measurements that fit well the deformation model are used for inversion. The fault geometry parameters and slip distributions obtained with these two strategies are analysed and compared. The two strategies provide consistent results in good agreement with previous studies: a 74 km long inverse fault characterized by a strike around  $321^\circ$ , a dip around  $31^\circ$ NE and two main zones of slip. However, in this study the maximum of slip appears slightly north-eastern and deeper compared to the slip distribution derived by Pathier et al. Moreover, in order to analyse the sensibility of fault geometry parameters and slip distribution to the noise present in the measurements in the context of each strategy, a series of synthetic tests with different types of noise are performed. For this, a random noise (white Gaussian noise) is added in the measurements from sub-pixel image correlation and a spatially correlated noise is added in the measurements from D-InSAR. The noise is generated according to the characteristics of noise estimated from three pre-seismic measurements. For each measurement, noise is generated and added 1000 times. And then, 1000 inversions are realised and 1000 values are obtained for each fault geometry parameter in each strategy. The distributions of fault geometry parameters in different strategies are analysed and compared. Joint inversions appear less sensitive to noise effects compared to pre-fusion calculations. Adding D-InSAR measurements tends to reduce the distribution spreading and to enhance the



dependence between given parameters. Some parameters are more dependent on the fusion strategy (rake, slip) whereas others are more dependent on the noise. Usually, the sensibility of slip distribution to the noise in the measurements is estimated by using the measurements with added noise and fixing the geometry of the fault (Funning et al., 2005, Pathier et al., 2006). In this paper, it is analysed in a different way. The slip distributions are estimated by using the 1000 sets of fault geometry parameters in each strategy and the original measurements without noise. Also, the results obtained in different strategies are analysed and compared. Finally, the advantage and disadvantage of each strategy is highlighted. Reference: E. Pathier, E. J. Fielding, T. J. Wright, R. Walker, B. E. Parsons, and S. Hensley. Displacement field and slip distribution of the 2005 Kashmir earthquake from SAR imagery. *Geophysical Research Letters*, 33(L20310), 2006. G. J. Funning and B. Parsons and T. J. Wright. Surface displacements and source parameters of the 2003 Bam (Iran) earthquake from Envisat advanced synthetic aperture radar imagery. *Journal of Geophysical Research*, 110 (B09406), 2005.

## The effects of vegetation coverage, topography and coastal orientation on the 2011 Tohoku-Oki (Japan) tsunami inundation investigated by satellite data

### Author(s)

Marco Chini <sup>(1)</sup>, Alessandro Piscini <sup>(1)</sup>, Francesca Romana Cinti <sup>(1)</sup>,  
Stefania Amici <sup>(1)</sup>, Rosa Nappi <sup>(1)</sup>, Paolo Marco De Martini <sup>(1)</sup>

### Department

<sup>(1)</sup>Istituto Nazionale di Geofisica e Vulcanologia , IT

### Abstract

We have studied the inland disastrous evidences of the tsunami triggered by the earthquake (M 9.0) occurred on March 11th, 2011 (at 05:46:23 UTC) offshore the coast of Honshu island (Japan). This large earthquake has been generated along the subduction plate boundary between the Pacific and the North America plates. The followed destructive tsunami caused casualties and severe damages along the coastline of most of Honshu Island. The dataset used in this work is composed of data in the visible spectral range, provided by ASTER (Advanced Spaceborne Thermal Emission and Reflection Radiometer) and Hyperion sensors, while for the microwave we have taken advantage of the active sensors such as Synthetic Aperture Radar (SAR). The capability to operate during daytime and nighttime and in almost all weather conditions are the key features that make SAR images useful for inundation mapping. In addition, the great sensitivity to water of the microwave band permits SAR to distinguish between land and water. In particular, both specular reflection, typical of open water, and double bounce backscattering, typical of vegetated and urban areas, are considered. The large amount of data available from different sensors onboard of different satellite missions have allowed to sample the gradual tsunami inundation receding during the days soon after it occurred. Unsupervised and supervised algorithms have been applied for land cover classification purposes, identifying and mapping the extent of the effects caused by the tsunami on the different land cover classes present on the scene nearby the Sendai coast. The change classes, which have been identified, are in particular the stressed vegetation, the structural/house damage, the flooded areas, the debris, the sand deposits and boulders. The synoptic view, which is peculiar of remote sensing satellite data, DTM analysis and the information extracted from such a broad spectral range data have allowed an analysis of the tsunami characteristics phenomenon, such as the minimum inundation distance and the minimum run-up, respect to physical characters of the coastal area, such as topography, vegetation coverage and coastal orientation. This study would contribute to the definition of the susceptible level of the coastal region to get devastated by tsunami wave.

# The September 2010, Darfield earthquake, and the February 2011, Christchurch “aftershock”: is there a cause and effect?

## Author(s)

Salvatore Stramondo <sup>(1)</sup>, Christian Bignami <sup>(1)</sup>, Marco Chini <sup>(1)</sup>,  
Christodoulos Kyriakopoulos <sup>(1)</sup>, Daniele Melini <sup>(1)</sup>, Marco Moro <sup>(1)</sup>,  
Matteo Picchiani <sup>(2)</sup>, Michele Saroli <sup>(3)</sup>

## Department

<sup>(1)</sup>Istituto nazionale di Geofisica e Vulcanologia - INGV , IT

<sup>(2)</sup>University Tor Vergata , IT

<sup>(3)</sup>University of Cassino , IT

## Abstract

We have investigated the possible causal relationship between two earthquakes occurred nearby Christchurch in New Zealand in September 2010 and in February 2011. The Mw 7.1 Darfield (Canterbury) event took place along a previously unrecognized east-west fault line, the strike slip Greendale fault. The Mw 6.3 Christchurch earthquake, generated by a blind thrust fault, occurred approximately five months later and about 6 km south-east of Christchurch centre. This second event is located at the easternmost limit of the Darfield aftershocks distribution. We have used a dataset composed of two pairs of ALOS PALSAR FBS (Fine Beam Single polarization) images acquired along two adjacent tracks. The pre-seismic images dated August 13, 2010, and January 1, 2011, respectively, while the post-seismic data were on September 28, 2010, and February 25, 2011. We then applied Differential SAR Interferometry (DInSAR) technique to measure the overall displacement fields from both shocks. In particular the September 2010 earthquake generated a complex pattern due to the activation of the Greendale fault and other secondary buried thrusts. Based on DInSAR outcomes we have then linearly inverted the coseismic displacement field. We subdivided the fault planes into a discrete number of rectangular patches and applied the Occam smoothing scheme to minimize the chi-square and the second order derivative to avoid oscillation in slip values. Once defined the geometries of the two seismogenic fault planes we have investigated the role of the first earthquake in promoting the rupture of the second by evaluating the Coulomb Failure Function. The result shows that the shallower part of the Christchurch fault has been unloaded by the Darfield earthquake. On the contrary, the deeper part of the fault has been brought closer to the rupture.

# The lowest place on Earth is rising due to Dead Sea water level drop: Evidence from SAR Interferometry

## Author(s)

Ran Nof <sup>(1)</sup>, Alon Ziv <sup>(1)</sup>, Marie-Pierre Doin <sup>(2)</sup>, Gidon Baer <sup>(3)</sup>, Yuri Fialko <sup>(4)</sup>, Shimon Wdowinski <sup>(5)</sup>,  
Yehuda Eyal <sup>(1)</sup>, Yehuda Bock <sup>(4)</sup>

## Department

<sup>(1)</sup>Ben-Gurion University of the Negev Geological and Environmental Sciences Ben-Gurion University of the Negev  
Mailbox 653 Beer-Sheva 8, IL

<sup>(2)</sup>L'Ecole normale supérieure 24 Rue Lhomond 75231 Paris CEDEX 5, France

<sup>(3)</sup>Geological Survey of Israel 30 Malkhe Israel, Jerusalem 95501, Israel, Israel

<sup>(4)</sup>University of California San Diego La Jolla, CA 92093-0225, USA

<sup>(5)</sup>University of Miami 4600 Rickenbacker Causeway Miami, FL 33149-1098, USA

## Abstract

The Dead Sea is located along the Dead Sea rift, between the Arabian plate to the east and the Sinai sub-plate to the west. The Dead Sea water level has been dropping in recent decades at an

average rate of about 1 meter per year. It is expected that such a water level change will be responded by lithospheric rebound and regional uplift, with spatial extent and amplitude that are controlled by the effective mechanical properties of the crust and upper mantle combined. In quest for the lithospheric response to water level drop, we analyzed 31 SAR images of satellites ERS-1 and ERS-2 descending track from the years 1993 to 2001, which were processed into 149 short perpendicular baseline (<300 m) interferograms. The expected annual ground displacement is small (a few millimeters), and the data is extremely noisy. In addition, the topography is almost a mirror image of the expected ground displacement, introducing a strong trade-off between the ground displacement and phase changes due to stratified atmosphere. To overcome the latter difficulty, we first solve for the phase contribution of each SAR acquisition with respect to the first acquisition. We then define a region of interest with limited spatial extension around the northern basin of the Dead-Sea, impose a linearity constraint on the LOS change, and simultaneously solve for the LOS change rate, DEM errors and the elevation-phase slope. While the LOS rate and DEM errors are solved for each pixel independently, the elevation-phase slope is solved for each SAR acquisition independently. We then remove the extracted phase-elevation slope of each acquisition from the original interferograms and independently recalculate for each pixel the LOS change rate and DEM errors. Using this approach we were able to remove the phase contribution from stratified atmospheric delay while recovering the ground displacement, the rate of which is constant. A time-series record of a GPS site, located west of the Dead Sea, shows an almost linear uplift, supporting our linearity constraint. We will present a map of LOS changes, showing uplift around the Dead Sea northern basin, with maximum LOS rates of 2.5 - 4 mm/yr near the shorelines. Such a clear picture cannot be observed in single interferograms, including those with the longest temporal baseline. A bootstrapping test indicates that our results are neither dominated, nor strongly affected by any single image. To examine whether crustal response to the Dead Sea water level drop is reproducible by purely elastic model, or should viscoelasticity be invoked, we first calculate the distribution of the total vertical load change resulting from the combined effect of water removal and chemical precipitation within the Dead Sea northern basin. We then model the effect of applying the inferred load change on homogeneous elastic half-space, and compare the modeled and observed LOS changes. A fairly good agreement between modeled and observed ground displacement is found when Poisson's ratio of 0.27 and a Young modulus of 46 GPa is used. The Young modulus value is lower than the average crustal modulus inferred from seismic and gravity data by almost a factor of two. Possible sources for this discrepancy will be discussed.

## An new approach for modeling fault dislocation from wrapped interferometric SAR data

### Author(s)

Gianfranco Fornaro <sup>(1)</sup>, Simone Atzori <sup>(2)</sup>, Fabiana Calò <sup>(1)</sup>, Diego Reale <sup>(1)</sup>, Stefano Salvi <sup>(2)</sup>

### Department

<sup>(1)</sup>CNR Via Diocleziano, 328, IT

<sup>(2)</sup>Istituto Nazionale di Geofisica e Vulcanologia Via di Vigna Murata 605, IT

### Abstract

The Differential Synthetic Aperture Radar Interferometry (DInSAR) technique has significantly increased the exploitation of remote sensed data in many geological and geophysical disciplines, particularly in tectonics. Co-seismic interferograms have provided in many cases "images of earthquakes", showing the surface displacement due to the deep fault dislocation and allowing to analyze the geometrical and kinematic characteristics of the fault, which are parameters of great interest for the earthquake hazard assessment and thus for the management of the associated

risk. Thanks to the availability and good spatial coverage of data acquired from ERS and ENVISAT satellites, for most of the regions struck by major earthquakes DInSAR techniques are applied almost routinely for investigating the surface deformation related to the seismic cycle before, during and after earthquakes, in order to analyze inter-seismic, co-seismic, and post-seismic signals of the fault activity. Typically DInSAR is jointly used with analytical fault models, such as the Okada solution, in order to extract valuable information on the dislocation mechanism at the fault level caused by the mainshock and significant aftershocks. In such case the modeling is currently performed at a post-processing stage, i.e. after the co-seismic displacements or post-seismic time series have been fully reconstructed with the DInSAR processing: contributions to the integration of geophysical model directly at the DInSAR processing stage are rather limited in the available literature. Temporal modeling is implemented during the multitemporal DInSAR processing, as for instance during the linear inversion from the unwrapped interferometric phase to the phase signal at the different acquisition times, or to facilitate critical processing steps such as the phase unwrapping. In particular, depending on the amount of the atmospheric and non linear deformation contributions, either at the pixel level or on arcs connecting pairs of pixels, the temporal evolution of the signal is approximated to be linear. This approximation is generally sound for the analysis of most of the deformation phenomena, but may be unsatisfactory in the presence of discontinuous temporal deformations, such as those associated with earthquakes. In such case deformation trends could be better approximated, both spatially and temporally, using well established geophysical models and algorithms aimed at integrating them in multitemporal DInSAR processing need to be developed. Furthermore, conventional analysis of earthquake source by using DInSAR interferograms requires carrying out Phase Unwrapping (PhU) procedures that allow the use of straightforward linear inversion of the surface displacements. This linear inversion may be preceded by a non-linear inversion step carried out to determine the parameters characterizing the fault geometry, mainly the fault position and orientation. However it should be highlighted that most interferograms corresponding to significant earthquakes suffer for the loss of signal coherence, often coupled with the presence of high fringe rates occurring near the surface outcrop of the co-seismic rupture. As result, in such cases PhU algorithms may fail. In this work an innovative contribution for the fault modelling based on the integration of geophysical models directly at the wrapped interferogram level is presented. In particular, the proposed approach is based on the inversion of DInSAR data with analytical dislocation models by minimizing a proper cost function defined at the interferometric complex level. As a consequence, the inversion problem from the data (i.e. the wrapped phase values) to the unknowns (the fault slip distribution) becomes non linear. Furthermore, such approach to inversion problem with spatial model requires a joint inversion with respect to all the parameter models since all of these latter concur to form the observed deformation of the surface. This fact, coupled to the non linear nature, makes the inversion problem from wrapped data particularly demanding from the computational point of view. As a consequence, we use the Singular Value Decomposition (SVD) technique in the non linear inversion in order to regularize the inversion as well as to significantly reduce the computational work. The proposed processing approach has been applied to the analysis of two earthquakes that stroke in 1999 the Attica region (Greece) and the area around the city of Izmit (Turkey) with a magnitude of 5.9 and 7.4 respectively, causing severe losses in terms of human life and urban damage. In the first case, associated with a dip-slip fault mechanism, the moderate earthquake magnitude (with no associated rupture) as well as the good coherence provided by the land cover of the area allowed to effectively performing the PhU of the co-seismic interferogram. Therefore, such case study has been used to develop and test the proposed technique, and to compare obtained results with those derived from classical analysis. In the second case, characterized by a strike-slip fault mechanism and higher magnitude, the co-seismic interferograms is particularly critical from a PhU standpoint due to the presence of fringe discontinuities and excessive fringe rates close to the surface fault rupture. As result, it is shown

as our non linear inversion from wrapped data outperforms the classical approach largely affected by unwrapping errors.

## Co-seismic deformation and Source characteristics of the Yushu Ms7.1 earthquake using InSAR and observation data

### Author(s)

Xinjian Shan <sup>(1)</sup>, Yunhua Liu <sup>(2)</sup>, Xiaogang Song <sup>(3)</sup>, Guifang Zhang <sup>(3)</sup>,  
Guohong Zhang <sup>(3)</sup>

### Department

<sup>(1)</sup>Institute of Geology,China Earthquake Administration Qijiahuozi St.,Dewai Av. CN

<sup>(2)</sup>Institute of Geology,China Earthquake Administration Qijiahuozi St.,Dewai Av., CN

<sup>(3)</sup>Institute of Geology, China Earthquake Administration Qijiahuozi St.,Dewai Av., CN

### Abstract

On 14 April 2010 the Ms7.1 earthquake occurred in Yushu county, Qinghai province, which is another destructive shock in the China mainland following the Wenchuan M8.0 event in 2008. This shock took place on the Ganze-Yushu fault within the Tibetan plateau. In this work, InSAR and offset-tracking methods were performed to retrieve the deformation field, distribution of surface ruptures. Then, we employ a dislocation model and the sensitivity- based iterative fitting (SBIF) method to calculation the source parameters of this event by inversion. The InSAR results show that the maximum dislocation is about 0.8m in LOS direction between two sides of the fault, corresponding to about horizontal dislocation of 1.5m, consistent with the result of field investigation. As revealed by field investigations, near the maximum dislocation site of InSAR, the surface rupture zone is composed of a series of fissures arranged in an en-echelon, with a measured maximum horizontal displacement of 1.8 m. In the deformation map, the range displacements on the north wall of the fault is moving to satellite, and the south wall is moving away from satellite, showing a left-lateral strike-slip. The rupture is identified by the offset-tracking method. Azimuth displacement analysis indicates that the surface rupture is about 75km long, running from the northwest to the southeast, trending N310°W, with a relative displacement of ~1 m in azimuth. The maximum dislocation in azimuth amounts to 1.3 m, located near the Harvard CMT solution, which is transformed to the actual horizontal dislocation about 1.7 m. The fault model is established by 2 segments, the inversion results show that the fault plane is 80km long, extending from northwest to southeast. Three peak-slip asperities are generated, which locate in 25km,50km and 65km from southeast point to northwest respectively, with depth less than 10km along dip. The largest slip area with the maximum slip 2m is located at the area 25km distant from the southeast point of the fault, with the depth less than 5km along dip, and reach the surface. Its location is consistent with the largest surface observation dislocation. The moment magnitude of the shock is about Mw 6.9. Keywords: Yushu earthquake; InSAR; offset;deformation field;surface rupture; Source characteristics

# Fault-slip evolution during the 2009 earthquake sequence in the northern Malawi Rift, East Africa

## Author(s)

Yariv Hamiel <sup>(1)</sup>, Gideon Baer <sup>(1)</sup>, Kondwani Dombola <sup>(2)</sup>, Patrick Chindandali <sup>(2)</sup>, Leonard Kalindekaffe <sup>(2)</sup>

## Department

<sup>(1)</sup>Geological Survey of Israel , IL

<sup>(2)</sup>Geological Survey Department of Malawi , MW

## Abstract

We use InSAR data, detailed ground observations, and elastic modeling to resolve the evolution and distribution of ground deformation and fault slip during the November 2009 to March 2010 seismic swarm in the Karonga region, northern Malawi Rift. The swarm included 17  $M \geq 4$  earthquakes (nine of which were larger than  $M_b 5$ ) and was accompanied by extensive surface deformation. The first month was characterized by a very low rate of seismic moment release. On December 6, the released seismic moment increased rapidly, continuing until December 19 with the occurrence of the largest,  $M_w 6$  event. The next few months are characterized by a very low seismic moment release rate. We find a very good agreement between the InSAR and field observations of surface ruptures. Our best fitted fault models indicate dip-slip displacements on a fault dipping 40° to the southwest with maximum slip of about 120 cm at 3-5 km depth. The rupturing segment migrated from the northern part of the fault between Dec. 6 and Dec. 17, to a deeper and southern segment during the Dec. 19 event, and continued as shallow creep above the southern segment until March 2010. Our results suggest that the fault was associated with a 0.8-1.1 km wide fracture zone having an effective shear modulus of 66-90% compared to the surrounding rocks.

# Recent tectonic activity over the Marmara sea region from time series InSAR

## Author(s)

Mahmut Arikan <sup>(1)</sup>, Andrew Hooper <sup>(1)</sup>, Miguel Caro Cuenca <sup>(1)</sup>, Ramon Hanssen <sup>(1)</sup>

## Department

<sup>(1)</sup>Delft University of Technology Kluyverweg 1, NL

## Abstract

The Anatolian micro-plate is undergoing continuous strain due to the collision of three major tectonic plates: the Eurasian, African and Arabian. In broad terms, it is being extruded towards the Hellenic Trench along the dextral North Anatolian and sinistral East Anatolian fault zones (NAFZ and EAFZ respectively). In 1999, a series of large earthquakes hit İzmit ( $M_w 7.4$ ) and Düzce ( $M_w 7.2$ ) cities along the western end of the NAFZ. Tens of thousands of people were killed and about half a million people were left homeless. Another earthquake of strong magnitude is foreseen on the NAFZ within the next 30 years along the main Marmara fault (MMF: the extension of the NAF in the Marmara sea) to the west, close to the megacity of Istanbul. Recently, GPS studies have shown slip rates of  $\sim 24$  mm/yr along the NAFZ and  $\sim 9$  mm/yr along the EAFZ. From a geophysical point of view, in order to forecast future earthquakes, it is valuable to thoroughly capture the magnitude and extent of tectonic deformation. In most previous studies,

this has been carried out using sparse GPS networks. Here, we apply time series (TS) InSAR analysis to the Marmara and surrounding regions to map the velocity field that results from the tectonic motion.

In our study, we used Envisat radar imagery from European Space Agency (ESA) between 2002 and 2010. In order to capture the whole deformation field, we processed 7 tracks of the ascending orbit and 6 tracks of the descending orbit, over an area that covers about 125,000 square kilometers in western Turkey. The radar data were provided in SLC format which we progressively concatenated to form 316 long swath SLCs for InSAR processing. During this process, for each track, we made use of the amplitude overlap between the successive frames to construct a long swath SLC. In addition, we updated the meta-information to be compatible with the newly formed image. Finally, we performed time series analysis on each track individually to produce velocity maps.

As the next step, we used GPS to combine individual velocity maps from each track onto a single reference frame. This is necessary, firstly, due to the Marmara Sea where there are no InSAR observations which introduces gaps in spatial point density causing unwrapping errors and secondly, to constrain the long wavelength deformation that is caused by orbital errors and atmospheric delay. We solved these in least-squares sense by integrating GPS and multi-track TS velocities. We also made use of geophysical parameters on active faults to constrain our models. The GPS velocities were obtained from recent studies in the region (Aktuğ09 et.al. and Ergintav09 et.al.).

As the final step, using our high-resolution velocity map, we identified strain accumulation zones in the Marmara sea region after the 1999 earthquakes. We then applied simple kinematic models to determine postseismic slip distribution and locking depth on actively deforming fault segments along the NAFZ, particularly the ones in the vicinity of İzmit and Düzce cities. We observed shallow slip deformation in the northern segment close to Düzce as well as deep slip deformation on the southern segment of the NAFZ.

To summarize, our results give improved estimates of the magnitude and extent of strain accumulation, which can be used to improve forecasting of a future earthquakes, particularly within the Marmara Sea region.

References:

1. Aktuğ, B., J. M. Nocquet, A. Cingöz, B. Parsons, Y. Erkan, P. England, O. Lenk, M. A. Gürdal, A. Kilicoglu, H. Akdeniz, A. Tekgül, 2009. Deformation of western Turkey from a combination of permanent and campaign GPS data: Limits to block-like behavior, *JGR* 114 (B10404).
2. Ergintav, S., S. McClusky, E. Hearn, R. Reilinger, R. Cakmak, T. Herring, H. Ozener, O. Lenk, and E. Tari (2009), Seven years of postseismic deformation following the 1999,  $M = 7.4$  and  $M = 7.2$ , İzmit-Düzce, Turkey earthquake sequence, *JGR* 114 (B07403).
3. Hooper, A., 2006. Persistent Scatterer Radar Interferometry for Crustal Deformation Studies and Modeling of Volcanic Deformation, PhD Thesis, Stanford University.
4. Arıkan, M., Hooper, A., Hanssen, R., 2010a. Large-scale tectonics in western Anatolia from time series InSAR. 7th EGU General Assembly 2010, Vienna 12, EGU2010-13909.
5. Arıkan, M., Hooper, A., Hanssen, R., 2010b. Radar time series analysis over West Anatolia. European Space Agency (Special Publication) ESA SP-677.

# Time series in Cascadia

## Author(s)

Rowena Lohman <sup>(1)</sup>

## Department

<sup>(1)</sup>Cornell 4130 Snee, US

## Abstract

Subduction zones accommodate the long-term convergence imposed by plate tectonics with a variety of mechanisms, including large earthquakes within the seismogenic zones that remain locked during most of the seismic cycle, and stable sliding or viscous deformation up-dip and down-dip of the locked regions. An additional style of behavior has been observed in subduction zones around the Pacific in recent years, where slow or silent earthquakes release strain equivalent in moment to M6-7 earthquakes. In the Cascadia subduction zone, the local continuous GPS array detects slow slip events at fairly regular intervals (~ every 14 months). The horizontal motions recorded by the GPS array have magnitudes of up to 6 mm, which should correspond to 5-10 mm of deformation in the nearly vertical satellite line-of-sight (LOS). Reported detection limits for the persistent scatterer method are ~ 1mm, so the expected signal is reasonably large. However, the length scales associated with slow slip events are large when compared to the frame size of available SAR data, which will reduce the ability to distinguish between satellite orbital errors, tectonic signal and the long-wavelength component of atmospheric noise. Here we compare the results of a range of point target and traditional time series approaches using both C- and L-band data. Much of our analysis involves the exclusion of signals that are either due to DEM errors resulting from the use of a C-band based SRTM DEM when examining L-band data, as well as double-bounce and other vegetation-related effects.

# DINSAR co-seismic and post-seismic analysis of the March,11th 2011 Tohoku (Japan) earthquake by using COSMO-SkyMed data

## Author(s)

Cristiano Tolomei <sup>(1)</sup>, John Peter Merryman <sup>(1)</sup>, Simone Atzori <sup>(1)</sup>, Stefano Salvi <sup>(1)</sup>

## Department

<sup>(1)</sup>Istituto Nazionale di Geofisica e Vulcanologia Via di Vigna Murata,605, IT

## Abstract

On Friday, 11 March 2011 Japan's most powerful earthquake since seismic records began has hit the north-east coast of the Country. The magnitude 9 earthquake has generated a destructive tsunami that caused several tens of thousands casualties. The earthquake and tsunami have also caused severe structural damage in Japan, including heavy damage to several nuclear power plants, in particular for that located near Fukushima. Shortly after the mainshock, we requested COSMO-SkyMed images for a large area, in the framework of the SIGRIS project (funded by the Italian Space Agency). We generated a few DINSAR interferograms showing the co-seismic displacement field, although, due to the scarcity of the pre-event image catalogue, the COSMO interferograms covered only a small sector of the area. Strong decorrelation phenomena occurred in most of the COSMO interferograms, thus we successfully applied the offset-tracking technique to obtain a better estimate of ground displacements. The COSMO acquisition plan is presently addressing the monitoring of post-seismic deformation, from the Northern Honshu to Tokyo, for both ascending and descending passes, with a revisit time of 16 days. As soon as a sufficient number of images is acquired, we will perform DINSAR multi-temporal analysis using the SBAS



(Small Baseline Subset) technique. We will show at the meeting the results of such analysis, as the mean ground velocity maps and the relative displacement time series.

## InSAR results from North America by the WInSAR Consortium

### Author(s)

Eric Fielding <sup>(1)</sup>, Non-profit research and educat <sup>(2)</sup>

### Department

<sup>(1)</sup>Jet Propulsion Laboratory, Caltech MS 300-233, US

<sup>(2)</sup>Various , USA

### Abstract

WInSAR is a consortium of non-commercial scientists engaged in radar remote sensing research and education, with major emphasis on InSAR studies in the western part of North America. We present here a summary of recent results by WInSAR scientists that are based largely or in part on ERS and Envisat SAR data analysis, with additional SAR data from other satellites and the NASA airborne InSAR system called UAVSAR. Studies have addressed deformation related to the earthquake cycle in the plate boundary system at the western edge of North America, including the San Andreas Fault (SAF) system, the Basin and Range province and the Cascadia subduction zone. The continuation of the SAF system into northern Mexico was the site of the Mw 7.2 El Mayor-Cucapah earthquake in April 2010. In addition to imaging coseismic deformation and damage, triggered slip, slip transients and postseismic processes are being studied, along with the interseismic buildup of stress on faults in the diffuse plate boundary. WInSAR scientists are also studying volcanic processes in the Cascade volcanic change, Long Valley, Yellowstone and the Big Island of Hawaii. Other research covers landslides, subsidence due to groundwater withdrawal and other subsurface processes, and wetland dynamics in a number of locations across North America. These studies target assessment of geologic hazards in response mode and risk of future events and also address fundamental questions of geological and geophysical structure of the Earth.

WInSAR is hosted by UNAVCO, and both organizations are non-profit, membership-governed groups funded by the National Aeronautics and Space Administration (NASA), the U.S. Geological Survey and the National Science Foundation (NSF). The WInSAR SAR data archive is in the process of being merged with the GeoEarthScope archive, also hosted by UNAVCO, which was funded by the NSF EarthScope project. The two archives combined contain about 17 TB of SAR data from ERS-1, ERS-2, Envisat and Radarsat-1. We have recently started an effort to implement an application programming interface to the WInSAR/GeoEarthScope archive to enable more efficient access to the data and metadata through machine-machine interfaces to supplement the existing web-based access. This will enable more efficient large-scale and time-series analysis of the archive data. The WInSAR consortium has an ALOS-1 PALSAR data allocation under the US Government Research Consortium Data Pool that is hosted at the Alaska Satellite Facility, covering parts of North America and some other regions in the Americas. WInSAR has also helped to create and maintain a prototype archive for the Group on Earth Observations Geohazard Supersite.

# Posters on Polarimetric Interferometry, Tomography and other Advanced Topics

## Just beyond PSI: Multi-dimensional SAR focusing for imaging and monitoring vertical structures

### Author(s)

Diego Reale <sup>(1)</sup>, Gianfranco Fornaro <sup>(2)</sup>, Antonio Pauciuolo <sup>(2)</sup>

### Department

<sup>(1)</sup>IREA - CNR Via diocleziano, 328, 80124 Naples Italy, IT

<sup>(2)</sup>IREA -CNR Via diocleziano, 328, 80124 Naples Italy, IT

### Abstract

Interferometric Synthetic Aperture Radar (InSAR) and particularly Differential InSAR (DInSAR), by exploiting large dataset of SAR images, have proven to be effective for the target localization and monitoring of deformation [1][2]. The high accuracy of the estimation and the large density of monitored targets make these technique highly cost effective with respect to classical terrestrial measurements typically carried out in environmental risk monitoring. The advantages of using interferometric approaches have pushed the major worldwide space agencies to develop new spaceborne SAR sensor, such as the operative TerraSAR-X and Cosmo-Skymed and the ESA SAR mission Sentinel-1 planned for the near future, characterized by larger bandwidth, resulting in improved spatial resolution nowadays reaching the meter level, and reduced revisiting times: All these improved features come out in increased monitoring capabilities. First results have shown the impressive increasing in the density of monitored targets both in rural [3] and urban areas [4]. Besides the sensor technology, also new and more effective processing algorithms have been proposed, in order to overcome limitation of classical interferometric approach: one of these is the SAR Tomography or multidimensional SAR imaging [5][6], that exploits both amplitude and phase information of SAR images, contrary to the phase only interferometric processing. Particularly, urban areas if on one side are full of manmade scatterers, which exhibit high persistency, are somehow adverse scenario for classical interferometry due to large density of vertical structures, such as buildings, resulting in a severe interference, typically referred to as layover, arising from the superposition of contribution from scatterers located at different heights, but at the same distance from the sensor. The imaging mechanism of radar is, in fact, based on the measure of distances (range) of the scatterers: If two targets, located at different positions, share the same range to the sensor, they are imaged into the same pixel. Standard interferometry, by assuming the presence of only one single phase centre, and particularly measuring the matching of the measured signal with the multipass signature, within each resolution cell (pixel), are not able to manage this kind of interference: as a consequence, the interference of contributions leads to misdetection of stable targets and incorrect estimations of position and displacement. This layover in urban areas has become of importance with the advent of the new high resolution sensors: thanks to the improved resolution, vertical structures are distributed over a larger number of pixel and then the interference is more frequent [7]. SAR tomography is a powerful extension of the interferometric concept: the exploitation of the full, amplitude and phase, measured signal leads to reconstructing the distribution of the backscattered energy along the slant height (elevation) / deformation mean velocity plane, allowing improving the detection of dominant scatterers and, above all, revealing the presence of possible interfering scatterers. In this work we present the an overview of the advances in the application of this technique on data

acquired by medium and high resolution SAR sensors to demonstrate the capability of this technique to overcome the limitations of classical PSI technique on vertical structures associated to the layover problem. REFERENCES [1] P. Berardino, G. Fornaro, R. Lanari, and E. Sansosti, "A new Algorithm for Surface Deformation Monitoring based on Small Baseline Differential SAR Interferograms", *IEEE Trans. Geosci. Remote Sens.*, vol. 40, pp.2375-2383, 2002. [2] A. Ferretti, C. Prati, F. Rocca, "Nonlinear subsidence rate estimation using permanent scatterers in differential SAR interferometry", *IEEE Trans. Geosci. Remote Sens.*, 38, nr. 5, pp.2202–2212, 2000. [3] D. Reale, D. O. Nitti, D. Peduto, R. Nutricato, F. Bovenga, G. Fornaro, "Post-seismic Deformation Monitoring With The COSMO/SKYMED Constellation," *IEEE Geosci. Remote Sens. Letters*, doi: 10.1109/LGRS.2010.2100364. [4] S. Gernhardt S, N. Adam, M. Eineder, and R. Bamler, "Potential of very high resolution SAR for persistent scatterer interferometry in urban areas," *Ann. GIS*, vol. 16, no. 2, pp. 103-111, Jun. 2010. [5] F. Lombardini, "Differential Tomography: a New Framework for SAR Interferometry", *IEEE Trans. Geosci. Remote Sens.*, 43, pp. 37-44, 2005. [6] G. Fornaro, D. Reale, F. Serafino, "Four-Dimensional SAR Imaging for Height Estimation and Monitoring of Single and Double Scatterers", *IEEE Trans. Geosci. Remote Sens.*, vol. 47, no. 1, Jan 2009. [7] X.X. Zhu and R. Bamler, "Very high resolution spaceborne SAR tomography in urban environment," *IEEE Trans. Geosci. Remote Sens.*, vol. 48, no. 12, pp. 4296-4308, Dec. 2010.

## Three Dimensional SAR Tomography in Shanghai Using High Resolution Space-borne SAR Data

### Author(s)

Lianhuan Wei <sup>(1)</sup>, Timo Balz <sup>(1)</sup>, Mingsheng Liao <sup>(1)</sup>, Kang Liu <sup>(1)</sup>

### Department

<sup>(1)</sup>Wuhan University State Key Lab. for Info. Eng. in Surveying, Mapping and Remote Sensing (LIESMARS) Wuhan Univer, CN

### Abstract

With the new generation of SAR satellites, like TerraSAR-X and COSMO-SkyMed, a data stack with up to 0.6 meter resolution can be built up in relatively short duration. The surveillance of buildings in urban areas benefits from the high spatial resolution, even details of buildings can be seen from space. However, the high resolution causes new problems due to the radar imaging geometry, for example, several different scatterers could be recorded in the same resolution cell. Our previous research results show that in areas with many high buildings, it is difficult to interpret the result from PS-InSAR technique. This is mainly due to the complicated backscattering and height estimation errors. Synthetic Aperture Radar (SAR) Tomography is a way of overcoming the limitations of the standard two dimensional SAR imaging, which aims at retrieving the distribution of scatterers in elevation direction and the corresponding reflectivity from a stack of SAR acquisitions. Small variations in the orbit are used to form a synthetic aperture in elevation direction, the so called elevation aperture. By spectral estimation, with special consideration of the difficulties caused by sparse and irregular sampling, a reflectivity profile is retrieved for each azimuth-range pixel. The reflectivity profile is used to estimate scattering parameters, such as the number of scatterers in a pixel, their elevations and their reflectivity strength. In this paper, the tomographic reconstruction of multiple scatterers from space-borne high resolution SAR images will be demonstrated in Shanghai test site. The high density of high-rise buildings in Shanghai leads to a rather complicated backscattering, which is difficult to handle in conventional interferometric processing. In order to reconstruct the 3D scatterer distribution from time-series of images, firstly we need to pre-process the data stack. The preprocessing procedure includes co-registration, atmospheric phase screen correction and baseline estimation. Then the non-parametric and parametric spectral estimation will be carried out to get three dimensional tomographic results. Due to the ill-conditioning of orbits, some

normalization tools are needed to overcome this problem. A primary tomographic experiments has been carried out in our research. The preliminary result shows the reconstructed reflectivity profile in elevation of two test points located on top of the Shanghai railway station from TerraSAR-X data is presented. The signal-to-noise ratio in the lower left example is still quite low, with normalized sidelobes strength of around 0.5, but nevertheless two clear signal peaks can be identified. The lower right example is worse, with one clear signal and with different secondary peaks depending on the reconstruction method: Wiener-SVD or TSVD. In the proposed presentation, we will show three dimensional tomographic results from both simulated data and real TerraSAR-X data, together with detailed analysis of the results. It will demonstrate the 3D reflectivity reconstruction capability and the multi-scatterers separation capability of SAR tomography.

## An improved crosstalk estimation algorithm of polarimetric and interferometric SAR calibration

Author(s)

Hong Zhang <sup>(1)</sup>, Fan Wu <sup>(2)</sup>

Department

<sup>(1)</sup>Chinese academy of Sciences , CN

<sup>(2)</sup>CAS , CN

### Abstract

Polarimetric SAR calibration includes crosstalk calibration and channel imbalance calibration, while the crosstalk and channel imbalance usually are coupled. So, it's difficult to estimate any of them separately. Among all kinds of polarimetric SAR calibration algorithms, Quegan's algorithm [1] can estimate the parameters easily without iteration, while Ainsworth's algorithm [2] can estimate the parameters accurately with iteration and this algorithm can calibrate any scene without choosing targets. Although Quegan's algorithm is more effective, it's more inaccurate because it omits lots of high order terms [3] [4]. Ainsworth's algorithm can estimate parameters in two ways. The first way is assuming co-polarization and cross-polarization have none correlation. Then the parameters can be estimated accurately if the crosstalk is low. However, if the crosstalk is high, the iteration may not converge, and the parameter cannot be estimated accurately, either. The second way is assuming co-polarization and cross-polarization are correlated. As the constraints reduce, the number of independent equations will also reduce, which will result in crosstalk parameters cannot be estimated accurately (usually underestimated). The Quegan's algorithm can estimate parameters stable but inaccurately, while the Ainsworth's algorithm can estimate crosstalk parameters accurately but unstable. This paper proposed an improved algorithm to estimate the parameters stable and accurately based on these two algorithms. Assuming co-polarization and cross-polarization have none correlation, we can get four equations to solve the four crosstalk parameters. Different from the Ainsworth's algorithm, the processing of this new algorithm is: 1) Initial the crosstalk parameters with the estimations of Quegan's algorithm. 2) Calculate the correction values of these four estimations with Newton iteration method. 3) Update the crosstalk parameters with these correction values. 4) If each term of the correction values is small enough, or if the number of iteration is big enough, exit the iteration; otherwise, return to 2). Since there is no approximate process when estimate the parameters, this algorithm can accurately solve all parameters, even if the crosstalk is high. To verify the effect of proposed algorithm, we use both simulated distorted PolSAR data and real distorted PolSAR data. The results confirm the proposed algorithm can accurately solve all parameters, even if the crosstalk is high. The PolSAR data used in experiments are acquired by East China Research Institute of Electronic Engineering over the test site near Sanya City, Hainan Province of China. Reference: [1] S. Quegan, A unified algorithm for phase and cross-talk

calibration of Polarimetric data-theory and observations, IEEE Transaction on Geoscience and Remote Sensing, vol.32, no.1, pp.89-99, Jan.1994. [2] T. L. Ainsworth, L. Ferro-Famil, and J.-S. Lee, Orientation angle preserving a posteriori Polarimetric SAR Calibration, IEEE Transaction on Geoscience Remote Sensing, vol.44, no.4, pp.994-1003, Apr.2006. [3] Lu Wuping, et al. Comparison of Polarimetric calibration techniques and their applications. IGARSS, 2010. [4] Alvin S. Goh, Comparison of Parameter Estimation Accuracy of Distributed-Target Polarimetric Calibration Techniques, IGARSS'07. Geosci. Remote Sensing, pp. 4175-4178, July. 2007.

## Accurate Interferometric processing of PALSAR Wide-Beam SCANSAR Data

### Author(s)

Charles Werner <sup>(1)</sup>, Urs Wegmüller <sup>(1)</sup>, Othmar Frey <sup>(1)</sup>, Maurizio Santoro <sup>(1)</sup>

### Department

<sup>(1)</sup>Gamma Remote Sensing AG , CH

### Abstract

SCANSAR interferometry is a central element in the next generation of interferometric SAR missions including Sentinel-1 [1]. The advantage of SCANSAR is the ability to achieve wide-swath coverage required for short repeat intervals with moderate increase of radar system complexity. Interferometry based applications are facilitated by wide swath widths that permit short revisit intervals and the potential for frequent acquisitions to reduce interferometric measurement errors due to atmospheric and ionospheric phase variability. The Japanese ALOS satellite includes the PALSAR radar operating at 1.27 GHz [2]. ALOS has acquired extensive SCANSAR data on a global basis over the last 5 years. We have developed an end-to-end phase-preserving interferometric processing system for SCANSAR-SCANSAR and SCANSAR-STRIPMAP data acquired by ALOS. SCANSAR-SCANSAR interferometry with PALSAR was first reported by Shimada using a SPECAN processor and other groups have described STRIPMAP based approaches for ALOS SCANSAR processing [3-5]. SCANSAR successively illuminates parallel overlapping swaths with bursts of radar pulses. The PALSAR instrument operates primarily in 5 data acquisition modes including the WB-1 SCANSAR mode with the following characteristics: PALSAR Acquisition Mode: ScanSAR (WB1) Central Frequency 1270 MHz PRF 1500 - 2500 Hz (discrete stepping) range Sampling Frequency 16 MHz Chirp bandwidth 14 MHz Polarisation HH Off-nadir angle [deg] 20.1-36.5 Incidence angle [deg] 18.0-43.3 Swath Width [Km] 350 Bit quantization [bits] 5 Number of Swaths: 5 Number of Pulses/Burst 247, 356, 274, 355, 327 Nominal Pulse Reptition Frequency (PRF): 1669.4, 2314.8, 1692.0, 2132.2, 1890.4 Starting slant range (m): 744337, 784210, 821384, 864104, 894533 Data rate [Mbps] 120 Data acquired during descending passes of ALOS are in SCANSAR WB mode. The PRF and starting slant range change in discrete steps during the acquisition. This requires that the data be resampled using a constant PRF along track for processing to avoid gaps. In the case of SCANSAR data rather than resampling each track to the nominal PRF value, our processor resamples the data in all 5 beams to a constant PRF value of 2150.5 Hz. The data are synchronized to a common time reference such that the images from the beams fall onto a common grid in azimuth and slant-range. The most critical factor in processing SCANSAR data for repeat-track interferometry is synchronization of the bursts as described by Bamler and Eineder [6]. A requirement for interferometric coherence is that the scene is viewed from the same azimuth aspect angle by corresponding pulses. Therefore, coherence is improved by nulling out echos in the two passes that do not overlap with respect to the aspect angle. The center-swath look-vector at the start and end of each burst in the reference track is calculated. Then the position and time on the track of the second acquisition is determined for these points. The burst overlap is then determined using the ideal start and stop times of the burst in the second track and the actual burst times. A phase-preserving strip-map SAR processor is used for

image formation in our system as proposed by Bamler and Eineder [6]. In this approach the time between bursts is filled with zeros and the data is processed as if it were continuous strip-mode data. One of the significant advantages of this approach is that no data are discarded at the start and end of the burst images as is the case with the SPECAN based SCANSAR processing. The SLC images are produced at the pixel spacing of 9.4 meters in range and 3.1 meters in azimuth. The actual azimuth resolution is reduced by a factor of approximately 5 to ~60 meters. The SLC data are detected and multi-looked using 3 range looks and 16 azimuth looks to produce MLI (multi-look intensity images) of each beam to give a pixel spacing of 29 meters in slant range and 51 meters in azimuth. These image strips are mosaicked without interpolation due to the common processing geometry to form the full 5-beam mosaic. Intensity offsets between the beams is corrected by matching the average intensity in the overlap region. The accuracy of the matching in the overlap depends on accurate knowledge of the range antenna patterns and low azimuth ambiguities. The full mosaic of the MLI images is then terrain geocoded using the SRTM DEM. For the purposes of terrain geocoding of the SAR image, the image can be processed without azimuth burst synchronization to maintain full resolution. One of the products of the terrain geocoding is the SRTM DEM resampled to the slant range coordinates of the MLI mosaic. Performing the geocoding refinement on the full mosaic avoids DEM offsets between the individual beams. The full DEM in radar coordinates (slant range) is sliced into the individual beams and used for SLC coregistration and resampling. The coregistration algorithm in our processing chain takes into account the local terrain to avoid loss of correlation and phase errors due to misregistration. Each SCANSAR beam is individually resampled to the matching beam in the second acquisition. We form the differential interferogram directly for each beam using the co-registered SLC produced using burst synchronization and the simulated interferogram produced using the timing and track data for each SLC and the DEM in radar coordinates. These 5 differential interferograms are mosaicked without requiring interpolation since the SLC data have a common geometrical reference. No further phase adjustment is required between the differential interferograms in the full differential interferogram mosaic. We have processed SCANSAR-SCANSAR data covering the New Zealand earthquake that occurred near Christchurch on 20100903 (UTC), and both SCANSAR-SCANSAR and SCANSAR-STRIPMAP data over Los Angeles in our initial tests. The Los Angeles SCANSAR-SCANSAR data are from 20061231 and 20070402 and the SCANSAR-STRIPMAP are from 20061231-20070703. Beam 4 of the SCANSAR data on 20061231 corresponds to the FBS mode data collected on 20070703. The SCANSAR acquisitions over Los Angeles were acquired with different PRFs with the result that the burst synchronization varies along-track, and is an excellent test of the burst-synchronization algorithm. The New Zealand data are from 20071020 and 20101028 and show reasonable correlation despite a 3 year time interval and ~1490 meter perpendicular baseline. References [1] De Zan, F., Guarnieri, A.M., Rocca, F., Advances in SAR interferometry for Sentinel-1 with TOPS, Radar Conference 2008, 26-30 May 2008 Rome doi:10.1109/RADAR.2008.4720871 [2] Rosenqvist, A, Shimada, M, Watanabe, M, ALOS PALSAR: A Pathfinder Mission for Global-Scale Monitoring of the Environment, IEEE Transactions on Geoscience and Remote Sensing, vol. 45, no. 11, Nov. 2007, pp. 3007-3316 doi: 10.1109/TGRS.2007.901027. [3] Shimada, M. [2008]. PALSAR ScanSAR ScanSAR Interferometry. in Proc. IGARSS conference 2008, pp IV-93–IV-96. [4] Liang, C, et al. ALOS PALSAR ScanSAR Interferometry and its Application in Wenchuan Earthquake, ESA Fringe Workshop 2009 [5] Mellors, R and Sandwell, D ScanSAR Interferometry With PALSAR, presentation at the 3rd ALOS PI Symposium, Fairbanks, Alaska, Nov 9-13 2009. [http://www.asf.alaska.edu/pi\\_symp/node/123](http://www.asf.alaska.edu/pi_symp/node/123) [6] Bamler, R and Eineder, M, ScanSAR processing using standard high precision SAR algorithms, IEEE Transactions on Geo. and Rem. Sensing, January 1996 vol. 34 pp. 212-218, doi: 10.1109/36.481905

# Evolutions of Diff-Tomo for Sensing Subcanopy Deformations and Height-varying Temporal Coherence

Author(s)

Fabrizio Lombardini <sup>(1)</sup>, Francesco Cai <sup>(1)</sup>

Department

<sup>(1)</sup>University of Pisa Dept. of Information Eng., via Caruso 16, 56122 Pisa, IT

## Abstract

Much interest is growing in techniques based on the coherent combination of complex (i.e. amplitude and phase) SAR data, extending the operative InSAR and D-InSAR methods [1] based on phase-only data, for the extraction of even more rich information on the observed scene. Among these techniques, 3-D SAR Tomography [2-4] (Tomo-SAR) is an experimental multibaseline (MB) interferometric mode achieving full 3-D images in the range-azimuth-height space through elevation beamforming, i.e. spatial (baseline) spectral estimation. Tomo-SAR resolves multiple scatterers in height in the same cell, overcoming a limitation of conventional InSAR processing and allowing the analysis of complex scenarios. This can be e.g. the estimation of forest height and biomass, derivation of sub-canopy topography, of soil humidity and ice thickness, and of heights and reflectivities in layover in natural or urban areas. Often, these complex scenes are also non-stationary, as deformation motions and temporal decorrelation can occur during the typical repeat-pass MB acquisition. Monitoring the former phenomenon is important, especially in the spaceborne sensor framework, and characterizing the latter can be useful to analyze and possibly reduce its perturbing effects [5]. However, although Tomo-SAR can separate multiple scatterers, it has neither measuring sensitivity to their deformation motions, nor separation capabilities of their possibly different temporal coherences. On the other hand, D-InSAR techniques sense deformations but degrade or cannot operate in multiple scattering scenes, in particular in presence of significant volumetric scattering. For these reasons, a novel coherent data combination mode termed Differential SAR Tomography (Diff-Tomo) has been recently originated by University of Pisa [6], synergically integrating the D-InSAR and the Tomo-SAR concepts to allow "opening" the SAR pixel in complex non-stationary scenes (patent pending). Diff-Tomo is based on two-dimensional space-time spectral analysis, deeply exploiting the information content of MB-multipass data. It allows the joint resolution of multiple elevation and deformation velocity components of the scatterers mapped in a SAR pixel, with applications e.g. in the monitoring of complex urban areas and infrastructures [7-8]. Diff-Tomo enables also "volumetric differential interferometry" capabilities [5], in which the continuous profiling may be possible of velocity versus height. From a more general point of view, Diff-Tomo has potentials of identifying scattering components intensity distributions in the joint domain of spatial (height) and temporal frequency (phase rate of change) of harmonics in which a signal from a scattering component with temporal decorrelation can be decomposed [5]. This may also avoid their misinterpretation in the tomographic processing (e.g. for temporal decorrelation-robust Tomography in forested scenes [9]). In this work, evolutions are presented of Diff-Tomo based techniques of coherent data combination for the separation and analysis of deforming or decorrelating components in complex volumetric scenarios. In particular, we focus on forest scenarios, characterized by the presence of a temporal decorrelating volumetric scattering component (the canopy), in layover with a ground scattering one, possibly affected by deformation motions. For developing these new functionalities, an approximated parametric Diff-Tomo algorithm matched to continuous spectral distributions is presented for estimation of the "spatial-temporal signatures" of a temporal decorrelating volume over ground [9]. With this, the challenging possibility is investigated of discriminating the amount of temporal decorrelation of

the canopy and ground scatterers, by identifying the temporal frequency distributions. The possible related phenomenological investigations are raising increasing attention, e.g. in the Pol-InSAR community, in the framework of the studies for the Earth Explorer Core Mission BIOMASS, and within the Tropiscat mission. Moreover, another possible application of Diff-Tomo in forest scenes is tested to estimate the velocity of possible ground subsidence under the canopy (e.g. from mining activities), decoupling the interfering volume effects through the presented parametric algorithm. Results are reported both for simulated scenarios and real data. In particular, first cut experiments of these challenging functionalities are shown with quasi-multistatic MB P-band E-SAR data, acquired over the boreal forest of Remningstorp (Sweden) over a 2 months time span. A quick subsidence motion is synthetically injected in the real data to investigate the subcanopy deformation sensing. First results show interesting potentials for this functionality, and give indication that separating height-varying temporal decorrelation mechanisms can be possible, even with sparsely sampled MB-multipass data. These Diff-Tomo evolutions may be fruitfully applied e.g. in the framework of the future mission TanDEM-L [10].

**ACKNOWLEDGEMENT** The authors thank the DLR team for providing the E-SAR data set that it acquired in the framework of the ESA project BIOSAR-1. **REFERENCES** [1] A. Ferretti, C. Prati, F. Rocca, "Nonlinear Subsidence Rate Estimation Using Permanent Scatterers in Differential SAR Interferometry," *IEEE Trans. on Geosci. Remote Sens.*, vol. 38(5), pp. 2202-2212, 2000. [2] A. Reigber, A. Moreira, "First Demonstration of Airborne SAR Tomography using Multibaseline L-band Data," *IEEE Trans. on Geosci. Remote Sensing*, vol. 38(5), pp. 2142-2152, 2000. [3] F. Lombardini, M. Montanari, F. Gini, "Reflectivity Estimation for Multibaseline Interferometric Radar Imaging of Layover Extended Sources," *IEEE Trans. on Signal Processing*, vol. 51(6), pp. 1508-1519, 2003. [4] G. Fornaro, F. Serafino, and F. Soldovieri, "Three Dimensional Focusing With Multipass SAR Data," *IEEE Trans. on Geosci. Remote Sens.*, vol. 41(3), pp. 507-517, 2003. [5] F. Lombardini, "Potentials of Volumetric Differential Interferometry and Robust Tomography," *ESA Fringe'07 Wrkshp.*, Frascati, 2007. [6] F. Lombardini, "Differential Tomography: A New Framework for SAR Interferometry", *IEEE Trans. on Geosci. Remote Sensing*, vol. 43(1), pp. 37-44, 2005. [7] G. Fornaro, F. Serafino, D. Reale, "4D SAR Imaging for Height Estimation and Monitoring of Single and Double Scatterers," *IEEE Trans. on Geosci. Remote Sens.*, vol. 47 (1), pp. 224-237, 2009. [8] F. Lombardini, M. Pardini, "Multiple Scatterers Identification in Complex Scenarios with Adaptive Differential Tomography," *Proc. of IEEE 2009 Int. Geosci. and Remote Sensing Symp. (IGARSS)*, Cape Town, South Africa, 2009. [9] F. Lombardini, F. Cai, M. Pardini, "Tomographic Analyses of Non-stationary Volumetric Scattering", *Proc. of 2010 European SAR Conference (EUSAR)*, Aachen, Germany, 2010. [10] A. Moreira, G. Krieger, I. Hajnsek, K. Papathanassiou, M. Eineder, F. De Zan, M. Younis, M. Werner, "Tandem-L: Monitoring the Earth's Dynamics with InSAR and PolInSAR", *Proc. of ESA POLinSAR Workshop*, Frascati (Italy), 2009.

## Urban 3D Reconstruction using COSMO-SkyMed high-resolution data

### Author(s)

Fabio Baselice <sup>[1]</sup>, Alessandra Budillon <sup>[1]</sup>, Giampaolo Ferraioli <sup>[1]</sup>, Gilda Schirinzi <sup>[1]</sup>, Vito Pascazio <sup>[1]</sup>

### Department

<sup>[1]</sup>Università Parthenope Centro Direzionale, Isola C4, IT

### Abstract

Three dimensional Synthetic Aperture Radar (SAR) imaging of earth surface has received a growing interest in recent years, thanks to the launch of new high-resolution radar sensors such as COSMO- SkyMed (C-S). 3-D SAR image formation provides the scattering scene estimation along azimuth, range and elevation co-ordinates. COSMO-SkyMed sensor provides SAR image stacks characterized by a much higher resolution than the ones of the previous generation



systems (ERS, ENVISAT), opening new applications. In particular, for 3-D reconstruction and, in general, applications exploiting the signal phase, thanks to the high resolution it is expected to find a larger number of coherent pixels per unit area, resulting in more accurate measurements. The aim of this paper is to exploit the peculiar characteristics of C-S system together with the recently developed algorithms for the generation of the 3-D models of earth surface. In particular, C-S data are used in the multi-pass interferometric configuration for non urban areas and in multi-pass tomographic configuration for urban areas.

**A. Multi-pass Interferometric Systems** To achieve high quality DEM reconstruction without imposing any constraint on the height profile of the ground surface, it is useful to adopt Multi-pass InSAR systems, exploiting the availability of many interferograms referred to the same scene, obtained using different baselines (using sensors watching the scene from different positions). The number of interferograms required to obtain reliable reconstructions depends significantly on the system parameters (frequencies, baselines, spatial and temporal coherence values). By the way, a large number of interferograms are not easy to obtain, since they are often characterized by small temporal and spatial correlation. In order to efficiently combine the different acquisitions, and thus to successfully solve the problem of the height reconstruction, a solution to this problem consists in adopting a statistical approach, based on Maximum Likelihood or on Maximum a Posteriori Estimation. The effectiveness of the Multi-pass approach for DEM reconstruction, in particular the capability to improve the precision of already available low resolution DEMs (SRTM case), has been proved with reference to ERS multi-baseline data. We expect that the use of C-S constellation data, and the favourable circumstance that the flying orbits will pass over the ground scene with low revisiting times, providing high coherence data sets (interferograms generated starting from correlated temporal/spatial acquisition), will result in a significant improvement of the DEM reconstructions.

**B. Multi-pass Tomographic Systems** The innovation introduced by SAR Tomography is the ability to reconstruct, in the same azimuth/range resolution cell, the scattering profile in a two-dimensional domain, elevation and mean deformation velocity, where the elevation is the direction orthogonal to the azimuth-range plane. The analysis of this reconstruction allows the detection of multiple scattering mechanisms interfering in the same pixel, and therefore provides both the location in space and the monitoring of movements through the mean deformation velocity and the estimation of deformation time series. The application of the tomographic technique is proving to be very effective particularly on urban areas, where phenomena of interference between buildings and reflective ground induced by the so-called phenomenon of layover are very common, due to the particular side-looking geometry. The technique, has been already applied to medium resolution SAR data provided by ERS and ENVISAT satellites, and it has demonstrated the validity of the method, allowing an increase in the density of monitored points thanks to the ability to distinguish interfering targets within the same pixel. Two different techniques exploiting stacks of multi-pass SAR images to retrieve the height of the different contributions that collapse in a layover cell in order to achieve 3-D SAR imaging have recently been proposed: Compressive Sensing and SAR Statistical Tomography . It is expected that the application of these two techniques to high resolution data of Cosmo-SkyMed, where the increase of the range resolution emphasizes the phenomena of layover, distributing the effect on a higher number of pixels, can return results even more significant.

# Different approaches for PSI target characterization for monitoring urban infrastructure

## Author(s)

Prabu Dheenathayalan <sup>[1]</sup>, Ramon Hanssen <sup>[1]</sup>

## Department

<sup>[1]</sup>Delft University of Technology Kluyverweg 1, 2629 HS Delft, NL

## Abstract

Persistent Scatterer Interferometry (PSI) can yield a positioning accuracy in the order of metres and millimetric deformation trends by exploiting coherent pixels. However, associating a Persistent Scatterer (PS) to a specific target such as a pole, building, ground or a building-to-ground interface is not straightforward [2]. If one could precisely associate each PS to an actual target, the observed deformation can be better interpreted, thereby creating a new range of applications. One such application is to find the relative motion between a building and the ground to detect the stress on underground infrastructures like pipes used for gas or sewer systems, potentially leading to damage or even gas explosions when left unnoticed. This building versus ground differential (BGD) motion detection can be used as one of the metrics to identify potentially unsafe urban zones and alert respective stakeholders.

To detect BGD motion, the reflections from buildings, ground, and the building to ground interfaces have to be separated. In our previous approach [1], we combined various types of information such as height estimated from PSI, scattering pattern (amplitude) variation over various incidence and squint angles, and polarimetric information to characterize and to detect the BGD motion. But polarization data is not available over all the regions and hence the BGD detection capability without using polarization data needs to be assessed. Towards the goal of BGD motion estimation, different approaches are introduced based on different set of information exploited: 1. Using only height, 2. Using height and amplitude, 3. Using height and polarization, and 4. Using height, amplitude and polarization. These approaches are compared and evaluated for target characterization and interpretation of deformation phenomena over a few urban areas in The Netherlands using TerraSAR-X time-series and polarimetric data. Later, this technique can also be applied on other urban areas using low resolution ENVISAT and ERS data to test its robustness.

## References:

[1] P. Dheenathayalan and R. Hanssen. Target characterization and interpretation of deformation using persistent scatterer interferometry and polarimetry. In the proceedings of the 5th International Workshop on Science and Applications of SAR Polarimetry and Polarimetric Interferometry, ESRIN, Frascati, Italy, 24-28 January 2011.

[2] D. Perissin. SAR super-resolution and characterization of urban targets. PhD thesis, Politecnico di Milano, Italy, March 2006.

# Theoretical Performance Bounds on the Estimation of Forest Structure Parameters From Multibaseline SAR Data

## Author(s)

Matteo Pardini <sup>(1)</sup>, Fabrizio Lombardini <sup>(2)</sup>, Konstantinos Papathanassiou <sup>(1)</sup>

## Department

<sup>(1)</sup>German Aerospace Center (DLR) , DE

<sup>(2)</sup>University of Pisa , IT

## Abstract

Given their central role in the carbon budget, the SAR remote sensing of forests has become during the last two decades a “hot” research topic. A powerful way to analyze forest scattering consists in the coherent combination of multibaseline (MB) SAR data, possibly also polarimetric. For instance, SAR Tomography is a powerful technique whose natural output is the 3-D imaging in the range-azimuth-height space, thus allowing the resolution of multiple scatterers in height in the same cell. As a consequence, the extraction of a high amount of information is made possible, e.g. forest height and biomass, radar reflectivities, sub-canopy topography, soil humidity, volume extinction [1].

In the last years, many tomographic algorithms have been conceived for the estimation of forest structure parameters in both parametric and non parametric frameworks and their performance have been judged against the available in-situ measurements [2-5]. However, not so many efforts have been spent in the analytical derivation of theoretical performance bounds, despite their primary importance. In fact, such tools provide a benchmark against which it is possible to compare the performance of any estimator. Not only, but they alert to the physical impossibility of finding an estimator whose performance is lower than the bounds.

This work offers a contribution to tackle the performance bounding problem by resorting to the Cramer-Rao bound (CRB) theory. The CRB is a result of the information theory which provides a lower bound on the variance of any unbiased estimator of an unknown parameter. Given also its relative easiness of calculation, the CRB is widely used in the statistical signal processing to judge the efficiency of the parameter estimators. In the specific MB SAR field, it could also be a very useful instrument to characterize the potentials of acquisition configurations and possibly as a guideline in designing acquisition patterns (mission planning) and systems. An interesting extension of the CRB is represented by the Hybrid CRB (HCRB), in which the presence of random phase offsets between different acquisitions (e.g. due to non perfect baseline estimation and/or propagation effects through the atmosphere) can be taken into account.

In particular, in this work the CRB and HCRB derivations are focused to the analysis of forest areas by assuming a two-layer model for the MB data vector, i.e. a ground layer and a canopy layer, with different characteristics of their vertical structure. Starting from the very general formulations of MB bounds in [6] and [7], ready-to-use CRB and HCRB formulas are given for forest scenarios. Moreover, the obtained precision limits on the parameters of interest are calculated numerically for some realistic acquisition patterns and for different observed scenarios. The presence of temporal decorrelation [8] it is also considered in the model, which is recognized to be one of the main application barriers of MB repeat-pass forest observations, especially from space.

## References:

[1] A. Reigber, A. Moreira, “First Demonstration of Airborne SAR Tomography Using Multibaseline L-Band Data,” *IEEE Trans. on Geoscience and Remote Sensing*, vol. 38, 2000.

[2] F. Lombardini, M. Pardini, “Experiments of Tomography-Based SAR Techniques with P-Band Polarimetric Data”, *Proc. of the 2009 ESA PolInSAR Workshop*.

- [3] M. Nannini, R. Scheiber, et al., "Estimation of the Minimum Number of Tracks for SAR Tomography," *IEEE Trans. on Geoscience and Remote Sensing*, vol. 47, 2009.
- [4] M. Neumann, L. Ferro-Famil, et al., "Estimation of Forest Structure, Ground, and Canopy Layer Characteristics From Multibaseline Polarimetric Interferometric Data," *IEEE Trans. on Geoscience and Remote Sensing*, vol. 48, 2010.
- [5] S. Tebaldini, "Single and Multipolarimetric SAR Tomography of Forested Areas: A Parametric Approach," *IEEE Trans. on Geoscience and Remote Sensing*, vol. 48, 2010.
- [6] F. Gini, F. Lombardini, M. Montanari, "Layover Solution in Multibaseline SAR Interferometry," *IEEE Trans. on Aerospace and Electronic Systems*, vol. 38, 2002.
- [7] M. Pardini, F. Lombardini, F. Gini, "The Hybrid Cramer-Rao Bound for Broadside DOA Estimation of Extended Sources in Presence of Array Errors," *IEEE Trans. on Signal Processing*, vol. 56, pp. 1726–1730, Apr 2008.
- [8] F. Lombardini, F. Cai, M. Pardini, "Parametric Differential SAR Tomography of Decorrelating Volume Scatterers," *Proc. of 2009 EURAD Conference*.

## A Modified Model Based SAR Target Decomposition Method for Polarimetric Data

### Author(s)

Hong Zhang <sup>(1)</sup>, Fan Wu

Department

<sup>(1)</sup>Chinese academy of Sciences , CN

### Abstract

1. INTRODUCTION As far as the incoherent decompositions are concerned, one of the important techniques is based on physical models, which separates the coherency or covariance matrix into several basic physical models of scattering mechanisms. Freeman et al. [1] modeled the covariance matrix as the contributions of three scattering mechanisms, namely the surface, double-bounce and volume scatterings. Yamaguchi et al. [2] proposed new volume models accounting for different tree trunk and branch distributions and added the helix scattering as the fourth component in his decomposition. In applications with respect to the urban districts, the model based decompositions are faced with negative values in the surface or double-bounce power as well as overestimation of the volume scattering power for some pixels. These problems will result in the misclassification between the ground objects such as the vegetations and the man-made structures. Therefore, we will propose a modified four-component decomposition to deal with these problems in this paper.

2. MODIFIED MODEL BASED SAR TARGET DECOMPOSITION Based on the coherency matrix, four kinds of scatterings are considered in the decomposition, namely the double bounce scattering, the volume scattering, the surface scattering and the helix scattering. After theoretical analysis and experiments, it can be found that the effect induced by the tilted buildings at a certain angle with respect to the radar illumination direction contributes to the overestimation of the volume scattering component in the urban areas. So an orientation angel compensation operation has been conducted over those areas covered by man-made structures, which can be discriminated by the H/A/| $\hat{A}$  classification. Although it is difficult to make a unified geometric assumption of man-made structures owing to the infinite variety of them, we still suppose the volume scattering to be the multi-scattering effect among the random little scatters of man-made structures. Based on the assumption of pure randomness contributes to pure volume scattering in the urban areas, a modified volume scattering model with the maximum entropy is applied in the decomposition. In theory, the modified volume scattering model also helps to reduce the overestimated volume scattering power in the urban areas, and hence decreases the negative powers. Finally, some ad hoc power constraints are added to eliminate the negative pixels completely.

3. EXPERIMENT OVERVIEW A

Radarsat-2 polarimetric image acquired over the Su Zhou city has been utilized in the experiments. Experiment results will verify the effectiveness of the orientation angle compensation, the modified volume model as well as the power constraints in dealing with the problems in the urban areas. To evaluate the proposed method further, a polarimetric SAR image classification method based on the decomposed scattering powers has also been conducted. The improvements in the classification result have also proved the feasibility of the proposed techniques. 4.

REFERENCES [1] A. Freeman, and S. L. Durden, "A three-component scattering model for polarimetric SAR data," *IEEE Trans. Geosci. Remote Sens.*, vol. 36, no. 3, pp. 963-973, May. 1998. [2] Y. Yamaguchi, T. Moriyama, M. Ishido, and H. Yamada, "Four component scattering model for polarimetric SAR image decomposition," *IEEE Trans. Geosci. Remote Sens.*, vol. 43, no. 8, pp. 1699-1706, Aug. 2005.

## Statistical Edge Detection in Urban Areas Exploiting X-Band SAR data

Author(s)

Fabio Baselice <sup>[1]</sup>, Giampaolo Ferraioli <sup>[1]</sup>, Vito Pascazio <sup>[1]</sup>

Department

<sup>[1]</sup>Università Parthenope Centro Direzionale, Isola C4, IT

### Abstract

Building edge detection is becoming a task of increasing importance in last decays. In literature, two classes of building edge detectors have been presented which exploit only the amplitude or only the phase of the SAR images, respectively. The techniques belonging to the first class perform the detection considering the difference in reflectivity map. Due to the multiplicative nature of speckle, gradient based techniques, such as Sobel filter, cannot be applied to SAR amplitude data, unless a previous speckle filter is performed, at the cost of a resolution reduction. The main approaches able to take into account the multiplicative nature of speckle are the ratio-based techniques for edge detection, which result to be effective in retrieving the correct shape of the ground structures, but are characterized by high false alarm rate. The techniques belonging to the second class perform the detection considering the strong phase changes in the interferogram, which are related to different heights of the structures. In literature different approaches have been proposed, showing interesting results. These methods start from the idea of finding building edges from the height information embodied in the interferometric phase. These methods are characterized by a low false alarm rate in terms of building edge reconstruction, but suffer some limitation about retrieving the shape of the buildings, requiring some a priori knowledge. The method proposed by [1] does not make any assumption about the scene under observation: buildings are well detected but the recovered shapes are not fully consistent with man made structures. In this work, we propose to jointly exploit the full complex SAR image, proposing two algorithms which work on real and imaginary parts and amplitude and phase, respectively. By jointly exploit the complex data, what we expect is to correctly identify the building and correctly recover their shapes while maintaining a low false alarm rate, combining the benefits of the existing techniques. To achieve this results, we extend to the complex case the approach of [1], where a stochastic approach based on the idea of finding building edges in an urban scenario by modeling the image as a Gaussian Markov Random Field (GMRF) with local hyperparameters is proposed. The local hyperparameters are seen as an indicator of the spatial correlation of the pixels. The detection of the building edges is carried out after the hyperparameter estimation, allowing to achieve interesting results in terms of detection accuracy. In urban areas, each couple of neighboring pixels involved in a building edge is characterized by both a reflectivity discontinuity (in SAR amplitude images) and a phase discontinuity (in interferometric SAR images). These discontinuities can also be found in the real and the imaginary parts of the complex SAR

signal. It is likely that the edges of one image are also present in the other one. The joint estimation allows to further improve the building edge detection both in terms of false alarm rate and detection probability. The performances of the proposed approach were tested on X-band data, showing interesting results using high resolution images. References [1] G. Ferraioli, "Multi-channel insar building edge detection," *Geoscience and Remote Sensing, IEEE Transactions on*, vol. 48, no. 3, pp. 1224 –1231, 2010.

## Posters on Ice and Snow

### Tide Model Accuracy in the Amundsen Sea, Antarctica, from InSAR Observations of Ice Shelf Motion

#### Author(s)

Malcolm McMillan

Department

<sup>(1)</sup>University of Leeds,

#### Abstract:

This study assesses the accuracy of tide model predictions in the Amundsen Sea Sector of West Antarctica. Tide model accuracy in this region is poorly constrained, yet tide models contribute to simulations of ocean heat transfer, and to the removal of tidal signals from satellite observations of ice shelves. We use two satellite-based interferometric synthetic aperture radar (InSAR) methods to measure the tidal motion of the Dotson Ice Shelf at multiple epochs; a single-difference technique that measures tidal displacement, and a double-difference technique that measures changes in tidal displacement. We use these observations to evaluate predictions from three tide models (TPX07.1, CATS2008a\_opt and FES2004). All three models perform comparably well, exhibiting root mean square deviations from the observations of ~ 9 cm (single-difference technique) and ~ 10 cm (double-difference technique). Care should be taken in generalising these error statistics because (1) the Dotson Ice Shelf experiences relatively small semidiurnal tides, and (2) our observations are not sensitive to all tidal constituents. An error analysis of our InSAR-based methods indicates measurement errors of 7 cm and 4 cm for the single- and double-difference techniques, respectively. A model-based correction for the effect of fluctuations in atmospheric pressure yields a ~ 6 % improvement in the agreement between tide model predictions and observations. This study suggests that tide model accuracy in the Amundsen Sea is comparable to other Antarctic regions where tide models are better constrained. These methods can be used to evaluate tide models in other remote Antarctic waters.

### The application of time Series InSAR on the Antarctic Peninsula: first results

#### Author(s)

Anneleen Oyen <sup>(1)</sup>, Matt King <sup>(2)</sup>, Andrew Hooper <sup>(1)</sup>

Department

<sup>(1)</sup>Delft University of Technology , NL

<sup>(2)</sup>Newcastle University , UK

#### Abstract

Providing reliable sea-level rise estimates requires precise knowledge on the mass balance of the Earth. This can be achieved by combining Gravity Recovery and Climate Experiment (GRACE) data and Glacial Isostatic Adjustment (GIA) models. These models estimate the amount of mass

change caused by the redistribution of mantle material due to past surface load changes (e.g. ice melt). Input parameters for such models are amongst others estimates of the viscosity of the upper mantle. The models can be constrained by measurements of the GIA-induced surface deformation. GPS has proven to be a suitable geodetic technique to measure GIA signal in Fennoscandia and Canada (Milne et al., 2001; van der Wal et al., 2009), but measuring such deformation is a real challenge, in the Antarctic, a continent which is remote and has the coldest climate on Earth. The climate and snow cover in Antarctica impede the realization of a dense network of GPS stations. Focusing on the Antarctic Peninsula (AP), the GPS measurements contradict the estimated GIA signal (Bevis et al., 2009). This suggests a large uncertainty in the GIA models due to a lack of knowledge about the ice history and Earth rheology below the AP. Here we use time series InSAR (TS-InSAR) techniques on the peninsula in order to catch the GIA signal over a much denser network. Specifically, we apply persistent scatterer interferometry combined with a small baseline approach (StaMPS; Hooper et al., 2004). The AP has experienced rapid ice melt, and, as a consequence, is undergoing high uplift rates. In addition, many rocky outcrops are present, and this makes the AP a perfect test side for the application of TS-InSAR with the aim of measuring GIA signal in the Antarctic. The resulting velocity maps will better constrain GIA models and ultimately lead to better sea level estimates.

Applying InSAR on the Antarctic Peninsula is not straightforward for the following reasons. First, the coregistration is often 'misled' by slow moving ice flows and ice sheets. This is solved by a-priori window selection for the coregistration steps.

Second, finding accurate topographic models for regions at high latitudes is difficult as most topographic missions, such as e.g. SRTM, do not reach such high latitudes. In addition, the map projection often leads to distortions of the DEM. At the AP, there is another issue. The peninsula itself is an elongated plateau, but the topography is very steep near the coasts. The slopes imply again problems for the coregistration, due to distortion of the pixels on the slopes. Solving this issue by DEM assisted coregistration is only possible when an accurate DEM is available.

Therefore, a composite DEM is created, with ASTER, RAMP, and GTOPO DEM's combined and if necessary topo-pairs from ERS ice phase data are added to improve the DEM.

A third challenge is the unwrapping of the resulting signal. Because the (coherent) rocky outcrops are scattered along the peninsula, the unwrapping algorithm is prone to unwrapping errors from one outcrop to another.

Despite the above-mentioned complications, we manage to create coherent time series with available Envisat images. The fact that coherence is also sometimes maintained, even during winter, is very promising. However, the expected GIA signal is a very long-wavelength signal and is smaller than the trends induced by the atmosphere and orbital errors. The fact that we are observing a polar region plays in our favour this time. The large overlap between the tracks increases the effective number of acquisitions significantly, which makes it possible to provide more reliable estimates on each of the signal contributions.

This work highlights the obstacles that occurred during the InSAR processing and gives suggested solutions. It demonstrates the potential for applying TS-InSAR approaches on the Antarctic Peninsula.

References:

Bevis, M., E. Kendrick, R. S. Jr, I. Dalziel, D. Caccamise, I. Sasgen, M. Helsen, F. W. Taylor, H. Zhou, A. Brown, D. Rayleigh, M. Willis, T. Wilson, and S. Konfal (2009). Geodetic measurements of vertical crustal velocity in west antarctica and the implications for ice mass balance. *Geochemistry, Geophysics, Geosystems*.

Hooper A., H. Zebker, P. Segall, and B. Kampes (2004) A new method for measuring deformation on volcanoes and other natural terrains using InSAR persistent scatterers. *Geophysical Research Letters*, Vol. 31

Milne G. A., J. L. Davis, Jerry X. Mitrovica, H.-G. Scherneck, J. M. Johansson, M. Vermeer, H. Koivula (2001) Space-Geodetic Constraints on Glacial Isostatic Adjustment in Fennoscandia. Science, Vol. 291

van der Wal, W., A. Braun, P. Wu, and G. Sideris (2009) Prediction of decadal slope changes in Canada by glacial isostatic adjustment modelling. Can. J. Earth Sci., Vol. 46

## Monitoring Glacial Rebound using InSAR in Iceland

### Author(s)

Wenliang Zhao <sup>(1)</sup>, Falk Amelung, Tim Dixon <sup>(2)</sup>

### Department

<sup>(1)</sup>University of Miami , USA

<sup>(2)</sup>University of South Florida , USA.

### Abstract

Various methods have been investigated to measure the crustal deformation in Iceland. The results show continuous uplift in recent years, and this rate is accelerating due to subglacier rebound, recent ice unloading and other geological events. The implementation of GPS provides millimeter precision at the stations. But the sparse density of the network is a problem preventing us from learning more details in spatial domain. Some work has been introduced to use InSAR to monitor volcanic and seismic deformation and get good results. Traditional satellites are very sensitive to these strong deformation signals. GPS time series for ice unloading has been introduced in recent years, while there is less paper describing InSAR techniques in this area. The main error sources of InSAR like atmosphere, orbital, phase unwrapping, decorrelation show the difficulties to measure 1-2 centimeter or sub-centimeter deformation. Here we did a test study of InSAR and InSAR time series based on small baseline subsets (SBAS) algorithm in Iceland. 4 tracks of ERS data were used for this study. We implemented the time series and got some information which is useful for further study. In the future we are going to get more data in this area. New generation satellites with shorter wavelength and repeat cycle should be better for slow deformation in glacier areas.

## Dynamics of fast glaciers in the Patagonia Icefields derived from TerraSAR-X and TanDEM-X data

### Author(s)

Dana Floricioiu <sup>(1)</sup>, Wael Abdel Jaber <sup>(1)</sup>, Helmut Rott <sup>(2)</sup>,

Nestor Yague-Martinez <sup>(1)</sup>

### Department

<sup>(1)</sup>German Aerospace Center (DLR) , DE

<sup>(2)</sup>University of Innsbruck , AT

### Abstract

The Patagonia Icefields are the largest mid-latitude ice masses in the Southern Hemisphere. The ice masses of the Northern and Southern Patagonia Icefields (NPI & SPI) are drained by outlet glaciers with fronts calving into fresh water lakes or Pacific fjords. Both ice fields were affected by significant downwasting in the last decades. Interferometric ice motion data have been obtained for outlet glaciers of SPI and NPI from 24h repeat pass L-band SIR-C data of SRL-2 in October 1994. ERS-1/-2 SAR tandem data could be applied for ice motion mapping only on few glaciers because of rapid decorrelation of the signal due to adverse meteorological conditions (snowfall, rain, melting) or strong shear in the terminal parts of the ice streams. With TerraSAR-X areal changes and ice motion are monitored since 2008. High resolution 2D velocity fields derived by means of amplitude correlation techniques reveal interesting features of ice motion and



deformation on the Patagonia glaciers. In June 2010 a second spacecraft, almost identical to the TerraSAR-X satellite, was launched to enable operation of the bistatic SAR mission TanDEM-X. During the first 2.5 months of the commissioning phase both satellites were separated in orbit by an along-track distance of 20 km enabling pursuit monostatic acquisitions. This formation allowed the validation of technical characteristics and performance of the new satellite without impacts of mutual SAR illumination. In parallel to the overall SAR system calibration activities a limited number of science data takes was acquired during several cycles of this phase. This work utilizes repeat pass TanDEM-X data acquired over Patagonia glaciers during three 11 day cycles of the pursuit monostatic commissioning phase. The same area on the ground was imaged by both satellites with a delay of 3 s, corresponding to the mentioned 20 km along track distance. This time lag is short enough to avoid temporal decorrelation and minimize atmospheric phase errors. The 3D-glacier topography is reconstructed from these data with large baselines and compared to SRTM DEMs from 2001. For some glaciers data from field work are available, as well as data from ice-free areas with accurate ground control points. By comparing the DEMs of 2001 and 2010 we will measure the surface lowering of the last decade for some of the main outlet glaciers, with expected thinning rates up to several m/a. The repeat pass data acquired by a single satellite are processed to obtain the 2D velocity field coincidentally with the topography information from the TanDEM-X acquisitions. The detailed ice flow patterns can thus be combined with topographic information derived from the DEMs, representing the basis for retrieving changes in the glacier mass and calving flux. The work demonstrates the excellent capabilities of high resolution, short revisit time X-band InSAR for assessing the dynamic state of glaciers. Although the pursuit monostatic mode will not be used for the global DEM generation these pre-operational TanDEM-X DEMs deliver important information about the system performance in areas with complex topography.

## Periglacial Mass Wasting in the Antarctic Peninsula: Displacement detection at the South Shetlands Islands with DInSAR

### Author(s)

Marco Jorge <sup>(1)</sup>, João Catalão <sup>(2)</sup>, Gonçalo Vieira <sup>(1)</sup>

### Department

<sup>(1)</sup>CEG-IGOT-University of Lisbon , PT

<sup>(2)</sup>LATTEX-IDL, University of Lisbon , PT

### Abstract

DInSAR is applied to the displacement detection and measurement of periglacial mass wasting processes, directly related with permafrost or seasonal frost conditions and/or the presence of ground-ice, at the South Shetlands Islands, near the northern tip of the Antarctic Peninsula, where climate and landscape are rapidly changing. Permafrost creep landforms, such as rockglaciers, and periglacial slope processes (i.e. solifluction), are some of the widespread phenomena in the recently deglaciated coastal-terrains, but very little is known on their activity (are they presently moving or are they relict features?) and kinematics. A priori knowledge on the location of the discrete processes/landforms is important to investigate and overcome limitations related to temporal decorrelation and troposphere delay related to strong weather variability and snowfalls. Also, in this type of medium-scale object-oriented analysis, acquisition geometry may bring about specific limitations; the relationship between the range direction, incidence angle, relative location of the landform (relief context) and the main displacement vector has to be properly acknowledged. The coherence and deformation signal of all the C and L band interferometric pairs from the ERS 1-2, ENVISAT and ALOS satellites is being searched and used

to classify the kinematics of the identifiable dynamic geomorphological features. C Band satellites provide coherent interferograms from the mid-1990's to the late 2000's, with temporal baselines ranging from tenths of days to around a year. Sometimes perpendicular baselines are less than 10 meters. L-band images clearly allow generating more coherent interferograms, but very few pairs exist. Even though summer snowfall is relatively frequent, it will be probably possible to get fairly coherent pairs with temporal baselines exceeding 1, 2 or even more years, because snow in the ground usually melts rapidly. Ideally, since different process rates manifest in distinct temporal baselines, the deformation signal can be used to classify kinematics. In the South Shetland Islands, DInSAR may allow pinpointing sites with specific dynamics and understanding if landforms that would be classified through field geomorphological observations as active, are indeed moving or are relict features.

## Studies of ice motion and drainage of glaciers in Iceland using high resolution X-Band SAR

### Author(s)

Florian Mueller <sup>[1]</sup>, Helmut Rott <sup>[2]</sup>, Eyjólfur Magnússon <sup>[3]</sup>, Thomas Nagler <sup>[1]</sup>, Dana Floricioiu <sup>[4]</sup>, Claudia Notarnicola <sup>[5]</sup>

### Department

<sup>[1]</sup>ENVEO IT GmbH Technikerstrasse 21a, 6020 Innsbruck, AT

<sup>[2]</sup>University of Innsbruck Innrain 52, 6020 Innsbruck, AT

<sup>[3]</sup>University of Iceland Dunhaga 3, 107 Reykjavik, IS

<sup>[4]</sup>DLR Münchner Straße 20, 82234 Oberpfaffenhofen-Wessling, DE,

<sup>[5]</sup>EURAC Drususallee 1, Bolzano, Italy, IT

### Abstract

Several outlet glaciers of the major ice caps in Iceland are affected by sub-glacial outburst floods, so-called jökulhlaups. Sources of these outbreaks are water accumulations beneath the glacier due to geothermal or volcanic activity. Outbreaks may also originate from lakes at glacier margins which drain into sub-glacial channels. One component of the project Northern Hydrology, carried out within the ESA STSE (Support to Science Element) programme, addresses techniques and applications of satellite data for studying drainage mechanisms and water outbreaks of sub-glacial lakes in Iceland. Such events are usually related to surface deformation and changes in ice velocities, sometimes occurring already well ahead of the peak of the flood wave. High resolution repeat pass SAR data are able to deliver spatially detailed information on surface motion and displacement, which are highly relevant for advancing the understanding of glacier hydraulics and jökulhlaup processes. In this paper we focus on methods and applications of high resolution X-band SAR data from the satellites TerraSAR-X and the COSMO-SkyMed for observing glacier motion and deformation of various glaciers in Iceland. Multiple 11-day repeat pass SAR data are available for TerraSAR-X from different seasons and years, covering different swathes. Because the signal phase decorrelates over this time span, cross-correlation of the incoherent amplitude signal is applied to obtain two components of the velocity vector for SAR data from one view direction. In several cases SAR data from both the ascending and descending swathes are available, enabling to derive the full 3D velocity vector. For the COSMO-SkyMed satellites repeat pass data over 1 day, 8 days and 14 days are available, depending on the constellation. This allows the application of interferometry over the short repeat interval, and of amplitude correlation for the longer time spans. One of the study glaciers is Skeidararjökull, a main outlet of the ice cap Vatnajökull, which has been affected by jökulhlaups in annual or bi-annual intervals during the last several years. Another study site is Eyjafjallajökull, where a water outbreak occurred shortly after start of the main volcanic eruption in April 2010. Ice motion and deformation are also analyzed for Breidamerkurjökull, another main outlet of the ice cap

Vatnajökull, which is calving into a major pro-glacial lake. The satellite data are of interest to study properties of surface deformation for the calving glacier. Furthermore, Breidamerkurjökull is the validation site for retrieval of 3D ice motion from multi-directional SAR data, as recording GPS stations and ablation measurements are available on several sites at the glacier tongue. The comparison between SAR velocities by means of amplitude correlation and GPS measurements shows agreement within 2 cm/day, confirming the high quality of image correlation products from high resolution SAR sensors.

## Ice flow mapping in Grove Mountains, East Antarctica using multi-temporal Interferometric SAR data

### Author(s)

Xiao Cheng <sup>(1)</sup>, Zhaohui Chi <sup>(2)</sup>

### Department

<sup>(1)</sup>Beijing Normal University, CN

<sup>(2)</sup>Texas A&M, USA

### Abstract

Satellite SAR interferometry is a very useful tool to measure ice flow in polar regions and help determine their state of mass balance and evolution in response to climate change. Grove Mountains is located on the east bank of Lambert Glacier, with an annual flow rate of about 10m. Previous research using four-pass interferometry with JERS-1 and ERS-1/2 data acquired in 1996 has revealed the quite complicated flow field in this area. In order to observe ice flow at long-term scale, 11 man-made corner reflectors were mounted in this area in early 2006 by China's Antarctic Expedition team and continuous ENVISAT ASAR acquisitions have been made since then. Under the support of Cryosat-2 AO, we collected continuous VV and HH-polarization ENVISAT ASAR data from 2006 to present. Supported by JAXA, we also collected a pair of ALOS PALSAR data in 2006 at L-band frequency. 6 of the 11 corner reflectors were installed on bare rocks and 5 of 11 were semi-buried in the snow. Those 5 moving reflectors lost high back-scattering capability gradually because of the rotation with the glacier. Since the whole time duration is too long (about 5 years) and the baselines are random, we adopted a cooperative registration strategy to match all the ASAR images acquired at different time. It is found that for C-band ASAR data, 35-d differential INSAR data are suitable for ice flow detection. With the time difference increase, relative flow speed and the de-correlation make the long-time INSAR data unusable. L-band offers longer times of coherence over snow and firn which make it superior in areas of rapid flow. A comparison of these results with ERS-1 data and JERS-1 data in 1996 shows very little change in speed in this sector. The final results are the distribution and movement of 11 corner reflectors, multi-temporal ice flow field in Grove Mountains. This work was performed at Beijing Normal University and Chinese Academy of Sciences under AO VECTRA 108, AO 2605 and 4091.

# Glacier-surface deformation in alpine terrain based on PS-InSAR method in Siachen Glacier

## Author(s)

Junchao Shi <sup>(1)</sup>, Massimo Menenti <sup>(1)</sup>, Roderik Lindenbergh <sup>(1)</sup>

## Department

<sup>(1)</sup>TU Delft Faculteit of Aerospace Engineering Building 62 Kluyverweg 1, NL

## Abstract

Abstract Accumulation gain is essential for mass balance of valley glaciers in Karakoram Himalaya. The higher elevation of this area received snowfall(>1000 cm a<sup>-1</sup>) annually, while the snowfall occupies 95% of total precipitation (75-150 cm a<sup>-1</sup>)[1]. Meanwhile, the air temperature ranging from -20°C to -40°C during December-February is also very suitable for accumulation of glacier mass. We choose ALOS/PALSAR from April, 2007, to September, 2009, in Siachen glacier to generate the interferograms and simulate the existing displacements. In this study, the surface deformation of upper part of Siachen glacier located in central Karakoram is estimated by using PS-InSAR method. Here, we implement the PS method, which uses spatial correlation of interferogram phase to find pixels with low-phase variance in the terrain. Prior knowledge of temporal variations in the deformation rate is not required for their identification. Through times series analysis of the interferograms we were able to reduce the impact of digital elevation model errors and extract the real surface change signal. Key words: PALSAR, Siachen glacier, surface deformation.

1. Introduction The Karakoram is situated at the western end of the trans-Himalaya and is one of the largest glaciated areas outside the polar regions, of which over 37% is covered by glaciers.[2] This study focuses on the upper part of Siachen Glacier(35.6°N 77.3°E), the eastern part of Karakoram range, it includes Teram Shehr Glacier, Lolofond Glacier and several other tributaries. Despite, Siachen Glacier is about 74 km long, and width varying from 1 to 8 km approximately, as the longest glacier in the Karakoram and second longest in the world's non-polar areas, the average winter snowfall is 10.5 m and temperatures can reach to -40°C. Including all tributary glaciers, the Siachen glacier system covers 700 km<sup>2</sup>. So, the observation of its glaciological process is limited by high attitude and remote and sophisticated meteorological conditions. Given these complex restraints, SAR data is an efficient source of this type glacier flow velocity estimation in general. The interferometric phase is as noted sensitive to both surface topography and coherent displacement of scatters along the radar look direction in the time between the acquisitions of the interferometric image pairs. For glacier surface, the coherence is affected by both meteorological conditions and glacier flow velocity and generally decreases rapidly with increasing time between the acquisitions of two SAR images. Meteorological causes of decorrelation include ice and snow melting, snowfall and wind redistribution of snow and ice. Moderate snowfall on the glaciated surface, extremely reduce temperatures and intense wind conditions give to harsh weather and climatic conditions over this region[3].

2. Dataset and surface deformation estimates We implemented 12 scenes of ALOS PALSAR FBS mode for interferograms generation to monitor the ice motion from April 2007 to September of 2009. All the 12 scenes are involved in orbits of 16026, track 523, ascending pass. The main advantages of the L-band (236-mm wavelength) PALSAR over C-band (56-mm wavelength) are as follows: deeper penetration of surface in less temporal decorrelation, enabling interferograms to have longer time separation the use of L-band PALSAR data.[4] This improves the coherence of interferometric pairs in winter, due to heavy snow cover attenuation. Moreover, the critical baseline is extended by the longer wavelength, so that we could produce more moderate quality interferograms. In addition to these fundamental wavelength-dependent issues, PALSAR is operated in a number of different modes that could both enhance and detract from its

interferometric capabilities[5]. In particular, the fine-beam single polarization (FBS—HH, 28-MHz bandwidth) has 2× better range resolution than most previous InSAR instruments, which further increases the critical baseline and could improve the spatial resolution of the interferograms. The fine-beam dual polarization (FBD—HH and HV, 14 MHz) has 2× worse range resolution than the FBS mode. Melting season of Siachen glacier starts beginning of May and culminates in July. Then, the coherence of interferograms will be decreased by this summer melt process. Considering these factors, we analyzed the perpendicular baseline before the co-registration and unwrapped phase generation. The principle improvement of Persistent scatter (PS) InSAR is that it overcomes the decorrelation problem by identifying resolution elements whose echo is dominated by a single scatterer within the resolution pixel in a series of interferograms. We select the scene of 20080610 as the only main master image, considering the Doppler centroid and temporal baseline synthetically. Then, pixels are multi-looked 5 times in range and 15 times in azimuth. We set criteria the performance of interferograms whose coherence is greater than 0.3, all the 11 interferograms correlated slave with masters matched finally. We processed the unwrapping depending on the optimization routines of SNAPHU[6]. After the unwrapping procedure, we select the candidate PS scatterers using StaMPS approach. In the end, we create the LOS (light of sight) velocity maps based on the master image 2007-2009. 3. Preclusion Here, PS-InSAR calculation shows its high accuracy (mm level) to determine ice movement in the slant-range direction. We produced the local maps of glacier surface deformation in time series over upper area of Siachen glacier. It is clear that Siachen Glacier and its tributaries are active, even over their upper regions where the temperature considerably low in winter. In general, ALOS-PASAR L-band SAR data combined PS-InSAR method overcomes the lower coherence decreased by snow cover in winter, which is very potential to describe the characteristics of glacier dynamics. Acknowledgement This research was founded by the European Commission (Call FP7-ENV-2007-1 grant 212921) as part of the CEOP-AEGIS project ([www.ceop-aegis.org/](http://www.ceop-aegis.org/)) coordinated by the Université de Strasbourg. All the ALOS-PALSAR data were provided by ESA. References [1] M. R. Bhutiyani, "Mass-balance studies on Siachen Glacier in the Nubra valley, Karakoram Himalaya, India," *Journal of Glaciology*, vol. 45, pp. 112-118, 1999. [2] C. Luke, et al., "Glacier velocities across the central Karakoram," *Annals of Glaciology*, vol. 50, pp. 41-49, 2009. [3] A. P. Dimri and S. K. Dash, "Winter temperature and precipitation trends in the Siachen Glacier," *Current Science*, vol. 98, pp. 1620-1625, Jun 2010. [4] D. T. Sandwell, et al., "Accuracy and Resolution of ALOS Interferometry: Vector Deformation Maps of the Father's Day Intrusion at Kilauea," *Ieee Transactions on Geoscience and Remote Sensing*, vol. 46, pp. 3524-3534, Nov 2008. [5] M. Shimada, et al., "PALSAR CALVAL summary and update 2007," *Igarss: 2007 Ieee International Geoscience and Remote Sensing Symposium*, Vols 1-12, pp. 3593-3596 5334, 2007. [6] A. Hooper, et al., "A new method for measuring deformation on volcanoes and other natural terrains using InSAR persistent scatterers," *Geophysical Research Letters*, vol. 31, pp. -, Dec 10 2004.

## Melt-induced speedup of Greenland Ice Sheet offset by efficient subglacial drainage

Author(s):

Aud Sundal <sup>(1)</sup>, Andrew Shepherd <sup>(1)</sup>, Steve Palmer <sup>(1)</sup>, Pete Nienow <sup>(2)</sup>,  
Edward Hanna <sup>(3)</sup>, Philippe Huybrechts <sup>(4)</sup>

Department

<sup>(1)</sup>University of Leeds, Leeds, LS2 9JT, <sup>(2)</sup>University of Edinburgh, <sup>(3)</sup>University of Sheffield, <sup>(4)</sup>Vrije Universiteit Brussels,

Abstract:

Fluctuations in surface melting are known to affect the speed of glaciers and ice sheets, but their impact on the Greenland Ice Sheet in a warming climate remains uncertain. While some studies suggest that greater melting produces greater ice sheet acceleration, others have identified a

long-term decrease in Greenland's flow despite increased melting. Here, we use satellite observations of ice motion recorded in a land-terminating sector of southwest Greenland to investigate the manner in which ice flow develops during years of markedly different melting. Although peak rates of ice speedup are positively correlated with the degree of melting, mean summer flow rates are not because glacier slowdown occurs when a critical runoff threshold of about 1.4 cm/day is exceeded. In contrast to the first half of summer, when flow is similar in all years, speedup during the latter half is  $62 \pm 16$  % less in warmer years. Consequently, in warmer years, the period of fast ice flow is three times shorter, and, overall, summer ice flow is slower. This behaviour is at odds with that expected due to basal lubrication alone. Instead, it mirrors that of mountain glaciers, where melt-induced acceleration of flow ceases during years of high melting once subglacial drainage becomes efficient. A model of ice sheet flow that captures switching between cavity and channel drainage modes is consistent with the runoff threshold, fast-flow periods, and later-summer speeds we have observed. Simulations of the Greenland Ice Sheet flow under climate warming scenarios should account for dynamic evolution of subglacial drainage; a simple model of basal lubrication alone misses key aspects of the ice sheet response to climate warming.

## Estimation of Ice Flow Velocity of Calving Glaciers Using Feature Tracking and SAR Interferometry

Author(s)

Chunxia Zhou <sup>(1)</sup>, Yu Zhou <sup>(1)</sup>, Dongchen E <sup>(1)</sup>, Zemin Wang <sup>(1)</sup>, Jiabing Sun <sup>(1)</sup>

Department

<sup>(1)</sup>Wuhan University No.129 Luoyu, Wuhan, CN

### Abstract

Antarctica is in very close relationship with the global climate, ecology environment, and the future of the human being. Changes in velocity of the large outlet glaciers and ice streams in Antarctica are important for ice sheet mass balance and hence sea level. Observations of Antarctica have revealed rapid changes occurring on the ice sheet on relatively short time scales. The increasing collapse of the ice shelf and glacier, the increasing rates of ice flow are indicators of the local effects of global changes. The ice flow velocity is also a critical variable in understanding glacier dynamics. At present, there are three effective ways to measure the ice flow velocity, which are GPS, feature tracking and SAR Interferometry. GPS-based velocity measurements are of high accuracy that can be used for an external validation of the other methods, while the coverage is restricted to discrete point and there are many inaccessible regions in Antarctica. Feature tracking is a popular way of extracting motion information from the image sequences, where the same feature can be detected reliably and consistently. But the disadvantage of this technique is that correspondence errors tend to be very large. Synthetic aperture radar Interferometry can detect the surface change in cm even mm level, while the loss of coherence in fast moving area could make the InSAR velocity irretrievable. Polar Record Glacier is about 50 km to the west of the Zhongshan Station, East Antarctica. It is the largest glacier along the Ingrid Christensen Coast. An enormous tongue of ice has broken free from Polar Record Glacier creating an iceberg tongue more than 25 km long. This paper will use a combination of InSAR and feature tracking to measure the ice velocity of the Polar Record Glacier and the calved iceberg. The multi-temporal satellite data, including Landsat, HJ-1A, ERS and Envisat, etc, cover from 1970s to now. Based on the geometric rectification, registration and overlay processing on different temporal remote sensing images, preliminary results are presented on the measurement of glacier surface velocity and changing characteristics analysis. In order to reduce coregistration error, the coregistrations are applied to optical images, ascending SAR images and descending SAR images respectively. The ice flow velocities are determined with several evident features.

According to the satellite image interpretation and the ice flow velocity, the interesting interaction between the glacier and iceberg are analyzed. Considering the relatively fast ice flow (over 680m/a) in this region, it is impossible to obtain the ice velocity field by using SAR images with 35-day temporal baseline. Fortunately, we can utilize ERS-1/2 tandem SAR data for InSAR velocity analysis. Differential InSAR measures only the displacement along the satellite line of sight (LOS). To estimate surface motion in three dimensions, both ascending and descending passes are required under the assumption of ice motion parallel to the ice surface. However, for Polar Record Glacier, horizontal velocity components can be estimated without yielding significant errors by InSAR because the slope is low and both accumulation and ablation are modest in one day. In the absence of SAR data of linearly independent directions, the velocity direction is estimated from the steepest slope. Feature tracking with SAR and optical images can be applied to derive absolute ice velocity, while the ice flow velocity are available only for the feature points. The InSAR velocity measurement presents the overall velocity field. The velocities derived from feature tracking and InSAR are in good agreement and they are complementary to each other.

## Posters on Terrain Subsidence and Landslides

### Local Phase Anomalies associated with the 2011 Tohoku-Oki Earthquake detected by PALSAR Interferometry

#### Author(s)

Satoshi Okuyama <sup>(1)</sup>, Masato Furuya <sup>(1)</sup>, Takahiro Abe <sup>(1)</sup>, Makoto Murakami <sup>(1)</sup>

#### Department

<sup>(1)</sup>Hokkaido University, JP

#### Abstract

We report local phase anomalies found in the co-seismic interferograms of the 2011 Tohoku-Oki Earthquake, Japan (M9.0). Such phase anomalies are mostly found in the mountainous region, suggesting that they are landslides triggered by the earthquake. In reality, the location of some phase anomalies do agree with known landslide regions. The largest phase anomaly found in the Miyagi prefecture, however, is not reported as the landslide region. Moreover, this phase anomaly covers multiple slopes, implying the deep-seated landslide. SAR interferometry is thus useful tool for finding, not just monitoring the landslide and it is important to investigate co-seismic interferograms carefully for the disaster prevention.

### Monitoring slow-movement landslides in Central Taleghan region, Iran, by using SAR Interferometry

#### Author(s)

Naghmeh Khavaninzadeh <sup>(1)</sup>, Mahdi Motagh <sup>(2)</sup>, Bahman Akbari <sup>(3)</sup>

#### Department

<sup>(1)</sup>Department of Surveying and Geomatics Engineering, University College of Engineering, University of Tehran, IR

<sup>(2)</sup>Department of Geodesy and Remote Sensing, Helmholtz Center Potsdam, Potsdam, GFZ German Research Center for Geosciences, DE ,

<sup>(3)</sup>Forests, range and watershed management organization, Agricultural ministry, Tehran, IR,

#### Abstract

Landslide is a geological phenomenon which refers to the downward sliding of mass of soil and rock, mostly occurring on the steep hills and slopes in the mountainous regions. This event leads to large human and economic losses in the world every year. Due to its special continental

conditions, topographical and tectonic situation Iran is among landslide-prone countries. Up to now, 32000 types of landslides have already been recognized in the country by the experts from Forests, Range and Watershed Management Organization (FRWMO). Damages to roadways, pipelines, buildings and etc from landslide are estimated at 50 millions of dollar/year. Most of the monitoring studies in landslide regions to date are performed by conventional techniques such as, tachometry, precise levelling and global positioning system (GPS) surveying. These techniques provide only point measurements and thus are not able to reveal the complex heterogeneities of landsliding. Nowadays, the novel technique of SAR Interferometry has gained increasing attention in scientific and engineering communities as a powerful geodetic technique to map small-scale surface deformation associated with landsliding and rockfall in mountainous regions. This paper is about the application of SAR Interferometry in monitoring landslides in Taleghan region, Iran. Taleghan is a mountainous region that is located northwest of Tehran, the capital of Iran. It is prone to landslides due to its special type of earth lithology, relatively high precipitation, relatively sharp slope and the presence of excess soil moisture. In order to understand the spatio-temporal characteristics of slope movements in Taleghan region, we applied the technique of SAR Interferometry

## Land subsidence in Mahyar plain, Central Iran, studied using SBAS-InSAR method

### Author(s)

Mansoureh Davoodijam <sup>(1)</sup>, Mahdi Momeni <sup>(1)</sup>, Mahdi Motagh <sup>(2)</sup>

### Department

<sup>(1)</sup>Isfahan university Isfahan university,surveying department, IR

<sup>(2)</sup>Department of Geodesy and Remote Sensing, Helmholtz Center Potsdam Department of Geodesy and Remote Sensing, Helmholtz Center Potsdam, DE

### Abstract

Subsidence is defined as the downward motion of a surface relative to a datum such as sea-level. Generally, compaction of sediments, extraction of ground water, oil and gas result in compression of the clay layers beneath the land surface and subsequently elevation of the land surface is lowered. In recent years, with the growing population of the world and lack of water caused by global warming there has been an increased request for groundwater to supply domestic, industrial and agricultural needs. Excess exploitation of this resource causes underground fluid pressure to decrease. Thus the supportive effective stress on the rock matrix increases and rock compaction or land surface subsidence occurs. Several problems are associated with land subsidence including damages to underground infrastructure and civil engineering structures such as buildings, roads, canals and bridges, and increasing inland flooding along streams and waterways due to changes in stream gradient. It has been addressed in the literature that land subsidence caused by over extraction of ground water is increasing around the world. It is also a widespread problem in Iran. Motagh et al (2008) did an InSAR survey and showed that several places in the country suffer from significant subsidence at the order of several cm/yr. They have found a correlation between ground deformations and level of ground water in those locations. This paper presents the result of InSAR time-series method, called SBAS, for monitoring land subsidence over Mahyar plain in south of Isfahan (Central part of Iran). Land subsidence and its associated fissures have been appeared in northern part of Mahyar plain since 3 decades ago. It has caused enormous damages to houses, farms, and channels in the region, causing continuous repairs to the major Isfahan-Shiraz Highway. Land subsidence monitoring is important in order to investigate the temporal and spatial extent of subsidence hazard and for mitigating related to it. The analysis done in this paper is based on both C-band and L-band radar images, acquired by



Envisat and ALOS satellites respectively. Envisat images include 21 ascending images spanning 2004- 2010 and 15 descending images spanning 2003-2006. ALOS data include 10 ascending images spanning 2008-2010 interval. For time-series analysis, the small baseline subset (SBAS) approach is used. Via this approach, mean deformation velocity maps and displacements time series are generated using least-squares inversion of differential interferograms.

## Landslide creep monitoring using the integration of GPS and InSAR

### Author(s)

Mehrdad Akbarimehr <sup>(1)</sup>, Mahdi Motagh <sup>(2)</sup>, Mohammad-Ali Sharifi <sup>(3)</sup>, Fardin Pashazadeh <sup>(4)</sup>

### Department

<sup>(1)</sup> University of Tehran Department of Surveying and Geomatics Engineering, University College of Engineering, Iran, IR

<sup>(2)</sup> Helmholtz Center Potsdam, GFZ, Potsdam, DE

<sup>(3)</sup> University of Tehran Department of Surveying and Geomatics Engineering, University College of Engineering, IR

<sup>(4)</sup> Watershed and Natural Resource of Western Azarbayajan, IR

### Abstract

Combination of different ground and space-based geodetic monitoring systems provide promising tools for the assessment and evaluation of landslide hazard. In this study, we apply space-born techniques of radar Interferometry and GPS to study the kinematics of two creeping landslides in Iran. The first one is located above the Sarcheshmeh village near Esfarayen city in the Khorasan province of northeast Iran and the other is located near Googerd village in the Azarbayejan province of northwest Iran. Differential Interferometric observations made using Envisat SAR data acquired since 2002 are analyzed together with repeated GPS measurements in network of ~ 20 stations to study the kinematics of these creeping landslides. GPS and InSAR measurements are complementary to each other with GPS providing precise horizontal movement at a few sparse locations while InSAR providing a semi-continues map of mass movement in the satellite line-of-sight direction.

## InSAR Products in Support of Urban Monitoring – Case Study: Lüneburg

### Author(s)

Iulia Dana <sup>(1)</sup>, Umut Günes Sefercik <sup>(2)</sup>

### Department

<sup>(1)</sup> Romanian Space Agency 21-25 Mendeleev Street, Sector 1, 010362, RO

<sup>(2)</sup> Zonguldak Karaelmas University 67100, Centre, TR

### Abstract

Urban monitoring based on high resolution synthetic aperture radar (SAR) data leads to very accurate results. Using SAR interferometric (InSAR) techniques, digital surface models (DSMs) and displacement maps can be generated. Standard (conventional) interferometry and other techniques derived from differential interferometry (for example, persistent scatterer interferometry or stacking) are applied for the generation of the InSAR products. The study uses a series of 18 images acquired by the German TerraSAR-X mission. The selected test site is Lüneburg (Germany), a town located in Lower Saxony. The interest area is characterized by the usual urban complex pattern: mixture of buildings, paved roads, vegetation, and the center of the town is located above a salt mine. Lüneburg has been previously affected by subsidence. The study is mainly focusing on the generation of an accurate digital surface model based on

interferometric pairs extracted from the TerraSAR-X time series. Also, the current subsidence in Lüneburg will be investigated using specific InSAR techniques.

## **Landslides monitoring by means of DInSAR, SBAS and PSI, in the Prefecture of Peloponnesus, Greece**

### **Author(s)**

Panagiotis Elias <sup>(1)</sup>, George Drakatos <sup>(1)</sup>

### **Department**

<sup>(1)</sup>National Observatory of Athens , GR

### **Abstract**

The risk induced from landslide events is considered to be increasing in the last decade. The means of monitoring the landslide evolution and record the pre and post micro-movements with remote sensed observations are nowadays more powerful with the advent of new high resolution SAR satellites. In the framework of the EOX-EL0071 project, two villages suffering from slow landsliding, have been selected for monitoring by exploiting ASAR/ENVISAT, RADARSAT-2 Ultra Fine and GPS data. Ten corner reflectors and a number of GPS benchmarks has been installed inside and outside the landslide bodies of the villages. Moreover two Permanent GPS stations have been installed inside the landslide bodies, are in operational mode and its measurements are being disseminated in real-time. Retrospective as well as near-real time studies has been carried out by means of SBAS, PSI and DInSAR methodologies for the assessment and demonstration of the potential use of such an observation system in a future operational mode. The main scope of the forthmentioned project was the education of decision makers, engineers and scientists of the local authorities of the Prefecture of Peloponnesus, Greece, in the subject of landslides. Topics as : the definition of the landslide, the cost in human and material losses, the importance of the operational use and description of the proposed observation system as well as issues related to the civil protection, were comprised the educational content. The project url is : <http://www.landslides.gr>

## **A geotechnical approach to the analysis of building settlements via DInSAR data**

### **Author(s)**

Dario Peduto <sup>(1)</sup>, Leonardo Cascini <sup>(1)</sup>, Settimio Ferlisi <sup>(1)</sup>, Livia Arena <sup>(1)</sup>, Gianfranco Fornaro <sup>(2)</sup>

### **Department**

<sup>(1)</sup>University of Salerno, Via Ponte Don Melillo, Fisciano (Salerno), IT

<sup>(2)</sup>National Council of the Research, Via Diocleziano, Napoli, IT

### **Abstract**

In the last decade the scientific literature extensively proved that subsidence phenomena affecting densely built-up areas can be analysed also with the contribution of the remote sensing techniques. Among these, space-borne Differential SAR Interferometry (DInSAR) can provide ground displacement measurements with comparable accuracy and more affordable costs than traditional techniques. The availability of image datasets with a world coverage since 1992 as well as the huge amount of ready-to-use processed data - delivered via several national and international projects - can help the geotechnical engineers with: i) the back-analysis of a given subsidence phenomenon; ii) the analysis of the effect on the ground of the variation of boundary conditions; iii) the control of the existing structures during underground excavations or water withdrawals; iv) the application of building damageability criteria, etc. In this work the enormous

potential of these techniques is tested with reference to a well-documented water-withdrawal induced subsidence phenomenon in Southern Italy, via the implementation of original procedures suited for DInSAR data use at different scales. In particular, whereas at regional scale just most critical areas are detected, at the municipal scale thematic maps of different parameters such as absolute cumulative settlements, settlement gradients, and relative rotations are generated via DInSAR data. These maps are then used to complement the analysis of the factors predisposing the phenomenon (i.e. the presence of highly deformable soils) and influencing the magnitude of related effects (i.e. the presence/absence of buildings, the shape or prevalent direction of built-up areas with reference to the subsidence bowl, the stiffness characteristics of the buildings, etc). Finally, focusing on single buildings exhibiting an adequate DInSAR data coverage the application of damageability criteria is shown also stressing the envisaged improvements derivable from the enhanced upcoming performances provided by the latest satellite sensors.

## Deformation monitoring in Aghajari oil field using DINSAR-SBAS approach

### Author(s)

Negin Fouladi Moghaddam, Mahdi Motagh <sup>(1)</sup>, Mostafa Esmaeili <sup>(2)</sup>

### Department

<sup>(1)</sup>Department of Geodesy and Remote Sensing, Helmholtz-Zentrum Potsdam ,DE

<sup>(2)</sup>Department of Surveying and Geomatics Engineering, University of Tehran, IR

### Abstract

In this paper, we investigate deformation rate and its spatial pattern in Aghajari Oil Field, Southwestern Iran, using Envisat InSAR time-series analysis. Earlier InSAR-based study of surface deformation in this oil field shows that accurate assessment of the rate and pattern of deformation in the area is hampered by strong contribution from atmospheric artifacts. In this study we use all Envisat ASAR data acquired in the region between 2003 and 2008 and focus on the time-series analysis of the Small Baseline (SBAS) approach for mitigating the effects from atmospheric artifacts in InSAR measurements and producing reliable time series of surface ground motion in Aghajari.

## Sinking cities in Indonesia: Space-geodetic evidence of rates and spatial distribution of land subsidence

### Author(s)

Estelle Chaussard <sup>(1)</sup>, Falk Amelung <sup>(1)</sup>, Sang Hoon Hong <sup>(2)</sup>, Hasanuddin Abidin <sup>(3)</sup>

### Department

<sup>(1)</sup>Rsmas , USA

<sup>(2)</sup>Korea Aerospace Research Institute (KARI) 115 Gwahangno Yuseong Daejeon, KR

<sup>(3)</sup>Institut Teknologi Bandung , ID

### Abstract

Land subsidence due to groundwater extraction, increased urban development, and natural consolidation of soil is known to occur in several cities of Indonesia. It is often causing damages to structures, making its consequences costly. Moreover, when associated with the predicted sea level rise, ground subsidence becomes a dramatic problem for many highly populated coastal metropolitan areas. Most of the evidences of rates and spatial distribution of ground subsidence in Indonesia are based on GPS and leveling campaigns, providing only spatially and temporally restricted data. InSAR has been applied to monitor ground subsidence in some areas, but these works have only looked at snapshots of deformation based on interferograms that can be biased

by atmospheric noise related to the water content of the atmosphere. Here we present a global survey of Sumatra and Java using differential SAR (D-InSAR) combined with SBAS-time series analysis to monitor ground subsidence on a large spatial scale and a continuous temporal scale. The D-InSAR survey of Sumatra and Java extends for about 3000km and covers an area of about 500,000km<sup>2</sup>. We used ALOS data from 35 ascending tracks and more than 1500 granules to generate more than 1000 interferograms spanning a period from late 2006 to early 2009. We identified 6 major cities undergoing ground subsidence. Our large-scale subsidence maps also present the spatial distribution of the subsidence within the cities for a continuous period of observation of 2 years. In Sumatra we observe linear subsidence in 2 cities, Lhokseumawe and Medan. In Java we observe linear subsidence in 1 city, Sidoarjo, and subsidence decreasing in time in 3 cities, Jakarta, Bandung and Semarang. We conclude that the phenomenon of cities subsidence is widely spread in Indonesia and rates are reaching from 2-3 cm/yr up to 24 cm/yr. In five of these six cities we suggest that ground water extraction is the main cause of high rates of ground subsidence.

## Long Term, Operational Monitoring of Enhanced Oil Recovery in Harsh Environments with InSAR

### Author(s)

Shiya Sato <sup>(1)</sup>, Michael Henschel <sup>(1)</sup>

### Department

<sup>(1)</sup>MDA Geospatial Services , CA

### Abstract

In 2004 Cenovus began monitoring the Foster Creek oil field in Northern Alberta, Canada with InSAR. The ground deformation measurements have been provided by MDA GSI from the RADARSAT series of satellites. Over the period, the monitoring has reliably shown the slow rise of the oil field due to enhanced oil recovery operations. The InSAR monitoring solution is essentially based on the observation of point and point-like targets in the field. The ground conditions in the area are almost continuously changing (in their reflectivity characteristics) making it difficult to observe coherent patterns from the ground. A sparse array of installed, trihedral corner reflectors and a wide range of targets of opportunity provide the basis for point monitoring of the area. The duration of the monitoring of the oil field has allowed us to transition from RADARSAT-1 to RADARSAT-2. The enhancement of the resolution of the monitoring as allowed by RADARSAT-2 has provided more targets of opportunity, as identified by a differential coherence method. This paper will provide an overview of the long term monitoring of the Foster Creek field. It will highlight the enhancements in the monitoring of the field available from RADARSAT-2 versus lower resolution sensors.

## INSAR Study of Landslides in the region of lake Sevan – Armenia

### Author(s)

Dimitar Minchev <sup>(1)</sup>, Andon Lazarov <sup>(1)</sup>, Dimitar Minchev <sup>(1)</sup>

### Department

<sup>(1)</sup>Burgas Free University , BG

### Abstract

The region of Lake Sevan in Armenia is of theoretical and practical interest due to its very high landslide phenomena caused by metrological and hydrological reasons. Based on the ESA Principal Investigator Number C1P-6051 and requested data from ASAR instrument of ESA ENVISAT satellite four single look complex images of the region of the Sevan Lake in Armenia are obtained

and thoroughly investigated, including two images from 2008 and two images from 2009. The one of them is pointed out as a master and the rest of them, three images as slaves. Hence, three interferometric pairs are produced. Then data of NASA SRTM mission is applied to the interferometric pairs in order to remove topography from the interferograms. Three interferograms generated illustrate decreasing of coherence caused by high temporary decorrelation, which means decreasing the level of coincidence of SLC's in each interferometric pair, according to the time of acquisition each of them.

## Detection and monitoring of landslide creep in Semirrom, Central Iran, using SAR Interferometry

### Author(s)

Behnaz Gozalpour <sup>(1)</sup>, Mahdi Motagh <sup>(2)</sup>, Mahdi Momeni <sup>(1)</sup>

### Department

<sup>(1)</sup>Department of Geomatics, Faculty of Engineering, University of Isfahan, Isfahan, Iran , IR

<sup>(2)</sup>Department of Geodesy and Remote Sensing, Helmholtz Center Potsdam, GFZ German Research Center for Geosciences, Potsdam, DE

### Abstract

Landslides are geological phenomena which are among the most catastrophic natural hazards in the world. Depending on their scales, they can cause heavy damages to human life and infrastructure. Landslide occurs when the stability of a slope changes from a stable condition to an unstable one. The major reason of this phenomenon is the change in gravity which is triggered by factors such as ground water pressure, river-induced erosions, and prolonged and heavy precipitation. Other environmental and man-made factors such as lack of vegetation cover, soil structure, and artificial vibration from heavy machinery or traffic also have great impacts on landslide occurrence. Detection and monitoring of mass movement in susceptible slopes play a key role in mitigating hazards and damages associated with landsliding. Various ground-based geodetic observations using techniques such as GPS and leveling have traditionally been used by engineers and scientists to monitor and assess landslide hazards. The main limitation of these methods is that they can't provide a high-resolution map of deformation illustrating the true extent and dimension of a moving slope. Synthetic Aperture Radar Interferometry (InSAR) has been widely used in recent decades to monitor movement of the ground surface associated with landslides, subsidence, earthquakes, volcanoes deformation, ice sheet and glacier movement. This technique relies on processing of two SAR images over the same area with a short baseline. The displacement is measured by calculating the phase difference between the two images acquired in the slant range geometry. The technique provides detailed maps of surface deformation with centimeter accuracy over wide areas (> 100 km<sup>2</sup>). In this study, we investigate the use of Envisat ASAR data to monitor landslide in Semirrom region in the Isfahan province of Central Iran. Our data consist of 28 ASAR images, which were acquired by the Envisat satellite in both descending and ascending orbits. We present two cases, confirmed by field observations, where the use of Envisat data led to the detection of previously unknown landslides, located along the only access road to the region. We examine the InSAR time-series technique of Small Baseline (SBAS) approach to assess the detailed spatio-temporal of slope creep in these landslides.

# Monitoring of the landslide in the vicinity of the railway - highway road to Sochi Olympic 2014 site "Krasnaya Polyana".

## Author(s)

Pavel Dmitriev <sup>(1)</sup>, Valentin Mikhailov <sup>(1)</sup>, Elena Kiseleva <sup>(1)</sup>,  
Ekaterina Smolyaninova <sup>(1)</sup>, Vasily Golubev <sup>(1)</sup>, Yuri Isaev <sup>(2)</sup>

## Department

<sup>(1)</sup>Schmidt Institute of Physics of the Earth of Russian Academy of Sciences, Moscow , RU

<sup>(2)</sup>«Lenmetrogiprotrans» St. Petersburg , RU

## Abstract

We present results of INSAR monitoring of displacements of a landslide slope at the exit from one of the tunnel systems of the new railway - highway road to the Sochi Olympic 2014 site "Krasnaya Polyana". The main problems of the SAR Interferometry in specific conditions of the Adler- Krasnaya Polyana area are: lack of reflectors, poor coherence due to dense vegetation in combination with strong topographic and atmospheric effects. The situation becomes even more complicated because many of existing reflectors (both man-made structures and natural objects) constantly change due to Olympic construction sites. We used images from two ENVISAT tracks (#85 ascending one covering the period from 01/08/2004 to 01/02/2009 and #35 descending one for the period 23/10/2003 - 08/07/2010) and one ALOS track (#588 ascending one starting at 22/01/2007 to 17/09/2010), and studied time-series for PS displacements employing StaMPS software. Estimates of DEM, atmospheric master and slave errors were subtracted. The important step in the StaMPS processing consists in appropriate choice of a reference area. We analyzed results of runs with different reference areas and chose one which provided close to zero average displacements of PS situated in the vicinity of the landslide in the area supposed to be stable. This area is a part of the highway at the foot of the opposite slope of the valley. We also tried different DEMs (SRTM3 and ACE2). Then we selected PS with the same coordinates identified from both ENVISAT ascending and descending tracks. To find full displacement vectors we used two assumptions. First, that vertical component of the displacement vector is small in comparison to horizontal ones. The second, that PS's move along topographic surface. In both cases mean displacement vectors appeared to be very close to vectors of the topography gradients. Then we applied an assumption that displacement occurs along the topography gradient vectors for all Ps's and estimated the absolute values of mean velocity which appeared to be between zero up to 5 cm/year. Results of geological and geodesic field studies showed that the landslide consists of many "patches" moving in different directions and at different rates. The results obtained by SAR methods fit well the surface data.

# InSAR assessment of pipeline stability using compact active transponders

## Author(s)

Jessica Hole <sup>(1)</sup>, Rachel Holley <sup>(2)</sup>, Giuseppe Giunta <sup>(3)</sup>, Gianpietro De Lorenzo <sup>(3)</sup>, Adam Thomas <sup>(1)</sup>

## Department

<sup>(1)</sup>Fugro NPA Ltd. , UK

<sup>(2)</sup>Fugro NPA Ltd. , UK

<sup>(3)</sup>Eni S.p.A , IT

## Abstract

This study examined the use of prototype Compact Active Transponders (CATs) to measure ground and pipeline motion at a known landslide in northern Italy. A network of 7 CAT units was deployed on and in the vicinity of a pipeline that transects a landslide prone slope. 29 Envisat and Radarsat-1 SAR images, acquired in different orbit and imaging modes were used to produce 41 short- and long-term interferograms from which motion across the CAT network was derived. The results showed that two of the CATs, located at the center of the study area, experienced higher rates of (satellite) line-of-sight (LOS) motion than the others. The spatial variation in the LOS motion rates could indicate that the central section of the slope moved at a higher rate, most likely in a westward and down-slope direction during the study. In addition to the InSAR measurements, some GPS campaigns were carried out, giving four epochs of motion measurements. Despite technical and environmental challenges, the study demonstrated the potential use of CATs to remotely map and monitor ground and structure motion.

# Recent results of subsidence in Khoy (Iran )- Ability of ALOS data in agricultural regions

## Author(s)

Morteza Sedighi <sup>(1)</sup>, Hamid Reza Nankali <sup>(1)</sup>, Farokh Tavakoli <sup>(1)</sup>

## Department

<sup>(1)</sup>National Cartographic Center NCC , IR

## Abstract

The subsidence of the Earth surface is a phenomenon that occurs in some places in the world which overuse underground sources of water. Iran has a semi-arid and arid climate and we detect an agricultural region (Khoy) subject to land subsidence due to over-exploitation of groundwater. Repeated levelling measurements of first order leveling network of Iran shows a 3.5 cm/yr for the rate of subsidence. Although, using the ENVISAT data we can recognise the subsidence area and also its rate in short temporal variation but ALOS data give us better results for subsidence detection in this vegetation area. InSAR processing the ALOS data shows the subsidence area is larger than that detected by levelling measurements and also has bigger rate for subsidence. For taking the reliable results for InSAR we used least square method for adjusting the individual InSAR observations. The InSAR shows the subsidence rate is about 12cm/yr during recent years.

# Monitoring anthropogenic and natural ground deformation in Grand Duchy of Luxembourg and the “Greater Region” by the advanced Interferometric Synthetic Aperture Radar

## Author(s)

Sergey Samsonov <sup>[1]</sup>, Nicoals D'Oreye <sup>[1]</sup>, Robert Colbach <sup>[2]</sup>

## Department

<sup>[1]</sup>European Center for Geodynamics and Seismology , LU

<sup>[2]</sup>Geological Survey of Luxembourg , LU

## Abstract

We present ongoing progress of the ESA CAT-1 project aiming monitoring anthropogenic and natural ground deformation in Luxembourg and the Greater Region (i.e. French and German bordering area) with ERS and ENVISAT Interferometric Synthetic Aperture Radar (InSAR). Previous remote sensing and terrestrial studies identified active ground deformations mainly in the South of Luxembourg and neighbouring northern part of France and in various parts of main river's valleys. These were mainly caused by former mining activities but other phenomena were observed at various scales such as landslides, rock instabilities, ground subsidence over soluble rocks or unconsolidated sediments etc. Monitoring of ground deformation in these regions is of a great importance because of their urbanization. Various man-made structures such as dams (e.g. Esch-sur-Sûre), bridges and large buildings (some structure are anchored in a rock cliff) will also be studied for deformation. By now ERS and Envisat historic data (1992-present) were acquired and processed. We performed time series analysis of calculated interferograms using SBAS technique and observed ground deformation. Large scale subsidence in former mining areas was identified and its temporal pattern was reconstructed. We also observed region of uplift but its cause is presently unknown. A variety of smaller scale signals were also observed and their causes are being investigated. We further intend to perform processing of this data using Persistent Scatterers Interferometry (PSI) approach and model observed signals.

# Land subsidence monitoring in the southern Spanish coast using satellite radar interferometry

## Author(s)

Antonio Miguel Ruiz Armenteros <sup>[1]</sup>, Miguel Caro Cuenca <sup>[2]</sup>,  
Joaquim Joao Moreira de Sousa <sup>[3]</sup>, Antonio J. Gil Cruz <sup>[1]</sup>, Ramon F. Hanssen <sup>[4]</sup>, Zbigniew Perski <sup>[5]</sup>,  
Jesús Galindo-Zaldivar <sup>[6]</sup>, Carlos Sanz de Galdeano Equiza <sup>[7]</sup>

## Department

<sup>[1]</sup>University of Jaén Campus Las lagunillas s/n 23071 Jaén, ES,

<sup>[2]</sup>Delft Institute of Earth Observation and Space Kluiverweg 1 PO Box 5058, NL <sup>[3]</sup>Universidade de Trás-os-Montes e Alto Douro Quinta de Prados, Apartado 1013, PT, <sup>[4]</sup>Delft Institute of Earth Observation and Space Systems Kluiverweg 1, NL

<sup>[5]</sup>Polish Geological Institute - NRI Carpathian Branch Skrzatow 1, 31-560 Cracow, PL <sup>[6]</sup>University of Granada Facultad de Ciencias, Campus de Fuentenueva s/n, ES

<sup>[7]</sup>CSIS-University of Granada Facultad de Ciencias, Campus de Fuentenueva s/n, ES

## Abstract

In the last decades, coastal areas in many parts of Spain have undergone a continuous urban expansion because of the growth of cities and development of new residential areas. The invasion of the sea, as a consequence of the rise of sea level and the subsidence of populated areas, may result in serious problems to many constructions situated in the coastline. This has an important impact on the economy, environment and society, representing a considerable natural hazard. This



paper investigates the applicability of satellite radar interferometry in studies of coastal dynamics. We use ERS SAR and Envisat ASAR datasets from 1992 to 2010 over the southern Spanish coast, and process them using persistent scatterer (PS), small baseline (SBAS) and a combined multi-temporal InSAR time-series methods to study the spatial and temporal evolution of some subsidence areas revealed from SAR observations.

## Persistent Scatterers Interferometry study of Roznow Lake area with ERS-1/2 archival data

### Author(s)

Zbigniew Perski <sup>(1)</sup>, Tomasz Wojciechowski <sup>(1)</sup>, Andrzej Borkowski <sup>(2)</sup>, Antoni Wojcik <sup>(1)</sup>

### Department

<sup>(1)</sup>Polish Geological Institute - National Research Institute , PL

<sup>(2)</sup>Wroclaw University of Environmental and Life Sciences , PL

### Abstract

In summer 2010 after very long and intensive rains occurred in May and June more than 90 landslides were reactivated in Roznow Lake area (Grodek nad Dunajcem municipality) causing heavy damages to properties, agriculture, buildings, roads and infrastructure. Many of reactivated landslides were already known and mapped. Few of them were continuously monitored using in-situ borehole instruments and GPS. However, major part of the damages has been caused by the landslides assumed to be inactive. The purpose of this work is to check the stability of those landslides prior to the event in 2010 over the period of 1992 - 2000 using archival ERS-1/2 data and Persistent Scatterer Interferometry (PSI) technique. The PSI method allows to detect millimeter displacements per year based on stable radar backscatter from individual objects like buildings, poles, rocks, etc. For the project purposes the same common area was processed using ERS-1/2 data acquired from two neighboring stacks: 179 and 408. Due to high relative elevations (up to 500 m) and different incidence angles (18° to 24°) not too many common scatterers were found. However, in most cases the scatterers were found within the same farm or group of the object allowing comparison of spatial pattern of deformation signal. The obtained results were interpreted in comparison with maps of existing landslides and geological data. PSI results might be used for detection of landslide movement at its early stage.

## InSAR and PSI results improvements with detailed LIDAR data

### Author(s)

Zbigniew Perski <sup>(1)</sup>, Andrzej Borkowski <sup>(2)</sup>, Tomasz Wojciechowski <sup>(1)</sup>

### Department

<sup>(1)</sup>Polish Geological Institute - National Research Institute , PL

<sup>(2)</sup>Wroclaw University of Environmental and Life Sciences , PL

### Abstract

In this paper the authors evaluate applicability of detailed elevation data for SAR Interferometric results improvement. LIDAR data – both airborne and terrestrial become more popular and available for scientific research and operational applications. With modern LIDAR systems it is possible to obtain very dense height measurements per square meter even in vegetated areas. Such data might be extremely useful to support interferometric processing of high resolution SAR systems and its spotlight mode. The application of LIDAR data might support InSAR research in following areas: - Source of improved elevation data: usually external DEMs represent terrain surface whereas radar signal is backscattered from all objects present on the surface (i.e.

buildings, vegetation etc.). Based on LIDAR point cloud we are able to easily generate various types of elevation surfaces that could be used for various analysis: - Source of data for backscatter properties modeling: based on the point cloud one can simulate the „scattering depth” for vegetated areas where volume scattering is occurring. Such “scattering depth” can be different according to the wavelength (e.g. X-band will backscatter from the leaves whereas C-band will backscatter from stem branches). - Better height estimation for individual persistent Scatterers: In case of PSI having very detailed elevation data we are able to better identify the Scatterers in the environment. We can also model its properties based on orientation and sub-pixel position. The applicability of LIDAR data has been evaluated for the area surrounding Roznow Lake in Southern Poland. This area is located in the Carpathian Mts. at 500 m relative heights. The area is mostly forested and rural with scattered urbanization (individual buildings and farms). Due to its geology the area is prone to landslides. In 2010 after very long and intensive rains in May and June about 90 landslides were reactivated in the Roznow Lake area (Grodzisk nad Dunajcem municipality) causing heavy damages to properties, buildings, roads and infrastructure.

## Landslide dynamics monitoring with TerraSAR-X interferometry and LIDAR data. Case studies of Klodne and Zbyszyce landslide (Southern Poland)

### Author(s)

Zbigniew Perski <sup>(1)</sup>, Antoni Wojcik <sup>(1)</sup>, Piotr Necsieruk <sup>(1)</sup>, Andrzej Borkowski <sup>(2)</sup>, Tomasz Wojciechowski <sup>(1)</sup>

### Department

<sup>(1)</sup>Polish Geological Institute - National Research Institute, PL

<sup>(2)</sup>Wroclaw University of Environmental and Life Sciences, PL

### Abstract

The Klodne and Zbyszyce landslides are located in the central part of Polish Carpathians in the Beskid Wyspowy Mountains. On June 1st 2010 after heavy and long-lasting rainfalls the Klodne landslide was triggered affecting the area that was considered as stable. Most of the landslide movement occurred within few days and destroyed 17 houses and two farm buildings. Landslide activity that occurred in 2010 caused in southern Poland significant material losses and damages to infrastructure and settlement. Zbyszyce landslide remains active since 1997 causing damages to the road and local settlement. After heavy rains occurred in summer 2010 the acceleration of some parts of the landslide was reported. Modern satellite, airborne and terrestrial remote sensing sensors theoretically allow to complete that task with high accuracy and large spatial coverage. With the example of Klodne landslide the authors compare the airborne data acquired prior to the landsliding (aerial stereophotographs and photogrammetric DEM) with newly acquired data (aerial photographs and LiDAR DEM) of July 2010. In case of Zbyszyce landslide, two LiDAR DEMs were acquired, in April and September 2010. The analysis of differential DEMs allowed to measure horizontal and vertical displacements and roughly estimates the volume of the colluvium. High Resolution satellite SAR (Synthetic Aperture Radar) data acquired by TerraSAR-X/TanDEM-X constellation in September, October and November 2011 and also March and April 2011. All scenes were used for interferometric analysis (differential interferometry) to measure the small scale displacements that occurred in different parts of both mentioned landslides. The further monitoring of Klodne landslide activity is continued in 2011 using new SAR data acquisitions and repeated terrestrial laser scanning campaigns. According to the airborne data analysis of Klodne landslide the horizontal displacements in upper part of the landslide between June and July 2010 reached 85 m. During the same period the vertical displacements vary from -20m to +8m in

various parts of the landslide. In autumn 2010 the displacement velocities measured with SAR interferometry show -0.76 mm/day to +0.57 mm/day. The observations are to be continued in the spring 2011 right after snowmelt season to get a better insight into the landslide dynamics.

## Bulging of the gypsum dome at Lesina Marina (Southern Italy) revealed by PSI techniques

### Author(s)

Alberto Refice <sup>(1)</sup>, Fabio Bovenga <sup>(1)</sup>, Guido Pasquariello <sup>(1)</sup>,  
Maria Dolores Fidelibus <sup>(2)</sup>, Giuseppe Spilotro <sup>(3)</sup>

### Department

<sup>(1)</sup>CNR , IT

<sup>(2)</sup>Politecnico di Bari , IT

<sup>(3)</sup>Università della Basilicata , IT

### Abstract

We apply DInSAR PSI techniques [1,2] to ascending and descending data from ERS and ENVISAT satellites to extract relevant information about mean velocities of stable points located on the Lesina Marina area. Sited in the Northern part of the Apulia Region, between the Lesina Lagoon and the mouth of the Fortore River, Lesina Marina lies not far from the Pietre Nere (Black Stones) Point, a very interesting site and the only outcrop of magmatic rocks in the Puglia region and in the whole Adriatic coast of Italy. The excavation of a canal through this area, performed in 1930, exposed grey micro- and meso-crystalline gypsum with intercalations of black limestones and marls of Upper Triassic age, mantled by loose sandy Quaternary deposits. The gypsum bedrock shows a high density of cavities, either dissolutional conduits or voids related to gravitational collapse processes. Starting from about 1970, a wide new touristic settlement was built over the area, which in turn, since about 1990, began to suffer for the increasing formation of sinkholes. We observe PS objects undergoing uplift displacements in both ascending and descending data over the Lesina Marina area. Relying on the relatively smooth nature of the observed phenomenon, and assuming negligible north-south movements, as justified by the overall geometry of the site geomorphological units, information coming from ascending and descending geometries was interpolated over a common geographic grid, then combined to obtain vertical and horizontal (east-west) velocity components. Derived vertical displacement rates exceed 4 mm/y on locations adjacent to the canal, gently decreasing to zero towards the western end of the built up area (about 600 m away). The east-west velocity component shows a W-SW trend with maximum rates of about 2 mm/y westwards over a belt about 200 m thick, starting about 200 m from the canal. The displacement seems to go on steadily in the entire monitored period from 1995 to 2010. High-precision leveling measurements, performed on topographic points distributed in the study area in 1999 and 2010, confirm the PSI data. These observations, supported by ancillary data and in situ investigations performed in the past [3], seem compatible with processes such as diapirism or the hydration of the residual anhydrite in the core of the gypsum mass. In this work, we try to sketch a model for the swelling process due to hydration, relying on statistical correlations between the uplift spatial pattern and the spatial distribution of geological features such as the gypsum layer surface. Based on these results, we speculate about the utility of DInSAR PSI techniques as early-warning tools in monitoring slow deformation processes leading to increased sinkhole hazard. ERS and ENVISAT data provided by European Space Agency – Category-1 project N. 5367. References [1] Ferretti A., Prati C. & Rocca F. (2001), "Permanent Scatterers in SAR Interferometry", IEEE Transactions on Geoscience and Remote Sensing, Vol. 39, No. 1, pp. 8-20. [2] Bovenga F. et al. (2004), "SPINUA: a flexible processing chain for ERS / ENVISAT long term interferometry", Proceedings of ESA-ENVISAT Symposium, Salzburg, Austria, 6-10 September 2004. [3] Fidelibus M.D., Gutiérrez F., Spilotro G. (2011), "Human-induced

## The SBAS-DInSAR approach for the spatial and temporal analysis of sinkhole phenomena

### Author(s)

Fabiana Calò <sup>(1)</sup>, Gianfranco Fornaro <sup>(1)</sup>, Mario Parise <sup>(2)</sup>

### Department

<sup>(1)</sup>CNR-IREA Via Diocleziano 328, Napoli, Italy, IT

<sup>(2)</sup>CNR-IRPI Via Amendola 122-I, Bari, Italy, IT

### Abstract

Sinkholes represent the main hazards in karst areas, characterizing such territories because of the presence of natural and anthropogenic caves. Dissolution in soluble rocks (carbonates, evaporites), and later evolution of karst caves due to breakdown processes cause sinkhole events related to underground voids of natural origin. In many regions of Italy, the presence of anthropogenic cavities, excavated underground for different reasons and in different epochs, and generally located at low depth from the ground surface, creates a further hazard, which becomes extremely dangerous in built-up areas. Loss of memory of these underground cavities results, as a matter of fact, in building above voids, which extension and stability conditions are not known. As a consequence, the upward evolution of instabilities phenomena occurring underground may reach the ground surface, thus creating sinkhole events. High demographic density and growing urbanization contribute to increase the vulnerability of many karst environments and the risk associated to sinkholes, which results in a significant threat to human life, property and infrastructures. In such a scenario, the risk management can be effectively addressed if risk prevention and mitigation measures are developed, based upon a deep knowledge of the sinkhole phenomena, from the mechanisms of formation to their spatial distribution and temporal evolution. To this aim, multi-pass space-borne Differential Synthetic Aperture Radar Interferometry (DInSAR) techniques provide a valid support to remotely investigate the sinkhole susceptibility at regional scale and for long time intervals, playing a key role in forecast strategies thanks to their capability of detecting and monitoring phenomena precursors. In spite of the suddenness of the final catastrophic collapse, in fact, sinkhole occurrence is typically preceded by slow surface displacements, that can be analyzed and monitored by DInSAR techniques by benefiting of large archive of SAR acquisitions. In this work, we apply the advanced DInSAR approach referred to as Small Baseline Subset (SBAS) for analyzing surface deformation in Apulia region (Southern Italy) where several sinkhole phenomena have been recorded in the last years, including the well known event occurred at Gallipoli on March 29, 2007. In particular, we exploit both ascending and descending ENVISAT images spanning the 2003-2010 period, and produce deformation maps and corresponding time series showing the temporal evolution of the ground displacements. The results so far obtained have been coupled with in situ data, suggesting as the institutions in charge of urban planning and environmental management can take relevant advantages if they move towards the development of integrated monitoring systems, based on the joint use of field surveys and geomorphological analysis and remote sensed data. Finally, it is worth to point out that such DInSAR analyses in sinkhole applications will significantly benefit by the availability of data acquired by SAR systems of new generation, thanks to their improved spatial resolution and reduced revisiting times. Further, the development of advanced full resolution processing techniques, as the 4-D (space velocity) imaging (Fornaro et alii,) exploiting both amplitude and phase information of SAR data, allows investigating very localized subsidence phenomena involving urban scenarios, and accordingly improving the assessment and mitigation of the associated risk. References BERARDINO, P., FORNARO, G., LANARI, R., SANSOSTI, E., 2002.

A new algorithm for surface deformation monitoring based on small baseline differential SAR interferograms. *IEEE Trans. Geosci. Remote Sens.*, 40 (11), pp. 2375–2383. FORNARO, G., REALE, D., SERAFINO, F., 2009, Four-Dimensional SAR Imaging for Height Estimation and Monitoring of Single and Double Scatterers. *IEEE Trans. Geosci. Remote Sens.*, 47, pp. 224 – 237.

## InSAR time series analysis of coal mining field in Zonguldak city, NW Turkey

### Author(s)

Saygin Abdikan <sup>(1)</sup>, Andrew Hooper <sup>(1)</sup>, Ramon Hanssen <sup>(1)</sup>, Fusun Balik Sanli <sup>(2)</sup>, Ziyadin Cakir <sup>(3)</sup>, Huseyin Kemaldere <sup>(4)</sup>

### Department

<sup>(1)</sup>Delft Institute of Earth Observation and Space Systems, Delft University of Technology Kluyverweg 1 2629 HS Delft, NL

<sup>(2)</sup>Department of Geomatics Engineering, Yildiz Technical University 34210, Istanbul, TR

<sup>(3)</sup>Department of Geological Engineering, Istanbul Technical University 34469, Istanbul, TR

<sup>(4)</sup>Department of Geodesy and Photogrammetry Engineering, Zonguldak Karaelmas University 67100, Zonguldak, TR

### Abstract

This paper presents preliminary results of subsidence monitoring of a coal-mining field in Zonguldak Province using the Interferometric Synthetic Aperture Radar (InSAR) time series. It is a coastal urban area in northwestern Turkey that is prone to human-induced environmental problems such as subsidence due to the coal-mining areas. Severe deformations in many buildings of the region have been known since the 1900s. The aim of this project is to investigate the subsidence that is damaging dwelling units and mining areas. Previous DInSAR studies show the subsidence monitoring at Zonguldak region (Deguchi et al, 2007, Akcin et al, 2010). A 204-mm deformation during 132 days around the Kozlu coalfield was found using one pair 1995 JERS-1 images and a 55-mm deformation over 15 months in an urban area near the Kozlu mining area was found using one pair 2005 Radarsat images. Surface deformations are also known to be taking place in the Uzulmez and Karadon mining fields but could not detect by previous DInSAR studies using C-band Radarsat. However, the lack of high coherence in these regions did provide reliable estimates of deformation. A total of 46 ENVISAT ASAR images acquired in two different geometries (17 in ascending track 343 and 29 in descending track 21) are used in this study. Persistent Scatterers Interferometry (PSI) and Small Baseline Interferometry (SB) time series analysis have been used between August 2003 and January 2010 for descending track and between May 2004 and July 2010 for ascending track (data from ESA Cat-1 project No: 6543). The raw ASAR data are focused using ROI\_PAC to form single look complex images, from which interferograms are calculated using DORIS. Time series are constructed using the StaMPS package with both PSI and SB approaches. Between 2003-2010 it is extracted approximately 50-60 mm which is less than in 1995 around the Kozlu coalfield. In urban area which is near the Kozlu mining area it is extracted approximately 120 mm for the period 2003-2010 years. Areas of subsidence with slower rates are also revealed at Karadon and Uzulmez regions. Maps of underground mining tunnels show that these surface deformations are most probably due to mining.

# Factors that have an influence on time series

## Author(s)

Davide Notti <sup>(1)</sup>, Claudia Meisina <sup>(1)</sup>, Francesco Zucca <sup>(1)</sup>, Michele Crosetto <sup>(2)</sup>

## Department

<sup>(1)</sup>University of Pavia Via Ferrata, 1 27100 Pavia, IT

<sup>(2)</sup>Instituto de Geomatica Av. Carl Friedrich Gauss, 11 - Castelldefels, ES

## Abstract

The development in elaboration of SAR persistent scatterer (PS) data has allowed an improvement in time series precision allow to study the behaviour in the time of different type process over a large area. The PS data over regional area until recent times give information about slow ground displacement related to different process like subsidence (Herrera et al, 2007), landslides (Colesanti and Wasowki, 2006) , tectonics or building deformations (Gernhar et al., 2009) . The quality of the data was very good regard the estimation of the average velocity over a certain period time, however was impossible to check the temporal evolution of the process because the elaboration made a with a linear regression smooth all the trends and a comparison with time series of other monitoring system was not possible. The more recent data are elaborated also with non-linear algorithms over wide regions and this allow, even if with many restrictions and problems, to study also the variation in the evolution of a process. For this work we have analyzed the time series of ERS (1992-2001) and (Novali et al, 2009)<sup>TM</sup>RADARSAT (2003-2010) elaborated over with SqueeSAR over three regions: Western Piedmont, Province of Pavia and Province of Imperia. We have analyzed different geological processes and factors that have an influence on time series also considering the errors related to the process of elaboration (i.e. algorithm or the phase unwrapping). The first problem in the analysis of a time series is to discriminate between noise, errors that affect time series and a true ground displacement trend. To make this is necessary to verify if the time series trend is compatible with the kinematic of the process analyzed. Another methodology is to compare many time series of different processes in different areas of the same dataset if we find a similar trend probably is related to algorithm used for the processing and not to a real deformation. More difficult is to verify the phase unwrapping in this case we need a comparison with a monitoring system that validate the effective acceleration of the process. Another factor that we consider is the period of analysis and the number of images if they increase the TS has a better quality. To reduce the effect of noise usually we did not analyzed a Time Series of a single PS but we calculate an average TS for the PS on the same process. The further step is to exploit the PS time series in order to understand the kinematic of the process. This type of analysis can be made for single process each time a regional analysis of TS trends is difficult because each process have a proper trend. The case histories analyzed are representative of different process: landslides, subsidence induced ground water extraction, settlement of new buildings, thermal oscillation. The cases under study represent usually process in which the TS trend is clear and easy to understand. In other cases we have the overlapping of different processes and the errors of related to noise. Also the different type of scatterer is difficult to evaluate Where it is possible we compared the TS with other direct or indirect monitoring data like rainfall, temperature, inclinometers data, piezometric data and we found some correlation between TS trend and some particular events.

# Integrated GNSS and InSAR processing over a landslide target near Koroška-Bela, NW Slovenia.

## Author(s)

Alan Fromberg <sup>(1)</sup>, Chris Prior <sup>(1)</sup>, Marko Komac, Blaz Milaniè <sup>(2)</sup>, Rachel Holley <sup>(3)</sup>, Pooja Mahapatra <sup>(4)</sup>, Hans Van der Marel <sup>(4)</sup>

## Department

<sup>(1)</sup>SEA As above, UK

<sup>(2)</sup>Geological Survey of Slovenia ,SI

<sup>(3)</sup>Fugro NPA , UK

<sup>(4)</sup>Technical University of Delft , NL

## Abstract

The I2GPS project has implemented a fully integrated unit and application for generating co-registered SAR interferometric and GNSS precision survey results by: • integrating the antenna of a GNSS receiver with a Compact Active Transponder (CAT) antenna to ensure millimetric co-registration and assure a coherent reference between the two precision surveying techniques; • developing the integrated application processing and conducting field trials to confirm the effectiveness of the technique. The Project was initiated in order to meet the needs of the Geological Survey of Slovenia which needed to exploit the high line of sight precision of InSAR together with the more frequent collection of horizontal displacements from GNSS data to detect sub-centimetric displacements of landslides as possible pre-cursors for mass debris flows, such as that in Stože in 2000 which destroyed 23 buildings and resulted in 7 casualties. This paper presents the design of the unit and summarises results from field trials conducted near Koroška-Bela in north-western Slovenia. The Potoška planina landslide is known to have produced at least four historical debris flows, some of which caused significant damage to a village down-slope. Current activity on the slide is presumed to be active slow-motion slip. The method and unit are equally applicable to measurements of 3D tectonic movements, glacier movement (maybe also melting) monitoring and infrastructure displacement monitoring. The I2GPS unit is based upon the integration of a CAT, together with an AsteRx2e GNSS receiver co-mounted on a plate that can be simply registered with a local surveying reference. This assures that measurements can be taken simultaneously using the two techniques and that synergies between the two (e.g. for resolving phase ambiguity when displacements exceed half a wavelength) can be exploited. The units are powered by a solar panel with secondary battery power supply, permitting autonomy over several months. Times, polarisations and viewing angles are programmed into the CATs in advance and reprogramming via a laptop and port . If raw data is required then GNSS receiver memory needs to be downloaded about once every two months of measurement time (need not be continuous). If RINEX format is acceptable then memory usage is improved by 50%. The methods using for installing the equipment in such a way that it could be reliably linked to displacements between reference targets off the landslide and units deployed such that they move with the landslide are described. Results of surveys conducted using Envisat data acquired between February and August 2011 using Envisat for InSAR and precision GPS techniques are summarised. Comparison between the results obtained by the techniques in isolation and the potential benefit obtained from integrated processing are described. The approaches for integrated processing considered including the atmospheric corrections available from GPS data processing to the InSAR results. I2GPS is supported by the European Union under its Seventh Framework Programme via the Galileo Supervisory Authority. The I2GPS consortium is composed of Systems Engineering and Assessment Limited (prime contractor), Delft University of Technology, Geological Survey of Slovenia, Septentrio Satellite Navigation NV, Société d'Applications

# Monitoring Stability of Levee with Time-series ENVISAT/ASAR Images

## Author(s)

Yuanyuan Pei <sup>(1)</sup>, Mingsheng Liao <sup>(1)</sup>, Teng Wang <sup>(1)</sup>, Lu Zhang <sup>(1)</sup>

## Department

<sup>(1)</sup>Wuhan University State Key Lab. for Info. Eng. in Surveying, Mapping and Remote Sensing (LIESMARS) Wuhan Univer, CN

## Abstract

Typhoon, tsunami and flood are, particularly in recent years, the top threats to coastal regions. Levees are constructed to protect coastal cities from typhoon, flood and sea tide. Since the stability of the levees is important during the extreme weather, it is necessary to monitor its deformation regularly. Levee stability can be negatively affected by the ground deformation adjacent to the levee. High subsidence rates adjacent to levee require more immediate attention than areas where there are lower subsidence rates. The advantages of radar remote sensing are frequently revisiting, wide area coverage, and displacement monitoring with high precision. It is well known that the intensity of the backscattering of the SAR image depends on slope, roughness, and dielectric constant of surface. The revetment and slopes form high intensity of backscattering, which are easy to be detected in SAR image. These conditions ensure coherent behavior for radar observations. Persistent Scatterer Interferometry (PSInSAR) technique is more useful for high density and large-scale monitoring. The interferometric phase is used as data input for PS-InSAR processing. Identification of PSs is one of the key procedures in both SAR image interpretation and analysis for monitoring surface deformation. The temporal coherence was introduced to identify PSs. The time series phases are unwrapped in a three-dimensional (3-D) way. The unwrapped phases were divided into DEM error phase, deformation phase, APS distribution of master and slave images and noisy parts. The image coverage is large and the levees are long, therefore we can split the differential interferograms into a number of overlapping patches in range and azimuth for computation efficiency. Each patch is processed independently to calculate deformation velocity. Then the results from these patches are combined together taking into account of different reference points. Shanghai sits on the Yangtze River Delta on China's eastern coast. Each year, the city is hit by typhoons from Pacific Ocean and threatened by the flood of the Yangtze River. With increasing economical investments in Shanghai, the creation of new land from sea is a hot topic. Lingang town of Shanghai lies in the junction of southeast of Yangtze River and Hangzhou bay, with area of about 296 km<sup>2</sup>. Thereinto, nearly 100km<sup>2</sup> of this area is tidal-flat. In the frame of Dragon II program, we collected 24 scenes of ENVISAT ASAR images (Ascending, Stripmap Mode, Track 497), acquired from October 2007 to February 2010. According to the PS-InSAR analysis, levees built on reclamation area show larger deformation velocity. Take Lingang town for instance, the subsidence in the west side is more serious than that of the east side. Moreover, the areas with the largest subsidence velocity are detected at the region near the levees. According to the geologic structure, the engineering geology condition in the whole eastern part were surpassed the west. The most serious subsidence area depending on our monitoring results should be paid for special attention. The results also suggest that the leveling measurements in Lingang town should be added into the land subsidence monitoring network system for the whole city.



# Geodynamic monitoring of oil-and-gas fields using radar Interferometric data

Author(s)

Anton Filatov <sup>(1)</sup>, Arkadi Yevtyushkin <sup>(1)</sup>

Department

<sup>(1)</sup>Ugra Research Institute of Information Technologies 151, Mira St., RU

## Abstract

Given work describes features of interferometric processing of the radar data on territory of Western Siberia, and also application of obtained results for monitoring of displacements of a ground surface around the area of intensive oil and gas production. The scientific side of work consists in research, developing and realization of methods of processing of radar measurements in the conditions of high temporal decorrelation. The practical side is connected with monitoring of a surface of oil and gas deposits and detection of motions caused by hydrocarbons extraction. Oil and gas reserves on the territory of Western Siberia are extracted in area of continuous and discontinuous permafrost, peatbogs, fully-frozen in winter shallow lakes, thermokarst provinces and in zone of ravine erosion as a result of technogenic top-soil failure. Negative geodynamic processes cause pipeline breakings at different depths in wells on active oil-and-gas fields, intrafield and main ground-surface pipelines. As a result of the spatial analysis of breakdown susceptibility of pipelines in connection with a site of local breaks it has been established, that a repeating breakdown susceptibility of oil pipelines is dated for these local breaks. From the point of view of physics and the geomechanics, studied structures prove as dynamically deformation processes, however without explosive infringements of thickness of breeds. Many researches show, that influence of local breaks of an earth crust on pipelines considerable, and can lead to destruction of pipelines. The importance of the given work is defined by necessity of decrease breakdown susceptibilities of oil and gas pipelines. At the same time Earth surface displacements monitoring in oil and gas fields areas is regulated by "The Instruction on Surveying Operations. RD-07-603-03" by Gosgortekhnadzor (Russian State Engineering Supervision Instance). This monitoring must include creation of the fixed reference points system both in limits of hydrocarbon field contour and outside of it (i.e. in the area of possible man-caused deformation and outside of this area). Traditional methods of regular measurements (mostly 2nd class leveling) should be applied on this system of points. Differential radar interferometry is an effective method for estimation of plane and vertical displacements in big areas caused by breakdown structure movements. High cloudiness and snow period duration caused by location of investigated territory in north latitudes make difficulties for monitoring of ground surface by optical remote sensing data. At the same time nature landscape features presented in that area place a certain limitation on interferometric processing and require more detailed data analysis. The main objective of the research work is construction of displacements maps of ground surface and detection of subsidences that have a negative impact on objects of oil and gas production. The complex of the researches spent using remote sensing data is addition to the land geological and geophysical works which are carried out by oil-extracting companies. Differential radar interferometry is an effective method for estimation of plane and vertical displacements caused by breakdown structure movements. At the same time nature landscape features presented in that area place a certain limitation on interferometric processing and require more detailed data analysis. During the research work ENVISATASAR, ERS-2SAR and ALOSPALSAR radar data were used. Complex analysis of temporal and spatial decorrelation depending on sensing conditions, sensing season and different natural landscapes of Western Siberia revealed the advantage of L-band radar data for research territory. ALOSPALSAR data allowed constructing displacements maps reflecting the ground surface dynamics of Samotlor and Gubkin oilfields during the 2007–2010 period. GPS measurements on points of geodynamic polygons were used as ground control

points during differential interferometric processing. Joint analysis of spatial profiles and displacements maps on territory of Samotlor and Gubkin deposits shows decreasing of subsidence forming the trough. The research work is supported by projects: ESA ENVISAT-AO ID 365, ESA Category-1 ID 3166, 07/JAXA/ASP.

## PSI helps to map relative susceptibility to ground and slope instabilities in the Lanzhou loess area of Gansu Province, China

### Author(s)

Janusz Wasowski <sup>(1)</sup>, Fabio Bovenga <sup>(1)</sup>, Davide Oscar Nitti <sup>(2)</sup>,  
Raffaele Nutricato <sup>(3)</sup>, Tom Dijkstra <sup>(4)</sup>, Xingmin Meng <sup>(5)</sup>

### Department

<sup>(1)</sup>CNR-IRPI Via Amendola 122, IT

<sup>(2)</sup>Politecnico di Bari, IT

<sup>(3)</sup>GAP srl, IT

<sup>(4)</sup>Loughborough University, UK

<sup>(5)</sup>Lanzhou University, CN

### Abstract

The advantages and limitations of PSI for ground/slope instability detection and mapping of relative susceptibility are evaluated for the semi-arid loess area of the city of Lanzhou (Gansu Province, China), home to over 3 million people. In this tectonically active region, characterized by high local relief (300-400 m), slope instability in the collapsible loess and underlying substratum is widespread and Lanzhou pays an increasingly high price due to lost lives and livelihoods as the city and its environs continue to develop in an unstable terrain. More than 40 ENVISAT ASAR datasets (period 2003-2010) were pre-processed to obtain stacks of co-registered differential SAR interferograms. Then the SPINUA algorithm was used to perform multi temporal analysis on the co-registered DInSAR stacks in order to correct for spurious effects such as atmospheric artifacts and DEM errors, and obtain precise displacement information over selected radar targets (PS). The analysis resulted in the identification of over 140,000 PS in the greater Lanzhou area (about 300 km<sup>2</sup>). The good news is that the central (and major) part of the city seems unaffected by instabilities. Nevertheless, the PSI displacement map reveals several zones, characterized by the presence of moving PS (with average velocities typically below 10 mm/yr). The interpretation of the PSI results in the lithological and geomorphological context of the Yellow River valley in the Lanzhou area shows that the lower, flat areas with floodplain and valley-fill deposits (Holocene terraces with mainly reworked loess at the surface) are stable, whereas some higher, gently sloping areas appear locally unstable, particularly where the Late Pleistocene terraces are covered by aeolian loess. Furthermore, PS with higher velocities appear to occur predominantly on the 4th and 5th order terraces (with clusters along the steep terraces risers denoting their instability), as well as locally on steep slopes in collapsible, aeolian loess. High velocity PS also appear to be clustered around areas of poor drainage and/or irrigation (e.g. Dongpingcun in West Lanzhou). This observation is supported by, e.g. the landslide history of the fourth Yellow River terrace at Heifantai (some 20 km west of the current study area) with large slope failures as recently as April 2011. Our reconnaissance field checks indicate that many of the detected movements could be associated with processes involving ground settlement/structure instability. However, it may often be difficult to ascertain the exact origin of low strain rates, especially when these are detected on slopes. Indeed, mm-cm/yr deformations can arise from different causes (e.g. subsidence and local settlements, shallow seasonal creep, pre-failure strains of incipient landslides, volumetric changes of geological/artificial materials, tectonics, and instability of structures that act as radar targets). Despite these interpretative difficulties, the PSI displacement results offer unique information, which, following expert judgment and correlations

with information on local geology, geomorphology and slope history, can be used for wide-area and site-specific assessments of relative susceptibility to ground and slope instabilities. Acknowledgements ENVISAT images were provided by ESA in the framework of CAT-1 project #7444 "Exploitation of ENVISAT radar data for ground and infrastructure instability hazard assessments in the Lanzhou area (Gansu Province,China)", PI - J. Wasowski.

## Soil water storage change inferred from clay expansion as detected by satellite radar interferometry

### Author(s)

Bram Te Brake <sup>(1)</sup>, Ramon Hanssen <sup>(2)</sup>, Martine Van der Ploeg <sup>(1)</sup>,  
Gerrit De Rooij <sup>(3)</sup>

### Department

<sup>(1)</sup> Wageningen University Droevendaalsesteeg 4, Wageningen, NL

<sup>(2)</sup> Delft University of Technology, NL

<sup>(3)</sup> Helmholtz Centre for Environmental Research, DE

### Abstract

Several InSAR studies over agricultural areas have observed phase changes between adjacent fields. Often it has been hypothesized that these phase changes may be related to soil moisture, with contribution of both surface elevation changes due to swell and shrinkage of clay rich soils and changes in penetration depth with soil moisture content. This hypothesis, however, does not fully explain the discrete differences in phase aligned with agricultural fields. Although these effects have been observed in some of the earliest InSAR studies, (e.g. Gabriel et al., 1989) the lack of ground truth prevents an unambiguous interpretation in terms of the driving mechanisms. In fact, we are not aware of any InSAR study where SAR acquisitions and field-specific in-situ measurements on soil moisture and elevation changes due to swell and shrinkage of clays were conducted simultaneously. In this study, we combine an extensive fieldwork campaign, monitoring soil moisture related parameters over individual agricultural fields, with C-band and X-band InSAR data over agricultural areas in the Netherlands. The objective is to assess the suitability of InSAR data for estimating water storage change in clay soils. Main factors of interest include the spatiotemporal resolution of SAR data, measurement accuracy obtained by InSAR and coherence preservation over arable land. We hypothesize that phase changes from C-band and X-band SAR interferometry over agricultural fields with clay-rich soils are caused by clay swell and shrinkage. The swell and shrink behaviour of these soils is highly related to the soil moisture content. Therefore surface elevation changes can be related to the amount of water stored in the unsaturated zone of the soil. The results suggest that InSAR observations using short wavelengths can reveal the detailed data on surface level motion of clay soils needed to estimate soil water storage change. This has high potential for large scale hydrological studies. References: Gabriel, A., Goldstein, R.M. & Zebker, H.A. (1989). Mapping small elevation changes over large areas: differential radar interferometry. *J. Geophys. Res.* 94, 9183-9191.

# Potential contribution of radar remote sensing for landslide monitoring in mountainous environment

## Author(s)

Mahdi Motagh <sup>(1)</sup>, Kanayim Teshebaeva <sup>(1)</sup>, Chris Chris Massey <sup>(2)</sup>,  
Sigrid Roessner <sup>(1)</sup>, Hannah Brackley <sup>(2)</sup>

## Department

<sup>(1)</sup>Department of Geodesy and Remote Sensing, Helmholtz Center Potsdam, GFZ German Research Center for Geosciences, Potsdam, Germany , DE

<sup>(2)</sup>GNS Science, Lower Hutt, NZ

## Abstract

Detailed information about the spatial and temporal pattern of mass movement is of fundamental importance for any landslide hazard assessment. Presently, most of the techniques for monitoring landslide displacements rely on ground-based measurements derived from conventional geodetic techniques such as GPS and electronic tachometers. This paper evaluates the capabilities of C-band, X-band and L-band space-borne radar interferometry for the investigation of landslide displacement. Two case studies are investigated. A first case focuses on measuring creep signal in 3 known landslides in New Zealand, namely Taihape, Poroa and Utiku landslides. German TerraSAR-X (X-band) and European's Envisat ASAR (C-band) data are utilized to detect and quantify ground surface deformation using advanced InSAR time-series analysis. The second case focuses on analyzing slope stability in Kyrgyzstan, Central Asia, where we evaluate the capability of X-band and L-band SAR interferometry for landslide assessment. Results show that high-resolution spaceborne radar imagery has a great potential for systematic monitoring and description of slope instabilities in landslide environments, as long as a good SAR data coverage in both space and time is available.

# Satellite vs Ground Based SAR Interferometry for landslide monitoring

## Author(s)

Paolo Mazzanti <sup>(1)</sup>

## Department

<sup>(1)</sup>NHAZCA S.r.l., spin-off "Sapienza" Università di Roma Via Cori snc, 00177 Rome, IT

## Abstract

In the last two decades SAR Interferometry significantly modified the concept of landslides monitoring and investigation. Collecting displacement data with a mm accuracy without any installation in the monitored area is opening new prospects in the analysis and control of landslides. Landslides are one of the most dangerous natural events and they can be considered as a global problem, more than other events like volcanoes and earthquakes (that are more localized in well know regions of the world). The World Bank considers landslides as difficult to be predicted as earthquakes. Nevertheless, several landslides can be predicted if suitable control is made. To this aim, displacement monitoring is a key point and techniques like InSAR can play an important role. Over the last years, several projects demonstrated the efficacy of Satellite SAR Interferometry in supporting landslides mapping and landslides hazard assessment at the regional scale. Otherwise, few studies has been done for forecasting purposes, due especially to some limitations of this technique (low temporal frequency of data ecc). However, new generation

satellites (e.g. Terra SAR-X, Cosmo-Sky Med) are opening new prospects in using such a technique for provisional purposes. Therefore, some projects have been recently dedicated to this specific aim. Successful experiences on Satellite InSAR lead in the last ten years to increasing efforts in developing Ground Based equipments, which are based on the same operational principles of Satellite based ones. First successful applications of this technique in landslides monitoring date back to the beginning of 2000, even if only in the last few years commercial equipments have been developed, thus allowing the use GBInSAR in common practice. Even if Satellite and Ground Based SAR Interferometry are based on the same operational principles there are several differences between them, especially in terms of achievable results. SInSAR is a suitable technique for the monitoring of large areas characterized by slow movement, while GBInSAR is more suitable for the detailed and continuous monitoring of small areas, up to few square kms, that are characterized by both slow and rapid movement (e.g. single unstable slopes and cliffs, volcanic flanks etc). As a matter of fact, GBInSAR equipments can collect SAR images with a sample rate of about 5 minutes and future equipments are expected to be faster. Temporal prediction of real landslides failure were performed over the last years by using GBInSAR data together with specific landslide models. Differently, SInSAR is hardly to be used for continuous emergency monitoring due to the low data sampling rate (about one image per month). Otherwise SInSAR is more appropriate as an investigation tool thanks to the historical database of satellite images available from 1992. Furthermore, must be considered that satellite and ground based SAR data are usually characterized by different point of views; therefore, SInSAR is more suitable for monitoring vertical displacements, while GBInSAR is more appropriate for the control of horizontal displacements. The combined use of these techniques is desirable for the reduction of landslide risks, and can allow to support decision makers at different levels (i.e. from the planning phase to the emergency phase). However, in facing with these techniques several limitations cannot be neglected. First of all, by InSAR monitoring only surface displacement can be measured and this is a strong limitation in landslide analysis. Furthermore, by advanced processing like PS InSAR the monitoring points are usually located over building and structures, hence, must be aware from misinterpretation of displacement causes, i.e. the displacement of a building is not necessarily related to ground displacement.

## Comparison of ground movements in coal mining areas (Belgium) observed by the PSI technique.

**Author(s)**

Pierre Yves Declercq <sup>(1)</sup>, Xavier Devleeschouwer <sup>(1)</sup>

**Department**

<sup>(1)</sup>GSB , BE

### **Abstract**

Thanks to the Terrafirma II program, one of ten services being supported by the European Space Agency's (ESA) under the Global Monitoring for Environment and Security (GMES) program. ERS1/2 and ENVISAT datasets from April 1992 - September 2005 have been processed around the city of Liège and in the Campine basin (Limburg region). Around 148,000 Permanent Scatterers (PS) are identified using 102 SAR images on a 2950 km<sup>2</sup> area. The studied areas are located both in old coal mining districts in the Province of Limburg in the NE of Belgium and along the river Meuse in the city of Liège. The PS density ranges from very low densities (<10 PS/km<sup>2</sup>) in rural zones to >300 PS/km<sup>2</sup> in urbanized areas. The main objective consists in the comparison of the recorded ground motions between these two old mining districts. In the Limburg area, the results of a kriging interpolation indicate a subsidence phenomenon in the western part, centered on the western coal mine district of the Campine collieries. It has a rectangular shape of 16 km long and 10 km wide. The lowest annual average velocities range between -4.63 and -16.07 mm/year. The

eastern zone, containing the abandoned collieries of the eastern mining district, reveals uplifting conditions. The result of the kriging interpolation reveals an uplift over two zones. The center of each zone corresponds to the highest annual average velocities ranging between 8.87 and 21.06 mm/year. A clear difference appears in terms of ground movements over the abandoned mines of the Campine coal basin. The last mining activities ended in 1992 in the western mining district and in 1988 in the eastern mining district. Around the Liège city, the mining activities stopped earlier with the last mine of “Blegny-Trembleur” closed in 1980. The kriging interpolation based on the annual average velocities of the PS reveals that the ground movements are related to the extension of the mining activities. In comparison with the Limburg region all the movement resulted in uplift except the soft sediments located in the alluvial plain of the river Meuse. The origin of the movements resides in the groundwater pumping activity, necessary to keep the active mines dry. In Liège, mining activities stopped sooner and shows only uplifting conditions with low velocities around 2 – 3 mm / year in some areas. The uplifting evolution is still visible 25 years after the closure of the coal mines. In the Limburg, pumps were switched off with a time difference of 5 years between eastern (years 1986-1988) and western (years 1991-1992) side of the coal mining basin, permitting a slow rise of the water level, first filling up the voids left by mining before pressurizing the aquifer. Both districts of the mining basin are in a different state. Residual subsidence continuing after the closure of mining activities in the Limburg indicates that mines are not yet completely flooded in the western mining district, whereas restored groundwater levels induced an elastic rebound highlighted by the positive velocities observed in Liège and the eastern mining district of the Campine basin.

## Application of advanced InSAR time series for monitoring seasonal and long-term peatland surface change

### Author(s)

Zhiwei Zhou <sup>(1)</sup>, Zhenhong Li <sup>(1)</sup>, Susan Waldron <sup>(1)</sup>, Noel Gourmelen <sup>(1)</sup>

### Department

<sup>(1)</sup>University of Glasgow School of Geographical and Earth Sciences, University of Glasgow, Glasgow, UK

### Abstract

Peatlands are an important reservoir in the global carbon cycle due to: (1) their capacity to store 30% of the global soil carbon or the equivalent of 50% of the carbon currently in the atmosphere [Gorham, 1991], and (2) their functioning ability to act as a source or sink for atmospheric carbon dioxide (CO<sub>2</sub>) and methane (CH<sub>4</sub>) [Charman. et al., 2008]. Studies related to greenhouse gas (GHG) emissions from peatlands and their response to climate changes have increased in the past few years [Frolking et al., 2002], with recent interest including assessments of surface level fluctuations in relation to the GHG fluxes [Fritz et al., 2008]. Interferometric Synthetic Aperture Radar (InSAR) has shown great capability and potential on measuring the Earth's surface movement [Massonnet and Feigl, 1998]. Here we investigate whether InSAR techniques can be used to map spatiotemporal deformation of peatlands. The peatland area in our study is located in the Monadhliath Mountains region, Scotland, where Keyworth et al [2009] mapped the extent and severity of erosion from 2006 to 2007 using optical remote sensing images and GPS. To date we have processed: (i) 30 scenes of Envisat C-Band ASAR images collected from two adjacent descending tracks (266 and 037) between March 2004 and September 2007; and (ii) 29 scenes of ALOS L-Band PALSAR images acquired from ascending tracks (664 and 665) between December 2006 and July 2010. The Small Baseline InSAR approach in the StaMPS/MTI [Hooper et al., 2007] package was used to generate mean velocity maps and deformation time series in the Line of Sight (LOS) direction. Both Envisat and ALOS datasets span the period from December 2006 to September 2007, which provided us an opportunity to investigate the feasibility of different bands of radar images to monitor peatland deformation. In addition, the consistency of LOS mean

velocity maps and deformation time series between adjacent tracks suggests that: (1) seasonal peatland surface level variations were observed in the Monadhliath Mountain area, ranging from -20 mm in the summer to +20 mm in the winter and; (2) peat surface level change is spatially variable. Thus it appears that InSAR can be employed to detect peatland surface deformation. To improve the reliability of InSAR-derived peatland deformation, two technical issues have been identified and will be addressed in the future: (1) phase unwrapping error; and (2) atmospheric effects. With these issues addressed, the next stage will link the observed seasonal peatland deformation signals with other environmental factors including water table level, atmospheric pressure and temperature to estimate the impacts on annual carbon balance. References Charman., D. J., H. Joosten., J. Laine., D. Lee., T. Minayeva., S. Opdam., F. Parish., M. Silvius., and A. Sirin. (2008), Assessment on Peatlands, Biodiversity and Climate Change: Main Report, Global Environment Centre, Kuala Lumpur & Wetlands International, Wageningen. Fritz, C., D. I. Campbell, and L. A. Schipper (2008), Oscillating peat surface levels in a restiad peatland, New Zealand - magnitude and spatiotemporal variability, *Hydrological Processes*, 22(17), 3264-3274. Frolking, S., N. T. Roulet, T. R. Moore, P. M. Lafleur, J. L. Bubier, and P. M. Crill (2002), Modeling seasonal to annual carbon balance of Mer Bleue Bog, Ontario, Canada, *Global Biogeochem. Cycles*, 16(3), 1030. Gorham, E. (1991), Northern Peatlands: Role in the Carbon Cycle and Probable Responses to Climatic Warming, *Ecological Applications*, 1(2), 182-195. Hooper, A., P. Segall, and H. Zebker (2007), Persistent scatterer interferometric synthetic aperture radar for crustal deformation analysis, with application to Volcán Alcedo, Galápagos, *J. Geophys. Res.*, 112, B07407. Keyworth, S., M. Jarman, and K. Medcalf (2009), Assessing the Extent and Severity of Erosion on the Upland Organic Soils of Scotland using Earth Observation: A GIFTSS Implementation Test: Final Report Rep. Massonnet, D., and K. L. Feigl (1998), Radar Interferometry and Its Application to Changes in the Earth's Surface, *Rev. Geophys.*, 36, 441-500.

## Application of SAR interferometric methods to identify the mobility of the area above salt diapir in Inowroclaw City , Kujawy Region (Poland)

Author(s)

Maria Surala <sup>(1)</sup>, Anna Piłtkowska <sup>(1)</sup>

Department

<sup>(1)</sup>Polish Geological Institute - National Research Institute Rakowiecka 4, Warsaw, PL

### Abstract

The presence of salt structures in the Inowroc<sup>3</sup>aw area (city of Poland) on the Kujawy Region constitutes an additional of the geological setting, which is also typical for Polish Lowlands. Remote Sensing interpretation presents the linear structural elements are supplementing the tectonic-structural picture and suggest a block – type character of the sub- Permian basement. They may also indicate the existence of active movements of salt bodies and point to tectonic zones active during the almost recent past. The selected test area is located above the salt dome, under the Inowroc<sup>3</sup>aw city. Since 1875 to 1991 in the Inowroclaw city was located the operated salt mine. In 1907 the mine was partly flooded and then since 1929 was re-opened and operated at the another levels. Finally, in 1991 the mine was closed and the empty cavities were filled with water. The mechanism of ground motion above the salt diapir is complex and have a few probable factors responsible for the uplift and the subsidence: lithology (uplift within the Triassic Clays perhaps due to loss of swelling and subsidence on the gypsum cap); tectonics (fault, diapir and specially salt tectonic); impact of the mining exploitation (e.g. convergence of the caverns); changes of the groundwater level. The research on terrain mobility in the region of salt dome was conducted using SAR interferometry techniques - PSinSAR and DinSAR. There were used all

available archival scenes (both descending and ascending) from the satellites ERS-1 / 2 and ENVISAT in order to determine the nature of displacement during the last 15 years. The structural geological analysis was performed in order to extend the prediction of tectonically active zones. The scope of work included analysis of archival studies of geological mapping, as well as cartographic materials relating to the area of geological structures and the salt mines documentary material. The database in GIS environment was created by tectonics, remote sensing, geophysical, geological, geodetic and structural information data. Therefore the mobility of the pilot study area using SAR interferometry techniques was analyzed together with all types of collected data. This gave preliminary conclusions about the uplift and subsidence in the salt dome area as well as gathered information about the types and causes (natural and induced) of mass movements and possibilities of preventing them in the vicinity of salt dome. During the analysis of PS dataset in the Inowroc<sup>3</sup>aw, the clear relationship was found between location of the salt generally showing uplift. In the middle of the salt structure covered by gypsum cap the subsidence was observed. Clearly, PS results should be further verified by using the precise geodetic measurements (leveling and GPS) as well as data on groundwater extraction. Nevertheless, the reported case studies show the importance of innovative PS methods and interferometry techniques for ground motion investigation above the salt structure in the Polish Lowland. Next steps in this investigation is demonstrate a potential of SAR interferometry to study terrain movements above the another areas of salt domes and diapires.

## Landslide mapping with SqueeSAR: from local to national scale

### Author(s)

Sara Del Conte <sup>(1)</sup>, Andrea Tamburini <sup>(1)</sup>, Simona Alberti <sup>(1)</sup>, Davide Colombo <sup>(1)</sup>, Massimo Broccolato <sup>(2)</sup>, Davide Carlo Guido Martelli <sup>(3)</sup>

### Department

<sup>(1)</sup>Tele-Rilevamento Europa T.R.E. s.r.l. Ripa di Porta Ticinese, 79- 20143 Milano, IT

<sup>(2)</sup>Regione Val d'Aosta Amérique, 33 - 11020 QUART, IT

<sup>(3)</sup>Imageo S.r.l. Via Valperga Caluso, 35 - 10125 Torino, IT

### Abstract

Mapping landslide distribution is traditionally based on geomorphological analysis, both from aerial-photo interpretation and field surveys. Thanks to its capability to detect millimetre level displacements over long periods and large areas, SqueeSAR analysis can be considered complementary to conventional geological and geomorphological studies. SqueeSAR represents the most recent advances of PSInSAR algorithm, and allows to obtain a significant increase in the spatial density of measurement points by exploiting signal returns from both Permanent and Distributed scatterers (PS and DS). In the framework of landslide detection and monitoring, SqueeSAR prove very helpful supporting the performance of landslide inventories at regional scale. In particular, the assessment of the degree of activity based on multi-year historical datasets can be invaluable. In case of very low (millimeters to centimeters per year) displacement rate, to assess the activity of a landslide is generally difficult or even impossible without the help of long-term displacement data. This is for example the case of Deep-seated Gravitational Slope Deformations (DGSD), characterized by large areal extent and surface displacements ranging from few millimeters to tens of millimeters per year. Thanks to its capability to detect small displacements over long periods and large areas, SqueeSAR™ analysis can be considered essential for accurate DGSD detection and monitoring at regional scale. The availability of surface displacement time series for all the radar benchmarks identified makes it also possible to change the scale of the analysis from regional to local, allowing an in depth study of the evolution of single instability phenomena, supporting the design of traditional monitoring networks, and even verifying the efficiency of remedial works. Furthermore SqueeSAR can provide valuable information on the behaviour of an area under study before the installation of any terrestrial measurement



system, provided data archives are available. During the last years several Italian Regions were studied with SqueeSAR in order to detect and monitor slope instability phenomena. One of the most successfully application was carried out on the whole Valle d'Aosta Region (NW Italy) area. Aim of the study was supporting the landslide inventory performed within the framework of the Italian Landslide Inventory (IFFI) Project, partly funded by APAT (Italian Agency for Environmental Protection and Technical Services). The study covered a time span of about twenty years, from mid 1992 to late 2010. As many unstable areas of the region were recently reactivated by the intense meteorological event, the surface displacement data provided by traditional monitoring networks were compared at local scale with the displacement measured provided by SqueeSAR. This helped in better understanding the effects of reactivation of the major landslides identified in the study area. The increasing interest of Italian regional and local authorities in the application of SqueeSAR as a standard monitoring tool to help hydrogeological risk assessment, resulted in a national project, Piano Straordinario di Telerilevamento (PST), founded by the Ministry of the Environment. Aim of the project was to create the first database of interferometric information on a national scale for mapping unstable areas. First stage of this project requested the processing of more than 12,000 ERS SAR scenes acquired over Italy, while the second stage will update these results with the Envisat images available up to 2010. In this paper, examples of integration of SqueeSAR data with other conventional geological and geomorphological studies at local and regional scale will be presented, with particular focus on DGSD which represent one of the most challenging type of landslide to be identified.

## Modeling of Small Scale Surface Deformation based on DInSAR result

**Author(s)**

Ryoichi Furuta <sup>[1]</sup>

**Department**

<sup>[1]</sup>RESTEC 1-9-9 Roppongi, Minatoku. Tokyo, 1060032, JP

### **Abstract**

Monitoring of small scale surface deformation as subsidence and landslides is very important to protect lifeline, manmade structures, buildings and houses, roads and railways, and so on. In order to monitor subsidence and landslides, several technologies were applied. However, these technologies cannot be applied to broad area and it is difficult to understand spatial distribution of affected area of subsidence and landslides. DInSAR analysis can be understand spatial distribution of affected area of subsidence and landslide, therefore, it has high prospect in Japan because Japan has a lot of sites of subsidence and landslides. However, DInSAR analysis cannot extract sub-surface information like depth of source of deformation. In order to enhance a capability of detection of small scale surface deformation as subsidence and landslide by DInSAR analysis, we proposed the integration use of DInSAR analysis and numerical model. Proposed model was applied to subsidence which was detected by ALOS PALSAR DInSAR. Target area is located in the North-East part of China. At the target area, large subsidence occurred due to coal mining activity and overuse of ground water. In order to consider way of countermeasure work for subsidence, it is important to know affected area of subsidence, depth of source of subsidence, and so on. Affected area of subsidence can be understood by the DInSAR analysis, however, depth of source of subsidence has difficult to understand by the DInSAR analysis. In order to understand the depth of source of subsidence, numerical model was necessary. Proposed model can be estimating affected area of subsidence and depth of source of subsidence, by a few parameters derived from DInSAR analysis. However, we confirmed that necessity of improvement of the model to estimate small scale surface deformation more accurately in the previous result. Proposed model was well performed in the simulation of subsidence pattern of 1-D space and it

could be estimated depth of subsidence source. However, it wasn't well performed to simulate subsidence pattern in 2-D space because we didn't consider the spatial distribution of ground stiffness. In this report, proposed model was improved to simulate subsidence pattern in 2-D space by considering the spatial distribution of ground stiffness. In order to estimate ground stiffness, DInSAR result were used. Assuming that ground subsidence pattern has related to ground stiffness, spatial distribution of ground stiffness was arranged. And based on the spatial distribution of ground stiffness, subsidence pattern of DInSAR was simulated. Through this method, effect of consideration of the spatial distribution of ground stiffness in the model was discussed by comparison of pre- and post-model. Additionally, modified model was applied to new test sites and validated by in-situ data.

## Subsidence due to fluid extraction, measured by small baseline InSAR in the Yellow River Delta, China

### Author(s)

Peng Liu <sup>(1)</sup>, Zhenhong Li <sup>(1)</sup>, Trevor Hoey <sup>(1)</sup>, Callum Dowds <sup>(1)</sup>

### Department

<sup>(1)</sup>University of Glasgow University Avenue, Glasgow, G12 8QQ, UK

### Abstract

The Yellow River, catchment area 752 000 km<sup>2</sup> and length 5464km, flows from the Tibetan Plateau through the Loess Plateau and North China Plain to reach the Bohai Sea in the Northwest Pacific. The aeolian sediment of the loess plateau is predominantly composed of 2-50 microns size particles. The plateau provides 90% of the total sediment load of the Yellow River with suspended sediment concentrations up to 37.4 kg.m<sup>-3</sup>. Before the construction of Xiaolangdi Reservoir in the middle reaches of Yellow River in 1999 more than a billion tonnes of sediment were discharged into the sea each year, generating a rapidly accreting and aggrading delta around the modern Yellow River mouth. The rate of aggradation is indicated by Borehole G-96 near the 1964-1976 (Gao et al., 1989) Diaokou Promontory of the Yellow River delta where a subaqueous delta stratum with 14C age of 3850±80 BP occurs at a depth of -17.2 m. Laser-diffraction particle size analysis and Scanning Electron Microscopy (SEM) imaging of 21 and 6 near-surface samples, respectively, from the Yellow River Delta showed that these samples share particle size characteristics and mineralogy with the Loess Plateau deposits. These properties suggest both that the delta sediments are sourced from the plateau, and that they have been changed little during transportation. Spirit level observations in the Yellow River Port between 1986 and 1997 show subsidence of 30.5 cm. This significant rate of subsidence shows the necessity of subsidence mapping in the Yellow River Delta. The Small Baseline Subset (SBAS) Interferometric Synthetic Aperture Radar (InSAR) technique identifies time series deformation of an area in a series of radar acquisitions by forming a robust small baseline Interferometric network. Small baseline interferograms are less affected by temporal and spatial decorrelation. In this study, we employ the SBAS InSAR technique in the StaMPS package to process Envisat ASAR images collected between 2007 and 2010. StaMPS selects the slowly decorrelating filtered phase (SDFP) pixels from small baseline interferograms to maintain the coherence of the interferograms over a long time interval. Radar echoes from SDFP pixels have Gaussian circular statistics and are independent from noise, and thus remain detectable over a long time period (Hooper et al., 2008). Consistent results between two descending tracks show subsidence with a mean velocity of up to 20 mm/yr in the radar line of sight direction, and also show that subsidence is not uniform across the delta. Field investigation shows an association between areas of subsidence and of petroleum extraction. In one area of the delta, the Gu-Dao Oilfield (9 square kms), we used the SBAS InSAR derived surface deformation to model the depth, location, geometry, and stress change of the deformation source using Yang's (1988) elastic Prolate Spheroid model. A prolate sphere with

semi major axis of 1.9 km and semi minor axis of 0.5 km provides a good first approximation to the InSAR derived deformation between 2007 and 2010. The subsidence observed in the vicinity of the oilfield is suggested to be caused by fluid extraction. Reference Gao, S.M., Li, Y.F., An, F.T., Wang, Y.M., Yan, F.H. (1989). The Formation and sedimentary environment of Yellow River Delta. S-Publishing Inc, Beijing. (in Chinese) Hooper, A. (2008). A multi-temporal InSAR method incorporating both persistent scatterer and small baseline approaches. GEOPHYSICAL RESEARCH LETTERS 35(L16302). Yang, X.M., P. M. Davis, J. H. Dieterich (1988). "Deformation from Inflation of a Dipping Finite Prolate Spheroid in an Elastic Half-Space as a Model for Volcanic Stressing." J. Geophys. Res. 93(B5): 4249-4257.

## Application of Differential SAR Interferometry technique in a Dynamic Neural Network-based simulation-optimization model for subsidence prediction

### Author(s)

Nazemeh Ashrafiyanfar <sup>(1)</sup>, Wolfgang Busch <sup>(1)</sup>, Mahmud Mohammad Rezapour Tabari <sup>(2)</sup>, Maryam Dehghani <sup>(3)</sup>

### Department

<sup>(1)</sup>Clausthal University of Technology Erzstr.18, DE

<sup>(2)</sup>Shahrekord University , IR

<sup>(3)</sup>K.N.Toosi University of Technolog (KNTU) , IR

### Abstract

Simulation is an interactive preview of a real system behavior. It is a powerful tool for analyzing and forecasting complex systems. In this research, the results of Differential SAR Interferometry (DInSAR) and groundwater system data were used to develop of a subsidence dynamic model in Hashtgerd plain between years 2003 and 2008. Hashtgerd area, in the vicinity of Tehran in Iran, is subject to the land subsidence due to groundwater over-exploitation in the recent years. The study area is mainly covered by cultivated lands and most of the water required for agriculture is provided by pumping wells. The lowering of the groundwater table shows that, there is excessive pumping. For detection and monitoring of subsidence in the area, a Differential SAR Interferometry (DInSAR) was used using 21 ENVISAT data ordered by ESA. To reach the temporal behavior of subsidence between years 2003 and 2008, time series of subsidence were calculated using the Small Baseline Subset (SBAS) algorithm. Moreover, to connect separate networks of the interferograms a smoothing constraint is integrated with the least square solution. This smoothing constraint reduces a part of atmospheric noise, orbital and unwrapping errors of the time series. Existing groundwater data between years 2003 and 2008 was collected and processed to use in a proper dynamic back-propagation neural network structure. The most important effective and accessible parameters on subsidence condition in Hashtgerd were groundwater table data from piezometric wells and aquifer system's discharge rate from operation wells. Groundwater table data for proper time intervals are extracted from piezometric well data. Using the position of piezometric wells, the groundwater table can be spatially interpolated for every pixel of the results of DInSAR. Furthermore, to calculate discharge rate of the aquifer system, operation wells are used. It is done based on pixel size of the results for subsidence from DInSAR and number of the existing operation wells in every pixel. Afterward, total value of discharged groundwater for every pixel will be calculated. With these data, time series of groundwater discharge is calculated. The dynamic neural network has memory and its response in any given time depends not only on the current input, but also on the history of the input sequence. The processed groundwater data and time series of DInSAR were used in a special way in the dynamic network. We defined inputs, output and decision variables of the simulator model to have the optimum objective function of the simulation. The results of the

simulation with Levenberg- Marquardt algorithm in dynamic network show comparable results with the results of time series of subsidence from DInSAR. However, we used a kind of Particle Swarm Optimization algorithm (PSO) to optimize the simulation procedures. The results of the simulation, using Particle Swarm Optimization algorithm (PSO) show highly similarity with the results of DInSAR. Based on the developed model, we can predict the subsidence for some time periods after 2008. This dynamic model helps us to formulate subsidence function and yield valuable information about relations of groundwater system and subsidence rates. The relation between groundwater condition and amount of subsidence in most parts of Iran has not been determined yet. This development will be done for the first time to study simultaneously both temporal and spatial behavior of subsidence and its interactions with the groundwater system by applying dynamic artificial neural networks. This model helps us to simulate and predict subsidence behavior in the area and to reduce possible impacts from the subsidence, especially in case with lacking ground measurements.

## Landslide detection in the Three Gorges region (China) using Small Baseline InSAR time-series techniques

### Author(s)

Andrew Singleton <sup>(1)</sup>, Zhenhong Li <sup>(1)</sup>, Trevor Hoey <sup>(1)</sup>

### Department

<sup>(1)</sup>University of Glasgow Geographical and Earth Sciences, East Quadrangle, University of Glasgow, University Avenue, Glasgow,, UK

### Abstract

Landslides have long been the most frequent and widespread geohazard in the Three Gorges region, predominantly caused by high slope gradients, susceptible lithologies, heavy summer rainfall and human activities. Over the last decade, the construction of the Three Gorges dam project has created a 600 km long reservoir with a bi-annual fluctuating water-level which has also been shown to reactivate ancient landslides (Wang et al., 2008a). Probabilistic hazard maps generated through GIS techniques can cover wide areas (e.g. Bai et al., 2010), while GPS monitoring systems can precisely monitor existing landslides (e.g. Li et al., 2010). However, the development of InSAR techniques has demonstrated the ability to monitor ground deformation with millimeter precision over large areas providing the coherence is high (Bamler & Hartl, 1998) and offers the most comprehensive method for detecting and monitoring landslides in the Three Gorges region. Within the Three Gorges region, major limitations include atmospheric water vapour, steep slopes and temporal decorrelation between SAR image acquisitions caused by dense vegetation which has led to previous studies installing corner reflectors on unstable slopes (e.g. Xia et al., 2004). The identification of persistent scatterers in a time-series of SAR images (Ferretti et al., 2001; Hooper et al., 2007) can create a wider network of stable phase measurements from which terrain displacement can be measured, and has been applied to urban areas within the Three Gorges (Wang et al., 2008b). This study therefore aims to extend slope stability analysis to non-urban areas using PS-InSAR time-series techniques.

Data from two sensors have been employed in this study to help verify the results without ground reference data. Ten descending TerraSAR-X High Resolution Spotlight images with a time interval of 11 days were collected between February 2009 and May 2009. In addition, 13 Envisat ASAR C-band images from the ascending track 068 were collected between December 2008 and March 2010 with a time interval of 35 days. Due to the dense vegetation coverage, the Small Baseline InSAR method implemented within the StaMPS/MTI package (Hooper et al., 2007) led to an acceptable density of highly coherent pixels in order to generate a mean velocity map and associated time-series graphs of surface deformation in the radar line of sight direction.

Despite the shorter wavelength, the faster repeat cycle and higher spatial resolution of the TerraSAR-X images lead to increased coherency and a greater density of PS points over a relatively small area. In contrast, the Envisat ASAR data cover much larger areas but suffer from a low density of PS points and are less sensitive to ground movements. These complementary data sources evidently show that slopes bordering the Yangtze River subsided by ~1 cm between February and April 2009 when the reservoir water-level was high. This movement seemingly stabilized after May when the water-level was lowered to accommodate the summer monsoonal rainfall. To improve the reliability of these measurements, four steps are required and will be the focus of future work: (1) extend the time-series to consider the effects of reservoir water-level lowering in other years; (2) apply the atmospheric correction models developed at the University of Glasgow to further reduce atmospheric water vapour effects on radar measurements; (3) model slope stability in response to geological and hydrological parameters; and (4) validate our results using field measurements.

With continued landsliding expected over the coming decades, accurate monitoring of slope stability over large areas of the Three Gorges region is vital to mitigate negative effects on local populations.

### References

- Bai, S., Wang, J., Lu, G., Zhou, P., Hou, S., and Xu, S., 2010. GIS-based logistic regression for landslide susceptibility mapping of the Zhongxian segment in the Three Gorges area, China. *Geomorphology* 115(1-2): 23 – 31.
- Bamler, R., and Hartl, P., 1998. Synthetic aperture radar interferometry. *Inverse Problems* 14: R1 – R54.
- Ferretti, A., Prati, C., and Rocca, F., 2001. Permanent scatterers in SAR interferometry. *Transactions on Geoscience and Remote Sensing* 39(1): 8 – 20.
- Hooper, A., Segall, P., and Zebker, H., 2007. Persistent scatterer interferometric synthetic aperture radar for crustal deformation analysis with application to Volcán Alcedo, Galápagos. *Journal of Geophysical Research* 112: B07407.
- Li, D., Yin, K., and Leo, C., 2010. Analysis of Baishuihe landslide influenced by the effects of reservoir water and rainfall. *Environmental and Earth Sciences* 60(4): 677 – 687.
- Wang, F., Zhang, Y., Huo, Z., Peng, X., Araiba, K., and Wang, G., 2008a. Movement of the Shuping landslide in the first four years after the initial impoundment of the Three Gorges Dam Reservoir, China. *Landslides* 5(3): 321 – 329.
- Wang, T., Perissin, D., Liao, M., and Rocca, F., 2008b. Deformation monitoring by long term D-InSAR analysis in Three Gorges Area, China. In: 2008 IEEE International Geoscience and Remote Sensing Symposium, Boston, 6th – 11th July 2008. Institute for Electrical and Electronics Engineers. pp. IV5 – IV8
- Xia, Y., Kaufmann, H., and Guo, X., 2004. Landslide monitoring in the Three Gorges area using D-InSAR and corner reflectors. *Photogrammetric Engineering and Remote Sensing* 70(10): 1167 – 1172.

### Acknowledgements

This work is supported by an EPSRC industrial scholarship to AS. Part of this work is supported by the Natural Environmental Research Council (NERC) through the GAS project (Ref: NE/H001085/1) as well as by a China NSFC Project (ID: 41074005/D0401). The TerraSAR-X and ENVISAT images were supplied through a TSX AO project (ID: LAN0112) and the ESA-MOST Dragon 2 Cooperation Program (ID: 5343) respectively.

# DInSAR analysis of aquifer compaction due to ground water extraction in the Segura River Basin

## Author(s)

Jose Fernandez <sup>(1)</sup>, Gerardo Herrera <sup>(2)</sup>, Pablo J. Gonzalez <sup>(3)</sup>, Roberto Tomás <sup>(4)</sup>

## Department

<sup>(1)</sup>Instituto de Geociencias, (CSIC-UCM), Fac. Cc. Matemáticas, Plaza de Ciencias, 3, Ciudad Universitaria, 28040 Madrid, Spain. , ES

<sup>(2)</sup>Área de Investigación en Peligrosidad y Riesgos Geológicos, Departamento de Investigación y Prospectiva Geocientífica, Instituto Geológico y Minero de España, ES

<sup>(3)</sup>Department of Earth Sciences, University of Western Ontario, Biological & Geological Sciences Building, London, Ontario, N6A 5B7, CN

<sup>(4)</sup>Departamento de Ingeniería de la Construcción, Obras Públicas e Infraestructura Urbana, Escuela Politécnica Superior, Universidad de Alicante, ES

## Abstract

The aim of this work is to analyze the subsidence affecting the whole Segura River Basin (1900 km<sup>2</sup>) using Differential Interferometry (DInSAR). This technique is capable of estimating mean deformation velocity maps of ground surface and displacement time series from Synthetic Aperture Radar (SAR) images. A dataset acquired between 1992 and 2008 from ERS and ENVISAT sensors has been processed measuring the highest rates of groundwater-related subsidence recorded in Europe (>10 cm/yr). These data have been validated against ground subsidence measurements and correlated with subsidence triggering and conditioning factors by means of a Geographical Information System (GIS). Retrieved results have permitted to improve the knowledge of the mechanisms that control aquifer compaction due to ground water extraction, and the associated effects in the buildings and infrastructures of exposed urban areas. As a consequence, the deeper understanding of this kind of phenomenon will be helpful to improve the management and control of the aquifer systems located in this part of the South-East Mediterranean, being applicable to any other similar region.

# Non-linear land subsidence in Morelia, Mexico, imaged through Synthetic Aperture Radar Interferometry

## Author(s)

Francesca Cigna <sup>(1)</sup>, Batuhan Osmanoğlu <sup>(1)</sup>, Enrique Cabral-Cano <sup>(2)</sup>, Timothy H. Dixon <sup>(1)</sup>, Shimon Wdowinski <sup>(1)</sup>

## Department

<sup>(1)</sup>University of Miami 4600 Rickenbacker Causeway, Miami, FL 33149-1098, USA

<sup>(2)</sup>Universidad Nacional Autónoma de México Ciudad Universitaria, 04510, MX

## Abstract

Synthetic Aperture Radar Interferometry (InSAR) and Persistent Scatterer Interferometry (PSI) are used to investigate spatial and temporal patterns of land subsidence in Morelia, Central Mexico. Past tectonics related to the Morelia-Acambay fault system controlled the overall development of the region and the formation of its horst-graben structure with variable thickness of sediment and volcanic products infill. Since the early 1980's the city of Morelia is experiencing subsidence associated with groundwater over-exploitation, leading to declining groundwater levels, compaction and loss of porosity in the aquifer, and ultimately land subsidence. ENVISAT ASAR images acquired between 2003 and 2010 are analyzed over the study area, 20 x 16 km.

The deformation field observed through PSI reflects both control from past tectonics and influence from groundwater withdrawal. Subsiding areas are distributed as either concentrated circular patterns centered around water wells, or as elongate patterns parallel to major faults (e.g., La Colina, La Paloma and Central Camionera). High subsidence rates are measured on the hanging wall of major normal faults coinciding with the thickest sediment deposits. Strong contrasts in subsidence rates are identified across major basin-bounding faults. For the PSI analysis the deformation is modeled to have a constant velocity through time, and agrees well with over 90% of the investigated area. We use four differential interferograms to investigate time variable deformation in selected areas. Time-lapse analysis of ground deformation with conventional InSAR reveals accelerations of subsidence north of the La Colina fault and the meander area of the Rio Grande river, in the central sector of the city. For this latter area, we identify well-marked patterns and very high displacements, corresponding to the location of the Prados Verdes II water well. Deformation rates as high as 10-15 mm/yr are measured in 2003-2004. Acceleration of subsidence is observed in 2005, corresponding to the recasing of the well and the consequent decrease of the static level. Measured rates reach 40-50 mm/yr in 2006-2007, and 75-80 mm/yr in 2008-2009. Profiles of cumulative LOS displacements, time-lapse velocities and accelerations between the different time spans are analyzed along a transect crossing both the water well and the Central Camionera fault. Up to 15 cm of cumulative deformations are measured in 2003-2009 near the water extraction location. Average acceleration ranges between 10-15 mm/yr<sup>2</sup> in 2003-2005 and 2008-2009, while maximum values are observed in 2005-2006, reaching 25 mm/yr<sup>2</sup>. Two circular and adjacent areas of intense land deformation are identified in 2008-2009, suggesting the existence of either a local change of the aquifer sediment hydraulic properties inducing a local decrease of subsidence between the two peak areas, or localized shallow groundwater recharge from the Rio Grande river, which would partially counteract the local water table decrease from groundwater extraction. A sharp gradient in ground subsidence values is also observed across the Central Camionera fault, highlighting higher subsidence rates in its hanging wall block. Although a recent accelerating subsidence feature is identified for this area, most of the city does not yet exhibit extreme subsidence rates, suggesting that improved water resource management could greatly reduce the long term subsidence.

## Operational Validation of the Accuracy of InSAR Measurements over an Enhanced Oil Recovery Field

### Author(s)

Michael Henschel <sup>(1)</sup>, Brad Lehrbass <sup>(1)</sup>, Shiya Sato <sup>(1)</sup>

### Department

<sup>(1)</sup>MDA Geospatial Services , CA

### Abstract

This paper presents a methodology for monitoring fast, strong ground deformation in a difficult environment with the RADARSAT-2 satellite. The original aim of the monitoring was to capture the ground change present due to an aggressive enhanced oil recovery program. The ground deformation was expected to be on the order of several centimetres per month with a spatial extent of a few hundreds of metres. In early 2010, a field of corner reflectors was installed over the oil field to be monitored in Northern Alberta. The spatial gradient of the ground change was originally assumed to be less than 2.5 cm/500 m (in one twenty-four day observation period) and the field of reflectors was installed with this assumption in mind. With observations, however, it has been shown that the spatial gradient can actually approach a maximum rate of three to four fringes between adjacent corner reflectors. If a single track of data (with observations every 24 days) had been employed in the monitoring, then the true extent of the ground change could not have been known using the corner reflector measurements alone. At times, even twice the

sampling rate would have missed the actual fringe rate. This is a key criterion for the design of a spatial sampling field over an enhanced oil recovery operation. To categorize the field, a series of 8 beam modes from the RADARSAT-2 satellite were used. The resulting time series of images provides interferometric measurements that are spaced over very short periods of time. That is, each series of images (each beam mode or track) provides an interferometric measurement over a period of 24 days but the image acquisition from each time series is staggered by approximately 3 days thus providing multiple observations of the same deformation signal. The agreement between the observed data provides an excellent characterization of the accuracy of the measurements made.

## Posters on Cross Interferometry

### ERS – ENVISAT cross-interferometry over the Athens metropolitan area

#### Author(s)

Ioannis Papoutsis <sup>(1)</sup>, Charalabos Kontoes <sup>(2)</sup>, Demitris Paradissis <sup>(1)</sup>

#### Department

<sup>(1)</sup>National Technical University of Athens , GR

<sup>(2)</sup>National Observatory of Athens , GR

#### Abstract

Cross-interferograms, formed by an ENVISAT ASAR and ERS-2 pair, present interesting characteristics, mainly due to the 28 minute time difference between the two SAR acquisitions. The inherent problem of cross-interferometry is the 31 MHz difference of the carrier frequency of the two sensors, leading to a large spectral shift. This shift can be cancelled by using those pairs that have a perpendicular baseline of about 2 km (sign sensitive). However such large baselines introduce an altitude of ambiguity of a few meters, giving rise to significant volume decorrelation effects and limiting the application of the technique to flat areas or in rolling topography. In this work the above characteristics of cross-interferometry are identified and examined for the Athens metropolitan area, which comprises of a mixture of topographic landscapes: flat, hilly and urban areas, aiming at DEM reconstruction and coherence map generation. Parameters that are taken into account include the land cover type and the terrain slope that affects the surface scattering mechanism. Additionally, an attempt to unwrap the noisy cross-interferograms is made, using existing phase unwrapping techniques, such as minimum cost flow, weighted least mean squares and residues branch cut. The processing of the data provided by ESA was mainly performed by the GAMMA SAR software.



# Poster Session II

## Posters on Atmosphere I and II

### Atmospheric effects detection by short baseline processing in RADARSAT time series over Manaus city, Amazon region

Author(s)

Fernanda Ledo G. Ramos <sup>(1)</sup>, Giovanni Nico <sup>(2)</sup>

Department

<sup>(1)</sup>Universidade Federal do Rio de Janeiro – COPPE/UFRJ Centro de Tecnologia, Bl. I214, Cid.Universitária, I. do Fundão, 21949-900 Rio de Janeiro BR

<sup>(2)</sup>Consiglio Nazionale delle Ricerche (CNR), Istituto per le Applicazioni del Calcolo (IAC) Via Amendola 122/D 70126 Bari, IT

#### Abstract

The preliminary results obtained by the first orbital interferometry study over Amazon region (Solimões Project) indicates an area of crustal movement located adjacently to a circular drainage feature inside Manaus city urban area. It's expected that the final analysis will include an improved understanding of the geological activities and crustal motion in the Amazon Basin that is characterized by an annual cycle of vertical displacement with amplitude of 50-75 mm measured by a GPS station near the centre of the basin. This is considered a large crustal oscillation and indicates the lithosphere is subsiding and rebounding in response to changes in the weight of the Amazon River system flow. The Amazon River annually cycles through a vertical height range of 10-15 m. The primary impediment to a wider application of InSAR technology is the traditional limitation to arid regions in the world. The moisture in the air column affects the SAR signal travelling speed and it's evidence is presented as false ramps or fringes in the interferograms. In temperate regions the rate of change of the moisture content is gradual (> 17 km) and can be removed with a high-pass filter. In tropical regions, as Amazon area, the depth of the atmosphere and rapid changes in moisture content produces highly variable results. A previous analysis of RADARSAT dataset over Manaus region evidenced important phase artefacts possibly due to the temporal variations of the Precipitable Water Vapour (PWV). Atmospheric artefacts are severe over regions such as Amazon, characterized by an important plant transpiration phenomenon. In this work we present an analysis of RADARSAT-1 and RADARSAT-2 times series acquired from 2006 to 2010 aiming to confirm the presence of atmospheric artefacts. The dataset was interferometrically processed using a short-baseline strategy, i.e. all interferometric pairs characterized by the shortest temporal baselines were identified. In this dataset the temporal baseline corresponds to the shortest temporal baseline which can be achieved using the Radarsat mission, 24 days. The InSAR processing of those pairs results in SAR interferograms containing the smallest contribution from possible terrain displacements due to geological phenomenon or anthropic activity. The interferometric phase was analysed to detect the presence of atmospheric artefacts. The rotational invariant spectrum of interferograms was computed and compared to the Kolmogorov spectrum typical of a turbulent medium to detect the signature of atmosphere. The scaling exponents of the power spectrum were computed and compared to that of the Kolmogorov power law. A statistical analysis of phase values was also conducted aiming to assess the gaussianity of the atmospheric artefacts in SAR interferograms. Furthermore, the Radon transform of the interferometric phase was analysed to detect the isotropic properties of atmospheric phenomena. The gaussianity of the atmospheric artefacts in

SAR interferograms was also tested. Topography effects were removed using the available SRTM Digital Elevation Model of the region. Besides this analysis, the presence of atmospheric artefacts in SAR interferograms was confirmed by the available measurements of the atmospheric parameters (air temperature, pressure, relative humidity, wind speed and direction, precipitation) over the studied area provided by the Brazilian Aeronautic Centre of Meteorology.

## Mitigation of atmospheric phase delay artefacts in interferometric SAR time series

### Author(s)

Pedro Mateus <sup>(1)</sup>, Giovanni Nico <sup>(2)</sup>, Ricardo Tomé <sup>(1)</sup>, João Catalão <sup>(1)</sup>, Pedro Miranda <sup>(1)</sup>

### Department

<sup>(1)</sup>Faculty of Sciences, University of Lisbon , PT

<sup>(2)</sup>Consiglio Nazionale delle Ricerche, Istituto per le Applicazioni del Calcolo , IT

### Abstract

Synthetic Aperture Radar (SAR) interferometry is a technique that through the measurement of the interferometric phase is able to furnish information about the displacement of terrain or man made structures. This information is useful to study the phenomena causing that displacement, both its spatial distribution and temporal variation. However, the interferometric phase does not contain only information on geometrical displacement. It is affected also by a temporal delay of the electromagnetic signal caused by temporal changes in spatial distribution refractive properties of the atmosphere which causes a phase delay. This delay introduces a further “displacement” which cannot be distinguished from the one affecting the terrain or the structure to be studied. There are two components of the atmospheric phase delay, a dry component related to atmospheric pressure of dry air and temperature, more stable in time, and a wet component related to different atmospheric parameters among which the water vapour fraction in atmosphere, which is much more variable both in time and space. The irregular variations of this last component of atmospheric phase delay are the main causes of atmospheric phase artefacts affecting interferometric SAR applications. In the last few years we conducted different experiments aiming to compare atmospheric phase delay measured by GPS, MERIS sensors and NWM as the WRF weather forecasting system. The experiments were conducted over the Lisbon region where a network of 12 permanent GPS receivers has been installed. The GPS time series of the dry and wet vertical delay estimations covers the time interval between the first and last interferogram. We found that the GPS estimates of the atmospheric phase delay are in good agreement with that computed from WRF numerical data. In particular, the wet component measured by GPS data is well explained in terms of WRF numerical data. The MERIS instrument on board of ENVISAT, provides maps of water vapour that can be used to mitigate the atmospheric effects in InSAR maps. The MERIS water vapour maps has a horizontal resolution as fine as 260 m × 290 m (FR, full resolution) and 1040 m × 1160 m (RR, reduced resolution). Limitations of MERIS are mainly related to the need for clear sky and sun illumination conditions. In this work we use the results of the above experiments to devise strategies to mitigate atmospheric phase delay artefacts in SAR interferograms. A set of 6 ENVISAT ASAR images were acquired during the period from April, 12 to November, 8 2009. The ASAR images were processed in a manner to minimize the temporal baseline resulting in 5 interferograms. Precise orbits were used. The topographic component was removed in all interferograms. Furthermore, in the studied period this area was not affected by tectonic movements giving rise to large scale terrain deformations. For this reason it is reasonable to assume that the phase measured in each interferogram is mainly related to temporal changes in the atmospheric phase delay properties, especially at large spatial scales. This InSAR dataset was used to quantify the mitigation of atmospheric phase artefacts. Three approaches were chosen to mitigate these artefacts. The first

approach is based on the GPS measurements interpolated in space in order to generate a synthetic phase image to be used in the mitigation operation. A second approach uses MERIS measurements of phase delay measurements. In this approach, algorithms have been developed to properly fill holes in MERIS maps due to presence of clouds or bad data in MERIS images, to estimate atmosphere phase delay maps. Also in this case the final product is a synthetic phase image computed from phase delay measurements. Finally, the third approach relies on WRF numerical data to compute the synthetic phase delay image used to mitigate atmospheric artefacts due to electromagnetic wave propagation. Effectiveness of the above approaches is quantified in terms of a statistical analysis of SAR interferograms before and after the mitigation operation. Advantages and disadvantages of the three approaches are discussed also in terms of their operational use. Keyword: Synthetic Aperture Radar (SAR), SAR interferometry (InSAR), Global Positioning System (GPS), MERIS, Weather Forecasting and Research System (WRF), Atmospheric phase delay.

## Estimating ASAR atmospheric propagation phase delay from MERIS data: a case study

Author(s)

Gianfranco Fornaro <sup>(1)</sup>, Luca Paglia <sup>(1)</sup>

Department

<sup>(1)</sup>CNR Via Diocleziano, 328, IT

### Abstract

Developments and applications of the Differential Interferometric SAR (DInSAR) technique have boosted the use of the SAR in support to quantitative analysis in many areas of the environmental risks such as: volcanic, seismic and landslides risks. Currently, coherent processing of long series of multipass SAR data via multitemporal DInSAR, also known as Advanced DinSAR (A-DInSAR) or DInSAR stacking, is a powerful and well recognized tool to monitor ground deformations, that provides a number of advantages over classical geodetic techniques in terms of data accessibility, coverage and costs. The availability of large SAR data archives and their easy accessibility allows A-DInSAR techniques to generate deformation time series spanning intervals of decades. In parallel to the systematic application of DInSAR, the current scientific literature in this field is addressing research topics whose aim is to improve the performance of the DInSAR processing chains, especially in terms of coverage and accuracy of measurements. DInSAR data are affected by many factors that cause the presence of spurious phase variations, which impact the quality of the estimated results. Among them the Atmospheric Propagation Delay (APD) impacts the accuracy of the final product. APD is mainly due to the presence of water vapor concentration in the troposphere that causes a variation of the refractive index from pass to pass and, as a consequence, a variation of the electromagnetic radiation propagation delay. APD variation is a phenomenon that in the past has dramatically limited the use of the DInSAR techniques based on the analysis of only individual or few differential interferograms. Modern interferometric SAR techniques are based on the joint use or, better, on the stacking of multipass SAR data stacking and effects of APD variation are tackled by filtering in accordance with the spatiotemporal statistical characterization of the noise source. More specifically by assuming that APD contributions are spatially correlated and temporally uncorrelated, the interferogram stacking techniques automatically estimate and subtract the APD contributions from the retrieved deformation signal. On one hand, it is thus evident that errors in the APD signal estimation lead to errors in the retrieved deformation signal. Typically such errors mainly affect the non linear component of the deformation signal: nonetheless erroneous APD estimations may also impact the evaluation of weak linear deformation components such as, for instance, those typically observable in the inter-seismic phase over faults. Another important limitation associated with

the presence of APD is related to the use of the multitemporal DInSAR techniques in emergency situations: In these cases typically only few acquisitions are available and therefore APD temporal filtering becomes critical. These motivations have recently stimulated the research in the use and integration of SAR data and information of other instruments commonly used for atmospheric radiation delay determination. By measuring radiation in the near-IR channels, multispectral imaging spectrometers allow obtaining, as a product, a rather accurate estimation of the Integrated Water Vapor (IWV). This product, after a proper calibration, is used as external information for reducing the effects of APD variations in the interferograms generated by using ASAR data, thus improving the estimation of ground deformation measurements. However, in any case the analysis is restricted to interferograms and no explicit comparison with the products derived via interferometric stacking techniques is carried out. The question regarding the "reliability" of the APD estimates from radar sensors and of the possible integration between radar and multispectral data for mitigation of the effects of APD, particularly in emergency situations, is still an open issue. In this work we performed an analysis aimed at comparing the APD product from a Small Baseline Subset (SBAS) DInSAR technique: The investigated area is in the Campania region in Italy

## Atmospheric corrections of Interferometric Synthetic Aperture Radar observations: comparison of GPS Radio Occultation, Global Atmospheric Models (GAM), MODIS and MERIS

### Author(s)

Aydin Shahbazi <sup>(1)</sup>, Mahdi Motagh <sup>(1)</sup>, Mohammad-Ali Sharifi <sup>(1)</sup>

### Department

<sup>(1)</sup>University College of Engineering, University of Tehran, IR

### Abstract

Phase delay caused by variable atmospheric conditions at the time of two SAR acquisitions presents one of the major limitations of repeat-pass Interferometric Synthetic Aperture Radar (InSAR) measurements, which can compromise the accuracy of deformation maps derived from InSAR. Great efforts have been made in the past to devise methods for properly estimating the extent to which InSAR measurements are affected by atmospheric artifacts. In this paper, we evaluate and compare advantages and disadvantages of 4 methodologies for atmospheric corrections in InSAR observations: (1) GPS Radio Occultation using data from Constellation Observing System for Meteorology Ionosphere and Climate (COSMIC) mission, (2) Global Atmospheric Models (GAM) using data from National Centers for Environmental Prediction (NCEP), (3) the near-IR water-vapor products provided by Moderate Resolution Imaging Spectroradiometer (MODIS) instrument and (4) water vapor content estimated from Envisat Medium Resolution Imaging Spectrometer (MERIS). Limitations and constrains of the above methodologies for mitigating atmospheric artifacts are investigated for a series of Envisat InSAR observations over Etna Mountain in Italy.

# Comparison of Interferometric SAR and Multispectral time series for determination of Atmospheric Phase Screen

Author(s)

Paolo Pasquali <sup>(1)</sup>, Alessio Cantone <sup>(1)</sup>, Paolo Riccardi <sup>(1)</sup>

Department

<sup>(1)</sup>Sarmap s.a. Cascine di Barico, 6989 Purasca, CH

## Abstract

Although SAR Differential Interferometry established in the last years as reliable tool for the measurement of very small land displacements, it has also become evident that the phase disturbances resulting from the propagation of the radio signals through a temporally and spatially varying atmosphere cannot be completely neglected. The so-called Atmospheric Phase Screen (APS) can introduce, in severe cases, errors as large as centimetres or even tens of centimetres in the estimated deformations. The introduction of Interferometric Stacking techniques, like the Small Baseline Subset (SBAS) and the Persistent Scatterers (PS) approaches, based on the analysis of Interferometric SAR time series, allowed both to extend the estimation of single displacements to their monitoring over long time periods, and to separate the temporally systematic effects, mainly due to geological phenomena, from temporally incoherent ones, ascribed in general to the APS. This process resulted in more accurate single deformation measurements and, indirectly, in estimates of the date-by-date contribution of the atmospheric variability. Recently, independent approaches based on the modelling of the phase effects due to the heterogeneity of the atmospheric water vapour as derived from Multispectral imagery have been successfully applied to the estimation of the APS, also improving the possibility of obtaining accurate deformation measurements from single differential interferograms. These approaches rely on the availability of Multispectral acquisitions, that are both as far as possible cloud - free and as temporally close as possible to the SAR acquisitions: for this reason the ESA ENVISAT mission, with both the Advanced SAR (ASAR) and the MEdium Resolution Imaging Spectrometer (MERIS) instrument on board, capable of simultaneous acquisitions, is a very interesting platform to exploit with such techniques. Typically, the APS estimation as performed during the Interferometric Stacking processing relies on some assumptions on and parameterizations of the type of spatial and temporal correlation of the signals that can be interpreted as land displacement or vice-versa as APS, and these assumptions can be made in general on a global basis; the exploitation of different and independent measures like those derived from multispectral datasets enables to relax these assumptions and to update them on a date - by - date basis. Vice - versa, the APS estimation as performed based on Multispectral (and MERIS in particular) imagery relies on assumptions about the geometrical location (height) of the water vapour fields that finally affect the interferometric phase. This paper compares the two approaches and results in the estimation of the APS, and the corresponding land displacement measurements as obtained from Interferometric Stacking techniques and from water vapour modelling from Multispectral acquisitions, based on a time series of 32 ENVISAT ASAR and MERIS data pairs, acquired in the period between 2002 and 2010 over the Dead Sea area. This analysis allows to better identify the advantages and disadvantages of the two approaches, to quantify the dependence of the quality of the estimated APS from different parameter settings and assumptions, and to draw better conclusions on the final accuracy that can be expected in the measured deformations. Furthermore, it can be shown how the combined exploitation of the two approaches can help in as far as possible relaxing the assumptions that are made during the separated estimation of the APS using the two single input (SAR and multispectral) data sources.

# Atmospheric phase delay estimation from multiple SAR interferometry measurements

Author(s)

Yo Fukushima <sup>(1)</sup>

Department

<sup>(1)</sup>Kyoto University, JP

## Abstract

The phase observed by most SAR interferograms includes stochastic fluctuations that are caused by radar signals propagating through disturbed atmosphere. Ionospheric phase delay is often the most prominent for L-band InSAR whereas tropospheric phase delay can be dominant for C-band. The present study focuses on estimation of such stochastic atmospheric phase signals. The detailed spatial pattern of the causes of the delay, i.e., the total electron content in the ionosphere or the water vapor in the troposphere, are important for studies such as planetary physics or meteorology as well as for weather forecasts. When the ground displacement signal is negligibly small, one can build a system of observation equations in a linear form  $d = Gm$ , where a column vector  $d$  is composed of unwrapped interferograms, a column vector  $m$  is composed of atmospheric delay for  $N$  SAR images, and the design matrix  $G$  acts as a differential operator. If one can form interferograms "connecting" all the SAR images, then the design matrix  $G$  has the maximum rank  $N-1$ , one minus the number of unknowns. This indicates that if one has an independent data set or a good guess that predict phase delay signals of one SAR acquisition, then one can solve for the phase delays of the other  $N-1$  SAR images. Alternatively, based on the philosophy that the phase delay signals should be as simple as possible, one can obtain the minimum norm solution of  $m$ . The minimum norm method was exploited in detail by performing synthetic tests. Synthetic "true" delay signals were created by assuming randomly correlated fluctuation that obeys Gaussian distribution and an exponential autocorrelation function. Then, synthetic interferograms were formed, and the linear inverse problem was solved. This test was repeated for different number of available SAR images  $N$ . A resolution analysis predicts that the standard deviation of the residuals (estimated - true) is equal to the standard deviation of the random fluctuation divided by the square root of the number of used SAR images  $N$ . The result of the synthetic test was consistent with this prediction. It is also found that the correlation coefficient for the true and estimated values becomes more than 0.9 when six or more SAR images were used ( $N \geq 6$ ). The proposed method can also be incorporated into InSAR time-series analyses for ground displacement measurements. One can first estimate the atmospheric fluctuation component from networks of small temporal baseline interferograms. Then, one can form long temporal baseline interferograms that span different networks to solve for the displacements.

# Water vapor distribution during heavy rain detected by InSAR and GPS

## Author(s)

Youhei Kinoshita <sup>(1)</sup>, Masanobu Shimada <sup>(2)</sup>, Masato Furuya <sup>(1)</sup>

## Department

<sup>(1)</sup>Hokkaido University Department of Natural History Sciences, N10W8, Kita-ku, Sapp, JP

<sup>(2)</sup>JAXA/EORC, JP

## Abstract

Interferometric Synthetic Aperture Radar (InSAR) phase signals allow us to map the Earth's surface deformation, but are also affected by the atmosphere. In particular, the heterogeneity of water vapor near the surface causes unpredictable phase changes in InSAR data. InSAR can therefore provide us with a spatial distribution of precipitable water vapor with unprecedented spatial resolution in the absence of deformation signals and other errors. On 2 September 2008, a torrential rain struck wide areas over the central Japan, and Japan Aerospace exploration Agency (JAXA) carried out an emergent observation of the heavy rain by PALSAR, an L-band synthetic aperture radar sensor. On January 2010, JAXA has carried out another PALSAR measurement of the very areas, so that we could generate InSAR image of the area and examine the detailed snapshot of the regional troposphere; the weather on January 21 2010 was dry and stable. Near Ibi River, we could detect localized signals, which changed 12.2 cm in radar line-of-sight over a spatial scale on the order of 8 km, and were unlikely to be an artifact of either ground deformation or DEM errors, or ionosphere. In the previous report (Kinoshita et al., 2010 AGU Fall Meeting), we validated this point, having shown other InSAR images as well as azimuth component of pixel-offset data. Then we concluded that the signal was due to neither ground deformation nor DEM errors, and we considered that the signal was probably not due to ionospheric effect. Now we compare the tropospheric delay in InSAR data with that derived from the GEONET data, the Japanese GPS network. The principle of atmospheric propagation delay in GPS is inherently the same as that of InSAR, therefore it is worth to compare of tropospheric delay between GPS and InSAR. We discuss what we could learn from the InSAR image and GPS zenith wet delay data.

# Atmospheric Water Vapor determination by the integration of InSAR and GNSS observations

## Author(s)

Fadwa Alshawaf <sup>(1)</sup>, Stefan Hinz <sup>(1)</sup>, Michael Mayer <sup>(1)</sup>

## Department

<sup>(1)</sup>Karlsruhe Institute of Technology, DE

## Abstract

Keywords: Interferometric SAR, GNSS, atmospheric water Vapor. High spatial and temporal variations of atmospheric water vapor cause an unknown delay on microwave signals transmitted by space-borne transmitters. This delay is considered as a major limitation in Interferometric Synthetic Aperture Radar (InSAR) applications as well as high-precision applications of the Global Navigation Satellite Systems (GNSS). Temporal variability of water vapor is well estimated from continuous GNSS measurements. On the other hand, InSAR can provide more information about the spatial variability of atmospheric water Vapor. The main goal of this work is to assimilate

InSAR phase observations and GNSS measurements collected from spatially-sparse sites to build up high spatially-resolved maps of atmospheric water Vapor. The Earth's atmosphere is divided into the ionosphere and the neutral atmosphere (neutrosphere). The ionosphere is a dispersive medium and its effect on radio signals can be eliminated by a linear combination of dual-frequency phase observations. Unlike the ionosphere, the neutrosphere is non dispersive and the neutrospheric delay has to be continuously quantified and compensated. The neutrospheric delay is divided into dry and wet delay components, the dry component can be calculated from empirical models (e.g., Saastamoinen) with high accuracy whenever air pressure observations are available. The wet component, however, is highly variable and is dominated by atmospheric water vapor. Therefore, GNSS and repeat-pass InSAR can be good sources for atmospheric water vapor sounding. Interferometric phase images derived from repeat-pass SAR systems show distortions most likely due to the temporal and spatial variations of atmospheric water vapor. These distortions are considered as a major limitation for Earth's topography and surface deformation studies. However, this effect can be dedicated for atmospheric studies. Atmospheric Phase Screens (APS) are extracted from InSAR interferograms. In this work, Persistent Scatterer Interferometry (PSI), particularly Stanford Method for Persistent Scatterers (StaMPS) is applied for that purpose. Digital elevation model of 5 m resolution is used to compensate the topographic phase and the surface deformation is minimal in the area of the study which makes its effect on the phase negligible. The atmospheric signal shown in the interferogram is the difference between two acquisitions and we aim at extracting an atmospheric image at each imaging time with the aid of an external source (currently, GNSS). In GNSS, the technique of Precise Point Positioning (PPP) is used for the purpose of water vapor calculation. PPP enables the reconstruction of the absolute excess in the signal path due to the propagation through the neutrosphere. Phase residuals are used for accurate calculation of water vapor. Site-specific effects such as Multipath errors and antenna phase center variations are compensated using a stacking method based on satellites geometries. More improvements on the results are achieved by weighing phase observations based on the signal-to-noise ratio. Results show that obtaining highly accurate series of water vapor from GPS phase observations requires involving metrological parameters in the solution. The area of Upper Rhine Graben (URG) is selected for this study since it is well-covered by homogeneously distributed permanent sites of the GNSS Upper Rhine Network (GURN). InSAR interferogram images are formed from seventeen ENVISAT acquisitions (track 294, descending orbit, and 100 km swath). Meteorological data, including 2D water vapor fields, from the numerical weather research and forecasting (WRF) model are used to validate the results achieved from GNSS and InSAR. Results show integrated water vapor values from GNSS phase observations with an accuracy of about 2-3 mm. Integrated water vapor values extracted from InSAR interferograms have to be validated using integrated water vapor maps simulated using the WRF model within the current stage of the work.

## Separating non-linear deformation and atmospheric phase screen (APS) for InSAR time series analysis using least-squares collocation

### Author(s)

Shizhuo Liu <sup>(1)</sup>, Ramon Hanssen <sup>(1)</sup>, Andrew Hooper <sup>(1)</sup>, Sami Samieiesfahany <sup>(1)</sup>, Freek VanLeijen <sup>(1)</sup>

### Department

<sup>(1)</sup>Delft University of Technology, NL

### Abstract

Effective separation of atmospheric phase screen (APS) and ground deformation is crucial for ground deformation monitoring based on InSAR time series analysis. The difficulty for APS



modeling mainly comes from the high spatial-temporal variation of water vapor in the lower troposphere. Moreover, ground deformations often show non-linear behaviors (in time) which are difficult to be modeled deterministically by functional models. Here, we propose a method based on least-squares collocation theory [1], which gives the best unbiased estimation and prediction of the parameters of interest, to estimate ground deformation with the best possible accuracy in the presence of APS. In many InSAR time series studies e.g., [2][3], ground deformation is often modeled deterministically via functional models (e.g., linear, quadratic and periodic, etc) based on a priori knowledge about the deformation in the area of interest. However, in practice many ground deformations are too complex to be completely modeled by functional models. In these cases, the stochastic characteristics of the complex deformations should be taken into account and modeled accordingly. A precise modeling of the APS should consider its temporal variability, i.e. some SAR images were acquired during bad weather when water vapor fluctuations are very strong and some were acquired when the local troposphere was calm. Moreover, the spatial variability of APS should also be taken into account. This is because the power of APS on average increases with an increase of the spatial distance between two pixels [4]. Such behavior of APS can usually be observed via a structure analysis based on tandem interferograms [4]. When the local land topography in the area of interest has a significant variation, e.g., in mountainous regions, the APS is also scaled by the height differences between ground pixels. Such height dependent phenomenon is known as the atmospheric vertical stratification [4]. The method proposed in this study only requires a time series of SAR interferograms as inputs. The method is implemented for PSInSAR [2] but can be adapted to other time series based approaches such as the small baseline approach [3]. Compared with the traditional spatial-temporal filtering method commonly used in many studies e.g., [2][3], our algorithm takes the spatial-temporal variability of APS into account. Moreover, it attempts to model the complex ground deformation not only with a functional model but also using a stochastic model. To evaluate our algorithm we carry out a case study over Mexico City that has been undergoing a rapid ground subsidence. The functional part of the subsidence is modeled by a quadratic polynomial. A Gaussian variance-covariance model is used to model the stochastic part of the subsidence. The spatial-temporal variation of APS is modeled by a variance-covariance function from the Matern-family [5]. The APS estimation based on our algorithm shows a good agreement with the MERIS water vapor products which were acquired simultaneously with the SAR images. Moreover, our algorithm is able to identify the areas that have been undergoing different subsiding processes (i.e., linear, quadratic and more complex), which is not possible using the traditional filtering method. References [1] P.J.G. Teunissen, "Least-squares prediction in linear models with integer unknowns," *Journal of Geodesy*, vol.81, pp.565-579,2007. [2] A. Ferretti, C. Prati, and F. Rocca, "Nonlinear subsidence rate estimation using permanent scatterers in differential SAR interferometry," *IEEE Transactions on Geoscience and Remote Sensing*, vol. 38, pp. 2202–2212, Sept. 2000. [3] P. Berardino, G. Fornaro, R. Lanari, and E. Sansosti, "A new algorithm for surface deformation monitoring based on small baseline differential SAR interferograms," *IEEE Transactions on Geoscience and Remote Sensing*, vol. 40, no. 11, pp. 2375– 2383, 2002. [4] R. F. Hanssen, *Radar Interferometry: Data Interpretation and Error Analysis*. Dordrecht: Kluwer Academic Publishers, 2001. [5] M. L. Stein, *Interpolation of Spatial Data; Some Theory for Kriging*. Springer Series in Statistics, Springer, 1999.

# Posters on Methods- General

## InSAR time series analysis of land deformation, North West of Iran

### Author(s)

Mohammad Mohseni Aref <sup>[1]</sup>, Mehdi Motgh <sup>[2]</sup>

### Department

<sup>[1]</sup>Department of Water Resources, Islamic Azad University, Branch Shiraz Iran, IR

<sup>[2]</sup>Department of Surveying and Geomatics Engineering, University College of Engineering, University of Tehran, IR

### Abstract

Interferometric Synthetic Aperture radar (InSAR) technique has proven to be a powerful technique for providing accurate measurement of ground deformation in developed aquifer systems. In this study, we use the integration of InSAR measurements with ground-based observations obtained from precise leveling and GPS techniques to study land surface deformation in Khoy, Salmas, Tasouj, Marand and Shabestar agricultural regions in Northwest of Iran. Earlier InSAR study showed that C-band Envisat Interferometry had very limited success to measure and map the spatial and temporal pattern of surface deformation in the region, mainly due to rapid temporal decorrelation associated with the agricultural field. Here we focus on L-band Interferometric data acquired in the area by the ALOS satellite during 2006 and 2010 to partially overcome the decorrelation sustained by the phase signal in C-band measurements, and apply modified SBAS and stacking techniques on ALOS data to derive the time-series and mean velocity of surface deformation.

## Landslides forecasting analysis by time series displacement derived from satellite InSAR data: preliminary results

### Author(s)

Paolo Mazzanti <sup>[1]</sup>, Alfredo Rocca <sup>[2]</sup>, Francesca Bozzano <sup>[2]</sup>, Roberto Cossu <sup>[3]</sup>, Mario Floris <sup>[4]</sup>

### Department

<sup>[1]</sup>NHAZCA s.r.l. - Spinoff "Sapienza" Università di Roma , IT

<sup>[2]</sup>"Sapienza" Università di Roma , Italy

<sup>[3]</sup>ESA, IT

<sup>[4]</sup>Università degli studi di Padova , IT

### Abstract

Slope instabilities are caused by several complex processes taking place at different level: geological and hydrogeological, climatic, (e.g. rainfall distribution or freeze-thaw cycles), earthquakes, volcanism, human activities etc. The combination of these factors and processes can lead to an instability condition that is manifested by mass movements of slopes occurring under the action of gravity. Landslides rarely behave as a rigid body that responds instantly to stresses. More frequently, especially in cases of large landslides (> 500.000 m<sup>3</sup>), they are characterized by a strain pattern (i.e. displacement), increasing over time. This particular behaviour is known as "creep". Starting from the basic theory of creep, several efforts have been done over the last decades in order to develop forecasting solutions for landslides. The most used approach to address the problem is the semi-empirical one, since it is the most reliable in forecasting analysis. Several semi-empirical models to predict the instant of collapse of slopes, as a function of velocity variation over time, have been proposed over the last decades (Uezawa, 1961, Saito, 1965,

Fukuzono, 1985, Voight, 1988, Crosta & Agliardi, 2003). Continuous acquisition of displacements data through time is a basic requirement for the application of the above-mentioned models. Terrestrial and aerial monitoring techniques can collect displacement data only after that suitable equipment has been installed. Satellite SAR data are available since 1992 and are continuously increasing over time in terms of quantity and quality. Hence, a large amount of displacement data can be obtained for several areas of the world. By the "Persistent Scatterers" (PS InSAR) processing technique the time series displacements of highly reflective targets with millimeter accuracy can be obtained. These data can help in the temporal prediction of landslide failure by applying semi-empirical models. The main limitations of using Ps InSAR techniques are: a) the presence of PS only in urbanized area and especially on man made structures; b) the monitoring of only surface displacements; c) the low data sample rate; d) the larger displacements in the final stage of movement; e) the non linear displacement trend before the failure. In the frame of the ESA CAT-1 project – ID: 9099 - "Landslides forecasting analysis by time series displacement derived from Satellite and Terrestrial InSAR data" long term SAR data stack provided by ERS and ENVISAT SAR satellites will be processed and analyzed to investigate large landslides recently occurred in Italy, with the aim to better define slope dynamics and forecasting modeling. More specifically, three slopes affected by large landslides, already collapsed, are being studied. In this work, SAR data are processed mainly by the Persistent Scatterers tool of SARscape commercial software. Furthermore processing will be performed also by the S-BAS processing algorithms integrated into the GENESI-DEC environment (<http://portal.genesi-dec.eu/>), which provides easy discovery and access to satellite and auxiliary data, as well as a user friendly interface for processing these data in Grid infrastructures. Time series of displacements derived from multi-stack data processing of SAR images are analyzed to obtain graphs of inverse of the velocity vs. time, and the back investigate landslides evolution over time. Hence, efficacy of satellite InSAR data for temporal prediction of landslides is analyzed and discussed, and the main limitations of InSAR data for the application of landslide time of failure forecasting models is assessed and investigated in detail. The expected results of this project are the following: a) identification of limits and potentiality of PS InSAR for landslide forecasting; b) identification of type of landslides that can be investigated by PS InSAR technique (for forecasting purposes); c) development of new landslide forecasting models specifically based on PS InSAR data.

## MATSAR: a Matlab-based INSAR processor

### Author(s)

Mozhdeh Shahbazi <sup>(1)</sup>, Mahdi Motagh <sup>(2)</sup>

### Department

<sup>(1)</sup>Department of Surveying and Geomatics Engineering, University College of Engineering, University of Tehran, IR

<sup>(2)</sup>Department of Geodesy and Remote Sensing, Helmholtz Center Potsdam, GFZ German Research Center for Geosciences, Potsdam, DE

### Abstract

Interferometric synthetic aperture radar (InSAR) uses interferogram of two or more SAR images to generate maps of surface deformation or digital elevation models. InSAR operational processing chain for displacement map generation comprises of five major stages: co-registration and resampling, interferogram generation, flat-earth correction, topography correction and phase unwrapping. In this paper, we discuss and evaluate new algorithms for SAR image matching and for topographic and reference-phase corrections, which improves conventional InSAR processing techniques in terms of increasing efficiency and reducing the time and computational effort. We implement and test our new codes and algorithms in MATLAB and evaluate them with respect to conventional INSAR processing implemented in DORIS software for a pair of Envisat ASAR data associated with the 2003 BAM earthquake.

# Application of novel SAR interferometry techniques for the retrieval of ice velocity and ice topography

## Author(s)

Noel Gourmelen <sup>(1)</sup>, Jeong-Won Park <sup>(2)</sup>, Andrew Shepherd <sup>(2)</sup>, Marcus Engdahl <sup>(3)</sup>

## Department

<sup>(1)</sup>University of Strasbourg 5 rue René Descartes, FR

<sup>(2)</sup>University of Leeds, UK

<sup>(3)</sup>ESA, IT

## Abstract

ERS2-ENVISAT cross-interferometry and Multiple Aperture InSAR are two novel techniques to exploit Synthetic Aperture Radar datasets that improve both surface topography and ice stream displacement retrieval. During cross interferometry campaigns, topography retrieval is improved thanks to the large perpendicular baseline (~2000m) between the ERS2 and ENVISAT instruments. Multiple Aperture InSAR allow an Interferometry based retrieval of ice stream displacement in the azimuth direction, increasing both resolution and precision of the retrieve velocity field when compare to conventional tracking methods. Here we exploit datasets from the SAR sensors onboard ERS1, ERS2 and ENVISAT to assess the potential of the two techniques for topography and ice displacement over sites in Greenland and Iceland. We focus particularly on datasets acquired during the ice phases of the ERS satellites and during the ERS2-ENVISAT cross-interferometry phases.

# Empirical study of the sensitivity of measuring horizontal displacements of point-like targets using C- and X-band SAR

## Author(s)

Jose Manuel Delgado Blasco <sup>(1)</sup>, Prabu Dheenathayalan <sup>(1)</sup>, Ling Chang <sup>(1)</sup>,  
Pooja Mahapatra <sup>(1)</sup>, Joana Esteves Martins <sup>(1)</sup>, Ramon Hanssen <sup>(1)</sup>

## Department

<sup>(1)</sup>Delft University of Technology Kluyverweg 1, 2629HS, Delft, The Netherlands, NL

## Abstract

Detecting a point-like target when it is horizontally displaced is of paramount importance in target tracking and in measuring the motion of glaciers over short intervals of time. This paper performs an experimental study of the accuracy, precision and sensitivity of the horizontal motion detectable using SAR. Therefore point-like targets such as corner reflectors (CR) are moved horizontally in a controlled manner over short time intervals to reproduce the real target motion. Such CR movements are monitored using SAR and the results are compared with the ground truth to arrive at the target horizontal motion determination parameters.

Towards this goal three CRs were installed each displaced by a few hundreds of metres in a farmland in Delft, The Netherlands. These corner reflectors are inclined for ERS-2 3-days ice-phase mission starting March 2011. Since the area does not exhibit horizontal motion, one of the CRs was moved horizontally stepwise in the order of a few centimeters to a few metres. At each step the CRs are imaged by SAR and also measured by campaign-style GPS (and with a few leveling campaigns) in order to provide the actual displacement in three dimensions. Then the motion is computed using SAR data and results are compared with the GPS measurements to validate the sensitivity of SAR in detection of motion of the targets. The experimental setup is such that the CRs are visible starting from March 2011 from both ascending and descending orbit TerraSAR-X satellite acquisitions over Delft. Hence similar parameters such as sensitivity, precision and

accuracy of motion detection will be derived for X-band SAR as well. Further, in order to substantially verify the reliability of our computations, data from three different field experiments with stable CRs performed with ERS-1/2 in 1996, with ENVISAT from 2003 to 2007 and with ENVISAT from March 2010 to January 2011 in the areas of Groningen, Delft and Cabauw respectively were exploited.

The outcome of our experiment will result in the empirical study of the sensitivity of motion detection of point-like targets in C- and X- bands. Also the influence of these parameters under varying imaging conditions such as change in Doppler and perpendicular baselines will be discussed.

## Joint inversion of INSAR and GPS times series : Application to monitoring ground motions related to volcanic or tectonic activities

### Author(s)

Dominique Remy <sup>(1)</sup>, Jean-Luc Froger <sup>(2)</sup>, Hugo Perfettini <sup>(1)</sup>

### Department

<sup>(1)</sup>IRD 14 av edouard Belin, FR

<sup>(2)</sup>Laboratoire Magmas et Volcans , FR

### Abstract

The understanding of many aspect of volcanic processes or of the earthquake cycle observed in South America has recently increased through the availability of large datasets of both ground-based geodetic and InSAR times series. These large datasets enable geodesists to accurately analyze the spatial and temporal evolution of surface deformation related to volcanic or tectonic processes. As they provide spatial constraints and temporal evolution history to the source model, they play a major role to better depict the present-day deformation style of active regions. Typically the time evolution of the source is derived from inverting the displacements available at each epoch. Nevertheless, such an approach could be computationally expensive and it could be difficult to retrieve a coherent time evolution. Recently a new statistical-based approach has been proposed by Kositsky and Avouac (2010) to overcome these limitations. We present here different studies conducted in South America where INSAR and GPS time series are jointly analyzed using this approach. We discuss the set of results in greater detail to illustrate the potentially of such an approach and we present our main conclusions.

## Impulse response correlation, a new method for Signal to Clutter Ratio estimation of point scatterers

### Author(s)

Piers Titus van der Torren <sup>(1)</sup>

### Department

<sup>(1)</sup>Delft University of Technology Netherlands, NL

### Abstract

Signal to Clutter Ratio (SCR) can be used as a measure for the selection of persistent scatterers. However, the current methods for SCR estimation require a big window for clutter estimation, or use related measures such as amplitude dispersion, and rely on secondary methods for sidelobe removal. In this paper a new method is proposed for SCR estimation using the impulse response function of the radar signal. With this method point scatterers can be detected in single radar images using a minimal window, causing a small resolution loss. Sidelobes are automatically

discarded based on their signal characteristics. Using temporal averaging persistent scatterers in a stack can be found. The single image based measure also provides a promising applicability for detection of quasi persistent scatterers. Tests show a small false detection rate and good performance on small to massive stacks.

## Automatic coregistration and simulated FRINGE removal by a direct estimation from high resolution DEM and ORBITAL data

### Author(s)

Fernanda Ledo G. Ramos <sup>(1)</sup>, Diana - Cristina Rosu <sup>(2)</sup>, Emmanuel Trouvé <sup>(2)</sup>, Flavien Vernier <sup>(2)</sup>, Jean-Marie Nicolas <sup>(3)</sup>, Renaud Fallourd <sup>(2)</sup>, Yajing Yan <sup>(2)</sup>, Fanny Ponton <sup>(4)</sup>, Fernando Miranda <sup>(5)</sup>

### Department

<sup>(1)</sup>Universidade Federal do Rio de Janeiro – COPPE/UFRJ Centro de Tecnologia, Bl. I214, Cid.Universitária, I. do Fundão, 21949-900 Rio de Janeiro, BR

<sup>(2)</sup>Université de Savoie, Polytech Annecy-Chambéry BP 80439, F-74944 Annecy-le-Vieux Cedex, FR

<sup>(3)</sup>Télécom ParisTech 75013 Paris, FR

<sup>(4)</sup>Université Joseph Fourier UMR 5559. B.P. 53, Grenoble, FR

<sup>(5)</sup>Centro de Pesquisas e Desenvolvimento da Petrobras Avenida Horácio Macedo, 950, Cid.Universitária, Ilha do Fundão, CEP 21941-915 RJ, BR

### Abstract

ABSTRACT For InSAR time-series deformation monitoring or change detection, an incorrect geo-localisation could lead to sub-optimal results as the orbital and topographic artefacts induce a misinterpretation of the derived signal. While being based on well known and documented algorithms [1], the coregistration and fringe simulation are influenced by the quality of parameters used in these computations. In this paper, we present an automatic coregistration and simulated fringe removal processing chain applied to RADARSAT-1, RADARSAT-2 and TERRASAR-X systems over two different regions in the globe: Chamonix Mont-Blanc massif (1000 to 4800m) and Manaus city in Brazilian Amazonia (up to 150m). The proposed purely geometric approach is based on the use of orbital data and digital elevation model (DEM) to compute the antenna-ground distances for master and slave images. This information is used to derive the coregistration offsets without any cross-correlation to avoid the lack of accuracy in decorrelated areas. The main processing steps and derived information can be described as follows: (a) state vector information extraction and orbit emulation by a polynomial model for each image; (b) acquisition time image and distance between the orbits and terrain image generation using a high resolution DEM and the Closest Point of Approach (CPA) with the zero Doppler hypotheses; (c) conversion of distance and time image into range and azimuth SAR image coordinates to derive radar-coding and geo-coding look-up tables (LUT), (e) calculation of orthogonal baseline Closest Point of Approach and local incidence angle images (useful sub-products); (f) Slave and Master coregistration by 1D or 2D interpolation based on range and azimuth differences, (g) conversion of distance differences into simulated fringes and projection into radar geometry (h) fringes removal with filtering and/or rescaling if necessary. These processing tools are implemented in the free distributed platform EFIDIR\_Tools [2] for providing an automatic D-InSAR generation chain compatible with different data format files as xml (currently used by new generation SAR systems) and also auxiliary files from Gamma and ROIPAC software. This approach was implemented in order to coregister a slave SAR image with respect to the master one, assuming that the geo-localisation for both master and slave are based on the satellite's trajectory in a precise manner from the metadata file. We have considered a polynomial regression in a least mean square sense. Firstly, the coefficients of the polynomial are calculated. The polynomial degree is specified by the end-user as an input parameter and should be adapted to the number of state vectors available in the metadata file, for example degree 7 for TerraSAR-X and degree 4 or less for RADARSAT-2. This stage also allows two specific tasks related to the resampling

procedure, namely: provides a visibility mask which marks the fold-over zones in the image (high relief application) [3] and generates an image of differences in range between the resampled slave SAR image and the master SAR image. The processing chain includes filtering and rescaling steps and simulated fringes extraction or not, based on the end-user decision. After the complex interferogram's computation, the outputs are presented in coherence, phase and amplitude values, filtered or not. The automatic processing proposed is being well performed in RADARSAT-2, TERRSAR-X and RADARSAT-1 data even if this latter one do not have zero Doppler calibration and precise orbits information. As a final objective, this processing chain permits the identification of remaining fringes due to atmospheric effects and terrain displacements. References [1] D. Massonnet and J.-C. Souyris, *Imaging with Synthetic Aperture Radar*. Lausanne: EPFL Press, 2008. [2] French National Research (ANR) project, "Extraction and Fusion of Information for measuring ground displacements with Radar Imagery (EFIDIR) project. online <http://www.efidir.fr>. [3] I. Pétilot, E. Trouvé, P. Bolon, A. Julea, Y. Yan, M. Gay, and J.-M. Vanpé, "Radar-coding and Geocoding Look Up Tables for the Fusion of GIS Data and SAR images in Mountain Areas," *IEEE Geoscience and Remote Sensing Letters*, vol. 7, pp. 309 - 313, 2010.

## An Adaptive and Iterative Filter Based on Local SNR for Strong Noise Reduction in SAR Interferogram

### Author(s)

Qian Sun <sup>(1)</sup>, Zhiwei Li <sup>(1)</sup>, Xiaoli Ding <sup>(2)</sup>, Jun Hu <sup>(1)</sup>, Jianjun Zhu <sup>(1)</sup>

### Department

<sup>(1)</sup>Central South University School of Geosciences and Info-Physics, Central South University, Changsha 410083, Hunan, CN

<sup>(2)</sup>The Hong Kong Polytechnic University, CN

### Abstract

Interferometric phase noise is a well-known error source for the InSAR measurements. Therefore, many kinds of filtering approaches have been proposed in order to suppress the noise effect in the interferogram during recent decades. Among these methods, Goldstein filter is prominent one which is implemented in the frequency domain of interferogram and commonly applied to the interferogram noise reduction. However, Goldstein filter does not have sufficient adaption since the filtering strength is determined by experience. An improved Goldstein filter had been developed by Baran et al., which exploit interferometric coherence to control the filtering strength. Although coherence can partially reflect the phase noise in an interferogram, it is an imperfect indication as phase noise can be affected by other factors, e.g. look number. Here we also present a modification algorithm for the Goldstein filter to dominate the filtering strength based on local signal-to-noise (SNR). Local SNR, which can be estimated according to the local statistic characteristics of interferometric phase, behaves as a better evaluation criterion for the quality of InSAR interferogram than interferometric coherence. We firstly construct the Goldstein filter's parameter depending on the local SNR of the interferogram. Then, a varying size filter window is used according to local SNR instead of fixed size window applied in the previous algorithm. Third, a second-iterative filtering procedure is adopted to recover the loss of phase signal. In this way, interferogram could be filtered with sufficient adaption and preserve the phase signal as much as possible while reducing the phase noise effectively in the interferogram. The new filter is applied to the coseismic ASAR interferogram concerned with 2009 L<sub>1</sub> Aquila earthquake in Italy. Dense fringes caused by the destructive earthquake require an effect filtering approach to retrieve deformation signal. In this study, we compare the results from the new filter to that from Goldstein and Baran filter. . The results demonstrate that our filter can significant diminish the noise effects in the interferogram and have a better performance than its competitors. Keywords: InSAR, interferogram, adaptive filter, iteration, local SNR

# Monitoring Ground Deformation on Carbon Sequestration Reservoirs in North America

## Author(s)

Wenliang Zhao <sup>(1)</sup>, Falk Amelung <sup>(2)</sup>, Tim Dixon <sup>(3)</sup>

## Department

<sup>(1)</sup>University of Miami , USA

<sup>(2)</sup>UMiami , USA

<sup>(3)</sup>University of South Florida , USA

## Abstract

The geological storage of carbon dioxide (CO<sub>2</sub>) is one of the most important methods for controlling the green house gas. The conception of this kind of storage is injecting large quantities of CO<sub>2</sub> (million tons) into deep reservoir like oil field, gas field or saline formation. Part of the use of CO<sub>2</sub> for secondary oil recovery suggests that the migration of carbon dioxide can be complicated, and can differ from the movement of injected water or hydrocarbons. Are these reservoirs safe? Will the carbon dioxide remain at depth? Can we know the movement of these flows? Due to these questions, there is a need to monitor the fate of CO<sub>2</sub> underground. Satellite based geodetic method such as InSAR taking advantages of lower cost, high spatial resolution, long-term monitoring, has been applied for ground deformation monitoring in recent two decades. It has been proved to be successful for centimeter level volcanic and earthquake deformation. More recently, InSAR is applied for the low rate deformation in central Nevada for long-term sub-centimeter post-seismic deformation using Small Baseline Subsets algorithm (SBAS). In this paper, we implement InSAR techniques to our carbon sequestration project in North America. Using JAXA's Alos-Palsar synthetic aperture radar image from 2007 to 2010, we generate ground motion time series at 5 carbon sequestration test sites. The results show clear ground uplift signals.

# Frequency and Space Domain Orbit Error Corrections: A case study in Coseismic Deformations of 2011 Tohoku Earthquake

## Author(s)

Mi Jiang <sup>(1)</sup>, Xiaoli Ding <sup>(1)</sup>, Guangcai Feng <sup>(1)</sup>, Zhiwei Li <sup>(1)</sup>

## Department

<sup>(1)</sup>Dept. of Land Surveying and Geo-Informatics, The Hong Kong Polytechnic University, HK

## Abstract

We experiment with both frequency and space domain algorithms for correcting orbit errors and apply them to study the coseismic deformations of the 2011 Tohoku earthquake. It is seen from the study that linear orbital errors can be effectively removed with maximum likelihood (ML) fringe frequency estimation and one-dimensional discrete Fourier transform (DFT) along both the azimuth and the range directions while for non-linear orbital errors, it is useful to employ a series of space domain algorithms, including iterative least squares fitting. The algorithms are applied to map the coseismic deformation of the 2011 Tohoku earthquake with data from two descending Envisat/ASAR tracks and two ascending ALOS/PALSAR tracks that cover most of the Northeastern part of Japan. The results are validated by using least squares residuals and independent GPS data. The detrended coseismic interferograms appear much more consistent with the GPS observations.



# Interferometric coherence analysis with high resolution space-borne synthetic aperture radar

## Author(s)

Sang-Hoon Hong <sup>(1)</sup>, Shimon Wdowinski <sup>(2)</sup>

## Department

<sup>(1)</sup>Korea Aerospace Research Institute , KR

<sup>(2)</sup>University of Miami , USA

## Abstract

Recently high spatial resolution space-borne synthetic aperture radar (SAR) systems with various polarizations have launched and have operated successfully. Interferometric SAR (InSAR) processing with the high resolution space-based observations acquired by these systems can provide more detail information for various geodetic applications. Coherence is regarded as a critical parameter in the evaluating the quality of an InSAR pair. In this study, we evaluate the coherence characteristics of high-resolution data acquired by TerraSAR-X (X-band) and ALOS (L-band) and intermediate-resolution data acquired by Envisat (C-band) over western Texas, U.S.A. Our coherence analysis reveals that the high-resolution X-band TSX (3.1 cm) data has a high coherence level (0.3-0.6), similar to that of the L-band ALOS data (23.5 cm) in short temporal baselines. Furthermore, the TSX coherence values are significantly higher than those of the C-band (5.6 cm) Envisat data. The higher coherence of the TSX dataset is a surprising result, because common scattering theories suggest that the longer wavelength SAR data maintain better coherence. In vegetated areas the shorter wavelength radar pulse interacts mostly with upper sections of the vegetation and, hence, does not provide good correlation over time in InSAR pairs. Thus, we suggest that the higher coherence values of the TSX data reflect the data's high-resolution, in which stable and coherent scatterers are better maintained. Although, however, the TSX data show a very good coherence with short temporal baseline (11-33 days), the coherences are significantly degraded as the temporal baselines are increased. This result confirms previous studies showing that the coherence has a strong dependency on the temporal baseline. We will continue this preliminary study by conducting additional coherence analyses over various environments and develop appropriate relationship that will account for data resolution in the coherence calculations.

# ALOS SAR interferometry for landslide monitoring in the Republic of Georgia

## Author(s)

Elena Nikolaeva <sup>(1)</sup>, Thomas R. Walter <sup>(2)</sup>, Manoochehr Shirzaei <sup>(3)</sup>

## Department

<sup>(1)</sup>Helmholtz Centre Potsdam GFZ German Research Centre for Geosciences, DE

<sup>(2)</sup>Physics of the Earth Helmholtzstraße 7, H7 318, DE

<sup>(3)</sup>Univ. of California, Berkeley , USA

## Abstract

Being a mountainous and a seismically active area, as a result of the collision of the Eurasian and the Arabian plates, the Republic of Georgia is particularly susceptible to landslides. Landslides in Georgia are one of the most devastating natural hazards, and cause substantial damage to society and infrastructure. Thus landslide detection and monitoring are of great importance. In this study we report on a previously unknown landslide area detected, by using InSAR and optical data over a site located close to the city of Sachkhere in central Georgia. To estimate the rate of the landslide, we use interferometric processing of eight ascending ALOS PALSAR scenes

spanning July 2007 through January 2010. Considering this data set we generated nine interferograms with spatial and temporal baseline smaller than 1700 m and 460 days, respectively. We estimated an annual displacement rate of up to 30 cm per year in Line-Of-Sight (LOS) for the landslide. The sliding area found to be elliptical in shape, being approximately 2 km long (north-south) and 0.5 km wide (east-west), affecting an area of 3 km<sup>2</sup>. Motion is assumed to be westward throughout. The movement extends to two villages and also affects a major sand mining area. To understand the dynamics of landslide, we developed a two dimensional (2D) model for estimating the volume and rate at the base of the landslide. The input of our 2D model were a height profile of the landslide area extracted from ASTER digital elevation model and the LOS velocity along a profile. The LOS velocity field displayed a gradient along a fairly flat surface, which is why we suggest a rotational landslide model. We further evaluated the maximum possible landslide volume, based on our presented model. The aerial photograph with a high resolution (~0.6 m) was used to infer the land cover and to detect kinematic indicators. These indicators are located within the area where movement was detected using InSAR, which is hence ground truth confirmation of the InSAR observations. This is the first radar interferometry work on Georgia. For the future, methods for monitoring landslide integrated by radar and optical satellite remote sensing will follow. We are going to continue to develop landslide models and to study the correlations between landslide dynamics and possible causative factors such as mining area, earthquakes, rainfall, which are typical for this area.

## Landslide Monitoring for German Infrastructure Construction Site using Concrete Corner Reflector InSAR

### Author(s)

Michael Riedmann <sup>(1)</sup>, Jan Anderssohn <sup>(1)</sup>, Oliver Lang <sup>(1)</sup>, Lutz Petrat <sup>(1)</sup>

### Department

<sup>(1)</sup>Astrium Services / Infoterra GmbH Platz der Einheit 14, 14467 Potsdam, DE

### Abstract

In this study, we use concrete Corner Reflector InSAR to monitor landslides at two different sites in Germany. The first site is a controversial infrastructure construction site, where a landslide is to be monitored before and during the construction phase. The second site is a risky landslide area in the Alps with movement rates of up to 2cm per year. The Corner Reflectors (CRs) were designed for TerraSAR-X satellite passes. They are made of concrete with integrated metal plates and are of triangular trihedral shape with minimal dimensions to obtain the necessary Radar Cross Section with respect to the surrounding area. The concrete guarantees stability against harsh weather conditions, and robustness with respect to vandalism or theft. Experiments are made with a black concrete CR and a CR with heating to judge their performance under winter conditions. First results will be presented at the conference.

# InSAR Time series Analysis of Interseismic deformation of Eastern part of Iran

## Author(s)

Zahra Mousavi <sup>(1)</sup>, Erwan Pathier <sup>(1)</sup>, Andrea Walpesrdorf <sup>(1)</sup>, Cecile Lassere <sup>(1)</sup>, Isabelle Manighetti <sup>(1)</sup>, Mathilde Vergnolle <sup>(1)</sup>, Farokh Tavakoli <sup>(2)</sup>,  
Hamidreza Nankali <sup>(2)</sup>

## Department

<sup>(1)</sup> Université Joseph Fourier LGIT - BP 53 , 38041, FR

<sup>(2)</sup> National Cartographic Center of Iran (NCC) , IR

## Abstract

The high seismicity of Iran, with large and shallow destructive earthquakes reflects its intense tectonic activity that takes place in the Alpine–Himalayan belt context. Active tectonics in Iranian plateau is dominated by the convergence between the Arabian and Eurasian plates, taking place inside the political borders of the country. The part of the convergence that is not absorbed in Zagros at its SW border must be accommodated by shear deformation between the Central Iran and the Helmand sub-plate to the east of Iran. Consequently, Eastern Iran has crucial role in accommodating N-S right-lateral shear between central Iran and Afghanistan. The tectonic deformation in eastern Iran is localized mainly on NS oriented right-lateral faults surrounding the aseismic Lut block, and EW left-lateral faults at the northern boundary of the Lut block. Previous studies on these major faults in Eastern Iran show discrepancies especially between the GPS interseismic slip rate (less than 1 mm/yr on the Dorouneh fault (Tavakoli et al. 2007) and geological slip rates ( $2.4 \pm 0.3$  mm/yr Fattahi et. al, 2007). Also according to rigid block model, it is expected to accommodate near 10 mm/yr slip rate somewhere on the Dorouneh and Dasht-e-Bayaz strike-slip faults. This discrepancy between the short time (GPS) and long term (geomorphological) and tectonic model motivated us to use another geodetic techniques to investigate how the deformation is distributed in the area. The spatial coverage, acceptable resolution and precision of Space-borne radar interferometry (InSAR) technique make it a powerful technique to resolve some open questions of fault mechanisms and their role in the regional tectonics. Several InSAR studies have been already successful in measuring long-wavelength ground displacements related to interseismic fault deformation on similar continental strike-slip fault (like the North Anatolian fault or the Haiyuan fault). The most important difficulty is the slow slip rate of the targeted faults (1 to 3 mm/yr). Even if the East-West orientation of the Dorouneh or Dasht-e-Bayaz strike-slip faults is favourable to the measurement from descending or ascending ENVISAT orbits, such low slip rate faults still require some methodological improvement with respect to conventional INSAR. In this study, we use ENVISAT ASAR images from 2003 to 2010, in descending orbits. The 400 by 400 km studied area that includes the eastern part of the Dorouneh fault is covered by four satellite tracks (435, 392, 163 and 120). The raw radar images are processed with ROI\_PAC to construct the interferograms and unwrapped them. The resulting differential interferogram phase is related to phase change to the deformation signal, tropospheric delay, orbital and DEM residual and noise. We correct for the stratified part of tropospheric delay correlated with elevation using the observed phase-elevation correlation. Large scale seasonal atmospheric correction will also be investigated using ERA-Interim meteorological model and GPS data. A twisted plane is also fitted to remove orbital errors. A careful visual inspection of the corrected interferograms is performed to investigate short wavelength signals (1-10 km scale) that could be related to superficial creep along faults. Local deformations related to subsidence phenomena were found in some valleys but there is no evidence over the 2003 to 2010 period for any sharp creep deformation signal located along fault.

To investigate the long wavelength tectonic signal due to interseismic strain accumulation, a time series analysis of the selected Images has been done on a pixel basis in order to enhance signal to noise ratio affected by remaining atmospheric signal. The selection and the weighting of the interferograms are based on a noise energy function that measures the quality of each interferogram. The resulting displacement time series and mean velocity map can be compared to GPS data. To interpret the InSAR observations it is helpful to assess the expected pattern of interseismic deformation for the given fault configuration. Our analysis is completed by a comparison of the interseismic velocity map derived from InSAR with simple direct elastic models based on the Savage and Burford model (1973) using different fault slip rates by assuming that the normal component of fault displacement is negligible.

## SAR inteferometry with seasonally changing snow cover

### Author(s)

Stephen Hobbs <sup>(1)</sup>, Anura Wickramanayake <sup>(2)</sup>, Jonny Sjöberg <sup>(3)</sup>, Tore Lindgren <sup>(2)</sup>, Priya Fernando <sup>(4)</sup>

### Department

<sup>(1)</sup>Cranfield University Whittle Building, Cranfield, MK43 0AL, UK

<sup>(2)</sup>Lulea University of Technology , SE

<sup>(3)</sup>Itasca Consultants AB , SE

<sup>(4)</sup>EADS Astrium Ltd , UK

### Abstract

Spaceborne radar interferometry is an established and very powerful method of measuring land subsidence over timescales of weeks to years. It has been demonstrated on natural and urban landscapes and is becoming an operational technique with accuracy better than 1 cm yr<sup>-1</sup>. The technique generally relies on having scatterers (which reflect the radar signal) which have stable properties over the timescale of interest. In some landscapes these scatterers occur naturally. However, at high latitudes there are particular difficulties because of the strong seasonal variation in the landcover – snow cover in particular can vary dramatically over periods of weeks to months – and the satellite orbits have particular features which are not generally significant at lower latitudes. It is unlikely that natural scatterers will be stable over long periods in these areas. The aim of this project is to develop methods of SAR interferometry suitable for use in landscapes with seasonal snow cover. The project has two themes: (1) improved understanding of SAR imaging at high latitudes and the use of interferometry in such landscapes, and (2) the development of artificial radar targets which can provide the necessary stability for long-term surface deformation monitoring. The sponsor runs a large mining operation at high latitudes. The study has a practical focus and is part of a larger project to provide a mining subsidence monitoring service for the sponsor. The project's aim is to achieve accurate monitoring of subsidence using radar interferometry at high latitudes. Techniques developed should be suitable for operational use. Test site The experiment test site is centred on the town of Kiruna in northern Sweden (67° 51' N, 20° 13' E). The ground is covered with snow (to a depth of 1 m or more) from October to May each year, and so the winter and summer periods have very different land cover properties. The site includes the town of Kiruna, a large mine, and areas of natural sparse forest with mainly birch and some coniferous trees up to several metres tall. Datasets Available Several datasets are available to support the research, these include: · GPS measurements from a network of control points · General weather observations · Mapping data for land cover / land use and topography · SAR images at approximately monthly intervals from 2009 (Radarsat-2, using up to 3 satellite tracks for imaging) · A network of corner reflectors across the test area The core data analysis tool is the MDA software package designed for processing Radarsat images (for both backscatter and interferometric products). The key resource for the research is the time series of high resolution SAR images suitable for interferometric

processing, which allows seasonal changes in backscatter to be observed directly. Methodology The project requires a mix of simulation and practical design and fieldwork. The main contributions will be in the area of target specification, design and validation. Achievements to date The project started late in 2009 and the main emphasis so far has been to establish the datasets needed for the research. Radarsat-2 images have been acquired and are being processed to derive interferometric products and to register them to standard projections compatible with each other and ancillary data. Field observations complementing the satellite imaging are also being made. Acknowledgements The project is sponsored in full by the LKAB mining company. The project also benefits from technical advice of MDA. Further information Contact Anura Wickramanayake (Anura.Wickramanayake@ltu.se)

## Interferometric Crossing Orbit Experiment using TerraSAR-X and TanDEM-X

### Author(s)

Steffen Wollstadt <sup>(1)</sup>, Francisco Lopez-Dekker <sup>(1)</sup>, Pau Prats <sup>(1)</sup>,  
Francesco De Zan <sup>(1)</sup>, Thomas Busche <sup>(1)</sup>, Gerhard Krieger <sup>(1)</sup>

### Department

<sup>(1)</sup>German Aerospace Center, DE

### Abstract

This paper discusses quasi repeat-pass space-borne SAR interferometry exploiting crossing orbits in order to obtain short revisit times of 1 and 5 days. Typical Repeat-pass as well as across-track SAR interferometry considers almost parallel orbit trajectories in order to obtain a common azimuth spectrum on ground which requires the whole repeat orbit cycle time for acquiring an interferometric pair of images. Taking the Earth rotation and a sun-synchronous orbit into consideration the orbits are crossing each other several times within a cycle, depending on the orbit design. This implies relatively close orbit trajectories as well as ground-tracks after an integer number of days, less than the repeat-orbit cycle time. Therefore baselines not exceeding the critical baseline are able to be achieved. The challenge of the small repeat pass time is to obtain a common ground spectrum. The azimuth spectrum as well as the spectrum in range must have a preferably large overlap in order to obtain a coherent interferogram. In range, the spectral overlap can be maximized by using the largest possible transmit bandwidth together with the crossing orbit approach where the across track baseline is small enough. This means that the possible acquisition areas are limited to very high latitudes as well as to a very narrow range of latitudes due to the small allowed difference between both incidence angles. Due to the angle between the orbit tracks, the same portions of the Doppler spectra do not map to common azimuth ground spectral components. Thus, in order to obtain a coherent pair of images, a relative squint (or Doppler centroid offset) between the individual acquisitions is required. For the geometries considered in this study, this relative squint is much larger than the azimuth beam-width. Therefore, it requires that the squint is applied physically during the acquisition. The uniquely flexible commanding capabilities of TerraSAR-X (TSX) and its twin satellite TanDEM-X (TDX) (TerraSAR-X add on for Digital Elevation Measurements), including their azimuth steering capability turns them into ideal platforms for an experiment with this type of non-parallel acquisitions. During the Commissioning Phase of TDX in July 2011 a crossing orbit experiment was already successfully acquired over the October Revolution Island, in the Russian Arctic. This data was acquired while TDX was approaching TSX to reach the 20 km along-track separated pursuit monostatic configuration. At the acquisition, the along-track separation was roughly 350 km. Due to the Earth rotation this caused a small but still significant crossing angle between the two space.craft. In order to perform the same within the nominal 11 day repeat cycle of TSX as explained above, it was found that the closest pairs of tracks correspond to a temporal lag of 5 or

6 days and the second closest pair to a 1-day lag. A reasonably flat test site located on the Antarctica, i.e. a high latitude in the southern hemisphere (78 deg S), was chosen due to low temporal decorrelation expected in the current local winter time. Three acquisitions were carefully planned over this single test site, where the first and the second exhibit a 5-day lag where the second and third a 1-day lag. The middle acquisition satisfies the requirements for both interferograms as the remaining two were designed in order to use the middle one as master. Here, the required squint angles of the three acquisitions for compensating the azimuth spectral shift were determined to be  $0.039^\circ$ ,  $-1.447^\circ$  and  $1.526^\circ$ , resulting a relative squint of  $1.486^\circ$  and  $2.973^\circ$ , respectively. In order to deal with the impact of the range spectral shift a high incidence angle of  $47^\circ$  was chosen together with a 300 MHz pulse-bandwidth. These acquisitions were repeated in the following 11-day cycle. The quasi repeat pass theory and acquisitions using crossing orbits offer a possibility to obtain new insight in the study of temporal decorrelation behavior of polar ice. The varying, but potentially large baselines could be exploited to measure topography and its changes in polar ice regions with a precise height accuracy in coherent areas. Additionally the results might offer a deeper knowledge of squinted SAR processing and interferometry under crossing orbits.

## InSAR interferogram real-time generation using optronic processor: initial concept

### Author(s)

Alain Bergeron <sup>(1)</sup>, Linda Marchese <sup>(1)</sup>, Martin Suess <sup>(2)</sup>, Bernd Harnisch <sup>(2)</sup>

### Department

<sup>(1)</sup>INO, CA

<sup>(2)</sup>ESA-ESTEC, NL

### Abstract

InSAR systems are of prime interest for disaster monitoring, providing valuable data to otherwise unreachable region at the moment of the disaster. Such systems are limited by the large volumes of data they generate that surpasses the satellite communication downlink capacity. Crucial data that the SAR system could otherwise provide must thus be discarded. Generation of final image/data generation is also time consuming. This introduces delays in the reception of the image used in disaster monitoring at the very moment when the data are urgently needed. An attractive option is to perform real-time image generation from the SAR raw data onboard and perform the interferometry onboard, for those cases where the SAR images are not required and an interferometric data pair is available. Alternatively, the same real-time processing on the ground would also provide rapid availability of the critical data. In addition to being smaller in size than the raw data, the SAR images and InSAR interferograms are easier to compress. Accordingly, such onboard processing will allow for more frequent science observations and allow for disaster response applications that are otherwise not possible. The hurdle for on-board SAR and InSAR processing is that a large volume of raw data must be processed. To be fast enough to process without bottleneck, digital processors require parallel processing schemes that consume large amounts of power and tend to be bulky. Satellites have tight constraints on payload power consumption, size and weight, thus often digital processors can not meet the demands for onboard processing. INO has developed a compact, lightweight optronic SAR processor prototype. The core of which is optics-based. The inherent parallel processing capabilities of lenses and the speed of light propagation allow for ultra-rapid SAR image generation and compression, resulting in a processing speed capability enough to process a complete ASAR scene over 20000 azimuth lines of 4000 range samples in less than 10 seconds. In addition to this image generation capabilities, a real-time technique to perform SAR interferometry using the SAR Optronic Processor has been developed and tested. It is an elegant

and compact alternative approach to adding an optical interferometer after the optronic processor, where image formation is performed first and then the interferogram is generated. In the case of the optronic processor, the SAR raw data interfere during processing and the result is an image overlaid with the interferogram. Such a combined processor would cut down on system complexity as the addition of the interferometer would require complex optomechanical components increasing the weight and the volume of the SAR processor system. Not only does this single optronic processor have the capability to generate a SAR image or an interferogram-combined SAR image, it performs the combined-interferogram image generation in essentially the same amount of time it takes to perform the SAR image generation. This paper discusses the feasibility of interferogram generation using the optronic SAR processing. It begins by presenting an overview of the optronic SAR processor. Next, full-scene ENVISAT/ ASAR image results are presented. Finally, results from the characterization of preliminary interferograms generated using simulated pairs from a single ASAR data set are reviewed.

## The InSAR Scientific Computing Environment: a processing tool for interferometric and polarimetric radar data

### Author(s)

Marco Lavallo <sup>(1)</sup>, Paul Rosen <sup>(1)</sup>, Walter Szeliga <sup>(1)</sup>, Sean Buckley <sup>(1)</sup>,  
Eric Gurrola <sup>(1)</sup>

### Department

<sup>(1)</sup>JPL/Caltech, USA

### Abstract

Synthetic Aperture Radars (SAR) are used to image the Earth's surface to extract structural and bio-physical properties of the natural environment. In order to extract a desired property, interferometric SAR (InSAR) data and polarimetric SAR (PolSAR) data have to be generated through accurate processing and with sufficient quality, e.g. free of distortions caused by the radar instrument or by the atmosphere. The availability of a software tool able to perform an automatic yet flexible interferometric and polarimetric processing is of primary importance for the development of geoscience applications, especially in view of the increasing number of spaceborne SAR missions. The InSAR Scientific Computing Environment (ISCE) is a new software tool developed collaboratively by Jet Propulsion Laboratory (JPL) and Stanford University within the NASA Advanced Information Systems and Technology program [1]. ISCE offers to the scientific community an open-source, modular and extensible computing environment for InSAR and PolSAR data processing, and will be freely available in the course of 2011. The tool is essentially a new version of ROI\_PAC (the repeat-orbit InSAR package) with new functionalities and improvements at the level of core algorithms, implementation strategy and user interface. Improvements of ISCE with respect to ROI\_PAC include a modular and extensible architecture, new focusing approach, better geocoding of the data, handling of multi-polarization data, radiometric calibration, and estimation and correction of ionospheric effects. The focusing approach is based on an ideal common trajectory defined for the InSAR data set; the InSAR processing is referenced to this ideal trajectory exploiting precise orbits information with a motion compensation algorithm, so that the geolocation of InSAR products results highly accurate. The software environment is composed by a set of C/Fortran core routines managed by a layer of Python modules that are modular, flexible and extensible, facilitating user contributions to the tool. By virtue of its modularity, it is possible to add new functionalities to ISCE in a relatively straightforward manner. Two of recently added functionalities are the support for PolSAR/Pol-InSAR products and the ionospheric module [2, 3]. The PolSAR and Pol-InSAR capabilities in ISCE allows simultaneous handling of multi-channel data, accurate co-registration among polarimetric channels, and polarimetric and radiometric calibration to meet the PolSAR quality requirements.

ISCE is able to generate a set of Pol-InSAR SLCs focused in the same exact geometry. The SLCs can be easily exported into polarimetric post-processing and analysis tool such as the ESA/PolSARPro or DLR/RAT. The extension of ISCE with polarimetric processing allows generating geocoded polarimetric time series, which are useful for the detection of scattering mechanism changes over time (e.g. to monitor deforestation activities and fires). The advanced Pol-InSAR capabilities can be used in combination with Pol-InSAR scattering models in order to retrieve forest characteristics such as the underlying topography beneath the canopy and the canopy height. The ionospheric module of ISCE provides a set of functions to estimate and mitigate the effects of the ionosphere on PolSAR and InSAR data. The module is also able to generate high-resolution maps of absolute and relative TEC. The advantage of estimating ionospheric effects using ISCE is twofold. First, the user is able to generate accurate geolocated maps of ionosphere starting from raw data and precise orbit information. Second, the knowledge of ionospheric-induced distortions can be exploited to re-focus the image and to re-form the interferogram in order to further improve the final product quality. Two methods of ionospheric estimation are implemented in ISCE, namely the Faraday rotation method and the range split-spectrum method, which provide a map of ionospheric distortions from PolSAR and InSAR data respectively. In this presentation we provide an overview of ISCE, describing its general characteristics and advantages with respect to other conventional InSAR processing tools. We show a sample InSAR/PolSAR processing chain and illustrate how the user can insert his own routines as part of the processing. We focus on the new functionalities of ISCE such as the handling of multi-polarization images, the generation of Pol-InSAR products and the estimation of ionospheric effects. Some of these components implement theoretical improvements that will be discussed. Results are shown using L-band ALOS/PALSAR data and the SRTM digital elevation model. [1] Gurrola, E., Rosen, P., Sacco, G., Szeliga, W., Zebker, H., Simons, M., Sandwell, D., Shanker, P., Wortham, C., Chen, A., "Interferometric Synthetic Aperture Radar (InSAR) Scientific Computing Environment," presented at AGU Fall Meeting, San Francisco, December 2010. [2] Rosen, P., Lavalley, M., Pi, X., Buckley, S., Szeliga, W., Zebker H., Gurrola E., "Techniques and tools for estimating ionospheric effects in interferometric and polarimetric SAR data", presented at IGARSS 2011, Vancouver, Canada, 25-29 July 2011. [3] Lavalley, M., and Simard, M., "Exploitation of dual and full Pol-InSAR PALSAR data", presented at the 4th Joint ALOS PI Symposium 2010, Tokyo, Japan, 15-18 Nov. 2010.

## DEM-based SAR pixel area estimation for enhanced geocoding refinement and radiometric normalization

### Author(s)

Othmar Frey <sup>(1)</sup>, Maurizio Santoro <sup>(1)</sup>, Charles L. Werner <sup>(1)</sup>, Urs Wegmüller <sup>(1)</sup>

### Department

<sup>(1)</sup>Gamma Remote Sensing, CH

### Abstract

Precise terrain-corrected georeferencing of SAR images and derived products in range-Doppler coordinates is relevant for data interpretation and for the combination with other geodata products. In addition, the transformation of data from map geometry to range-Doppler geometry is also very important, e.g., the transformation of terrain heights into SAR geometry as used in DInSAR applications.

A method for automated terrain-corrected SAR geocoding was described in [1]. This SAR geocoding method makes use of the satellite orbit, a digital terrain model, and the SAR imaging parameters to calculate the corresponding slant-range and along-track position for each grid point of the digital elevation model. These initial slant-range and along-track positions are stored in a look-up table. As a next step, a simulated SAR intensity image is calculated, similar to the



approach described by Ulander [2]. Then, offsets between the simulated image and the real SAR intensity image are determined and used to refine the look-up table. Eventually, the SAR image is transformed in one resampling step based on the refined look-up table.

The quality of the correlation-based look-up table refinement is strongly dependent on the availability of distinctive common features in both the real SAR intensity image and its simulated counterpart.

This SAR image intensity simulation makes use of the angular relationship between the surface normal of the local terrain patch, and the range-azimuth geometry, respectively. That type of algorithm leads to a realistic simulation of the terrain-induced variation of the backscattering coefficient except for areas with strong foreshortening and layover regions, which notably are the most distinctive terrain-induced radiometric features.

A much better simulation of layover regions is possible following ideas presented in [3]. We implemented such a DEM-based method for realistic SAR pixel area estimation and assessed the improvement achieved in both the geocoding refinement and the radiometric normalization.

The improvements obtained with regard to geocoding are: a higher robustness by making better use of available terrain features, in particular in the case where major parts of the area covered do not exhibit topographic variation, and an increase in geolocation accuracy. In terms of radiometric normalization an improved compensation of pixel area effects is achieved also for strong foreshortening and layover regions - however, it has to be noted that the spatial resolution remains low in these areas.

References:

[1] Wegmuller, U.; "Automated terrain corrected SAR geocoding," In: Proc. IEEE Int. Geosci. Remote Sens. Symp., vol.3, pp. 1712-1714, 1999. doi: 10.1109/IGARSS.1999.772070

[2] Ulander, Lars M. H.: "Radiometric slope correction of synthetic-aperture radar images," IEEE Transactions on Geoscience and Remote Sensing, 34(5):1115--1122, 1996.

[3] Small, D.; Miranda, N.; Meier, E.: "A revised radiometric normalisation standard for SAR", In: Proc. IEEE Int. Geosci. Remote Sens. Symp., vol. IV, pp. 566-569, July 2009.

## The Introduction Of ICDINSAR Software For DINSAR And PSINSAR Application

Author(s)

Yongsheng Li <sup>(1)</sup>, Jingfa Zhang <sup>(1)</sup>

Department

<sup>(1)</sup>China Earthquake Administration , CN

**Abstract**

The ICDINSAR (Institute of Crustal Dynamics INSAR ) is a open software designed for DINSAR and PSINSAR applications. The software was an executable tool to facilitate the use of DInSAR and PSInSAR technology. The software was well established based on multithreading, pipe communication mechanism for its flexible and smoothly operations. The software supported most SAR data formats, such as ASAR, ERS, ALOS, COSMO-SKYMED, TERRASAR-X, etc. The software has following main components: 1) SAR raw signal data image formation module The module could image formation the SAR raw signal date, such as ERS, ENVISAT,ALOS,etc. 2) Differential Interferometric SAR Processor module The DInSAR is the primary module in the ICDINSAR. It supports most SAR data format including TERRASAR-X and COSMO-SKYMED. 3) Permanent Scatterers Interferometric SAR Processor module This part is a new module, It contained basic process for PSInSAR analysis, It is still under the developing. The paper will demonstrate some DInSAR and PSInSAR results based on the software.

# On the Use of Radargrammetry in SAR Interferometry

## Author(s)

Cristian Rossi <sup>(1)</sup>, Fernando Rodriguez Gonzalez <sup>(1)</sup>, Thomas Fritz <sup>(1)</sup>

## Department

<sup>(1)</sup>German Aerospace Center (DLR), DE

## Abstract

Radargrammetry and interferometry provide the same information, the absolute range satellite-target, using respectively the geometric parallaxes and the unwrapped phase. In the Integrated TanDEM-X Processor (ITP) the radargrammetric information, exploiting the image shifts from the coregistration process, is used for the estimation of the absolute phase offset - i.e. what is missing to the unwrapped phase so that it represents the absolute range, allowing a subsequent precise geocoding and DEM generation. The estimation is performed in a DEM calibration approach, requested for the right connection of independently processed Raw DEMs belonging to the same data take, to avoid height discrepancies and discontinuities among them. A secondary but fundamental product coming from the comparison of the two measures is the identification of phase unwrapping errors, bringing to the mission a quality control parameter operationally useful for the ground segment. Finally, this information can be exploited for a fine absolute calibration of the end-to-end system yielding the detection of un-calibrated inaccuracies. In this paper the algorithms used in ITP are presented together with exemplary results and an accuracy analysis, demonstrating the effectiveness of the proposed approach.

# Multiple Aperture InSAR (MAI) With C-Band and L-Band Data: Noise and Precision

## Author(s)

Noah Bechor Ben Dov <sup>(1)</sup>, Thomas Herring <sup>(1)</sup>

## Department

<sup>(1)</sup>MIT 77 Mass Ave, Cambridge, MA 02139, USA

## Abstract

MAI is a technique to extract along-track (horizontal) phase-based displacements from InSAR data. MAI's theoretical precision can be at the CM level, an order of magnitude improvement over amplitude-based pixel offset approaches. However, MAI has been challenging to implement with most academic InSAR processors, and the theoretical precision difficult to reach for low to medium coherence terrains. We implement MAI with the JPL/CALTECH InSAR software ROI\_PAC. We study the MAI noise structure with Envisat, Radarsat-1, ERS, and ALOS data, and develop phase corrections and filtering based on the results. We study the MAI noise with both 'zero' signal, all noise data and with data presenting actual deformation signal. We process 11 Envisat pairs presenting low to medium coherence with less than 2 cm along track displacements, taken over the larger Los Angeles basin/San Gabriel Mountains in California, US. The test data contain a variety of decorrelation sources and cover different types of terrain, including urban, mountainous, vegetated and sea surfaces, as well as variety in temporal and spatial baselines. To test the MAI filter we superimpose the MAI noise images with signal simulating coseismic displacements from the 1812 Mw~7 Wrightwood earthquake sequence. The C-band results present a correlation dependent rms error ranging from 5 cm in correlation coefficient 0.3 to 1.5 cm in correlation coefficient 0.8. In an actual signal case (Hawaii, L-band), the random component of the noise ranged from 1.5 cm to 0.5 cm for correlation coefficients of 0.3, 0.9, respectively.

# Structure and Object Recognition using Very High Resolution InSAR Observations

Author(s)

Anca Popescu <sup>(1)</sup>, Mihai Datcu <sup>(2)</sup>

Department

<sup>(1)</sup>University Politehnica Bucharest Iuliu Maniu 1-3, RO

<sup>(2)</sup>DLR , DE

## Abstract

The article presents methods for scenes structure and object recognition using very High Resolution Interferometric SAR (InSAR) observations, and demonstrates their performance using TanDEM-X data. With the increased resolution of Synthetic Aperture Radar products provided by the new space missions, the complexity and heterogeneity of the scenes require new methods and approach for scene understanding and modeling. The variety of scattering mechanisms, from simple flat surface scattering to volume scattering in vegetated areas and double or multiple bouncing and corner reflections in urban environments, as well as the underlying geometrical effects make scene understanding and object recognition for data classification not a straightforward task to perform. While simple signal models can be employed for simple scattering mechanisms, the scattering models present in a very high resolution Synthetic Aperture Radar (SAR) image over urban areas are not available a priori and depend on a variety of factors. In this context the article proposes the use of InSAR observations and non-parametric models and discusses methods for structure and object recognition in very high resolution SAR images. The analysis is performed directly on the complex signal, making use of both the amplitude and the phase of the data. This is a very important aspect to consider, especially in high density urban scenes which contain an unpredictable number of structures, in particular man-made. Taking into account the coherent properties of the SAR acquisition system, the scene is modeled as a complex-valued random process, constructed by summing together two-dimensional complex exponential signals affected by noise. The proposed model is dependent on the imaged scene and the parameters to be estimated are the complex amplitudes and frequency components of the individual exponential terms. The estimates are computed in the frequency domain, in an iterative manner, from the InSAR signal periodogram. The estimation is performed in a mean-square sense, where an objective cost function is minimized when the estimated parameter vector is sufficiently descriptive for the imaged scene. The method finds the strongest complex sinusoid, cleans the sinusoid from the model and continues to iterate. At each step, all previously estimated exponentials are re-estimated until the relative change of the residue spectra of the model is conveniently small. In order to ensure the convergence of the algorithm, the number of components has to be previously known or estimated, or the estimation process stops when a desired spectral residue threshold is met. In our approach we start from a priori estimated number of components (or model order), based on the likelihood function, and by using an adaptive scheme we re-estimate the optimum number of components at each step. The estimated amplitudes and frequencies which are most dominant are retained as image descriptors and complete the set of features used for object classification. Further on, the optimum components are searched based on an Entropy Maximization Criterion, which ensures that the information contained in the estimated vectors of parameters is sufficiently discriminative for data classification. The experiments and discussions are conducted on very high resolution TanDEM-X data over urban scenes.

# Coregistration between Small Baseline InSAR Image Subsets using Pointwise Targets

Author(s)

Teng Wang <sup>(1)</sup>, Sigurjón Jónsson <sup>(1)</sup>

Department

<sup>(1)</sup>King Abdullah University of Science and Technology King Abdullah University of Science and Technology (KAUST), Thuwal, SA

## Abstract

Time-series InSAR analysis techniques such as Permanent (Persistent) Scatterer InSAR (PS-InSAR)[1], [2] and Small Baseline Subset (SBAS) analysis[3] are widely used to precisely measure ground deformation patterns and trends with high spatial resolution. It is well known that multi-image coregistration is the key procedure before starting time-series analysis. No matter whether PSlike or SBAS-like method is used, all the SAR images have to be coregistered and resampled onto the same grid of a single reference image (Master image). Mis-coregistration can severely reduce the interferometric coherence [7] and consequently result in incorrectly estimated ground deformation. Conventional InSAR coregistration consists of three main steps [4], [5], [6]: 1) estimation of the offsets between tie patches with amplitude cross-correlation, 2) fitting of a 2-D polynomial wrap function from a set of tie-patch offsets, and 3) resampling of the slave images. Generally speaking, there are three difficult situations for multi-image coregistration of SAR data: 1) coregistration between long temporal and/or normal baseline pairs, 2) coregistration between SAR images spanning a strong deformation event, such as a volcano eruption or a large earthquake, and 3) coregistration between images with seasonal feature changes, for example with and without snow coverage. To avoid coregistering long baseline InSAR images, Refice, A. et al. presented a method using a Minimum Spanning Tree (MST) to connect time-series SAR images[8]. Each interferogram (connection between SAR images) is weighted with their coherence, and then they search for the overall optimum tree i.e. the MST connecting all the images. Therefore, this MST connection strategy represents an attempt to coregister only short baseline SAR images for a given dataset. Coefficients of the polynomial warp functions are then transformed to map the coordinate of each image onto the Master image grid by inverting the incidence matrix of the MST. In [2], the same idea is used, despite that all the small baseline SAR image pairs are coregistered. Then the polynomial wrap function coefficients w.r.t. the master image are estimated by the weighted least squares approach. Nevertheless, for many datasets, we still face a large gap along either the temporal or normal baseline axis. In other words, coregistration approaches between highly decorrelated scenes still need to be studied. The corresponding research is mainly divided in two branches. One is trying to detect pointwise targets (PTs) from a single SAR image for better estimating the offsets [9], [10], [11], [12], and the other one focuses on the geometric wrap function, with which few tie patches are needed [13], [14]. Since the electromagnetic signature of a stable PT has been proved to be only slightly affected by the diversion of normal baselines [1], [15], [16], the amplitude cross-correlation can be reliable high on such targets. In [9], [12], feature detectors are used to locate PTs. Different from calculating the cross-correlation between the extended tie patches, in [11], the presented approach firstly detects PTs with an ideal 2-D impulse response function and then precisely estimates the offsets by maximizing the signal-to-clutter ratio (SCR). Nevertheless, it is difficult to detect enough PTs from a single SAR image that is strongly influenced by speckle noise. Alternatively, with the assistance of an external DEM and precise orbital data, geometrical wrap function can be used to estimate the offsets pixel by pixel [13]. Two benefits can be gained from this method: 1) only very few tie patches are needed to estimate the absolute offset (bias) in the

geometrical wrap function. 2) Ground topography is included in the model in order to reduce the high-order distortion effects related to the different imaging geometry. The analytical formulation and error propagation are given in [14]. However, since this algorithm needs to calculate the offset for each pixel, the computation burden is rather high. Still, at least one highly reliable tie patch has to be used for estimating the bias for the geometrical function. In this paper, we focus on the former two coregistration steps in the time-series InSAR scenario. A method is presented to coregister between small baseline SAR image subsets instead of between single SAR images. The connection strategy for the coregistration is similar as in [8], but we separate the MST into several sub-trees. The separation threshold depends on the coherence between image pairs. Applicably, a given baseline threshold or an occurrence of a strong deformation event is also possible to divide the MST into several sub-trees. All the images inside a single small baseline image subset are aligned firstly with conventional method, i.e. w.r.t. a temporal master image. And then the averaged amplitude map (incoherent mean amplitude map) is used for the next step. We use the sub-tree with the most SAR images (we call it Master subset) for detecting PTs and then search for the same targets in the other averaged amplitude maps to estimate the offsets between the subsets. For long normal baseline cases, a 3-D polynomial wrap function is proposed to fit the transformation geometry with an additional dimension of height coming from an external DEM. As we already have several coregistered images within the Master subset, Pointwise Target Candidates (PTCs) can at first be selected by coherence analysis. As shown in [17], PTs can be approximately detected by comparing the observed coherence with the estimated geometric coherence. Therefore, we can firstly use the decomposed coherence maps associated with small baseline interferograms to identify PTCs. In order to reduce the computation burden, only the PTCs are oversampled and used to carry out the following amplitude analysis. Since the speckle noise can be significantly reduced in the incoherent mean amplitude map without spatial resolution loss, the PTs can be located using the same response function in [11], but with a higher precision. The amplitude cross-correlation is then calculated with the detected PTs and a searching window on other subsets or images. The precise offsets can be estimated by searching for the maximum cross-correlation. Comparing with a single SAR image, many more PTs can be detected from the incoherent averaged amplitude analysis, allowing one to fit a 3-D polynomial wrap function with height for modeling the image transformation for long normal baseline image pairs. Finally, with the incidence matrix of the connection graph, we can easily align all the images onto the same Master grid. The proposed method is implemented on two test sites using ENVISAT ASAR images. One is a small volcano island Jewel at Tair in the southern Red Sea and the other is at the North Anatolian Fault in eastern Turkey. For both test sites, long normal baseline (> 500m) coregistration is unavoidable for the time series analysis. Moreover, for Jewel at Tair test site, an eruption happened during the data acquisition span, and for the North Anatolian Fault site, seasonal snow coverage strongly worsen the coregistration situation. The capability of our method is validated and evaluated by showing the coherence and amplitude stability improvement spanning the whole time-series dataset. Reference [1] Ferretti, A.; Prati, C.; Rocca, F.; , "Permanent scatterers in SAR interferometry," *IEEE Trans. Geosci. Remote Sens.* , vol.39, no.1, pp.8-20, Jan 2001 [2] Hooper, A., P. Segall, and H. Zebker, "Persistent Scatterer InSAR for Crustal Deformation Analysis, with Application to Volcán Alcedo, Galápagos", *J. Geophys. Res.*, 112, B07407, 2007. [3] Berardino, P.; Fornaro, G.; Lanari, R.; Sansosti, E.; , "A new algorithm for surface deformation monitoring based on small baseline differential SAR interferograms," *IEEE Trans. Geosci. Remote Sens.* , vol.40, no.11, pp. 2375- 2383, Nov 2002 [4] Q. Lin, J. F. Vesecky, and H. A. Zebker, "New approaches in interferometric SAR data processing," *IEEE Trans. Geosci. Remote Sens.*, vol. 30, no. 3, pp. 560–567, May 1992. [5] G. Fornaro and G. Franceschetti, "Image registration in interferometric SAR processing," *Proc. Inst. Elect. Eng., Radar, Sonar, Navig.*, vol. 142, no. 6, pp. 313–320, Dec. 1995. [6] R. F. Hanssen, *Radar Interferometry. Data Interpretation and Error Analysis*, Dordrecht, Kluwer Academic Publishers, 2001. [7] R. Touzi, A. Lopes, J. Bruniquel, and P.W. Vachon, "Coherence

estimation for SAR imagery", IEEE Trans. Geosci. Remote Sens., vol. 37, no. 1, pp. 135–149, Jan. 1999. [8] Refice, A.; Bovenga, F.; Nutricato, R.; , "MST-based stepwise connection strategies for multipass Radar data, with application to coregistration and equalization," IEEE Trans. Geosci. Remote Sens. , vol.44, no.8, pp.2029-2040, Aug. 2006 [9] Marinkovic, P.; Hanssen, R.; , "Advanced InSAR coregistration using point clusters," Geoscience and Remote Sensing Symposium, 2004. IGARSS '04. Proceedings. 2004 IEEE International , vol.1, no., pp.489-492, 20-24 Sept. 2004 [10] Bamler, R.; Eineder, M.; , "Accuracy of differential shift estimation by correlation and split-bandwidth interferometry for wideband and delta-k SAR systems," Geoscience and Remote Sensing Letters, IEEE , vol.2, no.2, pp. 151- 155, April 2005 [11] Serafino, F.; , "SAR image coregistration based on isolated point scatterers," Geoscience and Remote Sensing Letters, IEEE , vol.3, no.3, pp.354-358, July 2006 [12] Jinfeng Wang; Yiming Pi; Zongjie Cao; , "Level Set Method for SAR Image Coregistration," Geoscience and Remote Sensing Letters, IEEE , vol.5, no.4, pp.615-619, Oct. 2008 [13] Sansosti, E.; Berardino, P.; Manunta, M.; Serafino, F.; Fornaro, G.; , "Geometrical SAR Image Registration," IEEE Trans. Geosci. Remote Sens. , vol.44, no.10, pp.2861-2870, Oct. 2006 [14] Nitti, D.O.; Hanssen, R.F.; Refice, A.; Bovenga, F.; Nutricato, R.; , "Impact of DEM-Assisted Coregistration on High-Resolution SAR Interferometry," IEEE Trans. Geosci. Remote Sens. , vol.49, no.3, pp.1127-1143, March 2011 [15] F. Gatelli, A. M. Guamieri, F. Parizzi, P. Pasquali, C. Prati, and F. Rocca, "The wavenumber shift in SAR interferometry," IEEE Trans. Geosci. Remote Sens. , vol. 32, pp. 855-865, 1994. [16] D. Perissin, C. Prati, M. E. Engdahl, and Y. L. Desnos, "Validating the SAR Wavenumber Shift Principle With the ERS Envisat PS Coherent Combination," IEEE Trans. Geosci. Remote Sens. , vol. 44, pp. 2343-2351, 2006. [17] Teng Wang; Mingsheng Liao; Perissin, D.; , "InSAR Coherence-Decomposition Analysis," Geoscience and Remote Sensing Letters, IEEE , vol.7, no.1, pp.156-160, Jan. 2010.

## Posters on Methods - DInSAR/PSI

### Performance Evaluation of SBAS and PS to study land surface deformation in agricultural regions, case study: Western Tehran plain

#### Author(s)

Mostafa Esmaeili <sup>(1)</sup>, Mahdi Motagh <sup>(1)</sup>, Mahdi Motagh <sup>(1)</sup>

#### Department

<sup>(1)</sup>University of Tehran ,College of Engineering Tehran, North Amirabad, IR

#### Abstract

InSAR is a very effective tool for monitoring and measuring land surface deformations. However, due to spatial and temporal decorrelation, its applicability is limited to areas not much affected by geometric and temporal decorrelation. Multi-frame InSAR analysis using the two techniques of Small Baseline (SBAS) and Persistent Scatterer (PS) extends the capability of InSAR to deal with these limitations. Much study has been done in the past to apply these time-series techniques to study ground deformation associated with a wide range of natural and man-made phenomena. However, not much research has been done for detailed comparison between PS and SBAS applied to the same area, in particular in vegetated and agricultural regions with large deformation rates. In this paper we evaluate the performance of SBAS and PS to map regional subsidence rate in an agricultural region west of Tehran Plain, Iran. Our datasets includes 31 Envisat ASAR images, acquired in two tracks over the region during 2003-2008.

# Combining Continuous GPS and InSAR Data for the Analysis of Dynamic Aleutian Volcanoes

## Author(s)

Summer Miller <sup>(1)</sup>, Jeffrey Freymueller <sup>(1)</sup>, Wenyu Gong <sup>(1)</sup>, Franz Meyer <sup>(1)</sup>

## Department

<sup>(1)</sup>University of Alaska Fairbanks 903 Koyukuk Dr. Fairbanks AK 99775, USA

## Abstract

The application of InSAR to studying volcanic deformation is often limited. Especially volcanoes along Alaska's Aleutian chain are difficult targets for InSAR as their seasonal snow cover cause decorrelation close to the volcanic caldera, their exposed location in the North Pacific render them prone to severe atmospheric phase artifacts, and their location on small islands prevent the selection of suitable reference points necessary for deformation analysis. In this research, a combination of InSAR and GPS time-series data will be presented aimed at the following research goals: 1) through a comparison of GPS-based and InSAR-based deformation time series, what is the accuracy and precision of InSAR-derived deformation estimates in such challenging environments; 2) through a comparison between InSAR and GPS data, how accurate can the deformation of the InSAR reference point be estimated from a joint analysis of InSAR and GPS deformation signals; 3) can measurements of a local GPS network support the identification of residual atmospheric signals in InSAR-derived deformation time series. To achieve these research goals, the following work was performed: Time series of InSAR data were processed for two different test sites in Alaska, Okmok Volcano on Umnak Island, and Mt. Augustine located in the Cook Inlet. Short Baseline Subset (SBAS) processing was applied to extract deformation time series from the InSAR observations. Okmok volcano is one of the most active volcanoes in the Aleutian Island Chain and shows significant non-linear deformation behavior as it progresses through its eruption cycles. To analyze Okmok, two different InSAR data stacks were analyzed; a stack of L-band imagery acquired by the SAR sensor PALSAR on board the JAXA Advanced Land Observing Satellite produced deformation time series between 2006 and 2010; a stack of C-Band SAR data from the European Space Agency's Envisat satellite was used to produce a deformation time series between 2002 – 2009. These SAR-derived results were compared to measurements of GPS permanent stations as well as observations of a set of campaign GPS stations to address research goals 1) and 2) mentioned above. Four continuous GPS sites were available for this study that were installed on Okmok in 2002 and are located both within and around the caldera. Although Augustine volcano has shown several eruptions within the last decades, it is known to show very little deformation in between significant eruptions. This is evidenced by the observations of a dense continuous GPS network that is available on the island and that hasn't shown any significant deformation since its last eruption in 2006. A stack of ALOS PALSAR images was processed using SBAS and deformation signals were extracted. Due to the lack of significant deformation signals and due to the availability of spatially dense GPS observations, Augustine was the main test site for addressing research goal 3). From our research results we can conclude that combining InSAR and GPS measurements can significantly improve the capabilities of either technique especially in challenging environments as the one addressed here. Further research into more rigorous integration of both techniques in a joint analysis is needed to optimally exploit the synergies between these two geodetic tools.

# Towards repeatability, reliability and robustness in time-series InSAR

## Author(s)

Pooja Mahapatra <sup>(1)</sup>, Sami Samiei-Esfahany <sup>(1)</sup>, Ramon Hanssen <sup>(1)</sup>

Department

<sup>(1)</sup>Delft University of Technology, NL

## Abstract

As more and more excellent radar data are becoming available, InSAR techniques are being routinely applied on these data to measure ground deformation. The coloured deformation maps produced by (time-series) InSAR often seem to be uniquely interpretable, indubitable, and a result of objective data processing. Unfortunately, this proposition does not withstand critical assessment. Several comparative studies have been performed in the past for InSAR verification and validation, such as the Sardinia unwrapping study (1995), PSIC4 (Fringe 2003), the TerraFirma validation experiment (2007) and many other standalone experiments. However, a common feature of these studies has been that success in a particular case study does not necessarily imply success in another. This could be because of different radar data, locations, deformation and meteorological phenomena, processing methods, a priori information, and so on. Different methodologies, therefore, appear to produce significantly different results, which is unacceptable from a scientific point of view. Additionally, the current quality description of time-series InSAR deformation estimates is inadequate in terms of reliability, idealisation precision or a full variance-covariance matrix. There is thus a lack of transparency for end-users.

There are two main limitations of time-series InSAR techniques. First, there is a clear need for a match between the spatiotemporal sampling and extent of data in relation to the spatiotemporal variability of the deformation phenomenon. The availability of coherent scatterers is obviously not guaranteed in all cases. Secondly, and the main subject of this paper, there are a number of implicit assumptions one needs to make in order to perform successful interferometric data processing and parameter estimation. The results can depend on the data (number of images, their quality, temporal separation, homogeneity and extent), scatterer properties (number, quality, spatial separation, homogeneity and extent), signal (temporal and spatial smoothness, extent, abrupt changes in space and time) and the processing method used (conventional InSAR, time-series approaches such as persistent scatterer interferometry or PSI, small baselines and hybrid methods). Additionally, the parameter estimation problem is inherently underdetermined and ill-posed, making it solvable only by introducing a priori information. It is, therefore, important to know which information to use, how arbitrary they are, which assumptions to make, and how important or sensitive these assumptions are. These assumptions are not only limited to the well-known phase unwrapping conditions and paradigms, but also on a priori assumptions on atmospheric behaviour, (micro)topographic variability, direction of the deformation vector, and spatiotemporal behaviour of the deformation signal.

Using the test case of Harlingen in the Netherlands, we will show how changes in these assumptions affect the estimated parameters, and how sensitive the solution is to these assumptions. Owing to gas extraction and salt mining, areas around the town of Harlingen have experienced a cumulative subsidence of up to 32 cm over 18 years as measured by periodic levelling campaigns. ERS data over this region are processed using different PSI processing settings, which differ in their a priori choice of deformation model, network design, persistent scatterer selection method, atmosphere filter length and shape, noise filter length and orbit detrending. The influence of a posteriori filtering is also studied. The conclusion of this case-study



is that the only solution to improve the reliability of InSAR results is to make these assumptions explicit and falsifiable. This will be demonstrated and discussed.

## A Kalman Filter Based MTInSAR Methodology for Deriving 3D Surface Displacement Evolutions

### Author(s)

Jun Hu <sup>(1)</sup>, Xiaoli Ding <sup>(2)</sup>, Zhiwei Li <sup>(1)</sup>, Jianjun Zhu <sup>(1)</sup>, Qian Sun <sup>(1)</sup>, Lei Zhang <sup>(2)</sup>, Makoto Omura <sup>(3)</sup>

### Department

<sup>(1)</sup>Central South University, CN

<sup>(2)</sup>The Hong Kong Polytechnic University, CN

<sup>(3)</sup>Kochi Women's University, CN

### Abstract

Multi-temporal InSAR (MTInSAR), e.g., Permanent Scatterer (PS) and Small Baseline Subsets (SBAS) techniques, have been used widely for studying earth surface deformations related to many geophysical processes. However, MTInSAR techniques have been able to measure one-dimensional (1D) surface deformations in the direction of the line-of-sight (LOS) of the radar. As surface deformations are in three-dimension (i.e., up-down, east-west and north-south), one-dimensional observation apparently cannot always fully reflect the actual deformations. In addition, the temporal resolution of MTInSAR measurements is limited by the satellite orbit repeat period. More and more SAR satellites had been launched in recent years, including ENVISAT, PALSAR, TerraSAR and Cosmo-SkyMed. It is therefore very desirable to combine the multiple observations from the different SAR satellites and orbits to derive more comprehensive surface deformation measurements. We present a novel new MTInSAR approach for exploiting multi-sensor, multi-track and multi-temporal interferograms to infer three-dimensional (3D) surface displacement evolutions. Compared to the existing methodologies, our method can exploit and merge SAR interferograms regardless of the diversities of acquisitive tracks and cover times. The proposed approach is based on Kalman filter that has been widely used for modeling various dynamic processes. The one-dimensional LOS displacement measurements derived from multi-sensor, multi-track and multi-temporal unwrapped interferograms are adjusted by the observation and state models of Kalman filter. The former model is used to connect the observations in different LOS directions to the three-dimensional surface displacements, which is constructed according to imaging geometry. The latter model establishes relations between the displacements at adjacent time by assuming ground movements be characterized by high temporal correlation. Kalman filter is a recursive estimator, which is executed in a predicting and updating alternation. By computing a weighted average of the predicted value and the measured value, the 3D surface displacement at all the acquisition times can be estimated based on the models and a weighting scheme that reflects the noise levels of the observations and the deformations. The proposed MTInSAR method is first validated by simulated data. The three-dimensional surface displacement evolutions can be perfectly recovered by the designed Kalman filter from multi-sensor, multi-track and multi-temporal interferograms without errors. Then, the errors with different levels are added into the interferogram, respectively. We find that the root mean square errors (RMSE) of 3D estimations all grow up but with increasing rates for up-down, east-west and north-south vectors, respectively. Especially in the case of only right-looking interferograms being available, any reliable estimation is not expected in the north-south direction when the errors in interferograms are obviously. The accuracy of the measurements in the north-south directions is low due to the polar orbits of the current SAR satellites. In order to ensure the accuracy of the results in the up and east-west directions, we assume that the deformation in the north-south direction is negligible in the case study carried out for the Los Angeles area. The experiment uses total 21 SAR acquisitions from ENVISAT ascending and descending orbits and PALSAR ascending

orbit. The results indicate that the area suffered seasonal vertical surface deformations and accumulated horizontal motions, which agreed well with those from the SCIGN GPS measurements in the area. Keyword: InSAR, multi-sensor, multi-track, Kalman filter, three-dimension

## SBAS bounds evaluation: a case study

### Author(s)

Carmen Patrascu <sup>(1)</sup>, Mihai Datcu <sup>(2)</sup>

### Department

<sup>(1)</sup>University Politehnica of Bucharest Nr. 1-3, Blvd. Iuliu MANIU, Bucharest, RO

<sup>(2)</sup>German Aerospace Center DLR Oberpfaffenhofen, D-82234 Wessling, DE

### Abstract

The article presents the assessment and comparative evaluation of Persistent Scatterer (PS) and Small Baseline Subset (SBAS) algorithms by employing a case study over the area of Valencia, Spain (harbor and surrounding areas) and Bucharest, Romania. The data sets used for this study consist of very High Resolution Interferometric TerraSAR-X observations over the interest region. SAR interferometry is a special technique that uses the properties of coherent waves for measuring the relative distance to interest objects by using the phase difference when there are at least two observations available, which are separated in time or space. Despite the fact that InSAR techniques have been successfully applied for measuring effects of a large series of ground deformation phenomena, such results can't be used to monitor the interest regions over large periods of time due to spatial and temporal decorrelation effects. Multi-temporal InSAR techniques represent extensions of conventional InSAR algorithms that aim at addressing these problems and involve the simultaneous processing of multiple SAR acquisitions of the same area extended over large periods of time. The Persistent Scatterer (PS) method aims to identify pixels with a single dominant response that are less affected by decorrelation and use their associated interferometric phase to infer a deformation time series. Hence, a network of such single scatterer-dominant pixels may be used to extract information signatures from interferograms that have been severely compromised by decorrelation effects. Another analysis method is known as the small baseline subset algorithm (SBAS) and is used for the extraction of the latency of the data. The SBAS method has been successfully applied for data pairs with small baseline values, different independent datasets separated by large temporal baselines being successfully linked by using the singular value decomposition method (SVD). The differential interferograms required by the methods will be generated using the DORIS software, while the phase unwrapping for the small baseline subset algorithm will be performed using Snaphu. A priori information related to the region of interest will also be used to develop structural models for deformation signal estimation. For the SBAS technique, the authors verify if the data is normally distributed, by employing the Kolmogorov test, while for the PS technique several methods for increasing the number of persistent scatterers will be discussed. Moreover, the influence of the baselines' values over the results will be addressed. Furthermore, the influence of the atmospheric phase screen will be estimated and removed from the data sets. The variation, direction and velocity of the existing displacements will be measured. A comparison between the results obtained with both techniques will be performed by analyzing both the advantages and drawbacks. Moreover, the outcome of the designed algorithms will be compared to the more traditional GPS and leveling measurements performed over the interest regions. The authors also classify the error sources and give an estimate of the mean error value and Cramer-Rao bound. A thorough understanding of different causes for errors is extremely important especially in the case of persistent scatterers where scattering mechanisms need to be analyzed.

# Salt mining induced subsidence mapping of Lueneburg (DE) using PSI and SBAS techniques exploiting ERS and TERRASAR-X data

Author(s)

Kanika Goel <sup>(1)</sup>, Alessandro Parizzi <sup>(1)</sup>, Nico Adam <sup>(1)</sup>

Department

<sup>(1)</sup>Remote Sensing Technology Institute (IMF), German Aerospace Center (DLR), DE

## Abstract

This paper is a comparative study of the subsidence analysis of Lueneburg exploiting ERS and TerraSAR-X data using both the Persistent Scatterer Interferometry (PSI) and the Small Baseline Subset Algorithm (SBAS). Lueneburg is a town situated in the German state of Lower Saxony. The old part of the town lies on a salt dome. As a result of constant salt mining dating back to the 19th century, various areas of the town have experienced a gradual or high subsidence. Due to this sinking, various parts of the town became unstable and had to be demolished. The mine was finally closed in 1980, however, the subsidence still continues even today. Many ground stations have been established since 1946 to monitor the deformation, but due to the changing subsidence patterns and locations, space-borne differential SAR interferometric technique has been applied for subsidence mapping of Lueneburg. First, we present results using C-band ERS satellites' data from 1992 to 2003. We estimate the deformation time series using PSI as well as the SBAS technique, and compare the results. PSI focuses on resolution cells characterized by a single dominant scatterer and makes use of interferograms generated using a single master scene. In comparison, SBAS concentrates on a distributed scattering model and makes use of small baseline interferograms not limited to a single master. For PSI processing, we split the ERS dataset into two because of the high data amounts (1992-1997, 1998-2003) and assume a linear deformation model. For SBAS, the whole dataset is processed in one go without any modelling and we estimate the non-linear deformation time series. The subsidence phenomenon is observable using both the techniques and the results are similar and consistent with the ground based measurements. However, due to the low resolution of the C-band ERS sensors, the highly localized subsidence phenomenon cannot be detected sometimes. Thus, since October 2010, the X-band SAR satellite TerraSAR-X is used to monitor the subsidence at high resolution. TerraSAR-X provides a resolution of 0.6 m in slant range and 1.1 m in azimuth in the High Resolution Spotlight mode and even single buildings can be mapped from space. With a short repeat cycle of 11 days, stack of acquisitions can be acquired rapidly for time series analysis. We have processed a small dataset of 7 images from October 2010 to February 2011 using the SBAS approach, and have generated 21 differential interferograms. In most of the interferograms, the deformation fringes are clearly visible in the area of interest, and confirm to the ground based observations. We present the TerraSAR-X interferograms and the first deformation estimation results for the above mentioned time period. TerraSAR-X data looks ideal for the application and we are now collecting a larger stack of High Resolution Spotlight data for a better quantitative analysis. This paper demonstrates the applicability of differential SAR interferometry for observing such phenomena as salt mining induced subsidence and similar applications. Higher resolution satellites such as TerraSAR-X have a high potential for monitoring the deformation time series and the results can be used for further risk assessment. Additionally, the PSI and SBAS techniques provide comparable results in identifying the salient deformation patterns for Lueneburg and further comparative studies could be performed to better understand the limitations of these two techniques.

# Posters on Volcanoes

## The 2007-8 Volcanic Eruption on Jebel at Tair Island (Red Sea) studied by InSAR

Author(s)

Sigurjon Jonsson <sup>(1)</sup>, Chong Chen <sup>(1)</sup>, Teng Wang <sup>(1)</sup>

Department

<sup>(1)</sup>KAUST, SA

### Abstract

Jebel at Tair is a small (11 square-km) oval-shaped volcano island in the south-central part of the Red Sea. This stratovolcano rises from about 1200 m depth, has an elevation of ~250 m, and is mostly covered by basaltic lava flows. The remote island has been uninhabited except for a small Yemeni military base. On September 30th, 2007, an eruption started near the summit on Jebel at Tair, which was the first known eruption to occur on the island for more than a century. Reports state that the eruption destroyed the base and caused a few casualties. No geophysical instruments are installed on the island to monitor volcanic and earthquake activity. Therefore, we use radar and optical remote sensing to study the eruption. From a total of 19 ALOS (2006-2010), 11 ENVISAT (2003-2010), and 8 ERS (2000-2008) radar images, we formed multiple SAR interferograms (InSAR). No accurate Digital Elevation Model (DEM) exists for the island, so we had to begin by generating a DEM from the InSAR data, in order to correct our deformation observations. A pre-eruption DEM was obtained using 6 ENVISAT images from 2003-2006, and a post-eruption DEM was generated from another 6 images acquired in 2009-2010. Analysis of optical and SAR amplitude images show that a new prominent summit scoria cone was formed in the eruption. These images also show the extent of the new lavas, which reached the sea on both the western and northeastern flanks of the volcano and added a noticeable amount to the area of the island. We use interferometric decorrelation in the InSAR data to map the progress of the lava during the eruption and to estimate the total area and volume of the erupted products. The entire lava covers more than half of the island, or almost 6 sq-km of the 11 sq-km island. The early phase of the eruption in October 2007 was the most active with lava flows reaching the sea both on the western and northeastern flanks of the volcano. Lavas during the later phases of the eruption in November and December 2007 and in 2008 were deposited near the summit crater and onto the north flank. Assuming lava thickness of 2 m (based on local observations) the volume of the erupted lava is ~0.012 cubic-km. Since the local observations were mostly acquired near the coast, this volume does not include an unknown amount of lava that flowed into the sea nor thicker lavas near the summit crater. For the latter part, the DEMs before and after the eruption were at first cross-validated over the areas where no new lava flows were deposited, and then these two DEMs were compared to get an estimate of the lava thickness for the whole island. No volcano-wide pre- or post-eruption deformation is observed, suggesting a rather deep source of the magma. The co-eruptive deformation, where it can be seen away from the newly formed lavas, is complex and is not easily explained by standard models.

# SAR Interferometric analysis of ground deformation at Santorini Volcano (Greece)

## Author(s)

Elena Papageorgiou <sup>(1)</sup>, Michael Foumelis <sup>(2)</sup>, Issaak Parcharidis <sup>(2)</sup>

## Department

<sup>(1)</sup>National & Kapodistrian University Of Athens Panepistimiopolis 157 84, Zografou , GR

<sup>(2)</sup>Harokopio University of Athens 70, El. Venizelou Str., Athens, GR

## Abstract

SAR Interferometry was successfully used at Santorini Volcanic Complex (Greece), so as to obtain measurements of the surface displacement. The core of the study builds on volcano deformation monitoring, whereas secondary-linked effects such as potential slope instabilities, creeping along the high-elevated caldera walls and subsidence phenomena are monitored as well. Data-set used for this case study, include multi-sensor observations of C-Band. In detail, satellite based observations covering almost two decades (1992-2010), amount to 70 ERS -1/2 and 29 ENVISAT ASAR acquisitions. Deformation signals of millimeter-level accuracy were retrieved from the combination of SAR and ASAR images, by way of advanced interferometric techniques. Interferometric Stacking (IS) was applied for the first time at Santorini Volcanic Complex, in order to derive displacement information. Despite the small land coverage of the volcano, than its high relief, a selected range of baselines was considered during the processing of differential interferograms, to avoid residual topographic effect. Spatially unwrapped differential interferograms of low perpendicular baselines ( $B_p < 200$  m) were primarily stacked, in order to reduce the effect of atmospheric phases. Through this process, namely by combining different data-sets (SAR/ASAR) with different covering periods, the overall observation period increases in temporal-scale, thus a quite robust solution is finally achieved. The volcanic movements which were measured through the differential phases from multi-sensor data, show mainly subsidence in the central part of the Santorini Caldera, at Kammeni Islands, while different ground deformation patterns were recognized elsewhere on the volcano. The obtained interferometric results were additionally validated by geodetic GPS measurements that were conducted at the area from 1994 to 2005, presenting time dependent surface displacements of an 11-year spanning period. Finally, this work presents an attempt to obtain integrated interferometric results of ground deformation from both ERS and ENVISAT sensors in order to allow future investigations on the deformation sources of the volcanic complex, the Volcanic Hazard Assessment, and furthermore the risk resulting mostly by slope instabilities near residential areas, a first basis for defining a prevention and mitigation plan of the risk.

## Correlated volcano deformation detected by InSAR

## Author(s)

Thomas Walter <sup>(1)</sup>

## Department

<sup>(1)</sup>GFZ Potsdam Helmholtzstr. 7, DE

## Abstract

Volcanoes are often considered as isolated systems, however, evidences increase that magmatic and hydrothermal unrests periods may be closely related to the surrounding. We investigate ENVISAT satellite radar acquisitions at the Campanian volcanic arc to explore how the volcanoes Vesuvius, Campi Flegrei and Ischia Island display a kinematic link. The data is interferometrically

processed and provides a deformation time series that spans the period from 1992 to 2008, suggesting that all the studied volcano centers undergo slow subsidence, intermittently and synchronously interrupted by uplift periods. A wavelet based statistical cross correlation analysis allows to test the associated deformation behavior in the frequency domain. We identify pixels that show a similar deformation trend in the long term and in the short term, and substantiate that the long term subsidence as well as the short term uplift periods are correlated at the three volcanic systems. Similar deformation occurrence is found also at sites of buried tectonic faults in the surrounding, leading us to argue for a close interrelation of the volcanoes and their surrounding.

## Evaluation of deformation processes in Tenerife volcanic island: the role of the troposphere.

### Author(s)

Elena Gonzalez <sup>(1)</sup>, Alvaro Márquez <sup>(2)</sup>, Anselmo Fernández <sup>(2)</sup>, Veronica Fernández <sup>(2)</sup>

### Department

<sup>(1)</sup>National Geographic Institute General Ibañez Íbero, 3, ES

<sup>(2)</sup>Rey Juan Carlos University , ES

### Abstract

Tenerife (Canary Islands) is an active volcanic island where is located Teide volcano, the only active stratovolcano in the Canaries, which had experimented explosive volcanic activity in the past. Previous Insar studies have shown different active deformation processes in the island, interpreted as related to several no-magmatic processes. As deformations can be a sign of future volcanic reactivation we have analyzed a large collection of interferograms of the island in an attempt to evaluate the different factors involved in the detected deformations by Insar. Interferograms have been made using Doris software with ENVISAT ASAR SLC ascending and descending images from 2003 to 2010 in the scope of the Cat-1 Project "Ground deformation detection due to volcanic activity in Tenerife (The Canary Islands) using InSAR / GNSS combined techniques". The first results show that, in a great deal of interferograms, appear fringes which are clearly related to topography and which should imply a long-wavelength deformation of the whole island (both uplift and subsidence) of several centimeters in very short time periods. Using permanent GPS measurements we prove that those fringes can not be related to any kind of deformation process of such magnitude. In fact, we show that they reflect the so-called tropospheric effect which usually takes place in broad topographic environments when an InSAR analysis is performed. We have used precipitable water vapor contents data coming from one atmospheric radiosonde and two sun-photometers operated in Tenerife island, as well as some MODIS acquisitions. The correlation between the apparent uplift/subsidence of the whole island observed in the interferograms and the calculated tropospheric phase delays show that the long-wavelength effect detected is clearly caused by variations in the water vapor content in the troposphere. In the future, those data will be used to create a model in order to minimize the atmospheric effects in the interferograms for a better evaluation of magmatic and tectonic deformation processes in the island.

# Beyond elasticity: the continuous to discontinuous deformation transition and its importance for InSAR data modeling in volcanology

## Author(s)

Eoghan Holohan <sup>(1)</sup>, Thomas Walter <sup>(1)</sup>, Martin Schöpfer <sup>(2)</sup>, Henriette Sudhaus <sup>(1)</sup>, John Walsh <sup>(2)</sup>

## Department

<sup>(1)</sup>Helmholtz-Centre Potsdam - German Research Centre for Geosciences (GFZ) Helmholtzstrasse 7, Potsdam 14467, DE

<sup>(2)</sup>University College Dublin Fault Analysis Group, UCD School of Geological Sciences, Belfield, Dublin 4, IE

## Abstract

Continuum-based modeling of surface displacements measured from SAR interferograms sometimes lead to estimates of sub-surface deformation source geometries that have uncertain geological meaning. For example, recent studies of subsidence during a 2009 eruption at Fernandina volcano and during a 1997-2001 quiescence period at Alcedo volcano have linked the observed surface displacements, at least in part, to contraction of shallowly-inclined (4-25°) prolate ellipsoidal sources (i.e. cigar-like 'Yang sources'). Directly relating such sources to the shape and orientation of subterranean magma bodies is not readily reconcilable with field data typical of sub-volcanic igneous intrusions, however. A hypothesis proposed here is that such inclined source geometries may represent a deflating magma body that causes discontinuous (i.e. fracture-related) deformation in the surrounding host rock. To test this hypothesis, we extracted surface displacement data from Distinct Element Method (DEM) models of magma body deflation that simulate a transition from continuous to discontinuous deformation with fracture localization. We then performed continuum-based modeling of the DEM surface data to retrieve the apparent sub-surface deformation source. Our results show that discontinuous deformation at depth induces asymmetries in the model's free surface displacement profile even if no discontinuities reach the surface. This is because the accumulation of discontinuous deformation tends to be path-dependent and ultimately asymmetric. The deformation-induced asymmetry of the surface displacement profile can, in principle, give rise to inclined or prolate deformation source geometries, even if the original magma body itself was not inclined. Consequently, continuum-discontinuum models can provide a basis for more geologically-plausible interpretations of the observed InSAR data than in the case of purely elastic models.

# Analysis of long-wavelength deformation in central Kamchatka, Russia, with combined InSAR and GPS time series

## Author(s)

Judith Levy <sup>(1)</sup>

## Department

<sup>(1)</sup>University of Alaska Fairbanks, University Potsdam 903 Koyukuk Dr, USA

## Abstract

The Kamchatka Peninsula in far eastern Russia hosts one of the world's most active arc volcanic centers, the Klyuchevskaya Group (KG). Comprised of several volcanoes, the location of KG does not follow the general trend of the volcanic chain in eastern Kamchatka, but is offset to the west into the Central Kamchatka Depression. Several seismic studies tried to explain the origin of this exceptional position within the Kamchatka subduction zone, relating it to a gradual shallowing of

subducted slab (Gorbatov et al., 1997) or a deep low viscosity zone at 150 km (Nikulin et al., 2010). Yet, the mechanism of the magma source is still poorly understood. To study the geophysical mechanisms behind KG, a network of 8 continuous GPS stations and 6 additional campaign sites were established in the region. The measurements from these stations show a large-scale subsidence rate of 7-9 mm/yr between the time period 2005 to 2010 (analyzed in the International Terrestrial Reference Frame) that extends spatially beyond the coverage of the GPS network. In addition to the recorded vertical motion, GPS sites across Kamchatka also show a horizontal motion westwards. In this study, GPS observations are augmented with InSAR measurements. Although Interferometric Synthetic Aperture Radar (InSAR) has proven useful for obtaining high resolution sub-centimeter line-of-sight surface deformation information for local structures, difficulties arise for subtle large-scale deformation. Because the expected signal wavelength is much larger than orbit errors, it is a challenge for InSAR processing to accurately derive large-scale deformation rates. Therefore, in this study, we use GPS time series to 1) correct InSAR data for orbital errors while preserving any deformation related long-wavelength signal, 2) separate horizontal and vertical deformation signals in the InSAR data, and 3) interpolate deformation signals between the widely spread GPS stations to achieve improved sampling of the two-dimensional deformation pattern. In addition, the GPS-refined interferograms will be used to invert for geophysical model parameters of the magma source and a comparison to the GPS inversion will be presented. To allow for a seamless analysis of InSAR data over large areas, swaths of adjacent ALOS PALSAR frames have been concatenated and processed to large coverage interferograms. The results presented in this study show the benefit of GPS/InSAR combination for separating long-wavelength error signals from large-scale deformation patterns. Using a set of validation points, it could be shown that InSAR and GPS observations retrieved comparable subsidence figures.

## Permanent Scatterers and Small Baselines ( SBAS ) applications over ETNA

### Author(s)

Fabiano Costantini <sup>(1)</sup>, Antonios Mouratidis, Francesco Sarti <sup>(2)</sup>

### Department

<sup>(1)</sup>Tor Vergata University Via del politecnico 1 Roma, IT

<sup>(2)</sup> ESA, IT

### Abstract

In the last years Permanent Scatterers and SBAS techniques have been regarded as the new frontier on many InSAR applications. The potential of PS and SBAS in lava detection and classification is a relatively new issue. Recent lava flows in fact presents a higher concentration of PS ( or coherent points according to the SBAS approach ) which tends to decrease as the age of the lava increase. It is also observed that the concentration of PS varies according to different type of volcanic products ( lava and tephra or a combination of both ). Preliminary results are about a study of this behaviour, in fact concentration of PS ( investigated for the whole Envisat mission both in ascending and descending orbits ) has been related to both age and type of the lava. In particular two interesting lava flows ( both in the north and south side of the volcano ) were localised studied into depth. In the above mentioned areas a phase history of the selcted PS has been performed to better understand and quantify the residual noise ( Topographic and atmospheric errors mainly ). Etna lava detection and classification complemented with optical data ( Landsat ETM and Hyperion sensors ) for different lava type discrimination. A collaboration with INGV ( Italian National Institute of Geophysics and Volcanology ) and Technical University of Delft ( The Netherlands ) for in situ data validation campaigns and processing strategies suggestions.



# Time series of volcanic deformation in the Galápagos: A perspective from InSAR, GPS, and seismic data

## Author(s)

Marco Bagnardi <sup>(1)</sup>, Scott Baker <sup>(1)</sup>, Falk Amelung <sup>(1)</sup>, Dustin Coté <sup>(2)</sup>,  
Cynthia Ebinger <sup>(2)</sup>

## Department

<sup>(1)</sup>University of Miami 4600 Rickenbacker Cswy, 33149 Miami, FL, USA

<sup>(2)</sup>University of Rochester Rochester, NY 14627, USA

## Abstract

Located off the coast of Ecuador in the Pacific Ocean, the Galápagos Islands are home to some of the most active volcanoes in the world. Given their geographic location and difficult working conditions, the volcanoes have gone largely unmonitored until the last nineteen years. Interferometric synthetic aperture radar (InSAR) provided surface displacement measurements across the island chain since 1992 and measurements covering six eruptions at three different volcanoes. A continuous GPS network established at Sierra Negra in 2003 provided daily three component surface displacements measurements at the volcano allowing precise measurements during the 2005 eruption and provided a comparison for the InSAR measurements. The temporary broadband seismic network established in 2009 around Sierra Negra and Cerro Azul provided unprecedented measurements of the seismicity at the volcanoes. Using InSAR from ERS-1, ERS-2, Radarsat-1, Envisat, and ALOS satellites from 1992 to 2011, we measured surface displacements at the active volcanoes in the Galápagos Islands and generated time series using the small baseline subset (SBAS) method. A time history of surface displacements was measured at Wolf, Darwin, Alcedo, Sierra Negra, Cerro Azul, and Fernandina volcanoes. Combined with the GPS and seismic data, the InSAR time series allowed us to correlate surface and subsurface activity at individual volcanoes. In addition to activity at individual volcanoes, interactions between neighboring volcanoes were also evident. A brief period of subsidence at Sierra Negra occurred during the 2008 eruption of Cerro Azul seen in both the InSAR and GPS time series. An interaction between Fernandina and Alcedo is also present in the InSAR time series, and the location of seismicity between the two volcanoes provides evidence for a subsurface linkage between them. By combining the InSAR, GPS, and seismic datasets, we obtain details about the time-dependent relationship between what is being measured and the controlling processes beneath.

# Volcanic Deformation in Kenya, East African Rift

## Author(s)

Elsbeth Robertson <sup>(1)</sup>, Juliet Biggs <sup>(1)</sup>, Marie Edmonds <sup>(2)</sup>

## Department

<sup>(1)</sup>University of Bristol Department of Earth Sciences, Wills Memorial Building, Queens Road, BS8 2RJ, UK

<sup>(2)</sup>University of Cambridge Department of Earth Sciences, Downing Street, UK

## Abstract

The East African Rift (EAR) system is a 5,000 km long series of fault bounded depressions that run from Djibouti to Mozambique. In Kenya, the EAR hosts 12 Quaternary volcanoes that lie along its central rift axis. An earlier InSAR study, covering the period 1997-2008, discovered that four volcanoes underwent geodetic activity during this time. We present the results of an InSAR survey of the Kenyan Rift between 2008 to 2010. During this period, frequent Envisat acquisitions were scheduled under the ESA Changing Earth Science Network. We also process a parallel dataset collected by L-band satellite ALOS, which allows us to image volcanoes obscured by

vegetation at C-band. We find that there has been no subsequent periods of volcanic deformation since that of Paka in May 2006 to March 2007. The northern flank of Paka volcano uplifted by 21.3cm over the 9 month period between 2006-2007 and the interferograms suggest some lateral transport of magma prior to the main inflation pulse. No deformation was seen in interferograms before or after these dates. Due to the large number of overlapping Envisat wide-swath acquisitions, the temporal resolution possible with this data is significantly greater than in background image mode. For example, during the 9 month period of inflation at Paka, there are four image mode acquisitions from one track, whereas, during the same time period, there are six wide-swath acquisitions from three different tracks. Thus, by using Envisat wide-swath imagery, we will better constrain, temporally and spatially, the period during which Paka deformed. Volcanic surface deformation is traditionally interpreted as the change in volume due to the movement of incompressible magma. However, magmatic intrusions deep within the crust can provide an input of heat and volatiles perturbing an overlying hydrothermal system that may cause ground deformation. Future work will be concentrated on determining the driving mechanisms of the volcanic deformation in the Kenyan East Africa Rift between 1997-2008.

## Surface displacement time series at Kilauea volcano, Hawaii using space-based synthetic aperture radar

### Author(s)

Scott Baker <sup>(1)</sup>, Falk Amelung <sup>(1)</sup>

### Department

<sup>(1)</sup>University of Miami 4600 Rickenbacker Causeway, Miami, FL 33149, USA

### Abstract

Located in the middle of the Pacific ocean, Kilauea volcano, Hawaii is one of the most active volcanoes on Earth with continuous eruptive activity since 1983. Following the June 17, 2007 intrusion in the east rift zone, the summit caldera and Pu'u O'o exhibited broad areas of subsidence. A new vent opened within the Halema'uma'u crater at the summit caldera in March 2008 and experiences ongoing activity. With the use of Envisat, ALOS, and TerraSAR-X data, we acquire continuous measurements of the surface displacement over the entire area. We generate line-of-sight (LOS) InSAR time series using the small baseline subset (SBAS) method for ten Alos paths, eleven Envisat tracks, and two TerraSAR-X orbits. This data set provides dense spatial and temporal coverage at Kilauea and a detailed time history of displacement between the June 2007 and March 2011 intrusions. We observe broad areas of subsidence around the summit caldera and Pu'u O'o in 2008 and 2009. Re-inflation within the summit caldera begins in 2010 and accelerates leading up to the March 5, 2011 intrusion. Observations of the surface displacements related to the intrusion and the response of the summit caldera area provide insight into the shallow magmatic system and the connectivity of the system.

# 1993-2010 InSAR measurements at Aso caldera (Japan).

## Author(s)

Adriano Nobile <sup>(1)</sup>, Joel Ruch <sup>(1)</sup>, Valerio Acocella <sup>(1)</sup>, Eugenio Sansosti <sup>(2)</sup>,  
Sven Borgstrom <sup>(3)</sup>, Valeria Siniscalchi <sup>(3)</sup>, Yosuke Aoki <sup>(4)</sup>

## Department

<sup>(1)</sup>Università degli Studi Roma Tre Largo san leonardo murialdo 1, IT

<sup>(2)</sup>IREA - CNR , IT

<sup>(3)</sup>INGV - Osservatorio Vesuviano , IT

<sup>(4)</sup>University of Tokyo , JP

## Abstract

Aso volcano, located in Kyushu island (southern Japan), is one of the largest calderas in the world. Aso formed during four major explosive eruptions between 270 and 90 ka. Several volcanic vents are located in the central part of the caldera, among which the Naka-Dake, one of the most active volcanoes in Japan, characterized by strombolian and phreatic activities. Naka-Dake erupted six times in the past 20 years, the last time in February 2008. We used InSAR to analyze ground deformation at Aso over 17 years, from October 1993 to October 2010. We processed 72 SAR images acquired by different sensors (ERS 1-2, ENVISAT and ALOS) using ROI\_PAC software (Jet Propulsion Laboratory release). ERS and ENVISAT pairs have generally a low coherence, with signal restricted to inhabited areas. ALOS pairs are more coherent, however, we observed relevant atmospheric and ionospheric artifacts, and the detection of small displacements is reduced by the longer radar wavelength. For periods with consistent signal, we made velocity maps to increase the signal-to-noise ratio and improve the detection of deformation in the caldera using interferograms with coherent area coverage > 50%. This technique allows us to obtain useful information on deformation rate also from pixels which are not coherent in all the interferograms. To process velocity maps we correct the single interferogram by assuming a stable area in Kumamoto city as reference and then subtracted the average signal of this area to the interferogram. We then analyzed the signal/topography correlation and, assuming it is linear, we subtracted the signal calculated by the linear equation for each pixel. We converted each interferogram into an average deformation velocity map by dividing it by the time span of the images pair. Finally, we stacked all the resulting maps. In particular, we focused our work on three periods for which steady ground deformation was detected. 1) From January 1996 to November 1998 (ERS data), we observed a subsidence signal of 1.5 cm/yr (LOS) occurred in the central part of the caldera beneath Naka-Dake area, just after the May 1994 – November 1995 eruption. 2) From October 2003 to June 2006 (ENVISAT data) an uplift signal of 1-2 cm/yr (LOS) was observed in the central-southern part of the caldera. This period includes two eruptions, in January 2004 and April-August 2005. 3) Preliminary results for the period from December 2008 to September 2010 (ALOS data) suggest an uplift rate of 2 cm/yr (LOS) occurred in Naka-Dake area. These results are broadly consistent with available leveling data (Ohkura, Personal communication).

# The integration of multi-sensor interferometric observations for monitoring ground deformation in Damavand volcano, Iran

## Author(s)

Sanaz Vajedian <sup>(1)</sup>, Mahdi Motagh <sup>(1)</sup>, Faramarz Nilfouroushan <sup>(2)</sup>

## Department

<sup>(1)</sup>University Department of Surveying and Geomatics Engineering, Faculty of Engineering, University of Tehran, IR

<sup>(2)</sup>Department of Earth Sciences Uppsala University, SE

## Abstract

Monitoring of ground deformation resulting from natural and man-made hazards provide valuable information for various stages involved in the disaster cycle, from pre-disaster risk reduction to mapping the effects of an event for post-disaster management. Remote sensing geodetic monitoring using techniques such as SAR Interferometry are becoming increasingly important in such studies as they provide regional, and spatially continuous maps of deformation with great accuracy, without the need of performing much field work or expensive ground surveys. In this study, we used Envisat and ALOS InSAR observation to monitor ground deformation in Damavand Mountain, Iran. The time series of SAR images using both Persistent Scatterer (PS) and Small Baseline (SBAS) methodologies are performed to create a multi-sensor, long time-series of deformation. A validation has been carried out by comparing the estimated deformation with independent data set obtained from three permanent global positioning system (GPS) stations. Our InSAR results are in good agreement with existing ground-based dataset and indicate that time-series interferometric methods using observations from multiple SAR sensors provide promising tools for mitigating environmental and processing artifacts in InSAR, enhancing the capability of radar data to produce reliable and accurate deformation maps.

# Envisat Extended mission" continues the InSAR monitoring of Mt. Etna

## Author(s)

Francesco Guglielmino <sup>(1)</sup>, Giuseppe Puglisi <sup>(1)</sup>

## Department

<sup>(1)</sup>INGV Istituto Nazionale di Geofisica e Vulcanologia, Piazza Roma, 2, Catania, IT

## Abstract

The Envisat mission extension beyond the end of 2010 allows to (a) operate the mission for an additional 3 years (until end of 2013 or early 2014) and (b) ensure the continuity of the maximum number of Envisat applications, with the exception of ASAR Interferometry. The change of orbit, indeed, degraded the interferometric capabilities. Nevertheless, the new orbit configuration of Envisat has been refined, in order to ensure that the InSAR baselines will be kept at a minimum value at specific latitude, around 38° North for descending passes and 38° South for ascending passes. Etna area (latitude 37.5 °) is favored by this new orbital configuration of Envisat, and the new orbital repeat cycle of 30 days (instead of 35) will ensure more frequent acquisitions. In the framework of the CAT-1. 5843, we produced an interferogram relevant to the 12 December 2010 – 20 January 2011 passes. In this period, a fire fountain episode occurred on 12 January at the South Eastern Crater (SEC) of Mt. Etna, which produced an eastward flowing lava flow, within the Valle del Bove area and a large volcanic plume high several kilometers. The episode started at about 22:00 local time and ended at about 00:50 of 13 January (Behncke et al., internal report

INGV-CT). The deformations recorded in the interferogram are relatively small and limited around the summit area, at elevations above the 1500-2000 m. The interferometric fringes, suggest a deflation that might be related to the emptying of the shallow magmatic reservoir, although an atmospheric component cannot be definitively excluded. These preliminary analyses well fit with the data acquired by the monitoring systems managed by the Section of Catania of the INGV (GPS, tilt, seismic) and field and helicopter surveys (Behncke et al., internal report INGV-CT) as well as with the preliminary results of CSK interferogram produced by CNR-IREA in the framework of ASI-SRV project.

## InSAR observations of post-rifting deformation around the Dabbahu rift segment, Afar, Ethiopia.

### Author(s)

Ian Hamling <sup>(1)</sup>, Tim Wright <sup>(2)</sup>, Laura Bennatti <sup>(3)</sup>, Eric Calais <sup>(3)</sup>, Elias Lewi <sup>(4)</sup>, Carolina Pagli <sup>(2)</sup>

### Department

<sup>(1)</sup>ICTP Strada Costiera 11, IT

<sup>(2)</sup>University of Leeds, UK

<sup>(3)</sup>Purdue University, USA

<sup>(4)</sup>Addis Ababa University, ET

### Abstract

The 60-km-long Dabbahu segment of the Nubia-Arabia plate boundary lies in the Northern Ethiopian region of Afar. In September 2005 a major rifting episode resulted in the injection of a 60-km-long dyke with a maximum thickness of ~8 m. Subsidence observed at Dabbahu and Gabho volcanoes implied that some of the magma was sourced from shallow reservoirs beneath the volcanoes. Since the September 2005 intrusion, background displacement rates are significantly larger than the average secular divergence between Nubia and Arabia. Furthermore, between June 2006 and May 2010 a further 13 dykes were intruded in the Dabbahu segment, in the vicinity and to the south of Ado'Ale - a dissected, silicic volcanic complex at the centre of the rift segment. Using multiple ascending and descending interferograms, acquired regularly following the onset of rifting, we invert for the best fitting displacement, at every pixel, and at each epoch. We next solve for the best fitting displacement rate, taking into account different displacement rates before and after the June 2006 dyke intrusion and midway through 2008, and static offsets caused by each of the new intrusions. In a final step we combine both ascending and descending data and invert for the rift perpendicular and vertical displacement rates around the rift segment. To validate the result of the inversion we compare the displacement rates determined from InSAR with GPS sites located around the rift zone and find that there is a good agreement between the horizontal and vertical displacements calculated by InSAR with the GPS.

Deformation is concentrated around the rift segment, with the largest displacements observed in the vicinity of the Ado'Ale complex, presumably caused by the accumulation of magma in a mid-lower crustal (8-10 km) reservoir. Rift-perpendicular displacements vary from ~135 mm/yr to 180 mm/yr on the western and eastern flanks respectively, with peak displacements occurring ~20 km away from the rift axis. Vertical deformation is observed along most of the rift segment over a broad ~50 km zone. Peak displacements of ~240 mm/yr are found around Ado'Ale and, to the south east of the rift, segment we observe around 300 mm of subsidence over the observation period. Using a viscoelastic model, consisting of an elastic lid over a viscoelastic half-space, we simulate the deformation resulting from the September 2005 dyke intrusion. Using a simplified opening distribution to drive the model, we generate a series of forward models with varying elastic lid thickness's (10-30 km) and viscosities ( $10^{17}$  -  $10^{19}$  Pas). We find that, regardless of the elastic thickness and viscosity used, there are a number of deforming areas around the rift segment that cannot be explained by this simple viscoelastic model. To improve the fit to the

data, and to account for the magmatic sources around the rift segment, we include an inversion for four point sources located around the rift. We find that the residuals are reduced after we include magmatic sources around the rift segment. Our best fitting model suggests a crustal thickness of ~15-16 km with an underlying viscosity of  $10^{18.5}$  Pa s.

## Detachment depth revealed by rollover deformation: an integrated approach at Mount Etna

Author(s)

Joel Ruch <sup>(1)</sup>

Department

<sup>(1)</sup>Università Roma Tre Scienze Geologiche, IT

### Abstract

Flank instability is common at volcanoes, even though the subsurface structures, including the depth to a detachment fault, remain poorly constrained. Here, we use a multidisciplinary approach, applicable to most volcanoes, to evaluate the detachment depth of the unstable NE flank of Mt. Etna. InSAR observations of Mount Etna during 1995-2008 show a trapdoor subsidence of the upper NE flank, with a maximum deformation against the NE Rift. The trapdoor tilt was highest in magnitude in 2002-2004, contemporaneous with the maximum rates of eastward slip along the east flank. We explain this deformation as due to a general eastward displacement of the flank, activating a rotational detachment and forming a rollover anticline, the head of which is against the NE Rift. Established 2D rollover construction models, constrained by morphological and structural data, suggest that the east-dipping detachment below the upper NE flank lies at around 4 km below the surface. This depth is consistent with seismicity that clusters above 2-3 km below sea level. Therefore, the episodically unstable NE flank lies above an east-dipping rotational detachment confined by the NE Rift and Pernicana Fault. Our approach, which combines short-term (InSAR) and long-term (geological) observations, constrains the 3D geometry and kinematics of part of the unstable flank of Etna and may be applicable and effective to understand the deeper structure of volcanoes undergoing flank instability or unrest.

## The April 3, 2010 earthquake along the Pernicana Fault (mt. Etna - IT): analysis of satellite and in situ ground deformation data integrated by the system approach

Author(s)

Francesco Guglielmino <sup>(1)</sup>, Christian Bignami <sup>(2)</sup>, Salvatore Stramondo <sup>(1)</sup>, Alessandro Bonforte <sup>(1)</sup>, Giuseppe Puglisi <sup>(1)</sup>, Francesco Obrizzo <sup>(1)</sup>, Urs Wegmüller <sup>(3)</sup>, Pierre Briole <sup>(4)</sup>

Department

<sup>(1)</sup>INGV Istituto Nazionale di Geofisica e Vulcanologia, Piazza Roma, 2, Catania, IT

<sup>(2)</sup>Centro Nazionale Terremoti - Istituto Nazionale di Geofisica e Vulcanologia Via di Vigna Murata, IT

<sup>(3)</sup>Gamma Remote Sensing AG CH-3073 Gümligen, CH

<sup>(4)</sup>Ecole Normale Supérieure UMR-CNRS 8538, 24 Rue Lhomond, FR

### Abstract

Etna is worldwide known as one of the most studied and monitored active volcanoes. Flank instability along the eastern and southern portion of Mt. Etna has been observed and measured thanks to geodetic networks and InSAR data analysis. The spreading area is bordered to the north by the east-west Pernicana Fault System (PFS) which dynamic is often linked with the

eruptive activity, as recently observed during the 2002-2003 eruption. A seismic sequence occurred since April 2-3, 2010, along the PFS with two very shallow (a few hundred meters) mainshocks of magnitude 3.6 and 3.5. Explosions and ash emissions at the summit craters followed this swarm and culminated some days later (April 7-8). Despite the small magnitude, the earthquakes produced damage effects and relevant surface faulting along the PFS. In order to investigate the ground deformation pattern associated with the seismic swarm, we integrated the available satellite with ground deformation data acquired in situ. The comparison between the GPS surveys carried out in June 2009 and in April 2010 (at either periodic and permanent stations) has shown the ground deformation pattern of the whole northeastern flank of Mt. Etna: horizontal displacements of about 5-6 cm at all stations located on the PFS as well as in the eastern flank of the volcano. In this study, we also considered two leveling surveys carried out in November 2009 and April 2010 along a leveling route crossing perpendicularly the Pernicana fault at an altitude of about 1,400 m asl. The analysis performed on the height variations, shows a subsidence of the fault hangingwall (of about 7 cm) with respect to the footwall. Trying to investigate the deformation occurred along the PFS during the events of April 3rd 2010, we performed a DInSAR (Differential Interferometric Synthetic Aperture Radar) analysis of ascending and descending Envisat, and of ascending ALOS-PALSAR images encompassing the date of the earthquake. In particular, we analyzed the ENVISAT ascending pair referring to 07/10/2009 – 05/05/2010 and the ENVISAT descending pair referring to 18/11/2009 – 07/04/2010 time interval. The Envisat interferograms show very intense but local deformation on the Envisat ascending data and a low signal for the descending geometry, close to the Pernicana fault trace. This is probably due to the oblique normal/left-lateral kinematics of the PFS (as deduced also by GPS and leveling data), indeed both vertical (lowering) and horizontal (eastwards) components of motion produce a strong stretching of the LOS (Line Of Sight) distance for ascending geometry, while the two components act in opposite ways for the descending geometry, resulting in lower LOS distance variations compared to the ascending data set. We analyzed also the ALOS pair referring to 21/02/2010 – 08/04/2010 time and acquired along the ascending track number 638. The interferogram clearly show three fringes corresponding to roughly 35 cm LOS (Line Of Sight) displacement. In order to investigate the ground deformation pattern associated with this event, an application of the novel SISTEM (Simultaneous and Integrated Strain Tensor Estimation from geodetic and satellite deformation Measurements) approach is presented here. To achieve higher accuracy and get better constraint of the 3D components of the displacements, we improved the standard formulation of SISTEM approach, based on the GPS and a single DInSAR sensor, in order to take into account all the available dataset (GPS, leveling, ascending and descending ENVISAT C-Band interferograms and the ALOS L-Band data). The results show a max eastward movement (120 mm) associated with a max lowering ( -70 mm) in the area along strike of PFS. The 3D displacement maps well show the kinematics, and are able to reconstruct also the ground deformation affecting the whole investigated area, defining the movements of the whole north-eastern flank of the volcano. The proposed SISTEM method is satisfactorily applied to study the ground deformation related to the April, 2-3 earthquakes occurred on Mt. Etna. These results, which provide an accurate spatial characterization of ground deformation, are hence promising for future studies aimed at improving the knowledge about the kinematics of the active faults of Mt. Etna.

# Improving the determination of volumetric sources from InSAR data

## Author(s)

Valerie Cayol <sup>(1)</sup>, Aurelien Augier <sup>(2)</sup>, Jean-Luc Froger <sup>(2)</sup>, Thierry Souriot <sup>(2)</sup>

## Department

<sup>(1)</sup>CNRS UMR 6524 - Univ. B. Pascal Clermont-Ferrand, FR

<sup>(2)</sup>Laboratoire Magmas et Volcans Clermont-Ferrand, FR

## Abstract

When observed surface displacements are assumed to be caused by volume strain within the crust, they are often represented by the superposition of unit volume strain for a flat topography, leading to a linear relation between the displacements and the sources  $d=Gm$ . The best-fit solution is sought by minimizing a misfit function corresponding to least-squares between the data and the model  $\|d-Gm\|^2$ . In order to get consistent volume changes between neighboring sources, the volume change  $m$  is smoothed by additionally minimizing a roughness function defined as the Laplacian of the volume changes, weighted by a parameter  $\rho^2$ ,  $\rho^2\|Lm\|^2$ . Finally, the internal distribution of volume changes is determined, for each  $\rho^2$ , by a matrix product. Often, the smoothing parameter  $\rho^2$  is graphically determined from a trade-off curve between the misfit and the roughness functions, such that increasing  $\rho^2$  does not lead to a significantly better misfit. This whole procedure has several limitations. For instance, the topography is rarely flat. Logarithmic representations of the trade off curve shows that there can be several plausible values of  $\rho^2$ . This study proposes to improve the determination of volumetric sources in several ways. Firstly, in order to solve the problem for prominent topographies, we propose to construct  $G$  by computing each unit spherical volume strain numerically. Using synthetic sources and the associated interferograms, we investigate the conditions under which it is valid to add these spherical sources and to implement this semi-numerical method. Secondly, instead of using an empirical graphic method to determine  $\rho^2$ , we use a cross-validation sum of square method. Again, synthetic tests are used to determine the best way to implement the cross-validation. Thirdly, we determine, the sources which contribute to the observed displacements the most and compute the resolution matrices. Fourthly, we investigate the influence of data noise and the advantage of the simultaneous use of several viewing geometries. Finally, this method is applied to the summit deflation recorded by InSAR after a caldera collapse which took place at Piton de la Fournaise volcano in April 2007 and results are compared with those obtained using a 3D numerical method with a near neighborhood algorithm.



# High-resolution interferometric monitoring of Piton de la Fournaise with TERRASAR-X and COSMO-SKYMED data

## Author(s)

Jean-Luc Froger <sup>(1)</sup>, Mary Grace BATO <sup>(2)</sup>, Nicolas Villeneuve <sup>(3)</sup>,  
Thierry Souriot <sup>(4)</sup>, Thierry Rabaute <sup>(5)</sup>, Philippe Durand <sup>(6)</sup>, Valérie Cayol <sup>(7)</sup>, Andrea Di Muro <sup>(8)</sup>,  
Thomas Staudacher <sup>(8)</sup>, Bénédicte Fruneau <sup>(9)</sup>, Claire Tinel <sup>(6)</sup>

## Department

<sup>(1)</sup>Observatoire de Physique du Globe de Clermont-Ferrand & Université Blaise Pascal 5 rue kessler, FR

<sup>(2)</sup>University of the Philippines-Diliman QC, Philippines, Philippina

<sup>(3)</sup>CNRS 7154, Université de La Réunion, IPGP 15 avenue René Cassin, 97715 Saint-Denis cedex 9, La Réunion,

<sup>(4)</sup>Observatoire de Physique du Globe de Clermont-Ferrand, Université Blaise Pascal 5 rue Kessler, 63038 Clermont-Ferrand, France

<sup>(5)</sup>CS CS, Parc de la Grande Plaine, 5, rue Brindejonc des Moulinais, BP 15872, 31506 Toulouse, France, France

<sup>(6)</sup>CNES CNES, 18 av Ed Belin, 31401 TOULOUSE Cedex 9, France

<sup>(7)</sup>Observatoire de Physique du Globe de Clermont-Ferrand, CNRS 5 rue Kessler, 63038 Clermont-Ferrand, France

<sup>(8)</sup>IPGP 14 RN3, le 27ème, 97418 La Plaine des Cafres, La Réunion, France

<sup>(9)</sup>Université Paris-Est 5 bd Descartes 77454 Marne-la-Vallée cedex, France

## Abstract

We present preliminary results of a TerraSAR-X and COSMO-SkyMed interferometric survey of Piton de la Fournaise volcano (Reunion Island, Indian Ocean) for the period between September 2009 and September 2011. The radar data used for this survey are StripMap images provided to us by DLR through the LAN 0237 project and by ASI through the CSK 2080 project. The interferograms were produced using the Diapason software (©Altamira-Information). In a first part of our study, we analyze in detail the benefits for the interferometric coherence of using jointly X-band data with a recent Lidar DEM. These benefits are compared with those of C-band data, provided by a set of 340 Envisat-ASAR interferograms previously produced on Piton de la Fournaise in the framework of the ESA AO-ENVISAT 746 project. We demonstrate that, thanks to its improved resolution, X-band coherence is significantly better in areas without vegetation than that of C-band and that it declines quickly, as expected, in areas covered with vegetation. Moreover, we show that X-band coherence can be used to automatically map, with a good accuracy, lava flows emplaced during the time spanned by the interferogram. Our study also reveals the importance of using an up-to-date high-resolution DEM in the interferometric processing, in order to take full advantage of the X-band data capabilities. In a second part of the study, we investigate the sensitivity of X-band data to atmospheric perturbations with, in particular, a remarkable example of a heavy tropical rain imaged on a COSMO-SkyMed interferogram. In a third part, we show how TerraSAR-X interferograms provide new insight on displacements associated with an intrusion that happened on 18-19 October 2009 and with four successive eruptions that occurred on 5-6 November 2009, 14 December 2009, 2-12 January 2010 and 14-31 October 2010. This study was carried out in the framework of the InSAR Observatory of Indian Ocean (OI2) Service of the Observatoire de Physique du Globe de Clermont-Ferrand and of the French Space Agency CNES KALIDEOS programme. Keywords: Piton de la Fournaise, Indian Ocean, Volcanology, Geodesy, Radar interferometry, InSAR, TerraSAR-X, COSMO-SkyMed Acknowledgements: We thank ESA for providing us with ASAR-ENVISAT data through projects ENVISAT-AO #746, DLR for providing us with TerraSAR-X data through projects LAN #237 and ASI for providing us with COSMO-SkyMed data through project CSK #2080.

# Anatomy of an unstable volcano from InSAR: multiple processes affecting flank instability at Mt. Etna, 1994-2008

## Author(s)

Valerio Acocella <sup>(1)</sup>, Giuseppe Solaro <sup>(2)</sup>, Susi Pepe <sup>(2)</sup>, Joel Ruch <sup>(1)</sup>, Marco Neri <sup>(3)</sup>, Eugenio Sansosti <sup>(2)</sup>

## Department

<sup>(1)</sup>Università Roma Tre Scienze Geologiche , IT

<sup>(2)</sup>IREA - CNR , IT

<sup>(3)</sup>INGV CT, IT

## Abstract

Volcano deformation may occur under different conditions. To understand how a volcano deforms, as well as relations with magmatic activity, we study in detail Mt. Etna using InSAR data, from 1994 to 2008. From 1994 to 2000, the volcano inflates with a linear behaviour. The inflation is accompanied by eastward and westward slip on the E and W flanks, respectively. The portions proximal to the summit show higher inflation rates, whereas the distal portions show several sectors bounded by faults, in some cases behaving as rigid blocks. From 2000 to 2003, the deformation becomes non-linear, especially on the proximal E and W flanks, showing marked eastward and westward displacements, respectively. This behaviour results from the deformation induced by the emplacement of feeder dikes during the 2001 and 2002-2003 eruptions. From 2003 to 2008, the deformation approaches linearity again, even though the overall pattern continues to be influenced by the emplacement of the dikes from 2001 to 2002. The eastward velocity on the E flank shows a marked asymmetry between the faster sectors to the N and those, largely inactive, to the S. In addition, from 1994 to 2008 part of the volcano base (S, W and N lower slopes) experienced a consistent trend of uplift, on the order of 0.5 cm/yr. This study reveals that the flanks of Etna have undergone a complex instability resulting from three main processes. In the long-term (103-104 years), the load of the volcano is responsible for the development of a peripheral bulge. In the intermediate-term ( $\leq 101$  years, observed from 1994 to 2000), inflation due to the accumulation of magma induces a moderate and linear uplift and outward slip of the flanks. On the short-term ( $\leq 1$  year, observed from 2001 to 2002), the emplacement of feeder dikes along the NE and S rifts results in a non-linear, focused and asymmetric deformation on the E and W flanks. Deformation due to flank instability is widespread at Mt. Etna, regardless of volcanic activity, and remains by far the predominant type of deformation on the volcano.

# Volcanic activity in Eastern Turkey investigated by using InSAR

## Author(s)

Hannes Bathke <sup>(1)</sup>, Manoochehr Shirzaei <sup>(2)</sup>, Thomas Walter <sup>(3)</sup>

## Department

<sup>(1)</sup>GFZ German Research Centre for Geosciences , DE

<sup>(2)</sup>Berkeley Seismological Laboratory, University of California , USA

<sup>(3)</sup>GFZ German Research Centre for Geosciences , DE

## Abstract

Volcanoes of eastern Turkey have been historically active and are located in an active tectonic system with abundant faults and fissures. Tendürek is a low relief shield volcano with an edifice height of about 3580 m and covers an area of 650 km<sup>2</sup>. The volcano edifice has an elliptical shape; the two summit craters and a flank crater are arranged in the direction of the long axis. The summit crater is nested (1000 m in diameter) and of relatively low relief, whereas the

smaller eastern summit crater (800 m in diameter) is a more morphologically striking feature and has developed a small crater lake. The volcano mid flanks are encircled by an also elliptical ring fracture system with a 9 km long axis and a 6 km minor axis [Yilmaz et al. 1998]. This fracture system is more developed in the south than in the north, therefore can be considered as a partial cauldron. Such cauldron or calderas typically are the fault bounded surface expression of major magma chambers that have been (temporarily) subject to deflation. However, no such magma chamber has been constrained so far at Tendürek, and only little geophysical, geological and geodetic data is available. Because the last eruption occurred only some 150 years ago, there is vivid interest in investigating the volcano state of activity, and its deep magma plumbing system. The liberal data policy and continuous SAR scene acquisitions now allows exploring archived catalogues at this hitherto geodetically unrecognized volcano. Here we report on a radar interferometric study combining SAR images acquired by the Envisat satellite in the years from 2004- 2008 and 2003- 2010 in ascending and descending orbits, respectively. We used the softwares ROI\_Pac [Rosen et al. 2004] and Doris [Kampes & Usai 1999] to create interferograms, used the SRTM 90 m resolution dataset to remove the phase contributions due to topography and unwrapped the signal using snaphu [Chen & Zebker 2001]. The StaMPS software [Hooper et al. 2007] was used to analyse the temporal evolution and to estimate a mean annual velocity of the deformation signal in both tracks. Finally 53 small baseline interferograms in ascending orbit and 69 interferograms in descending orbit have been used. In the time series generation the orbital and the atmospheric phase contributions are estimated and removed from the deformation signal. Due to the poor coherence in the summit area, less stable pixels have been identified and could be filtered. At the mid and lower flanks and at distance from the volcanic edifice in the lower plains a large number of stable pixels have been retrieved. This has left us with a non uniformly sampled dataset, which however, allows us to investigate the ground deformation pattern at unprecedented spatial detail. We observed various localized but evident deformation occurrences, presumably associated with volcano-tectonic activity at Tendürek volcano. Deformation affected the upper region of the volcano, including the summit craters within the dimension of the previously mentioned ring fault system at a very low rate. The deformation region is elliptical in shape and suggests a continuous subsidence, in agreement with the cauldron type encircling fracture system. In order to make this large dataset available for physical modeling, we explored a variety of data subsampling methods. We performed inverse modeling utilizing the Genetic Algorithm described in Shirzaei and Walter (2010) to describe the source of the observed signal using different types of dislocation sources (Mogi, Okada). We find that an Okada source is best explaining the signal. The position of the Okada source is located beneath Tendürek summit and suggests a sill-like body. Future research is to explore the physical reasoning for such a continuously deflating source, which is possibly an older intrusion subject to deflation or cooling.

References: Chen, C. W., and H. A. Zebker (2001), Two-dimensional phase unwrapping with use of statistical models for cost functions in nonlinear optimization, *Journal of the Optical Society of America A*, 18, 338-351. Hooper, A., Segall, P., Zebker, H. (2007), Persistent scatterer interferometric synthetic aperture radar for crustal deformation analysis, with application to Volcón Alcedo, Galápagos, *J. Geophys. Res.*, 112, B07407, doi:10.1029/2006JB004763. Kampes, B., and S. Usai (1999), Doris: The Delft object-oriented radar interferometric software, paper presented at 2nd Operationalization of Remote Sensing Symposium, ITC, Enschede, Netherlands. Rosen, P. A., S. Henley, G. Peltzer, and M. Simons (2004), Updated Repeat Orbit Interferometry Package Released, *Eos Trans. AGU*, 85(5), 47. Shirzaei, M., and T. R. Walter (2009), Randomly iterated search and statistical competency as powerful inversion tools for deformation source modeling: Application to volcano interferometric synthetic aperture radar data, *J. Geophys. Res.*, 114, B10401, doi:10.1029/2008JB006071. Yilmaz, Y., Güner, Y., Saroglu, F. (1998), Geology of the quaternary volcanic centers of the east Anatolia, *Journal of Volcanology and Geothermal Research*, 85, 173-210.

# Deformation at Katla volcano, Iceland, 2003-2009: Disentangling surface displacements due to ice load reduction and magma movement using InSAR time series analysis

Author(s)

Karsten Spaans <sup>(1)</sup>, Andy Hooper <sup>(1)</sup>

Department

<sup>(1)</sup>Delft University of Technology Kluyverweg 1, Delft, NL

## Abstract

Katla volcano is located in the south of Iceland, and is one of the most active volcanoes in the country. The central caldera is completely covered by Mýrdalsjökull icecap and the largest ice cap in Europe, Vatnajökull, lies approximately 80 km to the north-east. Climate warming over the last century has resulted in a loss of ice mass from these and the other icecaps in Iceland, causing surface displacements over the whole country. Surface displacements caused by magma movements, landslides and plate spreading sum with this ice loss signal. GPS campaigns on and around Katla have been performed since the 1990's, and since 2000 several continuous stations have been installed. The GPS measurements indicated a magmatic intrusion beneath Katla's caldera, lasting until 2003. In the following years, two of the continuous stations on the south flank of the volcano showed unexpected horizontal movements when compared to the predicted plate spreading velocities. These horizontal movements are unlikely to be caused by continued magma intrusions, as they were still being detected up to summer of 2009, at which point deformations related to the 2010 eruption of the neighboring Eyjafjallajökull volcano affected the data. Besides magmatic intrusions, ice load reduction, local landslides and flank sliding could also explain the horizontal movements. Differentiating between these causes will not only reveal if Katla has been exhibiting increased volcanic activity in the last decade, but will also improve our understanding of ice mass unloading and other processes acting around Katla. We applied radar interferometry (InSAR) to Envisat ASAR data to generate 21 interferograms covering the Katla area between 2003 and 2009, using the superior spatial sampling of InSAR compared to the GPS data to differentiate between the different deformation sources. We used the Stanford Method for Persistent Scatterers (StaMPS) to select a set of pixels with stable phase behavior in time. Several interferograms with high decorrelation noise, mainly due to snow cover and, to a lesser extent, long perpendicular baselines, affected the Persistent Scatterer (PS) selection. This resulted in fewer PS pixels being selected, while at the same time the selected PS pixels in the low coherence interferograms exhibited high decorrelation noise. To mitigate the influence of the interferograms with increased decorrelation on the remainder of the stack, we processed them separately. After applying conventional StaMPS processing on the high coherence stack, we evaluated for every selected PS pixel the phase noise in each of the decorrelated interferograms individually, allowing us to select for every low coherence interferogram a (different) subset of the original set of PS. This resulted in more phase stable points in the set of high coherence interferograms, while at the same time improving the signal-to-noise ratio in the low coherence interferograms. We subtracted a model of ice mass unloading [Árnadóttir et al, 2009] from the unwrapped phase results, leaving an estimate of the deformation signal, which exhibits variation only over a relatively small spatial extent. We find no indications of residual deformation signals that could be related to magma movements on Katla's south flank, nor on any other part of the volcano. Furthermore, local causes of the residual movements at the two stations, such as land sliding, are not likely, as we detect no significant variation in the deformation signal in the area surrounding the GPS stations. We also find no difference between the residual mean displacement rates on the south flank and an area to the east, ruling out flank instability. We therefore conclude that the model of ice unloading at Vatnajökull and, to a lesser extent,

Mýrdalsjökull is able to explain the anomalous horizontal movement at the GPS stations on the south flank. At Eyjafjallajökull, which abuts Katla to the west, we find a previously undetected movement away from the satellite on the south flank. From the location and spatial pattern we infer that this signal is most likely deflation related to cooling magma volumes intruded in 1994 and 1999. At Torfajökull volcano to the north of Katla, we also detect an area moving away from the satellite, which has been attributed to the cooling of a large solidified magma chamber below the volcano, the presence of which was inferred from seismic studies.

## Posters on Cross-Interferometry

### ERS-ENVISAT Cross-Interferometry Results over the Jangtsekiang delta in China

#### Author(s)

Urs Wegmüller <sup>(1)</sup>, Maurizio Santoro <sup>(1)</sup>, Andreas Wiesmann <sup>(1)</sup>

#### Department

<sup>(1)</sup>Gamma Remote Sensing, CH

#### Abstract

In 2002 ESA launched the ENVISAT satellite with the Advanced SAR (ASAR). ENVISAT is operated in the same orbits as the ERS-2, preceding ERS-2 by approximately 28 minutes. One of the ASAR modes, namely IS2 at VV-polarization corresponds closely to the ERS SAR mode, except for the slightly different sensor frequency used. A unique opportunity offered by these two similar SAR instruments operated in the same orbital configuration is ERS – ENVISAT cross-interferometry (CInSAR). At perpendicular baselines of approximately 2 kilometers the look-angle effect on the reflectivity spectrum compensates for the carrier frequency difference effect. As was shown with examples over Germany, the Netherlands, Italy, and Switzerland [1] CInSAR has a good potential to generate accurate DEMs over relatively flat terrain.

In this contribution we report on ERS-ENVISAT Tandem (EET) CInSAR results over the Jangtsekiang delta, north of Shanghai, China. Three suited EET pairs, as listed in Table 1, were available.

Table 1: EET CInSAR parameters of pairs selected over Jangtsekiang delta. Indicated are the perpendicular baseline component,  $B_{\text{perp}}$ , and the Doppler Centroid difference,  $dDC$ .

track	date	$B_{\text{perp}}[\text{m}]$	$dDC[\text{Hz}]$
275	20081207	1460	320
-003	20081223	1443	407
-275	20090215	2168	970

Over the very flat delta area, the interferometric phase nicely shows smallest variations in the surface topography, thanks to its excellent sensitivity with a height ambiguity below 5m. Abrupt height changes of a few meters are clearly visible in the cross interferograms. For more gentle phase variations it is not clear if the cause is the topographic height or a varying phase delays in the atmosphere. In the coherence field boundaries are clearly visible. Possibly this is because of irrigation channels which are present. Overall the coherence is not very high over the cultivated fields. The likely explanation for this is the vegetation present. Higher values are observed along the coast and for dry tidal flats.

One of the pairs was acquired at low tide. Over the exposed tidal flats the interferometric coherence is high because both scenes are acquired during the same low tide within 28 minutes. The shape of the dry part of the tidal flats is clearly visible with coherence level very clearly above the low level observed over water. The width of the tidal flats is several kilometres. In between the dry or exposed parts there are water channels. The interferometric phase shows details of the elevation of dry parts of the tidal flats. Radar backscattering alone is much less suited than the EET CInSAR pairs. Water and very smooth dry surfaces show both very low

backscattering and can be confused. Furthermore, the details on the elevation provided by EET CInSAR is not available from backscatter alone. We conclude from this example that EET CInSAR has a good potential for the mapping of surface topography in tidal flats.

#### References

[1] Wegmüller U., M. Santoro, C. Werner, T. Strozzi, A. Wiesmann, and W. Lengert, "DEM generation using ERS-ENVISAT interferometry", *Journal of Applied Geophysics* Vol. 69, pp 51–58, 2009, doi:10.1016/j.jappgeo.2009.04.002.

## ERS-ENVISAT Cross-Interferometry signatures over deserts

### Author(s)

Urs Wegmüller <sup>(1)</sup>, Maurizio Santoro <sup>(1)</sup>, Christian Mätzler <sup>(1)</sup>

### Department

<sup>(1)</sup>Gamma Remote Sensing , CH

### Abstract

In this contribution we report on ERS-ENVISAT (EET) cross-interferometry (CInSAR) results achieved over deserts in Egypt, Algeria, USA and Mauretania. In flat areas these long baseline pairs can be used to generate digital elevation models with meter precision [1,2]. Related results were already reported for Egypt [3] and the Mohave desert [4]. In the meantime we also analyzed EET CInSAR pairs over the Sahara in Algeria and Mauretania.

Looking more carefully at the CInSAR phase we could consistently identify some surface features which were not visible in the optical imagery available in Google Earth. We think that we see fine differences in the surface elevation up to a few meters at most. Those are very likely related to subsurface structures such as craters.

Another focus of this paper is on the interpretation of the backscattering and the coherence with respect to the land cover. EET CInSAR is characterized by long 2km baselines and very short 28 minute time intervals. As compared to the "usual repeat pass interferograms" this is a much longer baseline on one hand and a very short time interval on the other hand. Over deserts we observed very low coherence for some areas and investigated for which surfaces this was the case and searched for explanations. For sand dunes very low backscattering and low coherence was observed. We relate this to the penetration of the microwaves into the very dry surfaces and related volume decorrelation effects. Due to the relatively low dielectric constant of dry sand there is very little backscattering from the air – sand interface. Most of the radiation propagates into the sand. There it get scattered and absorbed. As a result of absorption within the sand and relatively low volume scattering the resulting total backscattering remains very low. The coherence is also very low because of the scattering occurring at different depths. So, for the sand dunes volume decorrelation results in very low coherence. Based on the low backscattering and coherence sand dunes can be reliably identified in EET CInSAR data. Validation against optical data confirms the good potential.

#### References

[1] Wegmüller U., M. Santoro, C. Werner, T. Strozzi, A. Wiesmann, and W. Lengert, "DEM generation using ERS-ENVISAT interferometry", *Journal of Applied Geophysics* Vol. 69, pp 51–58, 2009, doi:10.1016/j.jappgeo.2009.04.002.

[2] Wegmüller U., M. Santoro, C. Werner, and Z. Lu, "Validation of ERS – ENVISAT Cross-Interferometry DEMs over New Orleans," *Proc. ESA Living Planet Symp.*, Bergen, Norway, 28. Jun. – 2. Jul. 2010.

[3] Wegmüller U. and M. Santoro, "ERS-ENVISAT Cross-Interferometry results over Egypt," *Proc. Fringe'09*, Frascati, Italy, 30. Nov – 4. Dec. 2009.

[4] Wegmüller U. A. Wiesmann, and M. Santoro, "Merging of an EET CInSAR DEM with the SRTM DEM," *Proc. Fringe'09*, Frascati, Italy, 30. Nov – 4. Dec. 2009.

# Posters on 3<sup>rd</sup> Party Missions

## An overview of MetaSensing SAR interferometric capabilities at L, C, X and Ku band

### Author(s)

Adriano Meta <sup>(1)</sup>, Ernesto Imbembo <sup>(1)</sup>, Christian Trampuz <sup>(1)</sup>, Alex Coccia <sup>(1)</sup>

### Department

<sup>(1)</sup>MetaSensing , NL

### Abstract

**Title:** An overview of MetaSensing SAR interferometric capabilities at L, C, X and Ku band **Authors:** Adriano Meta, Ernesto Imbembo, Christian Trampuz, Alex Coccia

In the last years MetaSensing has developed several Synthetic Aperture Radar systems at different bands, including fully polarimetric and interferometric sensors at L, C, X and Ku band. The new MetaSensing approach to SAR has reduced costs and time to deploy for radar data acquisitions. The sensors have been deployed on a range of aircrafts (Cessna 172, Cessna 182, Cessna 208, CASA 212 and integration on Learjet 35 is on going) acquiring data for commercial customers and space and scientific agencies in several countries. Several acquisitions have been performed in single pass, repeat pass and polarimetric interferometry configurations. A few examples are: repeat pass polarimetric interferometry at L-band, repeat pass interferometry at X-band (each acquisition acquired also with single pass interferometry), fully polarimetric simultaneous X and Ku- band (acquired by the SnowSAR in Lapland, the high radiometric accurate instrument MetaSensing has built for the ESA CoReH2O airborne support activities) Examples of along-track interferometry in X-band for moving target detection are also described. Data collected over highways and on moving ships in harbours are presented. The acquired data are processed by the MetaSensing proprietary SAR processor, which takes as input the navigation data and radar raw data and generate geocoded SAR complex images. Other products are easily obtained like sub Doppler processing for enhanced radiometric accuracy. Repeat pass or polarimetric data takes are automatically processed to generate coregistered images, in order to ease the subsequent post processing steps. Digital elevation models of the imaged terrain are also automatically incorporated in the SAR processing in order to get the highest accuracy in the phase preserving processor. MetaSensing has also recently purchased a dedicated Cessna 182 Turbo aircraft for SAR data acquisitions. The aircraft is equipped with the Garmin G1000 glass cockpit and the latest navigation instruments, including flight planning and autopilot

In conclusion, the paper reports on the results achieved by MetaSensing sensors in the last three years of campaigns at L, C, X and Ku band. The commercial products of MetaSensing are based on more than a decade of advanced research and development carried out in the most prominent radar institutes and agencies in Europe.

# Posters on Thematic mapping and DEM

## Inter-Tidal flats segmentation of SAR images using waterfall hierarchical algorithm

### Author(s)

Fernando Soares <sup>(1)</sup>, João Catalão <sup>(1)</sup>, Giovanni Nico <sup>(2)</sup>

### Department

<sup>(1)</sup>IDL, University of Lisbon Campo Grande, Ed. C8, Piso 2, 1749-016 Lisboa, PT

<sup>(2)</sup>Consiglio Nazionale delle Ricerche (CNR), Istituto per Applicazioni del Calcolo (IAC), IT

### Abstract

Knowledge of coastline is the basis for measuring and characterizing land and water resources, such as the area of the land, and the perimeter of coastline. Information about coastline position, orientation and geometric shape is also essential for autonomous navigation, geographical exploration, coastal erosion monitoring and modeling, and coastal resource inventory and management. Automated coastline extraction from digital image data belongs to the boundary detection problem in the field of computer vision and image processing, in which edge detection and image segmentation are two conventional approaches to the boundary detection. In this work we present a morphological-based segmentation approach driven by the waterfall hierarchical algorithm, in order to recognize the inter-tidal region in SAR images. Different time datasets from the same area are used: one corresponding to the low tide and the other one to the high tide. Generally the gradient line on water to land transition, of SAR coastal images, is degraded by noise, which makes difficult its identification by a pixel oriented segmentation approach. A grey level image is a discrete surface topography that can be analyzed in terms of its relief characteristics. Waterfall computation modifies that topography by a bottom-to-top tree process of basins flooding, which is done by means of watershed and dual reconstruction morphological transformations. Segmentation instability and feature randomness may stand regarding result accomplishment for the proposed features over the entire scene, when standard waterfall method is applied. To overcome this problem, hierarchical waterfall segmentation improvement is fostered, by doing marker constraint in each step of waterfall segmentation tree. When this is applied over noisy grey level images, regions with higher homogenous background grey signature emerge. Also, it should be noted that improvements are obtained by a previous signal (image) frequency filtering, using the Fourier transform. This algorithm was applied to a dataset consisting of two TerraSAR-X images acquired over the region of Lisbon (south bank of Tejo river) with a temporal baseline of 11 days. These SAR images have a spatial resolution of 3 m which is appropriate to identify the inter-tidal flats characterized by a small spatial extension.. A change detection approach was used to detect the location of inter-tidal flats. For each pixel of the two SAR images, registered on the same spatial grid, it was computed the normalized amplitude difference. This new image gives information about areas whose scattering properties changed between the acquisition times of the two SAR images. Among these areas there are also the inter-tidally lands which have the property of being covered by water in just one of the two SAR images and so have different scattering properties resulting in a different intensity in SAR images. The change detection image was thresholded to identify areas with high values of the normalized amplitude difference. The first results show that a proper recognition of the inter-tidal zone is achieved.



# Contribution of Flash Floods to the Interannual Variability of Dust Emission in the Sahara

## Author(s)

Kerstin Schepanski <sup>(1)</sup>, Tim Wright <sup>(1)</sup>, Peter Knippertz <sup>(1)</sup>

## Department

<sup>(1)</sup>University of Leeds Leeds, LS2 9JT, UK

## Abstract

Recent studies using satellite observations show that numerous dust sources are located in the foothills of the Saharan mountains. Generally, dust emission is closely related to sediment supply and wind speeds. Thus, dust emission can be inhibited by either lack of high wind speeds or by surface characteristics. Studies on the activity of potential dust sources show a marked interannual variability, the reasons of which are not fully understood. Significant rainfall and flash flood events are assumed to lead to changes in pluvial sediment supplies in mountain drainage systems. These sediments are suitable for dust uplift and assumed to have a main contribution to the dust emission fluxes over these areas. Here, results of a study investigating the role of pluvial sediment supply in drainage systems within the foothills of Saharan mountains for dust emission and its interannual variability will be presented. For selected areas, ENVISAT SAR measurements will be used to identify changes in surface sediments through loss of coherence between two subsequent repeat cycles. TRMM rainfall product will be used to identify days with significant rainfall in order to check on plausibility and if positive to give exact timing of flooding. Further, identified events will be related to (i) the frequency of surface wind conditions suitable for dust emission and (ii) actual observed dust emissions. Results of this study will aid the discussion of interannual variability of dustiness as well as the representation of soil processes in numerical dust models.

# High resolution digital surface model for production of airport obstruction charts using spaceborne SAR sensors

## Author(s)

Henrique Oliveira <sup>(1)</sup>, Marco Rodrigues <sup>(1)</sup>, Andrea Radius <sup>(2)</sup>

## Department

<sup>(1)</sup>ESTIG-IPB Escola Superior de Saúde, Rua Dr. José Correia Maltez, PT

<sup>(2)</sup>EDISOFT , PT

## Abstract

This research work is co-funded by the European Space Agency through the ITI TYPE C INICIATIVE: ESTEC Contract No. 22722/09/NL/CBi. Abstract Airport Obstruction Charts (AOCs) are graphical representations of natural or man-made obstructions (its locations and heights) around airfields, according to International Civil Aviation Organization (ICAO) Annexes 4, 14 and 15. One of the most important types of data used in AOCs production/update tasks is a Digital Surface Model (first reflective surface) of the surveyed area. The development of advanced remote sensing technologies provide the available tools for obstruction data acquisition, while Geographic Information Systems (GIS) present the perfect platform for storing and analyzing this type of data, enabling the production of digital AOCs, greatly contributing to the increase of the situational awareness of pilots and enhancing the air navigation safety level [1]. Data acquisition corresponding to the first reflective surface can be obtained through the use of Airborne Laser-Scanning and Light Detection and Ranging (ALS/LIDAR) or Spaceborne SAR Systems. The need of surveying broad areas, like the entire territory of a state, shows that Spaceborne SAR systems

are the most adequate in economic and feasibility terms of the process, to perform the monitoring and producing a high resolution Digital Surface Model (DSM). The high resolution DSM generation depends on many factors: the available data set, the used technique and the setting parameters. To increase the precision and obtain high resolution products, two techniques are available using a stack of data: the PS (Permanent Scatterers) technique [2], that uses large stack of data to identify many stable and coherent targets through multi-temporal analysis, removing the atmospheric contribution and to minimize the estimation errors, and the Small Baseline Subset (SBAS) technique ([3],[4]), that relies on the use of small baseline SAR interferograms and on the application of the so called singular value decomposition (SVD) method, in order to link independent SAR acquisition data sets, separated by large baselines, thus increasing the number of data used for the analysis. A tested area was established, corresponding to a 45 Km radius area from the Aerodrome Reference Point (ARP) of Faro Airport. Since few images are available for the tested area, the PS technique cannot be applied, and the attention was focused on the second technique, the SBAS. However, the SBAS technique was developed originally to generate deformation maps with differential interferometry (DINSAR); in our case, this technique was modified to find the solution in case of across track interferometry (INSAR) and implemented in SARSCAPE software. In the processing chain we selected relatively big baselines (between the 15% and 65% of the critical baseline) and used the same inversion scheme to retrieve a robust solution for the DEM, setting to zero the deformation contribute. After the selection of the high quality interferograms to use in the SBAS inversion, the resulting DSM was filtered to reduce the atmospheric contribution through the Wavelet method. The combination between the modified SBAS inversion algorithm, the selection of high quality interferograms and the atmospheric contribute removing allows generating high resolution DSM with relatively poor stack of data. Several data structures were used as ground truth data to evaluate the high resolution DMS, notably: a national raster model with a centimeter vertical accuracy and produced using human stereo-photogrammetric restitution validated by in situ topographic and geodetic observations; points from the Portuguese Geodetic Network (vector data) positioned inside the 45 Km radius area from the Aerodrome Reference Point (ARP) for Faro Airport; a set of specific points (vector data), corresponding to the highest points of well known and stable man-made objects (buildings, bridges, telecommunication's antennas, wind power stations, cranes, among others), randomly distributed inside the 45 Km radius area from the Aerodrome Reference Point (ARP) of Faro Airport, with a centimeter horizontal and vertical accuracies. Experimental results obtained shows that the DSM produced with the SBAS technique presents the accordance with the numerical requirements stated in ICAO's annex 15, chapter 10, with a vertical accuracy lower than 30 meters. Although, the presences of slivers near shoreline with extremely lower frequency were found, they can be eliminated using a special filter for this purpose.

Acknowledgments The authors acknowledge the support from ITT Visual Information Solutions GmbH, for the production of the Digital Surface Model using SARSCAPE Modules for ENVI [5].

REFERENCES [1] D. Damjanovic, "Using gis and remote sensing to enhance air navigation safety", Photogrammetric and Engineering & Remote Sensing, ASPRS, May 2003, pp 478-481. [2] A. Ferretti, C. Prati and F. Rocca, "Nonlinear subsidence rate estimation using permanent scatterers in differential SAR interferometry", Geoscience and Remote Sensing, IEEE Transactions on, vol. 38, no. 5, Part 1, Sept. 2000, pp. 2202 - 2212. [3] Perissin, D.; Rocca, F.; , "High-Accuracy Urban DEM Using Permanent Scatterers," Geoscience and Remote Sensing, IEEE Transactions on , vol.44, no.11, pp.3338-3347, Nov. 2006. [4] Berardino, P.; Fornaro, G.; Lanari, R.; Sansosti, E.; , "A new algorithm for surface deformation monitoring based on small baseline differential SAR interferograms," Geoscience and Remote Sensing, IEEE Transactions on , vol.40, no.11, pp. 2375- 2383, Nov 2002. [5] <http://www.ittvis.com/language/en-US/ProductsServices/ENVI/SARscape.aspx>

# Void filling and APS removal for DEM reconstruction from high-resolution INSAR data

## Author(s)

Mingsheng Liao <sup>(1)</sup>, Houjun Jiang <sup>(1)</sup>, Teng Wang <sup>(2)</sup>, Lu Zhang <sup>(1)</sup>

## Department

<sup>(1)</sup>Wuhan University State Key Lab. for Info. Eng. in Surveying, Mapping and Remote Sensing (LIESMARS) Wuhan Univer, CN

<sup>(2)</sup>King Abdullah University of Science and Technology King Abdullah University of Science and Technology (KAUST), Thuwal, SA

## Abstract

The quality and accuracy of DEMs derived from repeat-pass InSAR is limited by decorrelation and atmospheric phase screen (APS) difference between SAR images. The main sources of decorrelation over mountain areas are 1) geometric decorrelation induced by incidence angle variations, 2) and temporal decorrelation caused by physical changes on the terrain surface. Decorrelation usually results in data voids in interferometric DEMs. These void areas may have steep topography (layover and shadow regions), or, are covered by plants or water. Another limitation, the APS difference, introduces global and local phase errors. This kind of error is very difficult to remove and cannot be ignored. In this presentation, we show a compromising but effective approach to avoid DEM gaps and remove height errors induced by the atmosphere. Existing low resolution DEMs are used as external data to improve the quality of interferometric DEM. Our approach focuses on two aspects: 1) Fill data voids and calibrate the height with an external DEM. Data voids filling and height calibration are applied before geocoding to reduce positioning error. The external DEM is aligned to SAR coordinates via a coregistration between the simulated SAR image from external DEM and the interferogram amplitude image. The data voids are filled by the radarcoded DEM and the height are calibrated by using a linear model to eliminate systematic errors. 2) Estimate the APS from a differential interferogram with a low-pass filter in the frequency domain, and remove the height errors caused by APS. Differential interferograms are commonly used for ground surface deformation measurement. However, for topographic mapping, if deformation signals can be neglected from a differential interferogram with very short temporal baseline, the main power of low-frequency signals should come from the atmospheric artefacts. Therefore, the APS can be filtered out from a differential interferogram to improve DEM accuracy. In this step a fifth-order Butterworth filter, with a cutoff wavelength of 500 m, is adopted. The proposed method has been applied on high-resolution COSMO-SkyMed Tandem data with one-day temporal baseline over Mt.Qilian in north-western China. The images were acquired in stripmap (Himage) mode with 3 m resolution. Because of the one-day temporal baseline of our test data, the deformation signals were neglected in the experiment. A 10×10 km wide test area was selected. This area is characterized by an extremely rough terrain with elevation ranging from 3100m to 4300 m. An ASTER Global DEM (ASTER GDEM) with 30 m resolution was chosen as external data to facilitate the InSAR DEM procedures. After the radarcoding of ASTER GDEM, a differential interferogram and a height map in SAR coordinates were obtained to extract APS and fill data voids (severely decorrelated areas). The resultant DEM has been validated in comparison with an officially-issued 1:50000 DEM. The preliminary result shows that atmospheric artefacts and data voids have been removed effectively in resulted DEM.

# InSAR DEM Reconstruction with ICESat GLAS Data

## Author(s)

Yu Zhou <sup>(1)</sup>, Chunxia Zhou <sup>(2)</sup>, Dongchen E <sup>(2)</sup>, Zemin Wand <sup>(2)</sup>, Xin Tian <sup>(3)</sup>, Yuanzheng Cui <sup>(3)</sup>

## Department

<sup>(1)</sup>School of Geodesy and Geomatics, Wuhan University 129 Luoyu Road, Wuhan 430079, Hubei, China, CN

<sup>(2)</sup>Chinese Antarctic Center of Surveying and Mapping (CACSM), Wuhan University 129 Luoyu Road, Wuhan 430079, Hubei, CN

<sup>(3)</sup>State Key Laboratory of Information Engineering in Surveying, Mapping and Remote Sensing (LIESMARS), Wuhan University 129 Luoyu Road, Wuhan 430079, Hubei, CN

## Abstract

Antarctic ice sheet has gathered worldwide attention in the recent decades since its behavior is closely related to the global climate, ecology environment and even the future of our human beings. The technologies of the earth observation from space make it more accessible to study the mechanism of Antarctic ice sheet. However, the optical techniques based on parallax require the identification of homologous features in the terrain, which poses problems in snow areas in polar regions. Consequently, this paper will discuss the SAR technique and its application along with altimetry data used in Grove Mountains, east Antarctica. The Grove Mountains Area, located in Antarctic inland areas and 400km to the south of the Chinese Zhongshan Station, is one of the most valuable areas for research. Chinese National Antarctic Research Expedition (CHINARE) has carried out expeditions to the Grove Mountains four times stemming from scientific interests on its special terrain, blue ice and abundant meteorolites. In addition to the image and topographical map, remote sensing technology can also provide the meaningful information to other disciplines and to the expedition safety as well. In this paper we demonstrate the generation of digital elevation model (DEM) of Grove Mountains core area using ERS-1/2 SAR tandem data with the interferometric technique. The potential of using interferometric synthetic aperture radar (InSAR) to estimate the topography was first demonstrated in 1987 by Li and Goldstein. InSAR has the advantage of all time, all weather operation and cost-effective data acquisition over large areas, especially those more inaccessible areas. Moreover it can provide topography information with elevation accuracies comparable with optical methods. The topography information is considerably important especially for Antarctic ice sheet research. However, the DEM derived from InSAR includes some inclination errors and its accuracy is deteriorated to a certain extent. Although some field data are collected in the latest expeditions by Chinese geodetic surveyors, the field survey only covers the core area by 110 square kilometers. As a result, it is still difficult to generate an accurate DEM of the whole Grove Mountains over 8000 kilometers square because of the sloping terrains and the satellite baseline errors. Considering the drawbacks ICESat GLAS (Geoscience Laser Altimetry System) data of high precision are taken into account thereby removing the residual fringe in the interferogram. It is difficult to go on further study such as ice flow and mass balance without highly accurate DEM. For this purpose, we adjust the InSAR DEM using ICESat GLAS data and then compare the result to the GPS data and ASTER GDEM. It turns out to be coincident with GPS data and ASTER GDEM. The paper confirms that InSAR is a very valuable technique to be utilized in Antarctica, however some errors are introduced by layover, foreshortening, shadow surface decorrelation, and the atmospheric signal in the data. Fortunately, ICESat laser altimetry footprints can provide several highly accurate height points for calibrating the residuals in InSAR DEM. We conclude that the fusion of InSAR DEM and ICESat GLAS data is necessary to improve the quality of InSAR DEM. In that way InSAR can be introduced to complement field survey.

# Enhancing Building Reconstruction by Adaptive Filtering of Interferometric Phases

## Author(s)

Antje Thiele <sup>(1)</sup>, Clemence Dubios <sup>(2)</sup>, Erich Cadario, Stefan Hinz <sup>(2)</sup>

## Department

<sup>(1)</sup>Karlsruhe Institute of Technology (KIT) Englerstrasse 7, DE

<sup>(2)</sup>Institute of Photogrammetry and Remote Sensing (IPF) Englerstrasse 7, DE

## Abstract

The upgrading of the current generation of space borne high resolution SAR sensors (e.g., Cosmo-SkyMed and TerraSAR-X) provides next to very high spatial resolutions additionally short repeat-pass and single-pass interferometric data. This makes such data attractive for three-dimensional information extraction. Especially, the operation configuration of TerraSAR-X and TanDEM-X opens up new perspectives for this kind of applications. The presented work is part of an overall project, which includes the implementation and the evaluation of an approach for automatic 3D building detection for supporting the planning of energy supply in the future. Especially, the development of smart filtering of interferometric phases for enhancing building reconstruction will be discussed in the full paper. In most cases, man-made building detection from SAR and InSAR data presented in the literature was mainly based on magnitude data alone or a combination of magnitude and interferometric height data. These approaches exploit the magnitude of building signatures by analyzing the layover and shadow areas. The exploitation of the interferometric heights was restricted to mean height calculation within an estimated building footprint. But in high resolution InSAR data even the shape of the interferometric phase profiles at building locations contains valuable information. Our previous analysis of InSAR phase signatures of buildings was up to now restricted to high-resolution airborne data due to the lack of high-resolution coherent single-pass InSAR data from space, which is now relieved by the TanDEM-X mission of DLR. The concept of our approach was already presented, and it exploits GIS and InSAR data for 3D building reconstruction. Our reconstruction is subdivided in the processing steps: extraction of building footprint, extraction of real measured InSAR phases, definition of an initial building height, simulation of InSAR phases, assessment of real and simulated InSAR phases, and iterative adaptation of the building model to achieve best correlation. Our first results of building height estimation considering airborne InSAR data pointed out, that the assessment step between the simulated and real measured InSAR phases is the most crucial point. Depending on the quality of the real phase signature and the sensor configuration (e.g., baseline length), a high correlation and consequently a reliable reconstruction result can not be achieved. One possible solution enables a smart filtering of the noisy InSAR phases. Up to now, only a conventional multi-look filtering was used to smooth the phase signature. The filter shows acceptable results for large buildings, but the detailed signature of small buildings was destroyed in particular by the use of large square windows, due to the fact that all significant information is in the layover area. Furthermore, considering building orientations nonparallel to sensor flight direction, this filter is also inappropriate. Hence, we want to test standard InSAR filters and we also started to develop appropriate phase filters to support our 3D building reconstruction. The implementation focuses on two different strategies, on the one hand taking GIS information into account and on the other hand without additionally GIS information. The first group utilizes the building footprint information and the given range orientation to apply fix orientation filter, adaptive orientation filter, or specific filter combinations adapted to layover and roof statistics. For the development of the second group of filters, we consider work of Goldstein et al. 1998 and Baran et al. 2003 with focus on the preservation of the building signature and especially the layover shape in range direction. For now, high-resolution single-pass airborne data are considered as test data because real TanDEM-X data are not available yet. Furthermore, noisy

simulated InSAR phases are taken into account to describe and discuss the properties of the different filters in more detail. In the final paper results of our filter implementations will be presented and if possible also first results on TanDEM-X data.

## Posters on DInSAR & PSI

### Report on ENVISAT Wide Swath interferometry beyond 2010

#### Author(s)

Davide Giudici <sup>(1)</sup>, Davide D'Aria <sup>(1)</sup>, Nuno Miranda <sup>(2)</sup>

#### Department

<sup>(1)</sup>Aresys , IT

<sup>(2)</sup>ESA - ESRIN , IT

#### Abstract

The ENVISAT satellite orbit has entered in the extended mission phase in November 2010. To save the on-board fuel, the satellite orbit has been lowered by about 17 Km, and the SAR acquisition modes parameters have been updated to adapt to the new acquisition geometry. It was demonstrated in literature the possibility to perform interferometry both with the ASAR stripmap (IM) and Wide Swath (WS) acquisition modes. In the new orbit, the inclination is no more controlled, leading to a drift where the inclination is expected to increase almost linearly in time. This situation impacts on interferometry, and, referring to the specific case of the WS interferometry, the impacts to be considered are the normal baseline and the burst synchronization. Regarding the normal baseline, a proper design of the new orbit guarantees to have small baselines in latitudes where interferometry is mostly requested by the users (i.e. around 38 degrees). The paper focuses on the Wide Swath interferometric capability after orbit lowering. After an introduction related to the impact of the baseline and the burst-synchronization on WS interferometry, the results (obtained with the "WS-SYNCHRO" tool, already published in literature) on the available ASAR interferometric datasets are reported. The most representative interferograms, within the found cooperative datasets, are shown, in order to assess their quality.

### Ocean Tide Loading corrections applied to Persistent Scatterer Interferometry processing at tide gauges in the United Kingdom.

#### Author(s)

Ligia M. Adamska <sup>(1)</sup>, Andrew Sowter <sup>(1)</sup>, Richard M. Bingley <sup>(1)</sup>,  
Simon D. P. Williams <sup>(2)</sup>, Jonathan M. Leighton <sup>(1)</sup>, Douglas G. Tragheim <sup>(3)</sup>,  
F. Norman Teferle <sup>(4)</sup>

#### Department

<sup>(1)</sup>IESSG Nottingham Geospatial Building, University of Nottingham, UK

<sup>(2)</sup>Proudman Oceanographic Laboratory National Oceanography Centre, UK

<sup>(3)</sup>British Geological Survey British Geological Survey, Kingsley Dunham Centre, UK

<sup>(4)</sup>University of Luxembourg 6, Rue Richard Coudenhove-Kalergi L-1359 LU

#### Abstract

A recent study concluded that since the 1990s globally-averaged sea level rose at a rate near the upper end of the sea level projections of the Intergovernmental Panel on Climate Change's last two Assessment Reports. With many coastal areas being located close to or below Mean Sea Level (MSL), there is a greater threat for them to be engulfed. Series of tide gauges (TG) located

at coastal sites measure MSL. These measurements, however, contain deformation due to both sea level variation and vertical land motion (VLM). Vertical land movement estimates at or close to TG locations from precise levelling, Continuous Global Positioning System (CGPS) and Absolute Gravity (AG), are used to correct the sea level estimates. Thus, it is very important to be able to identify the contribution due to changes in land level at the tide gauge, in order to effectively plan for flood risk management. Ocean Tide Loading (OTL) is the elastic response of the Earth's crust following the water mass redistribution due to ocean tides. OTL can introduce displacement gradients of more than 3cm per 100km, which can significantly affect the VLM estimates. OTL corrections, which are applied as standard to CGPS and AG estimates, are currently not considered during deformation monitoring using Persistent Scatter Interferometry (PSI). Over the past few years, PSI has been successfully applied to urban and rural area deformation monitoring. With millimetric accuracy, it is proving to be a powerful technique for the measurement and monitoring of VLM through the analyses of time series of specially selected pixels in the radar data. Contrary to precise levelling, GPS and AG, PSI is capable of providing estimates over a wide spatial extent. However, like precise levelling, these estimates are relative as opposed to the absolute VLM provided by CGPS and AG. In this research, we investigate the suitability of PSI for monitoring benchmark and GPS/AG installations at tide gauges in the United Kingdom. Four study areas with various settings (different levels of urbanisation / vegetation) have been selected for testing: Newlyn, Sheerness, Liverpool and North Shields. Also, the impact of OTL corrections is assessed through their computation and application during PSI processing.

## Mapping of water level changes in Anzali wetland, North Iran, using multi-sensor InSAR observations

### Author(s)

Negar Pesian <sup>(1)</sup>, Mahdi Motagh <sup>(2)</sup>, Mohammad Ali Sharifi <sup>(1)</sup>

### Department

<sup>(1)</sup>Department of Surveying and Geomatics Engineering, University College of Engineering, University of Tehran, IR

<sup>(2)</sup>Department of Geodesy and Remote Sensing, Helmholtz Centre Potsdam, GFZ German Research Centre for Geosciences Potsdam, DE

### Abstract

Wetlands are variable and fluctuant ecosystems that are usually located in transition zones between dry land and water bodies, where the land may be covered by water, either permanently or seasonally. Wetlands are vital to the health of all other biomes and to wildlife and humans. They can prevent flooding and soil erosion, filter and purify surface water, and have economical, recreational, historical, scientific and cultural significance. However, many of these productive ecosystems are subject to degradation due to pressures caused by human activities. The most effective factor on these ecosystems is hydrology. Thus, monitoring of hydrological alterations in wetlands can help experts implement effective measures for their restorations and improved functioning. This study focuses on the use of multi-sensor InSAR observations to monitor water level changes in Anzali wetland, Iran. Anzali is a coastal wetland located in the southern parts of Caspian Sea near Bandar-e Anzali City, in the Gilan province of North Iran. This site has been registered as a wetland of international importance in the 1975 Ramsar Convention. It was included in the Montreux Record in 1993 due to change in water levels and increased nutrient-enrichment. We used 20 Envisat (C-band), 18 ALOS PALSAR (L-band) and 2 TerraSAR-X (X-band) SAR images and made all possible combination of interferograms with short and long temporal baselines to monitor water level changes in this wetland. ALOS data were available in two modes of HH and HV polarization, while Envisat and TSX data were available only in VV and HH polarization, respectively. Our results show that X-band TerraSAR-X and C-band Envisat interferograms do not remain coherent in Anzali wetland even for short time interval. In contrast

to TSX and Envisat interferograms, L-band ALOS interferograms maintain a good level of coherence in the wetland area. For the ALSO data, we find that the coherence of HH interferograms is higher than their equivalent HV interferograms; the fringe patterns in HV interferograms are similar to those in HH interferograms but at a lower quality. This research demonstrates once again the promising future of multi-temporal polarimetric SAR data for operational monitoring of hydrological conditions in wetlands.

## Models to predict Persistent Scatterers data distribution and their capacity to register movement along the slope

### Author(s)

Davide Notti <sup>[1]</sup>, Claudia Meisina <sup>[1]</sup>, Alessio Colombo <sup>[2]</sup>, Francesco Zucca <sup>[1]</sup>

### Department

<sup>[1]</sup>University of Pavia Via Ferrata, 1 27100 Pavia, IT

<sup>[2]</sup>Arpa Piemonte Via Trento 11 - 13900 Biella , IT

### Abstract

In the last years the use of persistent scatterers SAR data in the studies of some geological processes like subsidence (Herrera et al., 2007), landslides (Colesanti and Wasowsky, 2006) and tectonics (Bürgmann et al., 2006) has show a rapid growth. One of the major challenge in the analysis of geological processes by means of PS is to know if we'll have data and how and how much these data measure the effective ground movement. The general PS limitation are well know in literature (Meisina et al, 2008). These limitations are related to methodology of SAR image processing, to the characteristics of space born sensors (geometry of acquisitions, wave length used, revisit time,..) as well as topography and the land use. The topography has strong influences on PS distribution affecting the images with layover, foreshortening and shadowing effects. Therefore it would be interesting to know in advance if interferometry is convenient or not and what kind of solution (geometries of acquisitions, type of processing) will be better to choose. In this work we tested a model and the parameters to predict by means of a simple GIS process the potential PS distribution and a model that show the percentage of real displacement measurable in relation with topography. The first forecast model is called "CR- index" this model give a probabilistic value to have a PS over certain area, this model was firstly created for a small sample area (30 km<sup>2</sup>) in the Pyrenees measured with TerraSarX- (Notti et al, 2010) and then applied to other areas, using other sensors showed some incongruence related to an not precise weight assigned to the land use factor. So we have tried to improve this model testing it over three wide areas in North-West Italy using C-band data Radarsat and ERS sensors. This index is composed by two parts, the first is an index "R-index" that take in account the topographic effect on SAR images.. To test the efficiency of R index we compared the value of R index with the density of PS in different geomorphological sector (NW and Ligurian Alps, Apennines and Turin Hills) and with different LOS incidence angle (34° and 23°). The results are an argument of discussion about the better geometry of acquisition to use in relation to area studied. The second parameter is the land use "LU-index", developing the model purposed by (Colombo et al, 2007) to each class of land use is assigned a probabilistic value to have PS based on the experience and back analysis. For instance buildings have a high probability to have PS (100), forests area or lake have probability close to 0 to contain potential scatterer. We tested also the difference in PS and DS (distribute scatterer) detection using the new SqueeSAR (Novali et al., 2009) processing. A further step is the combination of LU and R indexes to obtain CR index the methodology was revised from the original model and it appears as the most difficult part to solve. To test the efficiency of the models we compare the CR index the real distribution of SAR data. The results are object of discussion about the quality of input data and the quality of processing. Another model developed "V slope Index" has the aim to calculate the percentage of the movement



detected along Vlos supposing that we have a slide parallel to the maximum slope line. Also this is a trigonometric model that combines slope and aspect parameters derived from DEM with LOS parameters. This index is also the coefficient that converts the Vlos into the velocity projected along the slope. An interesting application that we purpose for the indexes developed is for instance crossing their information with a landslides inventory so it is possible to forecast how many landslides in the area under study are in a good condition to be analyzed by SAR data.

## PS and SBAS Interferometry over the broader area of Thessaloniki, Greece, using the 20-year archive of ERS and Envisat data.

### Author(s)

Antonios Mouratidis <sup>(1)</sup>, Fabiano Costantini <sup>(2)</sup>

Department

<sup>(1)</sup>ESA , IT

<sup>(2)</sup>Tor Vergata University , IT

### Abstract

With ERS-2 close to its de-orbiting phase, previewed for summer 2011 and Envisat operating through 2013, an era of very successful ESA C-band missions is coming to its end. Although SAR data from these two missions are still being collected, their interferometric applications are limited (no gyroscopes for ERS-2 since 2001 and special restrictions to interferometry with Envisat/ASAR data during its mission extension). While waiting for the first Sentinel-1 C-band SAR data by 2013, archived ERS and Envisat acquisitions of the past 20 years comprise a particularly consistent, long time-series dataset, suitable for implementing PS and SBAS interferometry. The broader Thessaloniki area in northern Greece presents great interest for SAR interferometry; the Mygdonia Basin (approx. 30km east of the city of Thessaloniki), is basin of tectonic origin that constitutes the most seismically active region in Northern Greece and has been the epicentral area of the most recent severe earthquake in the region (1978, Ms=6.5); neotectonic (active) faults in and around the perimeter of the city impose considerable risk for this highly urbanized environment of more than 1 million inhabitants; subsidence phenomena have been occurring for several decades in the broader area of Kalohori, located at the extension of the western end of the city of Thessaloniki, while other deformation signals of various origins have been reported as well. Considering both ascending and descending time series datasets, the purpose of this study is to exploit the full archive of ERS and Envisat SAR data (1991-2010). Using the Stanford Method for Persistent Scatterers (StaMPS) and ENVI SARscape™, PS and SBAS techniques are implemented, in order to produce deformation maps of the study area, to comment on technical aspects and to connect the results with observations from independent sources.

# Satellite and ground based InSAR studies of the Åknes rockslide in Norway

## Author(s)

John Dehls <sup>(1)</sup>, Tom Rune Lauknes <sup>(2)</sup>, Lars Harald Blikra <sup>(3)</sup>, Lene Kristensen <sup>(3)</sup>, Carlo Rivalta <sup>(4)</sup>

## Department

<sup>(1)</sup> Geological Survey of Norway , NO

<sup>(2)</sup> Norut , NO

<sup>(3)</sup> Åknes/Tafjord Beredskap IKS , NO

<sup>(4)</sup> Ellegi srl , IT

## Abstract

On the west side of Sunnylvsfjord, just north of Geirangerfjord, is the Åknes rockslide. This rockslide is almost 1 km<sup>2</sup>, with a volume of possibly more than 50 million m<sup>3</sup> of rock in motion. The rockslide comprises multiple sectors, with velocities ranging up to 10 cm/year. In the event of a large failure, the resulting tsunami will travel throughout the fjord system, affecting many communities. The rockslide is currently being continuously monitored by multiple systems, including: • Extensometers and crackmeters • tiltmeters • laser total station • single lasers • permanent GPS network • ground-based interferometric radar • weather station • three deep boreholes with multisensor instruments recording movement and water level. In addition, four large corner reflectors are installed to assist in satellite-based InSAR measurements. The steep topography and vegetated lower slopes make Åknes site a challenge to monitor using both ground-based and satellite InSAR. Early attempts used the archive of ERS-1 and ERS-2 scenes. Insufficient ascending scenes were available and descending scenes provided very limited data on the southeast facing slope. For this study, we have used ascending data from Envisat, Radarsat-2 and TerraSAR-X, as well as the LiSALab ground based radar system. Ground based InSAR campaigns at Åknes have been carried out each summer since 2005, with the exception of 2007. The LiSALab radar has been installed directly across the fjord from the rockslide. Campaigns have varied from 78 to 114 days. GB-InSAR results have been consistent from year to year. The upper portion of the rockslide is clearly identified, and the spatial extent of the moving area is in agreement with field observations. The lower, vegetated portion of the rockslide does not give good results. Satellite InSAR processing has been done using the GSAR SBAS software. We have processed Envisat ASAR scenes, from 2003 until present, Radarsat-2 fine and ultrafine scenes, from 2008 to present, and TerraSAR-X stripmap scenes from 2010 to 2011. The TerraSAR-X and Radarsat-2 ultrafine datasets produce velocity maps that clearly match field observations. The lower resolution Radarsat-2 fine and Envisat ASAR datasets are less successful. A comparison of all ground-based and satellite-based InSAR results will be presented, along with in situ monitoring data. The displacement measurements, which are captured from different line-of-sight geometries, have been projected into a common reference system for comparison. The effects of spatial resolution and temporal sampling will be discussed.

# Urban deformation monitoring using X-band Persistent Scatterer Interferometry

## Author(s)

Michele Crosetto <sup>(1)</sup>, Oriol Monserrat <sup>(1)</sup>, María Cuevas <sup>(1)</sup>, Núria Devanthéry <sup>(1)</sup>, Bruno Crippa <sup>(2)</sup>

## Department

<sup>(1)</sup>Institut de Geomàtica Av. Canal Olímpic, s/n, ES

<sup>(2)</sup>University of Milan Via Cicognara 7, I-20129, IT

## Abstract

This work reviews the application of X-band Persistent Scatterer Interferometry (PSI) in urban areas, using SAR data coming from the TerraSAR-X and CosmoSkyMed sensors. PSI is a satellite-based remote sensing technique used to measure and monitor surface deformation. The main goal of this work is to identify and disseminate both the advantages and the limitations of X-band PSI in urban areas. From one hand it is important to properly highlight the powerful advantages offered by a satellite-based remote sensing technique that is sensitive to millimetric displacements; on the other one (hand) it is important to identify and explain to potential users the limitations of this technique. Both the opportunistic character (PSI only works over the so-called Persistent Scatterers, where the interferometric phase is good enough to get reliable deformation estimates) and the ambiguous nature of its observations, affect its capability to measure "fast" deformation phenomena. The work will include: - An analysis of the key characteristics of X-band PSI. - The discussion of several types of PSI results coming from a stack of StripMap TerraSAR-X images that cover the metropolitan area of Barcelona (Spain). - A preliminary comparison between TerraSAR-X and CosmoSkyMed over the same area.

# Mexico city subsidence monitoring aided by interferometry: summary and discussion of the different achieved results

## Author(s)

Penelope Lopez-Quiroz <sup>(1)</sup>, Marie-Pierre Doin <sup>(2)</sup>, Yajing Yan <sup>(3)</sup>, Virginie Pinel <sup>(4)</sup>

## Department

<sup>(1)</sup>Centro de Investigacion en Geografia y Geomatica Ing. Jorge L. Tamayo A.C. , MX

<sup>(2)</sup>Ecole Normale Supérieure 24 rue Lhomond Paris Cedex 05 75231 FR

<sup>(3)</sup>Polytech'Savoie LISTIC - Polytech'Savoie BP 8043974944 Annecy le Vieux Cedex , FR

<sup>(4)</sup>Universite de Savoie Campus Scientifique Universite de Savoie, FR

## Abstract

Mexico City subsidence rates reach up to 40 cm/yr mainly due to soil compaction led by the over exploitation of the Mexico Basin aquifer. The destructiveness of the displacement is due to the subsidence vertical gradients causing fractures on the main city urban infrastructure (buildings, gas, water and sewage networks). The need to continuously map and analyze, through space and time, Mexico city subsidence is evident and useful to assess the government stakeholder decisions. Since 2002, we have been monitoring the Mexico city subsidence through time series generated using different InSAR methods. First we develop a dedicated SBAS (Small BASeline) based algorithm (Lopez-Quiroz et al. 2009). Then we perform an intercomparison with results obtained employing IPTA from Gamma Remote Sensing (Yan Y., et al. 2011, in press) and StaMPS, developed by Andrew Hooper. Ground data, like leveling and GPS, were employed to assure the quality of the obtained measures. As a result, the Mexico city subsidence has been mainly represented using a model where a linear and a "small" quadratic components are present. The

quadratic behaviour of the displacement, seem to be correlated in some of the Mexico city areas, with the fractures system. This work intends to present a summary and a discussion of the different results obtained on the Mexico city subsidence phenomena thanks to the use of the interferometric technique.

## Thermal Response of Buildings with TerraSAR-X Stripmap Data

### Author(s)

Yoangel Torres <sup>(1)</sup>, Scott Baker <sup>(1)</sup>, Tim Dixon, Faulk Amelung <sup>(1)</sup>,  
Kamal Premaratne <sup>(1)</sup>

### Department

<sup>(1)</sup>University of Miami 5816 SW 5th St, USA

### Abstract

This work studies the thermal response of buildings in El Paso Texas using TerraSAR-X data. The data set consists of 19 Stripmap, single polarization ascending acquisitions (26 degree look angle) between December 28, 2009 and July 25, 2010. We use the small baseline subset (SBAS) method to generate line-of-sight (LOS) displacement time series using 40 interferograms. For certain areas, the time series show 2 to 3 cm of line-of-sight displacement towards the satellite between April and June. These areas were localized on large buildings that appeared to be warehouses. During this time the daily high temperatures increased from an average of 7 degrees Celsius to 32 degrees Celsius. We see a direct correlation between the observed displacement time series and daily high temperatures. We interpret these displacements as being related to thermal expansion of these buildings.

## Detection of ground deformation in the Porto metropolitan area with persistent scatterer interferometry (PSI)

### Author(s)

Joaquim Sousa <sup>(1)</sup>, Andrew Hooper <sup>(2)</sup>, Ramon Hanssen <sup>(2)</sup>, Luisa Bastos <sup>(3)</sup>, Antonio Ruiz <sup>(4)</sup>

### Department

<sup>(1)</sup>University of Tras-os-Montes e Alto Douro , PT

<sup>(2)</sup>TU Delft , NL

<sup>(3)</sup>Faculdade de Ciências da Universidade do Porto , PT

<sup>(4)</sup>Universidad de Jaén , ES

### Abstract

Differential SAR interferometry (DInSAR) is an alternative technique to obtain measurements of the surface displacement providing better spatial resolution and comparable accuracy while being less time consuming than conventional surveying methods. The Persistent Scatterer Interferometry (PSI) technique allow us to measure deformation with uncertainties of one millimeter per year, interpreting time-series of interferometric phases at coherent point scatterers (PS). Considering the regular revisit time and wide-area coverage of satellite radar sensors, and that PS usually correspond to buildings and other man-made structures, this technique is particularly suitable for applications in urban environments, which often represent a harsh setting for GPS or conventional topographic surveying. This study is the first attempt to apply the PSI technique to derive urban displacement information in the Porto Metropolitan area. We present the preliminary results exposed by the PSI analysis using all available ERS-1/2 and Envisat SAR scenes spanning from 1992 to 2010.

# InSAR for early warning of possible highway instability over undermined area of Ostrava

Author(s)

Milan Lazecky <sup>[1]</sup>

Department

<sup>[1]</sup>VSB-TUO 17. listopadu 15, Ostrava, CZ

## Abstract

A part of a relatively new czech highway D1 connecting Ostrava with Prague and Poland, is built over an undermined area of Ostrava-Svinov. Since the end of 2010, this part of the highway is fully operational. Because of undermining, a subsidence can be expected, however with a very slow rate since the mines are no more active in this area (the mining ended about 20 years ago in the place). Several TerraSAR-X images from 2011 are investigated interferometrically in order to estimate as precise deformation model as possible. Subjects of interest are movements of newly built highway bridges, banks and the subsidence activity in the area. Corner reflectors installed in the road banks closeby will provide additional stable points. Existing C-band multitemporal InSAR processing results of ERS and Envisat are available from an earlier period that can reveal a slow trend of residual subsidence. In this project, InSAR will be investigated as a tool for an early warning for highway stability.

# Long term monitoring of mining induced subsidence in Thuringia, Germany by DInSAR

Author(s)

Nesrin Salepci <sup>[1]</sup>

Department

<sup>[1]</sup>Friedrich-Schiller-University of Jena Loebdergraben 32 D-07743 Jena Germany, DE

## Abstract

In this study, Differential SAR Interferometry (DInSAR) technique is employed to detect and to monitor mining induced subsidence in different mining sites of Thuringia state of Germany. Multi-sensor and multi-frequency constellation of ERS-1, ERS-2, ENVISAT-ASAR and ALOS-PALSAR data covering the period of 1995 to 2010 is exploited to derive subsidence information. Because the combined observation of C-band and L-band data enables information benefit compared to single-sensor and single-frequency approach since the sensitivity of different wavelengths to surface displacement varies. As a consequence of long term and intensive underground mining activities, slow surface subsidence as well rapid and unwanted change in the landscape, e.g. a sinkhole formation, may take place. The impact of such activities has already been experienced in Thuringia. One example to the rapid subsidence, which is probably due to underground mining, is the sinkhole opened up suddenly in November 2011 in Schmalkaden area. Following this incident, one idea is to monitor the area before formation of the sinkhole and to investigate the possibility of detecting potentially dangerous areas in advance. In order to reduce dangerous rock movements and surface subsidence, backfilling is applied at some mining sites. One of the important backfill mine in Thuringia is the Sondernhausen salt mine. Accordingly, another idea of the study is to use DInSAR to monitor the change in subsidence rate and to verify the results of backfilling. Therefore, besides Schmalkaden, Sondernhausen mining site will also be investigated in the framework of this application. GAMMA RS software is used for the whole processing chain of 2 pass-interferometry from SLC data to generation of displacement map. ERS and ASAR data

will be combined by cross-interferometry to obtain one deformation model for C-band sensors. The deformation models derived from C-band and L-band scenes will then be compared.

## DInSAR Application: Subsidence of the Cerro Blanco Caldera

### Author(s)

Roberto Cuccu <sup>(1)</sup>, Fabiano Costantini <sup>(1)</sup>, Francesco Sarti <sup>(1)</sup>

### Department

<sup>(1)</sup>ESA, IT

### Abstract

The purpose of this study were to monitor the deformation of the Cerro Blanco Caldera, which is located in the northwest Argentina, near the border with Chile, in the province of Catamarca, by applying differential SAR interferometry (DInSAR). Its basic principles and applications have already been well documented. A previous DInSAR analysis in the study area, referring to the years 1992 to 2000 and performed by using ERS data, detected subsidence of the Cerro Blanco Caldera. In order to give continuity to that study, this work, using ASAR (Envisat – C Band) images, covers the period after the year 2000, spanning from 2003 to 2009 (first and last ASAR data acquisition available). Fourteen ASAR (Envisat) Single Look Complex (SLC) images have been used. A classical DInSAR approach was followed and the processing was carried out via the DORIS (Delft Object-oriented Radar Interferometric Software) software. In total, 67 differential interferograms were successfully computed, but not all of them have been useful to detect the subsidence due to the high phase noise and errors which affect them. After a selection of the useful differential interferograms, an estimate of the subsidence rate has been computed assuming that the deformation rate is constant during the time period of each differential interferogram. The result of this study is that the Cerro Blanco Caldera has continued to subside during the period between 2003 and 2009, but with a lower speed than the deformation rates evaluated in the previous study (1992-2000). Moreover, available GPS measurements, made between 2004 and 2005, allowed to validate in part this work, in fact the interferogram which cover the same period is in perfect agreement with them.

## Assessment of surface deformation associated with CO<sub>2</sub> Storage at the Ketzin test site, Germany: Results from TerraSAR-X time-series analysis

### Author(s)

Christin Lubitz <sup>(1)</sup>, Mahdi Motagh <sup>(1)</sup>, Sonja Martens <sup>(1)</sup>, Thomas Kempka <sup>(1)</sup>, Hermann Kaufmann <sup>(1)</sup>

### Department

<sup>(1)</sup>GFZ German Research Centre for Geosciences Telegrafenberg, 14473 Potsdam, DE

### Abstract

Ketzin is Europe's longest-running on-shore CO<sub>2</sub> storage site with the aim of increasing the understanding of geological storage of CO<sub>2</sub> in saline aquifers. The investigation and monitoring of the reservoir and CO<sub>2</sub> migration at various spatial and temporal scales plays a key role in the evaluation of environmental impacts associated with the Carbon Capture and Storage (CCS) technology. As of June 2008, 48,500 tons (April 2011) of CO<sub>2</sub> have been injected at Ketzin. The site is monitored by a comprehensive system consisting of geophysical, geochemical and microbiological measurements. This work presents the application of the space-borne Interferometric Synthetic Aperture Radar (InSAR) technique for evaluation of the spatio-temporal pattern of potential surface deformation associated with the CO<sub>2</sub> injection at Ketzin. Time series

analyses are applied to TerraSAR-X data, which have been acquired for the Ketzin site since March 2009. We also present preliminary results based on data from four corner reflectors recently installed at Ketzin to enhance the applicability of the Persistent Scatterer Interferometry (PSI) on this rural test site.

## Radar Interferometry Time Series Analysis to Evaluate the Source Modeling of the City Uplift in Staufen i. Br. (Germany)

### Author(s)

Christin Lubitz <sup>(1)</sup>, Mahdi Motagh <sup>(1)</sup>, Hans-Ulrich Wetzel <sup>(1)</sup>, Barbara Breuer <sup>(2)</sup>, Jan Anderssohn <sup>(3)</sup>, Ingo Sass <sup>(2)</sup>, Hermann Kaufmann <sup>(1)</sup>

### Department

<sup>(1)</sup>GFZ German Research Centre for Geosciences Telegrafenberg, 14473 Potsdam, DE

<sup>(2)</sup>Technical University Darmstadt Schnittspahnstraße 9, 64287 Darmstadt, DE

<sup>(3)</sup>Astrium Services Platz der Einheit 14, 14467 Potsdam, Germany, DE

### Abstract

The historical city of Staufen in Germany has been adversely affected in recent years by land uplift, at a rate of several cm per year. This has resulted in considerable damage to building structures, including large cracks in the Staufen Town Hall and in many other buildings. Preliminary geological and geophysical investigations attribute the source of uplift to a geochemical process called as anhydrite swelling, presumably triggered by a geothermal drilling operation conducted in the area in 2007 to provide climate-friendly geothermal heating to the city hall. The drilling operation caused the rise of the high-pressure groundwater to the Keuper-gypsum layer above, in turn causing the anhydrite to transform into gypsum, which then started to expand and to cause land uplift. The ongoing pattern of uplift in Staufen has been carefully monitored using conventional leveling surveys. In this study we present a new uplift map for the city, generated from interferometric analysis of TerraSAR-X StripMap data, acquired in the area between October 2008 and May 2010. We investigate the spatial distribution and temporal pattern of surface deformation using advanced InSAR processing techniques of Persistent Scatterer (PS) and Small Baseline (SBAS) methodologies and compare the results. The outcome of both techniques will be used to evaluate a recently updated source model that describes the underground processes in Staufen.

## Near Real-time Deformation Monitoring based on Persistent Scatterer Interferometry

### Author(s)

Ling Chang <sup>(1)</sup>, Ramon Hanssen <sup>(1)</sup>, Shizhuo Liu <sup>(1)</sup>

### Department

<sup>(1)</sup>Delft University of Technology Kluyverweg 1, 2629 HS Delft, NL

### Abstract

In this paper, we present a complete procedure for Near Real-time (NRT) deformation monitoring by Persistent Scatterer Interferometry (PSI). Frequent-update short-time interferograms (i.e., 11 or 22 days) are used. Persistent scatterers are long-term stable, but not necessarily over the full time series. In this study, the key focus is to identify and characterize all available points and to track their deformation time series. Moreover, according to the prior adapted deformation model of each point and their spatial distribution of deformation behavior, a robust testing approach is performed to discriminate between reliable deformation of points and error induced by noise. To

evaluate the algorithm, we carry out a case study over Delft, the Netherlands, using TerraSAR-X data (StripMap mode) with 3 meter resolution. Sixty descending images acquired between April 2009 to April 2011 are used. From this experiment, the feasibility of NRT deformation monitoring can be demonstrated, as well as the precision and reliability of the deformation time series for all tracked points. Meanwhile, as the sequential updating data join in the processing sets, an early alarm can be given once a certain tracked point has abnormal deformation which exceeds its deformation threshold.

## Testing with real data a weighted LEAST-SQUARES Method for PSI

### Author(s)

Fernando Vicente-Guijalba <sup>(1)</sup>, Juan Manuel Lopez-Sanchez <sup>(1)</sup>

### Department

<sup>(1)</sup>University of Alicante UA, C/San Vicente del Raspeig, S/N, P.O. Box 99 E-03080, ES

### Abstract

In this work we study the capabilities of a weighted least-squares method (WLS) to estimate ground deformation components in Persistent Scatterer Interferometry (PSI) over real scenarios. We have implemented an algorithm based on the one presented in [1], whose main contribution was the estimation of the linear components (deformation rate and DEM error) using a weighted least-squares method which allows detecting arcs with phase ambiguities (outliers), and hence avoiding integrating these arcs. Another contribution in [1] was the use of a more redundant network than the conventional Delaunay triangulation. We took this new framework as starting point to afford a realistic processing. The critical point using a WLS method to perform linear estimation is the selection of weights which must be related with phase noise of each point at each interferogram. Some known approaches are based on a priori covariance matrix of the images [1] or on deriving the image covariance matrix from unwrapped interferograms [2]. The former solution works in controlled situations like simulated ones, but it would fail in real scenarios. Regarding the latter one, since our goal is avoid using unwrapped interferogram stacks, we propose an alternative. Through the relationship between estimated coherence ( $\rho$ ) and phase probability density function (pdf) [3], interferometric phase standard deviation could be derived and its inverse is used as weight in our LS estimation. Therefore the linear components (increments of deformation rate and DEM error) for each link in the triangulated network are estimated using a WLS where the weights for each interferogram are obtained using the phase standard deviation through the estimated coherence. This approach allows us to present in this work results with real data in areas of known subsidence problems [4], instead of just simulations as in [1]. In addition, we have performed a comparison against the results obtained with the Coherence Pixel Technique (CPT), which estimates the linear components through the minimization of a model adjustment function [5-6]. CPT, and all methods based on the same approach, could yield incorrect solutions where phase ambiguities are present, and consequently result in an inconsistent integration. This new method enables us to cope with some scenarios where classical PSI techniques (e.g. CPT) may fail mainly due to phase ambiguities. Areas with high amount of atmosphere phase components or mountainous zones with a strong relief are sites where classical methods may produce inconsistent results. In this sense, the WLS approach avoids incorporating noisy or not reliable information in the processing, hence becoming more robust. References: [1] L. Zhang, X. Ding, and Z. Lu, "Modeling PSInSAR Time Series Without Phase Unwrapping", *IEEE Trans. Geosci. Remote Sensing* 49, pp. 547-556, 2011. [2] B.M. Kampes, "Radar Interferometry: Persistent Scatterer Technique", Springer, 2006. [3] D. Just and R. Bamler, "Phase statistics of interferograms with applications to synthetic aperture radar," *Appl. Opt.*, vol. 33, no. 20, pp. 4361-4368, 1994. [4] G. Herrera, R. Tomás, D. Monells, G. Centolanza, J.J. Mallorquí,



F. Vicente, V.D. Navarro, J.M. Lopez-Sanchez, M. Sanabria, M. Cano, J. Mulas, "Analysis of subsidence using TerraSAR-X data: Murcia case study", *Engineering Geology*, Volume 116, Issues 3-4, pp. 284-295, November 2010. [5] O. Mora, J.J. Mallorquí, and T. Broquetas, "Linear and nonlinear terrain deformation maps from a reduced set of interferometric SAR images", *IEEE Trans. Geosci. Remote Sensing* 41, pp. 2243–2253, 2003. [6] P. Blanco, J.J. Mallorquí, S. Duque, and D. Navarrete, "Advances on DInSAR with ERS and ENVISAT data using the Coherent Pixels Technique (CPT)", *Proc. IGARSS 2006, Denver (USA)*, 2006.

## Evaluation of spatial interpolation of PSI datasets for continuous displacement field characterization

### Author(s)

Michael Foumelis <sup>(1)</sup>, Stamatis Kalogirou <sup>(1)</sup>, Issaak Parcharidis <sup>(1)</sup>

### Department

<sup>(1)</sup>Harokopio University of Athens 70, El. Venizelou Str., Athens, GR

### Abstract

Over the last years spaceborne Synthetic Aperture Radar (SAR) interferometry reached some maturity, with various Permanent or Persistent Scatterers Interferometric (PSI) techniques developed for mapping and monitoring displacements at millimeter level accuracy. In spite of the advanced processing techniques, spatial coverage of the data is still questionable, especially over low-coherence areas, typically found in natural terrain environments. Spatial interpolation of PSI deformation estimates, under certain conditions and assumptions, can significantly assist further interpretation and improve the applicability of the results. A recently proposed spatial interpolation technique for heterogeneous datasets is the moving window kriging with geographically weighted variograms. It is based on the moving window kriging and aims to provide better predictions using a geographically weighted variograms that is expected to be information richer than the classic variogram analysis. The city of Patras was chosen as pilot area, due to the high density of the point targets identified and the complexity of the deformation, with various uplift and subsidence patterns, allowing detailed assessment of the proposed interpolation technique in terms of statistical error. For the definition of error and in turns the evaluation of the proposed technique two different approaches were realized. Initially, a random part of the original data was not considered in the interpolation to be used latter as mean for ground truthing. Further analysis involved the comparison between interpolated values and calculated deformation rate at expanded point target locations. Temporal unwrapping of these points was performed by regression analysis using local phase of neighboring high quality point targets as a reference. Apart from the evaluation of the interpolation itself, addressing the issue of the robustness of such technique for increasing the density of PSI results was enabled. Finally, a separation of the original dataset on the basis of scattering height was considered appropriate in order to recognize and differentiate possible local effects of individual construction stability from displacements corresponding to movements of the geological basement.

# Experiences about the COSMO-SkyMed Stripmap Himage data processing – First Results of COSMO-SkyMed AO research Project

## Author(s)

Angela Losurdo <sup>(1)</sup>, Valentina Sarli <sup>(2)</sup>, Annibale Guariglia <sup>(1)</sup>

## Department

<sup>(1)</sup>Geocart srl , IT

<sup>(2)</sup>CGIAM , IT

## Abstract

PSInSAR is a very useful remote-sensing technique for the detection and monitoring of surface deformations. Several different radar satellite missions have been launched providing different types of SAR images that can be used for ground movement detection and monitoring: C-Band satellites as ERS, ENVISAT or RADARSAT, L-Band satellite as ALOS PALSAR and X-band sensors as TerraSAR-X and in the last years COSMO-SkyMed. However the SAR data widely used are in C-band principally from the ERS-1, ERS-2 satellites. COSMO-SkyMed is a constellation composed of four satellites equipped with Synthetic Aperture Radar operating at X-band and the first satellite has been launched on June 2007. They use different sensor modes and polarizations in order to increase the application fields. We present first results from the COSMO-SkyMed AO research project (ID-1380): "A software tool in order to process SAR stripmap data and calculate the deformation map with subcentimeter precision". The overall purpose of the project is to test and adapt a own software called "SLIDE" (Sar Land Interferometry Data Exploitation) to process COSMO data. "SLIDE" is software tool which contains the complete processing chain in order to measure surface deformation using the PSInSAR technique. "SLIDE" has been developed to run on multitemporale ERS dataset; it was also tested and validated in different test sites like Maratea, a small sea town, and some villages in Val D'Agri (both sites are located in the Basilicata region, Southern Italy). Therefore, the project objective is the test-adjustment of the "SLIDE" to run COSMO data, by using - as innovative element - also a high-resolution Lidar DEM and artificial passive Corner Reflectors to be designed and installed under this research project. In the first year of the project, the activities carried out from the COSMO Project include the production of higher level Stripmap Himage (coregistered image, mean image, differential and synthetic interferogram, Geocoded Terrain Corrected Image ), the adaptation of basic procedures (orbital model, algorithm for calculating the topographical and deformation contributions) of SLIDE, the design of the prototypical passive artificial Corner Reflectors and their installation. The test sites are two and located in the Basilicata region, test site 1 -"Agri-Pollino", an area historically subject to landslides where there are divers villages (e.g. Maratea) and the test site 2-"Potenza". From the first results of the activities, it is interesting to compare the quality of the products obtained from the COSMO-SkyMed Data with the ERS data. The mean image made with only twelve COSMO data has naturally a higher resolution (about 3-5m) and appears very similar to an aerophotogrametric survey. By analyzing the synthetic and differential interferograms, it can be inferred a larger noise with respect to the same products resulted from the ERS data processing. This is certainly due to the use of X band which is more subject to atmospheric noise, to a higher pixel resolution which makes the relating coherence map particularly discontinuous and/or probably to an improper preliminary coregistration phase. Currently, no filter has been applied to the interferograms. The GTCs produced on the areas of Maratea and Potenza allow us to see a good overlap with the Google Earth maps. About the passive artificial Corner Reflector, a dihedral and a trihedral prototypes have been designed. They were installed and tested in a rural area of the "Potenza" test site. The analysis of the performances of the Corner Reflector prototype was carried out through the visual interpretation and statistical analysis of their Radar Cross Section

responses on SAR images. Good results have been calculated. Finally, couples of reflectors were installed in order to be visible along descending orbit and the other along ascending orbit. Sites of installation including areas with different characteristics (slope, aspect, altitude), are located in rural, urban and industrial zone and prone to landslides.

## Space based monitoring and analysis of the geological and geomorphological processes influencing the surficial dynamics of the Danube Delta

### Author(s)

Delia Teleaga <sup>(1)</sup>, Valentin Poncos <sup>(2)</sup>, Gheorghe Oaie <sup>(3)</sup>

### Department

<sup>(1)</sup>ASRC 19 Ion Luca Caragiale St., RO

<sup>(2)</sup>Advanced Studies and Research Center (ASRC) 19 Ion Luca Caragiale St., RO

<sup>(3)</sup>National Institute for Research and Development of Marine Geology and Geoecology, RO

### Abstract

The Danube Delta is one of the largest deltas in Europe and represents perhaps the newest added land to the continent. In recent times, due to Iron Gates I and II dams building, the Danube-borne sediments supply has been reduced and strong erosion processes have become the main dynamical factor. The DInSAR technique is used to monitor the following processes in the Danube Delta geosystem: · Detection of areas with flooded vegetation and measurements of the water level changes in these areas, · Detection of areas with ground level humidity variation (in porous and unconsolidated rocks) and estimation of depth changes of the dry/moist surface, · Measurements of the ground subsidence or uplift movements, · Indirect measurements of crustal motion in areas with consolidated rocks, · Beach erosion levels. For this study a set of 7 Alos Palsar images spanning the time interval of 2007-2009 and 22 ERS-1/2 radar images from 1992, 1993, 1995, 1996 and 1999 were used to obtain average deformation maps through an interferometric stacking technique.

## Complex investigation of the moderate seismicity in the Mediterranean

### Author(s)

Maya Ilieva <sup>(1)</sup>, Daniel Raucoules <sup>(2)</sup>, Panagiotis Elias <sup>(3)</sup>, Marcello De Michele <sup>(2)</sup>, Pierre Briole <sup>(4)</sup>

### Department

<sup>(1)</sup>National Institute of Geophysics, Geodesy and Geography, Bulgarian Academy of Sciences Acad. G. Bonchev str, block 3, 1113 Sofia, BG

<sup>(2)</sup>Bureau de Recherches Géologiques et Minières 3 avenue Claude-Guillemin, FR

<sup>(3)</sup>National Observatory of Athens Vas. Pavlou & I. Metaxa, 15236 Penteli, GR

<sup>(4)</sup>Ecole Normale Supérieure 24 rue Lhomond, 75231 Paris CEDEX 5, FR

### Abstract

The Mediterranean region is one of the most seismically active areas in the world, an effect which is associated with the conjunction between the Eurasian and African tectonic plates, as well as the drift of other plates like the Anatolian and Aegean. On the other hand, the movements of numerous other smaller tectonic features also contribute to the complex geotectonic situation in the region. The seismic events occurring in the region comprise the shocks in the vast range of magnitude and depth, but a big percentage of all events occur in the shallower lithospheric layers with moderate strength. The studying of this group of shocks is realizable by different

geophysical approaches and it contributes to the more precise determination of the plate boundaries. Moreover, the combination between different investigating methods enlarges the flexibility and reliability of the study. The present work is focused on the investigation of the advantages and disadvantages of the application and combination of different methods for examining several moderate shallow seismic events that occurred in the last 15 years in the Mediterranean. The data available for the study of the different earthquakes are InSAR, GPS and levelling measurements, seismological records, geological and tectonic information. The events used for the investigation are spread in the different parts of the Mediterranean region: Konitsa [1996], Boumerdes [2003], Lefkada [2003], L'Aquila [2009], and some others.

## PS-analysis of COSMO SAR data stacks through a fast and simple technique

### Author(s)

Daive Giudici <sup>(1)</sup>, Andrea Monti Guarnieri <sup>(2)</sup>, Davide D'Aria <sup>(1)</sup>, Davide Riva <sup>(1)</sup>, Nicolas Tagliani <sup>(1)</sup>, Andrea Recchia <sup>(2)</sup>, Stefano Tebaldini <sup>(2)</sup>

### Department

<sup>(1)</sup>Aresys , IT

<sup>(2)</sup>Politecnico di Milano , IT

### Abstract

The paper describes an accurate PS analysis technique that leads to the estimate of the PS velocity, phase and displacement from a SAR interferometric dataset, to be used for deformation analysis and coherent calibration. The technique is an original implementation of the Persistent Scatterers analysis, based on the correction of the atmospheric disturbance through the estimation of a differential velocity field to be integrated and removed from the original interferograms. This core step is important as it allows to obtain the atmospheric corrected phases while avoiding the direct estimation of the phase itself. The procedure exploits the initial set of PS candidates to estimate the spatial gradient of the phase and, after this step, the differential velocity field. Being this field estimated on the spatial gradient of the phases, it is smooth and can be unwrapped leading to a straight velocity analysis. The atmospheric phase screen is interpolated over all the pixels, allowing the densification of the PS set in a second iteration. The result of processing COSMO SKYMED high resolution Stripmap data (about 3 x 3 meters resolution) in the frame of the ASI-AO #1080 "SAR data Calibration and Validation by Natural Targets", are shown. Such processing aims to evaluate the PS densities and life time in both urban and rural area, as well as the exploitation of PS phases for calibration. The analysis is carried out by long strips acquired by the three sensors of the constellation over north Italy, from south Milan to north of Como.

# Presentation of the small baseline NSBAS processing chain on a case example: the Etna deformation monitoring from 2003 to 2010 using Envisat data.

## Author(s)

Marie-Pierre Doin <sup>(1)</sup>, Stephane Guillaso <sup>(2)</sup>, Romain Jolivet <sup>(3)</sup>, Cecile Lasserre <sup>(3)</sup>, Felicity Lodge <sup>(3)</sup>, Gabriel Ducret <sup>(1)</sup>, Raphael Grandin <sup>(1)</sup>

## Department

<sup>(1)</sup>Ecole Normale Supérieure 24 rue Lhomond, FR

<sup>(2)</sup>Technische Universität Berlin, DE

<sup>(3)</sup>Isterre, FR

## Abstract

In the framework of the ANR EFIDIR project, we assemble a processing chain that handles InSAR processing from RAW data to time series analysis. A large part of the chain (from RAW data to geocoded unwrapped interferograms) is based on ROI\_PAC modules, however re-arranged to process in series and in a common radar geometry all SAR images and interferograms. Additional modules concern the mitigation of atmospheric artifacts and residual orbital removal, followed by the inversion of interferograms into time series. We emphasize below the few particularities of this chain with respect to the standard ROI\_PAC processing (Rosen et al., 2004) and to the SBAS procedure described in Berardino et al. (2002). The first step goes from RAW data to differential interferograms. All SLCs are computed in a common doppler centroid geometry and band-pass filtered in azimuth. Master and slave SLCs are coregistered using an a priori distortion map in range derived from precise orbits and DEM, mixed with empirical offsets between slave and master images, obtained by amplitude image matching. An optimal small baseline network of interferograms is then defined using temporal and perpendicular baseline constraints, on which a maximum redundancy criteria is added. The latter criteria is useful to reduce the number of computed interferograms. A range spectral filter (Guillaso et al., 2011) is applied to the SLCs before producing differential interferograms. These small changes with respect to ROI\_PAC processing increases the coherence for large perpendicular baselines (350-500m) and in areas of large relief (one example is shown on Mount Etna). The second step involves phase filtering, unwrapping, and correction of interferograms. Various filters can be used, including simple looking and the adaptative filter of Goldstein and Werner (1998). In the case of Mount Etna interferograms, we implement a coherence and phase slope dependent filter that allows to extract useful phase information in incoherent areas away from the volcano. Empirical or model-based stratified atmospheric corrections can be performed before unwrapping to ease the unwrapping process in mountainous areas (Jolivet et al., 2011). After unwrapping, empirical corrections may be re-estimated, together with residual orbit error, and inverted to insure their consistency in the interferometric network. We then estimate the phase dispersion of each interferogram away from deforming areas. These values are inverted to quantify the amplitude of the atmospheric phase screen (APS) of each image. Interferograms are referenced to a stable pixel or to stable areas. In the third step, the phase delays of unwrapped interferograms are inverted pixel by pixel to solve for incremental phase delay between successive dates by least square, with additional constraints on the deformation. The additional constraints are a prescribed temporal evolution for the deformation (either smooth in time, or any parameterized function of time) plus a prescribed linear function of perpendicular baseline. The APS amplitude is used to inversely weight these additional constraints. We also make sure that additional constraints have a weight low enough to only impact the relative phase delay between separated image subsets. A first run with a few iterations (weighted by the residuum) is performed to map inconsistencies

in the interferometric network, thus detecting unwrapping errors. A second run corrects these unwrapping errors depending on the network redundancy. The output then consists of time series of raw and smoothed phase delay for each pixel that is coherent for at least half the interferograms. The above described procedure is applied and discussed on the Envisat ascending dataset given in the GEO Geohazards Supersite, that is already well studied and provides a good case example. It consists of 63 SAR data between 2003 and 2010. 222 interferograms were computed with perpendicular baselines lower than 500 m and temporal baselines lower than 1.3 year. Unwrapping takes into account creep on Pernicana Fault and a few other structures by delineating a "cut" along them. Stratified atmospheric effects are a priori corrected using the ECMWF ERAI atmospheric reanalysis. The average velocity pattern presents strong similarities with that described by Bonforte et al. [2011] for the 1995-2000 period of time. Non linear behavior of the deformation with time is also evident. Berardino, P., G. Fornaro, R. Lanari, and E. Sansosti [2002], "A new Algorithm for Surface Deformation Monitoring based on Small Baseline Differential SAR Interferograms", *IEEE Trans.Geosci. Remote Sens.*, Vol. 40, No 11, pp. 2375-2383. Bonforte A., F. Guglielmino, M. Coltelli, A. Ferretti, G. Puglisi, [2011] « Structural assessment of Mount Etna volcano from Permanent Scatterers analysis », *Geochem. Geophys. Geosyst.*, 12, Q02002, doi:10.1029/2010GC003213. R. M. Goldstein and C. L. Werner [1998], "Radar interferogram filtering for geophysical applications," *Geophys. Res. Lett.*, vol. 25, no. 21, pp. 4035–4038. Guillaso S. -P. Doin, R. Jolivet, C. Lasserre, G. Ducret, M. Kaban, and O. Hellwich, [2011] Time series differential SAR interferometry measurement of the Tien Shan mountain belt deformation a range spectral filter adapted to highly mountainous terranes, this issue. Jolivet R., R. Grandin, C. Lasserre, M.-P. Doin, G. Peltzer, [2011], Systematic InSAR tropospheric phase delay corrections from global meteorological reanalysis data, this issue. Rosen, P. A., S. Henley, G. Peltzer, and M. Simons [2004], Updated Repeat Orbit Interferometry Package Released, *Eos Trans. AGU*, 85(5), 47.

## Multi-scale InSAR Time Series (MInTS) analysis of the creeping section of the San Andreas Fault

### Author(s)

Piyush Agram <sup>(1)</sup>, Mark Simons <sup>(1)</sup>, Eric Hetland <sup>(2)</sup>

### Department

<sup>(1)</sup>California Inst of Tech MC 252-21, Caltech, Pasadena, CA, USA

<sup>(2)</sup>University of Michigan 2534 CC Little Bldg 1100 North University Ave, USA

### Abstract

Interferometric Synthetic Aperture Radar (InSAR) Time-series methods estimate the spatio-temporal evolution of surface deformation using multiple SAR interferograms. Traditional time-series analysis techniques [1,2] assume the statistical independence of InSAR phase measurements over space and time when estimating deformation. However, existing atmospheric phase screen models [3,4] clearly show that noise in InSAR phase observations is correlated over the spatial domain. Multi-scale InSAR Time Series (MInTS) [5] is an approach designed to exploit the correlation of phase observations over space to significantly improve the signal-to-noise ratio in the estimated deformation time-series compared to the traditional individual pixel-based time-series InSAR techniques. The MInTS technique reduces the set of InSAR observations to a set of almost uncorrelated observations at various spatial scales using wavelets. Traditional pixel-based inversion techniques can then be applied to the wavelet coefficients more effectively, thus significantly improving the signal-to-noise ratio.

Other salient features of MInTS include a weighting scheme which accounts for the presence of localized holes due to decorrelation or unwrapping errors in any given interferogram and the flexibility to explicitly parameterize known time-dependent processes that are expected to

contribute to a given set of observations (e.g., co-seismic steps and post-seismic transients, secular variations, seasonal oscillations, etc. like GPS). The estimation is regularized using a model resolution based smoothing so as to be able to capture rapid deformation where there are temporally dense radar acquisitions and to avoid oscillations during time periods devoid of acquisitions. MInTS also uses cross validation to choose the regularization penalty parameter in the inversion of for the time-dependent deformation field.

We demonstrate MInTS by applying it to three different ALOS PALSAR stacks acquired over the creeping section of the San Andreas Fault in California, USA in the time period spanning 2007-2010. Using the same data sets, we find that MInTS improves on conventional InSAR time-series approaches by increasing the spatial coverage of estimated deformation. MInTS improves the estimate of the secular inter-seismic creep rate across the creeping section by reliably separating out the seasonal signal in the estimated deformation.

#### References

1. Ferretti, A., Prati, C., Rocca, F., 2001. Permanent scatterers in sar interferometry. *IEEE TGRS* 39 (1), 8-20.
2. Berardino, P., Fornaro, G., Lanari, R., Sansosti, E., 2002. A new algorithm for surface deformation monitoring based on small baseline differential sar interferograms. *IEEE TGRS* 40 (11), 2375-2383.
3. Hanssen, R. F. 2001. *Radar Interferometry: Data Interpretation and Error Analysis*. First edn. Springer.
4. Emardson, T. R., Simons, M., Webb, F. H., 2003. Neutral atmospheric delay in interferometric synthetic aperture radar applications: Statistical description and mitigation. *JGR* 15 (B5), 2231.
5. Hetland, E., Muse, P., Simons, M., Shanker, P., Lin, N., & DiCaprio, C. J. 2011. A multi-scale approach to InSAR time-series analysis. In preparation.

## Applications using CEA SAR interferometry software package CIAO

#### Author(s)

Philippe Loreaux <sup>(1)</sup>, Béatrice Pinel-Puysegur <sup>(1)</sup>, Guillaume Quin <sup>(1)</sup>

#### Department

<sup>(1)</sup>CEA-Commissariat à l'Energie Atomique et aux Energies Alternatives CEA, DAM, DIF, F- 91297Arpajon, FR

#### Abstract

The CEA developed an interferometric software package called CIAO (Chaîne Interférométrique rAdar Opérationnelle). The objective is to obtain an automatic tool for sites monitoring. Using at least two radar images acquired on a same site, amplitude images, coherence images and differential interferograms are computed using CIAO. Those results are georeferenced to make relevant analyzes. CIAO includes also the possibility to blend radar and optical images. A CIAO user first collects the radar images for a given area (different radar satellites eventually) and then uses the software to generate automatically all the differential interferograms. Using a DEM database, CIAO takes into account the topographic effects as the orbitographic effects. Several options can be used. The two last modules developed relate to Permanent Scatterers and atmospheric compensation. Numerous Permanent Scatterers appear in VHR X band images, especially in areas containing man-made infrastructures. Exploiting these features in the algorithm will further improve the suitability of CIAO to compute deformation with sub-millimetric accuracy. In order to detect PS, we need a time series of stackable radar images. Thus, all images have the same range and azimuth resolution and every single pixel represent the same ground area in all the images. PS detection is then performed through a pixel by pixel analysis, studying amplitude variations of pixels along the time series. Amplitude stability is linked to phase stability when Signal to Noise Ratio (SNR) is high. This hypothesis is validated because PS have very high

amplitudes values. The amplitude dispersion index is defined as follows:  $D_p = \sigma_p / \bar{A}_p$  where  $\sigma_p$  is the standard deviation of the pixel amplitude along the time series,  $\bar{A}_p$  is the average value of the pixel amplitude along the time series. The more the amplitude is stable, the more the dispersion index is small. Thus, to determine if the pixel is a PS candidate or not, the amplitude dispersion index is compared to a threshold, typically 0.25. If the dispersion index of the pixel is lower than the dispersion threshold, the pixel is detected as PS candidate. Then the ground deformation is performed using the Spatio-Temporal Unwrapping Network (STUN) algorithm. Atmospheric effects, on the other hand, interfere with the radar signal. Taking them into account computationally will improve the interpretation of the deformation due to an earthquake for example. If the atmospheric data are available at the acquisition time, it is possible to compensate those effects. The idea of those methods is to simulate an "atmospheric interferogram" using meteorological modelling to estimate the tropospheric radar delay. The method implemented in CIAO uses the Weather Research and Forecasting (WRF) model to compute the atmospheric delay. WRF is suitable for a broad spectrum of applications across scales ranging from meters to thousands of kilometers. We can show that the method removes about 43% of the atmospheric signal. As an example of DInSAR applications using CIAO, the study of the 11 March 2011 Tohoku-oki earthquake is presented. Images acquired by ENVISAT, TerraSAR-X, Cosmo-SkyMed and ALOS were used. A joint exploitation of X-band and C-band data is used to interpret the deformation measurement. ENVISAT ASAR (C-band) differential interferogram of coseismic deformation between Feb. 19, 2011 and Mar. 21, 2011 shows 121 fringes between Tokyo and Sendai, which correspond to 3.40m displacement of Sendai w.r.t. Tokyo towards the satellite, mainly due to horizontal deformation towards East. The projection of deformation on TerraSAR-X and ENVISAT Line Of Sight (LOS) is performed. The differential deformation is projected in the vertical plane containing both LOS. The fringe rate is measured on both interferograms. Compared to C-band, it is smaller on TerraSAR-X than expected due to different incidence angle and residual orbital fringes in C-band. The angle  $\beta$  between differential deformation and horizontal plane can be derived from fringe rate ratio. Due to residual orbital fringes, more work is needed to exploit jointly X-band and C-band data. Another SAR application is change detection. The images acquired by different satellites on Japan area were used. With CIAO, the amplitude and coherence images are computed and can be used to detect changes. Before analyzing the changes, the images have to be registered using CIAO. This step is very important for this SAR application as for the deformation measurement. CIAO has several approaches to register coherent SAR images. One of the near future challenge is the registration of non-coherent SAR images (different look angle, different pass, and different band). Analyzing two registered TerraSAR-X images on Sendai area, a lot of changes can be detected. Post event features, debris and post event flood over the land can be clearly identified.

## 3-D phase unwrapping for satellite radar interferometry

### Author(s)

Batuhan Osmanoglu <sup>(1)</sup>, Timothy H. Dixon <sup>(2)</sup>, Shimon Wdowinski <sup>(1)</sup>

### Department

<sup>(1)</sup>University of Miami , USA

<sup>(2)</sup>University of South Florida , USA

### Abstract

Determining Earth's surface topography and deformation with interferometric Synthetic Aperture Radar (InSAR) involves measurement of phase, which, for a typical coherent radar signal, can only be done modulo  $2\pi$ . The cycle ambiguity inherent in the phase measurement has to be "unwrapped" over all observation dimensions (e.g. azimuth, range and time) of the data to remove the  $2\pi$  ambiguity of the phase measurements. For a time series of SAR images, useful for



reducing noise in topographic applications or measuring time-varying surface deformation, the necessary steps to connect ambiguous radar phase measurements are more challenging, and the operation may be termed 3-D phase unwrapping. Here we describe a 3-D unwrapping approach using an extended Kalman Filter. Our approach readily exploits existing information, and is robust in the presence of noise, providing improved accuracy compared to existing approaches for 3-D phase unwrapping under a wide range of conditions. In Morelia, Mexico, water withdrawal from the underlying aquifer induces surface displacements. A previous study conducted using persistent scatterer interferometry (PSI) indicates subsidence rates up to 50mm/yr and differential deformation along the faults across the basin. Time series of surface displacement observed in Morelia using the new 3-D unwrapping algorithm based on extended Kalman filters will be presented and effects of different filtering parameters will be studied.

## High Resolution Ground Deformations Monitoring by Cosmo-SkyMed PSP SAR Interferometry: Accuracy Analysis and Validation

### Author(s)

Mario Costantini <sup>(1)</sup>, Tingwu Chen <sup>(2)</sup>, Yongmin Xu <sup>(2)</sup>, Francesco Trillo <sup>(1)</sup>, Francesco Vecchioli <sup>(1)</sup>, Lingyan Kong <sup>(2)</sup>, Dong Jiang <sup>(3)</sup>, Qiong Hu <sup>(3)</sup>

### Department

<sup>(1)</sup>E-GEOS - an ASI/Telespazio Company Via Cannizzaro, 71, Rome, IT

<sup>(2)</sup>Beijing Institute of Surveying and Mapping Beijing, CN

<sup>(3)</sup>Eastdawn Beo Beijing, CN

### Abstract

1. INTRODUCTION Synthetic aperture radar (SAR) interferometry is a powerful technology for measuring slow terrain movements due to landslides, subsidence, and volcanic or seismic phenomena. Extraction of this information is a complex task, because the phase of the signal is measured only modulo 2 and is affected by random noise and systematic disturbances. The persistent scatterer (PS) approach brought important advances in the solution of this problem [1]. A new approach was recently proposed [2], named persistent scatterer pairs (PSP), for the identification of persistent scatterers (PS) in series of full resolution SAR images, and the retrieval of the corresponding terrain height and displacement velocity. The PSP technique overcomes problems related to the presence of atmospheric and orbital artifacts in the signal by exploiting only the relative properties of neighboring points both for identification and analysis of PS, thus removing the need for model-based interpolations starting from a preliminary set of measurements obtained by radiometric or low resolution analyses. In this work, after analyzing the qualifying characteristics of the PSP method, we will describe the validation performed by comparing the PSP measurements obtained from Envisat and high resolution COSMO-SkyMed SAR images over Beijing with optical leveling data. The results confirm the validity of the PSP approach and, for the first time, demonstrate the dramatic improvement brought in ground displacement measurements by high resolution COSMO-SkyMed data with respect to low resolution SAR data. In particular, not only the density of PS measurements increases, by two orders of magnitudes, but also the accuracy of PS measurements increases by about an order of magnitude. While the higher PS density is very important for monitoring of buildings and infrastructures, the higher accuracy of ground deformation measurements guaranteed by the high resolution COSMO-SkyMed data allows observing smaller ground deformations and with a shorter observation time. In addition, the COSMO-SkyMed constellation can provide an unprecedented frequency of observations, which allows monitoring also faster movements. In the following sections a summary of the method and of the validation results are given. 2. METHOD The central idea of the persistent scatterer pairs (PSP) method is to both identify and analyze PS working

only with pairs of points ("arcs"). Working only with pairs makes the methods insensitive to spatially correlated signals such as atmospheric or orbital artifacts, removing the need for data calibration and model-based interpolations starting from a preliminary set of measurements obtained by radiometric or low resolution analysis. Therefore, the PSP method is robust with respect to the density of the PS. In order to promote a pair of points to be a PSP the multi-temporal coherence is a possible test. In general the test can take into account both amplitude and phase information, and measures the similarity of the statistics of the two points. By applying the arc test to a limited set of arcs connecting close (but not only nearest neighboring) points it is possible to identify the so-called persistent scatterers pairs (PSPs), i.e. arcs connecting pairs of PS. The algorithm is designed in order to analyze the minimum number of arcs necessary to identify all PS. After identification of all coherent scatterers, the displacements and the 3D positions of the targets are obtained by integrating the differential estimates obtained corresponding to all the identified pairs (the PSPs). This set of arcs is highly redundant (not pairing only nearest neighboring points), which makes for a more reliable and accurate solution.

3. VALIDATION The PSP-IFSAR technology has been widely tested and used also for massive productions. We report here the results of an extensive validation performed by comparing the PSP-IFSAR measurements obtained from COSMO-SkyMed HIMAGE and Envisat SAR data with in situ optical leveling data over Beijing, China. The low resolution (5 x 25 sqm) Envisat result covered an area of about 100 x 100 km<sup>2</sup> including Beijing, China, and surroundings, while the high resolution (3 x 3 sqm) COSMO-SkyMed result covered about 7 x 5 km<sup>2</sup> in a central area of Beijing. The temporal span of the analysis was from March 2009 to March 2010. The area is affected by strong subsidence phenomena. The two sets of PSP-IFSAR ground displacement measurements were compared with precise optical leveling data relative to the same period. Two methods were used to analyze the PSP and leveling measurements in a unique coordinate system: (1) point-to-point and (2) contour-level to contour-level comparisons. The performed analysis showed a very good agreement between the COSMO-SkyMed PSP-IFSAR results and optical leveling measurements: an average difference of about 1.2 mm and a standard deviation of about 1.9 mm were measured. The average difference between the Envisat PSP-IFSAR measurements and the optical leveling data was about 6.5 mm, with a standard deviation of about 1 cm. The Envisat figures confirm the possibility of measuring mean velocities with accuracy of the order of millimeters per year over a time period of several years, as reported in the scientific literature. On the contrary, the performed analysis shows that the same accuracy on the mean velocities can be obtained with COSMO-SkyMed data already in a time span of a single year. The much better results obtained with COSMO-SkyMed with respect to Envisat data in the performed validation are explained by the smaller level of noise and disturbances that characterize each single displacement measurement obtained from COSMO-SkyMed data with respect to those from Envisat data. In fact, by analyzing time series of measurements, it can be observed that the magnitude of typical oscillations is about 1 cm in Envisat measurements and only 2 or 3 mm in COSMO-SkyMed ones. Finally, the performed analysis shows that the density of PS found with COSMO-SkyMed stripmap data is about 200 times higher than those obtained with Envisat data (Figure 2), and that a precise reconstruction of the 3D position of the PS is possible. These characteristics of the PSP COSMO-SkyMed measurements allow distinguishing different possible displacements of different parts of a building, which is essential for stability monitoring.

4. REFERENCES [1] A. Ferretti, C. Prati, and F. Rocca, "Permanent scatterers in SAR interferometry," *IEEE Trans. Geosci. Remote Sensing*, vol. 39, no.1, pp. 8-20, Jan. 2001. [2] M. Costantini, S. Falco, F. Malvarosa, F. Minati, "A new method for identification and analysis of persistent scatterers in series of SAR images," in *Proc. Int. Geosci. Remote Sensing Symp. (IGARSS)*, Boston MA, USA, pp. 449-452, 7-11 July 2008.

# Correction of Ionospheric Effects on InSAR Images Using Multiple Aperture InSAR

## Author(s)

Dong-Taek Lee <sup>(1)</sup>, Hyung-Sup Jung <sup>(1)</sup>, Zhong Lu <sup>(2)</sup>

## Department

<sup>(1)</sup>The University of Seoul Jeonnong 2-dong, Dongdaemun-gu, Seoul 130-743, KR

<sup>(2)</sup>U.S. Geological Survey Vancouver, Washington 98683-9589, USA

## Abstract

The Earth ionosphere is a shell of electrons and electrically charged atoms and molecules, surrounding the Earth from an altitude of approximately 50 - 1000 km [1]. The Earth ionospheric effects lead to geometry distortion, range delay, interferometric phase bias, range defocusing and Faraday rotation in synthetic aperture radar (SAR) and interferometric SAR (InSAR) systems [2]. Raucoules and de Michele [3] applied a method that reduced the ionospheric effects using azimuth offset maps from the relationship between the ionospheric effects and the azimuth offsets derived by Meyer et al. [4]. However, the method is not precise enough to extract ionospheric effects on InSAR images efficiently because the offset tracking technique has a reduced sensitivity to the azimuth offset field. Multiple aperture InSAR (MAI) technique has been recently developed by Bechor and Zebker [5] and improved by Jung et al. [6]. MAI is superior to the amplitude pixel offset method for imaging the azimuth offset field. We propose here an efficient method to correct ionospheric effects on InSAR images using MAI. We validate the proposed method using the ERS C-band InSAR images of the Galapagos volcanic islands.

REFERENCES [1] M. Jehle, M. Rüegg, D. Small, E. Meier and D. Nüesch, "Estimation of Ionospheric TEC and Faraday Rotation for L-Band SAR," in Proc. of SPIE, vol. 5979, pp. 252-260, 2005. [2] F. Meyer, R. Bamler, N. Jakowski and T. Fritz, "The Potential of Low-Frequency SAR Systems for Mapping Ionospheric TEC Distributions," IEEE Geosci. Remote Sens. Lett., vol. 3, no. 4, pp. 560-564, Oct. 2006. [3] D. Raucoules and M. de Michele, "Assessing Ionospheric Influence on L-Band SAR Data: Implications on Coseismic Displacement Measurements of the 2008 Sichuan Earthquake," IEEE Geosci. Remote Sens. Lett., vol. 7, no. 2, pp. 286-290, Apr. 2010. [4] F. Meyer, R. Bamler, N. Jakowski and T. Fritz, "Methods for small scale ionospheric TEC mapping from broadband L-band SAR data," in Proc. IGARSS 2006, Denver, CO, pp. 3755-3738, Jul. 31-Aug. 4, 2006. [5] N. B. D. Bechor and H. A. Zebker, "Measuring two-dimensional movements using a single InSAR pair," Geophys. Res. Lett., 33, L16311, 2006. [6] H.-S. Jung, J.-S. Won and S.-W. Kim, "An Improvement of the Performance of Multiple-Aperture SAR Interferometry (MAI)," IEEE Trans. Geosci. Remote Sens., vol. 47, no. 8, pp. 2859-2869, Aug. 2009.

# Estimation of the Persistent Scatterer density using optical remote sensing data and land cover data

## Author(s)

Simon Plank <sup>(1)</sup>, John Singer <sup>(1)</sup>, Kurosch Thuro <sup>(1)</sup>

## Department

<sup>(1)</sup>Technical University of Munich Arcisstr. 21, 80333 München, DE

## Abstract

In recent years persistent scatterer radar interferometry (PS-InSAR) has proven to be a powerful remote sensing technique to measure deformation of the Earth's crust with an accuracy of a few millimeters. However, to ensure a PS-InSAR processing with useable results, a stack containing at least 30 to 50 radar images (depending on the test site's land cover) is required. This high

amount of radar images is a very important cost factor when applying this method. In this paper we present two auxiliary methods for estimating the density of scatterers (possible persistent scatterers) before the area of interest is recorded by radar. The goal of this scatterer estimation is to find out, whether the scatterer density of a certain test site is high enough for PS-InSAR processing, or whether the scatterer density has to be artificially increased by corner reflectors – prior to the costly data acquisition. This scatterer density estimation is done in a geographical information system (GIS) by comparing the distribution of real PS targets (results of PS-InSAR processing) of several test sites with freely available (1) data of optical remote sensing sensors, such as Landsat and ASTER, and (2) land cover data, such as GlobCover and Corine land cover. Firstly, the optical remote sensing data were used to calculate the NDVI (Normalized Difference Vegetation Index) value of the test sites at various seasons. The paper shows a strong correlation of the NDVI value and the PS target distribution. Secondly, using the land cover data, the PS density of each single land cover class was calculated. To guarantee a wide usability of these methods, test areas with different types of land cover and of different climate were chosen. Therefore, both of the methods described above, enables the user to estimate the scatterer density (possible PS targets) before the area of interest is recorded by radar. The methods are intended for a first step evaluation whether the PS-InSAR technique can be applied for monitoring a certain test site. A great benefit of these methods is free availability and the (mostly) global coverage of the data used.

## Comparative analyses of PSI ground deformation measurements derived from multi-frequency satellite acquisitions

### Author(s)

Javier Duro <sup>(1)</sup>, Jose Raul Sabater <sup>(1)</sup>, David Albiol <sup>(1)</sup>, Fifamè N. Koudogbo <sup>(1)</sup>

### Department

<sup>(1)</sup>ALTAMIRA INFORMATION C/ Còrsega, 381-387 E-08037 Barcelona, ES

### Abstract

In recent years many new developments have been made in the field of SAR image analysis. The wider diversity in available SAR imagery allows now to cover a wider range of applications in the domain of risk management, damage assessment and monitoring at a large scale. The work that is proposed is based on the analysis of differences in ground deformation measurements extracted from the analysis of data stacks acquired at different frequencies. The overall aim of the project is the derivation of rules and the definitions of criteria for the selection of the appropriate SAR sensor for the each different type of region of interest. Key factors may be the geographic localization, the extension of the monitoring period and the land cover type. During the study, particular emphasis is placed on the study of the impact of the atmospheric artifacts at the different wavelengths. Moreover the analysis of the achieved density of PS and the capacity to detect and monitor fast and slow rate motions are also analyzed and discussed. The first topic of the study deals with the conditions of wave propagation at the different frequencies. As noticed from image analysis, absorption and disturbance that undergoes the signal during its propagation can significantly impair on the quality of the SAR images, and thus on the ground deformation measurements. Moreover the use of frequencies above 3GHz minimizes ionospheric impact on propagation, while tropospheric effects are increased at those wavelengths. The impact of those effects will be observed and compared at the different frequencies. A PS is any ground target that keeps its reflection properties along a set of SAR acquisitions. It is characterized by a strong and stable radar response that dominates the SAR resolution cell response. As a result those image pixels present a reduced noise level allowing reliable phase measurements in repeat passes interferometry. Generally, temporal changes of the scatterer or of its surroundings, difference in the look angles, volume scattering and thermal or processing noise result in a increase of the

phase noise within the resolution cell, leading in some cases into a loss of coherence in the repeat passes. However, in the case of PS-like pixels, all those effects do not have any impact or just a negligible influence in comparison with the response of the main target presented within the pixel. The second theme of the study will thus conduct to a review of the criteria for the selection of PSs and a qualitative analysis about their nature, depending on the frequency and the area of interest. The wavelength is directly linked with the sensitivity of the SAR images to detect ground motion, in consequence with the precision of the estimations. The last part of the study thus focuses on the analysis of the precision that could be achieved by PSI processing at different wavelengths. This analysis will be based on the monitoring of a same site considering SAR imagery acquired at different frequencies. Sites of interest are identified in urban and rural zones, where stacks of datasets acquired by different sensors (TerraSAR-X, Cosmo SkyMed, Envisat ASAR, Radarsat-2 and/or ALOS) over overlapping periods are available. The processing will be done using the PSI processing chain developed by Altamira and qualified in the framework of the GSE ESA project Terrafirma called Stable Points Network interferometric Process.

## Performance of a combined pixels selection method in DinSAR

### Author(s)

Giuseppe Centolanza <sup>(1)</sup>, Dani Monells <sup>(1)</sup>, Rubén Iglesias <sup>(1)</sup>, Jordi Mallorqui <sup>(1)</sup>, Juan M. Lopez-Sanchez <sup>(2)</sup>

### Department

<sup>(1)</sup>UPC C/ Jordi Girona 1-3, ES

<sup>(2)</sup>Universidad de Alicante, ES

### Abstract

Pixel selection is a crucial step in the DInSAR processing as the quality of the results depends on the phase quality of the selected pixels or, in other words, on how they preserve the coherence along time. The most used selection criteria are coherence stability ([1] [2]), amplitude stability (Permanent Scatterers, PS [3]) and spectral correlation ([4]). The results obtained with the different selection methods are similar in general terms but differences are noticeable as the methods are sensitive to different kinds of targets. Coherence is used to describe the temporal and spatial variations of the acquired signal. In order to estimate the coherence, a number of  $L$  neighbouring pixels are averaged and thus the resolution of the results is reduced. The interferograms are multi-looked and the speckle noise reduced but it does not work with spatial large baselines closer to the critical one. This approach is very well-suited for distributed targets but it can also be applied over urban areas with deterministic targets. It can be applied to any number of images. The amplitude selection is a technique developed by Politecnico di Milano and it estimates the phase stability of a pixel from its amplitude dispersion along the time. In order to get a reliable estimate a large number of images is required. The technique looks for point-like targets, the Permanent Scatterers, with an ideal isotropic response and not affected by restrictions on the maximum spatial baseline. The targets are smaller than a resolution cell and all the set of images can be used for interferometric applications. The method works at full resolution. The sublook correlation selection locates the so called Coherent Scatterers (CSs) that are characterised also by a point-like scattering behaviour, similar to PSs. It could be considered a method between the other two as it uses the sublook coherence to select the pixels. There is a reduction of the resolution depending on the number of sublooks used, typically a factor of two. The experience using the different methods has shown that a significant number of pixels are detected only by one method. A new selection method can be proposed in order to take advantage of all selected pixels. The aim is to increase the density of the pixels and get results with combined information of the three selection criteria. The first important step is to verify the intersection of the three maps of selected pixels. To increase the density, it would be necessary that there are uncommon

pixels for the three cases. Moreover, the phase standard deviation of the selected pixels should be similar for the three selection maps so that it allows a combined processing to retrieve deformation and DEM error results with comparable errors. The coherence values are directly linked to the phase dispersion depending on the effective number of looks. The entropy threshold for the sublook selection can be derived from the coherence threshold and related with the phase standard deviation. For the amplitude selection the phase dispersion can be estimated from the amplitude dispersion. In this way it is possible to select different kinds of pixels but characterized by a similar phase quality. In the final map each pixel is considered as the best case of the three selection methods. Moreover, with a multilayer processing it is possible to group pixels in different quality phase layers. The different approaches for the joint processing of the high and low resolution data will be presented and evaluated to determine which one provides a better performance. The joint processing of all pixels helps to improve the quality of the final results thanks to the redundancy provided. The city of Murcia has been selected to evaluate the performance of the method due to its high deformation rate, the set of extensometers deployed along the city that provide validation data and the large dataset of TerraSAR-X images available (project GEO0389). [1] Blanco, P.; Mallorquí, J.J.; Duque, S.; Monells, D.; "The Coherent Pixels Technique (CPT): an Advanced DInSAR Technique for Non-linear Deformation Monitoring", Pure and Applied Geophysics, 165, 1167-1193, 2008 [2] Lanari, R, Casu, F., Manzo, M., Zeni, G., Berardino, P., Manunta, M., and Pepe, A. (2007), " An Overview of the small baseline subset algorithm: A DInSAR technique for surface deformation analysis", Pure Appl. Geophys. 164(4), 637–661. [3] Ferretti, A.; Prati, C.; Rocca, F.; "Permanent scatterers in SAR interferometry", Geoscience and Remote Sensing Symposium, 1999. IGARSS '99 Proceedings. IEEE 1999 International , vol.3, no., pp.1528-1530 vol.3, 1999 [4] Schneider, R.Z.; Papathanassiou, K.P.; Hajnsek, I.; Moreira, A., "Polarimetric and interferometric characterization of coherent scatterers in urban areas", Geoscience and Remote Sensing, IEEE Transactions on, vol.44, no.4, pp. 971- 984, April 2006

## The thermal dilation component of X-band PSI observations

### Author(s)

María Cuevas <sup>(1)</sup>, Oriol Monserrat <sup>(1)</sup>, Michele Crosetto <sup>(1)</sup>, Guido Luzi <sup>(1)</sup>, Bruno Crippa <sup>(2)</sup>

### Department

<sup>(1)</sup>Institut de Geomàtica Av. del Canal Olímpic, s/n, ES

<sup>(2)</sup>University of Milan Via Cicognara 7, I-20129 , IT

### Abstract

Persistent Scatterer Interferometry (PSI) is a satellite-based remote sensing technique used to measure and monitor land deformation from a stack of interferometric SAR images. Its main products are the deformation maps (maps of the average displacement rates), the deformation time series and the maps of the so-called residual topographic error. This work focuses on X-band PSI and, in particular, PSI based on TerraSAR-X SAR imagery. Specifically, it concentrates on the thermal expansion component of PSI observations, which is caused by temperature differences in the observed scene between different SAR acquisitions. In order to properly model this component, we propose an extension of the standard two-parameter PSI model (deformation velocity and residual topographic error) with a third unknown parameter called the thermal dilation parameter. The map obtained from plotting this parameter is hereafter called "thermal map". In this work, we analyse the potentiality of this new PSI product. Some examples of thermal maps derived from a stack of 28 StripMap TerraSAR-X images that cover the metropolitan area of Barcelona (Spain) are discussed in depth.

# Retrieve ground parameters from QUASI-COHERENT targets for SAR interferometry

Author(s)

Hong Zhang <sup>(1)</sup>, Fan Wu, Yixian Tang <sup>(1)</sup>

Department

<sup>(1)</sup>Chinese academy of Sciences , CN

## Abstract

1. INTRODUCTION This study presents a multi-baseline InSAR method to retrieve terrain deformation and topography elevation from Quasi-Coherent Targets (Q-CTs), which distribute broadly on the earth surface with lower coherence compared to the permanent scatterers. The complex information of these targets is wholly exploited for system model establishment and precious parameters retrieval. For the large non-urban area where the ground information can not be well obtained due to the lack of Coherent Targets (CTs), the analysis from Q-CT InSAR approach can result effective parameters estimation, therefore bringing wider InSAR applications.

2. PROBLEM DESCRIPTIONS Multi-baseline DInSAR technique can generate long temporal ground deformation maps with high accuracy by jointly studying stacked SAR images of the same area [1, 5, 7, 8]. There are several well-known technologies, such as Permanent Scatterers technique [1], Small Baseline Subsets method [7], and Coherent Pixels technique [5], for deformation detection and terrain generation [3, 6] by exploiting the phase components of CTs. It should mention that the main drawback of CTs related techniques is the low spatial density of detectable coherent targets, particularly in vegetated non-urban areas. In other words, the lack of measured points can prevent from monitoring an area of interest affected by deformation with SAR techniques. Meanwhile the stable Q-CTs, with uniform scattering properties in the SAR resolution cell, exist broader and denser on the earth surface. With small normal baselines and temporal baselines, these targets can also be coherently observed in proper SAR image pairs. Recent studies have shown exciting information retrieval from Q-CTs SAR signals [2, 4]. In this study we mainly focus on the analysis of Q-CTs based on multi-baseline technique. The characteristic of these targets is fully exploited. A joint model is established by combining coherence and phase information to obtain more detailed surface deformation pattern and accurate topographic parameter. Considering the space related phase errors, such as atmospheric phase screen and orbit deviation errors, a weighted network for neighboring targets is built, which results simpler and effective parameter solutions.

3. EXPERIMENT AND RESULTS In this paper, 13 ascending ALOS PALSAR images relative to Tianjin, China are used to validate the algorithm. The dataset covers the period 2008/07/05-2010/08/26, and under short-baseline conditions there are 59 InSAR combinations. Due to over extraction of groundwater Tianjin has been suffering ground subsidence for long years. The experiment results show that there is obvious subsidence pattern detected during the period of 2008.07 to 2010.08. More importantly, the estimated ground displacement and topography can map the large non-urban regions with dense and precise information. Meanwhile the deformation pattern from CTs by conventional multi-baseline technique has also been obtained in this study to validate the Q-CTs results. Both are highly correlated. The denser deformation map retrieved by combining results from Q-CTs and CTs is well validated by filed survey measurements. Notice that because Q-CTs usually locate in the ground in non-urban area, this study can well obtain local terrain. The estimated terrain in our experiment is also in good consistence with the SRTM DEM relative to this area. With a broader non-urban area surface parameters inversion, this algorithm gives more practical application to SAR interferometry.

4. REFERENCES [1] A. Ferretti, C. Prati, and F. Rocca, "Nonlinear Subsidence Rate Estimation using Permanent Scatterers in Differential SAR Interferometry", IEEE Transactions on Geoscience and Remote Sensing, IEEE, USA, 38(5), pp. 2202-2212, September 2000. [2] A. M. Guarnieri and S. Tebaldini, "On the Exploitation of Target Statistics for SAR Interferometry Applications", IEEE

Transactions on Geoscience and Remote Sensing, IEEE, USA, 46(11), pp. 3436-3443, November 2008. [3] D. Perissin and F. Rocca, "High-accuracy Urban DEM using Permanent Scatterers", IEEE Transactions on Geoscience and Remote Sensing, IEEE, USA, 44(11), pp. 3338-3347, November 2006. [4] F. Rocca, "Modeling Interferogram Stacks", IEEE Transactions on Geoscience and Remote Sensing, IEEE, USA, 45(10), pp. 3289-3299, October 2007. [5] O. Mora, J.J. Mallorqui, and A. Broquetas, "Linear and Nonlinear Terrain Deformation Maps from a Reduced Set of Interferometric SAR Images", IEEE Transaction on Geoscience and Remote Sensing, IEEE, USA, 41(10), pp. 2243-2253, October 2003. [6] O. Mora, R. Arbiol, V. Pala, A. Adell, and M. Torre, "Generation of Accurate DEMs using DInSAR Methodology (TopoDInSAR)", IEEE Geoscience and Remote Sensing Letters, IEEE, USA, 3(4), pp. 551-554, October 2006. [7] P. Berardino, G. Fornaro, R. Lanari, and E. Sansosti, "A New Algorithm for Surface Deformation Monitoring based on Small Baseline Differential SAR Interferograms", IEEE Transactions on Geoscience and Remote Sensing, IEEE, USA, 40(11), pp. 2375-2383, November 2002. [8] T. Wu, C. Wang, H. Zhang, Y.X. Tang, and L. Tian, "Deformation Retrieval in Large Areas based on Multi-baseline DInSAR Algorithm: A Case Study in Cangzhou, Northern China", International Journal of Remote Sensing, Taylor & Francis, London, UK, 29(12), pp. 3633-3655, June 2008

## Ground Deformation Analysis by Persistent Scatterer Interferometry over the Whole Italian Territory: the Pst-A/2 Project

### Author(s)

Federico Minati <sup>(1)</sup>, Davide Colombo <sup>(2)</sup>, Mario Costantini <sup>(1)</sup>, Alessandro Ferretti <sup>(2)</sup>, Maria Grazia Ciminelli <sup>(1)</sup>, Salvatore Costabile <sup>(3)</sup>

### Department

<sup>(1)</sup>E-GEOS - an ASI/Telespazio Company Rome, Italy, IT

<sup>(2)</sup>TRE Milan, IT

<sup>(3)</sup>Ministero dell'Ambiente e della Tutela del Territorio e del Mare Rome, IT

### Abstract

1. INTRODUCTION Since the introduction of the fundamental ideas [1], persistent scatterer interferometry (PSI) has been successfully developed, validated and applied to detect and monitor slow ground movements due to subsidence, landslides, seismic and volcanic phenomena using satellite synthetic aperture radar (SAR) observations. In this work we will describe the first project devoted to create a persistent scatterer (PS) database at a national scale, a project that has required developing the most advanced PSI processing algorithms and suitable procedures to manage thousands of SAR images and hundreds of interferometric data-stacks, and represents a pioneering service for mapping and preventing geo-hazards. In 2008, the Italian Ministry of the Environment, in the framework of a programme called "Special Plan of Remote Sensing," awarded to an industrial team, led by e-GEOS and comprising TRE, a contract to provide the Italian Government with the first interferometric database for surface deformation analysis at a national level. This project, referred to as PST-A/2, is the first and only project in the world where terrain displacement monitoring at national scale (the whole Italian territory) is performed by means of SAR interferometry. Given this ambitious objective, e-GEOS and TRE had to rely on the most advanced PSI processing chains (based on developments of the algorithms described in [1], [2], [3]), and have developed suitable procedures to manage thousands of SAR images and hundreds of interferometric data-stacks. The PSI processing of the whole ERS and ENVISAT archives of SAR images (about 15,000 images) acquired over Italy (about 300,000 km<sup>2</sup>) from 1992 up to 2008 was already completed. Currently, the images acquired in 1999 and 2010 are being processed in order to update the PS database. Moreover, over three selected test sites, the PSI technology will be applied also to high resolution COSMO-SkyMed SAR data, in order to demonstrate the



possibility of upgrade the terrain displacement database with high resolution measurements. In the following sections we will summarize the overall project, the main challenges/problems (and relative solutions) related to such an ambitious objective, and the results already obtained.

**2. PROJECT DESCRIPTION** Italian research and industry have given a strong impulse to persistent scatterer interferometry developments and applications. The Italian Ministry of the Environment in 2008 awarded to an industrial team led by e-GEOS a contract to provide the Italian Government with the first interferometric database of surface deformations at a national level. This project, referred as PST-A/2, is part of a programme called "Special Plan of Remote Sensing," with the objective of mapping and preventing geo-hazards over the whole Italian territory (about 300.000 km<sup>2</sup>). PST-A/2 is the largest InSAR project ever funded, and it is the first and only project in the world where terrain displacement monitoring at national scale (the whole Italian territory) is performed by means of SAR interferometry. The final output of the project will be a database of displacement measurements from 1992 to 2010, and it will be provided to geologists and geophysicists for: identification of slow landslides possibly triggering faster phenomena; confirmation of the activation status of known landslides; mapping of new risk areas, not previously identified; quantitative analysis of other deformation phenomena like subsidence/compaction or seismic fault creeping; generation of a reference database for future investigations carried out using high-resolution sensors (e.g. COSMO SkyMed). For this ambitious objective, e-GEOS and TRE have counted on robust and parallel PSI processing chains (based on developments the algorithms described in [1], [2], [3]), capable of minimizing both user interaction (e.g. need for visual quality control) and processing time. Moreover, suitable techniques have been used to allow data calibration (possibly using prior information), to meet quality standards set by the Ministry and to guarantee the homogeneity of the results, properly mosaicking PS data in overlapping areas. The first phase of the project ended in May 2010, with the processing of the whole ERS and ENVISAT archive over the Italian territory from 1992 to 2008. The obtained products are made available to the Italian Regional Governments through the national cartographic portal (<http://www.pcn.minambiente.it/PCN/>) via WebGIS technology. The successful completion of the PST-A/2 project urged on the Italian Ministry of the Environment to commission to the same team the extension of the interferometric analysis till 2010. This update will be performed over the whole Italian territory with ENVISAT SAR data, and over a few selected test areas with high resolution COSMO-SkyMed SAR data. This second phase of the project is currently in progress and the end is scheduled by February 2012.

**3. CONCLUSIONS** Persistent scatterer interferometry is an effective technology for measuring slow ground deformation due to subsidence, landslides, earthquakes and volcanic phenomena. The project described in this work demonstrates that this cutting edge technology is already an operative tool for mapping and preventing geo-hazards. On the counter side, this work also demonstrates that the needs coming from professional and large scale applications further stimulate the research and the development of improvement to the PSI technology. This important experience should be capitalized and this kind of large area PSI analysis could be extended to other countries.

**4. REFERENCES** [1] A. Ferretti, C. Prati, and F. Rocca, "Permanent scatterers in SAR interferometry," *IEEE Trans. Geosci. Remote Sensing*, vol. 39, no.1, pp. 8-20, Jan. 2001. [2] A. Ferretti, C. Prati, and F. Rocca, "Non-linear subsidence rate estimation using permanent scatterers in differential SAR interferometry," *IEEE Trans. Geosci. Remote Sensing*, vol. 38, pp. 2202-2212, Sept. 2000. [3] M. Costantini, S. Falco, F. Malvarosa, F. Minati, "A new method for identification and analysis of persistent scatterers in series of SAR images," in *Proc. Int. Geosci. Remote Sensing Symp. (IGARSS)*, Boston MA, USA, pp. 449-452, 7-11 July 2008.

# Time Series InSAR: an Integer Least Squares approach for slowly decorrelating pixels

Author(s)

Sami Samiei Esfahany <sup>(1)</sup>, Ramon Hanssen <sup>(1)</sup>

Department

<sup>(1)</sup>Delft University of Technology , NL

## Abstract

During the last decade, different timeseries InSAR methodologies have been developed capable of detecting and monitoring various ground deformation mechanisms. The first generation of these techniques, called Persistent Scatterer Interferometry, focuses on targets with persistent behavior in time. These targets, named persistent scatterers, are coherent in the entire data stack and they are minimally affected by temporal and geometrical decorrelation. Persistent scatterers are usually small features (small with respect to the pixel size) with a dominant reflection in a resolution cell. Most of the PS are man made features, so there is a high density of them in urban areas and on infrastructures such as bridges, roads, dams and dikes. Also in mountain areas, some rocks and boulders can play the role of natural PS. However, the availability of persistent scatterers is not guaranteed. For example, in rural and agricultural areas, a low density of PS causes low spatial sampling of deformation processes. This limitation raised the question whether it is possible to extract useful information from resolution cells with distributed scattering mechanism in order to increase the spatial sampling of observed deformation signal. During the last couple of years, by processing more datasets and especially by availability of data with shorter satellite revisit times, it became evident that there are distributed scatterer (DS) resolution cells which contain coherent information not in the whole data stack but only in interferograms with short temporal baselines. That is, there are some areas which preserve coherence up to some time interval and gradually lose their coherence. We call them slowly decorrelating distributed scatterers. Consequently, a second generation of timeseries InSAR methodologies based on small baselines processing [ Berardino et al., 2002; Hooper 2008 ] and currently the SqueeSAR method were developed to extract information also from distributed scatterers. The goal of this contribution is to extend the geodetic mathematical model, which was developed for persistent scatterers, to a model which can exploit slowly decorrelating pixels. The main focus is on the integer least squares framework. This framework consists of a functional and a stochastic model. The functional model describes the relation between the observations and the unknown parameters, whereas the stochastic model describes the stochastic properties of the observation vector. The main challenge is to include the decorrelation effect in these models. In order to adapt the mathematical model for DS, we apply the following modifications: 1) changing the functional model from a single master to a multimaster configuration, 2) introducing the decorrelation effect in the stochastic model, and 3) introducing the effect of spatial filtering in the stochastic model. The temporal decorrelation effect is explained by a Wiener process as a random walk and is introduced in the covariance matrix of phase observations. As spatial filtering is a preferred step for extracting information from distributed scatterers, the effect of filtering is also introduced in the stochastic model. We perform an extensive simulation to test the algorithm and find a considerable improvement in correct estimation of ambiguities (i.e., correct unwrapping) for slowly decorrelating distributed pixels. We evaluate the performance of the algorithm over the Groningen area in the Netherlands. . Berardino, P., G. Fornaro, R. Lanari, and E. Sansosti (2002), A new algorithm for surface deformation monitoring based on small baseline differential SAR interferograms, IEEE Transactions on Geoscience and Remote Sensing, 40 (11), 2375 – 83, 2002.

## An improved persistent scatterer method for high deformation estimation

### Author(s)

Zahra Sadeghi <sup>(1)</sup>, Mohammad javad Valadan zouj <sup>(1)</sup>, Maryam Dehghani <sup>(1)</sup>

### Department

<sup>(1)</sup>K.n.toosi university Faculty of Geodesy and Geomatics Engineering, K.N.Toosi University of Technology, 1346, Vali-Asr Str, IR

### Abstract

Zahra Sadeghi<sup>1</sup>, Mohammad Javad Valadan Zouj<sup>1</sup>, Maryam Dehghani<sup>1</sup> <sup>1</sup> Faculty of Geodesy and Geomatics Engineering, K.N.Toosi University of Technology, 1346, Vali-Asr Street, Mirdamad Cross, Tehran , Iran, E-mail:atena\_sadeghi\_ak@yahoo.com, valadanzouj@kntu.ac.ir, dehghani\_rsgsi@yahoo.com In the most of the presented PSI algorithm the PS pixels are identified as those whose phase histories match an assumed model of how displacement varies with time. One of algorithm is developed by Delft University of Technology as DePSI (Delft implementation for Persistent Scatterer Interferometry), in which the PS candidates with amplitude analysis are selected. These PSI algorithms fail to identify PS pixels in rural areas lacking man-made structures. Hooper introduced a new PSI method called StaMPS (Stanford Method for PS) that uses amplitude and phase analysis in order to identify PS pixel and no prior knowledge of the variations in deformation rate is required. The required condition for phase unwrapping is not met due to high subsidence rate and this lead to significant phase unwrapping errors. Therefore, in this paper we present an enhanced algorithm based on PSI in order to estimate deformation rate in rural area undergoing high and nearly constant deformation rate. The proposed approach integrates the merits of all existing PSI algorithms in PS pixel selection and phase unwrapping. In our proposed algorithm , N interferograms from N+1 images acquired at different times are formed with respect to one master image maximizing the stack coherence. PS pixels are identified using amplitude and phase analysis according to StaMPS algorithm. After PS pixels selections, the spatially-uncorrelated part of the look angle error and the contribution of the master to the spatially-uncorrelated part of the signal are estimated and removed from the original phase before phase unwrapping. For deformation estimation, there are three principal steps. In the first step the linear component of deformation is obtained as preliminary estimation. PS pixels are connected to form a network and make double-difference phase. As long as atmospheric phase screen (APS) that is the contribution due to atmospheric delay and orbital errors, is strongly correlated in space, the contribution of APS to double-difference phase for arcs with length shorter than threshold value can be neglected. On the other hand, due to the nearly constant rate of the deformation in the study area, a constant-velocity model for targets motion is considered. Moreover, the influence of the noise on the time series of each arc is minimized by applying a temporal low-pass filtering method. Therefore, the principal goal is to estimate the relative constant velocity and integer ambiguity from wrapped phase. In order to estimate the unknowns, we use temporal unwrapping method presented in DePSI approach. The approach that is used for temporal unwrapping is least squares ambiguity decorrelation adjustment (LAMBDA). This approach yields an optimal solution, capable of using any variance-covariance matrix of observations . Moreover, it is very fast. The arcs with very low temporal coherence estimates are eliminated in order to detect unwrapping error. Consequently, some of the selected PS pixels are lost. The relative velocities and integer ambiguities spatially are then unwrapped in order to obtain the absolute values with respect to a reference PS pixel. As the residual phase as the result of the pervious step includes atmospheric delay, orbital errors, nonlinear deformation and

noise, in the next step it is tried to approximate the APS and nonlinear component of deformation by applying a temporal high pass filter and spatial low pass filter for remaining PS pixel. Moreover the kriging method is finally employed to spatially interpolate resulting phase due to APS and nonlinear deformation to approximate contributions of these phenomena to phase for all removed PS. After subtraction of the phases due to APS and nonlinear deformation, in the final step the linear component of deformation is obtained as in first step is explained . Tehran basin is located in the north of Iran, between the Alborz Mountains to the north and the Arad and Fashapouye mountains to the south. The test area is a sub-selection of Southwestern Tehran basin with the maximum subsidence rate due to the over-exploitation of groundwater. The approach is applied to the 22 descending ENVISAT ASAR images of track 149 spanning between 2003 and 2008. The maximum estimated velocity was- 24.95 cm/year. Moreover, by analysis of an additional adjacent track (378) including 14 ENVISAT ASAR images between 2003 to 2005 using conventional SBAS algorithm, the deformation rate of the area was extracted and was compared to the deformation rate obtained from proposed algorithm. The absolute maximum of the difference between both deformation rates is 4.30 cm/yr. However, the mean value and the standard deviation of the histogram are estimated as near zero and 1.2 cm/yr, respectively, demonstrating the high performance of the presented algorithm. Moreover using leveling observation, the obtained results are evaluated and the results show the pattern of deformation along the leveling station is identical that it indicates success of our proposed algorithm in deformation estimation. In this paper, we have presented an enhanced algorithm based on PSI in order to estimate the high subsidence rate in southwestern Tehran basin and The results illustrated the significant improvement to the PSI method.

## Ground Deformation Time Series Analysis from Temporarily Coherent Point InSAR

### Author(s)

Lei Zhang <sup>(1)</sup>, Zhong Lu <sup>(2)</sup>, Xiaoli Ding <sup>(3)</sup>, Hyung-Sup Jung <sup>(4)</sup>

### Department

<sup>(1)</sup>The Hong Kong Polytechnic Univeristy Hung Hom, KLN, HK

<sup>(2)</sup>U.S. Geological Survey , USA

<sup>(3)</sup>The Hong Kong Polytechnique University , HK

<sup>(4)</sup>The University of Seoul , KR

### Abstract

Phase unwrapping, a vital step in current multi-temporal InSAR (MT-InSAR) techniques (e.g., PSI and SBAS), is usually performed either by searching a predefined solution space, LAMBDA, or 2D/3D sparse Minimum Cost Flow (MCF) algorithms. However, the success rate of phase unwrapping can never be guaranteed. Considering the fact that the SAR data are increasingly available and new sensors (e.g. TerraSAR-X and COSMO-Skymed, and future Sentinel-1) can acquire data in rather short repeat intervals, why should we still be bothered by the estimation of phase ambiguities to retrieve the deformation time series? In this paper we propose a novel MT-InSAR approach termed as Temporarily Coherent Point InSAR (TCPInSAR) that can isolate the coherent points from a small set of SAR images and estimate the deformation time series without phase unwrapping. The approach has a series of innovations including TCP identification, TCP networking and TCP least squares estimator. The parameter estimation utilizes a well-known fact that there is usually no phase ambiguity at relatively short arcs constructed by densely distributed coherent points in interferograms with short baselines. Although the core algorithms related to TCP identification and deformation parameter estimation have been documented in [1, 2] using synthetic datasets, processing details on the application of TCPInSAR to real datasets and the retrieval of time evolutionary deformation patterns have not been fully discussed. Here

from several case studies where our TCPIInSAR approach has been successfully applied, we present the one related to Los Angeles basin in southern California. More than 40 Envisat/ASAR images (Track 170 Frame 2925) acquired from 2003 to 2010 are processed to demonstrate the performance of the TCPIInSAR approach. The estimated deformation time series has been adequately validated by the CGPS observations from Southern California Integrated GPS network (SCIGN). References: [1] Zhang, L., Ding, X.L., & Lu, Z. (2011a). Ground settlement monitoring based on temporarily coherent points between two SAR acquisitions. *ISPRS Journal of Photogrammetry and Remote Sensing*, 66, 146-152 [2] Zhang, L., Ding, X.L., & Lu, Z. (2011b). Modeling PSIInSAR time series without phase unwrapping. *IEEE Transactions on Geoscience and Remote Sensing*, 49, 547-556

## DInSAR Pixel Selection based on Spectral Correlation in Time between Sublooks

### Author(s)

Dani Monells <sup>(1)</sup>, Rubén Iglesias <sup>(1)</sup>, Giuseppe Centolanza <sup>(1)</sup>, Jordi Mallorqui <sup>(1)</sup>, Juan M López-Sánchez <sup>(2)</sup>, Paco López-Dekker <sup>(3)</sup>

### Department

<sup>(1)</sup>Universitat Politècnica de Catalunya (UPC), ES

<sup>(2)</sup>Universidad de Alicante P.O.Box 99, ES

<sup>(3)</sup>DLR Oberpfaffenhofen, DE

### Abstract

Interferogram phase quality is a key issue in SAR Differential Interferometry (DInSAR) processing in order to obtain reliable results. Deformation information cannot be extracted from all the pixels within the area under study since, due to decorrelation, only part of them would have enough phase quality along the stack. The main agents that reduce phase stability are the spatial and temporal decorrelation. For this reason prior the application of DInSAR techniques an adequate pixel selection over the available data is mandatory. This paper presents a high resolution pixel selection alternative to the traditional Coherence Selection Method [1] and the Permanent Scatterers (PS) Technique [2], based on the study of the spectral correlation in time between different Sublooks of the image spectrum. This DInSAR pixel criterion has been developed from the concept of the so-called Coherent Scatterers (CS) [3], characterized by a deterministic point-like scattering behavior in a single acquisition, but considering now its temporal stability. This method reduces the resolution loss due to the multilook processing in the coherence method, reduces the restriction on the required number of images and eliminates the radiometric calibration step for amplitude selection. As in the latter, reliability of the phase estimator depends on the number of acquisitions available so the performance of both estimators with respect the available number of images will be studied. The method is more suitable for urban areas, where the density of temporal stable point-like scatterers is higher. The proposed method uses the unweighted sinc impulse response SAR image so any windowing applied during the focusing have to be undone to obtain a rectangular spectrum. The next step is to divide each image spectrum into 2 or more Sublooks. Stable Point-like scatterers are characterized by a correlated spectrum in range and azimuth along all the stack of interferograms. The temporal stable point-like scatterers will preserve a constant spectrum along time so the estimated temporal spectral correlation between Sublooks will be high and these targets will take part in the final selection. Two different estimators have been studied to obtain the temporal spectrum correlation: the coherence and the entropy. The entropy estimator has demonstrated to be better due to its major sensitivity in high quality values, i.e. high coherence or low entropy. Finally, a multi-layer processing is applied over the selected pixels using the Coherent Pixels Technique algorithm [1]. Selected pixels are divided in different layers according to their quality for the temporal spectral

correlation value. After that, beginning with the top layer, the linear block (linear velocity and topographic error estimation) is iteratively executed by adding successive layers, so obtained absolute velocity and topographic error values of each layer act as the seed values to the following integration process improving linear results and rising pixel density but preserving quality. Another aspect is that not all the points detected in the pixel selection are related to real targets. Undesired artifacts appear due to the SAR characteristics: redundant information around the main lobe and the side lobes of high power scatterers in zones of limited coefficient of backscattering. In order to face this problem, the use of a Spatially Variant Apodization (SVA) algorithm is proposed [4]. This method uses non-linear operators to reduce the width of the main lobes and also to suppress the side lobes. Several datasets from different sensors (ERS-2, Envisat, TerraSAR-X and Radarsat-2) over urban areas will be used to test the wellness of the method, taking as a reference the Permanent Scatterers Technique for comparison purposes. This comparison will be performed both in terms of selected pixels, checking both the number and the coincidence, and in terms of deformation and DEM error retrieved. [1] Blanco, P.; Mallorquí, J.J.; Duque, S.; Monells, D.; "The Coherent Pixels Technique (CPT): an Advanced DInSAR Technique for Non-linear Deformation Monitoring", *Pure and Applied Geophysics*, 165, 1167-1193, 2008 [2] Ferretti, A.; Prati, C.; Rocca, F.; "Permanent scatterers in SAR interferometry", *Geoscience and Remote Sensing Symposium*, 1999. IGARSS '99 Proceedings. IEEE 1999 International , vol.3, no., pp.1528-1530 vol.3, 1999 [3] Schneider, R.Z.; Papathanassiou, K.P.; Hajnsek, I.; Moreira, A., "Polarimetric and interferometric characterization of coherent scatterers in urban areas", *Geoscience and Remote Sensing, IEEE Transactions on*, vol.44, no.4, pp. 971- 984, April 2006 [4] Smith, B.H.; "Generalization of spatially variant apodization to noninteger Nyquist sampling rates," *Image Processing, IEEE Transactions on* , vol.9, no.6, pp.1088-1093, Jun 2000

## A simulated annealing (SA) algorithm to efficiently select the interferometric SAR data pairs used by the EMCF phase unwrapping technique

Author(s)

Antonio Pepe <sup>(1)</sup>

Department

<sup>(1)</sup>IREA-CNR , IT

### Abstract

Yang Y 1,2, Pepe A 1, Manzo M 1, and Lanari R 1 [1] Istituto per il Rilevamento Elettromagnetico dell'Ambiente, CNR, 328 Diocleziano, I-80124 Napoli, Italy; e-mail:{yang.y, pepe.a, manzo.mr, lanari.r@irea.cnr.it} [2] National University of Defense Technology, P.R. China Abstract We present a new procedure to properly select the interferometric SAR data pairs involved in the generation of deformation time series by using the Small BAseline Subset (SBAS) algorithm [1]. In particular, we propose an approach that is thought to be fully compatible with the Extended Minimum Cost Flow (EMCF) Phase Unwrapping strategy [2]. The EMCF technique exploits two Delaunay triangulations, the former is relevant to the SAR acquisition distribution in the "temporal-perpendicular baseline" plane, allowing us to identify the sequence of multilook interferograms to be generated, the latter is computed in the azimuth/range plane and involves a set of coherent pixels common to the generated interferograms. Compared to conventional MCF phase unwrapping operations [3], which are independently performed on each single interferogram, the EMCF technique jointly exploits both the spatial characteristics and the temporal relationships among the differential interferograms. The core of the EMCF algorithm is represented by the "temporal" PhU step, which is carried out by exploiting the distribution of the selected SAR data pairs in the temporal/perpendicular baseline plane. However, the Delaunay triangulation has the

most uniform distribution of the angles, but may also involve interferograms corrupted by severe decorrelation phenomena [4]. To circumvent this problem, we propose in this work a new method to efficiently search, among all the possible triangulations in the temporal/perpendicular baseline domain, the one that minimizes the decorrelation noise. In particular, we have implemented a procedure based on the application of a Simulated Annealing (SA) searching algorithm [5]. The starting point is the selection of the most appropriate “fitness” function to be exploited by the SA algorithm. To this purpose, we observe that each triangle of a generic triangulation identifies an “elementary loop” composed by three (multilook) interferograms. Accordingly, if we consider the  $t$ -th elementary loop involving the SAR acquisitions labeled to as A, B, C in the temporal/perpendicular baseline domain, the corresponding three A-B), f(B-C), and f(C-A).(multilook) differential interferograms are  $f_A$ s evident, the sum of these three phase differences is a random signal with a zero mean value and a standard deviation that depends on the decorrelation noise in the interferograms. Therefore, small values of such differences correspond to interferograms less affected by noise. Accordingly, we use as the fitness function to be maximized by the SA algorithm a factor strictly dependent on such differences, defined similarly to the temporal coherence [2] and hereinafter referred to as “congruence”. The starting point of the implemented SA procedure is the computation of the “congruence” of the standard Delaunay triangulation in the temporal/perpendicular baseline plane. Then, the SA algorithm mutates the triangulations as long as the maximum value of the fitness function is reached; the mutation is performed through a simple flip-edge operation [6]. It is worth to remark that no constraints on the temporal and perpendicular baseline of the involved SAR data pairs are imposed. Subsequently, in order to further reduce the impact of the decorrelation noise, we discard from the obtained triangulation the triangles that still involve too much noisy interferograms. To do this efficiently, we analyze the sum of the phases over each elementary loop  $t$  of the retrieved triangulation  $T_r$  in the temporal/perpendicular baseline domain. We present in this work the results of the first experiment we have carried out on a set of 39 descending ENVISAT SAR data relevant to the Abruzzi area (Italy), spanning the 2002-2009 time interval. The improvement of the phase unwrapping performances clearly demonstrate the effectiveness of the proposed method.

REFERENCES [1] P. Berardino, G. Fornaro, R. Lanari, and E. Sansosti, “A new algorithm for surface deformation monitoring based on small baseline differential SAR interferograms,” *IEEE Trans. Geosci. Remote Sens.*, vol. 40, no. 11, pp. 2375–2383, Nov. 2002. [2] A. Pepe, and R. Lanari R., “On the extension of the minimum cost flow algorithm for phase unwrapping of multitemporal differential SAR interferograms,” *IEEE Trans. Geosci. Remote Sens.*, vol. 44, no. 9, pp. 2374-2383, Sept. 2006. [3] M. Costantini and P. A. Rosen, “A Generalized Phase Unwrapping Approach for Sparse Data”, in *Proc. Geosc. and Rem. Sensing Symposium (IGARSS)*, Hamburg (Germany), Jun. 1999, pp. 267–269. [4] H. A. Zebker and J. Villasenor, “Decorrelation in interferometric radar echoes,” *IEEE Trans. Geosci. Remote Sens.*, vol. 30, no. 5, pp. 950–959, 854 Sep. 1992. [5] D. Bertsimas and J. Tsitsiklis, “Simulated Annealing, “ *Statistical Science*, vol. 8, n.1, pp. 10-15, 1993. [6] O. Aichholzer, F. Aurenhammer, T. Hackl and B. Speckmann, “On minimum weight pseudo-triangulations,” *Computational Geometry*, doi:10.1016/j.comgeo.2008.10.002, 2008.

---





# NOTES

























